MAY 2025
VOLUME 84

ISSUE
5

ANNALS OF THE **RHEUMATIC DISEASES**

THE EULAR JOURNAL

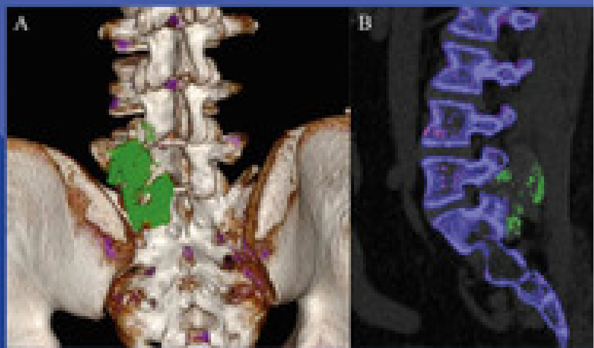

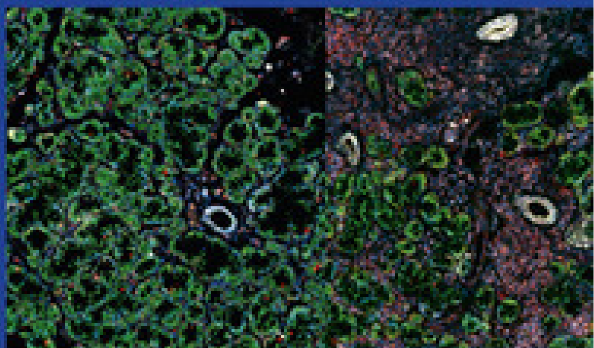

ELSEVIER

eular
EUROPEAN ALLIANCE OF ASSOCIATIONS FOR RHEUMATOLOGY

The home of innovative rheumatology research

Ann Rheum Dis 84 (2025) 657−659

Contents lists available at ScienceDirect

Annals of the Rheumatic Diseases

journal homepage: https://www.sciencedirect.com/journal/annals-of-the-rheumatic-diseases

Editorial

Molecular endotypes and theratypes in osteoarthritis: transforming a concept into reality with deep learning and multiomics

Osteoarthritis (OA) is now understood as a heterogeneous disease in many respects, including its clinical presentation, underlying pathophysiological mechanisms, and response to treatments. Distinct phenotypes, shaped by key risk factors such as metabolic dysfunction, ageing, and prior joint injury, suggest divergent pathophysiological pathways. This challenges the conventional view of OA as a singular disease process and raises a critical question: does OA represent a single, multifactorial disease with shared endpoints or a spectrum of distinct pathological mechanisms converging on a common clinical outcome [1]?

To better capture this heterogeneity, initial efforts focused on defining clinical phenotypes based on established risk factors [2,3]. Advances in systems biology, high-dimensional analytics, and omics technologies have shifted the focus towards identifying OA *endotypes*—subgroups characterised by distinct molecular or cellular signatures offering deeper insight into the complex mechanisms driving OA pathophysiology and precise disease stratification [4,5].

More recently, the concept of theratypes has emerged, referring to endotypes associated with treatment response prediction [6]. However, applying a theratype-driven approach to OA remains challenging, as no treatment effectively slows OA progression, and more than 40% of patients report dissatisfaction with their treatment [7]. This underscores the need to refine therapeutic strategies, particularly in the context of analgesia or multimodal management. Theratype-based approaches may be particularly relevant in end-stage knee OA, where total knee arthroplasty (TKA) remains the final option for many patients. Despite its widespread use, 20% to 34% of patients report persistent postoperative pain [8], underscoring the need for better risk stratification. Predicting TKA response remains a critical, unmet need. While several risk factors, such as high body mass index, smoking, widespread pain or depression, and opioid use, have been associated with poor outcomes [9−11], these factors alone are insufficient to reliably predict TKA response. Additionally, they fail to capture the underlying molecular and cellular complexity of OA and its symptoms, notably pain. Identifying theratypes could enable more precise patient stratification, ultimately optimising postoperative outcomes and improving patient satisfaction [12].

While these concepts are well-defined in theory, supporting data remain limited. Rockel et al [13] address this gap by providing experimental evidence and data to advance these concepts. In a cohort of 414 patients with late-stage knee OA eligible for TKA, the authors collected pre- and per-operative clinical variables and multiomics data, including 2727 molecular features that consisted of microRNA (miRNA) from plasma, synovial fluid, and urine and metabolites from plasma. They developed a multimodal deep learning model with a variational autoencoder (VAE) architecture to identify patient clusters and key molecular signatures. VAEs are unsupervised deep learning algorithms that reduce high-dimensional data via latent space representation, enabling pattern recognition while preserving heterogeneity through probabilistic modelling. These models are particularly powerful for integrating diverse multiomics data.

Using their VAE-based algorithm, Rockel et al [13] identified 3 distinct preoperative clusters, each characterised by unique molecular signatures and pathway associations. Cluster 1 was enriched for metabolites and pathways related to development and regeneration and nervous system function. Cluster 2 was associated with features of ageing and cellular community dynamics, while cluster 3 was linked to catabolic processes, immune activation, and lipid metabolism. Clinical characteristics exhibited minimal variation across clusters, suggesting that these groupings capture underlying biological differences not reflected in standard clinical assessments, supporting the concept of molecular endotypes extending beyond traditional clinical phenotypes.

The authors then explored whether these endotypes could serve as theratypes predictive of TKA response. Using multimodal machine learning modelling, the primary outcome was an improvement in the Western Ontario and McMaster Universities Arthritis Index (WOMAC) pain and function scores at 1 year, with response defined as a ≥33.3% improvement. While overall pain and functional outcomes did not differ significantly across clusters, the predictors of response varied: plasma miRNAs were most informative in cluster 1, clinical variables in cluster 2, and urinary miRNAs in cluster 3. Notably, integrative multiomics analysis identified key predictive features, including synovial fluid miRNAs (hsa-miR-1265 and hsa-miR-642a) and plasma miRNAs (hsa-miR-3942-5p), underscoring the potential of multilayered molecular profiling to refine patient stratification. Furthermore, combining clinical and biological data improved predictive performance, increasing the area under the curve in each cluster analysis and reinforcing the value of multimodal integration over single-modality approaches.

Rockel et al [13] highlight the potential of deep learning and multiomics in personalised medicine and TKA outcome

https://doi.org/10.1016/j.ard.2025.03.009
Received 23 February 2025; Revised 11 March 2025; Accepted 17 March 2025

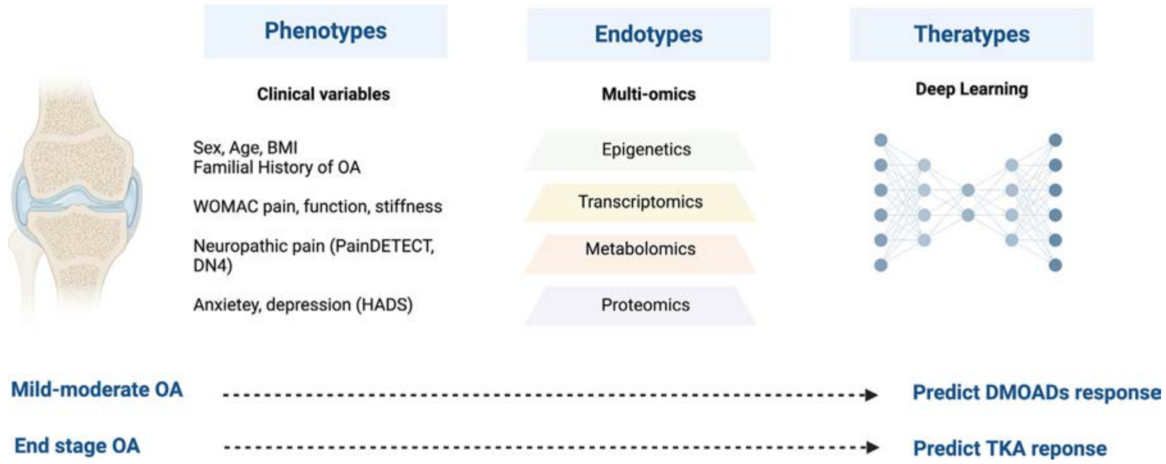

Figure. Application of multiomics and machine learning in endotypes and theratypes identification. BMI, body mass index; DMOAD, disease-modifying osteoarthritis drugs; HADS, Hospital Anxiety Depression Score; OA, osteoarthritis; TKA, total knee arthroplasty; WOMAC, Western Ontario and McMaster Universities Arthritis Index; DN4, Douleur Neuropathic 4.

prediction. These approaches require large-scale, high-quality omics datasets, which are inherently complex and heterogeneous. Additionally, broad clinical implementation remains challenging, as multiomics methods may not be feasible for every patient due to cost and scalability constraints. Rockel et al [13] successfully integrated data from over 400 patients, demonstrating the feasibility of large-scale multiomics analysis in OA. However, these approaches remain challenging for external validation and multicenter studies due to the lack of standardised datasets and reproducibility concerns. Notably, Rockel et al [13] addressed this challenge by ensuring data transparency through the public availability of their dataset and code, facilitating further research and validation efforts.

Machine learning and deep learning are playing an expanding role in OA research, facilitating multiomics integration through dimensionality reduction techniques that bridge the gap between high-dimensional data and biological understanding [14,15]. Effective integration of these datasets is critical, enhancing model accuracy while mitigating both experimental and biological noise. The strength of this study lies in its ability to combine multiomics layers, offering a more comprehensive view of the biological mechanisms underlying TKA response while addressing a practical clinical challenge beyond theoretical biological concepts.

This integrative strategy is essential for advancing precision medicine and deepening our understanding of complex diseases such as OA. However, deep learning models are inherently susceptible to a lack of interpretability, as described by the black box effect [16]. These models predict outcomes without necessarily identifying the mechanistic pathways responsible for success or failure. There is a pressing need to develop explainable machine learning and causal inference models to uncover the mechanistic pathways driving TKA outcomes. Additionally, defining a 33% improvement in WOMAC scores as a threshold for success may be overly stringent for a surgical intervention. Arthroplasty outcomes are increasingly assessed using dedicated patient-centred metrics, such as the ‘forgotten knee’ concept, which can be evaluated through a simple closed question (ie, ‘Does the operated knee feel always normal in all everyday activities?’) or a specific questionnaire, further emphasising the need for robust and clinically meaningful predictive models [17,18]. Furthermore, given the risks associated with TKA, including infection and prosthesis loosening, theratype-driven approaches may ultimately prioritise safety and tolerability as much as efficacy [19].

Despite these challenges, multiomics integration remains a powerful tool for identifying key phenotypes, endotypes, and theratypes, offering new opportunities for personalised OA treatment. Once effective disease-modifying OA drugs become available, theratypes could help identify patients most likely to benefit from these costly treatments, ensuring more personalised and efficient therapeutic strategies. Rockel et al [13] pave the way for translating this concept into clinical reality, marking a significant step towards data-driven treatment optimisation in OA care (Fig).

Funding

JS funding: Going Inside Osteoarthritis-Related Pain Phenotyping (GO-PAIN) 2022 ERA-NET NEURON grant and Pfizer ADVANCE 2020 grant, ANR-24-CE14-1824 CholinOA.

Competing interests

MB reports no competing interests. JS reports personal fees from Merck Sharp & Dohme (MSD), Pfizer, AbbVie, Fresenius Kabi, Bristol Myers Squibb (BMS), Lilly, Novartis, Union Chimique Belge (UCB), Grunenthal, Nordic Pharma, Biogen, and Janssen.

Patient consent for publication

Non applicable

Ethics approval

Non applicable

Provenance and peer review

Not commisioned; externally peer reviewed

Declaration of generative AI and AI-assisted technologies in the writing process

During the preparation of this editorial, the authors used ChatGPT in order to correct English (spelling, syntax and grammar). After using this tool, the author reviewed and edited the content as needed and took full responsibility for the content of the publication.

Orcid

Jérémie Sellam: http://orcid.org/0000-0002-1814-6003

Marie Binvignat[1,2], Jérémie Sellam[1,*]
[1] *Rheumatology Department, Sorbonne Université, Saint-Antoine Hospital Assistance Publique Hôpitaux de Paris (AP-HP), Centre de Recherche Saint-Antoine (CRSA) Inserm UMRS-938, Paris, France*
[2] *Immunology, Immunopathology, Immunotherapy I3 Lab, Inserm UMRS-959, Sorbonne Université, Paris, France*
*__Correspondence to__ Prof Jérémie Sellam, Rheumatology Department, Sorbonne Université, Saint-Antoine Hospital, Assistance Publique Hôpitaux de Paris (AP-HP), Centre de Recherche Saint-Antoine (CRSA) Inserm UMRS-938, Paris, France.
E-mail address: jeremie.sellam@aphp.fr (J. Sellam).

REFERENCES

[1] Deveza LA, Loeser RF. Is osteoarthritis one disease or a collection of many? Rheumatology (Oxford) 2018;57 iv34-42. doi: 10.1093/rheumatology/kex417.
[2] Courties A, Berenbaum F, Sellam J. The phenotypic approach to osteoarthritis: a look at metabolic syndrome-associated osteoarthritis. Joint Bone Spine 2019;86:725–30. doi: 10.1016/j.jbspin.2018.12.005.
[3] Dell'Isola A, Allan R, Smith SL, Marreiros SSP, Steultjens M. Identification of clinical phenotypes in knee osteoarthritis: a systematic review of the literature. BMC Musculoskelet Disord 2016;17:425. doi: 10.1186/s12891-016-1286-2.
[4] Kraus VB, Hsueh MF. Molecular biomarker approaches to prevention of post-traumatic osteoarthritis. Nat Rev Rheumatol 2024;20:272–89. doi: 10.1038/s41584-024-01102-y.
[5] Berenbaum F. Deep phenotyping of osteoarthritis: a step forward. Ann Rheum Dis 2019;78:3–5. doi: 10.1136/annrheumdis-2018-213864.
[6] Hunter DJ, Deveza LA. Deconstructing the "types" of osteoarthritis. Osteoarthritis Imaging 2025;5:100257. doi: 10.1016/j.ostima.2024.100257.
[7] Vitaloni M, Botto-van Bemden A, Sciortino R, Carné X, Quintero M, Santos-Moreno P, et al. A patients' view of OA: the Global Osteoarthritis Patient Perception Survey (GOAPPS), a pilot study. BMC Musculoskelet Disord 2020;21:727. doi: 10.1186/s12891-020-03741-0.
[8] Beswick AD, Wylde V, Gooberman-Hill R, Blom A, Dieppe P. What proportion of patients report long-term pain after total hip or knee replacement for osteoarthritis? A systematic review of prospective studies in unselected patients. BMJ Open 2012;2:e000435. doi: 10.1136/bmjopen-2011-000435.
[9] Li J, Guan T, Zhai Y, Zhang Y. Risk factors of chronic postoperative pain after total knee arthroplasty: a systematic review. J Orthop Surg Res 2024;19:320. doi: 10.1186/s13018-024-04778-w.
[10] Boyce L, Prasad A, Barrett M, Dawson-Bowling S, Millington S, Hanna SA, et al. The outcomes of total knee arthroplasty in morbidly obese patients: a systematic review of the literature. Arch Orthop Trauma Surg 2019;139:553–60. doi: 10.1007/s00402-019-03127-5.
[11] Mohammad HR, Gooberman-Hill R, Delmestri A, Broomfield J, Patel R, Huber J, et al. Risk factors associated with poor pain outcomes following primary knee replacement surgery: analysis of data from the clinical practice research datalink, hospital episode statistics and patient reported outcomes as part of the STAR research programme. PLoS One 2021;16:e0261850. doi: 10.1371/journal.pone.0261850.
[12] Mobasheri A, Loeser R. Clinical phenotypes, molecular endotypes and theratypes in OA therapeutic development. Nat Rev Rheumatol 2024;20:525–6. doi: 10.1038/s41584-024-01126-4.
[13] Rockel JS, Sharma D, Espin-Garcia O, Hueniken K, Sandhu A, Pastrello C, et al. Deep learning−based clustering for endotyping and post-arthroplasty response classification using knee osteoarthritis multiomic data. Ann Rheum Dis 2025 Published online February 12. doi: 10.1016/j.ard.2025.01.012.
[14] Binvignat M, Pedoia V, Butte AJ, Louati K, Klatzmann D, Berenbaum F, et al. Use of machine learning in osteoarthritis research: a systematic literature review. RMD Open 2022;8:e001998. doi: 10.1136/rmdopen-2021-001998.
[15] Bonaguro L, Schulte-Schrepping J, Ulas T, Aschenbrenner AC, Beyer M, Schultze JL. A guide to systems-level immunomics. Nat Immunol 2022;23:1412–23. doi: 10.1038/s41590-022-01309-9.
[16] Rudin C. Why black box machine learning should be avoided for high-stakes decisions, in brief. Nat Rev Methods Primers 2022;2:1–2. doi: 10.1038/s43586-022-00172-0.
[17] Eymard F, Charles-Nelson A, Katsahian S, Chevalier X, Bercovy M. Predictive factors of "Forgotten Knee" acquisition after total knee arthroplasty: long-term follow-up of a large prospective cohort. J Arthroplasty 2017;32:413–418.e1. doi: 10.1016/j.arth.2016.06.020.
[18] Lan RH, Bell JW, Samuel LT, Kamath AF. Evolving outcome measures in total knee arthroplasty: trends and utilization rates over the past 15 years. J Arthroplasty 2020;35:3375–82. doi: 10.1016/j.arth.2020.06.036.
[19] Sweerts L, Hoogeboom TJ, van Wessel T, van der Wees PJ, van de Groes SAW. Development of prediction models for complications after primary total hip and knee arthroplasty: a single-centre retrospective cohort study in the Netherlands. BMJ Open 2022;12:e062065. doi: 10.1136/bmjopen-2022-062065.

Ann Rheum Dis 84 (2025) 660−663

Contents lists available at ScienceDirect

Annals of the Rheumatic Diseases

journal homepage: https://www.sciencedirect.com/journal/annals-of-the-rheumatic-diseases

Viewpoint

Statistical review: frequently given comments updated

Stian Lydersen *

Regional Centre for Child and Youth Mental Health and Child Welfare, Department of Mental Health, Faculty of Medicine and Health Sciences, Norwegian University of Science and Technology (NTNU), Trondheim, Norway

ARTICLE INFO

Article history:
Received 19 December 2024
Received in revised form 3 February 2025
Accepted 4 February 2025

ABSTRACT

From 2006 to 2024, I have carried out statistical reviews of about 700 manuscripts for *Annals of the Rheumatic Diseases* and *RMD open*. My most frequent review comments concern the following:

1. Report how missing data were handled.
2. Limit the number of covariates in regression analyses.
3. Do not use stepwise selection of covariates.
4. Validate prediction models.
5. Adjust for baseline values in randomised controlled trials.
6. Do not adjust for baseline values in observational studies.
7. Dichotomising a continuous variable can be a bad idea.
8. Student *t* test is better than nonparametric tests.
9. Mean (SD) are also relevant for nonnormally distributed data.
10. Adjusting *P* values for multiplicity.
11. Report estimate, CI, and (possibly) *P* value—in that order of importance.
12. Do not test for baseline imbalances in a randomised controlled trial.
13. Format for reporting CIs.
14. Mind the number of reported decimal places.
15. Report absolute numbers where relevant.

INTRODUCTION

From 2006 to 2024, I have carried out statistical reviews of about 700 manuscripts for *Annals of the Rheumatic Diseases* and *RMD open*. Some errors and weaknesses occur more often than others and have been listed in my viewpoint in *Annals of the Rheumatic Diseases* in 2015 [1]. This viewpoint is an update of this list. Compared with the list from 2015, most items on the list remain, Yates correction and post hoc power are deleted as they occur more seldom, and prediction model validation, multiplicity adjustment, and reporting of absolute numbers have been added. Furthermore, references are updated.

I hope this can help authors to avoid these statistical errors and weaknesses in future manuscripts. Some statistical terms are explained in the Appendix.

1. REPORT HOW MISSING DATA WERE HANDLED

Report the amount of missing data in the different variables [2,3] and how this was handled in the analyses. Commonly used methods are, from the less to the more complex ones, complete case analysis (disregarding cases with partially missing data), single imputation methods like expectation-maximation imputation, multiple imputation, and full information maximum likelihood. In longitudinal studies, mixed models may be appropriate, while

*Correspondence to Prof. Stian Lyderson.

E-mail address: stian.lydersen@ntnu.no

Handling editor Josef S. Smolen.

https://doi.org/10.1016/j.ard.2025.02.007

last observation carried forward is almost always biased and should be avoided where possible [4].

2. LIMIT THE NUMBER OF COVARIATES IN REGRESSION ANALYSES

Some authors attempt to include too many covariates compared with the number of cases in a regression model, for example, 17 covariates in a study with 64 cases. Traditional rules of thumb state that the ratio of cases per covariate ought to be at least in the size of order 10. Some authors recommend 15, some 20, and others state that 5 is sufficient. In logistic regression and Cox regression, 10 events per variable is usually sufficient [5], and in many situations, 5 events per variable is sufficient [6]. Note that in logistic regression, this is not the total number of observations, but the smallest of the two outcome groups. Similarly, in Cox regression, one should have at least 5-10 events per variable, disregarding censored observations.

3. DO NOT USE STEPWISE SELECTION OF COVARIATES

Automated variable selection procedures like stepwise selection used to be very popular. Today an increasing number of analysts criticise such methods. For example Rothman [7] page 419, state the following: 'There are several systematic, mechanical, and traditional algorithms for finding models (such as stepwise and best-subset regression) that lack logical and statistical justification and that perform poorly in theory, simulations and case studies... One serious problem is that the *P* values and standard errors ... will be downwardly biased, usually to a large degree'.

Selection of covariates should be based on the research question at hand and on substantial knowledge such as what is biologically plausible. Chapter 10 'Predictor selection' in the book 'Regression methods in biostatistics linear, logistic, survival, and repeated measures models' [8] gives good guidance on this matter.

4. VALIDATE PREDICTION MODELS

When a prediction model has been developed, it ought to be validated on data which were not used in model development. Split-sample validation is done by first dividing the data set into a training set, say a random sample of 80% of the data, used for model development. The prediction model is subsequently validated using the remaining data, often referred to as the validation set. However, training and validation set approaches have weaknesses and are more and more replaced by resampling and bootstrapping approaches. These are still seen as internal validation, performed during the development. In addition to internal validation, there ought to be external validation in 1 or more separate data sets in order to assess the general applicability of the prediction model [9].

5. ADJUST FOR BASELINE VALUES IN RANDOMISED CONTROLLED TRIALS

Consider a randomised controlled trial (RCT) comparing 2 or more treatments, where the outcome variable is measured before randomisation and after treatment. Testing whether there is a significant change (difference) from before to after treatment within each treatment arm separately is not an appropriate analysis method [10]. One can compare the mean change between the treatment arms. But better approaches exist: One can use regression with the outcome variable after treatment as dependent variable, and baseline value of the outcome and treatment group as covariates [11]. This method is often called analysis of covariance (ANCOVA). Alternatively, one can use a linear mixed model with the outcome as dependent variable and time point and the interaction between treatment and time as categorical covariate. In this model, the interaction term represents the treatment effect [12,13]. If there are missing values, a linear mixed model generally gives less bias than ANCOVA [14].

6. DO NOT ADJUST FOR BASELINE VALUES IN OBSERVATIONAL STUDIES

In an observational study, on the contrary, adjusting for baseline values cannot be generally recommended [15], page 124 to 127. In fact, this can produce different conclusions than analysing a score difference (after score minus before score), a phenomenon also known as Lord's paradox [16]. A central issue is that in a randomised trial, the treatment is applied after measuring the baseline score. Hence, the treatment cannot have affected the baseline score. In an observational study, the exposure may have been present also before the baseline score was measured. Then, adjusting for the baseline value can introduce bias. But, one can compare the mean change between the exposed and unexposed individuals. Alternatively, one can use a linear mixed model with time point, exposure, and the interaction between time point and exposure.

7. DICHOTOMISING A CONTINUOUS VARIABLE CAN BE A BAD IDEA

Avoid to dichotomise continuous variables if possible [17,18]. Dichotomising implies loss of information and hence loss of statistical power. Moreover, dichotomising a covariate implies that the analysis tacitly assumes that the effect of that covariate changes abruptly at the threshold, and else is constant. In reality, most effects are smooth functions of the covariate. However, sometimes, it can be sensible to dichotomise, for example, according to some predefined clinical threshold. Data-driven categorisation such as above/below the median of the observations is never a good idea. The same weaknesses are valid for categorising into more than 2 categories, although the harm is then somewhat less than by dichotomising. Section 13.5 in the book statistical analysis of contingency tables [18] gives good guidance on this matter.

8. STUDENT'S *t* TEST IS BETTER THAN NONPARAMETRIC TESTS

Student's *t* test has major advantages over nonparametric tests such as the Wilcoxon test [19]: First, the method allows to compute a CI for the mean of interest, not only a *P* value. Second, Student's *t* test is more powerful, particularly in small samples [20]. A widespread misunderstanding is that Student's *t* test should not be used in small samples. Third, Student's *t* test is readily generalised into regression analysis and other analyses.

Student's *t* test is rather robust to deviations from normality, as long as there are no residuals extremely distant, say much more than 4-5 SDs, from zero. This is particularly the case for the version of the *t* test not assuming equal variances. [21] Visual inspection of Q-Q plots is well suited to detect such deviations. Visual inspection of P-P plots is not suited for detecting such deviations. When the data deviate substantially from the normal distribution, one can, for example, use bootstrapping to obtain CIs and *P* values [22]. Bootstrapping has been available in standard statistical software for many years, and it is an underused technique in many applications of statistics.

9. MEAN (SD) ARE ALSO RELEVANT FOR NONNORMALLY DISTRIBUTED DATA

The mean and SD are meaningful descriptive statistics for data following all types of continuous distributions and sometimes even for ordinal data, not only the normal distribution [23]. A widespread misunderstanding is that one must use other measures such as median and IQR if data do not follow the normal distribution. In fact, the mean and SD has several favourable properties. For example, the mean and SD from different studies can readily be combined in a possible later meta-analysis. This is not the case for the quantile-related measures.

10. ADJUSTING *P* VALUES FOR MULTIPLICITY

When there are multiple hypotheses in a study, state whether an adjustment of *P* values to protect the familywise error rate (FWER) or false discovery rate (FDR) was carried out. If you use adjustment, state which method was used and for how many hypotheses. The choice of method for multiplicity adjustment must be specified before the researcher carries out the analysis, to avoid choosing a method that gives the desired or expected results. Some relevant methods for multiplicity adjustment are described previously [24], along with recommendations.

11. REPORT ESTIMATE, CI, AND (POSSIBLY) *P* VALUE—IN THAT ORDER OF IMPORTANCE

P values are overused and overemphasised in medical research as well as many other applied sciences. Sometimes authors report only the *P* value, for example: ‘Patients exposed to E were more likely than the unexposed to develop the disease D ($P = .04$)’. The Vancouver guidelines [25] state the following: ‘When possible, quantify findings and present them with appropriate indicators of measurement error or uncertainty (such as confidence intervals). Avoid relying solely on statistical hypothesis testing, such as P values, which fail to convey important information about effect size and precision of estimates’.

12. DO NOT TEST FOR BASELINE IMBALANCES IN AN RCT

A table of baseline characteristics per treatment group is essential in any RCT report. A statistical test at baseline is conceptually meaningless because, by definition, any imbalance will be due to the play of chance. Such significance testing is futile and can be misleading, although reported in some medical journal articles [24,26]. We can expect 5% of the variables to differ significantly between the groups (at level 5%).

13. FORMAT FOR REPORTING CIs

Commonly used separators between confidence limits are comma (,), semicolon (;), and hyphen (-). The comma and hyphen should be avoided, since they resemble a decimal separator, a thousands’ separator, or a minus sign. A good and much used choice is to use ‘to’ (eg, 0.16 to 0.25). The same advice applies for other intervals, such as IQR and minimum to maximum values.

14. MIND THE NUMBER OF REPORTED DECIMAL PLACES

Reporting too few decimals makes the results inaccurate. Moreover, an unnecessarily large number of decimals conceals the message—the results are drowned by a surfeit of figures. Some general advice is found in [27]. Regarding *P* values, avoid reporting them as ‘n.s.’ or $P < .05$ or $P < .01$. The exception is extremely small *P* values, which ought to be reported as, for example, $P < .001$. A much used recommendation is to report *P* values with up to 2 significant digits and maximum 3 decimals, such as $P = .12$, $P = .035$, $P = .006$, and $P < .001$.

15. REPORT ABSOLUTE NUMBERS WHERE RELEVANT

The Vancouver guidelines [25] state the following: ‘Give numeric results not only as derivatives (for example, percentages) but also as the absolute numbers from which the derivatives were calculated’. Where applicable, this is a very simple and sensible advice.

Competing interests

The author declares no competing interests.

Funding

This research did not receive any specific grant from funding agencies in the public, commercial, or not-for-profit sectors.

Patient consent for publication

Not applicable.

Ethics approval

Not applicable.

Provenance and peer review

Commissioned; externally peer reviewed.

APPENDIX

Some statistical terms used in this article are explained below.

Expectation-maximation imputation of missing data

Missing values in the data set are estimated as their expected values, given all observed values in the data set. This results in a complete data set with singly imputed values. Single imputation can be an acceptable procedure if there is a low proportion of missing values.

Familywise error rate

The probability of a type I error in at least one of the hypothesis tests.

False discovery rate

This is the expected proportion of false positive findings, among the claimed positive findings. Use of the FDR instead of FWER is most relevant in studies with a large number of hypotheses but can be relevant also in studies with as few as, for example, 8-16 hypothesis tests.

Multiple imputation of missing data

Several complete data sets, for example m = 100 data sets, are created. The missing values are in principle drawn randomly from their expected distributions, given all observed values in the data set. Subsequently, analysis results from each of the m complete data sets are combined to give estimates, CIs and *P* values taking the variability within and between the imputed data sets into account. Older texts on multiple imputation stated that m = 3 to 5 imputed data sets can be sufficient. Today, a larger number is recommended [28] page 58 to 60. A total of m = 20 imputations can be sufficient in many situations. A safe choice is m = 100 imputations, unless computing time is an issue.

Last observation carried forward

Consider a longitudinal study where the patients are scheduled to visit the clinic at certain time points. If data are missing at a time point, data from the last available time point are filled in. For example, the scheduled visits are at 1, 2, 3, and 6 months, and a patient missing data at 3 months gets the values from 2 months filled in also at 3 months. If data are also missing at 6 months, the same values are carried forward 6 months as well.

Stepwise selection of covariates

From a given set of candidate covariates for a regression analysis, only those fulfilling a given data-driven criterion are included in the final analysis. A common criterion is that the *P* value must be below a threshold, such as P>0.10. Several variants of stepwise selection exist, including forward selection, backwards elimination, and all subsets regression.

Analysis of covariance

In this context, analysis of covariance (ANCOVA) means regression analysis with outcome after treatment (or exposure) as dependent variable, including baseline value and treatment group as covariates. Some authors use ANCOVA in a slightly different meaning.

Q-Q plot

A plot of the observed values versus the expected values under an assumed probability distribution, usually the normal distribution. If the graph is close to a straight line, the data agree well with the assumed probability distribution.

P-P plot

A plot of the observed cumulative probabilities versus the expected ones under an assumed probability distribution, usually the normal distribution. If the graph is close to a straight line, the data agree well with the assumed probability distribution.

Orcid

Stian Lydersen: http://orcid.org/0000-0001-6613-8596

REFERENCES

[1] Lydersen S. Statistical review: frequently given comments. Ann Rheum Dis 2015;74(2):323–5.
[2] STROBE Statement. Strengthening the reporting of observational studies in epidemiology 2014 https://www.strobe-statement.org/ Accessed December 19, 2024.
[3] CONSORT guidelines. 2010. https://www.bmj.com/content/388/bmj-2024-080472. Accessed December 19, 2024.
[4] Lydersen S. Last observation carried forward. Tidsskr Nor Laegeforen 2019;139(9) Norwegian, English.
[5] Peduzzi P, Concato J, Kemper E, Holford TR, Feinstein AR. A simulation study of the number of events per variable in logistic regression analysis. J Clin Epidemiol 1996;49(12):1373–9.
[6] Vittinghoff E, McCulloch CE. Relaxing the rule of ten events per variable in logistic and Cox regression. Am J Epidemiol 2007;165(6):710–8.
[7] Rothman KJ. Epidemiology an introduction. 2nd ed. New York: Oxford University Press; 2012.
[8] Vittinghoff E, Glidden DV, Shiboski SC, McCulloch CE. Regression methods in biostatistics linear, logistic, survival, and repeated measures models. Statistics for biology and health. 2nd ed. New York: Springer; 2012.
[9] Steyerberg EW. Clinical prediction models. A practical approach to development, validation, and updating. 2nd ed. New York: Springer; 2019.
[10] Bland JM, Altman DG. Comparisons against baseline within randomised groups are often used and can be highly misleading. Trials 2011;12:264.
[11] Vickers AJ, Altman DG. Statistics notes: analysing controlled trials with baseline and follow up measurements. BMJ 2001;323(7321):1123–4.
[12] Twisk J, Bosman L, Hoekstra T, Rijnhart J, Welten M, Heymans M. Different ways to estimate treatment effects in randomised controlled trials. Contemp Clin Trials Commun 2018;10:80–5.
[13] Coffman CJ, Edelman D, Woolson RF. To condition or not condition? Analysing 'change' in longitudinal randomised controlled trials. BMJ Open 2016;6(12):e013096.
[14] Lydersen S. Adjustment for baseline value in longitudinal randomised trials. Tidsskr Nor Legeforen 2022;142(6).
[15] Fitzmaurice GM, Laird NM, Ware JH. Applied longitudinal analysis. Wiley series in probability and statistics. 2nd ed. Hoboken: Wiley; 2011.
[16] Lord FM. A paradox in the interpretation of group comparisons. Psychol Bull 1967;68(5):304–5.
[17] Altman DG, Royston P. The cost of dichotomising continuous variables. BMJ 2006;332(7549):1080.
[18] Fagerland M, Lydersen S, Laake P. Statistical analysis of contingency tables. Boca Raton: Chapman and Hall/CRC; 2017.
[19] Altman DG, Bland JM. Parametric v non-parametric methods for data analysis. BMJ 2009;338:a3167.
[20] Bland JM, Altman DG. Analysis of continuous data from small samples. BMJ 2009;338:a3166.
[21] Fagerland MW, SandvikL. Performance of five two-sample location tests for skewed distributions with unequal variances. Contemp Clin Trials 2009;30(5):490–6.
[22] Bland JM, Altman DG. Statistics notes: bootstrap resampling methods. BMJ 2015;350:h2622.
[23] Lydersen S. Mean and standard deviation or median and quartiles? Tidsskr Nor Laegeforen 2020;140(9).
[24] Lydersen S. Avoid significance tests for background variables in randomised controlled trials. Tidsskr Nor Laegeforen 2020;140(4).
[25] Recommendations for the conduct, reporting, editing, and publication of scholarly work in medical journals [Internet] 2024 [updated 2024 January; cited 2024 Nov 12]. Available from: http://www.icmje.org/icmje-recommendations.pdf.
[26] de Boer MR, Waterlander WE, Kuijper LD, Steenhuis IH, Twisk JW. Testing for baseline differences in randomized controlled trials: an unhealthy research behavior that is hard to eradicate. Int J Behav Nutr Phys Act 2015;12:4.
[27] Lydersen S, Skovlund E. Do we need all the decimals? Tidsskrift for den Norske Laegeforening 2023;143(7).
[28] van Buuren S. Flexible imputation of missing data. 2nd ed. Boca Raton: CRC Press; 2018.

Ann Rheum Dis 84 (2025) 664–679

Contents lists available at ScienceDirect

Annals of the Rheumatic Diseases

journal homepage: https://www.sciencedirect.com/journal/annals-of-the-rheumatic-diseases

Recommendation

Expert consensus statement on the treatment of immune-mediated inflammatory diseases with Janus kinase inhibitors: 2024 update

Peter Nash[1], Andreas Kerschbaumer[2], Victoria Konzett[2], Daniel Aletaha[2], Thomas Dörner[3], Roy Fleischmann[4], Iain McInnes[5], Jette Primdahl[6], Naveed Sattar[7], Yoshiya Tanaka[8], Michael Trauner[9], Kevin Winthrop[10], Maarten de Wit[11], Johan Askling[12], Xenofon Baraliakos[13], Wolf-Henning Boehncke[14,15], Paul Emery[16], Laure Gossec[17], John D. Isaacs[18], Maria Krauth[19], Eun Bong Lee[20], Walter Maksymowych[21], Janet Pope[22], Marieke Scholte-Voshaar[23,24], Karen Schreiber[25,26,27], Stefan Schreiber[28], Tanja Stamm[29], Peter C. Taylor[30], Tsutomu Takeuchi[31], Lai-Shan Tam[32], Filip Van den Bosch[33,34], Rene Westhovens[35], Markus Zeitlinger[36], Josef S. Smolen[2,*]

[1] *Griffith University School of Medicine, Nathan, Brisbane, QLD, Australia*
[2] *Division of Rheumatology, Department of Medicine 3, Medical University of Vienna, Vienna, Austria*
[3] *Department of Medicine/Rheumatology and Clinical Immunology, Charité University Hospital, Berlin, Germany*
[4] *Metroplex Clinical Research Center and University of Texas Southwestern Medical Center, Dallas, TX, USA*
[5] *Institute of Infection, Immunity and Inflammation, University of Glasgow, Glasgow, UK*
[6] *Department of Regional Health Research, University of Southern Denmark, Odense, Denmark*
[7] *School of Cardiovascular and Metabolic Health, University of Glasgow, UK*
[8] *First Department of Internal Medicine, University of Occupational and Environmental Health, Kitakyushu, Japan*
[9] *Division of Gastroenterology and Hepatology, Department of Medicine 3, Medical University of Vienna, Vienna, Austria*
[10] *Division of Infectious Diseases and School of Public Health, Oregon Health and Science University, Portland, OR, USA*
[11] *Medical Humanities, Amsterdam University Medical Centre, Amsterdam, Netherlands*
[12] *Department of Medicine Solna, Karolinska Institutet, Stockholm, Sweden*
[13] *Rheumazentrum Ruhrgebiet, Herne, Germany*
[14] *Division of Dermatology and Venereology, Geneva University Hospitals, Geneva, Switzerland*
[15] *Department of Pathology and Immunology, Faculty of Medicine, University of Geneva, Geneva, Switzerland*
[16] *Leeds NIHR Biomedical Research Centre, LTHT, Leeds Institute of Rheumatic and Musculoskeletal Medicine, University of Leeds, Leeds, UK*
[17] *Sorbonne Université, INSERM, Institut Pierre Louis d'Epidémiologie et de Santé Publique, Paris France, AP-HP, Pitié-Salpêtrière Hospital, Rheumatology Department, Paris, France*
[18] *Translational and Clinical Research Institute, Newcastle University, Newcastle upon Tyne, UKNIHR Newcastle Biomedical Research Centre and Musculoskeletal Unit, Newcastle upon Tyne Hospitals, Newcastle upon Tyne, UK*
[19] *Division of Haematology and Haemostaseology, Department of Medicine 1, Medical University of Vienna, Vienna, Austria*
[20] *Seoul National University College of Medicine, Seoul, Republic of Korea*
[21] *Medicine, University of Alberta Faculty of Medicine and Dentistry, Edmonton, AB, Canada*
[22] *Medicine, Division of Rheumatology, The University of Western Ontario, London, ON, Canada*

Correspondence to Dr. Josef S. Smolen, Division of Rheumatology, Department of Medicine 3, Medical University of Vienna, Vienna, Austria.
E-mail address: josef.smolen@meduniwien.ac.at (J.S. Smolen).

Handling editor Dimitrios Boumpas.

https://doi.org/10.1016/j.ard.2025.01.032

[23] *Department of Pharmacy, Sint Maartenskliniek, Netherlands*
[24] *Department of Pharmacy, Radboudumc, Nijmegen, Netherlands*
[25] *Danish Centre for Expertise in Rheumatology (CeViG), Danish Hospital for Rheumatic Diseases, Sønderborg, Denmark*
[26] *Department of Regional Health Research (IRS), University of Southern Denmark, Odense, Denmark*
[27] *Thrombosis and Haemostasis, Guy's and St Thomas' NHS Foundation Trust, London, UK*
[28] *Department Internal Medicine I, University Hospital Schleswig-Holstein, Kiel University, Kiel, Germany*
[29] *Section for Outcomes Research, Center for Medical Statistics, Informatics, and Intelligent Systems, Medical University of Vienna, Vienna, Austria*
[30] *Botnar Research Centre, Nuffield Department of Orthopaedics, Rheumatology and Musculoskeletal Sciences, University of Oxford, Oxford, UK*
[31] *Division of Rheumatology, Department of Internal Medicine, Keio University School of Medicine, Tokyo, and Saitama Medical University, Saitama, Japan*
[32] *Rheumatology, Department of Medicine and Therapeutics, Chinese University of Hong Kong Shaw College, New Territories, Hong Kong*
[33] *VIB-UGent Center for Inflammation Research, Department of Internal Medicine and Pediatrics, Ghent University, Ghent, Belgium*
[34] *Ghent University Hospital, Department of Rheumatology, Ghent, Belgium*
[35] *Department of Development and Regeneration, Skeletal Biology and Engineering Research Center, KU Leuven, Leuven, Belgium*
[36] *Department of Clinical Pharmacology, Medical University of Vienna, Vienna, Austria*

ARTICLE INFO

Article history:
Received 6 August 2024
Received in revised form 30 November 2024
Accepted 16 December 2024

ABSTRACT

In light of the introduction of new Janus kinase inhibitors (JAKi), new indications for JAKi and recent safety considerations that have arisen since the preceding consensus statement on JAKi therapy, a multidisciplinary taskforce was assembled, encompassing patients, health care professionals, and clinicians with expertise in JAKi therapy across specialties. This taskforce, informed by two comprehensive systematic literature reviews, undertook the objective to update the previous expert consensus for using JAKi developed in 2019. The taskforce deliberated on overarching principles, indications, dosage and comedication strategies, warnings and contraindications, screening protocols, monitoring recommendations, and adverse effect profiles. The methodology was based on the European Alliance of Associations for Rheumatology standard operating procedures, with voting on these important elements. Furthermore, an updated research agenda was proposed. The task force did not address when a JAKi should be prescribed but rather considerations once this decision has been made. This update aimed to equip clinicians with the necessary knowledge and guidance for the efficient and safe administration of this expanding and significant class of drugs.

INTRODUCTION

Immune-mediated inflammatory diseases (IMIDs) comprise a variety of diseases, including not only rheumatoid arthritis (RA), psoriatic arthritis (PsA); axial spondyloarthritis (AxSpA)/ankylosing spondylitis; connective tissue diseases, also called systemic autoimmune rheumatic diseases, such as systemic lupus erythematosus (SLE) and systemic sclerosis, but also inflammatory skin diseases such as psoriasis (PsO); atopic dermatitis (AD) and autoimmune alopecia; inflammatory bowel diseases (IBDs) namely Crohn disease (CD) and ulcerative colitis (UC); and others, including multiple sclerosis. Each of these represents a distinct, organ-specific or systemic clinical entity with a genetic predisposition mostly linked to the presence of certain immune response genes, which under specific environmental conditions allows immunologic tolerance to be broken [1,2]. For some, we may have a clue on this breaking point [3], and for others, there are indications for viral involvement [4,5]. All of the listed conditions share the pathogenesis of an immune-mediated inflammatory response involving a variety of common and disparate cytokines, among them those related to the polarisation of T cells, various lymphokines, as well as proinflammatory cytokines [6,7].

Cytokines, after binding to their cell membrane−associated cognate receptors, activate a variety of intracellular signal transduction mechanisms. Important proinflammatory cytokines use mitogen-activated protein kinases (MAPK) and/or nuclear factor kappa B (NFκB) for this purpose [8], whereas the majority of cytokines involved in immune cell activation and various proinflammatory messenger molecules act via the Janus kinase (JAK) pathway [9]. Interestingly, neither inhibitors of MAPK nor NFκB have been successfully translated as therapeutics in people with IMIDs [10,11] In contrast, Janus kinase inhibitors (JAKi) have been approved for a variety of IMIDs over the last decade and continue to be studied in others.

In order to account for the complexity of using JAKi in various diseases, a large taskforce has developed an expert consensus statement on the use of JAKi in IMIDs a few years ago [12]. However, since its publication, JAKi have been approved for a variety of new indications and, even more importantly, safety issues when compared with tumour necrosis factor (TNF) inhibitors (TNFi) have arisen [13] and warnings and precautions for the use of JAKi have been updated. Therefore, it was deemed important to revisit the efficacy and safety of JAKi and develop an update of the consensus statement. It should be clarified that diseases other than IMIDs in which JAKi may also be indicated, such as haematologic malignancies or COVID-19, will not be addressed in this study. The result of the taskforce's deliberations and decisions are presented in this article.

METHODS

The expert consensus statement was developed in line with the general methodology provided by the European Alliance of Associations for Rheumatology (EULAR) in its standard operating procedures (SOPs) for the development of recommendations [14]. First a steering committee (PN, AK, VK, DA, TD, RF, IM, JP, NS, YT, MT, KW, MdW, JSS) was formed to address all necessary aspects for a systematic literature research (SLR) in a face-to-face meeting on April 16, 2023; the SLR, which included all articles published between March 1, 2019 (the data cut of the 2019 SLR), and October 14, 2023, focused on the efficacy and safety of all JAKi across indications. The results of the SLR were presented to the steering group on November 10, 2023, in another face-to-face meeting. The steering group then prepared proposals for changes of the consensus statement that were to be presented to the full taskforce. Levels of evidence (LoE) were assessed according to the Oxford Centre for Evidence-Based Medicine [15]. On January 10, 2024, the taskforce met at 2 different times to discuss the SLR results, review the steering group's proposals, and update the previous statement. The morning session (Central European time) was designated to accommodate mainly participants from Asia, while the afternoon session was set to enable experts from the Americas to contribute. Patients and nonphysician health care professionals were also present.

The overarching principles (OAPs) and individual recommendations address issues related to JAKi treatment of patients diagnosed with IMIDs. Of note, the taskforce did not discuss when to initiate JAKi therapy, as this should be covered by the respective disease-specific management recommendations. The taskforce focused on assessing if the items previously established were still valid based on the information accrued over the past 4 years and, consequently, on changes from the prior publication if deemed pertinent. The voting rules adhered to the EULAR SOPs, which stipulate to accept a proposal if a 75% majority is reached; if a 75% majority is not reached, the discussion continues and an amendment is presented which is again voted for, with a >66% majority of participants necessary for acceptance; again, if this next proposal is not approved, another round of discussions takes place, after which the new proposal has to be voted on by >50% of the members present in the room. The deliberations and changes were noted and recorded to allow their presentation in this report. After the meeting, all taskforce members received the ultimately approved version of the recommendations together with information on the LoE for each item to allow for a final vote on the level of agreement (LoA) for each of the items. Of note, an individual item which includes more than one aspect may have more than one LoE assigned, as will be seen in the individual items.

The last results of the LoA voting were received in February 2024. For the OAPs, only the voting results and LoA are presented, since they are general, explanatory statements mostly related to good clinical practice that do not require specific assessment of evidence.

RESULTS

In the prior consensus statement, published in 2019 [12], the process leading to the OAPs and recommendations outlined below was explained in detail [12] and in an abbreviated form in the methods' section above. As before, the recommendations were divided into a number of elements judged to be important in clinical practice and for the use of these points of guidance (Table 1).

These elements include: 4 OAPs (4 in 2019), 2 points on indications (2 in 2019), 4 items on treatment dose and comedications in different IMIDs (4 in 2019), 6 entries related to contraindications (5 in 2019), 7 items on prescreening and risks (7 in 2019), 3 entries regarding laboratory and clinical monitoring (3 in 2019) and 5 points on adverse effects (5 in 2019). While the number of bullet points has remained the same for most elements, many of these underwent changes based on recent insights. Further, each recommendation is accompanied by its associated LoEs, strength of recommendation (SoR), vote (% final approval), and the taskforce's LoA with the final wording. Please note that for some recommendations, the LoEs, and thus SoRs, are low despite a strong vote and agreement by the task force members. Such results generally reflect the absence of a study or studies performed to specifically investigate the point(s) raised, even if secondary indications are present. Therein, we rely on expert opinion, although often supported by some underlying data.

For readers who are familiar with the previous version of this expert consensus statement, we have indicated which changes have been made and why. Nevertheless, Table 1 with all recommendations is a stand-alone new version without any reference to the previous publication.

Overarching principles

Of the 4 OAPs, 3 were unchanged, and for 1, a slight wording change was applied to maintain uniformity with other principles. Key points of the discussions, taskforce voting results and LoAs are addressed further.

Item A: Initiation of JAKi therapy and the treatment target to be achieved should be based on a shared decision between the patient and the clinician, fully informing the patient on the potential benefit and risks of this therapy (vote, 100%; LoA, 9.94)

The term medical specialist in the previous version was altered to clinician to keep uniformity with the term used in OAP 3 and 4. It acknowledges that a variety of specialties and health professionals are involved in the management of patients taking JAKi. The importance of shared decision making between clinician and patient was again emphasised as was the necessity to provide the patient with full and adequate information on the risk and benefit of JAKi therapy. However, there was a slight amendment from the previous 'which requires full information of the patient' to the new 'fully informing the patient' to streamline the wording. The SLRs provided the latest evidence on efficacy and safety, building upon the 2019 SLR [16], to guide the taskforce. Clinicians interested in the details are referred to the separate publications [17,18]. Long-term safety data with a number of JAKi now extends to over a decade particularly in rheumatologic and dermatologic diseases [19−23].

Item B: Therapeutic approaches to treating patients with chronic inflammatory conditions should be in line with international/national recommendations (algorithms) for the management of the respective disease (vote, 100%; LoA, 9.72)

The taskforce continues to recommend general management principles for individual diseases in line with international and national guidelines. The minor change made was to eliminate 'and' between 'international' and 'national' to simply read 'international/national', since these are not always fully aligned. Thus, when international or national recommendations differ, the

Table 1

Overarching principles and individual recommendations by different categories

Item	Recommendation	LoE/SoR	Final vote (%)	LoA
Overarching principles				
A	Initiation of JAKi therapy and the treatment target to be achieved should be based on a shared decision between the patient and the clinician, fully informing the patient on the potential benefit and risks of this therapy.	NA	100	9.9 ± 0.4
B	Therapeutic approaches to treating patients with chronic inflammatory conditions should be in line with international/national recommendations (algorithms) for the management of the respective disease.	NA	100	9.7 ± 0.6
C	The points-to-consider when initiating JAKi therapy do not provide information on when JAKi should be used in the treatment algorithm, but rather attempt to assist the clinician once the decision to prescribe a JAKi has been made.	NA	100	9.7 ± 0.5
D	These points-to-consider address specific (but not all) aspects related to the application of JAKi therapy and the clinician should additionally refer to the disease-specific product information.	NA	100	9.8 ± 0.5
I. Indications				
1.	Patients with immune-mediated inflammatory diseases (IMIDs); as of 2024, depending on the specific drug, these include rheumatoid arthritis, psoriatic arthritis, axial spondyloarthritis, ulcerative colitis, Crohn disease, psoriasis, atopic dermatitis, vitiligo, and alopecia areata.	1a/A	100	9.9 ± 0.3
2.	Currently, there is no direct evidence from head-to-head comparisons to show efficacy or safety superiority of one JAKi over another.	5/D	94	9.9 ± 0.3
II. Treatment dose and comedication				
1.	Use the dose recommended for the specific disease.	1a/A	100	9.8 ± 0.5
2.	Consider dose adjustments in patients with higher age,* significant renal or hepatic impairment,* other comorbidities and/or at risk of drug interactions.	2b/C, *5/D	100	9.6 ± 1.0
3.	Regarding comedication, follow specific recommendations for the respective disease.	1a/B	100	9.8 ± 0.5
4.	Consider dose reduction of the JAKi in patients in sustained remission according to established assessment instruments (regarding use of such instruments, see recommendation V/3).	1b/B	94	9.1 ± 1.3
III. Warnings or contraindications				
1.	Severe active (or recurrent)* infections, including tuberculosis and opportunistic infections.	2b/B, *4/D	94	9.7 ± 0.6
2.	Current (or history of) malignancies.	5/D	94	9.2 ± 0.9
3.	Severe organ dysfunction such as advanced chronic liver disease and severe renal disease (creatinine clearance of <30 mL/min).	5/D	100	9.7 ± 0.6
4.	Pregnancy and lactation.	5/D	100	9.8 ± 0.6
5.	History of arterial and venous thromboembolic events.	2b/B	100	9.5 ± 0.8
6.	Vaccination with live vaccines.	5/D	100	9.6 ± 1.0
IV. Pretreatment screening and risks				
1.	Patient history and physical examination, with a focus on warnings and contraindications.	5/D	100	9.9 ± 0.4
2.	Consider risk factors for venous thromboembolic events, especially a history of thromboembolism; cardiovascular risk such as a history of cardiovascular event; risk for malignancy, such as smoking history*.	2b/B, *5/D	100	9.9 ± 0.3
3.	Routine laboratory testing (full and differential blood counts, liver blood tests, renal function); and lipid levels as a baseline.	5/D	100	9.7 ± 0.6
4.	Hepatitis B virus (HBV) testing (HBV surface antigen, HBV surface antibody, HBV core antibody, and with/without HBV DNA testing) and hepatitis C virus (HCV) testing (HCV antibody, with HCV RNA testing if antibody positive).	2b/B	100	9.9 ± 0.3
5.	HIV testing in high-risk populations.	2b/B	100	9.6 ± 1.0
6.	Tuberculosis screening as per national recommendations.	2b/B	100	9.9 ± 0.3
7.	Assess and update vaccination status in accordance with national recommendations; consider vaccination against herpes zoster.	5/D	100	9.7 ± 0.5
V. Laboratory and clinical monitoring				
1.	Periodic minimal laboratory monitoring: full and differential blood counts, liver and renal function tests, lipid levels.	2b/B, *5/D	100	9.8 ± 0.5
2.	Regular skin examination (for detection of skin cancer), as per national recommendations.	5/D	94	8.9 ± 1.5
3.	Evaluate response using validated, disease-specific measures of disease activity; for evaluation and definition of response, be aware that C-reactive protein and erythrocyte sedimentation rate may be reduced by JAKi independently of reduction of disease activity and possibly even in infections*.	2b/B, *5/D	100	9.9 ± 0.7
VI. Adverse effects				
1.	Serious infections (similar to biological disease-modifying antirheumatic drugs), opportunistic infections including TB, herpes zoster (increased rates compared with biological disease-modifying antirheumatic drugs) may occur; the risk of infectious events can be lowered with reduction or elimination of concomitant glucocorticoid use.	2b/B	100	9.7 ± 0.7
2.	Rates of malignancy may be higher with JAK inhibition compared with TNF inhibitors; the risk of non−melanoma skin cancer is elevated.	2b/B	94	9.5 ± 0.7
3.	Lymphopenia, thrombocytopenia, neutropenia, and anaemia may occur; anaemia especially occurring with JAKi that inhibit JAK2.	1b/B	100	9.5 ± 1.1
4.	There is a dose-dependent risk of venous thromboembolic events, especially pulmonary embolism with JAK inhibition, particularly in patients with risk factors for venous thromboembolic events.	2b/B	100	9.7 ± 0.6
5.	Elevations of creatine phosphokinase are noted with JAKi but have usually not been associated with clinical events; elevations of creatinine have been noted with JAKi but have not been associated with renal failure or hypertension.	2b/B	100	9.6 ± 0.7

JAK, Janus kinase; JAKi, Janus kinase inhibitor; LoA, level of agreement; LoE, level of evidence; SoR, strength of recommendation; TNF, tumour necrosis factor.

clinician should choose the most appropriate recommendations considering individual country and access limitations.

Item C: The points-to-consider when initiating JAKi therapy do not provide information on when JAKi should be used in the treatment algorithm but attempt to assist the clinician once the decision to prescribe a JAKi has been made (vote, 100%; LoA, 9.72)

The usage of the terminology 'consensus statement' or 'recommendations' or 'points-to-consider' and not 'guidelines' throughout was regarded as an important distinction when opinion and low LoE are used and for medicolegal implications, since a decision to use a given drug in a specific patient is always one that relates to that individual in a patient-clinician relationship and does not require strict guidelines but rather general considerations related to safety and efficacy in each specific circumstance. No guideline can address all circumstances that may be pertinent in a particular patient with a particular diagnosis, unique comorbidities, a personal disease history as well as treatment history, and concomitant medications or similar aspects (see also item D).

Item A: These points-to-consider address specific (but not all) aspects related to the application of JAKi therapy and the clinician should additionally refer to the disease-specific product information (vote, 100%; LoA, 9.81)

The importance of disease-specific product information should be carefully considered. As new data emerge, updates to recommendations are necessary over time. A large number of clinical trials investigating JAKi are currently being conducted, with 487 trials involving JAKi therapy registered on clinicaltrials.gov at the time of writing.

I. Indications

Item 1: Patients with IMIDs; as of 2024, depending on the specific drug, these include those with RA, juvenile idiopathic arthritis, PsA, AxSpA, UC, CD, PsO, AD, vitiligo, and alopecia areata (LoE, 1A; SoR, A; vote, 100%; LoA, 9.91)

Since 2019, different JAKi have been approved for several additional IMIDs. The taskforce noted that treatment dose and comedications are important considerations in different IMIDs, and the status quo (2024) is mentioned. This list may soon be expanded. For example, while clinical trial evidence of efficacy of JAKi for patients with hidradenitis suppurativa exists, this is not an approved indication as yet [24]. Deucravacitinib has been approved for PsO, might be approved for PsA once phase 3 trials are successfuly finalized and has been investigated in a phase 2 trial of SLE and demonstrated significant efficacy at 3 mg twice daily [25]. Moreover, positive phase 2 randomised controlled trial (RCT) data have been presented for upadacitinib in SLE at 30 mg daily dose [26]. Further, JAKi are under active investigation in other IMIDs including interferonopathies, dermatomyositis, vasculitis, polymyalgia rheumatic, and giant cell arteritis among many others. Of note, AxSpA includes both radiographic and nonradiographic spondyloarthritis. Further, baricitinib has received regulatory approval in combination with remdesivir for the treatment of suspected or laboratory-confirmed COVID-19 infection in hospitalised adult and paediatric patients requiring supplemental oxygen, mechanical ventilation, or extracorporeal membrane oxygenation. However, similar to other non-IMID indications such as haematologic malignancies, COVID-19 is not considered an IMID nor was it included in the SLR, which is the reason why it has been excluded from the present indication list [27]. The different JAKi and their approved indications are listed in Table 2, while the different IMIDs for which JAKi are approved and the respective JAKi are shown in Table 3.

Item 2: Currently, there is no direct evidence from head-to-head comparisons to show efficacy or safety superiority of one JAKi over another (LoE, 5; SoR, D; vote, 94%; 1 abstention; LoA, 9.91)

The taskforce debated whether this recommendation should be a note in the text but agreed that it should be included to assuage attempts to claim superior efficacy between JAKi, as there is no evidence at the present time from multinational, multicenter RCTs that one JAKi is more efficacious clinically, structurally, or functionally than any other JAKi. There remain no clinical trials of JAKi after intolerance or lack of efficacy of another JAKi. This item has been minimally adjusted compared with the previous statement to make clear that any potential

Table 2
JAK inhibitors approved primarily by EMA and/or FDA at the time of writing

Drug	Main target	Indications	Metabolism and dose
Abrocitinib	JAK1, JAK2	AD	100-200 mg daily
Baricitinib	JAK1, JAK2	RA, AD, AA, JIA, COVID-19[a]	>66% renal excretion; 2-4 mg daily
Delgocitinib	Pan-JAK	AD[b]	Topical
Deucravacitinib	TYK2	PsO	CyP1A2 13% renal excretion, active metabolite BMT-153261; 6 mg daily
Fedratinib	JAK1-FLT3	Myelofibrosis	400 mg daily
Filgotinib	JAK1	RA	CES2, active metabolite (1:10 potency); 100-200 mg daily
Gusacitinib	JAK/Syk	AD	2-4 mg daily
Momelotinib	JAK1, JAK2/ACRV1	Myelofibrosis	200 mg daily
Oclacitinib	JAK1, JAK2, JAK3	Canine AD	0.4-0.6 mg/kg chewable tablet
Paricitinib	JAK2/Flt3	Myelofibrosis	200 mg twice daily
Peficitinib	Pan-JAK	RA[b]	NNMT, SULT2A1, 16% renal excretion; 150 mg daily
Ritlecitinib	JAK3, TEC	AA	50 mg daily
Ruxolitinib	JAK1, JAK2	Myelofibrosis, Polycythemia vera, GvHD, vitiligo (topical)	CyP3A4; 5-10 mg twice daily
Tofacitinib	JAK1, JAK3, JAK2	RA, PsA, AxSpA, ulcerative colitis, JIA	CyP3A4, 30% renal excretion; 5 mg twice daily
Upadacitinib	JAK1, JAK2	RA, PsA, AD, JIA UC, CD, AxSpA (including nr AxSpA)	CyP3A4 20% renal excretion; 15-30 mg daily

AA, alopecia areaty; ACRV1, activin A receptor, type 1; AD, atopic dermatisis; AxSpA, axial spondyloarthritis; CD, Crohn disease; CES, carboxyesteraseisoform; CyP cytochrome P; EMA, European Medicines Agency; ER, extended release; FDA, Food and Drug Administration; FLT-3, fms like tyrosine kinase 3; JAK, Janus kinase; JIA, juvenile idiopathic arthritis; NNMT, nicotinamide N-metbyltransferase; nr, nonradiographic; PsA, psoriatic arthritis; PsO, psoriasis; RA, rheumatoid arthritis; SULT, sulfotransferase; Syk, spleen typrosine kinase; TYK2, tyrosine kinase 2; TEC, tyrosine kinase expressed in hepatocellular carcinoma; UC, ulcerative colitis.

[a] Approved by FDA in combination with remdesivir.

[b] Approved in Japan.

Table 3
Approved JAK inhibitors for specific IMID indications (at the time of writing)

Indication	Approved JAKi
Rheumatologic diseases	
Rheumatoid arthritis	Baricitinib (JAK1, JAK2), filgotinib (JAK1), peficitinib (pan-JAK), tofacitinib (JAK 1, JAK3, JAK2), upadacitinib (JAK1, JAK2)
Psoriatic arthritis	Tofacitinib (JAK1, JAK3, JAK2), upadacitinib (JAK1, JAK2)
Axial spondyloarthritis	Tofacitinib (JAK1, JAK3, JAK2), upadacitinib (JAK1, JAK2)
Juvenile idiopathic arthritis	Tofacitinib (JAK1, JAK3, JAK2), baricitinib (JAK1, JAK2)
Dermatologic diseases	
Psoriasis	Deucravacitinib (TYK2)
Atopic dermatitis	Abrocitinib (JAK1, JAK2), baricitinib (JAK1, JAK2), gusacitinib (JAK/Syk), upadacitinib (JAK1, JAK2)
Alopecia areata	Baricitinib (JAK1, JAK2), ritlecitinib (JAK3, TEC)
Vitiligo	Ruxolitinib (JAK1, JAK2) – topical
Inflammatory bowel disease	
Crohn disease	Upadacitinib (JAK1, JAK2)
Ulcerative colitis	Tofacitinib (JAK1, JAK3, JAK2), upadacitinib (JAK1, JAK2)

IMID, immune-mediated inflammatory disease; JAK, Janus kinase; TEC, tyrosine kinase expressed in hepatocellular carcinoma.

difference would have to be shown in trials directly comparing 2 or more drugs ('from head-to-head comparisons to show efficacy or safety superiority' now replaces 'of superiority regarding efficacy or safety') (Table 1).

II. Treatment dose and comedications in different diseases

Item 1: Use the dose recommended for the specific disease (LoE, 1a; SoR, A; vote, 100%; LoA, 9.84)

This recommendation (unchanged) highlights dose adjustments per disease indication; for example, in the treatment of IBD differing induction and maintenance dosing are clearly defined.

Item 2: Consider dose adjustments in patients with higher age, significant renal or hepatic impairment, other comorbidities, and/or at risk of drug interactions (LoE, 2b/5; SoR C/D; vote, 100%; LoA, 9.61)

JAKi metabolism is summarised in Table 2. As previously described in the 2019 consensus paper, JAKi that are metabolised by the hepatic cytochrome P (CYP) 450 pathway lead to drug interactions with other inhibitors of this pathway, such as ketoconazole, and promoters, such as rifampicin, necessitating dosage adjustments. Baricitinib is 70% renally excreted, so dosage should be reduced in patients with kidney disease and reduced glomerular filtration rate. Filgotinib is metabolised by hepatic carboxylesterases, and its less potent major metabolite GS-829845 (by a factor of 10) is a pharmacologically active, selective inhibitor of JAK1. Upadacitinib undergoes hepatic oxidation with minor CYP metabolism, and peficitinib undergoes hepatic conjugation. Organic anion transporter 3 inhibitors, such as probenecid, interact with baricitinib requiring a dose reduction to 2 mg/d. Rifampicin, when used in latent tuberculosis (TB) prophylaxis or therapy for active TB, increases hepatic metabolism of tofacitinib and upadacitinib, so that a dose increase needs to be considered. Ketoconazole has the opposite effect, inhibiting tofacitinib and upadacitinib metabolism, so a dose reduction is suggested.

The general meaning of this item remains unchanged, but some details have been amended. Higher age is no longer specified as '>70 years' as age-related health status is relative to comorbidities, frailty, and re-definition of meaningful age groups [28]. The taskforce debated the designation 'impaired hepatic function' as this was considered to be not meaningfully measurable; for example, transaminase monitoring does not adequately measure hepatic function. Aadvanced chronic liver disease' would be the preferred term [29], but it is less well recognised [10,11], and therefore, it was agreed to keep the previous terminology. Comorbidities include those relevant to JAKi therapy, such as cardiovascular disease, malignancy, or high thrombosis risk (eg, past thromboembolic events, obesity, use of contraceptives, or recent surgery). Reduced renal function may necessitate dose reduction. It is also noted that some haematologic abnormalities that may affect the JAKi dose, such as neutropenia and lymphopenia, may be drug induced rather than a comorbidity.

Item 3: Regarding comedication, follow specific recommendations for the respective disease (LoE, 1a; SoR, B; vote, 100%; LoA, 9.79)

This bullet that included only a statement about RA in 2019 was shortened so as to not single out a specific disease, since comedication will depend on the specific disease, and this was felt to be sufficiently covered in the new formulation of this item. Of note, for many indications, combination with methotrexate (MTX) shows superior efficacy to JAKi monotherapy; examples include RA [13,14,30–32] and CD [33]. Immunogenicity, which is an important issue for combining biological agents with MTX [34], is not an issue with oral small molecules. Since data on the added efficacy of comedication are not available for all diseases for which JAKi are approved, the LoE(SoR is mixed.

Item 4: Consider dose reduction of the JAKi in patients in sustained remission according to established assessment instruments (regarding use of such instruments, see recommendation V/item 3; LoE, 1b; SoR, B; vote 94%; 1 abstention; LoA, 9.12)

This bullet point previously focused on RA, but, since this is relevant in other diseases too, such as UC, this part of the respective item I/4 in the previous recommendations was deleted and text about pertinent assessment instruments added to be more general. In a large randomised phase 3 trial in RA patients, after reaching low disease activity/remission (LDA/REM) for several months, maintenance of LDA/REM was greater with continued baricitinib 4 mg daily compared with tapering to 2 mg. Nevertheless, a large proportion of patients receiving the reduced dosing could maintain LDA/REM and among those who flared, the majority recaptured these treatment targets after reinitiating the 4-mg dosage [35]. Patients with UC who are treated with tofacitinib-induced stable remission could de-escalate the dose and maintain remission, especially in those in deep endoscopic remission and those without previous TNFi failure [36].

III. Warnings and contraindications

The heading was altered to 'warnings and contraindications' as 'contraindications' are not always absolute and depend upon the patient journey and comorbidities, *Item 1: Severe active (or recurrent) infections, including TB and opportunistic infections (LoE, 2b/5; SoR, B/D; vote, 94%; 1 abstention; LoA, 9.73)*

JAKi therapy may still be appropriate, taking safety issues into consideration. 'Chronic' infection was changed to 'recurrent' infection as a warning that also active infections may recur without being chronic (ie, chronic infections are always also 'active'). The risk of infections is similar among the currently approved JAKi, with filgotinib having a lower risk of herpes zoster on systematic review of RA trials [37], which was, however, not confirmed by sensitivity analyses [38,39]. Asian patient populations are more prone to develop herpes zoster than non-Asian patients [40,41]. TB and opportunistic infections were observed during JAKi therapy, with higher rates at increased doses and in older patients [20,41,42].

Item 2: Current (or history of) malignancies (LoE, 5; SoR, D; vote, 94%; 1 abstention; LoA, 9.15)

Differing from the 2019 version (describing 'current malignancies') and given the ORAL Surveillance results [13] with a numerical imbalance in rates of some malignancies when compared with TNFi, the term 'or history of' malignancies was added to this recommendation. Long-term registry follow-up data are needed to provide more evidence. This is important as patients with previous malignancies (typically within the last 5 years before study inclusion) are usually excluded from clinical trials. Registries including patients with comorbidities and concomitant medications that would exclude them from clinical trials, however, show no signal that JAKi therapy increases lymphoproliferative or solid tissue malignancy apart from an increase in non–melanoma skin cancer (NMSC) when compared with MTX and placebo [43,44]. However, in the ORAL Surveillance trial, a population particularly prone to develop major cardiovascular events was studied and an imbalance in lung cancer (but not breast cancer) incidence seen [13]. Many of these patients had a history of current or past smoking with a small imbalance in baseline smoking rates compared with the group treated with TNFi. Moreover, it is currently unknown whether JAKi could be used to treat checkpoint inhibitor–associated side effects (eg, checkpoint inhibitor–induced arthritis and IBD).

Item 3: Severe organ dysfunction such as decompensated advanced chronic liver disease and severe renal disease (creatinine clearance < 30 mL/min; LoE, 5; SoR, D; vote, 100%; LoA, 9.67)

The term 'severe hepatic disease' was now replaced by 'decompensated advanced chronic liver disease', the designation preferred by hepatologists over the older term 'liver cirrhosis' since this is defined by noninvasive criteria such as liver stiffness [29]. In this respect, JAKi should not be used in patients with a Child score of ≥9 points or a history or presence of hepatic decompensation (eg, ascites, hepatic encephalopathy grade of ≥2, and variceal bleeding); and for those with creatinine clearance of <30 mL/min, dose adjustments should be made. Of note, certain JAKi (baricitinib, filgotinib, and upadacitinib) are contraindicated for patients with creatinine clearance of <15 mL/min.

Item 4: Pregnancy and lactation (LoE, 5; SoR, D; vote, 100%; LoA, 9.76)

No change was made to this point compared with the previous consensus statement. Women of childbearing age should adhere to effective contraception while taking JAKi because of evidence of animal teratogenicity. Further, evidence from animal models on lactational pharmacokinetics showed an excretion of JAKi in breast milk. Sufficient human data on inadvertent pregnancies during JAKi therapy are currently lacking. An insufficient human database on lactation rather than evidence of harm is the reason for recommending to avoid JAKi during breastfeeding. Previous concerns on spermatogenesis based on animal data for filgotinib have been refuted in the filgotinib spermatogenesis studies, MANTA and MANTA-RAy. Filgotinib at 200 mg daily for 13 weeks had no impact on semen variables or sex hormones in men with active IBD or inflammatory rheumatic disease [45]. Paternal fertility appears unaffected by other JAKi in animal studies, but again, there are only limited human data available. 'The EULAR points-to-consider for the use of antirheumatic therapy in reproduction, pregnancy and lactation' [46] have been updated recently; this update will be available soon and can provide further guidance.

Item 5: History of arterial and venous thromboembolic events (LoE, 2b; SoR, B; vote, 100%; LoA, 9.45)

This recommendation was changed from 'recurrent VTE' to 'history of' arterial 'or' venous thromboembolic events to emphasise that arterial as well as venous thromboembolism (VTE) are increased in a dose-dependent manner with JAKi compared with using TNFi [47]. While it is notable that active inflammation is thrombogenic [48], the data on increased thromboembolic risk stem from placebo-controlled and active controlled trials [49], although this has not been studied as a primary outcome. Thus, careful risk/benefit assessment is needed in this clinical situation.

Item 6: Vaccination with live vaccines (LoE, 5; SoR, D; vote, 100%; LoA, 9.55)

This recommendation was added given increased use of recombinant and live vaccination in particular as far as herpes zoster is concerned.

IV. Pretreatment screening and risks

Item 1: Patient history and physical examination, with a focus on warnings and contraindications (LoE, 5; SoR, D; vote, 100%; LoA, 9.91)

The second half of the recommendation was added for consistency. Risk factors for adverse events of interest such as major adverse cardiac events (MACEs), VTE, TB, hepatitis B virus (HBV) and hepatitis C virus (HCV) infections, complicated diverticulitis, and herpes zoster history should be considered. Basic skin checks for NMSC should be performed for those at risk.

Item 2: Consider risk factors for venous thromboembolic events, especially a history of thromboembolism and whether this was provoked or unprovoked, as well as cardiovascular risk factors such as a history of cardiovascular event and the risk for malignancy, including smoking history (LoE, 2b/5; SoR, B/D; vote, 100%; LoA, 9.91)

This item was the last in this category in 2019. Based on the importance of thromboembolism considerations, it was moved up and expanded regarding other risk factors, including cardiovascular events and malignancy, especially lung cancer. The taskforce was aware that there is some redundancy with item 1 in this section, but this is deliberate, and the repetition and expansion should prompt higher vigilance, given that subanalyses of the ORAL Surveillance trial showed that those with a previous cardiovascular event are at particular risk to develop MACEs [50,51]. Of note, registry and cohort data, even when looking at patients at risk, did not show such increased risks [52,53]; however, the LoE of cohort studies compared with that of an RCT is lower, and more data will have to come from further RCTs.

Item 3: Routine laboratory testing (full and differential blood counts, liver blood tests, renal function, and lipid levels as a baseline; LoE, 5; SoR, D; vote, 100%; LoA, 9.73)

This item, like that of other points with a low LoE, is solely based on expert opinion, since no study investigated which laboratory tests are indispensable before starting JAKi therapy. The taskforce felt that, for example, creatine phosphokinase (CPK) testing was not routinely needed, although asymptomatic CPK increases may occur under JAKi treatment [54,55]. Of note in this respect, myalgia without rhabdomyolysis has been occasionally reported, so CPK testing should be done if respective symptoms develop [20]. Regarding liver blood tests (bilirubin, albumin, aspartate transaminase, alanine transaminase, alkaline phosphatase, and γ-glutamyl transferase), most clinicians are using aspartate transaminase/alanine transaminase at baseline and during monitoring.

Item 4: HBV testing (HBV surface antigen, HBV surface antibody, HBV core antibody, and with/without HBV DNA testing) and HCV testing (HCV antibody, with HCV RNA testing if antibody test was positive; LoE, 2b; SoR, B; vote, 100%; LoA, 9.88)

Hepatitis serology is recommended for all patients. While this recommendation has remained the same as in 2019, hepatitis D (δ) virus should also be tested in all patients with HBV infection. Patients with chronic HBV infection should receive JAKi only after consultation with a hepatologist for potential combination with antiviral agents. Similarly, patients with positive-result HCV RNA, should have HCV treated before JAKi therapy with hepatologist involvement.

Item 5: HIV testing in high-risk populations (LoE, 2b; SoR, B; vote, 100%; LoA, 9.58)

No new data exist since 2019, and the readers are referred to the previous deliberations for further details [12].

Item 6: TB screening as per national recommendation (LoE, 2b; SoR, B; vote, 100%; LoA, 9.91)

Risk of reactivation or new infection is similar to TNFi [13,56,57], so that screening according to national guidelines is recommended. Patients with latent TB should have initial concomitant anti-TB therapy; generally, isoniazid for 4 to 8 weeks is recommended and continued as per national guidelines.

Item 7: Assess and update vaccination status in accordance with national recommendations; consider vaccination against herpes zoster (LoE, 5; SoR, D; vote, 100%; LoA, 9.73)

The EULAR vaccination recommendations may assist clinicians treating IMIDs [58]. As mentioned in the 2019 recommendations, virus reactivation has been documented with JAKi therapy particularly herpes zoster (but also simplex and human papilloma viruses), in a dose-dependent manner. Herpes zoster vaccination is recommended, either using the live-attenuated vaccine with 2 to 4 weeks cessation of JAKi therapy or with the recombinant vaccine. Studies suggest that pausing MTX for 1 to 2 weeks at the time of vaccination reduces blunting of vaccine response [59,60].

V. Laboratory and clinical monitoring

This section has been moved from its previous position as number VI to now become element V for reasons of logical flow. The taskforce simply felt that the laboratory portion would fit better immediately after the section on pretreatment screening and before dealing with adverse events (now section VI).

Item 1: Periodic minimal laboratory monitoring: full and differential blood counts, liver and renal tests, and lipid levels (LoE, 2b/5; SoR, B/D; vote, 100%; LoA, 9.76)

In the previous version of the consensus statements, specific time points were recommended, but the taskforce felt that this was too prescriptive, and this debate was resolved by simply stating ‘periodic’, as was previously done after specifying initial detailed time points. With regard to lipid levels, it was suggested to measure these periodically, preferably also at baseline, and if levels are increased to suggest lipid lowering therapy as per national guidelines. With testing of liver and renal function, it was acknowledged that not all instruments (eg, liver enzyme tests) are practically adequate to assess ‘function’.

Item 2: Regular skin examination (for detection of skin cancer), as per national recommendations (LoE, 5; SoR, D; vote, 94%; 1 abstention; LoA, 8.88)

This bullet point was changed from the previous recommendation of ‘annual skin examinations’, since it was felt that this depended on local risks and, therefore, national recommendations should be adhered to.

Item 3: Evaluate response using validated, disease-specific measures of disease activity; for evaluation and definition of response, be aware that C-reactive protein and erythrocyte sedimentation rate may be reduced by JAK inhibitors independently of reduction of disease activity and possibly even for infections. (LoE 2b/5, SoR B/D, Vote 100%, LoA 9.97)

Several instruments used to assess disease activity include C-reactive protein (CRP) as one of the components. Since JAKi inhibits interleukin (IL)-6 signalling and IL-6 is a direct (hepatic) activator of acute phase reactants (APRs), APR/CRP decreases, and even their normalisation can often occur in the absence of significant clinical changes, suggesting the presence of LDA/REM without respective clinical evidence. Therefore, instruments should be used that do not include APRs to preclude such erroneous results [61]. For example, the American College of Rheumatology (ACR) and EULAR have recommended to not use the disease activity score (DAS; original or using 28 joint counts) to determine remission but rather other measures, such as Boolean criteria without CRP or clinical disease activity index (CDAI) definitions of remission [62]. The same caveat may pertain to the use of Axial Spondyloarthritis Disease Activity Score (ASDAS) in AxSpA [63], although it is otherwise a more reliable instrument than other ones used previously, or Minimal Disease Activity (MDA), Psoriatic Arthritis Disease Activity Score (PASDAS), and Disease Actvity Index for Psoriatic Arthritis (DAPSA) (although not clinical DAPSA) in PsA [64]. Indeed, claims that one drug may be better than another one could be (and are) made when using such measures [65], without such superiority being necessarily reflected in other objective assessments of disease activity, such as swollen joint counts in RA; at the least, potential small and clinically irrelevant differences may be highly exaggerated when using instruments comprising APRs. Regarding infections, one should be aware of the possibility that the CRP response may be blunted, but there are some data suggesting that CRP does increase in the course of infections in patients treated with JAKi [66].

VI. Adverse effects

This element was moved from its previous position as section V to now become group VI of the recommendations (see earlier).

Item 1: Serious infections (similar to biologic disease-modifying antirheumatic drugs), opportunistic infections including TB, and herpes zoster (increased rates compared to biological disease-modifying antirheumatic drugs) may occur; the risk of infectious events can be lowered with reduction or elimination of concomitant glucocorticoid use (LoE, 2b; SoR, B; vote, 100%; LoA, 9.70)

This item remained essentially unchanged, simply reflecting the currently available data regarding infections under JAKis. As mentioned earlier, herpes zoster rates may be lower with filgotinib than those with the other JAKis, but this is an impression, albeit based on the data from placebo and active controlled trials and not deducted from head-to-head comparisons of different JAKi. Dose-dependent risks for serious infections were observed in several trials [13,41,56,67,68] with higher age being an important risk factor [21,57,69,70].

Item 2: Rates of malignancy may be higher with JAK inhibition compared with those with TNF inhibitors; the risk of NMSC is elevated (LoE, 2b; SoR, B; vote, 94%; 1 abstention; LoA, 9.52)

This recommendation was reformulated to reflect data from the ORAL Surveillance trial on patients enriched for cardiovascular risk factors [13,71]. The wording ‘may’ was used despite the fact that this was an RCT comparing a JAKi, tofacitinib, with TNFi, but a confirmatory RCT is needed to change ‘may’ to ‘is’, especially since data from registries, which have primarily been implemented to find rarer adverse events, do not show an increased malignancy risk with JAKi [43,72]. As indicated earlier, the ORAL Surveillance trial included a particular group of patients at risk for developing malignancies due to a high prevalence of current or past smokers.

Item 3: Lymphopenia, thrombocytopenia, neutropenia, and anaemia may occur − anaemia especially occurring with JAKi that inhibit JAK2 (LoE, 1b; SoR, B; vote, 100%; LoA, 9.52)

Since anaemia of chronic disease is improved at the group level with filgotinib [39,73,74], the second half of this recommendation was added to reflect the fact that anaemia occurs primarily upon inhibition of JAK2, since erythropoietin signals via the JAK2 homodimer. Lymphocyte counts of $<0.5 \times 10^9$/L are associated with increased risk of serious and opportunistic infection. Neutropenia 0.5 to 1.0×10^9/L is common with JAKi, but rarely associated with infections [55,75]. Only a few haematologic abnormalities were observed in deucravacitinib-treated patients; however, larger studies are still ongoing [76−78].

Item 4: There is a dose-dependent risk of venous thromboembolic events, especially pulmonary embolism with JAK inhibition, particularly in patients with risk factors for venous thromboembolic events (LoE, 2b; SoR, B; vote, 100%; LoA, 9.67)

This point, which focused on high-dose tofacitinib and on baricitinib in 2019 [47,79,80], was expanded to reflect that the increased VTE risk may pertain to all JAKi, as long as no opposing data from RCTs have become available. It remains unknown whether this is an effect of JAK2 inhibition or a JAK class effect, nor is the exact mechanism for this adverse effect understood [52,53,81]. Risk factors for VTEs have been mentioned earlier.

Table 4
Research agenda

1. What is the efficacy and safety of switching between JAKi in nonresponders or due to lack of tolerability?
2. What are the predictors of response to JAKi when compared with other disease-modifying antirheumatic drugs used for RA?
3. Do JAKi reduce cardiovascular risk by interfering with inflammation, despite the results of the ORAL Surveillance study?
4. Is VTE a class effect or a JAK2 inhibition effect and what is the mechanism of VTE? What is the actual risk of VTE when treating with a JAKi?
5. What is the safety of JAK inhibition in patients with previous or current malignancy or who develop a malignancy while on therapy?
6. Are JAKi effective and safe as therapy for autoimmune diseases induced by checkpoint inhibitors in patients with malignancy?
7. How safe are JAKi in HBV/HCV−infected patients and other viral infections such as human papilloma virus? In case of active infections, especially COVID-19, should JAKi be temporarily discontinued? If so for how long?
8. How safe are JAKi in pregnancy and lactation? What should be recommended if a woman taking a JAKi becomes pregnant?
9. Safety of JAKi in elective surgery − should they be discontinued and if so for how long and when should they be restarted?
10. What is the efficacy of JAKi in extra-articular (EA) RA manifestations including vasculitis, nodulosis, lung involvement, overlap syndromes, and EA manifestations of axial spondyloarthritis and inflammatory bowl diseases?
11. What is the efficacy and safety of combination therapies with JAKi and other targeted therapies, especially biological disease-modifying antirheumatic drugs in patients with severe RA or other diseases?
12. What are the distinct molecular *in vivo* downstream effects of JAK inhibition in the setting of individual diseases?
13. What are the differences between different JAKi (eg, TyK2i) regarding safety?
14. Are JAKi plus methotrexate (MTX) more efficacious than MTX + glucocorticoids (GC) in disease-modifying antirheumatic drug −naive RA (at least in the short term)?
15. What is the mechanism for JAKi-induced acne?
16. Can the dose of all JAKi be tapered or discontinued in remission?
17. Do drug levels of JAKi correlate with adherence to drug?
18. What is the mechanism leading to JAKi-induced creatinine and creatine phosphokinase elevations?
19. Will JAKi be efficacious in pre-RA or in preventing RA?
20. What is the effect of JAKi on pain and fatigue and what are the mechanisms?
21. How long should one interrupt JAKi therapy before and/or after vaccination?
22. Are there clinically meaningful efficacy differences between the different JAKi (including deucravacitinib)?

HBV, hepatitis B virus; HCV, hepatitis C virus; JAK, Janus kinase; JAKi, Janus kinase inhibitor; RA, rheumatoid arthritis.

Item 5: Elevations of CPK are noted with JAKi but have usually not been associated with clinical events; elevations of creatinine have been noted with JAKi but have not been associated with renal failure or hypertension (LoE, 2b; SoR, B; vote, 100%; LoA, 9.55)

This last recommendation remained essentially the same as in 2019. The data accrued since the last SLR further strengthen and confirm this conclusion [54,55]. Moreover, acne occurs more frequently on JAKi than that on placebo [82], although this analysis did not include filgotinib, which may have a different profile in this respect. Finally, a research agenda was discussed during and after the meeting, tabulated in Table 4.

DISCUSSION

This update presents an amended version of the consensus statement for using JAKi in IMIDs, developed in 2019. The update became necessary because despite the short time since the development of the original document, new JAKi have been approved and licensed for several new indications. Most importantly, new safety issues have arisen, especially on cardiovascular and malignancy risks [13].

This statement differs from disease management recommendations in two important ways: first, as already pointed out, it does not deal with how a particular disease should be managed but rather with how JAKi should be used once the respective decision has been made; and second, it does not address a specific disease but rather the range of IMIDs for which JAKi have been approved. To this end, the taskforce included not only experienced clinicians from relevant specialties but also health care professionals and patients across nations and continents who focused on changes since the previous publication. The amendments were based on SLRs over the intervening period, which covered efficacy and safety aspects across IMIDs, being published separately in the future [17,18].

The taskforce discussions and decisions addressed general principles, indications and contraindications, screening, and monitoring, as well as a research agenda for the usage of JAKi therapy in patients with IMIDs. They cover the significant advances in JAKi therapy since 2019 regarding the development of novel agents such as the Tyk2 inhibitors; new approvals for novel indications, such as AxSpA, AD, and IBD; economic aspects given the advent of generics with implications for effective affordable therapy (especially for low income countries); data from trials focusing on safety, long-term extension studies of clinical trials, as well as registry data including patients with comorbidities and concomitant medications that would preclude their enrolment in clinical trials; as well as black box warnings from the Food and Drug Administration and European Medicines Agency adding safety concerns and dictating the place of JAK inhibition in therapy for a number of countries.

Since COVID-19 is not an IMID, it has not been addressed in this update, but it should be pointed out that baricitinib, in combination with remdesivir, has been approved for COVID-19 treatment and that EULAR has published recommendations that include advice for the management using immunomodulatory therapy such as JAKi in the setting of acute COVID-19 infection [83].

Baricitinib, deucravacitinib, filgotinib (in Europe and Japan), peficitinib (in Japan), tofacitinib, and upadacitinib are licensed for one or more autoimmune inflammatory diseases. Integrated safety analyses of tofacitinib up to 9.5 years (22 875 patient-years of exposure) [21,84], baricitinib up to 9.3 years (13 148 patient-years of exposure) [19,85−87], filgotinib to 5.6 years (5493 patient-years of exposure) [39,88], and upadacitinib (4020 patient-years of exposure) [20,56] have been published to complement the SLR safety analysis [89].

JAK selectivity has led to the development of novel molecules. Tyk2 inhibitors target signal transduction by IL-12, IL-23, IL-10, and type 1 interferons. Some of them, like deucravacitinib, bind covalently to the pseudokinase domain rather than reversibly to the adenosine triphosphate (ATP) pocket of the kinase domain [90]. Deucravacitinib has approval for PsO, a comprehensive PsA clinical trial programme [91,92], and is currently under investigation in SLE [25]. Also under development are beprocitinib and SAR-20347, which are inhibitors of Tyk2 and JAK1, while ropsacitinib inhibits Tyk2 and JAK2 and was under investigation in PsO and hidradenitis suppurativa, at the time of writing.

Follow-up data from long-term extensions of clinical trials and registry data has yet to demonstrate that ‘JAK 1 selectivity/preferred’ convincingly shows advantages in efficacy or safety between JAKi − apart from possibly reduced zoster and thromboembolic rates as well as less anaemia for filgotinib [22]. However, whether increased cardiovascular and thrombosis risk, as suggested by a head-to-head safety study (compared with TNF inhibition) [13] is a JAKi class effect or rather a specific JAK2 inhibition effect remains an unsettled question for the research agenda as does the possible mechanism for increased malignancy risk compared with that of TNFi. The safety and contraindication statements outlined in the respective sections of this update have been crafted to manage that risk until more definitive data are available. The task force encouraged the design of new outcome trials in this space to generate high-quality data.

Since drugs should generally be used at the minimum effective dose, the recommendations also address dose reduction once the desired state has been achieved. As far as this has been studied, good outcomes are maintained in most patients upon dose reduction, and in those in whom disease activity then increases, the good disease state is usually recaptured by returning to the previously more effective dose. Moreover, as indicated in the monitoring section, for all JAKi that interfere with IL-6 signal transduction and thus directly with CRP production, instruments that include CRP should presumably not be used in clinical trials and with caution in clinical practice to prevent potentially false trial results and erroneous continuation of an insufficiently efficacious JAKi. This is not an issue for Tyk2-selective inhibition.

Generic JAKi are now available in a number of countries, and the first clinical equivalence study of originator tofacitinib and a generic has been published [93]. Generic small molecules have the potential to provide highly effective therapy at a more affordable price particularly for countries where access is a major limitation due to cost, especially when long-term therapy is required, although cost containment is also an issue in high-income countries. In any case, recommendations remain as for the originator drugs.

The current consensus statement is certainly not a final one. Many other indications and many other JAKi are currently being investigated, and some of these studies are listed in Table 5.

In conclusion, this update acknowledges that a variety of specialists and health professionals are involved in the management of patients taking JAKi and emphasises the need for adequate information to provide informed consent. The update stresses the use of national and international guidelines and recommends dose adjustments in the setting of comorbidities like renal impairment and concomitant medications like rifampicin. Evidence for JAKi tapering while maintaining efficacy and recapture on flare has been updated. Given the ORAL Surveillance trial as well as extensive registry data, when JAKi therapy is considered, safety considerations like thrombosis, MACE, and malignancy must be taken into account, as well as individual risk and benefit, the patients disease journey, comorbidities, and concomitant medications. The research agenda remains important to answer questions of risk, mechanistic issues, safety in pregnancy and lactation, and adequacy of monitoring and more high-quality outcome trials are highly recommended. Once these data or other new information become available, a further update of this consensus statement will be desirable.

Competing interests

PN received grants for research, clinical trials, and for advice and lectures from Pfizer, Novartis, Janssen, UCB, Lilly, AbbVie, Samsung, BMS, Servatus, and Amgen. AK reports speakers bureau and consultancy for AbbVie, Amgen, Galapagos, Janssen, Eli Lilly, MSD, Novartis, Pfizer, and UCB. DA reports consultancy

Table 5
Status of using JAK inhibitors in IMIDs (green: approved, white: in trial; at the time of writing)

	TOFA	BARI	UPA	FILGO	PEFI	DEUC	RITLE	ABRO	RUXO
RA	Ph3	Ph3 Completed FDA 2 mg EMA 4 mg approved	Ph3 Completed FDA,EMA approved	Ph3 Completed EMA approved FDA pending	Ph2 Completedmultinational Ph3 Asia approved in Japan. China/Taiwan/Sth Korea ongoing				
PsA	Ph3 completed FDA,EMA approved		Ph3 Completed FDA,EMA approved	Ph2 completed, Ph3 term early		Ph2 completed, Ph3 ongoing			
rAxSpA	Ph3 completed FDA,EMA approved		Ph3 Completed FDA,EMA approved	Ph2 completed, Ph3 withdrawn					
nrAxSpA			Ph3 Completed FDA,EMA approved						
SLE		Ph3 completed, (SLE-BRAVE)	Ph3 ongoing (SELECT-SLE)			Ph2 completed, Ph3 ongoing			
DLE				Ph2 completed		Ph2 ongoing POETYK-SLE			Ph 2 single arm ongoing
LN				Ph2 completed		Ph2 terminated low recruitment			
SjS	Ph2 ongoing	Ph2 ongoing		Ph2 completed		Ph3 ongoing POETYK-SJS-1			
JIA	Ph3 completed FDA,EMA approved	Ph3 Completed, EMA approved							
UC	Ph3 completed FDA,EMA approved		Ph3 completed FDA,EMA approved	Ph3 completed, EMA approved	Ph2 completed	Ph2 completed	Ph2 completed		
CD	Ph2 completed		Ph3 Completed FDA,EMA approved	Ph2 completed		Ph 2 ongoing			
PsO	Ph3 completed				Ph2 completed	Ph3 completed FDA, EMA approved			

(*continued*)

Table 5
(Continued)

	TOFA	BARI	UPA	FILGO	PEFI	DEUC	RITLE	ABRO	RUXO
AD	Ph2 completed for topical TOFA	Ph3 completed, EMA approved 4 msg	Ph3 Completed FDA,EMA approved					Ph3 completed FDA EMA approved	Ph3 completed TRuE AD1-3
AA	Ph2 pilot study	Ph3 completed FDA 2 mg EMA 4 mg approved	Ph3 ongoing UPA-AA			Ph 2 ongoing	Ph3 completed FDA, EMA approved (>age 12)		Ph2 completed
Vit							Ph2 completed Ph3 ongoing, Tranquillo & Tranquillo 2		Ph3 completed FDA, EMA approved (also >age12)
HS			Ph2 completed, Ph3 ongoing Step-Up-HS)			Single centre Ph2 ongoing			Single arm single centre Ph2 ongoing

AA, alopecia areata; ABRO, abrocitinib; AD, atopic dermatitis; BARI, baricitinib; CD, Crohn disease; DEUCRA, deucravacitinib; DLE, discoid erythematosus; EMA, European Medicines Agency; FDA, Food and Drug Administration; FILGO, filgotinib; HS, hidradenitis supprativa; JAK, Janus kinase; JIA, juvenile idiopathic arthritis; LN, lupus nephritis; nrAxSpA, nonradiographic axial spondylarthropathy; PEFI, peficitinib; Ph, phase; PsA, psoriatic arthritis; PsO, psoriasis; RA, rheumatoid arthritis; rAxSpA, radiographic axial spondylarthropathy; RITLE, ritlecitinib; RUXO, ruxolitinib; SjS, Sjogren syndrome; SLE, systemic lupus erythematosus; TOFA, tofacitinib; UC, ulcerative colitis; UPA, upadacitinib; Vit, vitiligo.

fees, speakers' bureau fees, and grant/research support from AbbVie, Eli Lilly, Galapagos, Gilead, Janssen, Merck, Novartis, Pfizer, Sandoz and Sanofi. TD reports consulting fees from Roche, Novartis, GSK, and Astra Zeneca and participation in advisory boards of GNE, Roche, and Novartis. RF is a consultant for AbbVie, Pfizer, and BMS. IM reports honoraria/consultation fees and grants/research supports from AbbVie, Amgen, BMS, Causeway Therapeutics, Cabaletta, Eli Lilly, Gilead, Janssen, Novartis, Pfizer, Sanofi, UCB, Evelo, Compugen, AstraZeneca, and Moonlake. JP reports honoraria from BMS and Pfizer. NS consulted for and/or received speaker honoraria from Abbott Laboratories, AbbVie, Amgen, AstraZeneca, Boehringer Ingelheim, Eli Lilly, Hanmi Pharmaceuticals, Janssen, Menarini-Ricerche, Novartis, Novo Nordisk, Pfizer, Roche Diagnostics, and Sanofi and received grant support paid to his University from AstraZeneca, Boehringer Ingelheim, Novartis, and Roche Diagnostics outside the submitted work. YT has received speaker fees and/or honoraria from Eli Lilly, AstraZeneca, AbbVie G.K., Gilead Sciences K.K., Chugai Pharmaceutical, Boehringer-Ingelheim, GlaxoSmithKline K.K, Eisai, Taisho Pharmaceutical, Bristol-Myers Squibb, and Pfizer and research grants from Mitsubishi Tanabe Pharma, Eisai, Chugai Pharmaceutical, and Taisho Pharmaceutical. MT is a speaker and/or consultant and/or advisory board member for Albireo, BiomX, Falk, Boehringer Ingelheim, Bristol-Myers Squibb, Falk, Genfit, Gilead, Intercept, Janssen, MSD, Madrigal, Novartis, Phenex, Pliant, Regulus, and Shire and reports grants/research support from Albireo, Alnylam, Cymabay, Falk, Gilead, Intercept, MSD, Takeda, and UltraGenyx. KW reports consultant honoraria or research grants from Pfizer, AbbVie, Lilly, BMS, and Galapagos. MdW has received honoraria for consultancies and speaking through Stichting Tools from AbbVie, BMS, Celgene, Janssen, Lilly, Novartis, Pfizer, and Roche. JA reports Karolinska Institutet has entered into agreements with the following entities, with JA as PI, regarding the ARTIS national safety monitoring of rheumatology immunomodulators: Abbvie, BMS, Eli Lilly, Galapagos, MSD, Pfizer, Roche, Samsung Bioepis, and Sanofi. XB reports grant/research support from AbbVie and Novartis; consulting fees from AbbVie, BMS, Chugai, MSD, Novartis, Pfizer, and UCB Pharma; speakers' bureau fees from AbbVie, BMS, Celgene, Chugai, Merck, Novartis, Pfizer, and UCB Pharma. W-HB reports honoraria as a speaker and/or advisor from AbbVie, BMS, Pfizer, and Sanofi. PE reports advisory roles for AbbVie, Activa, AstraZeneca, BMS, Boehringer Ingelheim, Galapagos,Gilead, Immunovant, Janssen, Lilly, and Novartis and participation in clinical trials for AbbVie, BMS, Lilly, Novartis, Pfizer, and Samsung. LG reports grants from AbbVie, Biogen, Lilly, Novartis, and UCB; personal fees from AbbVie, BMS, Celltrion, Janssen, Novartis, Pfizer, and UCB; honoraria for lectures from AbbVie, Amgen, BMS, Celltrion, Janssen, Lilly, MSD, Novartis, Pfizer, Stada, and UCB; and nonfinancial support from AbbVie, Amgen, Biogen, Janssen, MSD, Pfizer, and UCB, outside the submitted work. JDI reports consultant in AbbVie, Anaptys Bio, Annexon Biosciences, AstraZeneca, BMS, Cyxone AB, Dragonfly, Eli Lilly, Galapagos NV, Gilead Sciences Ltd, GSK, Istesso, Janssen, Kenko International, Kira Biotech, Ono Pharma, Pfizer, Revelo Biotherapeutics, Roche, Sail, Sanofi, Sonoma Biotherapeutics, Topas, and UCB. MK reports advisory boards/consultancy for Novartis, BMS, and GSK. WM has acted as a paid consultant/participated in advisory boards for AbbVie, Boehringer Ingelheim, Celgene, Eli Lilly, Galapagos, Janssen, Novartis, Pfizer, and UCB; received research and/or educational grants from AbbVie, Novartis, Pfizer, and UCB; and received speaker fees from AbbVie, Janssen, Novartis, Pfizer and UCB. JP reports grants/research from BMS, Janssen, Mallinckrodt, and Pfizer (Seattle Genetics); is a consultant for AbbVie, Amgen, Astra Zeneca, Boehringer Ingelheim, Boxer Capital, Bristol Myers Squibb, Celltrion Healthcare, Eli Lilly, Frensenius Kabi, GSK, Janssen, Merck, Mitsubishi Tanabe Pharma, Novartis, Pfizer, Sandoz, Samsung, and Sanofi; is a speaker or in advisory board for AbbVie, Amgen, Boehringer Ingelheim, Bristol Myers Squibb, Certa, Eli Lilly, Frensenius Kabi, Janssen, Nordic Pharma, Novartis, Organon, Otsuka, Palleon, Pfizer, Sandoz, Sanofi, UCB, and Zura. MS-V received a grant for her PhD research from Roche and fees for lectures from Pfizer, outside the submitted work. KS reports speakers fees from UCB, Eli Lilly, and Rovi; research grants from Novo Nordic Foundation; and research support from the Danish Association for Rheumatism (Gigtforeningen). TS reports personal fees from AbbVie, Janssen, MSD, Novartis, and Roche, outside the submitted work. PCT reports research support from Galapagos (Alfasigma) and consultancy fees from Galapagos (Alfasigma), Gilead, Pfizer, AbbVie, and Lilly. TT reports speaking fee from AbbVie GK, Chugai, Eli Lilly Japan, Eisai, Gilead Sciences, Pfizer Japan, and Taisho Pharma and consultancy fees from AbbVie GK, Eli Lilly Japan, Gilead Sciences, Mitsubishi-Tanabe, and Taisho Pharma. FvdB reports speaker and/or consultancy fees from AbbVie, Amgen, Eli Lilly, Fresenius Kabi, Galapagos, Janssen, Novartis, and UCB. RW acted as a PI and advisor for Celltrion and Galapagos. JSS reports research grants to his institution from AbbVie, AstraZeneca, Galapagos, and Lilly and honoraria for consultancies and/or speaking engagements from AbbVie, Ananda, AstraZeneca, Astro, BMS, Celgene, Celltrion, Chugai-Roche, Galapagos-Gilead, Immunovant, Janssen, Lilly, Novartis- Sandoz, Pfizer, R-Pharma, and Samsung. VK, EBL, LS-T, and MZ: none.

Acknowledgements

The support of Martina Seidel from the Vienna Medical Academy regarding the logistics of organising the meetings is gratefully acknowledged.

Contributors

PN and JSS wrote the first drafts of the manuscript, and all authors provided input and provided final approval for submission. PN and JSS are guarantors in this respect.

Funding

The meetings for this work were supported by unrestricted grants from AbbVie, Galapagos, and Lilly to the Medical University of Vienna. No representative of any of the companies was present at any of the meetings (neither in meetings for the initial nor in the course of the work for the updated consensus statements) and they had no influence on the wording of the recommendations.

Patient consent for publication

Patient involvement and participation in voting as well as commenting on the manuscript occurred throughout the process.

Ethical approval

Ethics approval was not sought nor needed for this study that involved a literature search, meetings, and voting procedures.

Data availability statement

All data obtained during the process have been disclosed in this article, and there is nothing else to share.

Orcid

Laure Gossec: http://orcid.org/0000-0002-4528-310X

REFERENCES

[1] Theofilopoulos AN, Kono DH, Baccala R. The multiple pathways to autoimmunity. Nat Immunol 2017;18(7):716–24. doi: 10.1038/ni.3731.
[2] Gutierrez-Arcelus M, Rich SS, Raychaudhuri S. Autoimmune diseases - connecting risk alleles with molecular traits of the immune system. Nat Rev Genet 2016;17(3):160–74. doi: 10.1038/nrg.2015.33.
[3] Petersen J, Ciacchi L, Tran MT, Loh KL, Kooy-Winkelaar Y, Croft NP, et al. T cell receptor cross-reactivity between gliadin and bacterial peptides in celiac disease. Nat Struct Mol Biol 2020;27(1):49–61. doi: 10.1038/s41594-019-0353-4.
[4] Harley JB, Chen X, Pujato M, Miller D, Maddox A, Forney C, et al. Transcription factors operate across disease loci, with EBNA2 implicated in autoimmunity. Nat Genet 2018;50(5):699–707. doi: 10.1038/s41588-018-0102-3.
[5] Zhang L. A common mechanism links Epstein-Barr virus infections and autoimmune diseases. J Med Virol 2023;95(1):e28363. doi: 10.1002/jmv.28363.
[6] Smolen JS, Aletaha D, Barton A, Burmester GR, Emery P, Firestein GS, et al. Rheumatoid arthritis. Nat Rev Dis Primers 2018;4:18001. doi: 10.1038/nrdp.2018.1.
[7] McInnes IB, Gravallese EM. Immune-mediated inflammatory disease therapeutics: past, present and future. Nat Rev Immunol 2021;21(10):680–6. doi: 10.1038/s41577-021-00603-1.
[8] Smolen JS, Steiner G. Therapeutic strategies for rheumatoid arthritis. Nat Rev Drug Discov 2003;2(6):473–88. doi: 10.1038/nrd1109.
[9] Bonelli M, Kerschbaumer A, Kastrati K, Ghoreschi K, Gadina M, Heinz LX, et al. Selectivity, efficacy and safety of JAKinibs: new evidence for a still evolving story. Ann Rheum Dis 2024;83(2):139–60. doi: 10.1136/ard-2023-223850.
[10] Yu H, Lin L, Zhang Z, Zhang H, Hu H. Targeting NF-κB pathway for the therapy of diseases: mechanism and clinical study. Signal Transduct Target Ther 2020;5(1):209. doi: 10.1038/s41392-020-00312-6.
[11] Ganguly P, Macleod T, Wong C, Harland M, McGonagle D. Revisiting p38 mitogen-activated protein kinases (MAPK) in inflammatory arthritis: a narrative of the emergence of MAPK-activated protein kinase inhibitors (MK2i). Pharmaceuticals (Basel) 2023;16(9):1286. doi: 10.3390/ph16091286.
[12] Nash P, Kerschbaumer A, Dörner T, Dougados M, Fleischmann RM, Geissler K, et al. Points to consider for the treatment of immune-mediated inflammatory diseases with Janus kinase inhibitors: a consensus statement. Ann Rheum Dis 2021;80(1):71–87. doi: 10.1136/annrheumdis-2020-218398.
[13] Ytterberg SR, Bhatt DL, Mikuls TR, Koch GG, Fleischmann R, Rivas JL, et al. Cardiovascular and cancer risk with tofacitinib in rheumatoid arthritis. N Engl J Med 2022;386(4):316–26. doi: 10.1056/NEJMoa2109927.
[14] The European Alliance of Associations for Rheumatology. EULAR SOPs – standard operating procedures for task forces [Internet]. 2024. Available from: https://wwweularorg/web/static/lib/pdfjs/web/viewerhtml?file=https://wwweularorg/document/download/702/412c1a86-96e4-4089-86a6-c6554204c6f9/679. Accessed January 8, 2024.
[15] OCEBM Levels of Evidence Working Group, Center for Evidence-based Medicine. OCEBM Levels of Evidence. Oxford: University of Oxford; 2011.
[16] Kerschbaumer A, Smolen JS, Nash P, Doerner T, Dougados M, Fleischmann R, et al. Points to consider for the treatment of immune-mediated inflammatory diseases with Janus kinase inhibitors: a systematic literature research. RMD Open 2020;6(3):e001374. doi: 10.1136/rmdopen-2020-001374.
[17] Konzett VK, Efficacy of Janus kinase inhibitors in immune-mediated inflammatory diseases a systematic literature review informing the 2024 update of an international consensus statement, https://doi.org/10.1016/j.ard.2025.01.023.
[18] Konzett VK, Safety of Janus kinase inhibitors in immune-mediated inflammatory diseases – a systematic literature review informing the 2024 update of

an international expert consensus statement, https://doi.org/10.1016/j.ard.2025.01.024.
[19] Taylor PC, Takeuchi T, Burmester GR, Durez P, Smolen JS, Deberdt W, et al. Safety of baricitinib for the treatment of rheumatoid arthritis over a median of 4.6 and up to 9.3 years of treatment: final results from long-term extension study and integrated database. Ann Rheum Dis 2022;81(3):335–43. doi: 10.1136/annrheumdis-2021-221276.
[20] Burmester GR, Cohen SB, Winthrop KL, Nash P, Irvine AD, Deodhar A, et al. Safety profile of upadacitinib over 15 000 patient-years across rheumatoid arthritis, psoriatic arthritis, ankylosing spondylitis and atopic dermatitis. RMD Open 2023;9(1):e002735. doi: 10.1136/rmdopen-2022-002735.
[21] Cohen SB, Tanaka Y, Mariette X, Curtis JR, Lee EB, Nash P, et al. Long-term safety of tofacitinib up to 9.5 years: a comprehensive integrated analysis of the rheumatoid arthritis clinical development programme. RMD Open. 2020;6(3):e001395. doi: 10.1136/rmdopen-2020-001395.
[22] Tanaka Y, Genovese MC, Matsushima H. Long-term safety, efficacy, and patient-centered outcomes of filgotinib in the treatment of rheumatoid arthritis: current perspectives. Patient Prefer Adherence 2023;17:2499–516. doi: 10.2147/PPA.S417677.
[23] Corbella-Bagot L, Riquelme-McLoughlin C, Morgado-Carrasco D. Long-term safety profile and off-label use of JAK inhibitors in dermatological disorders. Actas Dermosifiliogr 2023;114(9):T784–801. doi: 10.1016/j.ad.2023.08.002.
[24] Martora F, Scalvenzi M, Ruggiero A, Potestio L, Battista T, Megna M. Hidradenitis suppurativa and JAK inhibitors: a review of the published literature. Medicina (Kaunas) 2023;59(4):801. doi: 10.3390/medicina59040801.
[25] Morand E, Pike M, Merrill JT, van Vollenhoven R, Werth VP, Hobar C, et al. Deucravacitinib, a tyrosine kinase 2 inhibitor, in systemic lupus erythematosus: a phase II, randomized, double-blind, placebo-controlled trial. Arthritis Rheumatol 2023;75(2):242–52. doi: 10.1002/art.42391.
[26] Merrill JT, Tanaka Y, D'Cruz D, Vila-Rivera K, Siri D, Zeng X, et al. Efficacy and safety of upadacitinib or elsubrutinib alone or in combination for patients with systemic lupus erythematosus: a phase 2 randomized controlled trial. Arthritis Rheumatol 2024;76(10):1518–29. doi: 10.1002/art.42926.
[27] Kalil AC, Patterson TF, Mehta AK, Tomashek KM, Wolfe CR, Ghazaryan V, et al. Baricitinib plus remdesivir for hospitalized adults with Covid-19. N Engl J Med 2021;384(9):795–807. doi: 10.1056/NEJMoa2031994.
[28] Geifman N, Cohen R, Rubin E. Redefining meaningful age groups in the context of disease. Age (Dordr) 2013;35(6):2357–66. doi: 10.1007/s11357-013-9510-6.
[29] de Franchis R, Bosch J, Garcia-Tsao G, Reiberger T, Ripoll C, Faculty Baveno VII. Baveno VII - renewing consensus in portal hypertension. J Hepatol 2022;76(4):959–74. doi: 10.1016/j.jhep.2021.12.022.
[30] Maini RN, Breedveld FC, Kalden JR, Smolen JS, Davis D, Macfarlane JD, et al. Therapeutic efficacy of multiple intravenous infusions of anti-tumor necrosis factor alpha monoclonal antibody combined with low-dose weekly methotrexate in rheumatoid arthritis. Arthritis Rheum 1998;41(9):1552–63.
[31] Burmester GR, Mariette X, Montecucco C, Monteagudo-Sáez I, Malaise M, Tzioufas AG, et al. Adalimumab alone and in combination with disease-modifying antirheumatic drugs for the treatment of rheumatoid arthritis in clinical practice: the Research in Active Rheumatoid Arthritis (ReAct) trial. Ann Rheum Dis 2007;66(6):732–9.
[32] Emery P, Burmester GR, Bykerk VP, Combe BG, Furst DE, Barré E, et al. Evaluating drug-free remission with abatacept in early rheumatoid arthritis: results from the phase 3b, multicentre, randomised, active-controlled AVERT study of 24 months, with a 12-month, double-blind treatment period. Ann Rheum Dis 2015;74(1):19–26. doi: 10.1136/annrheumdis-2014-206106.
[33] Vermeire S, Noman M, Van Assche G, Baert F, D'Haens G, Rutgeerts P. Effectiveness of concomitant immunosuppressive therapy in suppressing the formation of antibodies to infliximab in Crohn's disease. Gut 2007;56(9):1226–31. doi: 10.1136/gut.2006.099978.
[34] Jani M, Barton A, Warren RB, Griffiths CEM, Chinoy H. The role of DMARDs in reducing the immunogenicity of TNF inhibitors in chronic inflammatory diseases. Rheumatology (Oxford) 2014;53(2):213–22. doi: 10.1093/rheumatology/ket260.
[35] Takeuchi T, Genovese MC, Haraoui B, Li Z, Xie L, Klar R, et al. Dose reduction of baricitinib in patients with rheumatoid arthritis achieving sustained disease control: results of a prospective study. Ann Rheum Dis 2019;78(2):171–8. doi: 10.1136/annrheumdis-2018-213271.
[36] Vermeire S, Su C, Lawendy N, Kobayashi T, Sandborn WJ, Rubin DT, et al. Outcomes of tofacitinib dose reduction in patients with ulcerative colitis in stable remission from the randomised RIVETING trial. J Crohns Colitis 2021;15(7):1130–41. doi: 10.1093/ecco-jcc/jjaa249.
[37] Winthrop K, Isaacs J, Calabrese L, Mittal D, Desai S, Barry J, et al. Opportunistic infections associated with Janus kinase inhibitor treatment for rheumatoid arthritis: a structured literature review. Semin Arthritis Rheum 2023;58:152120. doi: 10.1016/j.semarthrit.2022.152120.
[38] Winthrop K, Buch MH, Curtis J, Burmester GR, Aletaha D, Amano K, et al. POS0092. Herpes zoster in the filgotinib rheumatoid arthritis program. Ann Rheum Dis 2021;80(Suppl 1) 255.1-6. doi: 10.1136/annrheumdis-2021-eular.1408.
[39] Winthrop KL, Tanaka Y, Takeuchi T, Kivitz A, Matzkies F, Genovese MC, et al. Integrated safety analysis of filgotinib in patients with moderately to severely active rheumatoid arthritis receiving treatment over a median of 1.6 years. Ann Rheum Dis 2022;81(2):184–92. doi: 10.1136/annrheumdis-2021-221051.
[40] van Oorschot D, Vroling H, Bunge E, Diaz-Decaro J, Curran D, Yawn B. A systematic literature review of herpes zoster incidence worldwide. Hum Vaccin Immunother 2021;17(6):1714–32. doi: 10.1080/21645515.2020.1847582.
[41] Winthrop KL, Nash P, Yamaoka K, Mysler E, Khan N, Camp HS, et al. Incidence and risk factors for herpes zoster in patients with rheumatoid arthritis receiving upadacitinib: a pooled analysis of six phase III clinical trials. Ann Rheum Dis 2022;81(2):206–13. doi: 10.1136/annrheumdis-2021-220822.
[42] Winthrop KL, Loftus EV, Baumgart DC, Reinisch W, Nduaka CI, Lawendy N, et al. Tofacitinib for the treatment of ulcerative colitis: analysis of infection rates from the ulcerative colitis clinical programme. J Crohns Colitis 2021;15(6):914–29. doi: 10.1093/ecco-jcc/jjaa233.
[43] Huss V, Bower H, Hellgren K, Frisell T, Askling J, Behalf of the ARTIS group. Cancer risks with JAKi and biological disease-modifying antirheumatic drugs in patients with rheumatoid arthritis or psoriatic arthritis: a national real-world cohort study. Ann Rheum Dis 2023;82(7):911–9. doi: 10.1136/ard-2022-223636.
[44] Molina-Collada J, Alonso F, Otero L, Bohórquez C, Díaz Torné C, Pérez García C, et al. Cancer risk with biologic and targeted synthetic DMARDs in patients with rheumatic diseases and previous malignancies: results from the BIOBADASER register. Semin Arthritis Rheum 2024;64:152341. doi: 10.1016/j.semarthrit.2023.152341.
[45] Reinisch W, Hellstrom W, Dolhain R, Sikka S, Westhovens R, Mehta R, et al. Effects of filgotinib on semen parameters and sex hormones in male patients with inflammatory diseases: results from the phase 2, randomised, double-blind, placebo-controlled MANTA and MANTA-RAy studies. Ann Rheum Dis 2023;82(8):1049–58. doi: 10.1136/ard-2023-224017.
[46] Götestam Skorpen C, Hoeltzenbein M, Tincani A, Fischer-Betz R, Elefant E, Chambers C, et al. The EULAR points to consider for use of antirheumatic drugs before pregnancy, and during pregnancy and lactation. Ann Rheum Dis 2016;75(5):795–810. doi: 10.1136/annrheumdis-2015-208840.
[47] Mease P, Charles-Schoeman C, Cohen S, Fallon L, Woolcott J, Yun H, et al. Incidence of venous and arterial thromboembolic events reported in the tofacitinib rheumatoid arthritis, psoriasis and psoriatic arthritis development programmes and from real-world data. Ann Rheum Dis 2020;79(11):1400–13. doi: 10.1136/annrheumdis-2019-216761.
[48] Molander V, Bower H, Frisell T, Askling J. Risk of venous thromboembolism in rheumatoid arthritis, and its association with disease activity: a nationwide cohort study from Sweden. Ann Rheum Dis 2021;80(2):169–75. doi: 10.1136/annrheumdis-2020-218419.
[49] Center for Drug Evaluation and Research. Statistical review – clinical studies – olumiant (baricitinib) [Internet]. 2019. Available from: https://www.accessdata.fda.gov/drugsatfda_docs/nda/2018/207924Orig1s000StatR.pdf
[50] Charles-Schoeman C, Buch MH, Dougados M, Bhatt DL, Giles JT, Ytterberg SR, et al. Risk of major adverse cardiovascular events with tofacitinib versus tumour necrosis factor inhibitors in patients with rheumatoid arthritis with or without a history of atherosclerotic cardiovascular disease: a post hoc analysis from ORAL Surveillance. Ann Rheum Dis 2023;82(1):119–29. doi: 10.1136/ard-2022-222259.
[51] Kristensen LE, Danese S, Yndestad A, Wang C, Nagy E, Modesto I, et al. Identification of two tofacitinib subpopulations with different relative risk versus TNF inhibitors: an analysis of the open label, randomised controlled study ORAL Surveillance. Ann Rheum Dis 2023;82(7):901–10. doi: 10.1136/ard-2022-223715.
[52] Hoisnard L, Pina Vegas L, Dray-Spira R, Weill A, Zureik M, Sbidian E. Risk of major adverse cardiovascular and venous thromboembolism events in patients with rheumatoid arthritis exposed to JAK inhibitors versus adalimumab: a nationwide cohort study. Ann Rheum Dis 2023;82(2):182–8. doi: 10.1136/ard-2022-222824.
[53] Meissner Y, Schäfer M, Albrecht K, Kekow J, Zinke S, Tony H-P, et al. Risk of major adverse cardiovascular events in patients with rheumatoid arthritis treated with conventional synthetic, biologic and targeted synthetic disease-modifying antirheumatic drugs: observational data from the German RABBIT register. RMD Open 2023;9(4):e003489. doi: 10.1136/rmdopen-2023-003489.
[54] Panaccione R, Isaacs JD, Chen LA, Wang W, Marren A, Kwok K, et al. Characterization of creatine kinase levels in tofacitinib-treated patients with

ulcerative colitis: results from clinical trials. Dig Dis Sci 2021;66(8):2732–43. doi: 10.1007/s10620-020-06560-4.
[55] Charles-Schoeman C, Giles JT, Lane NE, Choy E, Furst DE, Vencovský J, et al. Impact of upadacitinib on laboratory parameters and related adverse events in patients with RA: integrated data up to 6.5 years. Rheumatol Ther 2024;11(1):157–75. doi: 10.1007/s40744-023-00624-3.
[56] Cohen SB, van Vollenhoven RF, Winthrop KL, Zerbini CAF, Tanaka Y, Bessette L, et al. Safety profile of upadacitinib in rheumatoid arthritis: integrated analysis from the SELECT phase III clinical programme. Ann Rheum Dis 2021;80(3):304–11. doi: 10.1136/annrheumdis-2020-218510.
[57] Winthrop KL, Harigai M, Genovese MC, Lindsey S, Takeuchi T, Fleischmann R, et al. Infections in baricitinib clinical trials for patients with active rheumatoid arthritis. Ann Rheum Dis 2020;79(10):1290–7. doi: 10.1136/annrheumdis-2019-216852.
[58] Furer V, Rondaan C, Heijstek MW, Agmon-Levin N, van Assen S, Bijl M, et al. 2019 update of EULAR recommendations for vaccination in adult patients with autoimmune inflammatory rheumatic diseases. Ann Rheum Dis 2020;79(1):39–52. doi: 10.1136/annrheumdis-2019-215882.
[59] Araujo CSR, Medeiros-Ribeiro AC, Saad CGS, Bonfiglioli KR, Domiciano DS, Shimabuco AY, et al. Two-week methotrexate discontinuation in patients with rheumatoid arthritis vaccinated with inactivated SARS-CoV-2 vaccine: a randomised clinical trial. Ann Rheum Dis 2022;81(6):889–97. doi: 10.1136/annrheumdis-2021-221916.
[60] Park JK, Lee YJ, Shin K, Kang EH, Ha YJ, Park JW, et al. A multicenter, prospective, randomized, parallel-group trial on the effects of temporary methotrexate discontinuation for one week versus two weeks on seasonal influenza vaccination in patients with rheumatoid arthritis. Arthritis Rheumatol 2023;75(2):171–7. doi: 10.1002/art.42318.
[61] Aletaha D, Smolen JS. Remission in rheumatoid arthritis: missing objectives by using inadequate DAS28 targets. Nat Rev Rheumatol 2019;15(11):633–4. doi: 10.1038/s41584-019-0279-6.
[62] Studenic P, Aletaha D, de Wit M, Stamm TA, Alasti F, Lacaille D, et al. American College of Rheumatology/EULAR remission criteria for rheumatoid arthritis: 2022 revision. Ann Rheum Dis 2023;82(1):74–80. doi: 10.1136/ard-2022-223413.
[63] Sieper J, Porter-Brown B, Thompson L, Harari O, Dougados M. Assessment of short-term symptomatic efficacy of tocilizumab in ankylosing spondylitis: results of randomised, placebo-controlled trials. Ann Rheum Dis 2014;73(1):95–100. doi: 10.1136/annrheumdis-2013-203559.
[64] Kerschbaumer A, Smolen JS, Aletaha D. Disease activity assessment in patients with psoriatic arthritis. Best Pract Res Clin Rheumatol 2018;32(3):401–14. doi: 10.1016/j.berh.2018.08.004.
[65] Rubbert-Roth A, Enejosa J, Pangan AL, Haraoui B, Rischmueller M, Khan N, et al. Trial of upadacitinib or abatacept in rheumatoid arthritis. N Engl J Med 2020;383(16):1511–21. doi: 10.1056/NEJMoa2008250.
[66] Hendricks OC, Chrysidis S, Gerwien J, Saifan C, de Leonardis F, Lopez-Romero P, et al. CRP changes during bacterial infections in baricitinib-treated patients with RA. Arthritis Rheumatol 2018;70(Suppl 9):1683.
[67] van Vollenhoven R, Takeuchi T, Pangan AL, Friedman A, Mohamed MF, Chen S, et al. Efficacy and safety of upadacitinib monotherapy in methotrexate-naive patients with moderately-to-severely active rheumatoid arthritis (SELECT-EARLY): a multicenter, multi-country, randomized, double-blind, active comparator-controlled trial. Arthritis Rheumatol 2020;72(10):1607–20. doi: 10.1002/art.41384.
[68] McInnes IB, Kato K, Magrey M, Merola JF, Kishimoto M, Haaland D, et al. Efficacy and safety of upadacitinib in patients with psoriatic arthritis: 2-year results from the phase 3 SELECT-PsA 1 study. Rheumatol Ther 2023;10(1):275–92. doi: 10.1007/s40744-022-00499-w.
[69] Balanescu AR, Citera G, Pascual-Ramos V, Bhatt DL, Connell CA, Gold D, et al. Infections in patients with rheumatoid arthritis receiving tofacitinib versus tumour necrosis factor inhibitors: results from the open-label, randomised controlled ORAL Surveillance trial. Ann Rheum Dis 2022;81(11):1491–503. doi: 10.1136/ard-2022-222405.
[70] Winthrop KL, Citera G, Gold D, Henrohn D, Connell CA, Shapiro AB, et al. Age-based (<65 vs ≥65 years) incidence of infections and serious infections with tofacitinib versus biological DMARDs in rheumatoid arthritis clinical trials and the US Corrona RA registry. Ann Rheum Dis 2021;80(1):134–6. doi: 10.1136/annrheumdis-2020-218992.
[71] Curtis JR, Yamaoka K, Chen YH, Bhatt DL, Gunay LM, Sugiyama N, et al. Malignancy risk with tofacitinib versus TNF inhibitors in rheumatoid arthritis: results from the open-label, randomised controlled ORAL Surveillance trial. Ann Rheum Dis 2023;82(3):331–43. doi: 10.1136/ard-2022-222543.
[72] Khosrow-Khavar F, Desai RJ, Lee H, Lee SB, Kim SC. Tofacitinib and risk of malignancy: results from the safety of tofacitinib in routine care patients with rheumatoid arthritis (STAR-RA) study. Arthritis Rheumatol 2022;74(10):1648–59. doi: 10.1002/art.42250.
[73] Favalli EG, Buch MH, Galloway J, Constantin A, Durez P, Van Hoek P, et al. AB0454: safety of filgotinib in patients with RA: laboratory analysis results from a long-term extension study. Ann Rheum Dis 2023;82(Suppl 1):1417–8. doi: 10.1136/annrheumdis-2023-eular.2129.
[74] Loveikyte R, de Haas A, Oortwijn A, Eskens B, Jamoul C, Muller K, et al. P393 effect of filgotinib on anaemia in patients with ulcerative colitis in SELECTION. J Crohns Colitis 2023;17(Suppl 1):i525–7. doi: 10.1093/ecco-jcc/jjac190.0523.
[75] Kay J, Harigai M, Rancourt J, Dickson C, Melby T, Issa M, et al. Changes in selected haematological parameters associated with JAK1/JAK2 inhibition observed in patients with rheumatoid arthritis treated with baricitinib. RMD Open. 2020;6(3):e001370 doi:10.1136/rmdopen-2020-001370
[76] Morand E, Merola JF, Tanaka Y, Gladman D, Fleischmann R. TYK2: an emerging therapeutic target in rheumatic disease. Nat Rev Rheumatol 2024;20(4):232–40. doi: 10.1038/s41584-024-01093-w.
[77] Fleischmann RM, Thaçi D, Gooderham M, Strober B, Korman NJ, Banerjee S, et al. POS1040: safety of deucravacitinib, an oral, selective tyrosine kinase 2 inhibitor: as assessed by laboratory parameters − results from a phase 2 trial in psoriatic arthritis and 2 phase 3 trials in psoriasis. Ann Rheum Dis 2022;81(Suppl 1):835–6. doi: 10.1136/annrheumdis-2022-eular.1862.
[78] Strober B, Blauvelt A, Warren RB, Papp KA, Armstrong AW, Gordon KB, et al. Deucravacitinib in moderate-to-severe plaque psoriasis: pooled safety and tolerability over 52 weeks from two phase 3 trials (POETYK PSO-1 and PSO-2). J Eur Acad Dermatol Venereol 2024;38(8):1543–54. doi: 10.1111/jdv.19925.
[79] Salinas CA, Louder A, Polinski J, Zhang TC, Bower H, Phillips S, et al. Evaluation of VTE, MACE, and serious infections among patients with RA treated with baricitinib compared to TNFi: a multi-database study of patients in routine care using disease registries and claims databases. Rheumatol Ther 2023;10(1):201–23. doi: 10.1007/s40744-022-00505-1.
[80] Molander V, Bower H, Frisell T, Delcoigne B, Di Giuseppe D, Askling J, et al. Venous thromboembolism with JAK inhibitors and other immune-modulatory drugs: a Swedish comparative safety study among patients with rheumatoid arthritis. Ann Rheum Dis 2023;82(2):189–97. doi: 10.1136/ard-2022-223050.
[81] Ingrassia JP, Maqsood MH, Gelfand JM, Weber BN, Bangalore S, Lo Sicco KI, et al. Cardiovascular and venous thromboembolic risk with JAK inhibitors in immune-mediated inflammatory skin diseases: a systematic review and meta-analysis. JAMA Dermatol 2024;160(1):28–36. doi: 10.1001/jamadermatol.2023.4090.
[82] Martinez J, Manjaly C, Manjaly P, Ly S, Zhou G, Barbieri J, et al. Janus kinase inhibitors and adverse events of acne: a systematic review and meta-analysis. JAMA Dermatol 2023;159(12):1339–45. doi: 10.1001/jamadermatol.2023.3830.
[83] Alunno A, Najm A, Machado PM, Bertheussen H, Burmester GRR, Carubbi F, et al. 2021 update of the EULAR points to consider on the use of immunomodulatory therapies in COVID-19. Ann Rheum Dis 2022;81(1):34–40. doi: 10.1136/annrheumdis-2021-221366.
[84] Burmester GR, Nash P, Sands BE, Papp K, Stockert L, Jones TV, et al. Adverse events of special interest in clinical trials of rheumatoid arthritis, psoriatic arthritis, ulcerative colitis and psoriasis with 37 066 patient-years of tofacitinib exposure. RMD Open 2021;7(2):e001595. doi: 10.1136/rmdopen-2021-001595.
[85] Bieber T, Katoh N, Simpson EL, de Bruin-Weller M, Thaçi D, Torrelo A, et al. Safety of baricitinib for the treatment of atopic dermatitis over a median of 1.6 years and up to 3.9 years of treatment: an updated integrated analysis of eight clinical trials. J Dermatolog Treat 2023;34(1):2161812. doi: 10.1080/09546634.2022.2161812.
[86] King B, Mostaghimi A, Shimomura Y, Zlotogorski A, Choi GS, Blume-Peytavi U, et al. Integrated safety analysis of baricitinib in adults with severe alopecia areata from two randomized clinical trials. Br J Dermatol 2023;188(2):218–27. doi: 10.1093/bjd/ljac059.
[87] Guttman-Yassky E, Thyssen JP, Silverberg JI, Papp KA, Paller AS, Weidinger S, et al. Safety of upadacitinib in moderate-to-severe atopic dermatitis: an integrated analysis of phase 3 studies. J Allergy Clin Immunol 2023;151(1):172–81. doi: 10.1016/j.jaci.2022.09.023.
[88] Winthrop K, Aletaha D, Caporali R, Tanaka Y, Takeuchi T, Van Hoek P, et al. POS0844: integrated safety analysis of filgotinib in patients with moderate to severe active rheumatoid arthritis with a maximum exposure of 8.3 years. Ann Rheum Dis 2023;82(Suppl 1):721–2. doi: 10.1136/annrheumdis-2023-eular.1553.
[89] Szekanecz Z, Buch MH, Charles-Schoeman C, Galloway J, Karpouzas GA, Kristensen LE, et al. Efficacy and safety of JAK inhibitors in rheumatoid arthritis: update for the practising clinician. Nat Rev Rheumatol 2024;20(2):101–15. doi: 10.1038/s41584-023-01062-9.
[90] Jensen LT, Attfield KE, Feldmann M, Fugger L. Allosteric TYK2 inhibition: redefining autoimmune disease therapy beyond JAK1-3 inhibitors. EBioMedicine 2023;97:104840. doi: 10.1016/j.ebiom.2023.104840.

[91] Armstrong AW, Gooderham M, Warren RB, Papp KA, Strober B, Thaçi D, et al. Deucravacitinib versus placebo and apremilast in moderate to severe plaque psoriasis: efficacy and safety results from the 52-week, randomized, double-blinded, placebo-controlled phase 3 POETYK PSO-1 trial. J Am Acad Dermatol 2023;88(1):29–39. doi: 10.1016/j.jaad.2022.07.002.

[92] Strober B, Thaci D, Sofen H, Kircik L, Gordon KB, Foley P, et al. Deucravacitinib versus placebo and apremilast in moderate to severe plaque psoriasis: efficacy and safety results from the 52-week, randomized, double-blinded, phase 3 program for evaluation of TYK2 inhibitor psoriasis second trial. J Am Acad Dermatol 2023;88(1):40–51. doi: 10.1016/j.jaad.2022.08.061.

[93] Zhao J, Huang H, Wang Y, Deng X, Geng Y, Zhang X, et al. Real-world clinical equivalence of generic and branded tofacitinib: a prospective longitudinal cohort study in patients with rheumatoid arthritis. Mayo Clin Proc 2024;99(1):26–38. doi: 10.1016/j.mayocp.2023.08.029.

Ann Rheum Dis 84 (2025) 680−696

Contents lists available at ScienceDirect

Annals of the Rheumatic Diseases

journal homepage: https://www.sciencedirect.com/journal/annals-of-the-rheumatic-diseases

Rheumatoid arthritis

Efficacy of Janus kinase inhibitors in immune-mediated inflammatory diseases a systematic literature review informing the 2024 update of an international consensus statement

Victoria Konzett[1,*], Josef S. Smolen[1], Peter Nash[2], Daniel Aletaha[1], Kevin Winthrop[3], Thomas Dörner[4], Roy Fleischmann[5], Yoshiya Tanaka[6], Jette Primdahl[7], Xenofon Baraliakos[8], Iain B. McInnes[9], Michael Trauner[10], Naveed Sattar[11], Maarten de Wit[12], Jan W. Schoones[13], Andreas Kerschbaumer[1]

[1] *Department of Medicine III, Division of Rheumatology, Medical University of Vienna, Vienna, Austria*
[2] *Griffith University School of Medicine, Gold Coast, QLD, Australia*
[3] *Oregon Health & Science University, Portland, OR, USA*
[4] *Rheumatology, Charite Medical Faculty Berlin, Berlin, Germany*
[5] *Metroplex Clinical Research Center, University of Texas Southwestern Medical Center at Dallas, Dallas, TX, USA*
[6] *The First Department of Internal Medicine, University of Occupational and Environmental Health, Japan, Kitakyushu, Japan*
[7] *Danish Hospital for Rheumatic Diseases, University Hospital of Southern Denmark, Sønderborg, Denmark*
[8] *Rheumazentrum Ruhrgebiet, Ruhr University Bochum, Herne, Germany*
[9] *College of Medical Veterinary and Life Sciences, University of Glasgow, Glasgow, UK*
[10] *Department of Medicine III, Division of Gastroenterology and Hepatology, Medical University of Vienna, Vienna, Austria*
[11] *Cardiovascular and Metabolic Health, University of Glasgow, Glasgow, UK*
[12] *Stichting Tools, Patient Research Partner, Amsterdam, The Netherlands*
[13] *Directorate of Research Policy, Leiden University Medical Center, Leiden, The Netherlands*

A R T I C L E   I N F O

Article history:
Received 29 September 2024
Received in revised form 9 November 2024
Accepted 11 November 2024

A B S T R A C T

Objective: This systematic literature review (SLR) on efficacy outcomes was performed to inform the 2024 update of the expert consensus statement on the treatment of immune-mediated inflammatory diseases (IMIDs) with Janus kinase inhibitors (JAKi).
Methods: An update of the 2019 SLR was performed in MEDLINE, Embase, and the Cochrane Library. For efficacy, randomised, placebo (PLC)- or active-controlled trials on all JAKi investigated in IMIDs, as well as cohort and claims data for conditions where such studies were not available, were included.
Results: In total, 10,556 records were screened, and 182 articles were included in the final analysis, investigating 21 JAKi in 51 IMIDs. Forty-three phase 2 and 59 phase 3 trials as well as 9 strategic trials and 72 pilot or cohort studies and case series were considered. JAKi demonstrated efficacy both in PLC-controlled trials as well as in head-to-head comparisons against active comparators, with 93 of 102 randomised controlled trials (RCTs) meeting their primary endpoints. Since 2019, 8 JAKi have received approval by the Federal Drug Agency and the European Medicine Agency for treatment of 11 IMIDs; of these, for 2, no approved disease-modifying antirheumatic drug (DMARD) therapy had previously been available.

*__Correspondence to__ Dr. Victoria Konzett, Department of Medicine III, Division of Rheumatology, Medical University of Vienna, Austria.
E-mail address: victoria.konzett@meduniwien.ac.at (V. Konzett).
Handling editor Dimitrios T. Boumpas.

https://doi.org/10.1016/j.ard.2025.01.023

Conclusions: JAKi are effective for treating IMIDs, and various compounds have recently been approved. The impact of Janus kinase (JAK) selectivity for distinct JAK-STAT pathways needs further investigation, and few data are also available on sustained disease control upon tapering or withdrawal or on the optimal strategic placement of JAKi in international treatment algorithms.

WHAT IS ALREADY KNOWN ON THIS TOPIC

- The 2019 consensus statement on 'points to consider for the treatment of immune-mediated inflammatory diseases (IMIDs) with Janus kinase inhibitors (JAKi)' had drawn upon good efficacy data for JAKi in immune-mediated inflammatory conditions. Since then, a broad range of previously known and novel compounds with varying selectivity for different JAK-STAT pathways have been investigated.

WHAT THIS STUDY ADDS

- We here provide a summary of efficacy outcomes with JAKi investigated in IMIDs and published between 2019 and 2023. Twenty-one compounds were investigated in a total of 43 phase 2 and 59 phase 3 studies, of which most were placebo (PLC)-controlled.
- Twelve studies included an active comparator, of which 5 were designed as noninferiority trials.
- Nine strategic trials on treatment tapering or withdrawal as well as induction therapy with JAKi were further included, albeit predominantly conducted in open-label trial designs, which warrants further investigation of this important topic.
- Further analyses are also needed in IMIDs where numeric benefits were observed with JAKi in pilot or cohort studies as well as case series, but where no randomised controlled trial (RCT) data had been available at data cut.

HOW THIS STUDY MIGHT AFFECT RESEARCH, PRACTICE OR POLICY

- This review informed an international task force formulating the 2024 update of the expert consensus statement on the use treatment of IMIDs with JAKi, by summarising efficacy and safety outcomes of JAKi across all IMIDs published since the original 2019 consensus.

INTRODUCTION

Various physiologic and pathophysiologic immune mechanisms are regulated by cytokines that signal via the Janus kinase (JAK)-STAT pathways, making JAK inhibitors (JAKis) compelling agents for treating immune-mediated inflammatory diseases (IMIDs) [1−4]. Many compounds targeting this pathway have been investigated in a broad spectrum of IMIDs and patient populations, although their complex involvement in numerous biologic processes and potential off-target effects have repeatedly been reviewed and discussed [5−8].

To provide practical guidance for treating physicians in this complex and constantly evolving field, an international task force formulated a consensus statement on the treatment of IMIDs with JAKi in 2019, focusing both on their efficacy and safety across different diseases and in different patient populations [9,10]. At that point in time, tofacitinib (TOFA) was already approved for rheumatoid arthritis (RA), psoriatic arthritis (PsA), and ulcerative colitis (UC) and baricitinib (BARI), upadacitinib (UPA), and peficitinib (PEFI) were licensed for RA (PEFI only in Japan, Korea and Taiwan).

Since then, new drugs have been studied and some also approved. Further, new efficacy data, in particular for new indications, as well as new safety findings, have ignited discussions around the appropriate use of JAKi and have prompted regulators to not only approve new indications but also to release warnings regarding the safety of these compounds [11−15]. Considerations about the optimal balance of benefits and risks of JAKi have thus arisen across all medical disciplines [16−19].

These developments, as well as the large amount of recently published literature, warrant an update of the 2019 consensus statement, and a systematic literature review (SLR) was performed to inform the task force on efficacy and safety outcomes of JAKi published since the original 2019 consensus. This study summarises new efficacy aspects, while the SLR on safety outcomes as well as the updated consensus statement on the use of JAKi in IMIDs are reported separately (P. Nash et al, manuscript in press, Ann Rheum Dis, 2025; V. Konzett et al, manuscript in press, Ann Rheum Dis, 2025).

METHODS

Previously established principles for the conduction of recommendations and points to consider as well as the Cochrane Handbook for Systematic Literature Reviews and Preferred Reporting Items for Systematic Reviews and Meta-Analyses (PRISMA) guidelines were adhered to in this project [20−24]. The task force consisted of over 30 members, most of whom were clinicians representing different specialties, and included patient representation and nonphysician health care professionals (for details see, P. Nash et al, manuscript in press, Ann Rheum Dis, 2025). A steering committee (the authors of this article) defined the scope of the review in Population, Intervention, Comparator, Outcomes (PICO) format in an initial in-person meeting on April 16, 2023 [25]. After development of a search strategy based on this protocol, 3 database searches were conducted by an experienced librarian (JWS) using MEDLINE, Embase, and the Cochrane Library. All articles published between March 1, 2019 (the last date searched for the previous SLR), and October 27, 2023, were screened. In addition, the initial search for the 2019 SLR was extended to the broader scope of the current SLR. Conference abstracts presented at international rheumatology, gastroenterology, and dermatology conferences between 2021 and 2023 were included as well. The initial search was performed in June 2023 and updated on October 27, 2023, to include the most recent data. Articles were screened by 1 researcher (VK), and all doubts were discussed with the methodologist (AK).

PICO criteria, research questions, and the detailed search strategy are provided in Supplemental Appendix (Section 1). All patient populations and efficacy outcomes were prespecified, and records were then screened for randomised, double-blind (DB), placebo (PLC)-controlled or active-controlled, phase 2 to phase 4 trials (randomised controlled trials [RCTs]) on all JAKi investigated in IMIDs. Myeloproliferative disorders and other malignancies, graft-vs-host disease, posttransplant immunosuppression and treatment of COVID-19 disease were not considered in this project because these do not constitute IMIDs. Studies with a duration of at least 6 months and a sample size of at least 50 participants were included, as well as open-label (OL)

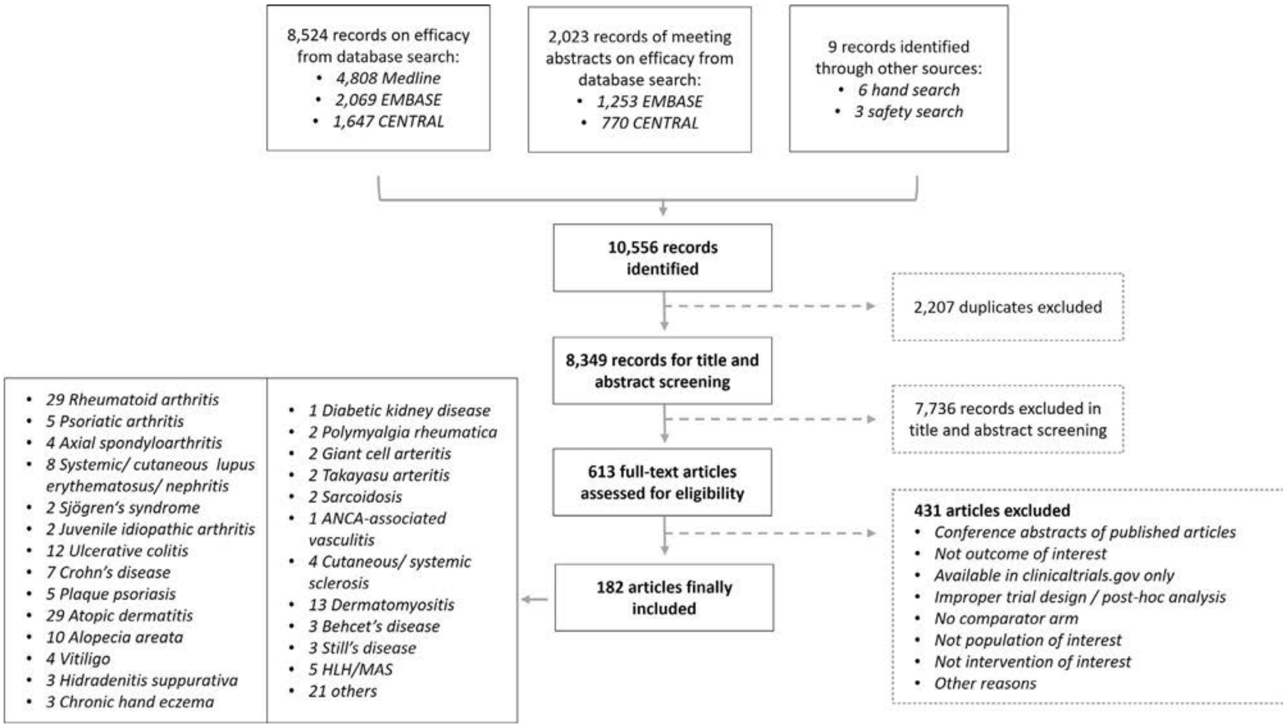

Figure 1. Flowchart illustrating the systematic literature search and manuscript selection process. ANCA, antineutrophil cytoplasmic antibody; HLH, haemophagocytic lymphohistiocytosis; MAS, macrophage activation syndrome.

strategic trials on treatment induction or withdrawal. Shorter and/or smaller trials as well as observational cohort studies and case series of at least 5 patients were considered in rare diseases and conditions where RCT data were not available. Only studies with published manuscripts or conference abstracts available in English language were considered.

Study and baseline characteristics, methodological summaries and efficacy outcomes from finally included articles were extracted using standardised spreadsheets. Efficacy outcomes of interest were distinctly defined for all indications before starting the literature search (Supplemental Appendix, Section 1.1.4). Risk of bias (RoB) assessment was done using the Cochrane Collaboration's tool for assessing RoB in randomised trials [26] and the Hayden Tool for observational studies [27]. Owing to the heterogeneity of diseases and patient populations investigated, we refrained from performing meta-analyses on efficacy outcomes.

Because this SLR includes many different disorders and the outcome instruments used for each of these disorders may not be widely known, a supplementary list of these instruments for the different diseases is provided for better clarity of the subsequent results presentation (Supplemental list of abbreviations and outcomes measures).

RESULTS

From a total of 10,556 records identified, 613 were selected for full-text assessment, of which 182 were included in the final analysis; 29 articles assessed JAKi in RA or RA interstitial lung disease (ILD), 9 in PsA or axial spondyloarthritis (axSpA), 10 in systemic lupus erythematosus (SLE) and cutaneous or discoid lupus erythematosus (CDLE), lupus nephritis or Sjögren syndrome (SjS), 2 in juvenile idiopathic arthritis (JIA), 19 in inflammatory bowel disease (IBD), 54 in dermatologic conditions, and 59 in other IMIDs like polymyalgia rheumatica (PMR) or Behçet disease, with the latter group including predominantly nonrandomised cohort and registry studies.

Details on the literature search and selection process are shown in Figure 1. The main reasons for exclusion of articles from the analysis were studies investigating JAKi in non−immune-mediated (eg, haematologic or oncologic) conditions or in infectious diseases; conference abstracts on articles subsequently published in full; reports on nonrandomised studies, cohort studies or case reports (if evidence from randomised studies was available), as well as post hoc or pooled analyses of RCT data.

Table 1 provides an overview of all JAKi studied in RCT across IMIDs included in the 2024 update of the consensus statement. The trials addressed in the previous SLR were not re-evaluated and the reader is referred to that publication for more details [10]. All data published since are summarised further and provided in more detail in Supplemental Appendix (Section 5; efficacy outcomes). Tabular overviews of head-to-head studies as well as tapering and withdrawal trials are further shown in Tables 2 and 3 [28−39] and in Supplemental Appendix (Section 6.2; Supplemental Table S1), as are timelines of all published JAKi efficacy trials (Supplemental Appendix; Section 6.3.1). Overviews of systemic and topical therapies tested in phase 2 and phase 3 trials, as well as of completed and pending drug approvals processed by major regulators like the Federal Drug Agency (FDA) or the European Medicines Agency (EMA), are provided in Figure 2 and in Supplemental Appendix (Section 6.2; Supplemental Tables S2 and S3). For an overview of outcome instruments and abbreviations used in this manuscript, we refer the reader to an additionally provided reference book (Supplemental list of abbreviations and outcomes).

Rheumatologic diseases

Rheumatoid arthritis

The current SLR revealed 10 new phase 2 and phase 3 efficacy trials as well as 6 strategic trials, mainly on tapering or treatment induction. Eight studies assessed JAKi in

Table 1

Overview of JAKi studied in RCTs of various IMID included in the 2024 consensus

JAKi	Abbreviation	Target	Indications in which compound was studied in 2019-2023 (SLR update)
JAK1-3 inhibitors			
Tofacitinib	TOFA	JAK1-3	RA, PsA, AS, JIA, UC
Peficitinib	PEFI	JAK1-3	RA
Gusacitinib	GUSA	SYK/JAK1-3	CHE
JAK1/2 inhibitors			
Baricitinib	BARI	JAK1/2	RA, SLE, LN, SjS, JIA, AD, AA, DMell
Upadacitinib	UPA	JAK1(/2)	RA, PsA, AS, nr-axSpA, UC, CD, AD, HS
ABBV-599 (Elsubrutinib/Upadacitinib)	ABBV	BTK/JAK1(/2)	RA, SLE
Deuruxolitinib	DEURUXO	JAK1/2	AA
JAK1 inhibitors			
Filgotinib	FILGO	JAK1	RA, LN, CDLE, SjS, UC, CD
Abrocitinib	ABRO	JAK1	AD
Ivarmacitinib	IVAR	JAK1	UC, AD, AA
Itacitinib	ITA	JAK1	—
Povorcitinib	POVOR	JAK1	HS
JAK3 inhibitors			
Ritlecitinib	RITLE	JAK3/TEC	RA, UC, AA, vitiligo
TYK2 inhibitors			
Deucravacitinib	DEUCRA	TYK2	PsA, SLE, PsO
Ropsacitinib	ROPSA	TYK2	PsO
JAK1/TYK2 inhibitors			
Brepocitinib	BREPO	JAK1/TYK2	PsA, UC, PsO, AA
TLL-018	TLL-018	TYK2/JAK1	RA
Topical JAK inhibitors			
Izencitinib (gut-selective)	IZE	pan-JAK	UC, CD
Topical brepocitinib	tBREPO	JAK1/TYK2	PsO, AD
Topical ruxolitinib	tRUXO	JAK1/2	AD, AA, vitiligo
Topical delgocitinib	tDELGO	pan-JAK	AD, AA, CHE
Topical tofacitinib	tTOFA	JAK1-3	—

AA, alopecia areata; ABBV-599, elsubrutinib/upadacitinib fixed combination; AD, atopic dermatitis; AS, ankylosing spondylitis; BTK, Bruton tyrosine kinase; CD, Crohn disease; CDLE, cutaneous/discoid lupus erythematosus; CHE, chronic hand eczema; DMell, diabetes mellitus; HS, hidradenitis suppurativa; JAK, Janus kinase; JIA, juvenile idiopathic arthritis; LN, lupus nephritis; nr-axSpA, nonradiographic axial spondyloarthritis; PsA, psoriatic arthritis; PsO, psoriasis; RA, rheumatoid arthritis; SjS, Sjögren syndrome; SLE, systemic lupus erythematosus; SYK, spleen tyrosine kinase; TEC, Tec-kinase; TYK, tyrosine kinase; UC, ulcerative colitis.

methotrexate (MTX) insufficient responders (IRs) or conventional-synthetic disease-modifying antirheumatic drugs (csDMARDs) IR, 4 in disease-modifying antirheumatic drug (DMARD) naïve patients, 4 in biologic DMARD (bDMARDs) IR, and 3 in previous responders to JAKi therapy. Ten DB trials were graded as low RoB, 1 as unclear RoB, 2 as high RoB, and 1 abstract was included. All 5 OL trials were graded as high RoB. The primary endpoint was met in all efficacy trials.

In SELECT-EARLY, UPA was superior to PLC in DMARD naïve patients (low RoB) [40] and in SELECT-CHOICE to abatacept (ABA) in bDMARD IR (high RoB), as DAS28 was used as primary outcome, which is highly weighted on C-reactive protein (CRP), while JAKi interfere with the signalling pathway to CRP production, which ABA does not [28,41]. The efficacy of UPA was further confirmed in patients from China, Brazil, and South Korea (low RoB) [42] and a combination therapy of UPA with elsubrutinib (EBT; a Bruton tyrosine kinase inhibitor [BTKi]) showed significant benefits on disease outcomes in a phase 2 trial. However, treatment effects were most likely attributable to the JAKi (UPA), since EBT monotherapy failed to demonstrate superiority over PLC (high RoB) [43]. Moreover, BARI efficacy was confirmed in a phase 3 study from China, Brazil, and Argentina in MTX IR patients (unclear RoB) [44].

The FINCH phase 3 programme tested filgotinib (FILGO) against PLC and adalimumab (ADA) in MTX IR (FINCH1) [29], as well as against PLC in bDMARD IR and in MTX naïve patients (FINCH2 and FINCH3) (all low RoB) [45,46]. In MTX IR patients, both FILGO doses demonstrated superiority over PLC, FILGO 200 mg (but not 100 mg) was noninferior to ADA, and radiographic progression was higher in PLC than that in FILGO or ADA-treated patients [29]. Superiority over PLC was also achieved in FINCH2 in bDMARD IR [45] and in FINCH3 in MTX naïve patients, when combined with background MTX, whereas FILGO 200 mg every day monotherapy only showed numeric but not statistical superiority over MTX monotherapy in FINCH3 [46].

PEFI demonstrated superiority over PLC in MTX IR patients from China, Taiwan, and South Korea (low RoB) [47], and ritlecitinib (RITLE), a JAK3/TEC inhibitor, showed positive data in an 8-week phase 2a study [48].

TOFA 5 mg twice a day was tested as active comparator in a phase 2a study from China evaluating TLL-018, a novel TYK2/JAK1 inhibitor (abstract) [49], where TLL-018 was superior to TOFA, but which warrants further exploration in a multinational phase 3 programme. TOFA was also used as active comparator in 2 phase 3 studies on otilimab (OMB), a granulocyte-monocyte colony stimulating factor inhibiting antibody (GM-CSFi), where OMB was not superior to TOFA (both low RoB) [30].

In ORAL SHIFT, a blinded withdrawal study of background MTX in TOFA + MTX patients who had achieved low disease activity or remission (REM) (Clinical disease activity index [CDAI], ≤10) after 24 weeks of OL treatment, REM could be sustained in the majority of patients over a 24-week follow-up period in both trial arms (TOFA + MTX combination and TOFA monotherapy; low RoB) [50,51]. Other OL trials compared TOFA with MTX induction therapy in standard and high dose

Table 2

Overview of head-to-head studies: rheumatic conditions and inflammatory bowel disease (IBD)

Study ID	Study arms	No	Patients	RoB	PEP	Week	*P* value	Outcomes			
Rheumatoid arthritis								ACR20	ACR50	ACR70	DAS28-CRP < 2.6
Rubbert-Roth et al, 2020 (SELECT-CHOICE) [28]	ABA 500/1000 mg weekly + csDMARD	309	bDMARD IR	High	ΔDAS28-CRP [NI vs ABA]	12	REF	66.3%	34.3%	13.6%	13.3% Δ −2.00
	UPA 15 mg every day + csDMARD	303					<.001 [NI and S]	75.6%	46.2%	21.5%	30.0% Δ −2.52
Combe et al, 2021 (FINCH 1) [29]	PLC + MTX	475	MTX IR	Low	ACR20 [S vs PLC]	12	REF	49.9%	19.8%	6.7%	9.0%
	FILGO 100 mg every day + MTX	475					<.001 [S vs PLC] .054 [NI vs ADA] in DAS28-CRP ≥ 3.2	69.8%	36.5%	18.5%	24.0%
	FILGO 200 mg every day + MTX	480					<.001 [S vs PLC] .054 [NI vs ADA] in DAS28-CRP ≥ 3.2	76.6%	47.2%	26.1%	34.0%
	ADA 40 mg every other week + MTX	325					<.001 [S vs PLC]	70.5%	35.1%	14.2%	24.0%
Fleischmann et al, 2023 (contRAst 1) [30]	PLC + csDMARD	256	csDMARD/bDMARD IR	Low	ACR20 [S vs PLC]	12	REF	42.7%			
	OMB 90 mg every day + csDMARD	513					.0023 [S vs PLC]	54.7%			
	OMB 150 mg twice a day + csDMARD	510					.0362 [S vs PLC]	50.9%			
	TOFA 5 mg twice a day + csDMARD	258				24	.0061[S vs OMB90)] .007 [S vs OMB150]	63.6%			
Fleischmann et al, 2023 (contRAst 2) [30]	PLC + csDMARD	270	csDMARD/bDMARD IR	Low	ACR20 [S vs PLC]	12	REF	23.5%			
	OMB 90 mg every day + csDMARD	545					<.0001 [S vs PLC]	54.9%			
	OMB 150 mg twice a day + csDMARD	539					<.0001 [S vs PLC]	54.5%			
	TOFA 5 mg twice a day + csDMARD	271				24	<.0001 [S vs OMB90/150]	71.1%			
Psoriatic arthritis								ACR20	ACR50	ACR70	PASI75
McInnes et al, 2021 (SELECT-PsA 1) [31]	PLC ± csDMARD	423	csDMARD IR	Low	ACR20 [S vs PLC]	12	REF	36.2%	13.2%	2.4%	21.3[a]
	UPA 15 mg every day ± csDMARD	429					<.001 [S vs PLC] <.001 [NI vs ADA] >.05 [S vs ADA]	70.6%	37.5%	15.6%	62.6 [a]
	UPA 30 mg every day ± csDMARD	423					<.001 [S vs PLC] <.001 [NI vs ADA] <001 [S vs ADA]	78.5%	51.8%	25.3%	62.4 [a]
	ADA 40 mg every other week ± csDMARD	429					REF	65.0%	37.5%	13.8%	53.1 [a]
Lupus nephritis								≥50% proteinuria reduction			
Hassanien et al, 2023 [32]	BARI	30	Lupus nephritis class III or IV, proteinuria ≥ 0.5 g/24 h; SOC IR	Abstract	≥50% proteinuria reduction [S vs CYC]	12		70.0%			
	CYC 0.7 mg/m^2 every month	30						43.4%			

Table 2 (Continued)

								Composite remission (TMS/endoscopic remission)	Clinical remission (TMS)
Ulcerative colitis									
Singh et al, 2023 (ORCHID) [33]	TOFA 10 mg twice a day Prednisolone 40 mg every day (taper)	43 35	Moderate UC (TMS 6-9, endoscopic remission MS 2/3)	High (OL)	Composite remission (TMS ≤2; endoscopic remission MS 0; faecal calprotectin <100 μg/g)	8	.31 (between-group comparison)	16.28% 8.57%	41.9% 37.1%

ABA, abatacept; ACR20/50/70, American College of Rheumatology 20%/50%/70% response criteria [34]; ADA, adalimumab; BARI, baricitinib; CRP, C-reactive protein; CYC, cyclophosphamide; csDMARD, conventional-synthetic disease-modifying antirheumatic drug; DAS28, disease activity index of 28 joints; FILGO, filgotinib; MS, Mayo score; MTX, methotrexate; NI, noninferiority; OMB, otilimab; OL, open label; PASI, psoriasis area and severity index; PEP, primary endpoint; PLC, placebo; REF, reference arm; RoB, risk of bias; S, superiority; TMS, total Mayo score; TOFA, tofacitinib; UPA, upadactinib.
Outcome criteria are explained in detail in the Supplemental Material (list of outcomes and definitions).

[a] Week 16

regimens in DMARD naïve patients [52,53] as well as MTX and TOFA withdrawal in treatment responders: In CDAI responders (CDAI ≤ 2.8), sustained CDAI REM through weeks 52 and 104 could be achieved in 23 of 34 patients upon MTX withdrawal vs 13 of 45 upon TOFA withdrawal [54]. TOFA tapering or withdrawal in DAS28 responders (DAS28-ESR LDA) allowed sustained disease control through week 24 in 27 of 42 patients tapering TOFA to 5 mg once daily, 8 of 39 completely withdrawing TOFA, as compared with 40 of 41 patients who continued TOFA 5 mg twice daily (all high RoB) [55]. Factors associated with loss of REM upon TOFA withdrawal were prior bDMARD exposure, disease duration, and autoantibody titres [54], as well as baseline disease activity (LDA vs REM) [55].

High-level prospective data or RCT data are lacking to date for JAKi in RA-ILD, but retrospective analyses and pooled trial data did not show increased risks for ILD development in patients with RA [56–58]. Instead, stable functional and structural outcomes were observed in patients with RA-ILD on JAKi treatment [59–61], also when compared with RTX [62] or ABA [63,64]. Detailed data on retrospective analyses are presented in the Supplemental Appendix (Section 6.1.1).

Psoriatic arthritis

Since 2019, 5 phase 2 and 3 studies have been published, assessing JAKi in csDMARD IR (4) and in bDMARD or tumour necrosis factor α inhibitor (TNFi) IR patients (2). All were graded as low RoB, and the primary endpoint was met in all trials.

SELECT-PsA 1 and 2 studied efficacy of UPA on signs and symptoms of PsA (both low RoB). In SELECT-PsA 1, UPA was tested against PLC and ADA in csDMARD IR patients and showed superiority over PLC for both UPA arms, as well as superiority over ADA for the UPA 30 mg arm [31]. In SELECT-PsA 2, UPA was evaluated against PLC, in bDMARD IR patients [65]. Significant benefits of UPA on other disease domains like skin disease, enthesitis, and radiographic progression as well as patient-reported outcomes (PROs) and composite outcome measures (like the disease activity in PsA index [DAPSA] or minimal disease activity [MDA]) were observed in both trials [31,65].

Superiority over PLC was further demonstrated in a phase 2 study on deucravacitinib (DEUCRA), a selective TYK2 inhibitor (low RoB) [66], as well as in a phase 2b study on brepocitinib (BREPO), a TYK2/JAK1 inhibitor, in a dose-dependent manner (low RoB) [67]. An additional phase 3 study was conducted on TOFA in patients from China, which confirmed superiority of TOFA over PLC in this population [68].

Radiographic and nonradiographic axial spondyloarthritis

Four phase 2 and 3 trials on TOFA and UPA were published since 2019, studying both bDMARD naïve and bDMARD IR patients, in radiographic as well as nonradiographic axSpA (nr-axSpA). All trials were graded as low RoB, and all primary endpoints were met.

TOFA was studied in a phase 3 trial in patients with ankylosing spondylitis (AS) and insufficient response to ≥2 nonsteroidal anti-inflammatory drugs (NSAIDs) (including also 20% bDMARD-experienced patients) (low RoB) [69].

Efficacy on signs and symptoms of both radiographic and nr-axSpA was further shown for UPA in bDMARD naïve patients with AS and insufficient response to NSAIDs in SELECT-AXIS 1 [70], while SELECT-AXIS 2 was split into a trial on UPA in AS (77% TNFi or interleukin [IL] 17i IR) [71] and 1 in nr-axSpA (33% TNFi or IL-17i IR) [72]. Primary and secondary (including

Table 3

Overview of head-to-head studies: dermatologic conditions (psoriasis and atopic dermatitis)

Study ID	Study arms	No	Patient population	RoB	PEP	Wk	*P*	Outcomes			
Psoriasis								PASI75	PASI90	PASI100	sPGA 0/1)
Armstrong et al, 2023 (POETYK PSO-1) [35]	PLC	166	sPGA ≥ 3, PASI ≥ 12, BSA ≥ 10%, disease duration ≥ 6 mo	Unclear	PASI75	16	REF	12.7%	4.2%	0.6%	7.2%
	DEUCRA 6 mg twice a day	332			sPGA 0/1 (plus ≥2-point improvement)		<.0001 [S vs PLC] <.0001 [S vs APRE]	58.4%	35.5%	14.2%	53.6%
	AML 30 mg twice a day (uptitration)	168			[S vs PLC]		REF	35.1%	19.6%	3.0%	32.1%
Strober et al, 2023 (POETYK PSO-2) [36]	PLC	255	sPGA ≥ 3, PASI ≥ 12, BSA ≥ 10%, disease duration ≥ 6 mo	Unclear	PASI75	16	REF	9.4%	2.7%	1.2%	8.6%
	DEUCRA 6 mg twice a day	511			sPGA 0/1 (plus ≥2-point improvement)		<.0001 [S vs PLC] <.001 [S vs APRE]	53.0%	27.0%	10.2%	49.8%
	AML 30 mg twice a day (uptitration)	254			[S vs PLC]		REF	39.8%	18.1%	4.3%	29.5%
Atopic dermatitis								EASI75	EASI100	vIGA-AD 0/1	% ΔItch NRS
Blauvelt et al, 2021 (HEADS Up) [37]	DUPI 300 mg every other week	344	EASI ≥ 16; IGA-AD ≥ 3; BSA ≥ 10%; Itch NRS ≥ 4	Unclear	EASI75 [S vs DUPI]	16	REF	61.1%	7.6%		−49.0
	UPA 30 mg every day	348					.006 [S vs DUPI]	71.0%	27.9%		−66.9
Bieber et al, 2021 (JADE COMPARE) [38]	PLC	131	EASI ≥ 16; IGA-AD ≥ 3; BSA ≥ 10%; Itch NRS ≥ 4; age ≥ 18; disease duration ≥ 1 y; TGC/TCNI IR	Unclear	vIGA-AD 0/1 (plus ≥2 grade improvement) EASI75 [S vs PLC]	12	REF	27.1%	1.6%	14.0%	28.9%
	ABRO 100 mg every day	238					<.001 [S]	58.7%	8.1%	36.6%	47.5%
	ABRO 200 mg every day	226					<.001 [S]	70.3%	12.3%	48.4%	63.1%
	DUPI 300 mg every other week	243					<.001 [S]	58.1%	6.6%	36.5%	54.5%
Reich et al, 2022 (JADE DARE) [39]	DUPI 300 mg every other week	365	EASI ≥ 16; IGA-AD ≥ 3; BSA ≥ 10%; Itch NRS ≥ 4; age ≥ 18 y; disease duration ≥ 0.5 y; TGC/TCNI IR	Low	Itch NRS ≥ 4 point improvement EASI90 [S vs DUPI]	2 4	REF		15.0%		26.0%
	ABRO 200 mg every day	362					<.001 [S]		29.0%		48.0%

ABRO, abrocitinib; AML, apremilast; BSA, body surface area; csDMARD, conventional-synthetic disease-modifying antirheumatic drug; DEUCRA, deucravacitinib; DUPI, dupilumab; EASI, eczema area and severity index; IR, insufficient responder; NI; noninferiority; NRS, numeric rating scale; PASI, psoriasis area and severity index; PEP, primary endpoint; PLC, placebo; REF, reference arm; RoB, risk of bias; S, superiority; sPGA, static physician global assessment of disease activity; TCNI, topical calcineurin inhibitor; TGC, topical glucocorticoid; vIGA-AD, validated investigator global assessment of atopic dermatitis.

Outcome criteria are explained in detail in Online Supplemental Material (list of outcomes and definitions).

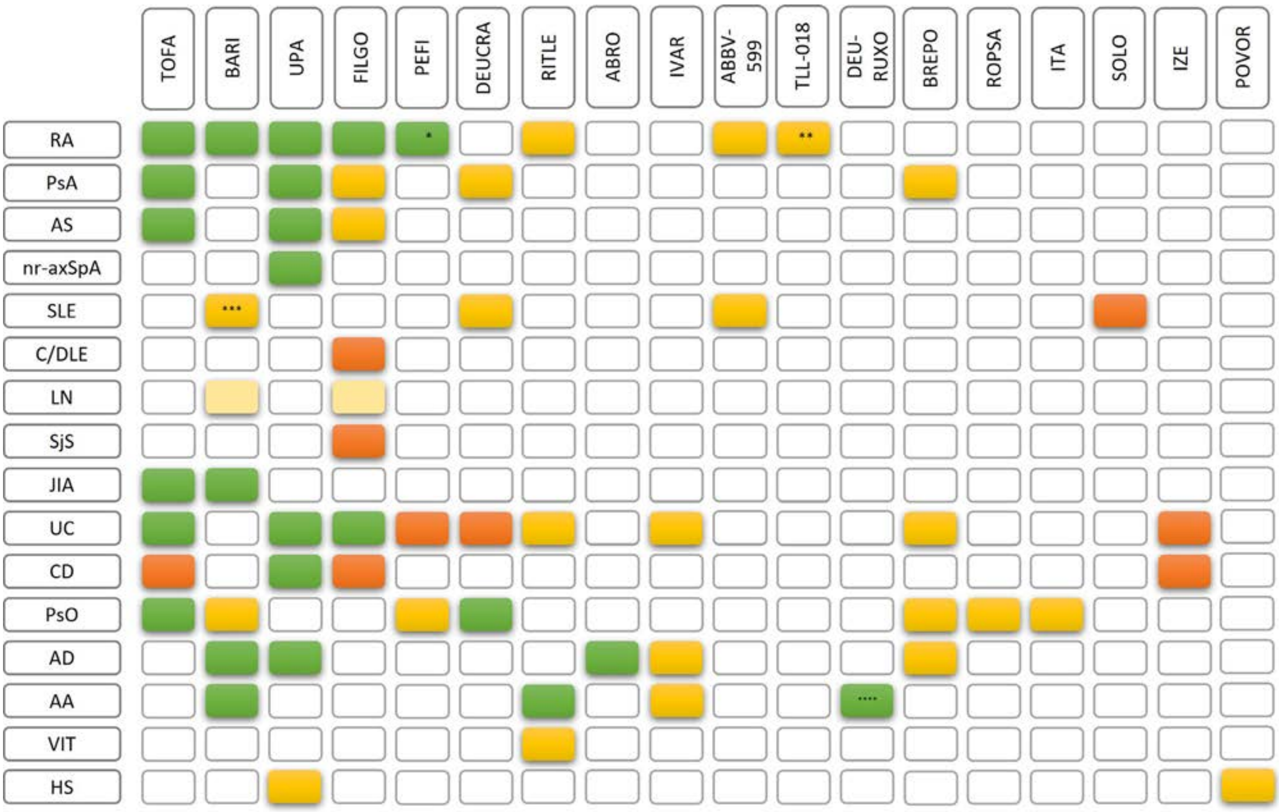

Figure 2. Systemic therapies tested in phase 2 and phase 3 trials. Green indicates that primary endpoint was met in phase 3; yellow indicates that primary endpoint was met in phase 2; red indicates that primary endpoint was not met in phase 2 or phase 3; *phase 3, only Asia; **phase 2a, only China, comparison against tofacitinib; ***phase 3 partially met; ****phase 3 available only as abstract. An overview of topical therapies is provided in the Supplemental Appendix (Section 6.2; Supplemental Table S2). AA, alopecia areata; ABBV-599, elsubrutinib/upadacitinib fixed combination; ABRO, abrocitinib; AD, atopic dermatitis; AS, ankylosing spondylitis; BARI, baricitinib; BREPO, brepocitinib; CD, Crohn disease; C/DLE, cutaneous/discoid lupus erythematosus; DEUCRA, deucravacitinib; DEURUXO, deuruxolitinib; FILGO, filgotinib; HS, hidradenitis suppurativa; ITA, itacitinib; IVAR, ivarmacitinib; IZE, izencitinib; JIA, juvenile idiopathic arthritis; LN, lupus nephritis; nr-axSpA, nonradiographic axial spondyloarthritis; PEFI, peficitinib; POVOR, povorcitinib; PsA, psoriatic arthritis; PsO, psoriasis; RA, rheumatoid arthritis; RITLE, ritlecitinib; ROPSA, ropsacitinib; SjS, Sjögren syndrome; SLE, systemic lupus erythematosus; SOLO, solocitinib; TOFA, tofacitinib; UC, ulcerative colitis; UPA, upadacitinib; VIT, vitiligo.

imaging) endpoints at week 14 were met in all 3 studies (all low RoB) [70−72].

Systemic lupus erythematosus and Sjögren's syndrome

Two phase 2 and 2 phase 3 trials were available for SLE, 1 phase 2 trial and 1 pilot study for CDLE, 2 phase 2 trials for lupus nephritis, as well as 1 phase 2 trial and 1 pilot study for SjS. Five of these RCTs were assessed as low RoB and 1 as unclear; 2 abstracts as well as the pilot studies were not graded for RoB. Five RCTs met their primary endpoints, while 3 did not.

For BARI, phase 2 data had been positive in SLE [73], but this could not be confirmed in the subsequent phase 3 SLE-BRAVE programme. The primary endpoint was met for BARI 4 mg every day in SLE-BRAVE-I, but not in SLE-BRAVE-II, and major secondary endpoints were not met in both trials (both low RoB) [74,75].

Efficacy was demonstrated for selective TYK2 inhibition in a phase 2 study on DEUCRA (low RoB) [76], and positive results were also observed in a phase 2 trial on ABBV-599, an EBT/UPA fixed combination; with effects driven predominantly by the JAKi, not the BTKi (abstract) [77].

Some numeric benefits were observed for FILGO in a phase 2 trial in cutaneous lupus (low RoB) [78], and a pilot study was available for TOFA in discoid lupus [79]. FILGO was also studied in lupus nephropathy [80], and BARI demonstrated superiority over cyclophosphamide (CYP) in lupus nephritis for proteinuria reduction in a recently completed phase 2 trial (abstract) [32]. Symptomatic improvements were further seen in a pilot study on BARI in SjS [81], while a phase 2 trial on FILGO failed to show relevant benefits in this disease (unclear RoB) [82].

Juvenile idiopathic arthritis

Two phase 3 trials assessed efficacy and safety of TOFA and BARI in JIA (both low RoB) [83,84]. TOFA demonstrated efficacy for achievement and maintenance of treatment targets in an 18-week OL run-in and 26-week DB treatment withdrawal study in children and adolescents with polyarticular JIA, extended oligoarthritis, juvenile PsA and enthesitis-associated arthritis [83]. Efficacy was also demonstrated for BARI in this population [84] and trials on BARI in systemic JIA (NCT04088396) and in juvenile arthritis−associated uveitis (NCT04088409) are currently ongoing.

Inflammatory bowel diseases

Ulcerative colitis

Since 2019, 4 phase 2, 6 phase 3, 4 phase 3b/4, and 1 OL strategic trial became available in UC. Eight trials were graded as low RoB, 1 as unclear, 2 as high, and the abstract was not assessed for RoB. The primary endpoint was met in all phase 3 trials and in 2 of the 4 phase 2 trials.

UPA was studied in the phase 3 U-ACHIEVE programme and demonstrated superiority over PLC for induction and maintenance of clinical REM in adults with moderate-to-severe UC (all low RoB) [85,86]. Superiority over PLC for induction and maintenance was further demonstrated for FILGO in the phase 2b/3 SELECTION programme, again in biologics-naïve as well as biologics-experienced adults with moderate-to-severe UC [87].

TYK2 inhibition with DEUCRA failed to demonstrate significant benefits in the LATTICE-UC study (abstract) [88,89], while selective JAK1 inhibition with ivarmacitinib (IVAR) showed superiority over PLC in the phase 2 AMBER2 study (low RoB) [90]. Efficacy was also demonstrated in the phase 2 VIBRATO trial for RITLE and BREPO, again in moderate-to-severe UC (unclear RoB) [91], while a phase 2 study on izencitinib (IZE), a gut-selective pan-JAK inhibitor, did not meet the primary endpoint (abstract) [92].

Dose reduction of TOFA 10 mg twice a day to TOFA 5 mg twice a day in patients with stable clinical REM for at least 6 months was evaluated in a phase 3b/4 maintenance trial. REM through week 24 was sustained in most patients upon dose reduction, with higher success rates achieved in those with deep endoscopic REM or without previous TNFi failure (low RoB) [93]. An OL, parallel-group, pilot study further demonstrated that successful induction of clinical REM could be achieved with both glucocorticoids and TOFA, thereby supporting the use of JAKi for induction of REM in UC [33].

Crohn's disease

Four phase 2 studies and 3 phase 3 studies were considered for CD. Four trials were graded as low RoB, 1 as high, and 2 abstracts were not assessed. Four studies met their primary endpoint, and 3 did not.

The phase 3 programme on UPA confirmed phase 2 results in adults with moderate-to-severe CD, where UPA demonstrated superiority over PLC in 2 12-week induction trials (U-EXCEL and U-EXCEED), as well as in 1 maintenance trial through week 52 (U-ENDURE) (all 3 low RoB) [94].

Two phase 2 trials of FILGO could not confirm positive results of the 2017 FITZROY study [95]. DIVERGENCE 1 assessed FILGO in adults with moderate-to-severe CD (high RoB) [96] and DIVERGENCE 2 in adults with perianal fistulising CD (1-3 external openings with drainage) (abstract) [97,98]. Both trials were underpowered, as DIVERGENCE 1 included an early nonresponder discontinuation at week 10, and DIVERGENCE 2 was preterminated due to recruitment problems [96−98]. Gut-selective pan-JAK inhibition with IZE did not demonstrate superiority over PLC in a recent phase 2 study in moderate-to-severe CD (abstract) [99].

Dermatologic diseases

Chronic plaque psoriasis

Three phase 2 studies and 2 phase 3 studies have become available in psoriasis (PsO) since 2019. One study was graded as low RoB, 2 as unclear, and 2 assessed with some concerns on RoB. Four studies met their primary endpoint, and 1 did not.

DEUCRA was investigated in the phase 3 POETYK-PSO programme, and benefits of selective inhibition of IL12/23 and type 1 interferon (IFN) signalling demonstrated in patients with moderate-to-severe plaque PsO; with superiority of DEUCRA over PLC as well as apremilast shown in both POETYK PSO-1 and POETYK PSO-2 (both unclear RoB) [35,36]. POETYK PSO-2 additionally included a tapering and withdrawal period from study weeks 24 to 52, where psoriasis area and severity index (PASI) 75-responders were re-randomised to PLC or DEUCRA 6 mg every day; 80% of patients sustained PASI75 response in the DEUCRA continuation arm, vs 31.3% in the DEUCRA withdrawal arm (high RoB) [36].

Ropsacitinib (ROPSA), another selective TYK2 inhibitor, was assessed in a phase 2b trial in adults with moderate-to-severe PsO and demonstrated dose-dependent superiority over PLC (some concerns on RoB) [100]. Systemically targeting JAK1 in addition to TYK2 with oral BREPO resulted in a significant decrease in PASI scores through week 12 in a phase 2 trial (some concerns on RoB) [101], whereas topical treatment with BREPO failed to significantly improve signs and symptoms of PsO in a phase 2a study (low RoB) [102].

Atopic dermatitis

Nine systemic and topical JAKi were evaluated in phase 2 and phase 3 trials in atopic dermatitis (AD) over the past years, in a total of 28 studies (7 phase 2, 20 phase 3, and 1 phase 3b/4). Twenty studies were graded as low RoB, 2 with some concerns on RoB, 2 as high RoB, and 4 as unclear. For BARI, UPA, abrocitinib (ABRO), topical ruxolitinib (RUXO), and topical delgocitinib (DELGO) therapy, children and/or adolescents were included in parts of the trial development programme. The primary endpoint was met in all studies, indicating an overall strong therapeutic benefit of JAKi in this highly prevalent disease.

Efficacy was demonstrated for BARI in 1 phase 2 trial [103], as well as in the BREEZE-AD phase 3 programme: BREEZE-AD1, 2, and 5 tested BARI monotherapy in topical glucocorticoid (TGC) IR patients with moderate-to-severe AD, with topical background therapy allowed only as rescue medication (BREEZE-AD1/2 low RoB; BREEZE-AD5 high RoB) [104,105], while BREEZE-AD4 and 7 tested BARI against PLC in a fixed combination with TGC, again in moderate-to-severe AD (both low RoB) [106,107]. BREEZE-AD PEDS then confirmed efficacy and tolerability of BARI in children and adolescents with AD [108], and treatment responders from BREEZE-AD1, 2, and 7 were further enrolled in the DB long-term BREEZE-AD3 extension study [109]. BREEZE-AD3 included a BARI continuation vs dose reduction substudy in 168 treatment responders through weeks 52 to 104, where efficacy could be sustained in the majority of patients upon dose reduction from BARI 4 mg every day to BARI 2 mg every day (unclear RoB) [110].

ABRO was evaluated in a phase 2 trial [111] and in the phase 3 JADE programme, again in adults and adolescents with moderate-to-severe AD and IR to topical therapies. ABRO monotherapy demonstrated efficacy against PLC in a dose-dependent manner in JADE MONO-1 and -2 (both low RoB) [112,113], as well as in combination with TGC in JADE COMPARE and JADE DARE, where it was also tested against dupilumab (DUPI), an IL-4/13−inhibiting monoclonal antibody [JADE COMPARE: unclear RoB; and JADE DARE: low RoB) [38,39]. JADE TEEN further evaluated efficacy and safety of ABRO + TGC in adolescents with AD (low RoB) [114], and JADE REGIMEN showed that blinded tapering to ABRO 100 mg every day or treatment withdrawal after a 12-week induction period resulted in disease flares in 43% and 81%, respectively, compared with 19% in the treatment continuation group (low RoB) [115]. DUPI nonresponders from JADE COMPARE were further enrolled in the OL JADE EXTEND trial [116].

Moreover, UPA was superior to PLC as monotherapy in a phase 2 trial [117] and in the phase 2b/3 Measure Up 1 and 2 trials (both low RoB) [118] as well as in combination with TGC in the phase 3 AD Up (low RoB), and in Rising Up (a safety trial on UPA from Japan) (low RoB) [119,120]. UPA was further superior to DUPI in HEADS Up (unclear RoB) [37] as well as to PLC when tested in adolescents with moderate-to-severe AD included in the Measure Up 1 and 2 and AD Up studies [121].

Positive phase 2 data were also available for IVAR, a selective JAK1 inhibitor (low RoB) [122]. As for topical treatment of AD, significant and early benefits could be observed in phase 2 and phase 3 trials on topical RUXO, a JAK1/JAK2 inhibitor, in TRuE-AD 1 and 2 (validated investigator global assessment of AD [vIGA-AD] 2-3; body surface area [BSA] 3%-20%; age ≥12 years; all low RoB) [123−125], as well as in a phase 2 trial on topical BREPO, a JAK1/TYK2 inhibitor (high RoB) [126] and for topical DELGO, in phase 2 and phase 3 trials on children with AD from Japan (low RoB) [127,128].

Alopecia areata

For alopecia areata (AA), 6 phase 2 studies and 4 phase 3 studies were included. Two studies were graded as low RoB, 3 with some concerns on RoB, 2 as high RoB, 2 as unclear, and 1 abstract was not assessed. Eight studies met their primary endpoint, and 2 studies did not (both on topical therapies).

BARI in 2022 became the first FDA-approved systemic treatment for AA, after showing significant benefits on disease outcomes in patients with moderate-to-severe AA (severity of alopecia tool [SALT, ≥50) in the phase 2 BRAVE-AA1 (unclear RoB) [129] as well as the phase 3 BRAVE-AA1 and 2 trials (some concerns on RoB) [130].

The phase 2a ALLEGRO trial further showed significant improvements in total SALT scores with RITLE, a combined JAK3/TEC inhibitor, and BREPO, a JAK1/TYK2 inhibitor (low RoB) [131]. This was confirmed for RITLE in the phase 3 study of the ALLEGRO programme, where dose-dependent efficacy was shown for both primary and secondary outcomes (low RoB) [132].

Positive phase 2 trials were further performed on deuruxolitinib (DEURUXO), a JAK1/2 inhibitor (unclear RoB), as well as on IVAR, a selective JAK1 inhibitor (some concerns on RoB), where significant benefits were observed in a dose-dependent manner [133,134]. DEURUXO efficacy was recently also confirmed in the THRIVE-AA1 phase 3 trial (presented as abstract) [135].

Despite the encouraging results of topical treatment with RUXO and DELGO in other autoimmune skin conditions, neither RUXO 1.5% cream (JAK1/2 inhibition) nor DELGO 30 mg/g ointment (pan-JAK inhibition) therapy significantly improved SALT scores in 2 DB, vehicle-controlled, phase 2 trials, in patients with moderate-to-severe AA (both high RoB) [136,137].

Vitiligo

For vitiligo, 1 phase 2 and 2 phase 3 studies were available on topical JAKi, as well as 1 phase 2 study on systemic treatment. All studies were graded as low RoB, and all met their primary endpoints.

Significant benefits on stable and progressive vitiligo were observed with RUXO cream in a phase 2 trial [138], as well as the phase 3 TRuE-V1 and TRuE-V2 trials, in adults and adolescents with moderate nonsegmental vitiligo (both low RoB) [139]. Oral JAK inhibition with RITLE further showed dose-dependent benefits in a phase 2 study in adults with active disease (low RoB) [140].

Hidradenitis suppurativa and chronic hand eczema

ADA is to date the only FDA-approved systemic agent for hidradenitis suppurativa (HS), albeit only partially effective [141]. Three phase 2 trials now investigated selective JAK1 inhibitors in adults with mild or moderate-to-severe HS, 2 studied povorcitinib (POVOR) (both low RoB) and 1 studied UPA (abstract). All 3 trials met their primary endpoints [142,143].

For chronic hand eczema (CHE), only TGC and alitretinoin had been available to date. Symptomatic improvements were now observed with topical DELGO [144,145] as well as with systemic, an oral spleen tyrosine kinase (SYK)/pan-JAK inhibitor, in 3 phase 2 studies (all low RoB) [146].

Other diseases

Diabetic kidney disease

One phase 2 RCT assessed efficacy and safety of BARI in type II diabetes−associated chronic kidney disease (CKD). A 41% decrease in first morning urine albumin-creatinine ratio was observed through week 24 with BARI 4 mg every day (P = .022 vs PLC) (some concerns on RoB) [147]. Another phase 2 study on BARI in type I diabetes was published after the data cut of this SLR, warranting further exploration of JAKi in this disease [148].

Other immune-mediated inflammatory conditions

JAKi were also tested in various other hereditary and acquired autoimmune conditions (see further), but no RCTs had been published in these conditions upon the data cut of this SLR. All cohort data and exploratory analyses are summarised below and provided in more detail in the Supplemental Appendix (Section 6.1.2).

We found studies on TOFA in PMR [149,150] on BARI, TOFA, and UPA in giant cell arteritis (GCAs) [151,152], as well as on TOFA in Takayasu arteritis (TAKs) [153,154]. TOFA was also investigated in sarcoidosis [155,156] in antineutrophil cytoplasmic antibody (ANCA)−associated vasculitis [157], in systemic sclerosis (SSc) [158−160], and in SSc-ILD [161]. In dermatomyositis (DM), improvement of cutaneous manifestation was observed with TOFA (as well as BARI and RUXO), while muscular manifestations did not seem comparably affected [162−167]. TOFA was further evaluated in anti-MDA −associated ILD, where it was assessed for induction, maintenance, dose escalation in progressive disease, and compared against TAC in a retrospective analysis [168−174]. Both TOFA and BARI improved cardiac, vascular, and articular manifestations of Behçet disease, while intestinal symptoms responded better to BARI treatment [175−177]. Pilot data and case series were also available for patients with Still disease [178−180] as well as for haemophagocytic lymphohistiocytosis (HLH), especially in autoimmune- and infection-associated, less so in malignancy-associated disease [181−186].

Other diseases investigated were IFN-associated autoinflammatory diseases [187−192], synovitis, acne, pustulosis, hyperostosis, and osteitis (SAPHO) [193−195], and vacuoles, e1-enzyme, x-linked, autoinflammatory, somatic (VEXAS) syndrome [196], primary biliary cholangitis (PBC) [197], as well as noninfectious uveitis and dry-eye disease [198,199], chronic Epstein-Barr virus infection [200], chronic/refractory pouchitis and proctitis [201−203], refractory autoimmune encephalitis [204], hypereosinophilic syndrome [205], lichen planus and sclerosus [206,207], and various other dermatologic conditions [208−211]. Details on these studies are provided in the Supplemental Appendix (Section 6.1.2).

DISCUSSION

This SLR informed an international task force for an update of the expert consensus statement on the treatment of IMIDs with JAKi (P. Nash et al, manuscript in press, Ann Rheum Dis, 2025). Since 2019, various JAKi have been tested across different IMIDs, and a substantial amount of compounds have gained approval by the FDA and EMA, also in conditions where no DMARD therapy had previously been approved, or in patient subgroups where the conduction of large pharmaceutical trials has always been difficult, like children and adolescent [83,84,121].

JAKi in RA and PsO had been studied most extensively in 2019 already, while predominantly phase 2 data had been available for many other IMIDs, like IBD or SLE [9,10]. In these conditions, larger phase 3 trials have often confirmed phase 2 data but also deflated early hopes, like in SLE, where the phase 3 SLE-BRAVE I and II trials failed to meet most major endpoints [74,75].

The recent data further underlined the efficacy of differentially selective JAKi in various IMIDs, with, for example, preferentially JAK1 selective inhibitors demonstrating good overall efficacy outcomes in IBD [85,87,94], and TYK2 selective inhibitors appearing promising in psoriatic conditions or SLE, potentially due to their selective inhibition of IFN and IL12/23 pathways, while endpoints were not met in UC [76,212].

Albeit limited by studies with only low levels of evidence, this SLR could also inform the task force on the use of JAKi in less prevalent and therefore more difficult to study rheumatic conditions like myositis or SSc [158,165], as well as on extra-musculoskeletal manifestations of rheumatic conditions, like skin manifestations of connective tissue diseases or PsA, as well as RA-ILD [56,58,170].

Our study has 2 major limitations: title and abstract screening, RoB analyses, and data extraction were performed by 1 researcher only (VK) but discussed with the methodologist (AK) and the steering group in cases of doubt. Moreover, efficacy data were not meta-analysed due to the heterogeneity of the data across diseases, study types, and patient populations.

The strength of our work lies clearly in the broad synopsis of all available data on JAKi across diseases and patient populations, which allows for a complete overview of all available evidence as well as a detailed investigation of distinct signals found in different immune-mediated conditions, patients subgroups, and study types. A substantial amount of high-level evidence was published on JAKi in recent years, which highlights the relevance of these pharmaceutical compounds for treatment of IMIDs. The potential differences between variably selective JAK-STAT pathway inhibitors in various conditions and patient populations, which were observed in our work, warrant further exploration.

In summary, this SLR provides an extensive overview of currently available efficacy data on JAKi in IMIDs, informing an international task force on the update of the expert consensus statement on the treatment of IMIDs with JAKi (P. Nash et al, manuscript in press, Ann Rheum Dis, 2025). More trials are currently being conducted or planned, and high-level data are especially needed in immune-mediated conditions where no or few effective therapies are available to date.

Competing interests

VK received speaker fees from Eli Lilly and AstraZeneca. JSS received grants from AbbVie, AstraZeneca, Eli Lilly, and Galapagos and speaker or consultancy fees from AbbVie, Amgen, Anada, Astro Pharma, BMS, Celltrion, Chugai, Eli Lilly, Gilead, Immunovant, MSD, Novartis, Pfizer, Roche, R-Pharma, Samsung, Sanofi, and Union Chimique Belge (UCB). PN received grants from AbbVie, BMS, Pfizer, Novartis, Eli Lilly, UCB, and Janssen and speaker or consultancy fees from Eli Lilly, Novartis, AbbVie, Pfizer, BMS, Novartis, Janssen, and UCB. DA received grants from Eli Lilly and Galapagos and speaker or consultancy fees from AbbVie, Gilead, J&J, Eli Lilly, MSD, Novartis, and Sandoz. KW received grants from BMS and Pfizer and speaker or consultancy fees from BMS, Pfizer, AbbVie, UCB, Eli Lilly & Company, Galapagos, GlaxoSmithKline (GSK), Roche, Gilead, Regeneron, Sanofi, AstraZeneca, Novartis, and Moderna. TD received grants from BMS, Eli Lilly, and J&J and speaker or consultancy fees from BMS, Eli Lilly, J&J, Pfizer, Novartis, Roche/GNE, and Remegen. RF received grants from AbbVie, BMS, Galvani, GSK, Gilead, Janssen, Eli Lilly, Novartis, Pfizer, and UCB and consultancy fees from AbbVie, Almirall, Artiva, Biotherapeutics, Atomwise, Biohaven, Pharmaceuticals, BMS, Cyoxone, Deep Cure, Dren Bio, Galvani, Gates Bio, Gilead, GSK, Halia, Immunovant, ImmuneMed, InventisBio, Istesso, Janssen, Janux, Eli Lilly, Monte Rosa, Novartis, Overland, Pfizer, Spyre, Synact, Teijin Pharma, TPG, UCB, Vyne, and Xencor. YT received grants from Mitsubishi Tanabe, Eisai, Chugai, and Taisho and speaker or consultancy fees from Eli Lilly, AstraZeneca, AbbVie, Gilead Sciences, Chugai, Boehringer Ingelheim, GSK, Eisai, Taisho, BMS, and Pfizer. XB received speaker or consultancy fees from AbbVie, Alphasigma, Amgen, BMC, Cesas, Celltrion, Galapagos, Janssen, Eli Lilly, Moonlake, Novartis, Pfizer, Roche, Sandoz, Springer, Stada, Takeda, UCB, and Zuellig. IBM received grants from AbbVie, Amgen, BMS, Causeway Therapeutics, Cabaletta, Dextera, Eli Lilly, Gilead, Janssen, Novartis, Montai, Pfizer, Sanofi Regeneron, UCB, Compugen, AstraZeneca, and Moonlake and speaker or consultancy fees from AbbVie, Amgen, BMS, Causeway Therapeutics, Cabaletta, Dextera, Eli Lilly, Gilead, Janssen, Novartis, Montai, Pfizer, Sanofi Regeneron, UCB Pharma, Compugen, AstraZeneca, and Moonlake. MT received grants from Albireo, Alnylam, Cymabay, Falk Pharma, Genentech, Gilead, Intercept, MSC, Takeda, and UltraGenyx and speaker or consultancy fees from AbbVie, Agomab, Albireo, BiomX, Boehringer Ingelheim, Chemomab, Cymabay, Falk, Gilead, Genit, Hightide, Intercept, Ipsen, Janssen, LoopLab, Mirum, MSD, Novartis, Phenex, Pliant, Rectify, Regulus, Shire, and Siemens. NS received grants from AstraZeneca, Boehringer Ingelheim, Novartis, and Roche Diagnostics and speaker or consultancy fees from Abbott Laboratories, AbbVie, Amgen, AstraZeneca, Boehringer Ingelheim, Eli Lilly, Hanmi Pharmaceuticals, Janssen, Menarini-Ricerche, Novartis, Novo Nordish, Pfizer, Roche Diagnostics, and Sanofi. MdW received speaker fees from Evidera, UCB, Zürich Hospital, and the REMEDI Consortium. AK received speaker or consultancy fees from AbbVie, Eli Lilly, Gilead, Janssen, UCB, Galapagos, MSD, Novartis, and Pfizer. JP and JWS have nothing to declare.

Acknowledgements

The meetings for this work were supported by unrestricted grants from AbbVie, Galapagos, and Eli Lilly to the Medical University of Vienna. No representative of any of the companies was present at any of the meetings (neither in meetings for the initial nor in the course of the work for the updated consensus statements), and they had no influence on the wording of the recommendations. The support of Martina Seidel from the Vienna Medical Academy regarding the logistics of organising the meetings is also gratefully acknowledged.

Contributors

All authors contributed and finally approved the current manuscript. VK is the guarantor of the study. The guarantor accepts full responsibility for the finished work and the conduct of the study, had access to the data, and controlled the decision to publish the manuscript together with the methodologist (AK) and the convenor of the taskforce (JSS).

Funding

The meetings for this work were supported by unrestricted grants from AbbVie, Galapagos, and Eli Lilly to the Medical University of Vienna. No representative of any of the companies was present at any of the meetings (neither in meetings for the initial nor in the course of the work for the updated consensus statements), and they had no influence on the wording of the recommendations.

Patient consent for publication

Owing to the nature of the analyses, this is not applicable for the current work. All patients gave informed consent to participation in the studies included and publication of study results.

Ethics approval

Owing to the nature of the analyses performed in this study, this is not applicable for the current project. All studies included in this work were approved by respective ethics committees.

Provenance and peer review

This manuscript was not commissioned and independently submitted to the journal by the authors. It underwent external peer review and editorial review.

Data availability statement

Not applicable because no datasets were generated for this study. All data relevant to the study are available in public, and are included in the article or uploaded as online supplemental information.

Patient and public involvement

Patients and/or the public were not involved in the design, or conduct, or reporting, or dissemination plans of this research. Details are provided in the methods section.

Supplementary materials

Supplementary material associated with this article can be found in the online version at doi:10.1016/j.ard.2025.01.023.

REFERENCES

[1] Bonelli M, Kerschbaumer A, Kastrati K, Ghoreschi K, Gadina M, Heinz LX, et al. Selectivity, efficacy and safety of JAKinibs: new evidence for a still evolving story. Ann Rheum Dis 2024;83(2):139–60.

[2] Benucci M, Bernardini P, Coccia C, De Luca R, Levani J, Economou A, et al. JAK inhibitors and autoimmune rheumatic diseases. Autoimmun Rev 2023 Apr;22(4):103276.

[3] Tanaka Y, Luo Y, O'Shea JJ, Nakayamada S. Janus kinase-targeting therapies in rheumatology: a mechanisms-based approach. Nat Rev Rheumatol 2022 Mar;18(3):133–45.

[4] Coskun M, Salem M, Pedersen J, Nielsen OH. Involvement of JAK/STAT signaling in the pathogenesis of inflammatory bowel disease. Pharmacol Res 2013 Oct;76:1–8.

[5] Vincenti F, Tedesco Silva H, Busque S, O'Connell P, Friedewald J, Cibrik D, et al. Randomized phase 2b trial of tofacitinib (CP-690,550) in de novo kidney transplant patients: efficacy, renal function and safety at 1 year. Am J Transplant 2012 Sep;12(9):2446–56.

[6] Winthrop KL. The emerging safety profile of JAK inhibitors in rheumatic disease. Nat Rev Rheumatol 2017 Apr;13(4):234–43.

[7] McLornan DP, Pope JE, Gotlib J, Harrison CN. Current and future status of JAK inhibitors. Lancet 2021 Aug 28;398(10302):803–16.

[8] Russell MD, Stovin C, Alveyn E, Adeyemi O, Chan CKD, Patel V, et al. JAK inhibitors and the risk of malignancy: a meta-analysis across disease indications. Ann Rheum Dis 2023 Aug;82(8):1059–67.

[9] Nash P, Kerschbaumer A, Dörner T, Dougados M, Fleischmann RM, Geissler K, et al. Points to consider for the treatment of immune-mediated inflammatory diseases with Janus kinase inhibitors: a consensus statement. Ann Rheum Dis 2021 Jan;80(1):71–87.

[10] Kerschbaumer A, Smolen JS, Nash P, Doerner T, Dougados M, Fleischmann R, et al. Points to consider for the treatment of immune-mediated inflammatory diseases with Janus kinase inhibitors: a systematic literature research. RMD Open 2020 Nov;6(3):e001374.

[11] Ytterberg SR, Bhatt DL, Mikuls TR, Koch GG, Fleischmann R, Rivas JL, et al. Cardiovascular and cancer risk with tofacitinib in rheumatoid arthritis. N Engl J Med 2022 Jan;386(4):316–26.

[12] US Federal Drug Administration. FDA requires warnings about increased risk of serious heart-related events, cancer, blood clots, and death for JAK inhibitors that treat certain chronic inflammatory conditions [Internet]; 2021 [cited 08-02-2024]. Available from: https://www.fda.gov/drugs/fda-drug-safety-podcasts/fda-requires-warnings-about-increased-risk-serious-heart-related-events-cancer-blood-clots-and-death.

[13] European Medical Agancy. Xeljanz (tofacitinib) summary of product characteristics [Internet]; 2021 [cited 08-02-2024]. Available from: https://www.ema.europa.eu/en/medicines/human/EPAR/xeljanz.

[14] US Federal Drug Administration. Xeljanz (tofacitinib) highlights of prescribing information [Internet]; 2021 [cited cited 08-02-2024]. Available from: https://www.accessdata.fda.gov/drugsatfda_docs/label/2021/203214s028,208246s013,213082s003lbl.pdf.

[15] US Federal Drug Administration. FDA requires warnings about increased risk of serious heart-related events, cancer, blood clots, and death for JAK inhibitors that treat certain chronic inflammatory conditions [Internet]; 2021 [cited cited 08-02-2024]. Available from: https://www.fda.gov/drugs/drug-safety-and-availability/fda-requires-warnings-about-increased-risk-serious-heart-related-events-cancer-blood-clots-and-death.

[16] Winthrop KL, Cohen SB. Oral surveillance and JAK inhibitor safety: the theory of relativity. Nat Rev Rheumatol 2022 May;18(5):301–4.

[17] Atzeni F, Popa CD, Nucera V, Nurmohamed MT. Safety of JAK inhibitors: focus on cardiovascular and thromboembolic events. Expert Rev Clin Immunol 2022 Mar;18(3):233–44.

[18] Smolen JS, Landewé RBM, Bergstra SA, Kerschbaumer A, Sepriano A, Aletaha D, et al. EULAR recommendations for the management of rheumatoid arthritis with synthetic and biological disease-modifying antirheumatic drugs: 2022 update. Ann Rheum Dis 2023 Jan;82(1):3–18.

[19] Kragstrup TW, Glintborg B, Svensson AL, McMaster C, Robinson PC, Deleuran B, et al. Waiting for JAK inhibitor safety data. RMD Open 2022 Feb;8(1):e002236.

[20] van der Heijde D, Aletaha D, Carmona L, Edwards CJ, Kvien TK, Kouloumas M, et al. 2014 Update of the EULAR standardised operating procedures for EULAR-endorsed recommendations. Ann Rheum Dis 2015 Jan;74(1):8–13.

[21] Page MJ, McKenzie JE, Bossuyt PM, Boutron I, Hoffmann TC, Mulrow CD, et al. The PRISMA 2020 statement: an updated guideline for reporting systematic reviews. Rev Esp Cardiol (Engl Ed) 2021 Sep;74(9):790–9.

[22] Higgins JP, Thomas J, Chandler J, Cumpston M, Li T, Page MJ, et al. Cochrane handbook for systematic reviews of interventions. 2nd ed. Chichester (UK): John Wiley & Sons; 2019.

[23] European Alliance of Associations for Rheumatology. Project Grant Application [Internet]; 2024 [cited 2024 Aug 18]. Available from: https://www.eular.org/recommendations/points-to-consider-task-forces-project-applications.

[24] European Alliance of Associations for Rheumatology. Standard operating procedures for task forces [Internet]; 2024 [cited 2024 Sep 19]. Available from: https://www.eular.org/web/static/lib/pdfjs/web/viewer.html?file=https://www.eular.org/document/download/680/b9eb08d0-faca-4606-8ed9-d0539b3f312a/660.

[25] Sackett D, Richardson W, Rosenberg W, Haynes MD. Evidence-based medicine: how to practice and teach EBM. London (UK): Churchill Livingstone; 2005.
[26] Higgins JPT, Altman DG, Gøtzsche PC, Jüni P, Moher D, Oxman AD, et al. The Cochrane Collaboration's tool for assessing risk of bias in randomised trials. BMJ 2011 Oct;343:d5928.
[27] Hayden JA, Côté P, Bombardier C. Evaluation of the quality of prognosis studies in systematic reviews. Ann Intern Med 2006 Mar;144(6):427–37.
[28] Rubbert-Roth A, Enejosa J, Pangan AL, Haraoui B, Rischmueller M, Khan N, et al. Trial of upadacitinib or abatacept in rheumatoid arthritis. N Engl J Med 2020 Oct;383(16):1511–21.
[29] Combe B, Kivitz A, Tanaka Y, van der Heijde D, Simon JA, Baraf HSB, et al. Filgotinib versus placebo or adalimumab in patients with rheumatoid arthritis and inadequate response to methotrexate: a phase III randomised clinical trial. Ann Rheum Dis 2021 Jul;80(7):848–58.
[30] Fleischmann RM, van der Heijde D, Strand V, Atsumi T, McInnes IB, Takeuchi T, et al. Anti-GM-CSF otilimab versus tofacitinib or placebo in patients with active rheumatoid arthritis and an inadequate response to conventional or biologic DMARDs: two phase 3 randomised trials (contRAst 1 and contRAst 2). Ann Rheum Dis 2023 Dec;82(12):1516–26.
[31] McInnes IB, Anderson JK, Magrey M, Merola JF, Liu Y, Kishimoto M, et al. Trial of upadacitinib and adalimumab for psoriatic arthritis. N Engl J Med 2021 Apr;384(13):1227–39.
[32] Hassanien M, Moshrif A, Hetta H. OP0053 efficacy and safety of baricitinib in patients with active lupus nephritis: a double-blind, randomized, placebo-controlled phase 3 trial. Ann Rheum Dis 2023;82(Suppl 1):34–5.
[33] Singh A, Midha V, Kaur K, Mahajan R, Singh D, Kaur R, et al. Tofacitinib versus oral prednisolone for induction of remission in moderately active ulcerative colitis [ORCHID]: a prospective, open-label, randomized, pilot study. J Crohns Colitis 2023 Feb;18(2):300–7.
[34] Felson DT, Anderson JJ, Boers M, Bombardier C, Furst D, Goldsmith C, et al. American College of Rheumatology. Preliminary definition of improvement in rheumatoid arthritis. Arthritis Rheum 1995 Jun;38(6):727–35.
[35] Armstrong AW, Gooderham M, Warren RB, Papp KA, Strober B, Thaçi D, et al. Deucravacitinib versus placebo and apremilast in moderate to severe plaque psoriasis: efficacy and safety results from the 52-week, randomized, double-blinded, placebo-controlled phase 3 POETYK PSO-1 trial. J Am Acad Dermatol 2023 Jan;88(1):29–39.
[36] Strober B, Thaçi D, Sofen H, Kircik L, Gordon KB, Foley P, et al. Deucravacitinib versus placebo and apremilast in moderate to severe plaque psoriasis: efficacy and safety results from the 52-week, randomized, double-blinded, phase 3 program for evaluation of TYK2 inhibitor psoriasis second trial. J Am Acad Dermatol 2023 Jan;88(1):40–51.
[37] Blauvelt A, Teixeira HD, Simpson EL, Costanzo A, De Bruin-Weller M, Barbarot S, et al. Efficacy and safety of upadacitinib vs dupilumab in adults with moderate-to-severe atopic dermatitis: a randomized clinical trial. JAMA Dermatol 2021 Sep;157(9):1047–55.
[38] Bieber T, Simpson EL, Silverberg JI, Thaçi D, Paul C, Pink AE, et al. Abrocitinib versus placebo or dupilumab for atopic dermatitis. N Engl J Med 2021 Mar;384(12):1101–12.
[39] Reich K, Thyssen JP, Blauvelt A, Eyerich K, Soong W, Rice ZP, et al. Efficacy and safety of abrocitinib versus dupilumab in adults with moderate-to-severe atopic dermatitis: a randomised, double-blind, multicentre phase 3 trial. Lancet 2022 Jul;400(10348):273–82.
[40] van Vollenhoven R, Takeuchi T, Pangan AL, Friedman A, Mohamed MF, Chen S, et al. Efficacy and Safety of Upadacitinib Monotherapy in Methotrexate-Naive Patients With Moderately-to-Severely Active Rheumatoid Arthritis (SELECT-EARLY): a multicenter, multi-country, randomized, double-blind, active comparator-controlled trial. Arthritis Rheumatol 2020 Oct;72(10):1607–20.
[41] Felson D, Smolen JS. Trial of upadacitinib or abatacept in rheumatoid arthritis. N Engl J Med 2021 Jan;384(1):83.
[42] Zeng X, Zhao D, Radominski SC, Keiserman M, Lee CK, Meerwein S, et al. Upadacitinib in patients from China, Brazil, and South Korea with rheumatoid arthritis and an inadequate response to conventional therapy. Int J Rheum Dis 2021;24(12):1530–9.
[43] Fleischmann R, Friedman A, Drescher E, Singhal A, Cortes-Maisonet G, Doan T, et al. Safety and efficacy of elsubrutinib or upadacitinib alone or in combination (ABBV-599) in patients with rheumatoid arthritis and inadequate response or intolerance to biological therapies: a multicentre, double-blind, randomised, controlled, phase 2 trial. Lancet Rheumatol 2022;4(6):e395–406.
[44] Li Z, Hu J, Bao C, Li X, Li X, Xu J, et al. Baricitinib in patients with rheumatoid arthritis with inadequate response to methotrexate: results from a phase 3 study. Clin Exp Rheumatol 2020 Jul-Aug;38(4):732–41.
[45] Genovese MC, Kalunian K, Gottenberg JE, Mozaffarian N, Bartok B, Matzkies F, et al. Effect of filgotinib vs placebo on clinical response in patients with moderate to severe rheumatoid arthritis refractory to disease-modifying antirheumatic drug therapy: the FINCH 2 randomized clinical trial. JAMA 2019 Jul;322(4):315–25.
[46] Westhovens R, Rigby WFC, van der Heijde D, Ching DWT, Stohl W, Kay J, et al. Filgotinib in combination with methotrexate or as monotherapy versus methotrexate monotherapy in patients with active rheumatoid arthritis and limited or no prior exposure to methotrexate: the phase 3, randomised controlled FINCH 3 trial. Ann Rheum Dis 2021;80(6):727–38.
[47] Yang Y, Li J, Liu J, Liu L, Wang Y, Hu J, et al. Safety and efficacy of peficitinib in Asian patients with rheumatoid arthritis who had an inadequate response or intolerance to methotrexate: results of a multicenter, randomized, double-blind, placebo-controlled phase 3 study. Lancet Reg Health West Pac 2023 Oct;42:100925.
[48] Robinson MF, Damjanov N, Stamenkovic B, Radunovic G, Kivitz A, Cox L, et al. Efficacy and safety of PF-06651600 (ritlecitinib), a novel JAK3/TEC inhibitor, in patients with moderate-to-severe rheumatoid arthritis and an inadequate response to methotrexate. Arthritis Rheumatol 2020 Oct;72(10):1621–31.
[49] Zeng X, Wu C, Hu J, Liu S, Jiang Z, Li J, et al. LB0001 head-to-head comparison of TLL-018 and tofacitinib in patients with active rheumatoid arthritis: interim results from a phase IIa study. Ann Rheum Dis 2023;82(Suppl 1):200.
[50] Cohen SB, Pope J, Haraoui B, Irazoque-Palazuelos F, Korkosz M, Diehl A, et al. Methotrexate withdrawal in patients with rheumatoid arthritis who achieve low disease activity with tofacitinib modified-release 11 mg once daily plus methotrexate (ORAL Shift): a randomised, phase 3b/4, non-inferiority trial. Lancet Rheumatol 2019;1(1):e23–34.
[51] Cohen SB, Pope J, Haraoui B, Mysler E, Diehl A, Lukic T, et al. Efficacy and safety of tofacitinib modified-release 11 mg once daily plus methotrexate in adult patients with rheumatoid arthritis: 24-week open-label phase results from a phase 3b/4 methotrexate withdrawal non-inferiority study (ORAL Shift). RMD Open 2021;7(2):e001673.
[52] Zhao J, Wang Y, Zhang Z. AB0493 the efficacy and safety of tofacitinib in the treatment of dmards naive rheumatoid arthritis patients (Eastern study). Ann Rheum Dis 2023;82(Suppl 1):1441.
[53] Khan MM, Ahmed S, Hasan Sajib MK, Morshed AA, Mahbub-Uz-Zaman K, Haq SA. Tofacitinib versus methotrexate as the first-line disease-modifying antirheumatic drugs in the treatment of rheumatoid arthritis: an open-label randomized controlled trial. Int J Rheum Dis 2023 Sep;26(9):1729–36.
[54] Kubo S, Miyazaki Y, Amano K, Matsui K, Kameda H, Inoue Y, et al. Sustained remission following the discontinuation of tofacitinib in patients with rheumatoid arthritis (XANADU study): an open-label randomised study. RMD Open 2023 Apr;9(2):e003029.
[55] Wang M, Xue Y, Du F, Ma L, Lu LJ, Jiang L, et al. Continuation, reduction, or withdrawal of tofacitinib in patients with rheumatoid arthritis achieving sustained disease control: a multicenter, open-label, randomized controlled trial. Chin Med J (Engl) 2023 Feb;136(3):331–40.
[56] Baker MC, Liu Y, Lu R, Lin J, Melehani J, Robinson WH. Incidence of interstitial lung disease in patients with rheumatoid arthritis treated with biologic and targeted synthetic disease-modifying antirheumatic drugs. JAMA Netw Open 2023 Mar;6(3):e233640.
[57] Citera G, Mysler E, Madariaga H, Cardiel MH, Castañeda O, Fischer A, et al. Incidence rates of interstitial lung disease events in tofacitinib-treated rheumatoid arthritis patients: post hoc analysis from 21 clinical trials. J Clin Rheumatol 2021 Dec;27(8):e482–90.
[58] Salvarani C, Sebastiani M, Dieude P, Garcia M, Deberdt W, Rogai V, et al. Baricitinib and the risk of incident interstitial lung disease: a descriptive clinical case report from clinical trials. Rheumatol Ther 2021 Sep;8(3):1435–41.
[59] Kalyoncu U, Bilgin E, Erden A, Satış H, Tufan A, Tekgöz E, et al. Efficacy and safety of tofacitinib in rheumatoid arthritis-associated interstitial lung disease: TReasure real-life data. Clin Exp Rheumatol 2022 Nov;40(11):2071–7.
[60] Venerito V, Stefanizzi P, Cantarini L, Lavista M, Galeone MG, Di Lorenzo A, et al. Immunogenicity and safety of adjuvanted recombinant zoster vaccine in rheumatoid arthritis patients on anti-cellular biologic agents or JAK inhibitors: a prospective observational study. Int J Mol Sci 2023 Apr;24(8):6967.
[61] Lee SK, Shin K, Jung JY, Suh CH, Kim JW, Kim HA. Retention rate and safety of biologic and targeted synthetic DMARDs in patients with RA-associated interstitial lung disease: a KOBIO registry study. BioDrugs 2023 Mar;37(2):247–57.
[62] Cronin O, McKnight O, Keir L, Ralston SH, Hirani N, Harris H. A retrospective comparison of respiratory events with JAK inhibitors or rituximab for rheumatoid arthritis in patients with pulmonary disease. Rheumatol Int 2021 May;41(5):921–8.
[63] Mochizuki T, Yano K, Ikari K, Okazaki K. Radiological evaluation of interstitial lung disease in patients with rheumatoid arthritis treated with abatacept or JAK inhibitors for 1 year. Respir Investig 2023 May;61(3):359–63.

[64] Tardella M, Di Carlo M, Carotti M, Ceccarelli L, Giovagnoni A, Salaffi F. A retrospective study of the efficacy of JAK inhibitors or abatacept on rheumatoid arthritis-interstitial lung disease. Inflammopharmacology 2022 Jun;30 (3):705–12.

[65] Mease PJ, Lertratanakul A, Anderson JK, Papp K, Van den Bosch F, Tsuji S, et al. Upadacitinib for psoriatic arthritis refractory to biologics: SELECT-PsA 2. Ann Rheum Dis 2021 Mar;80(3):312–20.

[66] Mease PJ, Deodhar AA, van der Heijde D, Behrens F, Kivitz AJ, Neal J, et al. Efficacy and safety of selective TYK2 inhibitor, deucravacitinib, in a phase II trial in psoriatic arthritis. Ann Rheum Dis 2022 Jun;81(6):815–22.

[67] Mease P, Helliwell P, Silwinska-Stanczyk P, Miakisz M, Ostor A, Peeva E, et al. Efficacy and safety of the TYK2/JAK1 inhibitor brepocitinib for active psoriatic arthritis: a phase IIb randomized controlled trial. Arthritis Rheumatol 2023 May;75(8):1370–80.

[68] Leng X, Lin W, Liu S, Kanik K, Wang C, Wan W, et al. Efficacy and safety of tofacitinib in Chinese patients with active psoriatic arthritis: a phase 3, randomised, double-blind, placebo-controlled study. RMD Open 2023 Jan;9 (1):e002559.

[69] Deodhar A, Sliwinska-Stanczyk P, Xu H, Baraliakos X, Gensler LS, Fleishaker D, et al. Tofacitinib for the treatment of ankylosing spondylitis: a phase III, randomised, double-blind, placebo-controlled study. Ann Rheum Dis 2021 Aug;80(8):1004–13.

[70] van der Heijde D, Song IH, Pangan AL, Deodhar A, van den Bosch F, Maksymowych WP, et al. Efficacy and safety of upadacitinib in patients with active ankylosing spondylitis (SELECT-AXIS 1): a multicentre, randomised, double-blind, placebo-controlled, phase 2/3 trial. Lancet 2019 Dec;394 (10214):2108–17.

[71] van der Heijde D, Baraliakos X, Sieper J, Deodhar A, Inman RD, Kameda H, et al. Efficacy and safety of upadacitinib for active ankylosing spondylitis refractory to biological therapy: a double-blind, randomised, placebo-controlled phase 3 trial. Ann Rheum Dis 2022 Nov;81(11):1515–23.

[72] Deodhar A, Van den Bosch F, Poddubnyy D, Maksymowych WP, van der Heijde D, Kim TH, et al. Upadacitinib for the treatment of active non-radiographic axial spondyloarthritis (SELECT-AXIS 2): a randomised, double-blind, placebo-controlled, phase 3 trial. Lancet 2022 Jul;400(10349):369–79.

[73] Wallace DJ, Furie RA, Tanaka Y, Kalunian KC, Mosca M, Petri MA, et al. Baricitinib for systemic lupus erythematosus: a double-blind, randomised, placebo-controlled, phase 2 trial. Lancet 2018 Jul;392(10143):222–31.

[74] Petri M, Bruce IN, Dörner T, Tanaka Y, Morand EF, Kalunian KC, et al. Baricitinib for systemic lupus erythematosus: a double-blind, randomised, placebo-controlled, phase 3 trial (SLE-BRAVE-II). Lancet 2023 Mar;401 (10381):1011–9.

[75] Morand EF, Vital EM, Petri M, van Vollenhoven R, Wallace DJ, Mosca M, et al. Baricitinib for systemic lupus erythematosus: a double-blind, randomised, placebo-controlled, phase 3 trial (SLE-BRAVE-I). Lancet 2023 Mar;401(10381):1001–10.

[76] Morand E, Pike M, Merrill JT, van Vollenhoven R, Werth VP, Hobar C, et al. Deucravacitinib, a tyrosine kinase 2 inhibitor, in systemic lupus erythematosus: a phase II, randomized, double-blind, placebo-controlled trial. Arthritis Rheumatol 2023 Feb;75(2):242–52.

[77] Merrill JT, Tanaka Y, D'cruz D, Vila K, Siri D, Zeng X, et al. OP0139 efficacy and safety of ABBV-599 high dose (elsubrutinib 60 mg and upadacitinib 30 mg) and upadacitinib monotherapy for the treatment of systemic lupus erythematosus: a phase 2, double-blind, placebo-controlled trial. Ann Rheum Dis 2023;82(Suppl 1):91–2.

[78] Werth VP, Fleischmann R, Robern M, Touma Z, Tiamiyu I, Gurtovaya O, et al. Filgotinib or lanraplenib in moderate to severe cutaneous lupus erythematosus: a phase 2, randomized, double-blind, placebo-controlled study. Rheumatology (Oxford) 2022 May;61(6):2413–23.

[79] Alsukait S, Learned C, Rosmarin D. Open-label phase 2 pilot study of oral tofacitinib in adult subjects with discoid lupus erythematosus (DLE). J Drugs Dermatol 2023 Apr;22(4):425–7.

[80] Baker M, Chaichian Y, Genovese M, Derebail V, Rao P, Chatham W, et al. Phase II, randomised, double-blind, multicentre study evaluating the safety and efficacy of filgotinib and lanraplenib in patients with lupus membranous nephropathy. RMD Open 2020 Dec;6(3):e001490.

[81] Bai W, Liu H, Dou L, Yang Y, Leng X, Li M, et al. Pilot study of baricitinib for active Sjogren's syndrome. Ann Rheum Dis 2022 Jul;81(7):1050–2.

[82] Price E, Bombardieri M, Kivitz A, Matzkies F, Gurtovaya O, Pechonkina A, et al. Safety and efficacy of filgotinib, lanraplenib and tirabrutinib in Sjogren's syndrome: a randomized, phase 2, double-blind, placebo-controlled study. Rheumatology (Oxford) 2022 Nov;61(12):4797–808.

[83] Ruperto N, Brunner HI, Synoverska O, Ting TV, Mendoza CA, Spindler A, et al. Tofacitinib in juvenile idiopathic arthritis: a double-blind, placebo-controlled, withdrawal phase 3 randomised trial. Lancet 2021 Nov;398 (10315):1984–96.

[84] Ramanan AV, Quartier P, Okamoto N, Foeldvari I, Spindler A, Fingerhutová Š, et al. Baricitinib in juvenile idiopathic arthritis: an international, phase 3, randomised, double-blind, placebo-controlled, withdrawal, efficacy, and safety trial. Lancet 2023 Aug;402(10401):555–70.

[85] Danese S, Vermeire S, Zhou W, Pangan AL, Siffledeen J, Greenbloom S, et al. Upadacitinib as induction and maintenance therapy for moderately to severely active ulcerative colitis: results from three phase 3, multicentre, double-blind, randomised trials. Lancet 2022 Jun;399 (10341):2113–28.

[86] Vermeire S, Danese S, Zhou W, Ilo D, Klaff J, Levy G, et al. Efficacy and safety of upadacitinib maintenance therapy for moderately to severely active ulcerative colitis in patients responding to 8 week induction therapy (U-ACHIEVE Maintenance): overall results from the randomised, placebo-controlled, double-blind, phase 3 maintenance study. Lancet Gastroenterol Hepatol 2023 Nov;8(11):976–89.

[87] Feagan BG, Danese S, Loftus Jr. EV, Vermeire S, Schreiber S, Ritter T, et al. Filgotinib as induction and maintenance therapy for ulcerative colitis (SELECTION): a phase 2b/3 double-blind, randomised, placebo-controlled trial. Lancet 2021 Jun;397(10292):2372–84.

[88] Danese S, Panaccione R, D'Haens G, Peyrin-Biroulet L, Schreiber S, Kobayashi T, et al. DOP42 Efficacy and safety of deucravacitinib, an oral, selective tyrosine kinase 2 inhibitor, in patients with moderately-to-severely active ulcerative colitis: 12-week results from the Phase 2 LATTICE-UC study. J Crohns Colitis 2022;16(Suppl 1):i091–2.

[89] Danese S, Panaccione R, D'Haens G, Pyrin-Biroulet L, Schreiber S, Kobayashi T, et al. Efficacy and safety of deucravacitinib, an oral, selective tyrosine kinase 2 inhibitor, in patients with moderately to severely active ulcerative colitis: 12-week results from the phase 2 LATTICE-UC study. Gastroenterol Hepatol (N Y) 2022 Jul;18(7)(Suppl 2):6.

[90] Chen B, Zhong J, Li X, Pan F, Ding Y, Zhang Y, et al. Efficacy and safety of ivarmacitinib in patients with moderate-to-severe, active, ulcerative colitis: a phase II study. Gastroenterology 2022 Dec;163(6):1555–68.

[91] Sandborn WJ, Danese S, Leszczyszyn J, Romatowski J, Altintas E, Peeva E, et al. Oral ritlecitinib and brepocitinib for moderate-to-severe ulcerative colitis: results from a randomized, phase 2b study. Clin Gastroenterol Hepatol 2023 Sep;21(10) 2616-28.e7.

[92] Tirumalaraju D. Theravance's izencitinib fails in phase IIb ulcerative colitis trial [Internet]; [cited 09-06-2023]. Available from: https://www.clinicaltrialsarena.com/news/theravance-izencitinib-ulcerative-colitis/

[93] Vermeire S, Su C, Lawendy N, Kobayashi T, Sandborn WJ, Rubin DT, et al. Outcomes of tofacitinib dose reduction in patients with ulcerative colitis in stable remission from the randomised RIVETING trial. J Crohns Colitis 2021 Jul;15(7):1130–41.

[94] Loftus Jr EV, Panés J, Lacerda AP, Peyrin-Biroulet L, D'Haens G, Panaccione R, et al. Upadacitinib induction and maintenance therapy for Crohn's disease. N Engl J Med 2023 May;388(21):1966–80.

[95] Vermeire S, Schreiber S, Petryka R, Kuehbacher T, Hebuterne X, Roblin X, et al. Clinical remission in patients with moderate-to-severe Crohn's disease treated with filgotinib (the FITZROY study): results from a phase 2, double-blind, randomized, placebo-controlled trial. Lancet 2017 Jan;389 (10066):266–75.

[96] D'Haens GR, Lee S, Taylor SA, Serone A, Rimola J, Colombel JF, DIVERGENCE 1 Study Group. Filgotinib for the treatment of small bowel Crohn's disease: the DIVERGENCE 1 trial. Gastroenterology 2023 Jul;165(1) 289-92.e3.

[97] Reinisch W, Colombel JF, D'Haens GR, Rimola J, DeHaas-Amatsaleh A, McKevitt M, et al. Efficacy and safety of filgotinib for the treatment of perianal fistulizing Crohn's disease: results from the phase 2 DIVERGENCE 2 study. J Crohns Colitis 2022 Jan;16:I019–21.

[98] Morison B, Reinisch W, Colombel J-F, D'Haens G, Rimola J, DeHaas-Amatsaleh A, et al. P48 filgotinib for perianal fistulizing Crohn's disease: the phase 2 DIVERGENCE 2 study. Gut 2022;71(Suppl 1):A62–3.

[99] Schreiber S, Reinisch W, Nguyen D, Guerin T, Kierkus J, Rozpondek P, et al. P375 Izencitinib induction treatment in patients with moderately-to-severely-active Crohn's disease: a phase 2 double-blind, randomized, placebo-controlled study. J Crohns Colitis 2023;17(Suppl 1):i505–7.

[100] Tehlirian C, Singh RSP, Pradhan V, Roberts ES, Tarabar S, Peeva E, et al. Oral tyrosine kinase 2 inhibitor PF-06826647 demonstrates efficacy and an acceptable safety profile in participants with moderate-to-severe plaque psoriasis in a phase 2b, randomized, double-blind, placebo-controlled study. J Am Acad Dermatol 2022 Aug;87(2):333–42.

[101] Forman SB, Pariser DM, Poulin Y, Vincent MS, Gilbert SA, Kieras EM, et al. TYK2/JAK1 inhibitor PF-06700841 in patients with plaque psoriasis: phase IIa, randomized, double-blind, placebo-controlled trial. J Invest Dermatol 2020 Dec;140(12) 2359-70.e5.

[102] Landis MN, Smith SR, Berstein G, Fetterly G, Ghosh P, Feng G, et al. Efficacy and safety of topical brepocitinib cream for mild-to-moderate chronic

plaque psoriasis: a phase IIb randomized double-blind vehicle-controlled parallel-group study. Br J Dermatol 2023 Jul;189(1):33–41.
[103] Guttman-Yassky E, Silverberg JI, Nemoto O, Forman SB, Wilke A, Prescilla R, et al. Baricitinib in adult patients with moderate-to-severe atopic dermatitis: a phase 2 parallel, double-blinded, randomized placebo-controlled multiple-dose study. J Am Acad Dermatol 2019 Apr;80(4) 913-21.e9.
[104] Simpson EL, Lacour JP, Spelman L, Galimberti R, Eichenfield LF, Bissonnette R, et al. Baricitinib in patients with moderate-to-severe atopic dermatitis and inadequate response to topical corticosteroids: results from two randomized monotherapy phase III trials. Br J Dermatol 2020 Aug;183 (2):242–55.
[105] Simpson EL, Forman S, Silverberg JI, Zirwas M, Maverakis E, Han G, et al. Baricitinib in patients with moderate-to-severe atopic dermatitis: results from a randomized monotherapy phase 3 trial in the United States and Canada (BREEZE-AD5). J Am Acad Dermatol 2021 Jul;85(1):62–70.
[106] Bieber T, Reich K, Paul C, Tsunemi Y, Augustin M, Lacour JP, et al. Efficacy and safety of baricitinib in combination with topical corticosteroids in patients with moderate-to-severe atopic dermatitis with inadequate response, intolerance or contraindication to ciclosporin: results from a randomized, placebo-controlled, phase III clinical trial (BREEZE-AD4). Br J Dermatol 2022 Sep;187(3):338–52.
[107] Reich K, Kabashima K, Peris K, Silverberg JI, Eichenfield LF, Bieber T, et al. Efficacy and safety of baricitinib combined with topical corticosteroids for treatment of moderate to severe atopic dermatitis: a randomized clinical trial. JAMA Dermatol 2020 Dec;156(12):1333–43.
[108] Torrelo A, Rewerska B, Galimberti M, Paller A, Yang CY, Prakash A, et al. Efficacy and safety of baricitinib in combination with topical corticosteroids in paediatric patients with moderate-to-severe atopic dermatitis with an inadequate response to topical corticosteroids: results from a phase III, randomized, double-blind, placebo-controlled study (BREEZE-AD PEDS). Br J Dermatol 2023 Jul;189(1):23–32.
[109] Silverberg JI, Simpson EL, Wollenberg A, Bissonnette R, Kabashima K, DeLozier AM, et al. Long-term efficacy of baricitinib in adults with moderate to severe atopic dermatitis who were treatment responders or partial responders: an extension study of 2 randomized clinical trials. JAMA Dermatol 2021 Jun;157(6):691–9.
[110] Thyssen JP, Werfel T, Barbarot S, Hunter HJA, Pierce E, Sun L, et al. Maintained improvement in physician- and patient-reported outcomes with baricitinib in adults with moderate-to-severe atopic dermatitis who were treated for up to 104 weeks in a randomized trial. J Dermatolog Treat 2023 Dec;34(1):2190430.
[111] Gooderham MJ, Forman SB, Bissonnette R, Beebe JS, Zhang W, Banfield C, et al. Efficacy and safety of oral janus kinase 1 inhibitor abrocitinib for patients with atopic dermatitis: a phase 2 randomized clinical trial. JAMA Dermatol 2019 Dec;155(12):1371–9.
[112] Simpson EL, Sinclair R, Forman S, Wollenberg A, Aschoff R, Cork M, et al. Efficacy and safety of abrocitinib in adults and adolescents with moderate-to-severe atopic dermatitis (JADE MONO-1): a multicentre, double-blind, randomised, placebo-controlled, phase 3 trial. Lancet 2020 Jul;396 (10246):255–66.
[113] Silverberg JI, Simpson EL, Thyssen JP, Gooderham M, Chan G, Feeney C, et al. Efficacy and safety of abrocitinib in patients with moderate-to-severe atopic dermatitis: a randomized clinical trial. JAMA Dermatol 2020 Aug;156(8):863–73.
[114] Eichenfield LF, Flohr C, Sidbury R, Siegfried E, Szalai Z, Galus R, et al. Efficacy and safety of abrocitinib in combination with topical therapy in adolescents with moderate-to-severe atopic dermatitis: the JADE TEEN randomized clinical trial. JAMA Dermatol 2021 Oct;157(10):1165–73.
[115] Blauvelt A, Silverberg JI, Lynde CW, Bieber T, Eisman S, Zdybski J, et al. Abrocitinib induction, randomized withdrawal, and retreatment in patients with moderate-to-severe atopic dermatitis: results from the JAK1 Atopic Dermatitis Efficacy and Safety (JADE) REGIMEN phase 3 trial. J Am Acad Dermatol 2022 Jan;86(1):104–12.
[116] Shi VY, Bhutani T, Fonacier L, Deleuran M, Shumack S, Valdez H, et al. Phase 3 efficacy and safety of abrocitinib in adults with moderate-to-severe atopic dermatitis after switching from dupilumab (JADE EXTEND). J Am Acad Dermatol 2022 Aug;87(2):351–8.
[117] Guttman-Yassky E, Thaçi D, Pangan AL, Hong HCH, Papp KA, Reich K, et al. Upadacitinib in adults with moderate to severe atopic dermatitis: 16-week results from a randomized, placebo-controlled trial. J Allergy Clin Immunol 2020 Mar;145(3):877–84.
[118] Guttman-Yassky E, Teixeira HD, Simpson EL, Papp KA, Pangan AL, Blauvelt A, et al. Once-daily upadacitinib versus placebo in adolescents and adults with moderate-to-severe atopic dermatitis (Measure Up 1 and Measure Up 2): results from two replicate double-blind, randomised controlled phase 3 trials. Lancet 2021 Jun;397(10290):2151–68.
[119] Reich K, Teixeira HD, de Bruin-Weller M, Bieber T, Soong W, Kabashima K, et al. Safety and efficacy of upadacitinib in combination with topical corticosteroids in adolescents and adults with moderate-to-severe atopic dermatitis (AD Up): results from a randomised, double-blind, placebo-controlled, phase 3 trial. Lancet 2021 Jun;397(10290):2169–81.
[120] Katoh N, Ohya Y, Murota H, Ikeda M, Hu X, Ikeda K, et al. A phase 3 randomized, multicenter, double-blind study to evaluate the safety of upadacitinib in combination with topical corticosteroids in adolescent and adult patients with moderate-to-severe atopic dermatitis in Japan (Rising Up): an interim 24-week analysis. JAAD Int 2022 Mar;6:27–36.
[121] Paller AS, Ladizinski B, Mendes-Bastos P, Siegfried E, Soong W, Prajapati VH, et al. Efficacy and safety of upadacitinib treatment in adolescents with moderate-to-severe atopic dermatitis: analysis of the Measure Up 1, Measure Up 2, and AD Up randomized clinical trials. JAMA Dermatol 2023 May;159(5):526–35.
[122] Zhao Y, Zhang L, Ding Y, Tao X, Ji C, Dong X, et al. Efficacy and safety of SHR0302, a highly selective Janus kinase 1 inhibitor, in patients with moderate to severe atopic dermatitis: a phase II randomized clinical trial. Am J Clin Dermatol 2021 Nov;22(6):877–89.
[123] Kim BS, Sun K, Papp K, Venturanza M, Nasir A, Kuligowski ME. Effects of ruxolitinib cream on pruritus and quality of life in atopic dermatitis: results from a phase 2, randomized, dose-ranging, vehicle- and active-controlled study. J Am Acad Dermatol 2020 Jun;82(6):1305–13.
[124] Kim BS, Howell MD, Sun K, Papp K, Nasir A, Kuligowski ME. INCB 18424-206 Study Investigators. Treatment of atopic dermatitis with ruxolitinib cream (JAK1/JAK2 inhibitor) or triamcinolone cream. J Allergy Clin Immunol 2020 Feb;145(2):572–82.
[125] Papp K, Szepietowski JC, Kircik L, Toth D, Eichenfield LF, Leung DYM, et al. Efficacy and safety of ruxolitinib cream for the treatment of atopic dermatitis: results from 2 phase 3, randomized, double-blind studies. J Am Acad Dermatol 2021 Oct;85(4):863–72.
[126] Landis MN, Arya M, Smith S, Draelos Z, Usdan L, Tarabar S, et al. Efficacy and safety of topical brepocitinib for the treatment of mild-to-moderate atopic dermatitis: a phase IIb, randomized, double-blind, vehicle-controlled, dose-ranging and parallel-group study. Br J Dermatol 2022 Dec;187 (6):878–87.
[127] Nakagawa H, Nemoto O, Igarashi A, Saeki H, Oda M, Kabashima K, et al. Phase 2 clinical study of delgocitinib ointment in pediatric patients with atopic dermatitis. J Allergy Clin Immunol 2019 Dec;144(6):1575–83.
[128] Nakagawa H, Nemoto O, Igarashi A, Saeki H, Kabashima K, Oda M, et al. Delgocitinib ointment in pediatric patients with atopic dermatitis: a phase 3, randomized, double-blind, vehicle-controlled study and a subsequent open-label, long-term study. J Am Acad Dermatol 2021 Oct;85(4):854–62.
[129] King B, Ko J, Forman S, Ohyama M, Mesinkovska N, Yu G, et al. Efficacy and safety of the oral Janus kinase inhibitor baricitinib in the treatment of adults with alopecia areata: Phase 2 results from a randomized controlled study. J Am Acad Dermatol 2021 Oct;85(4):847–53.
[130] King B, Ohyama M, Kwon O, Zlotogorski A, Ko J, Mesinkovska NA, et al. Two phase 3 trials of baricitinib for alopecia areata. N Engl J Med 2022 May;386(18):1687–99.
[131] King B, Guttman-Yassky E, Peeva E, Banerjee A, Sinclair R, Pavel AB, et al. A phase 2a randomized, placebo-controlled study to evaluate the efficacy and safety of the oral Janus kinase inhibitors ritlecitinib and brepocitinib in alopecia areata: 24-week results. J Am Acad Dermatol 2021 Aug;85(2):379–87.
[132] King B, Zhang X, Harcha WG, Szepietowski JC, Shapiro J, Lynde C, et al. Efficacy and safety of ritlecitinib in adults and adolescents with alopecia areata: a randomised, double-blind, multicentre, phase 2b-3 trial. Lancet 2023 May;401(10387):1518–29.
[133] King B, Mesinkovska N, Mirmirani P, Bruce S, Kempers S, Guttman-Yassky E, et al. Phase 2 randomized, dose-ranging trial of CTP-543, a selective Janus kinase inhibitor, in moderate-to-severe alopecia areata. J Am Acad Dermatol 2022 Aug;87(2):306–13.
[134] Zhou C, Yang X, Yang B, Yan G, Dong X, Ding Y, et al. A randomized, double-blind, placebo-controlled phase II study to evaluate the efficacy and safety of ivarmacitinib (SHR0302) in adult patients with moderate-to-severe alopecia areata. J Am Acad Dermatol 2023 Nov;89(5):911–9.
[135] Senna MM, King B, Mesinkovska N, Mostaghimi A, Hamilton C, Cassella J. Efficacy of the oral JAK1/JAK2 inhibitor CTP-543 (deuruxolitinib) in adult patients with moderate to severe alopecia areata: results from the multinational double-blind, placebo-controlled THRIVE-AA11 phase 3 trial. In: Poster presented at: American Academy of Dermatology's 2023 annual meeting; March 17-21, 2023; 2023.
[136] Mikhaylov D, Glickman JW, Del Duca E, Nia J, Hashim P, Singer GK, et al. A phase 2a randomized vehicle-controlled multi-center study of the safety and efficacy of delgocitinib in subjects with moderate-to-severe alopecia areata. Arch Dermatol Res 2023 Mar;315(2):181–9.

[137] Olsen EA, Kornacki D, Sun K, Hordinsky MK. Ruxolitinib cream for the treatment of patients with alopecia areata: a 2-part, double-blind, randomized, vehicle-controlled phase 2 study. J Am Acad Dermatol 2020 Feb;82(2):412–9.
[138] Rosmarin D, Pandya AG, Lebwohl M, Grimes P, Hamzavi I, Gottlieb AB, et al. Ruxolitinib cream for treatment of vitiligo: a randomised, controlled, phase 2 trial. Lancet 2020 Jul;396(10244):110–20.
[139] Rosmarin D, Passeron T, Pandya AG, Grimes P, Harris JE, Desai SR, et al. Two phase 3, randomized, controlled trials of ruxolitinib cream for vitiligo. N Engl J Med 2022 Oct;387(16):1445–55.
[140] Ezzedine K, Peeva E, Yamaguchi Y, Cox LA, Banerjee A, Han G, et al. Efficacy and safety of oral ritlecitinib for the treatment of active nonsegmental vitiligo: a randomized phase 2b clinical trial. J Am Acad Dermatol 2023 Feb;88(2):395–403.
[141] Kimball AB, Okun MM, Williams DA, Gottlieb AB, Papp KA, Zouboulis CC, et al. Two phase 3 trials of adalimumab for hidradenitis suppurativa. N Engl J Med 2016 Aug;375(5):422–34.
[142] Alavi A, Hamzavi I, Brown K, Santos LL, Zhu Z, Liu H, et al. Janus kinase 1 inhibitor INCB054707 for patients with moderate-to-severe hidradenitis suppurativa: results from two phase II studies. Br J Dermatol 2022 May;186(5):803–13.
[143] Kirby JS, Okun MM, Alavi A, Bechara FG, Zouboulis CC, Brown K, et al. Efficacy and safety of the oral Janus kinase 1 inhibitor povorcitinib (INCB054707) in patients with hidradenitis suppurativa in a phase 2, randomized, double-blind, dose-ranging, placebo-controlled study. J Am Acad Dermatol 2024 Mar;90(3):521–9.
[144] Worm M, Bauer A, Elsner P, Mahler V, Molin S, Nielsen TSS. Efficacy and safety of topical delgocitinib in patients with chronic hand eczema: data from a randomized, double-blind, vehicle-controlled phase IIa study. Br J Dermatol 2020 May;182(5):1103–10.
[145] Worm M, Thyssen JP, Schliemann S, Bauer A, Shi VY, Ehst B, et al. The pan-JAK inhibitor delgocitinib in a cream formulation demonstrates dose response in chronic hand eczema in a 16-week randomized phase IIb trial. Br J Dermatol 2022 Jul;187(1):42–51.
[146] Jimenez PA, Sofen HL, Bissonnette R, Lee M, Fowler J, Zammit DJ, et al. Oral spleen tyrosine kinase/Janus kinase inhibitor gusacitinib for the treatment of chronic hand eczema: results of a randomized phase 2 study. J Am Acad Dermatol 2023 Aug;89(2):235–42.
[147] Tuttle KR, Brosius 3rd FC, Adler SG, Kretzler M, Mehta RL, Tumlin JA, et al. JAK1/JAK2 inhibition by baricitinib in diabetic kidney disease: results from a phase 2 randomized controlled clinical trial. Nephrol Dial Transplant 2018 Nov;33(11):1950–9.
[148] Waibel M, Wentworth JM, So M, Couper JJ, Cameron FJ, MacIsaac RJ, et al. Baricitinib and beta-cell function in patients with new-onset type 1 diabetes. N Engl J Med 2023 Dec;389(23):2140–50.
[149] Zhang L, Li J, Yin H, Chen D, Li Y, Gu L, et al. Efficacy and safety of tofacitinib in patients with polymyalgia rheumatica: a phase 2 study. Ann Rheum Dis 2023 May;82(5):722–4.
[150] Ma X, Yang F, Wu J, Xu B, Jiang M, Sun Y, et al. Efficacy and Safety of Tofacitinib in Patients with Polymyalgia Rheumatica (EAST PMR): an open-label randomized controlled trial. PLoS Med 2023 Jun;20(6):e1004249.
[151] Koster MJ, Crowson CS, Giblon RE, Jaquith JM, Duarte-García A, Matteson EL, et al. Baricitinib for relapsing giant cell arteritis: a prospective open-label 52-week pilot study. Ann Rheum Dis 2022 Jun;81(6):861–7.
[152] Álvarez-Reguera C, Loricera J, Tofade T, Prieto-Peña D, Romero-Yuste S, Miguel ED, et al. AB0709 effectiveness of janus kinase inhibitors in giant cell arteritis in clinical practice. Real-world clinical practice study and literature review. Ann Rheum Dis 2023;82(Suppl 1):1559–60.
[153] Kong X, Sun Y, Dai X, Wang L, Ji Z, Chen H, et al. Treatment efficacy and safety of tofacitinib versus methotrexate in Takayasu arteritis: a prospective observational study. Ann Rheum Dis 2022 Jan;81(1):117–23.
[154] Wang J, Dai X, Ma L, Wu S, Jin X, Ji Z, et al. Efficacy and safety of tofacitinib versus leflunomide with glucocorticoids treatment in Takayasu arteritis: a prospective study. Semin Arthritis Rheum 2022 Aug;55:152018.
[155] Friedman MA, Le B, Stevens J, Desmarais J, Seifer D, Ogle K, et al. Tofacitinib as a steroid-sparing therapy in pulmonary sarcoidosis, an open-label prospective proof-of-concept study. Lung 2021 Apr;199(2):147–53.
[156] Damsky W, Wang A, Kim DJ, Young BD, Singh K, Murphy MJ, et al. Inhibition of type 1 immunity with tofacitinib is associated with marked improvement in longstanding sarcoidosis. Nat Commun 2022 Jun;13(1):3140.
[157] Liu Y, Ji Z, Yu W, Wu S, Chen H, Ma L, et al. Tofacitinib for the treatment of antineutrophil cytoplasm antibody-associated vasculitis: a pilot study. Ann Rheum Dis 2021 Dec;80(12):1631–3.
[158] Karalilova RV, Batalov ZA, Sapundzhieva TL, Matucci-Cerinic M, Batalov AZ. Tofacitinib in the treatment of skin and musculoskeletal involvement in patients with systemic sclerosis, evaluated by ultrasound. Rheumatol Int 2021 Oct;41(10):1743–53.
[159] You H, Xu D, Hou Y, Zhou J, Wang Q, Li M, et al. Tofacitinib as a possible treatment for skin thickening in diffuse cutaneous systemic sclerosis. Rheumatology (Oxford) 2021 May;60(5):2472–7.
[160] Khanna D, Padilla C, Tsoi LC, Nagaraja V, Khanna PP, Tabib T, et al. Tofacitinib blocks IFN-regulated biomarker genes in skin fibroblasts and keratinocytes in a systemic sclerosis trial. JCI Insight 2022 Sep;7(17):e159566.
[161] Junfei Z, Meihua G, Shuai Z, Xiangting L, Zhidan L, Tianming C, et al. Retrospective comparative study of the efficacy of JAK inhibitor (tofacitinib) in the treatment of systemic sclerosis-associated interstitial lung disease. Clin Rheumatol 2023 Oct;42(10):2823–32.
[162] Paik JJ, Casciola-Rosen L, Shin JY, Albayda J, Tiniakou E, Leung DG, et al. Study of tofacitinib in refractory dermatomyositis: an open-label pilot study of ten patients. Arthritis Rheumatol 2021 May;73(5):858–65.
[163] Shneyderman M, Ahlawat S, Christopher-Stine L, Paik JJ. Calcinosis in refractory dermatomyositis improves with tofacitinib monotherapy: a case series. Rheumatology (Oxford) 2021 Nov 3;60(11):e387–8.
[164] Min MS, Alsarheed A, Kassamali B, Mazori DR, Schaefer M, Merola JF, et al. Tofacitinib as treatment for refractory dermatomyositis: a retrospective study from 2 academic medical centers. J Am Acad Dermatol 2022 Feb;86(2):423–5.
[165] Landon-Cardinal O, Guillaume-Jugnot P, Toquet S, Sbeih N, Rigolet A, Champtiaux N, et al. JAK inhibitors for the treatment of adult dermatomyositis: a pilot study. J Am Acad Dermatol 2023 Apr;88(4):924–6.
[166] Beckett M, Tan J, Bonnardeaux E, Dutz J, Shojania K, To F, et al. Tofacitinib therapy in refractory inflammatory myositis: a retrospective cohort study of 41 patients. Rheumatology (Oxford) 2024 May;63(5):1432–6.
[167] Zhang J, Sun L, Shi X, Li S, Liu C, Li X, et al. Janus kinase inhibitor, tofacitinib, in refractory juvenile dermatomyositis: a retrospective multi-central study in China. Arthritis Res Ther 2023 Oct;25(1):204.
[168] Chen Z, Wang X, Ye S. Tofacitinib in amyopathic dermatomyositis-associated interstitial lung disease. N Engl J Med 2019 Jul;381(3):291–3.
[169] Fan L, Lyu W, Liu H, Jiang H, Chen L, Liu Y, et al. A retrospective analysis of outcome in melanoma differentiation-associated gene 5-related interstitial lung disease treated with tofacitinib or tacrolimus. J Rheumatol 2022 Dec;49(12):1356–64.
[170] Kurasawa K, Arai S, Namiki Y, Tanaka A, Takamura Y, Owada T, et al. Tofacitinib for refractory interstitial lung diseases in anti-melanoma differentiation-associated 5 gene antibody-positive dermatomyositis. Rheumatology (Oxford) 2018;57(12):2114–9.
[171] Ida T, Furuta S, Takayama A, Tamura J, Hayashi Y, Abe K, et al. Efficacy and safety of dose escalation of tofacitinib in refractory anti-MDA5 antibody-positive dermatomyositis. RMD Open 2023 Jan;9(1):e002795.
[172] Xue Y, Zhang J, Deng J, Kuang W, Wang J, Tan X, et al. Efficiency of tofacitinib in refractory interstitial lung disease among anti-MDA5 positive juvenile dermatomyositis patients. Ann Rheum Dis 2023 Nov;82(11):1499–501.
[173] Wang Y, Luo J, Lv X, Li Y, An Q, Mo L, et al. Tofacitinib for new-onset adult patients with anti-melanoma differentiation-associated 5 gene antibody positive dermatomyositis. Clin Rheumatol 2023 Jul;42(7):1847–53.
[174] Li S, Li S, Wang J, Zhang L, Duan J, Lu X, et al. Efficacy and safety of tofacitinib in anti-melanoma differentiation-associated 5 gene antibody-positive dermatomyositis. J Clin Rheumatol 2023 Sep;29(6):281–4.
[175] Liu J, Hou Y, Sun L, Li C, Li L, Zhao Y, et al. A pilot study of tofacitinib for refractory Behcet's syndrome. Ann Rheum Dis 2020 Nov;79(11):1517–20.
[176] Wang Z, Wang X, Liu W, Wang Y, Liu J, Zhang L, et al. Baricitinib for the treatment of refractory vascular Behcet's disease. Clin Immunol 2023 May;250:109298.
[177] Liu J, Yu X, Wang Z, Liu W, Liu X, Wang X, et al. Baricitinib for the treatment of intestinal Behcet's disease: a pilot study. Clin Immunol 2023 Feb;247:109241.
[178] Hu Q, Wang M, Jia J, Teng J, Chi H, Liu T, et al. Tofacitinib in refractory adult-onset Still's disease: 14 cases from a single centre in China. Ann Rheum Dis 2020 Jun;79(6):842–4.
[179] Gillard L, Pouchot J, Cohen-Aubart F, Koné-Paut I, Mouterde G, Michaud M, et al. JAK inhibitors in difficult-to-treat adult-onset Still's disease and systemic-onset juvenile idiopathic arthritis. Rheumatology (Oxford) 2023 Apr;62(4):1594–604.
[180] Sun Z, Li R, Wang Y, Han F, Wei W, Li X. Efficacy of baricitinib in patients with refractory adult-onset Still's disease. Drugs R D 2023 Jun;23(2):109–20.
[181] Ahmed A, Merrill SA, Alsawah F, Bockenstedt P, Campagnaro E, Devata S, et al. Ruxolitinib in adult patients with secondary haemophagocytic lymphohistiocytosis: an open-label, single-centre, pilot trial. Lancet Haematol 2019 Dec;6(12):e630–7.
[182] Boonstra PS, Ahmed A, Merrill SA, Wilcox RA. Ruxolitinib in adult patients with secondary hemophagocytic lymphohistiocytosis. Am J Hematol 2021 Apr;96(4):E103–5.
[183] Zhou D, Huang X, Xie M, Zhu L, Huang X, Li X, et al. Ruxolitinib combined with dexamethasone in adult patients with newly diagnosed hemophagocytic

lymphohistiocytosis: a single-center pilot trial. Am J Hematol 2023 May;98 (5):E106–9.
[184] Zhang Q, Wei A, Ma HH, Zhang L, Lian HY, Wang D, et al. A pilot study of ruxolitinib as a front-line therapy for 12 children with secondary hemophagocytic lymphohistiocytosis. Haematologica 2021 Jul;106 (7):1892–901.
[185] Zhang Q, Zhao YZ, Ma HH, Wang D, Cui L, Li WJ, et al. A study of ruxolitinib response-based stratified treatment for pediatric hemophagocytic lymphohistiocytosis. Blood 2022 Jun;139(24):3493–504.
[186] Wang J, Zhang R, Wu X, Li F, Yang H, Liu L, et al. Ruxolitinib-combined doxorubicin-etoposide-methylprednisolone regimen as a salvage therapy for refractory/relapsed haemophagocytic lymphohistiocytosis: a single-arm, multicentre, phase 2 trial. Br J Haematol 2021 May;193 (4):761–8.
[187] Sanchez GAM, Reinhardt A, Ramsey S, Wittkowski H, Hashkes PJ, Berkun Y, et al. JAK1/2 inhibition with baricitinib in the treatment of autoinflammatory interferonopathies. J Clin Invest 2018 Jul;128(7):3041–52.
[188] Vanderver A, Adang L, Gavazzi F, McDonald K, Helman G, Frank DB, et al. Janus kinase inhibition in the Aicardi-Goutieres syndrome. N Engl J Med 2020 Sep;383(10):986–9.
[189] Kanazawa N, Ishii T, Takita Y, Nishikawa A, Nishikomori R. Efficacy and safety of baricitinib in Japanese patients with autoinflammatory type I interferonopathies (NNS/CANDLE, SAVI, and AGS). Pediatr Rheumatol Online J 2023 Apr;21(1):38.
[190] Forbes LR, Vogel TP, Cooper MA, Castro-Wagner J, Schussler E, Weinacht KG, et al. Jakinibs for the treatment of immune dysregulation in patients with gain-of-function signal transducer and activator of transcription 1 (STAT1) or STAT3 mutations. J Allergy Clin Immunol 2018 Nov;142 (5):1665–9.
[191] Deyà-Martínez A, Rivière JG, Roxo-Junior P, Ramakers J, Bloomfield M, Guisado Hernandez P, et al. Impact of JAK inhibitors in pediatric patients with STAT1 gain of function (GOF) mutations-10 children and review of the literature. J Clin Immunol 2022 Jul;42(5):1071–82.
[192] Nikishina IP, Arsenyeva SV, Matkava VG, Arefieva AN, Kaleda MI, Smirnov AV, et al. Successful experience of tofacitinib treatment in patients with fibrodysplasia ossificans progressiva. Pediatr Rheumatol Online J 2023 Aug;21(1):92.
[193] Li C, Li Z, Cao Y, Li L, Li F, Li Y, et al. Tofacitinib for the treatment of nail lesions and palmoplantar pustulosis in synovitis, acne, pustulosis, hyperostosis, and osteitis syndrome. JAMA Dermatol 2021 Jan;157(1):74–8.
[194] Liu S, Yu Y, Liu Y, Ma M, Li C. Efficacy of baricitinib in synovitis, acne, pustulosis, hyperostosis, and osteitis syndrome: a case series. Joint Bone Spine 2023 Sep;90(5):105587.
[195] Li Y, Huo J, Cao Y, Yu M, Zhang Y, Li Z, et al. Efficacy of tofacitinib in synovitis, acne, pustulosis, hyperostosis and osteitis syndrome: a pilot study with clinical and MRI evaluation. Ann Rheum Dis 2020 Sep;79(9):1255–7.
[196] Heiblig M, Ferrada MA, Koster MJ, Barba T, Gerfaud-Valentin M, Mékinian A, et al. Ruxolitinib is more effective than other JAK inhibitors to treat VEXAS syndrome: a retrospective multicenter study. Blood 2022 Aug;140 (8):927–31.
[197] Gordon SC, Trudeau S, Regev A, Uhas JM, Chakladar S, Pinto-Correia A, et al. Baricitinib and primary biliary cholangitis. J Transl Autoimmun 2021;4:100107.
[198] Srivastava SK, Watkins T, Nguyen QD, Sharma S, Scales D, Dacey M, et al. A phase 2 randomized controlled trial of the Janus kinase (JAK) inhibitor filgotinib in patients with noninfectious uveitis. Invest Ophthalmol Vis Sci 2022;63(7):2678.
[199] Liew SHM, Nichols KK, Klamerus KJ, Li JZ, Zhang M, Foulks GN. Tofacitinib (CP-690,550), a Janus kinase inhibitor for dry eye disease: results from a phase 1/2 trial. Ophthalmology 2012 Jul;119(7):1328–35.
[200] Song Y, Wang J, Wang Y, Wang Z. Ruxolitinib in patients with chronic active Epstein-Barr virus infection: a retrospective, single-center study. Front Pharmacol 2021;12:710400.
[201] Uzzan M, Nachury M, Amiot A, Peyrin-Biroulet L, Kirchgesner J, Bouhnik Y. GETAID TOFA-POUCH study group. Effectiveness and safety of tofacitinib in patients with chronic pouchitis multirefractory to biologics. Dig Liver Dis 2023 Aug;55(8):1158–60.
[202] Uzzan M, Nachury M, Nuzzo A, Amiot A, Caron B, Benezech A, et al. Tofacitinib for patients with anti-TNF refractory ulcerative proctitis: a multicentre cohort study from the GETAID. J Crohns Colitis 2024 Mar;18(3):424–30.
[203] Akiyama S, Cohen NA, Kayal M, Dubinsky MC, Colombel JF, Rubin DT. Treatment of chronic inflammatory pouch conditions with tofacitinib: a case series from 2 tertiary IBD centers in the United States. Inflamm Bowel Dis 2023 Sep;29(9):1504–7.
[204] Jang Y, Lee WJ, Lee HS, Chu K, Lee SK, Lee ST. Tofacitinib treatment for refractory autoimmune encephalitis. Epilepsia 2021 Apr;62(4):e53–9.
[205] Faguer S, Groh M, Vergez F, Hunault-Berger M, Duployez N, Renaudineau Y, et al. JAK inhibition for $CD3^{-}$ $CD4^{+}$ lymphocytic-variant hypereosinophilic syndrome. Clin Immunol 2023 Jun;251:109275.
[206] Brumfiel CM, Patel MH, Severson KJ, Zhang N, Li X, Quillen JK, et al. Ruxolitinib cream in the treatment of cutaneous lichen planus: a prospective, open-label study. J Invest Dermatol 2022 Aug;142(8) 2109-16.e4.
[207] Bao C, Xu Q, Xiao Z, Wang H, Luo R, Cheng B, et al. Abrocitinib as a novel treatment for lichen sclerosus. Br J Dermatol 2023 Jul;189(1):136–8.
[208] Liu T, Chu Y, Wang Y, Zhong X, Yang C, Bai J, et al. Successful treatment of prurigo nodularis with tofacitinib: the experience from a single center. Int J Dermatol 2023 May;62(5):e293–5.
[209] Han Y, Tu P. Baricitinib is potentially effective in the treatment of refractory livedoid vasculopathy. Front Immunol 2022;13:1008392.
[210] Sun YH, Man XY, Xuan XY, Huang CZ, Shen Y, Lao LM. Tofacitinib for the treatment of erythematotelangiectatic and papulopustular rosacea: a retrospective case series. Dermatol Ther 2022 Nov;35(11):e15848.
[211] Ju T, Labib A, Vander Does A, Yosipovitch G. Topical Janus kinase-signal transducers and activators of transcription inhibitor tofacitinib is effective in reducing nonatopic dermatitis chronic itch: A case series. J Am Acad Dermatol 2022 Aug;87(2):400–3.
[212] Mease P, Deodhar A, van der Heijde D, Behrens F, Kivitz A, Neal J, et al. Safety and efficacy of deucravacitinib, an oral, selective tyrosine kinase 2 inhibitor, in patients with psoriatic arthritis: 52-week results from a randomized phase 2 trial. Arthritis Rheumatol 2022;74:1598.

Ann Rheum Dis 84 (2025) 697−715

Contents lists available at ScienceDirect

Annals of the Rheumatic Diseases

journal homepage: https://www.sciencedirect.com/journal/annals-of-the-rheumatic-diseases

Rheumatoid arthritis

Safety of Janus kinase inhibitors in immune-mediated inflammatory diseases – a systematic literature review informing the 2024 update of an international expert consensus statement

Victoria Konzett[1,*], Josef S. Smolen[1], Peter Nash[2], Kevin Winthrop[3], Daniel Aletaha[1], Thomas Dörner[4], Roy Fleischmann[5], Yoshiya Tanaka[6], Jette Primdahl[7], Xenofon Baraliakos[8], Iain B. McInnes[9], Michael Trauner[10], Naveed Sattar[11], Maarten de Wit[12], Jan W. Schoones[13], Andreas Kerschbaumer[1]

[1] *Department of Medicine III, Division of Rheumatology, Medical University of Vienna, Vienna, Austria*
[2] *Griffith University School of Medicine, Gold Coast, QLD, Australia*
[3] *Oregon Health and Science University, Portland, OR, USA*
[4] *Rheumatology, Charite Medical Faculty Berlin, Berlin, Germany*
[5] *Metroplex Clinical Research Center, University of Texas Southwestern Medical Center at Dallas, Dallas, TX, USA*
[6] *The First Department of Internal Medicine, University of Occupational and Environmental Health, Japan, Kitakyushu, Japan*
[7] *Danish Hospital for Rheumatic Diseases, University Hospital of Southern Denmark, Sønderborg, Denmark*
[8] *Rheumazentrum Ruhrgebiet, Ruhr University Bochum, Herne, Germany*
[9] *College of Medical Veterinary and Life Sciences, University of Glasgow, Glasgow, UK*
[10] *Department of Medicine III, Division of Gastroenterology and Hepatology, Medical University of Vienna, Vienna, Austria*
[11] *Cardiovascular and Metabolic Health, University of Glasgow, Glasgow, UK*
[12] *Stichting Tools, Patient Research Partner, Amsterdam, the Netherlands*
[13] *Directorate of Research Policy, Leiden University Medical Center, Leiden, the Netherlands*

ARTICLE INFO

Article history:
Received 29 September 2024
Received in revised form 19 November 2024
Accepted 25 November 2024

ABSTRACT

Objectives: This systematic literature review (SLR) on safety outcomes was performed to inform the 2024 update of the expert consensus statement on the treatment of immune-mediated inflammatory diseases (IMIDs) with Janus kinase inhibitors (JAKi).
Methods: An update of the 2019 SLR was performed in MEDLINE, Embase, and the Cochrane Library. For safety, randomised, placebo-controlled or active-controlled trials on all JAKi investigated in IMIDs, long-term extension (LTE) studies, pooled trial data analyses, and cohort and claims studies were included.
Results: We screened 13,905 records, of which 209 were finally included. Three safety trials and 13 post hoc analyses, 83 efficacy randomised controlled trials (RCTs) with adequate safety reporting, 56 integrated safety analyses and LTE of RCTs, 20 additional conference abstracts on RCT data, as well as 37 real-world cohort studies were presented to the task force. Safety profiles of JAKi were overall consistent across compounds and indications, but impacts of patient profiles, treatment dosing, and other cofactors like background medications on drug safety could be

*Correspondence to Dr. Victoria Konzett, Department of Medicine III, Division of Rheumatology, Medical University of Vienna, Austria.
E-mail address: victoria.konzett@meduniwien.ac.at (V. Konzett).

Handling editor Dimitrios T. Boumpas.

https://doi.org/10.1016/j.ard.2025.01.024

observed. Furthermore, differential effects of variously selective JAKi on distinct adverse events of special interest (AESI) and laboratory outcomes were discerned.
Conclusion: A substantial amount of literature was published on JAKi safety since 2019. A comprehensive overview of these data supports the optimal use of JAKi in patients with IMIDs, by consideration and balance of their benefits as well as risks in every patient.

WHAT IS ALREADY KNOWN ON THIS TOPIC

- Janus kinase inhibitors (JAKi) are effective for treating immune-mediated inflammatory diseases (IMIDs), but their optimal use has been debated in recent years due to safety signals detected in trial development programmes as well as the ORAL Surveillance safety study.
- In 2019, an international task force formulated a consensus statement on 'points to consider for the treatment of IMIDs with JAKi'. In light of the recent developments in the field, this statement will now be updated.

WHAT THIS STUDY ADDS

- We here provide a comprehensive overview of all safety data published on JAKi in IMIDs since 2019. The recent years brought about the introduction of novel and increasingly selective compounds to the market, as well as safety signals from the ORAL Surveillance trial that had generated both black-box warnings for the whole drug class as well as extensive subsequent analyses of safety outcomes in broader patient populations and at-risk cohorts.

HOW THIS STUDY MIGHT AFFECT RESEARCH, PRACTICE OR POLICY

- This review informed an international task force formulating the 2024 update of the expert consensus statement on points to consider for the treatment of IMIDs with JAKi, by summarising efficacy and safety outcomes of JAKi across IMIDs published since the original 2019 consensus.

INTRODUCTION

Janus kinase inhibitors (JAKi) are highly effective for the treatment of immune-mediated inflammatory diseases (IMIDs). This has been demonstrated across various multinational trial development programmes as well as in registry data and has led to the approval of different JAKi for treatment of various IMIDs, such as rheumatoid arthritis (RA), psoriatic arthritis (PsA), axial spondyloarthritis (axSpA), juvenile idiopathic arthritis (JIA), ulcerative colitis (UC), Crohn's disease (CD), psoriasis (PsO), atopic dermatitis (AD), alopecia areata (AA), and vitiligo [1,2].

While JAKi convey significant benefits by broadly downregulating inflammatory responses via inhibition of JAK-STAT pathways, they have also been associated with various side effects − some of which have been expected in light of their pharmacologic properties, while others had been discovered only during the drug development processes [3−7]. Optimal use of JAKi therefore requires careful consideration of their benefits and risks, as well as the integration of multiple cofactors that systematically impact this balance in every individual patient [8−10].

An expert consensus statement on points to consider (PtCs) for the optimal use of JAKi in IMIDs has been formulated by an international task force in 2019 [11,12]. Since then, a substantial amount of additional literature on JAKi safety has been published, including a safety-endpoint trial comparing JAKi with tumour necrosis factor alpha inhibitors (TNFis) in patients with RA [13], followed by black-box warnings prompted by regulators in reaction to safety signals detected in this study [14−18]. Beyond this, however, many more outcomes and datasets have been investigated, and post hoc as well as subgroup analyses have furthered our understanding of mediators and cofactors that impact JAKi safety and efficacy in different patient populations [19−30].

The task force therefore decided to update the 2019 consensus statement, and systematic literature reviews (SLRs) were performed to summarise all recently published data on efficacy as well as safety outcomes of JAKi studied in IMIDs. Efficacy outcomes as well as the updated consensus statement are published separately (V. Konzett et al, manuscript in press, Ann Rheum Dis, 2025; P. Nash et al, manuscript in press, Ann Rheum Dis, 2025). This paper focuses on the safety of JAKi in patients with IMIDs, and summarises all data published since 2019.

METHODS

For this SLR, we adhered to established principles for the conduction of recommendations and PtCs as well as the Cochrane Handbook for Systematic Literature Reviews and Preferred Reporting Items for Systematic Reviews and Meta-Analyses (PRISMA) guidelines [31−35].

A steering committee consisting of physicians from different medical specialties, a patient and a nonphysician health professional met in person on April 16, 2023, to define the scope of the SLR in Population, Intervention, Comparator, Outcomes (PICO) format [36]. For the safety SLR, we searched for safety-endpoint trials, phase 2 to phase 4 clinical trial data with adequate safety reporting as well as long-term extension (LTE) studies with an active comparator (both double-blind and open-label trial designs), integrated safety analyses of randomised controlled trial (RCT) data, and registry data from cohort and claims studies. Conference abstracts on high-level clinical trial data that were presented at international rheumatology, gastroenterology, and dermatology conferences between 2021 and 2023 were considered as well, whereas cohort and claims studies were only included when published in peer-reviewed journals. For all conference abstracts that were presented to the task force, full publications that became available in subsequent months leading to manuscript finalisation were further included.

We searched for trials with a sample size of at least 50 participants and a treatment duration of at least 6 months. Only studies on JAKi in IMIDs were considered. Trials on JAKi studied in myeloproliferative disorders and other malignancies, graft-vs-host disease, posttransplant immunosuppression, or treatment of COVID-19 disease were excluded, as the patient population was considered as highly different from our population of interest. Only articles or conference abstracts published in English language were taken into consideration, and trials registered only in trial databases were excluded from this SLR if not published.

A search strategy was developed in accordance with these guidelines, and a library search was conducted in 3 databases (MEDLINE, Embase, and the Cochrane Library) by an experienced librarian (JWS). All articles published between March 1, 2019 (the data cut of the 2019 SLR) [12], and October 14, 2023, as well as all studies that were published before March 2019 but had not been within the scope of the original SLR were then screened by 1 researcher (VK), and all doubts were discussed with the methodologist (AK). A first search was conducted in June 2023 and was updated in October 2023 for inclusion of more recent publications.

Safety outcomes of special interest considered in this SLR were major cardiovascular events (MACEs), malignancies (excluding nonmelanoma skin cancer [NMSC]), NMSC, venous thromboembolic events (VTEs) and arterial thromboembolic events (ATEs), serious infectious events (SIEs), opportunistic infections events (OIE), including latent and active tuberculosis (TB), herpes zoster (HZ), gastrointestinal perforations (GIPs), and all-cause mortality (ACM). Other safety outcomes of interest were acne, hepatic disorders, interstitial lung disease (ILD), conjunctivitis, reproductive health, bone density and osteoporosis, weight changes, vaccination response rates and safety, as well as COVID-19 infections and associated morbidity and mortality.

PICO criteria, research questions, and the detailed search strategy are summarised in the Supplemental Appendix (Section 1). For all studies included, study characteristics and methodological summaries were extracted onto standardised spreadsheets, which are listed in the Supplemental Appendix (Sections 2-7).

In RCTs, event rates (ERs) were predominantly shown as numbers and proportions of patients with the event in predefined safety analysis sets (most commonly, all patients who received at least 1 dose of the study drug). In safety trials and integrated safety analyses, ERs were commonly given as exposure adjusted incidence rates (IRs) or ERs, per 100 patient-years (PYs) of exposure. IRs are commonly calculated as the number of patients with at least 1 event, whereas ER usually summarise the total number of events in the safety population and therefore tend to be higher, as the ratio could consider multiple events in a single patient. IRs were further either censored at time of first occurrence of the event of interest or calculated as uncensored ratios over the whole analysis period, which was considered as well in this SLR. For integrated safety data and LTE studies on individual drugs, only the most recent publication (highest number of PYs of exposure) was considered.

Baseline characteristics, safety outcomes and risk of bias (RoB) assessments were additionally extracted onto standardised spreadsheets and are again provided in the Supplemental Appendix (Sections 3-7). For RCT data, RoB was assessed using the Cochrane Collaboration's tool for assessing RoB in randomised trials [37], whereas the Hayden Tool was used for observational studies [38].

Meta-analyses of mean changes in laboratory outcomes were performed for all parameters where sufficient RCT data were available at week 12 or week 24. Owing to heterogeneity between patient populations, analyses were only performed in RA populations, but data were pooled from all eligible RA RCTs included in this SLR as well as the previous 2019 SLR. Mean differences of active treatments vs comparators (placebo [PLC] or methotrexate [MTX]) were calculated, and a random-effects model using restricted maximum likelihood estimators (REML) was used to account for between-study heterogeneity. Missing SDs up to 5% were imputed, and CIs calculated using the Hartung-Knapp method to provide robust estimates. All analyses and visualisations were done using R (R Core Team, version 4.4.1, Vienna, Austria), and the 'meta' package (G. Schwarzer, version 7.0) [39,40]. No meta-analyses were performed on other adverse events of special interest (AESIs), as events and patient populations were heterogeneously defined, and inclusion and exclusion of at-risk patients varied across studies.

RESULTS

For the safety SLR, we identified 13,905 records focusing on safety only, of which 644 were selected for full-text reading, and 130 finally included. Of the 10,556 articles screened for the efficacy SLR, 79 records on 83 RCTs were additionally included also for the safety SLR, as safety data were adequately reported (V. Konzett et al, manuscript in press, Ann Rheum Dis, 2025). This sums up to a total of 209 records on JAKi safety that were presented to the task force, of which 2 were on open-label safety-endpoint trials (3 trials), 13 on post hoc analyses of these trials, 79 were on RCT data (83 trials), 56 on pooled safety analyses, and 2 on additionally included LTE studies with active comparator; 20 abstracts not yet available as full publication and 37 analyses of cohort and claims databases were also included.

Figure 1 summarises the literature search and record selection process. The main reasons for exclusion of manuscripts from the analysis were inadequate safety reporting, lack of an active comparator arm, more recently published data available, as well as studies on populations, interventions, or outcomes beyond the scope of this review.

One safety-endpoint trial studied tofacitinib (TOFA) in RA, 2 studied filgotinib (FILGO) in men with inflammatory bowel disease (IBD) or rheumatic conditions. Concerning RCT data, 12 articles assessed JAKi safety and efficacy in RA, 5 in PsA, 4 in axSpA, 4 in systemic lupus erythematosus (SLE) and Sjögren syndrome (SjS), 2 in JIA, 5 in UC, 3 in CD, 43 in dermatologic conditions, and 1 in diabetic kidney disease (DKD), since the last SLR performed in 2019. Of these, 65 were considered as having low RoB, 6 as high RoB, 4 with some concerns on RoB, and 8 as unclear (Supplemental Appendix; Section 4.3).

Pooled RCT data were available for TOFA, baricitinib (BARI), upadacitinib (UPA), FILGO, peficitinib (PEFI), and abrocitinib (ABRO). Two LTE studies comparing UPA with active comparators (adalimumab [ADA] and MTX) and 20 conference abstracts on TOFA, UPA, FILGO, ABRO, and deucravacitinib (DEUCRA) were also included. Data from cohort and claims studies were predominantly available for TOFA and BARI, studied in RA or UC. Of these studies, none was graded as low RoB, 15 as moderate, and 22 as high RoB (Supplemental Appendix; Sections 6.3 and 7.3).

Safety-endpoint trials

Three safety-endpoint trials were included in this SLR [13,41]. ORAL Surveillance was an event-driven, randomised, open-label, noninferiority study conducted in patients with active RA despite MTX therapy, aged at least 50 years, and with at least 1 cardiovascular (CV) risk factor (current smoking, hypertension, high-density lipoprotein [HDL] cholesterol < 40 mg/dL, diabetes, family history of premature coronary heart disease, RA-associated extra-articular disease, and/or history of coronary artery disease). Patients were randomised to TOFA 5 mg twice daily (n = 1455), TOFA 10 mg twice daily (n = 1456), or TNFi (n = 1451; ADA in North America; etanercept [ETA] in the rest of the world). Primary endpoints were the noninferiority of MACE and malignancies (excluding NMSC) for combined TOFA vs TNFi, defined as the upper bound (UB) of the 95% CI not crossing 1.8. These primary endpoints were not

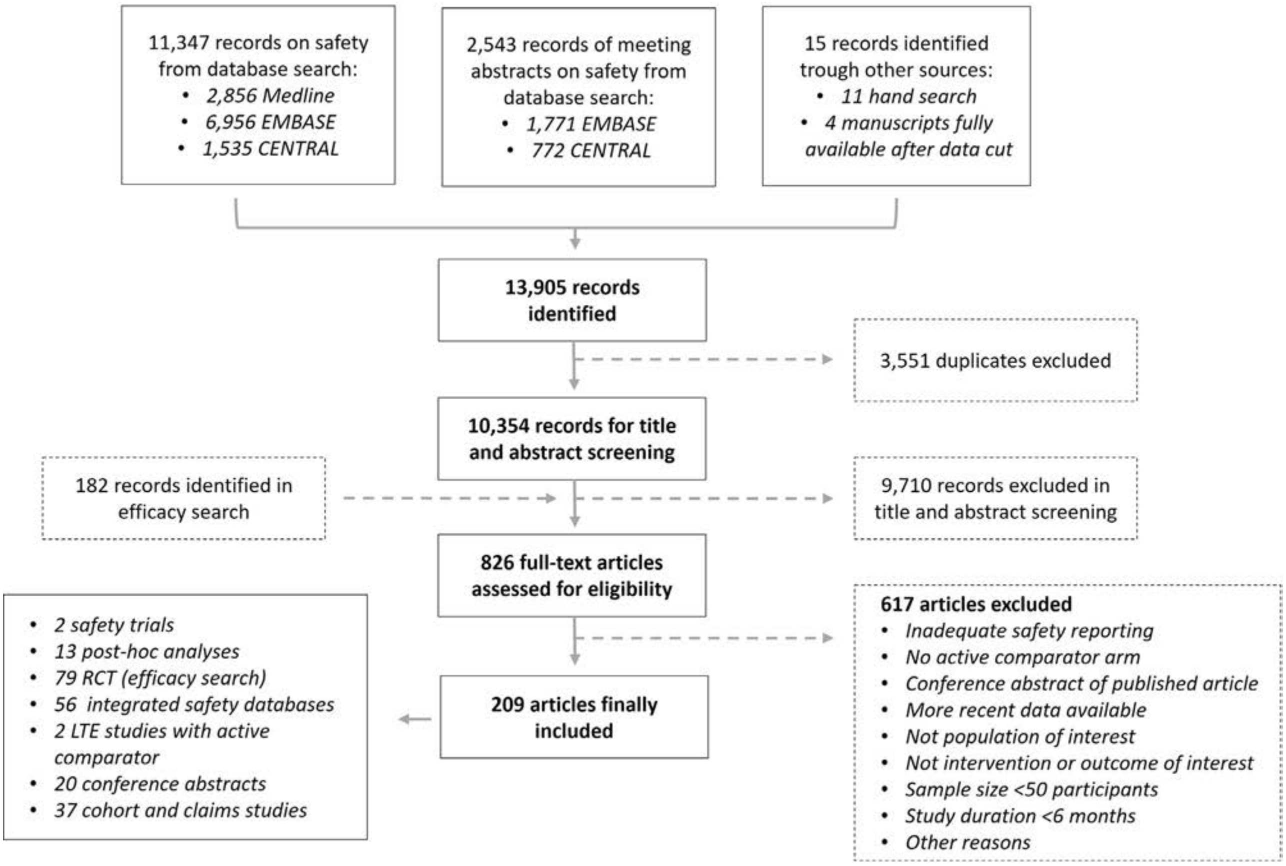

Figure 1. Flowchart summarising the systematic literature review and manuscript selection process. LTE, long-term extension; RCT, randomised controlled trial.

met, indicating that TOFA was not noninferior to TNFi for risk of MACE and malignancies (excluding NMSC) in this study [13].

An increased risk with TOFA vs TNFi was also observed for various secondary endpoints. Overall, serious adverse events (SAEs) were reported in 24.1%, 26.8%, and 21.1% of patients treated with TOFA 5 mg twice daily, TOFA 10 mg twice daily, and TNFi, respectively. Moreover, 45.7%, 50.5%, and 39.7% temporarily discontinued the studied drug (<2 months) and 14.4%, 20.9%, and 14.5% did so permanently, for TOFA 5 mg twice daily, TOFA 10 mg twice daily, and TNFi, respectively. All patients were asked to remain in the study for at least 3 years even if treatment was discontinued. If originally randomised to TOFA 10 mg twice daily, safety endpoints were continued to be counted in the 10-mg twice daily arm, despite a mandated dose reduction to TOFA 5 mg twice daily in 2019 [13,42].

MANTA and MANTA-RAy trials [41,43] were conducted to assess the impact of FILGO 200 mg every day on male reproductive health in men aged 21 to 65 years with IBD or RA, PsA and ankylosing spondylitis (AS), due to safety concerns that arose in the preclinical development phase of the drug [41,43]. As AESI, these outcomes will be discussed in more detail later.

Integrated safety analyses of RCT data

RCT on JAKi were commonly powered for efficacy outcomes, but safety signals were subsequently summarised in pooled analyses of the overall trial development programmes, including LTE studies. An overview of these integrated safety analyses is provided in Table 1 [19−21,25,45−59], as well as in the Supplemental Appendix (Section 2.4 and Section 5).

ERs were commonly given as IR per 100 PYs of exposure (IR/100PY), reflecting the number of patients with the respective event in the follow-up period, censored at time of event, death, or end of study, or as ER per 100 PYs (E/100PY), where multiple events were considered in a single patient.

AEs were usually categorised using the Medical Dictionary for Regulatory Activities (MedDRA) terminology [60]. The most commonly involved organ class was ‘infections and infestations’, and pneumonia was the most frequently reported SAEs in most analyses [19−21,52,53].

Overall, safety profiles were consistent across times and indications, but differences in distinct AESI were observed between various patient populations (Figs 2-4) [19,22,61,62]. Higher rates of CV events and malignancies were, for example, observed in RA and UC compared with axSpA, AD, or AA [19,20,47,51,54], whereas SIEs were more frequently observed in SLE [52], OIE rates were highest for UC [20], and acne or eczema herpeticum most commonly reported in patients with dermatologic conditions [7,19]. Treatment dosage as well as JAK selectivity further seemed to impact safety profiles, which will be discussed in more detail later.

LTE studies

The SELECT COMPARE study as well as the SELECT-PSA 1 study on UPA maintained active comparator arms over a 10- and 5-year period, respectively, of which 5-year as well as 2-year results were available at data cut [63−65]. The analyses were consistent with the pooled RCT data and did not show significant risk increases over time for various AESI. In comparison with the ORAL Surveillance trial, dropouts and dose switches were usually possible in LTE studies, which needs to be considered when interpreting these results.

Table 1

Overview of integrated safety data analyses

JAKi	Disease	Study ID	Trials summarised	N total	PY total
TOFA	PsO	Strober et al, 2019 [44]	Phase 2-3, LTE (6 trials)	3623	5204
	RA	Cohen et al, 2020 [45]	Phase 1-4, LTE (21 trials)	7061	22,875
	PsA	Burmester et al, 2020 [46]	Phase 3, LTE (3 trials)	783	776
	RA/PsA/UC/PsO	Burmester et al, 2021 [20]	Phase 1-4, LTE (38 trials)	13,567	37,066
	AS	Deodhar et al, 2022 (A) [47]	Phase 2-3 (2 trials)	420	
	UC	Sandborn et al, 2023 [48]	Phase 2-4, LTE (6 trials)	1157	3000
	UC	Panés et al, 2024 [49]	Phase 2-4, LTE (6 trials)	1157	3202
BARI	RA	Taylor et al, 2022 [21]	Phase 1-4, LTE (10 trials)	3770	14,744
	AD	Bieber et al, 2023 [50]	Phase 2-4, LTE (8 trials)	2636	4628
	AA	King et al, 2023 [51]	Phase 2-3, LTE (2 trials)	1303	1868
	SLE	Morand et al, 2023 [52]	Phase 2-3, LTE (4 trials)	2164	1655
UPA	RA	Cohen et al, 2021 [53]	Phase 3 (5 trials)	3834	4020
	AD	Guttman-Yassky et al, 2023 [54]	Phase 2-3, LTE (4 trials)	2485	2787
	RA/PsA/AS/AD	Burmester et al, 2023 [19]	Phase 2-3, LTE (12 trials)	6991	15,425
	RA	Fleischmann et al, 2023 [25]	Phase 3 (6 trials)	3209	10,135
FILGO	RA	Winthrop et al, 2022 [22]	Phase 2-3, LTE (5 trials)	3691	6081
	UC	Schreiber et al, 2023 [79]	Phase 2-3, LTE (3 trials)	1348	3326
	RA	Burmester et al, 2024 [55]	Phase 2-3, LTE (5 trials)	3691	12,541
PEFI	RA	Takeuchi et al, 2021 [56]	Phase 2-3, LTE (4 trials)	1052	2336
	RA	Tanaka et al, 2022 [57]	Phase 2-3, LTE (4 trials)	1052	2999
ABRO	AD	Simpson et al, 2021 [58]	Phase 2-3, LTE (6 trials)	2856	1641
	AD	Simpson et al, 2024 [59]	Phase 2-3 (8 trials)	2089	2109

A, abstract; AA, alopecia areata; ABRO, abrocitinib; AD, atopic dermatitis; AS, ankylosing spondylitis; BARI, baricitinib; FILGO, filgotinib; JAKi, Janus kinase inhibitor; LTE, long-term extension study; PEFI, peficitinib; PsA, psoriatic arthritis; PsO, psoriasis; PY total, total patient-years of exposure; RA, rheumatoid arthritis; SLE, systemic lupus erythematosus; TOFA, tofacitinib; UC, ulcerative colitis; UPA, upadacitinib.

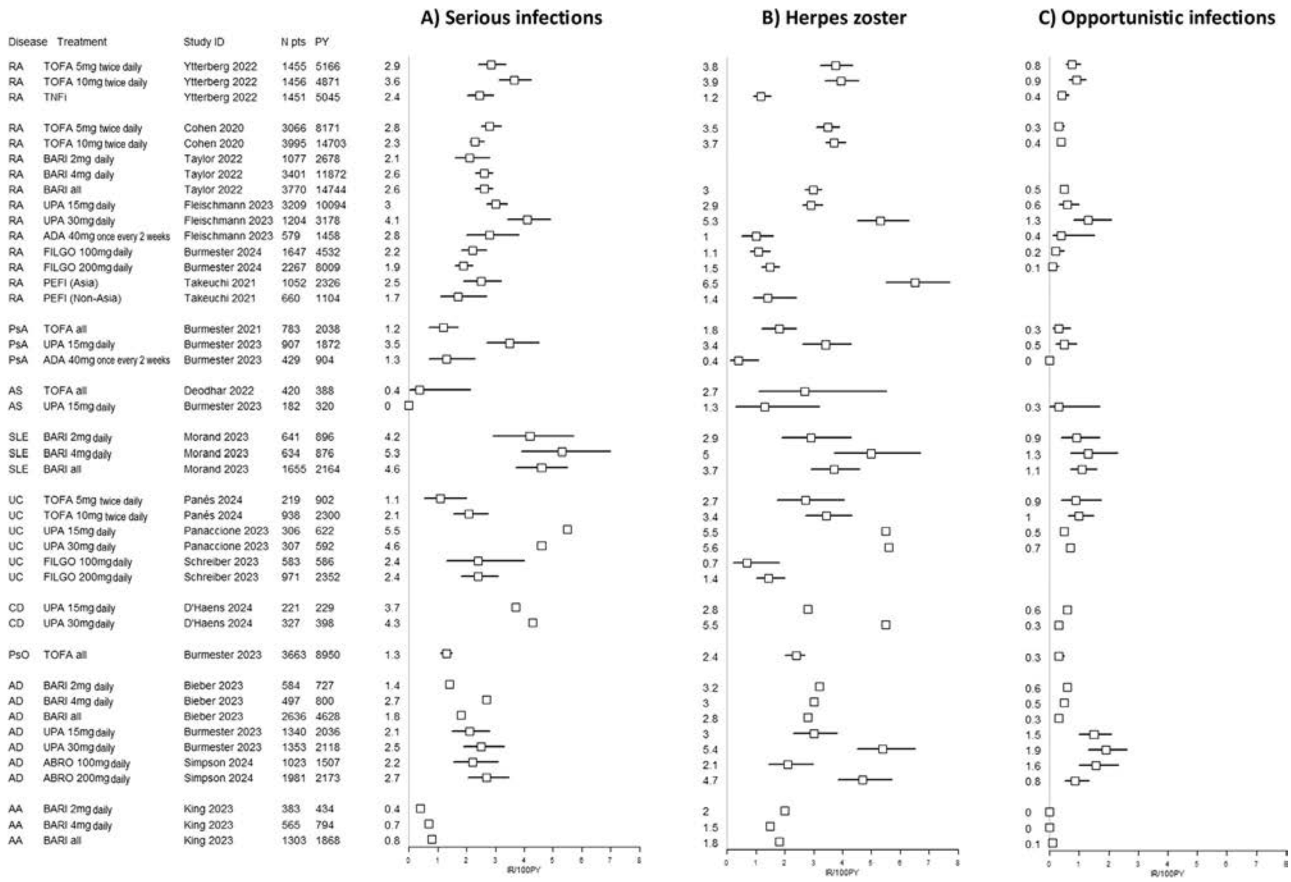

Figure 2. Infection rates in ORAL Surveillance and integrated safety analyses of randomised controlled trial (RCT) data. Event rates are shown as censored incidence rates per 100 patient-years of exposure (IR/100PY) or as events per 100 patient-years (E/100PY) for upadacitinib (UPA) in ulcerative colitis (UC) and Crohn's disease (CD) [61,62]. AA, alopecia areata; ABRO, abrocitinib; AD, atopic dermatitis; ADA, adalimumab; AS, ankylosing spondylitis; BARI, baricitinib; FILGO, filgotinib; PEFI, peficitinib; PsA, psoriatic arthritis; PsO, psoriasis; PY, patient-years of exposure; RA, rheumatoid arthritis; SLE, systemic lupus erythematosus; TOFA, tofacitinib; TNFi, tumour necrosis factor alpha inhibitor.

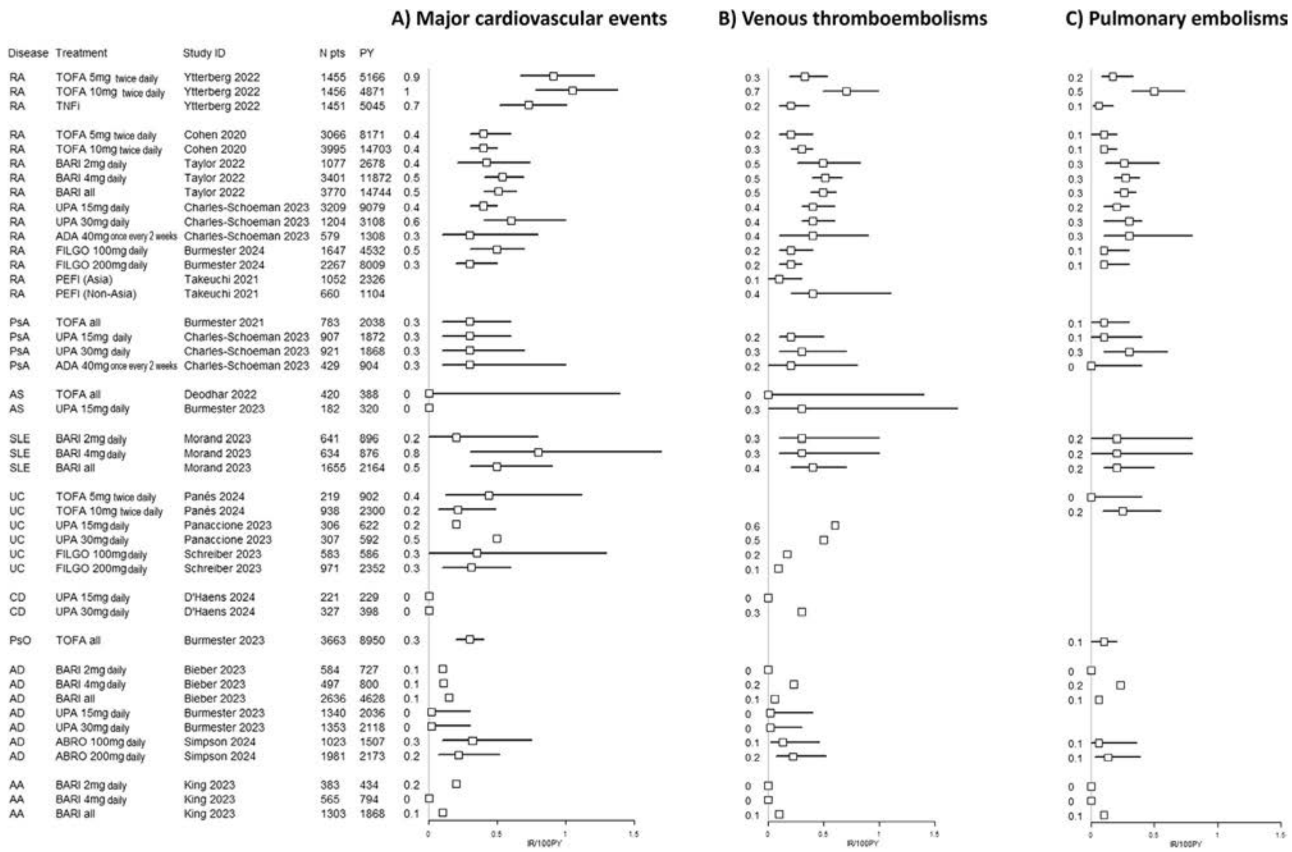

Figure 3. Major cardiovascular events and thromboembolic events in ORAL Surveillance and integrated safety analyses of randomised controlled trial (RCT) data. Event rates are shown as censored incidence rates per 100 patient-years of exposure (IR/100PY) or as events per 100 patient-years (E/100PY) for upadacitinib (UPA) in ulcerative colitis (UC) and Crohn's disease (CD) [61,62]. Venous thromboembolisms include deep vein thrombosis (DVT) and pulmonary embolisms (PE); PE rates for filgotinib (FILGO) in rheumatoid arthritis (RA) from Winthrop et al [22]. AA, alopecia areata; ABRO, abrocitinib; ADA, adalimumab; AD, atopic dermatitis; AS, ankylosing spondylitis; BARI, baricitinib; PEFI, peficitinib; PsO, psoriasis; PsA, psoriatic arthritis; PY, patient-years of exposure; SLE, systemic lupus erythematosus; TNFi, tumour necrosis factor alpha inhibitor; TOFA, tofacitinib.

Cohort and claims registries

Twenty-one cohort studies were additionally presented to the task force, of which 15 compared JAKi with biologic disease-modifying antirheumatic drugs (bDMARDs), 5 compared JAKi with conventional synthetic disease-modifying antirheumatic drugs (csDMARDs), and 4 compared one JAKi with another JAKi. Seventeen studies assessed patients with RA, 1 assessed patients with PsA, 1 assessed patients with UC, and 3 included various IMIDs. Twelve studies had a prospective, and 9 had a retrospective character. Seventeen analyses of claims data were additionally included, of which 13 studied patients with RA, 2 studied UC, 1 studied AA, and 1 various IMIDs (Supplemental Appendix; Sections 6.1 and 7.1).

The largest registries available for patients with RA using disease-modifying antirheumatic drugs (DMARDs) were the US claims cohorts (up to 130,718 patients) [29,30,66,67] as well as US Corrona registry (10,357 patients) [68], the German RABBIT registry (13,991 patients) [69,70], the Swedish ARTIS registry (27,610 patients) [27,28,71], the French SNDS registry (15,835 patients) [72], as well as the Korean national health insurance database for UC (21,821 patients) [73,74]. Median follow-up times commonly ranged from 6 months to 1 or 2 years, although patients on JAKi were usually numerically underrepresented and sometimes followed for shorter periods of time compared with csDMARD- or bDMARD-treated patients in these databases, due to their later introduction to the markets. Because of that, cohort and claims data were also predominantly available for TOFA and BARI, the earlier JAKi.

Adverse events of special interest

Serious infections

A dose-dependent increase in SIE was observed over time in ORAL Surveillance, especially in elderly patients. Crude hazard ratios (cHRs) against TNFi were 1.29 (95% CI, 0.94-1.79) and 1.08 (95% CI, 0.74-1.58) for TOFA 5 mg twice daily, as well as 1.44 (1.05-1.99) and 1.55 (95% CI, 1.10-2.19) for TOFA 10 mg twice daily, in patients aged ≥50 years and ≥65 years, respectively. IRs of 2.9, 3.6, and 2.4/100PY were observed in the overall trial population, as well as of 4.0, 5.9, and 3.7/100PY in patients aged ≥65 years, in the TOFA 5-mg twice daily, in the TOFA 10-mg twice daily, and in TNFi arms, respectively [13,75].

This dose dependence for SIE in elderly patients was also established in integrated safety data on TOFA [76], albeit not in the overall RA population [45], as well as for BARI [21,50,77], UPA [25,78], and PEFI in Asia [57], for BARI in SLE [52], and for TOFA in UC [49]. No dose dependence was established for FILGO in RA and UC [55,79]. In general, IRs were higher in RA and in SLE compared with other conditions (Fig 2A) [19,20,52].

Aside from age, underlying disease entity and comorbidities, baseline glucocorticoid (GC) dose, geographic region, male sex, body mass index, and lymphopenia were identified as important risk factors for SIE [13,20,45,75,77]. Commonly observed SIE in RCTs were pneumonia, serious HZ, urinary tract infection, and serious COVID-19 infection [19,45,77]. LTE studies did not show an increased risk for SIE over time [21,22,45,63,65,77,80].

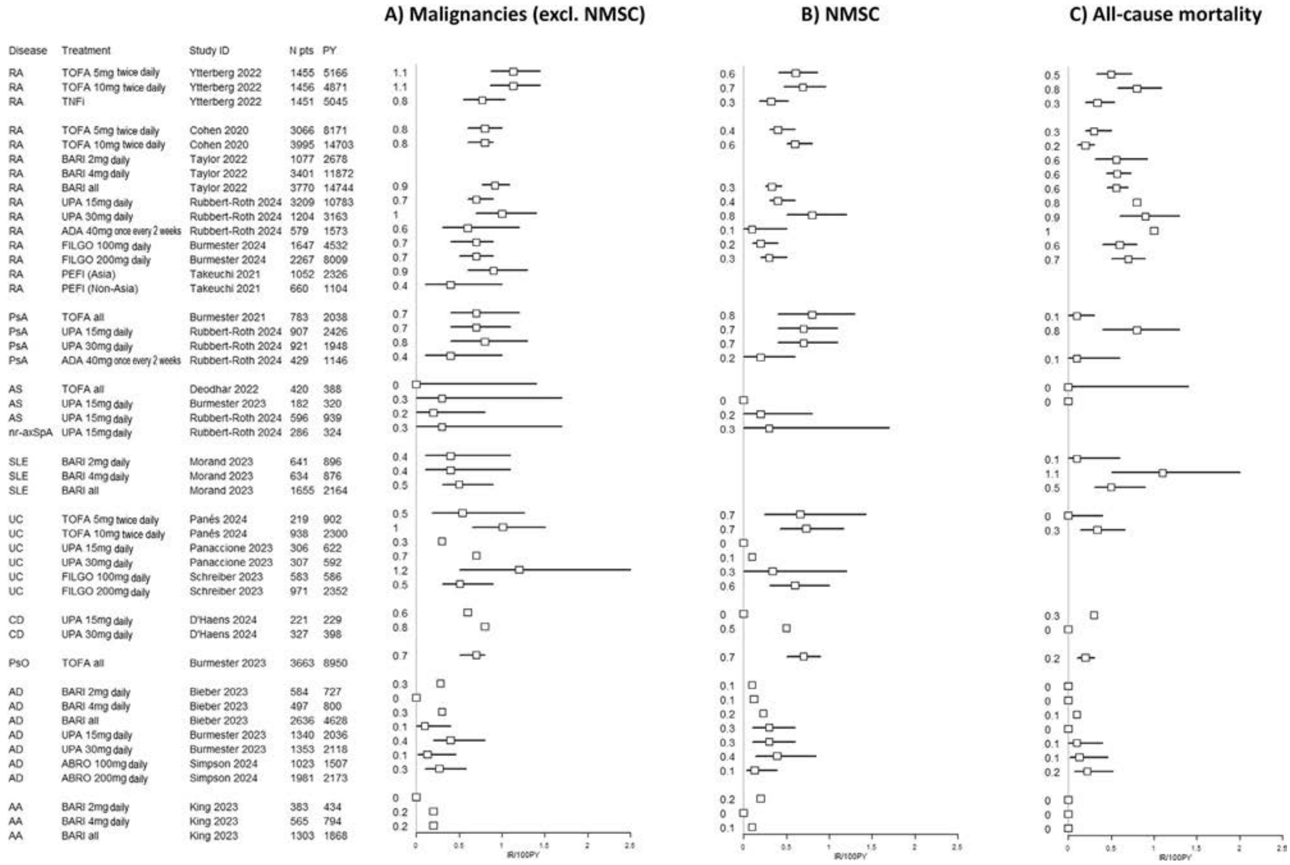

Figure 4. Malignancies and all-cause mortality in ORAL Surveillance and integrated safety analyses of randomised controlled trial (RCT) data. Event rates are shown as censored incidence rates per 100 patient-years of exposure (IR/100PY) or as events per 100 patient-years (E/100PY) for upadacitinib (UPA) in ulcerative colitis (UC) and Crohn's disease (CD) [61,62]. Mortality rates for UPA in psoriatic arthritis (PsA) from Burmester et al [19]. AA, alopecia areata; ABRO, abrocitinib; ADA, adalimumab; AD, atopic dermatitis; AS, ankylosing spondylitis; BARI, baricitinib; FILGO, filgotinib; NMSC, nonmelanoma skin cancer; PEFI, peficitinib; PsO, psoriasis; PY, patient-years of exposure; RA, rheumatoid arthritis; SLE, systemic lupus erythematosus; TNFi, tumour necrosis factor alpha inhibitor; TOFA, tofacitinib.

Cohort and claims data were largely consistent with integrated safety data. No significant associations with increased risks for SIE were observed in various analyses comparing JAKi with bDMARDs or csDMARDs [27,68,81−84]. In a large observational study of 6278 and 124,440 TOFA and bDMARD initiators from 3 US claims registries, SIE rates were comparable between TOFA and most bDMARDs (TOFA vs ADA: adjusted HR [adjHR], 1.06; 95% CI, 0.87-1.30), albeit higher than that with ETA (adjHR, 1.41; 95% CI, 1.15-1.73) and lower than that with infliximab (adjHR, 0.81; 95% CI, 0.65-1.00) [66].

Herpes zoster

Risk of HZ infections was increased with JAKi both in RCT as well as in registry data [13,25,29,52,66]. Weighted HR (wHR) were 3.82 (95% CI, 2.05-7.09) for BARI vs ETA, and 4.00 (95% CI, 1.59-10.06) for TOFA vs ETA, in a prospective multicentre RA cohort from Sweden (34,279 treatment episodes) [27], as well as 3.66 (95% CI, 2.38-5.63) for JAKi vs csDMARDs in the German RABBIT registry (713 patients with RA on JAKi and 3851 on csDMARD therapy) [69].

In ORAL Surveillance, cumulative probabilities for HZ increased predominantly in the first 6 months and subsequently plateaued [75]. No cumulation of events was observed over time in LTE studies [21,45,77,80].

Important risk factors for HZ infections were age and geographic region, with significantly higher rates observed in elderly patients as well as in Asian populations [44,57,75]. Other relevant risk factors were smoking, prior DMARD exposure, and the underlying disease entity, with higher rates in RA and UC vs PsA or PsO [20,85,86] or in AD vs AA [51], while conflicting data were found on the impact of concomitant GC or csDMARD background therapies [45,78,87]. Compared with other JAKi, ERs were lower with FILGO, and no dose dependence was observed in integrated safety data (Fig 2B) [55,79].

Across all studies, HZ cases were mostly mild and involved only a single dermatome, but disseminated manifestations and complications like ocular or ophthalmic involvement, zoster meningitis, and persistent neuralgia were also observed [19,21,78,88]. HZ vaccination rates were low (<10%) in all JAKi trials [53].

Opportunistic infections

OIEs were heterogeneously defined across studies, and inclusion and exclusion of at-risk patients as well as adjudication or external reviews of events varied, which complicates the comparison of results. Most commonly, multidermatomal and/or disseminated HZ events were considered as OIEs, whereas oral candidiasis was not included, and TB cases were analysed separately.

In general, OIEs were infrequent across all study populations, but numerically higher in patients with UC, SLE, and AD than in other cohorts (Fig 2C) [20,48]. Commonly reported OIEs were disseminated HZ and oesophageal candidiasis, as well as eczema herpeticum (Kaposi varicelliform eruption) in AD [19].

In ORAL Surveillance, cHRs against TNFi were 1.82 (95% CI, 1.07-3.09) and 2.17 (95% CI, 1.29-3.66), potentially due to higher rates of opportunistic HZ infections in the TOFA arms [13]. A dose dependence was established for TOFA and UPA in UC and RA [19,20,49,53,61], as well as for UPA in AD, due to higher rates of eczema herpeticum in the UPA 30-mg every day arm [19]. This dose dependence was not observed for BARI in RA or AD [50,77], where patients with a history of eczema herpeticum were excluded [89], and also not for ABRO in AD [59]. As with HZ, IRs were numerically lower for FILGO compared with other JAKi in RA [22,55,90].

Tuberculosis

No significant risk increase for TB infections or reactivations was observed for JAKi compared with bDMARDs. A total of 38 and 210 active and latent TB cases were reported in the overall TOFA trial programme, most of them in endemic regions. Of those latent cases receiving prophylaxis, 4 developed active TB during the study, all in the TOFA 10-mg twice daily arm [45]. In ORAL Surveillance, 1 active TB case was reported in the TOFA 5-mg twice daily arm and 5 in the TOFA 10-mg twice daily as well as 5 in the TNFi arm, respectively [13]. Similarly, ERs were low for TOFA in other diseases (1 case in PsO; no cases in PsA or UC) [20], as well as for other JAKi, with IR of 0.1/100PY or lower observed in RA, PsA, AS, and UC for UPA [19,61,78], as well as in RA and SLE for BARI [21,52], and no cases observed for BARI and ABRO in AD or AA [50,51,58]. Comparisons with bDMARD showed numerically lower rates for UPA vs ADA in RA [19,53].

In observational data, wHR of 0.60 (95% CI, 0.22-1.62) was estimated for TB infections for TOFA vs TNFi, as well as 0.25 (95% CI, 0.09-0.73) for OIE, for JAKi vs TNFi, in Taiwanese and in Korean national health registry data [91,92].

COVID-19

BARI is approved for treatment of hospitalised patients with COVID-19 [93], and positive data had also been published for TOFA [94]. On the contrary, increases in COVID-19−related morbidity and mortality were observed both in RCTs on JAKi that were conducted during the pandemic, as well as in observational data.

Serious and fatal COVID-19 was observed in 28.4% and 4.2% of patients on UPA 15 mg every day in RA and 31.2% and 6.5% on UPA 15 mg every day in PsA, respectively, compared with 15.6% and 0% on ADA in RA, 9.1% and 0% on MTX in RA, and 10.8% and 0% on ADA in PsA [19]. In the UPA RA programme, COVID-19−related pneumonia was observed in 2.3% of patients on UPA 15 mg every day, compared with 0.3% on ADA and 0.6% on MTX [25].

The COVID-19 global alliance registry (2869 patients with RA on biologic or targeted synthetic DMARD therapy) showed higher odds ratios (ORs) for COVID-19−related hospitalisations for JAKi and rituximab (RTX) vs other bDMARDs (OR, 2.06; 95% CI, 1.60-2.65, for JAKi vs TNFi; OR, 4.15; 95% CI, 3.16-5.44, for RTX vs TNFi) [95], and an adjHR of 1.81 (95% CI, 1.09-3.01) for hospitalisations was observed in the nationwide British cohort study (181,694 patients with IMID on standard therapies, 871 patients on JAKi) [96], as well as of 1.19 (95% CI, 1.00-1.42) in the TriNetX database, a retrospective analysis of globally collected electronic health record (EHR) data (2676 propensity score−matched pairs of patients with RA on JAKi vs TNFi) [97]. Overall rates of COVID-19 infections were comparable between JAKi and bDMARD groups in these studies [19,97], and it is to date unclear whether JAKi should be discontinued after COVID-19 infection, as subsequent effects on immunomodulation are unclear [98].

Other infections

Analyses of influenza rates with TOFA in the RA, PsA, and UC trial programmes showed higher overall infection rates in UC, but comparable rates within indications for TOFA, PLC, or active comparators, albeit numerically lower with ADA in PsA. Most influenza cases were nonserious, and no clear age or dose dependence was established [99].

Respiratory events were comparable over a 1-year to 2-year follow-up period in 28 and 19 patients with RA and ILD treated with JAKi or RTX, respectively, in a retrospective single-centre cohort study [100]. No increased risk for *Clostridium difficile* infections or associated complications was observed with TOFA in the UC programme [101].

MACEs

ORAL Surveillance showed a numeric increase of MACE (CV death, nonfatal myocardial infarction, and nonfatal stroke) with TOFA vs TNFi, and noninferiority of TOFA vs TNFi was not met in this study (cHR, 1.33; 95% CI, 0.91-1.94, for combined TOFA vs TNFi) [13], which had until then not been observed in smaller RCT or registry data on JAKi [20,45]. Indeed, IR were higher in ORAL Surveillance compared with RCTs (Fig 3A). One reason for this lies likely within patient populations included, with ORAL Surveillance studying a large at-risk cohort of 4362 patients for more than 3 years, while efficacy RCTs commonly include a much smaller and highly selected patient population with a more favourable CV risk profile and are conducted with much shorter follow-up periods [13,23,24,102,103]. Of note, a similar trial was performed to compare tocilizumab, an anti−interleukin (IL)-6 receptor antibody, with TNFi, where no difference in MACE or malignancies was observed, albeit higher overall ERs compared with those in ORAL Surveillance [104].

Within the ORAL Surveillance cohort, MACEs were predominantly observed in elderly patients with a history of smoking or other CV risk factors, and significant risk differences between the JAKi and TNFi occurred predominantly in these subgroups (cHR, 1.98; 95% CI, 0.95-4.14, in patients with a history of atherosclerotic CV diseases [hxASCVDs]; vs cHR, 1.14; 95% CI, 0.73-1.78, in those without hxASCVDs) [13,23,105−108]. Comparable trends were also observed in trial development programmes, where stratified analyses of CV events were subsequently repeated [24,102,103,109,110]. The continued ADA arm in the SELECT COMPARE study on UPA enabled a post hoc analysis of safety outcomes comparable with the ORAL Surveillance design, albeit of course not powered for these safety outcomes. Moreover, ERs were higher in patients at risk or with a history of CV events, while HR were comparable between UPA and ADA in this study [25].

Concerning dosage, a dose dependence for MACE was observed for TOFA in ORAL Surveillance [13], but not in RCT data in RA and UC [45,48,49], and a dose dependence was seen for BARI and UPA in RA and SLE [21,23,52,53], but not in PsA, AD, or AA [19,23,50,51,57]. No dose dependence was established for FILGO in RA and in UC [55,79], but higher ERs were again observed in elderly patients and in those with unfavourable CV disease risk profiles [111−114]. Data were consistent also for other JAKi, shown in the Supplemental Appendix (Section 8) [56,88,115].

Various cohort and claims studies investigating CV outcome in routine care populations have recently been published, like the Safety of Tofacitinib in Routine Care Patients With Rheumatoid Arthritis (STAR-RA) trial, an analysis of US claims data [30], as well as data from the US Corrona registry [68], and prospective multicentre cohorts from Sweden and Germany [27,70]. In summary, no associations with increased risks were observed for JAKi vs TNFi in these studies, also when adjusting for various baseline covariates [27,30,68,70,72,74,83,84,91,116,117]. STAR-RA included an RCT duplicate cohort where the ORAL Surveillance trial design was emulated. As in ORAL Surveillance, wHR for TOFA vs TNFi were higher in a CV risk−enriched population (wHR, 1.24; 95% CI, 0.90-1.69, in the RCT duplicate cohort; vs 1.01, 95% CI, 0.83-1.23, in the overall population), although comparability is of course limited due to the retrospective character of the analysis [30].

VTEs

Interim analyses of the ORAL Surveillance study showed increased rates of pulmonary embolisms (PEs) and ACM with TOFA 10 mg twice daily, which had also not been observed previously in efficacy trials [12,67,118], and led to a mandatory dose reduction to TOFA 5 mg twice daily in the ongoing safety trial in 2019 [42].

Pathophysiologic mechanisms that drive thromboembolic events with JAKi as well as biomarkers to predict disease onsets are elusive to date [119]. In general, risk for thromboembolic events is higher in patients with autoimmune diseases [120], and as described previously for MACE, baseline CV risk was identified as a major risk factor [42,106], as were age, history of VTE, and concomitant therapies like oral contraceptives or GC [42,45,121,122]. Moreover, treatment dosing was important, as observed, for example, for TOFA in ORAL Surveillance [13,122], as well as in the TOFA trial programmes in RA and UC [45,123], whereas drawing clear conclusions on dose dependence from RCT data in general were difficult due to low overall ERs in most trials (Fig 3B) [19−21,45,47,49−52,55].

Interestingly, it was predominantly PE events that drove risk differences between TOFA and TNFi in ORAL Surveillance, whereas deep vein thrombosis (DVT) rates seemed comparable between study groups [13]. The same was observed in a large multicentre cohort study from Sweden, where a total of 2249 and 30,383 patients starting JAKi or bDMARDs were prospectively followed for a median of 2 years. AdjHR for JAKi vs TNFi were 1.73 (95% CI, 1.24-2.42), 3.21 (95% 2.11-4.88), and 0.83 (95% CI, 0.47-1.45), for VTE, PE, and DVT, respectively, indicating a significant risk association for VTE and especially PE, but not DVT, in this observational study [71].

Significant risk increases for VTE were also observed for BARI vs TNFi, in a pooled analyses of 14 registry and claims databases from Europe, the United States, and Japan, with an IR ratio (IRR) of 1.51 (95% CI, 1.10-2.08) estimated in 7606 propensity score−matched pairs [83]. This risk difference was in fact predominantly driven by the aforementioned Swedish cohort (the ARTIS registry) as well as data from the French national health insurance registry (SNDS database), where cHR and adjHR for inpatient VTE of 1.9 (95% CI, 1.2-2.8) and 1.2 (95% CI, 0.8-1.8) were estimated for TNFi vs ADA, in 8481 and 7354 patients, respectively [72]. Within the SNDS cohort, a case-control substudy was performed on 92 patients with IMIDs (predominantly RA) on JAKi, who had experienced at least 1 thromboembolic event during the follow-up period. An association with higher risk for VTE was observed after start of JAKi therapy (IRR, 8.27; 95% CI, 3.41-20.04), as well as up to 30 days after stopping the treatment [124].

ATEs

Aside from MACE, fewer data were available on ATEs. No increased risk was observed for ATEs in ORAL Surveillance (cHR, 1.12; 95% CI, 0.74-1.70; and cHR, 1.14; 95% CI, 0.75-1.74 for TOFA 5 mg twice daily and TOFA 10 mg twice daily vs TNFi, respectively) [13], but IRs were again higher in the safety trial compared with the RA trial programme (0.92, 0.94, and 0.82/100PY for TOFA 5 mg twice daily, TOFA 10 mg twice daily, and TNFi in ORAL Surveillance, vs 0.4/100PY in integrated TOFA RCT data) [13,45], and elevated in CV risk−enriched patients in the pooled RA population [42].

Malignancies (excluding NMSC)

Malignancies (excluding NMSC) were the second major endpoint analysed in the ORAL Surveillance trial, and as for MACE, noninferiority of TOFA vs TNFi could not be shown (cHR, 1.48; 95% CI, 1.04-2.09, for combined TOFA vs TNFi) [13].

Hypotheses to explain that differences reached from protective effects of TNFi to oncogenic potentials of JAKi, for example, via involvements in the Natural killer (NK)-cell metabolisms downstream JAK-STAT pathways [1,26,125,126]. As for MACE and VTE, subgroup analyses showed higher ERs in distinct at-risk cohorts (higher age, smoking, geographic region, comorbidities, and suboptimal CV risk profile) [26,106], and ORAL Surveillance detected an increased risk for lung cancers (cHR, 2.17; 95% CI, 0.95-4.93), which were the most commonly observed malignancies in the TOFA arm, whereas breast cancers were most commonly seen with TNFi [13,26]. IRs were again generally lower in the trial programmes, and dependent amongst other factors on the patient population studied (Fig 4A) [19,20,47,52,50,51,125].

Lung cancers, breast cancers and gastrointestinal cancers were also the most commonly reported malignancies in the trial development programmes [19,21], and no increased risk for lymphomas was observed with JAKi to date [25,54,61,125]. Registry data did not show associations with increased risks for malignancies (excluding NMSC) with JAKi so far (Table 2) [28,29,68,82,84,91,116,127]. In STAR-RA, wHR of 1.01 (95% CI, 0.83-1.22) and 1.17 (95% CI, 0.85-1.62) were estimated in the real-world cohort as well as in the RCT duplicate cohort [29], and an adjHR of 0.94 (95% CI, 0.65-1.38) was recently reported in a prospective, longitudinal cohort study comparing JAKi (predominantly TOFA and BARI) with TNFi in the nationwide Swedish RA registry [28].

These data need to be interpreted in consideration of the timeframes when malignancies started to occur in ORAL Surveillance [13]. Post hoc analyses showed that risk curves for TOFA and TNFi only started to diverge after 2 to 3 years (cHR for months 0-18, 0.93; 95% CI, 0.53-1.62; vs cHR for months 18 onwards, 1.93, 95% CI, 1.22-3.06; interaction P = .0469) [13,26]. Shorter follow-up times therefore do not allow for detection of middle- to long-term effects or risk accumulation over time in cohort and claims studies. An overview of these studies comparing JAKi with active comparators as well as their respective follow-up times is provided in Table 2.

NMSC

For NMSC, numeric increases were observed both in the ORAL Surveillance trial as well as in integrated safety data and in registry data, and IRs were comparable between the safety trial and RCT data (Fig 4B) [13,19,20,47,50−52,125].

The most commonly reported NMSC events in ORAL Surveillance were basal and squamous cell carcinomas, with unexpectedly high rates of especially squamous skin cancers observed in the safety trial. Age and dosage were again observed as important risk factors [26]. A dose dependence was also established for UPA in RA, but not in PsA [125], as well as for FILGO in elderly patients [111]. IRs were generally lower in axSpA, CD, AD, and AA [19,47,50,51,62,125].

Table 2

Registry databases comparing malignancy rates (excluding nonmelanoma skin cancer [NMSC]) on JAKi with active comparators[a]

Study ID	Comparison	No. Of patients	Hazard ratio (95% CI)	Mean follow-up time
Kremer et al, 2021 [68]	TOFA vs bDMARDs	TOFA: 1420 bDMARD: 4820	adjHR, 1.04 (0.68-1.61)	TOFA: 1.58 y TNFi: 1.54 y
Khosrow-Khavar et al, 2022 (STAR-RA) [29]	TOFA vs TNFi (RCT duplicate cohort)	TOFA: 10,504 TNFi: 72,791 (TOFA: 2706) (TNFi: 24,329)	wHR, 1.01 (0.83-1.22) (wHR, 1.17 [0.85-1.62])	TOFA: 10 mo TNFi: 11 mo
Hirose et al, 2022 [127]	TOFA vs ABA	TOFA: 187 ABA: 183	TOFA, 0 malignancies ABA, 1 malignancy	TOFA/ABA: 1 y
Fang et al, 2022 [91]	TOFA vs TNFi	TOFA: 822 TNFi: 2357	TOFA IR, 0.39/100PY TNFi IR, 0.35/100PY	JAKi: 2.02 y TNFi: 2.10 y
Min et al, 2023 [116]	JAKi vs TNFi	JAKi: 2498 TNFi: 9267	adjHR, 0.59 (0.39-0.89)	–
Uchida et al, 2023 [82]	JAKi vs TNFi	JAKi: 296 TNFi: 203	adjHR, 0.39 (0.1-1.55)	1.3 y (median)
Mok et al, 2023 [84]	JAKi vs TNFi	JAKi: 551 TNFi: 1920 (treatment courses)	adjHR, 0.87 (0.39-1.95)	Duration of treatment courses
Huss et al, 2023 [28]	JAKi vs TNFi	JAKi: 1967 TNFi: 7343 other bD: 3520	adjHR, 0.94 (0.65-1.38)	JAKi: 1.95 y TNFi: 2.83 y other bD: 2.49 y (median)

ABA, abatacept; adjHR, adjusted hazard ratio; bDMARD/bD, biologic disease-modifying antirheumatic drug; IR, incidence rate; JAKi, Janus kinase inhibitor; PY, patient-years of exposure; STAR-RA, Safety of Tofacitinib in Routine Care Patients With Rheumatoid Arthritis; TNFi, tumour necrosis factor alpha inhibitor; TOFA, tofacitinib; wHR, weighted hazard ratio.

[a] Hazard ratios as well as mean/ median follow-up periods are given.

Observational studies found conflicting results. A wHR of 1.15 (95% CI, 0.96-1.39) was observed in the overall STAR-RA cohort for TOFA vs TNFi [29], and no significant risk increases were observed in US and Taiwanese claims cohorts [68,91], whereas a prospective RA cohort study from Sweden estimated an adjHR of 1.39 (95% CI, 1.01-1.91) for JAKi (predominantly TOFA and BARI) vs TNFi, which was not seen for non-TNFi bDMARDs vs TNFi (adjHR, 1.00; 95% CI, 0.78-1.28). The study also showed a numeric trend towards risk accumulation over time, in a median follow-up period of about 2 years [28].

ACM

The most commonly observed causes of death across various analyses were CV events, SIE, respiratory disorders, and malignancies [22,45]. ACM was higher with TOFA than with TNFi in ORAL Surveillance, although a significant difference was only observed in the TOFA 10-mg twice daily arm (cHR, 1.49; 95% CI, 0.81-2.74 with TOFA 5 mg twice daily vs TNFi; and cHR, 2.37; 95% CI, 1.34-4.18 for TOFA 10 mg twice daily vs TNFi) [13]. A numeric risk increase was again established in a CV risk−enriched population [106]. This trend was also observed in RCT data, for example, when stratifying by baseline CV risk in the SELECT trials on UPA in RA (IR 0.8-0.9/100PY in the overall population, vs 1.3-1.4 in CV at-risk patients) [25], or in the FINCH trials on FILGO in RA [112].

For trials conducted during the COVID-19 pandemic, an increased risk for COVID-19−related mortality was observed with JAKi vs active comparators, especially for UPA in the RA and PsA trials [19,25].

No clear trends on JAKi-related mortality were observed in most cohort studies [68,84,91,116]. A significant association with increased risk was found for BARI vs ETA in the Swedish ARTIS registry (wHR, 2.27; 95% CI, 1.51-3.40), but this was also observed for RTX, abatacept, and tocilizumab, whereas no risk increase was found for TOFA (wHR, 1.09; 95% CI, 0.40-2.92), in 1837 patients on BARI, 426 on TOFA, and 8748 on ETA, respectively [27]. In STAR-RA, cHR and wHR were 1.57 (95% CI, 1.31-1.90) and 1.20 (95% CI, 0.98-1.46) for TOFA vs TNFi, respectively, in 12,852 TOFA-treated and 89,411 TNFi-treated patients [30]. COVID-19−related mortality was higher with JAKi and RTX vs csDMARDs but not for TNFi vs csDMARDs in a prospective multicentre cohort from Sweden [128].

GIPs

Nine GIPs were adjudicated to TOFA 5 mg twice daily, 5 to 10 mg TOFA twice daily, and 4 to TNFi in ORAL Surveillance, resulting in IR of 0.17, 0.10, and 0.08/100PY for TOFA 5 mg twice daily, TOFA 10 mg twice daily, and TNFi, respectively [13]. In RA RCTs, 27 events were adjudicated to TOFA in the trial programme (7964 patients; IR 0.1/100PY) [20], and 9 cases were confirmed by medical review in the BARI programme (3770 patients; IR 0.06/100PY) [21]. Data for other JAKi were consistent with these findings, with reported IR of 0.1/100PY or lower [19,48,49,53], except for CD, where rates were higher due to the diseases general pathophysiologic phenotype [62]. For comparison, estimated IR from clinical trials on tocilizumab in RA were 0.19/100PY, calculated in 17,906 patients [129].

Acne

Significant increases in acne rates were observed with JAKi in AD and AA [130−132], and acne was the most commonly reported AE in the UPA 30-mg arm in AD (events observed in >10% of included patients) [19,133]. Increased risks were also observed for ABRO and BARI, although numerically lower than with UPA [134], and even higher rates were reported in AA (IR for BARI 4.5/100PY in AA vs 3.3/100PY in AD) [51,134].

This had not been observed in earlier JAKi trials or in ORAL Surveillance [13,21,53], but when reported more consistently, increased acne rates were also found for UPA in the UC and CD (up to 7% in the induction trials) [135,136], for DEUCRA across all diseases [137−140], as well as for various other compounds, in not only dermatologic but also rheumatologic conditions [141−145].

Overall, a recent meta-analysis calculated a weighted OR of 3.8 (95% CI, 2.76-5.32) across all JAKi and diseases, with highest risks estimated for preferentially JAK1 selective inhibitors

(ABRO und UPA), as well as in dermatologic vs nondermatologic conditions [7]. Most acne cases were mild and did not lead to treatment discontinuation or significant impacts of patients' health-related quality of life [133].

Reproductive health, pregnancy, and lactation

The impact of FILGO 200 mg every day on male reproductive health was assessed in the MANTA and MANTA-RAy studies, which were conducted due to safety signals detected in preclinical stage animal models [43]. The primary endpoint (≥50% decrease in sperm concentration at week 13) was met in 8 of 120 patients with FILGO 200 mg every day and 10/120 patients with PLC (Δ, −1.7%; 95% CI, −9.3% to 5.8%), and no significant impact of FILGO 200 mg every day on semen variables and sex hormones was therefore detected [41].

No new studies on female reproductive health or JAKi safety during pregnancy and lactation have been published since 2019 [12]. Additional data on outcomes of accidental pregnancies in trial development programmes were recently provided by sponsors, but they were beyond the scope of this review and commonly confounded by intake of background medications like MTX. Detailed summaries are provided elsewhere [146,147].

Hepatic disorders

In ORAL Surveillance, 46, 72, and 35 hepatic events were reported with TOFA 5 mg twice daily, TOFA 10 mg twice daily, and TNFi, respectively, without a significant risk increase established for the JAKi vs TNFi [13]. No dose dependence or systematic signals were detected for UPA in integrated safety data [19,53,65], and liver enzyme elevations were comparable between FILGO and MTX in an early RA population [148]. Across all trials, reported events were mostly abnormalities in liver function tests, while drug-induced liver injuries (DILIs) or Hy's law cases were generally infrequent [13].

One study assessed hepatitis B reactivations in the BARI trial programme and showed a positive hepatitis B virus (HBV) DNA (>29 IU/mL) in 3.7% of patients with serums markers suggestive of previous HBV infection, half of them meeting the criteria for HBV reactivation (HBV DNA, >100 IU/mL). BARI was permanently or temporarily stopped in the majority (75%) of cases with less than half also receiving antiviral treatment. No patients developed clinically evident hepatitis [149].

Conjunctivitis

Conjunctivitis is a commonly observed AE with dupilumab (DMB), an IL-4/13 inhibiting antibody licensed for the treatment of AD [150]. This was not seen with JAKi [50,151], and switching from DMB to UPA in 14 patients with DMB-associated conjunctivitis in a retrospective AD cohort study resulted in symptom resolution in all patients within 1 month [152].

Other safety outcomes

No increased risk for fractures or osteoporosis was observed in the TOFA trials [153], and analyses of bone mineral density over a 52-week treatment period with BARI showed stable to improved values in a prospective single-centre study [154].

No significant weight changes were observed with FILGO in the FINCH RA trials, and baseline body mass index did not significantly impact efficacy outcomes in this cohort [155]. AE related to gastrointestinal tolerability seemed numerically higher for ABRO compared with other JAKi, with, for example, nausea reported in 6.1% and 14.6% of patients with AD on ABRO 100 mg and ABRO 200 mg every day, respectively, vs 2.0% in the PLC arm [134].

Background therapies

The impact of background therapies on JAKi safety remains unclear to date. In a post hoc analysis of 6 phase 3 RA trials on TOFA, selected AESI were reported more frequently in studies that included background csDMARDs vs monotherapies [156], while similar ERs were observed in monotherapy and combination arms, for example, in the UPA trials, with exceptions being hepatic disorders and creatine phosphokinase (CPK) elevations [19,87]. No significant impact of background MTX on malignancies or HZ infections was observed in other distinct analyses [26,78].

Conflicting results were also found for GC treatment, which is a well-known risk factor for many AE and comorbidities and was associated with increased risks for SIE in ORAL Surveillance and integrated TOFA data [20,75], but, for example, not in post hoc analyses of the ORAL Strategy trial [157]. Both GC as well as MTX background therapies might impact vaccination response rates [158−160], but more data are needed to provide further insights.

Vaccine immunogenicity

Satisfactory humoral responses (≥2-fold increase in antibody titres) to pneumococcal vaccine (PCV-13) through weeks 4 to 12 were observed in patients on BARI and UPA in RCT substudies (68% with BARI and UPA 15 mg every day) [161,162], as well as in a prospective single-centre cohort study from Japan, where comparable response rates were seen for JAKi and MTX, whereas combination therapy slightly decreased humoral responses (90% on MTX, 95% on JAKi, 52% on MTX+ JAKi) [158]. Modest effects were found for live zoster vaccine in patients with RA on TOFA [159], but higher humoral immunogenicity was achieved with recombinant zoster vaccine in recent LTE substudies (88% of 4-fold increase in antibody titres on UPA 15 mg every day + MTX through week 16) [163], as well as in real-world cohorts [164−166]. Nonetheless, antibody titres were lower than those measured in healthy individuals in pivotal trials [167−169].

Concerning COVID-19 vaccinations, humoral response rates were comparable between JAKi and bDMARDs in various cohort studies, albeit generally lower in patients with IMIDs than those in healthy controls [160,170−172]. Vaccines were generally well tolerated, and serious adverse reaction or disease flares were infrequent. Data on infections disease outcomes of vaccinated patients were sparse [158−166,170−172].

Laboratory outcomes

A descriptive overview of mean changes in major laboratory outcomes across JAKi trials is provided in the Supplemental Appendix (Section 15.2; Supplemental Figs S1 and S2). For RA, we further performed meta-analyses of mean differences in haemoglobin, neutrophil, platelet, and low-density lipoprotein (LDL) changes through weeks 12 and 24, with active treatments vs PLC and/or MTX, which are shown in Figure 5 as well as in the Supplemental Appendix (Section 15.3; Supplemental Fig S3).

For some outcomes, like haemoglobin, leucocytes, or platelets, contrasting effects were observed for the various compounds, suggesting differences in signalling downstream selective JAK-STAT pathways, while others, like lipoproteins or transaminases, consistently changed across all JAKi trials, indicating a class effect.

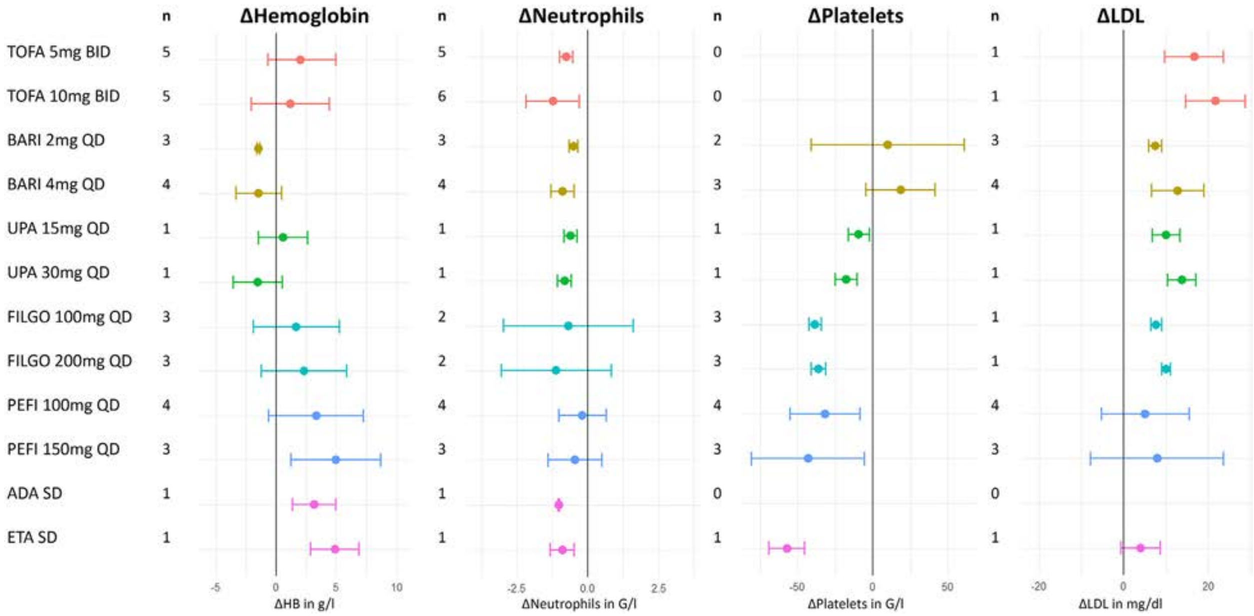

Figure 5. Meta-analysis of mean changes in laboratory outcomes through week 12, in randomised controlled trials on Janus kinase inhibitor (JAKi) in rheumatoid arthritis; figure shows mean differences of active treatment vs respective comparator arms (placebo and/or conventional synthetic disease-modifying antirheumatic drug). ADA, adalimumab; BID, twice daily; BARI, baricitinib; ETA, etanercept; FILGO, filgotinib; HB, haemoglobin; LDL, low-density lipoprotein; n, number of study arms analysed; PEFI, peficitinib; QD, once daily; SD, standard dose; TOFA, tofacitinib; UPA, upadacitinib.

Most changes in laboratory outcomes were mild to moderate and not related to clinically relevant adverse reactions. LDL increases paralleled with HDL increases, maintaining stable LDL:HDL ratios over time [173−175], and were not associated with increased atherogenicity or CV events [176−178], as well as responsive to statin therapy [176,179].

CPK elevations were common with JAKi (11.2% with TOFA in the UC programme), but mostly mild and not associated with an increased rates of myositis or rhabdomyolysis cases [19,20,180,181]. Mild to moderate increases in liver enzymes and creatinine levels were observed with JAKi, but not associated with decreases in hepatic or renal function [181,182]. Cases of hypophosphatemia were further observed in the FILGO trials [183].

Concerning haematologic parameters, slight decreases in haemoglobin levels were observed for UPA and BARI [181,184,185], whereas slight increases were seen for most other compounds [22,183,186]. Platelet levels transiently increased with BARI [184], while they commonly decreased with other JAKi [22,58]. Changes in neutrophils and lymphocytes were mostly mild, transient, and not associated with serious infections [181,183,184, 187], whereas the impact of JAKi on NK-cell activation and function needs further exploration, especially in light of the aforementioned concerns on malignancy outcomes with JAKi [126]. Only minimal changes were observed for DEUCRA, a selective Tyrosine Kinase 2 (TYK2) inhibitor [188−190].

DISCUSSION

We conducted a SLR on safety outcomes with JAKi, across all IMIDs in which JAKi have been approved (or studied) hitherto, to inform the 2024 update of the expert consensus statement on the treatment of IMIDs with JAKi (P. Nash et al, manuscript in press, Ann Rheum Dis, 2025). A large safety trial as well as integrated safety data of all major trial development programmes and LTE studies were considered; as were extensive analyses of registry data from cohort and claims studies, which complemented our work with a substantial amount of PYs collected in real-world conditions. Visualisation of ERs and mean changes in major laboratory outcomes across various compounds provides insights into differential pharmacodynamics of variously selective JAKi, as well as distinct effects that apply to the whole drug class, like increased rates of HZ infections or changes in lipid parameters and CPK levels.

The articles included in our summary need to be interpreted with consideration of their characteristics regarding data collection, analysis, and RoB. Even though integrated safety data include a large number of PYs of follow-up, they are nonetheless cumulative analyses of single efficacy trials, which are not powered for safety analyses. A highly selected patient population is usually followed up for about 12 to 52 weeks, with patients usually dropping out of the studies when adverse reactions occur, meaning that LTE predominantly include patients with good tolerability and treatment response. Furthermore, dose switching and rescue therapies are commonly allowed in LTE studies.

ORAL Surveillance, on the contrary, is a safety-endpoint trial that was better powered to detect differences in rates of rare events by following an at-risk cohort of approximately 4500 patients for more than 3 years. Different to efficacy trials, patients were asked to remain in the study despite treatment discontinuations due to AEs for further follow-up [13].

It was predominantly in these at-risk patients where AESI occurred in the safety trial, while more subtle safety impacts or risk accumulation over many years in younger patients without comorbidities remain elusive to date. Moreover, the noninferiority design of the trial on TOFA vs TNFi did not allow for differentiation between harmful impacts of the former and protective effects of the latter; in other words, are both TNFi and TOFA effective but TNFi more so?

Risk for AEs such as infections or CV events is generally higher in patients with IMIDs compared with the overall population due to chronic inflammatory loads as well as associated comorbidities and background therapies like MTX or GC [191−193]. Control of the active inflammatory disease therefore remains the major goal of immunotherapy, and JAKi clearly constitute highly effective tools in that context. Their use in patients with IMID therefore calls for a delicate balance of benefit and risk that needs to be addressed individually in every patient, a task that requires a clear overview of the distinct safety impacts that respective molecules have on the individual patients. Generation of these safety profiles was a major aim of our current work.

Our project is subject to 2 major limitations: first, only 1 researcher (VK) performed title and abstract screening as well as RoB assessments and data extraction. However, all doubts were discussed with the methodologist (AK) as well as the steering group, a panel of long-standing experts in the field. Second, inclusion and exclusion criteria varied across studies, and safety outcomes were not always consistently defined, as were methodological approaches to statistical analyses of safety outcomes, despite the latter having become more consistent in recent years for all major analyses. Additionally, on one hand, RCT data should always be interpreted in consideration of the highly selected patient population included, while real-world studies, on the other hand, are subject to common RoB, like bias by indication, information, detection, or confounding, which were diversely addressed across the considered studies.

This project's strength is clearly the broad overview of safety data across all indications and compounds. It is to date unclear to what extent findings from the ORAL Surveillance trial can be extrapolated to all JAKi and patient populations, but the complete review of the available literature allowed us to elaborate distinct safety signals for differently selective JAKi and in different patient cohorts, like contrasting changes in haematologic variables, higher HZ rates with UPA or ABRO compared with FILGO, or lower CV ERs and infections in younger patient populations, like axSpA or dermatologic conditions. We could also investigate dose dependences for various AESI, which clearly support use of the lowest effective doses. Moreover, positive data on prophylactic treatments, like HZ vaccination or consistent use of statins for CV risk prevention will be informative for treating physicians [163,194], as will be the overview of safety signals that are commonly observed with JAKi but do not usually result in clinically meaningful adverse reactions, like CPK elevations or creatinine changes.

Established standard operating procedures (SOPs), research checklists, and RoB tools were used in this project. As done previously, the task force was informed on the level of evidence for all PtCs, as well as the strength of all recommendations [31−33,35,37,38].

In summary, we provide here a comprehensive overview of safety outcomes with JAKi, which was presented to an international task force to update an expert consensus statement on the optimal use of JAKi in IMIDs. This synopsis is relevant in light of the extensive developments on JAKi safety and efficacy that have happened over the recent years, and shall provide a concise overview for treating physicians.

Competing interests

VK received speaker fees from Eli Lilly and AstraZeneca. JSS received grants from AbbVie, AstraZeneca, Eli Lilly, and Galapagos and speaker or consultancy fees from AbbVie, Amgen, Anada, Astro Pharma, BMS, Celltrion, Chugai, Eli Lilly, Gilead, Immunovant, MSD, Novartis, Pfizer, Roche, R-Pharma, Samsung, Sanofi, and UCB. PN received grants from AbbVie, BMS, Pfizer, Novartis, Eli Lilly, UCB, and Janssen and speaker or consultancy fees from Eli Lilly, Novartis, AbbVie, Pfizer, BMS, Novartis, Janssen, and UCB. DA received grants from Eli Lilly and Galapagos and speaker or consultancy fees from AbbVie, Gilead, J&J, Eli Lilly, MSD, Novartis, and Sandoz. KW received grants from BMS and Pfizer and speaker or consultancy fees from BMS, Pfizer, AbbVie, Union Chimique Belge (UCB), Eli Lilly & Company, Galapagos, GlaxoSmithKline (GSK), Roche, Gilead, Regeneron, Sanofi, AstraZeneca, Novartis, and Moderna. TD received grants from BMS, Eli Lilly, and J&J and speaker or consultancy fees from BMS, Eli Lilly, J&J, Pfizer, Novartis, Roche/GNE, and Remegen. RF received grants from AbbVie, BMS, Galvani, GSK, Gilead, Janssen, Eli Lilly, Novartis, Pfizer, and UCB and consultancy fees from AbbVie, Almirall, Artiva, Biotherapeutics, Atomwise, Biohaven, Pharmaceuticals, BMS, Cyoxone, Deep Cure, Dren Bio, Galvani, Gates Bio, Gilead, GSK, Halia, Immunovant, ImmuneMed, InventisBio, Istesso, Janssen, Janux, Eli Lilly, Monte Rosa, Novartis, Overland, Pfizer, Spyre, Synact, Teijin Pharma, TPG, UCB, Vyne, and Xencor. YT received grants from Mitsubishi Tanabe, Eisai, Chugai, and Taisho and speaker or consultancy fees from Eli Lilly, AstraZeneca, AbbVie, Gilead Sciences, Chugai, Boehringer Ingelheim, GlaxoSmithKline, Eisai, Taisho, BMS, and Pfizer. XB received speaker or consultancy fees from AbbVie, Alphasigma, Amgen, BMC, Cesas, Celltrion, Galapagos, Janssen, Eli Lilly, Moonlake, Novartis, Pfizer, Roche, Sandoz, Springer, Stada, Takeda, UCB, and Zuellig. IBM received grants from AbbVie, Amgen, BMS, Causeway Therapeutics, Cabaletta, Dextera, Eli Lilly, Gilead, Janssen, Novartis, Montai, Pfizer, Sanofi Regeneron, UCB, Compugen, AstraZeneca, and Moonlake and speaker or consultancy fees from AbbVie, Amgen, BMS, Causeway Therapeutics, Cabaletta, Dextera, Eli Lilly, Gilead, Janssen, Novartis, Montai, Pfizer, Sanofi Regeneron, UCB Pharma, Compugen, AstraZeneca, and Moonlake. MT received grants from Albireo, Alnylam, Cymabay, Falk Pharma, Genentech, Gilead, Intercept, MSC, Takeda, and UltraGenyx and speaker or consultancy fees from AbbVie, Agomab, Albireo, BiomX, Boehringer Ingelheim, Chemomab, Cymabay, Falk, Gilead, Genit, Hightide, Intercept, Ipsen, Janssen, LoopLab, Mirum, MSD, Novartis, Phenex, Pliant, Rectify, Regulus, Shire, and Siemens. NS received grants from AstraZeneca, Boehringer Ingelheim, Novartis, and Roche Diagnostics and speaker or consultancy fees from Abbott Laboratories, AbbVie, Amgen, AstraZeneca, Boehringer Ingelheim, Eli Lilly, Hanmi Pharmaceuticals, Janssen, Menarini-Ricerche, Novartis, Novo Nordish, Pfizer, Roche Diagnostics, and Sanofi. MdW received speaker fees from Evidera, UCB, Zürich Hospital, and the REMEDI Consortium. AK received speaker or consultancy fees from AbbVie, Eli Lilly, Gilead, Janssen, UCB, Galapagos, MSD, Novartis, and Pfizer. JP and JWS have nothing to declare.

Acknowledgements

The meetings for this work were supported by unrestricted grants from AbbVie, Galapagos, and Eli Lilly to the Medical University of Vienna. No representative of any of the companies was present at any of the meetings (neither in meetings for the initial nor in the course of the work for the updated consensus statements), and they had no influence on the wording of the recommendations. The support of Martina Seidel from the Vienna Medical Academy regarding the logistics of organising the meetings is also gratefully acknowledged.

Contributors

All authors contributed and finally approved the current manuscript. VK is the guarantor of the study. The guarantor accepts full responsibility for the work and the conduct of the study, had access to the data, and controlled the decision to publish the manuscript together with the methodologist (AK) and the convenor of the taskforce (JSS).

Funding

The meetings for this work were supported by unrestricted grants from AbbVie, Galapagos and Eli Lilly to the Medical University of Vienna. No representative of any of the companies was present at any of the meetings (neither in meetings for the initial nor in the course of the work for the updated consensus statements), and they had no influence on the wording of the recommendations.

Patient consent for publication

Owing to the nature of the analyses, this is not applicable for the current work. All patients gave informed consent to participation in the studies included and publication of study results.

Ethics approval

Owing to the nature of the analyses performed in this study, this is not applicable for the current project. All studies included in this work were approved by respective ethics committees.

Provenance and peer review

This manuscript was not commissioned and independently submitted to the journal by the authors. It underwent external peer review and editorial review.

Data availability statement

Not applicable because no datasets were generated for this study. All data relevant to the study are available in public and are included in the article or uploaded as online supplemental information.

Patient and public involvement

Patients and/or the public were not involved in the design, or conduct, or reporting, or dissemination plans of this research. Details are provided in the methods section.

Supplementary materials

Supplementary material associated with this article can be found in the online version at doi:10.1016/j.ard.2025.01.024.

REFERENCES

[1] Szekanecz Z, Buch MH, Charles-Schoeman C, Galloway J, Karpouzas GA, Kristensen LE, et al. Efficacy and safety of JAK inhibitors in rheumatoid arthritis: update for the practising clinician. Nat Rev Rheumatol 2024;20(2):101–15.
[2] Bonelli M, Kerschbaumer A, Kastrati K, Ghoreschi K, Gadina M, Heinz LX, et al. Selectivity, efficacy and safety of JAKinibs: new evidence for a still evolving story. Ann Rheum Dis 2024;83(2):139–60.
[3] Vincenti F, Tedesco Silva H, Busque S, O'Connell P, Friedewald J, Cibrik D, et al. Randomized phase 2b trial of tofacitinib (CP-690,550) in de novo kidney transplant patients: efficacy, renal function and safety at 1 year. Am J Transplant 2012;12(9):2446–56.
[4] Winthrop KL. The emerging safety profile of JAK inhibitors in rheumatic disease. Nat Rev Rheumatol 2017;13(4):234–43.
[5] Atzeni F, Popa CD, Nucera V, Nurmohamed MT. Safety of JAK inhibitors: focus on cardiovascular and thromboembolic events. Expert Rev Clin Immunol 2022;18(3):233–44.
[6] Russell MD, Stovin C, Alveyn E, Adeyemi O, Chan CKD, Patel V, et al. JAK inhibitors and the risk of malignancy: a meta-analysis across disease indications. Ann Rheum Dis 2023;82(8):1059–67.
[7] Martinez J, Manjaly C, Manjaly P, Ly S, Zhou G, Barbieri J, et al. Janus kinase inhibitors and adverse events of acne: a systematic review and meta-analysis. JAMA Dermatol 2023;159(12):1339–45.
[8] Winthrop KL, Cohen SB. ORAL Surveillance and JAK inhibitor safety: the theory of relativity. Nat Rev Rheumatol 2022;18(5):301–4.
[9] Gossec L, Kerschbaumer A, Ferreira RJO, Aletaha D, Baraliakos X, Bertheussen H, et al. EULAR recommendations for the management of psoriatic arthritis with pharmacological therapies: 2023 update. Ann Rheum Dis 2024;83(6):706–19 18.
[10] Smolen JS, Landewé RBM, Bergstra SA, Kerschbaumer A, Sepriano A, Aletaha D, et al. EULAR recommendations for the management of rheumatoid arthritis with synthetic and biological disease-modifying antirheumatic drugs: 2022 update. Ann Rheum Dis 2023;82(1):3–18.
[11] Nash P, Kerschbaumer A, Dörner T, Dougados M, Fleischmann RM, Geissler K, et al. Points to consider for the treatment of immune-mediated inflammatory diseases with Janus kinase inhibitors: a consensus statement. Ann Rheum Dis 2021;80(1):71–87.
[12] Kerschbaumer A, Smolen JS, Nash P, Doerner T, Dougados M, Fleischmann R, et al. Points to consider for the treatment of immune-mediated inflammatory diseases with Janus kinase inhibitors: a systematic literature research. RMD Open 2020;6(3):e001374.
[13] Ytterberg SR, Bhatt DL, Mikuls TR, Koch GG, Fleischmann R, Rivas JL, et al. Cardiovascular and cancer risk with tofacitinib in rheumatoid arthritis. N Engl J Med 2022;386(4):316–26.
[14] US Federal Drug Administration. FDA requires warnings about increased risk of serious heart-related events, cancer, blood clots, and death for JAK inhibitors that treat certain chronic inflammatory conditions. Maryland: US FDA; 2021.
[15] US Federal Drug Administration. Xeljanz (tofacitinib) highlights of prescribing information. Maryland: US FDA; 2021.
[16] US Federal Drug Administration. FDA requires warnings about increased risk of serious heart-related events, cancer, blood clots, and death for JAK inhibitors that treat certain chronic inflammatory conditions 12/2021 update. Maryland: US FDA; 2021.
[17] European Medical Agancy. Xeljanz (tofacitinib) summary of product characteristics. Amsterdam, Netherlands: EMA; 2021.
[18] European Medical Agency. European Medicines Agency Meeting highlights from the Pharmacovigilance Risk Assessment Committee (PRAC), 9–12 January 2023. Amsterdam, Netherlands: EMA; 2023.
[19] Burmester GR, Cohen SB, Winthrop KL, Nash P, Irvine AD, Deodhar A, et al. Safety profile of upadacitinib over 15 000 patient-years across rheumatoid arthritis, psoriatic arthritis, ankylosing spondylitis and atopic dermatitis. RMD Open 2023;9(1):e002735.
[20] Burmester GR, Nash P, Sands BE, Papp K, Stockert L, Jones TV, et al. Adverse events of special interest in clinical trials of rheumatoid arthritis, psoriatic arthritis, ulcerative colitis and psoriasis with 37 066 patient-years of tofacitinib exposure. RMD Open 2021;7(2):e001595.
[21] Taylor PC, Takeuchi T, Burmester GR, Durez P, Smolen JS, Deberdt W, et al. Safety of baricitinib for the treatment of rheumatoid arthritis over a median of 4.6 and up to 9.3 years of treatment: final results from long-term extension study and integrated database. Ann Rheum Dis 2022;81(3):335–43.
[22] Winthrop KL, Tanaka Y, Takeuchi T, Kivitz A, Matzkies F, Genovese MC, et al. Integrated safety analysis of filgotinib in patients with moderately to severely active rheumatoid arthritis receiving treatment over a median of 1.6 years. Ann Rheum Dis 2022;81(2):184–92.
[23] Charles-Schoeman C, Buch MH, Dougados M, Bhatt DL, Giles JT, Ytterberg SR, et al. Risk of major adverse cardiovascular events with tofacitinib versus tumour necrosis factor inhibitors in patients with rheumatoid arthritis with or without a history of atherosclerotic cardiovascular disease: a post hoc analysis from ORAL Surveillance. Ann Rheum Dis 2023;82(1):119–29.
[24] Dougados M, Charles-Schoeman C, Szekanecz Z, Giles JT, Ytterberg SR, Bhatt DL, et al. Impact of cardiovascular risk enrichment on incidence of major adverse cardiovascular events in the tofacitinib rheumatoid arthritis clinical programme. Ann Rheum Dis 2023;82(4):575–7.
[25] Fleischmann R, Curtis JR, Charles-Schoeman C, Mysler E, Yamaoka K, Richez C, et al. Safety profile of upadacitinib in patients at risk of cardiovascular disease: integrated post hoc analysis of the SELECT phase III rheumatoid arthritis clinical programme. Ann Rheum Dis 2023;82(9):1130–41.
[26] Curtis JR, Yamaoka K, Chen YH, Bhatt DL, Gunay LM, Sugiyama N, et al. Malignancy risk with tofacitinib versus TNF inhibitors in rheumatoid

arthritis: results from the open-label, randomised controlled ORAL Surveillance trial. Ann Rheum Dis 2023;82(3):331–43.

[27] Frisell T, Bower H, Morin M, Baecklund E, Di Giuseppe D, Delcoigne B, et al. Safety of biological and targeted synthetic disease-modifying antirheumatic drugs for rheumatoid arthritis as used in clinical practice: results from the ARTIS programme. Ann Rheum Dis 2023;82(5):601–10.

[28] Huss V, Bower H, Hellgren K, Frisell T, Askling J, ARTIS group. Cancer risks with JAKi and biological disease-modifying antirheumatic drugs in patients with rheumatoid arthritis or psoriatic arthritis: a national real-world cohort study. Ann Rheum Dis 2023;82(7):911–9.

[29] Khosrow-Khavar F, Desai RJ, Lee H, Lee SB, Kim SC. Tofacitinib and risk of malignancy: results from the Safety of Tofacitinib in Routine Care Patients With Rheumatoid Arthritis (STAR-RA) Study. Arthritis Rheumatol 2022;74 (10):1648–59.

[30] Khosrow-Khavar F, Kim SC, Lee H, Lee SB, Desai RJ. Tofacitinib and risk of cardiovascular outcomes: results from the Safety of TofAcitinib in Routine care patients with Rheumatoid Arthritis (STAR-RA) study. Ann Rheum Dis 2022;81(6):798–804.

[31] van der Heijde D, Aletaha D, Carmona L, Edwards CJ, Kvien TK, Kouloumas M, et al. 2014 Update of the EULAR standardised operating procedures for EULAR-endorsed recommendations. Ann Rheum Dis 2015;74(1):8–13.

[32] Page MJ, McKenzie JE, Bossuyt PM, Boutron I, Hoffmann TC, Mulrow CD, et al. The PRISMA 2020 statement: an updated guideline for reporting systematic reviews. Rev Esp Cardiol (Engl Ed) 2021;74(9):790–9.

[33] Higgins JP, Thomas J, Chandler J, Cumpston M, Li T, Page MJ, et al. Cochrane handbook for systematic reviews of interventions. 2nd ed. Chichester (UK): John Wiley & Sons; 2019.

[34] EULAR. Project grant application [Internet]. 2024 [cited 2024 August 18]. Available from: https://www.eular.org/recommendations/points-to-consider-task-forces-project-applications

[35] EULAR. Standard operating procedures for task forces [Internet]. 2024 [cited 2024 September 19]. Available from: https://www.eular.org/web/static/lib/pdfjs/web/viewer.html?file=https://www.eular.org/document/download/680/b9eb08d0-faca-4606-8ed9-d0539b3f312a/660

[36] Sackett D, Richardson W, Rosenberg W, Haynes MD. Evidence-based medicine: how to practice and teach EBM. London (UK): Churchill Livingstone; 2005.

[37] Higgins JP, Altman DG, Gotzsche PC, Juni P, Moher D, Oxman AD, et al. The Cochrane Collaboration's tool for assessing risk of bias in randomised trials. BMJ 2011;343:d5928. Oct 18.

[38] Hayden JA, Côté P, Bombardier C. Evaluation of the quality of prognosis studies in systematic reviews. Ann Intern Med 2006;144(6):427–37 21.

[39] R Core Team 2024. R: A Language and Environment for Statistical Computing. Vienna, Austria: R Foundation for Statistical Computing; 2024. [Internet]Available from: https://www.R-project.org.

[40] Balduzzi S, Rücker G, Schwarzer G. How to perform a meta-analysis with R: a practical tutorial. Evid Based Ment Health 2019;22(4):153–60.

[41] Reinisch W, Hellstrom W, Dolhain RJEM, Sikka S, Westhovens R, Mehta R, et al. Effects of filgotinib on semen parameters and sex hormones in male patients with inflammatory diseases: results from the phase 2, randomised, double-blind, placebo-controlled MANTA and MANTA-RAy studies. Ann Rheum Dis 2023;82(8):1049–58.

[42] Mease P, Charles-Schoeman C, Cohen S, Fallon L, Woolcott J, Yun H, et al. Incidence of venous and arterial thromboembolic events reported in the tofacitinib rheumatoid arthritis, psoriasis and psoriatic arthritis development programmes and from real-world data. Ann Rheum Dis 2020;79 (11):1400–13.

[43] Hellstrom WJG, Dolhain RJEM, Ritter TE, Watkins TR, Arterburn SJ, Dekkers G, et al. MANTA and MANTA-RAy: rationale and design of trials evaluating effects of filgotinib on semen parameters in patients with inflammatory diseases. Adv Ther 2022;39(7):3403–22.

[44] Strober BE, Gottlieb AB, van de Kerkhof PCM, Puig L, Bachelez H, Chouela E, et al. Benefit-risk profile of tofacitinib in patients with moderate-to-severe chronic plaque psoriasis: pooled analysis across six clinical trials. Br J Dermatol 2019;180(1):67–75.

[45] Cohen SB, Tanaka Y, Mariette X, Curtis JR, Lee EB, Nash P, et al. Long-term safety of tofacitinib up to 9.5 years: a comprehensive integrated analysis of the rheumatoid arthritis clinical development programme. RMD Open 2020;6(3):e001395.

[46] Burmester GR, Curtis JR, Yun H, FitzGerald O, Winthrop KL, Azevedo VF, et al. An integrated analysis of the safety of tofacitinib in psoriatic arthritis across phase III and long-term extension studies with comparison to real-world observational data. Drug Saf 2020;43(4):379–92.

[47] Deodhar A, Akar S, Curtis J, Zorkany B, Magrey M, Wang C, et al. POS0296 integrated safety analysis of tofacitinib in ankylosing spondylitis clinical trials. Ann Rheum Dis 2022;81(Suppl 1):394–5.

[48] Sandborn WJ, D'Haens GR, Sands BE, Panaccione R, Ng SC, Lawendy N, et al. Tofacitinib for the treatment of ulcerative colitis: an integrated summary of up to 7.8 years of safety data from the Global Clinical Programme. J Crohns Colitis 2023;17(3):338–51.

[49] Panés J, D'Haens GR, Sands BE, Ng SC, Lawendy N, Kulisek N, et al. Analysis of tofacitinib safety in ulcerative colitis from the completed global clinical developmental program up to 9.2 years of drug exposure. United European Gastroenterol J 2024;12(6):793–801.

[50] Bieber T, Katoh N, Simpson EL, de Bruin-Weller M, Thaçi D, Torrelo A, et al. Safety of baricitinib for the treatment of atopic dermatitis over a median of 1.6 years and up to 3.9 years of treatment: an updated integrated analysis of eight clinical trials. J Dermatolog Treat 2023;34(1):2161812.

[51] King B, Mostaghimi A, Shimomura Y, Zlotogorski A, Choi GS, Blume-Peytavi U, et al. Integrated safety analysis of baricitinib in adults with severe alopecia areata from two randomized clinical trials. Br J Dermatol 2023;188(2):218–27.

[52] Morand E, Smolen JS, Petri M, Tanaka Y, Silk M, Dickson C, et al. Safety profile of baricitinib in patients with systemic lupus erythematosus: an integrated analysis. RMD Open 2023;9(3):e003302.

[53] Cohen SB, van Vollenhoven RF, Winthrop KL, Zerbini CAF, Tanaka Y, Bessette L, et al. Safety profile of upadacitinib in rheumatoid arthritis: integrated analysis from the SELECT phase III clinical programme. Ann Rheum Dis 2021;80(3):304–11.

[54] Guttman-Yassky E, Thyssen JP, Silverberg JI, Papp KA, Paller AS, Weidinger S, et al. Safety of upadacitinib in moderate-to-severe atopic dermatitis: an integrated analysis of phase 3 studies. J Allergy Clin Immunol 2023;151 (1):172–81.

[55] Burmester GR, Gottenberg J-E, Caporali R, Winthrop KL, Tanaka Y, Ekoka Omoruyi EV, et al. Integrated safety analysis of filgotinib in patients with moderate-to-severe rheumatoid arthritis over a treatment duration of up to 8.3 years. Ann Rheum Dis 2024;83(9):1110–7.

[56] Takeuchi T, Tanaka Y, Rokuda M, Izutsu H, Kaneko Y, Fukuda M, et al. A pooled safety analysis of peficitinib (ASP015K) in Asian patients with rheumatoid arthritis treated over a median of 2 years. Mod Rheumatol 2021;31 (3):543–55.

[57] Tanaka Y, Takeuchi T, Kato D, Kaneko Y, Fukuda M, Izutsu H, et al. A pooled analysis of serious infections and herpes zoster-related disease in Asian patients with rheumatoid arthritis treated with peficitinib (ASP015K) over a median of 3 years. Mod Rheumatol 2022;32(4):708–17.

[58] Simpson EL, Silverberg JI, Nosbaum A, Winthrop KL, Guttman-Yassky E, Hoffmeister KM, et al. Integrated safety analysis of abrocitinib for the treatment of moderate-to-severe atopic dermatitis from the phase II and phase III clinical trial program. Am J Clin Dermatol 2021;22(5):693–707.

[59] Simpson EL, Silverberg JI, Nosbaum A, Winthrop K, Guttman-Yassky E, Hoffmeister KM, et al. Integrated safety update of abrocitinib in 3802 patients with moderate-to-severe atopic dermatitis: data from more than 5200 patient-years with up to 4 years of exposure. Am J Clin Dermatol 2024;25(4):639–54.

[60] MedDRA, Medical Dictionary for Regulatory Activities [Internet]. [accessed 2024 Jul 9]. Available from: https://www.meddra.org

[61] Panaccione R, Lichtenstein G, Nakase H, Armuzzi A, Kucharzik T, Levy G, et al. P518 Safety of upadacitinib in ulcerative colitis: long-term data from the phase 3 open-label extension study (U-ACTIVATE). J Crohns Colitis 2023;17(Suppl 1):i644–6.

[62] D'Haens G, Louis E, Loftus Jr. EV, Regueiro M, Jairath V, Magro F, et al. OP10 efficacy and safety of upadacitinib in patients with moderately to severely active Crohn's disease: results from the U-ENDURE long-term extension. J Crohn Colitis 2024;18(Suppl 1):i17–8.

[63] Fleischmann R, Blanco R, Van den Bosch F, Bessette L, Song Y, Penn SK, et al. Long-term efficacy and safety following switch between upadacitinib and adalimumab in patients with rheumatoid arthritis: 5-year data from SELECT-COMPARE. Rheumatol Ther 2024;11(3):599–615.

[64] Fleischmann R, Mysler E, Bessette L, Peterfy CG, Durez P, Tanaka Y, et al. Long-term safety and efficacy of upadacitinib or adalimumab in patients with rheumatoid arthritis: results through 3 years from the SELECT-COMPARE study. RMD Open 2022;8(1):e002012.

[65] McInnes IB, Kato K, Magrey M, Merola JF, Kishimoto M, Haaland D, et al. Efficacy and safety of upadacitinib in patients with psoriatic arthritis: 2-year results from the phase 3 SELECT-PsA 1 study. Rheumatol Ther 2023;10(1):275–92.

[66] Pawar A, Desai RJ, Gautam N, Kim SC. Risk of admission to hospital for serious infection after initiating tofacitinib versus biologic DMARDs in patients with rheumatoid arthritis: a multidatabase cohort study. Lancet Rheumatol 2020;2(2):e84–98.

[67] Desai RJ, Pawar A, Khosrow-Khavar F, Weinblatt ME, Kim SC. Risk of venous thromboembolism associated with tofacitinib in patients with

rheumatoid arthritis: a population-based cohort study. Rheumatology (Oxford) 2021;61(1):121–30.
[68] Kremer JM, Bingham III CO, Cappelli LC, Greenberg JD, Madsen AM, Geier J, et al. Postapproval comparative safety study of tofacitinib and biological disease-modifying antirheumatic drugs: 5-year results from a United States-Based Rheumatoid Arthritis Registry. ACR Open Rheumatol 2021;3 (3):173–84.
[69] Redeker I, Albrecht K, Kekow J, Burmester GR, Braun J, Schäfer M, et al. Risk of herpes zoster (shingles) in patients with rheumatoid arthritis under biologic, targeted synthetic and conventional synthetic DMARD treatment: data from the German RABBIT register. Ann Rheum Dis 2022;81(1):41–7.
[70] Meissner Y, Schäfer M, Albrecht K, Kekow J, Zinke S, Tony HP, et al. Risk of major adverse cardiovascular events in patients with rheumatoid arthritis treated with conventional synthetic, biologic and targeted synthetic disease-modifying antirheumatic drugs: observational data from the German RABBIT register. RMD Open 2023;9(4):e003489.
[71] Molander V, Bower H, Frisell T, Delcoigne B, Di Giuseppe D, Askling J, ARTIS study group. Venous thromboembolism with JAK inhibitors and other immune-modulatory drugs: a Swedish comparative safety study among patients with rheumatoid arthritis. Ann Rheum Dis 2023;82(2):189–97.
[72] Hoisnard L, Pina Vegas L, Dray-Spira R, Weill A, Zureik M, Sbidian E. Risk of major adverse cardiovascular and venous thromboembolism events in patients with rheumatoid arthritis exposed to JAK inhibitors versus adalimumab: a nationwide cohort study. Ann Rheum Dis 2023;82(2):182–8.
[73] Cheng D, Kochar BD, Cai T, Ananthakrishnan AN. Risk of infections with ustekinumab and tofacitinib compared to tumor necrosis factor alpha antagonists in inflammatory bowel diseases. Clin Gastroenterol Hepatol 2022;20 (10) 2366−72.e6.
[74] Kochar BD, Cheng D, Cai T, Ananthakrishnan AN. Comparative risk of thrombotic and cardiovascular events with tofacitinib and anti-TNF agents in patients with inflammatory bowel diseases. Dig Dis Sci 2022;67 (11):5206–12.
[75] Balanescu AR, Citera G, Pascual-Ramos V, Bhatt DL, Connell CA, Gold D, et al. Infections in patients with rheumatoid arthritis receiving tofacitinib versus tumour necrosis factor inhibitors: results from the open-label, randomised controlled ORAL Surveillance trial. Ann Rheum Dis 2022;81 (11):1491–503.
[76] Winthrop KL, Citera G, Gold D, Henrohn D, Connell CA, Shapiro AB, et al. Age-based (<65 vs >/=65 years) incidence of infections and serious infections with tofacitinib versus biological DMARDs in rheumatoid arthritis clinical trials and the US Corrona RA registry. Ann Rheum Dis 2021;80 (1):134–6.
[77] Winthrop KL, Harigai M, Genovese MC, Lindsey S, Takeuchi T, Fleischmann R, et al. Infections in baricitinib clinical trials for patients with active rheumatoid arthritis. Ann Rheum Dis 2020;79(10):1290–7.
[78] Winthrop KL, Nash P, Yamaoka K, Mysler E, Khan N, Camp HS, et al. Incidence and risk factors for herpes zoster in patients with rheumatoid arthritis receiving upadacitinib: a pooled analysis of six phase III clinical trials. Ann Rheum Dis 2022;81(2):206–13.
[79] Schreiber S, Rogler G, Watanabe M, Vermeire S, Maaser C, Danese S, et al. Integrated safety analysis of filgotinib for ulcerative colitis: results from SELECTION and SELECTIONLTE. Aliment Pharmacol Ther 2023;58 (9):874–87.
[80] Winthrop KL, Loftus EV, Baumgart DC, Reinisch W, Nduaka CI, Lawendy N, et al. Tofacitinib for the treatment of ulcerative colitis: analysis of infection rates from the ulcerative colitis clinical programme. J Crohns Colitis 2021;15(6):914–29.
[81] Machado MAÁ, Moura CS, Guerra SF, Curtis JR, Abrahamowicz M, Bernatsky S. Effectiveness and safety of tofacitinib in rheumatoid arthritis: a cohort study. Arthritis Res Ther 2018;20(1):60.
[82] Uchida T, Iwamoto N, Fukui S, Morimoto S, Aramaki T, Shomura F, et al. Comparison of risks of cancer, infection, and MACEs associated with JAK inhibitor and TNF inhibitor treatment: a multicentre cohort study. Rheumatology (Oxford) 2023;62(10):3358–65.
[83] Salinas CA, Louder A, Polinski J, Zhang TC, Bower H, Phillips S, et al. Evaluation of VTE, MACE, and serious infections among patients with RA treated with baricitinib compared to TNFi: a multi-database study of patients in routine care using disease registries and claims databases. Rheumatol Ther 2023;10(1):201–23.
[84] Mok CC, So H, Yim CW, To CH, Lao WN, Wong SPY, et al. Safety of the JAK and TNF inhibitors in rheumatoid arthritis: real world data from the Hong Kong Biologics Registry. Rheumatology (Oxford) 2024;63(2):358–65.
[85] Yun H, Yang S, Chen L, Xie F, Winthrop K, Baddley JW, et al. Risk of herpes zoster in autoimmune and inflammatory diseases: implications for vaccination. Arthritis Rheumatol 2016;68(9):2328–37.
[86] Gupta G, Lautenbach E, Lewis JD. Incidence and risk factors for herpes zoster among patients with inflammatory bowel disease. Clin Gastroenterol Hepatol 2006;4(12):1483–90.
[87] Nash P, Richette P, Gossec L, Marchesoni A, Ritchlin C, Kato K, et al. Upadacitinib as monotherapy and in combination with non-biologic disease-modifying antirheumatic drugs for psoriatic arthritis. Rheumatology (Oxford) 2022;61(8):3257–68.
[88] Winthrop KL, Curtis JR, Yamaoka K, Lee EB, Hirose T, Rivas JL, et al. Clinical management of herpes zoster in patients with rheumatoid arthritis or psoriatic arthritis receiving tofacitinib treatment. Rheumatol Ther 2022;9 (1):243–63.
[89] Werfel T, Irvine AD, Bangert C, Seneschal J, Grond S, Cardillo T, et al. An integrated analysis of herpes virus infections from eight randomized clinical studies of baricitinib in adults with moderate-to-severe atopic dermatitis. J Eur Acad Dermatol Venereol 2022;36(9):1486–96.
[90] Winthrop K, Buch MH, Curtis J, Burmester GR, Aletaha D, Amano K, et al. POS0092 Herpes zoster in the filgotinib rheumatoid arthritis program. Ann Rheum Dis 2021;80(Suppl 1):255–6.
[91] Fang YF, Liu JR, Chang SH, Kuo CF, See LC. Comparative safety of Janus kinase inhibitors and tumor necrosis factor inhibitors in patients undergoing treatment for rheumatoid arthritis. Int J Rheum Dis 2022;25(11):1254–62.
[92] Choi SR, Shin A, Ha YJ, Lee YJ, Lee EB, Kang EH. Comparative risk of infections between JAK inhibitors versus TNF inhibitors among patients with rheumatoid arthritis: a cohort study. Arthritis Res Ther 2023;25(1):129.
[93] Rubin R. Baricitinib is first approved COVID-19 immunomodulatory treatment. JAMA 2022;327(23):2281.
[94] Guimaraes PO, Quirk D, Furtado RH, Maia LN, Saraiva JF, Antunes MO, et al. Tofacitinib in patients hospitalized with Covid-19 pneumonia. N Engl J Med 2021;385(5):406–15.
[95] Sparks JA, Wallace ZS, Seet AM, Gianfrancesco MA, Izadi Z, Hyrich KL, et al. Associations of baseline use of biologic or targeted synthetic DMARDs with COVID-19 severity in rheumatoid arthritis: results from the COVID-19 Global Rheumatology Alliance physician registry. Ann Rheum Dis 2021;80 (9):1137–46.
[96] MacKenna B, Kennedy NA, Mehrkar A, Rowan A, Galloway J, Matthewman J, et al. Risk of severe COVID-19 outcomes associated with immune-mediated inflammatory diseases and immune-modifying therapies: a nationwide cohort study in the OpenSAFELY platform. Lancet Rheumatol 2022;4(7): e490–506.
[97] Tsai JJ, Liu LT, Chen CH, Chen LJ, Wang SI, Wei JC. COVID-19 outcomes in patients with rheumatoid arthritis with biologic or targeted synthetic DMARDs. RMD Open 2023;9(3):e003038.
[98] Sparks JA, Wallace ZS, Seet AM, Robinson PC, Machado PM, Yazdany J. Response to: correspondence on "Associations of baseline use of biologic or targeted synthetic DMARDs with COVID-19 severity in rheumatoid arthritis" by van Vollenhoven et al. Ann Rheum Dis 2023;82(8):e178.
[99] Winthrop KL, Yndestad A, Henrohn D, Danese S, Marsal S, Galindo M, et al. Influenza adverse events in patients with rheumatoid arthritis, ulcerative colitis, or psoriatic arthritis in the tofacitinib clinical development programs. Rheumatol Ther 2023;10(2):357–73.
[100] Cronin O, McKnight O, Keir L, Ralston SH, Hirani N, Harris H. A retrospective comparison of respiratory events with JAK inhibitors or rituximab for rheumatoid arthritis in patients with pulmonary disease. Rheumatol Int 2021;41(5):921–8.
[101] Loftus EV, Baumgart DC, Gecse K, Kinnucan JA, Connelly SB, Salese L, et al. *Clostridium difficile* infection in patients with ulcerative colitis treated with tofacitinib in the ulcerative colitis program. Inflamm Bowel Dis 2023;29 (5):744–51.
[102] Kristensen LE, Strober B, Poddubnyy D, Leung YY, Jo H, Kwok K, et al. Association between baseline cardiovascular risk and incidence rates of major adverse cardiovascular events and malignancies in patients with psoriatic arthritis and psoriasis receiving tofacitinib. Ther Adv Musculoskelet Dis 2023;15 1759720X221149965.
[103] Schreiber S, Rubin DT, Ng SC, Peyrin-Biroulet L, Danese S, Modesto I, et al. Major adverse cardiovascular events by baseline cardiovascular risk in patients with ulcerative colitis treated with tofacitinib: data from the OCTAVE Clinical Programme. J Crohns Colitis 2023;17(11):1761–70.
[104] Giles JT, Sattar N, Gabriel S, Ridker PM, Gay S, Warne C, et al. Cardiovascular safety of tocilizumab versus etanercept in rheumatoid arthritis: a randomized controlled trial. Arthritis Rheumatol 2020;72(1):31–40.
[105] Buch M, Bhatt D, Charles-Schoeman C, Giles J, Mikuls T, Koch G, et al. Risk of extended major adverse cardiovascular event endpoints with tofacitinib vs TNF inhibitors in patients with rheumatoid arthritis: a post hoc analysis of a phase 3b/4 randomized safety study [abstract]. Arthritis Rheumatol 2022;74:L06.

[106] Kristensen LE, Danese S, Yndestad A, Wang C, Nagy E, Modesto I, et al. Identification of two tofacitinib subpopulations with different relative risk versus TNF inhibitors: an analysis of the open label, randomised controlled study ORAL Surveillance. Ann Rheum Dis 2023;82(7):901–10.

[107] Charles-Schoeman C, Buch M, Dougados M, Bhatt D, Giles J, Vranic I, et al. Risk factors for major adverse cardiovascular events in patients aged ≥ 50 years with RA and ≥ 1 additional cardiovascular risk factor: results from a phase 3b/4 randomized safety study of tofacitinib vs TNF inhibitors [abstract]. Arthritis Rheumatol 2021;73:0958.

[108] Szekanecz Z, Giles JT, Buch MH, Ytterberg SR, Dougados M, Bhatt DL, et al. POS0110 incidence of major adverse cardiovascular events stratified by geographic region and baseline cardiovascular risk: a post hoc analysis of ORAL Surveillance. Ann Rheum Dis 2022;81(Suppl 1):278–9.

[109] Charles-Schoeman C, DeMasi R, Valdez H, Soma K, Hwang LJ, Boy MG, et al. Risk factors for major adverse cardiovascular events in phase III and long-term extension studies of tofacitinib in patients with rheumatoid arthritis. Arthritis Rheumatol 2019;71(9):1450–9.

[110] Taylor PC, Bieber T, Alten R, Witte T, Galloway J, Deberdt W, et al. Baricitinib safety for events of special interest in populations at risk: analysis from randomised trial data across rheumatologic and dermatologic indications. Adv Ther 2023;40(4):1867–83.

[111] Mariette X, Borchmann S, Aspeslagh S, Calvo J, Moriggl R, Szekanecz Z, et al. POS0824 cardiovascular (CV) and malignancy events in the filgotinib (fil) rheumatoid arthritis (RA) clinical development program up to 8.3 years. Ann Rheum Dis 2023;82(Suppl 1):707–8.

[112] Buch MH, Gómez-Puerta JA, Burmester GR, Combe B, Rajendran V, Stiers PJ, et al. POS0308 long-term clinical profile of filgotinib (FIL) in patients (PTS) with rheumatoid arthritis (RA) by cardiovascular (CV) risk factors: a post hoc subgroup analysis. Ann Rheum Dis 2023;82(Suppl 1):397–8.

[113] Aletaha D, Westhovens R, Combe B, Gottenberg JE, Buch MH, Caporali R, et al. POS0676 efficacy and safety of filgotinib in patients aged ≥75 years: a post hoc subgroup analysis of the finch 4 long-term extension (LTE) study. Ann Rheum Dis 2022;81(Suppl 1):612–3.

[114] van der Woude J, Schreiber S, Peyrin-Biroulet L, Szekanecz Z, Choy EH, Stiers PJ, et al. P520 thromboembolic and major adverse cardiovascular events among patients in the filgotinib clinical trial programme. J Crohns Colitis 2023;17(Suppl 1):i646–9.

[115] Simpson EL, Silverberg JI, Nosbaum A, Winthrop K, Guttman-Yassky E, Hoffmeister KM, et al. 330 Safety of abrocitinib in 3582 patients with moderate-to-severe atopic dermatitis with over 900 patients exposed for almost 2 years. Br J Dermatol 2023;188(Suppl 2):ljac140.025.

[116] Min HK, Kim H, Jeong HJ, Kim SH, Kim HR, Lee SH, et al. Risk of cancer, cardiovascular disease, thromboembolism, and mortality in patients with rheumatoid arthritis receiving Janus kinase inhibitors: a real-world retrospective observational study using Korean health insurance data. Epidemiol Health 2023;45:e2023045.

[117] Tong X, Shen CY, Jeon HL, Li Y, Shin JY, Chan SC, et al. Cardiovascular risk in rheumatoid arthritis patients treated with targeted synthetic and biological disease-modifying antirheumatic drugs: a multi-centre cohort study. J Intern Med 2023;294(3):314–25.

[118] Desai RJ, Pawar A, Weinblatt ME, Kim SC. Comparative risk of venous thromboembolism in rheumatoid arthritis patients receiving tofacitinib versus those receiving tumor necrosis factor inhibitors: an observational cohort study. Arthritis Rheumatol 2019;71(6):892–900.

[119] Weitz JI, Szekanecz Z, Charles-Schoeman C, Vranic I, Sahin B, Paciga SA, et al. Biomarkers to predict risk of venous thromboembolism in patients with rheumatoid arthritis receiving tofacitinib or tumour necrosis factor inhibitors. RMD Open 2022;8(2):e002571.

[120] Avouac J, Fogel O, Hecquet S, Daien C, Elalamy I, Picard F, et al. Recommendations for assessing the risk of cardiovascular disease and venous thromboembolism before the initiation of targeted therapies for chronic inflammatory rheumatic diseases. Joint Bone Spine 2023;90(5):105592.

[121] Charles-Schoeman C, Fleischmann RM, Mysler E, Greenwald M, Wang C, Chen AS, et al. POS0239 risk of venous thromboembolic events in patients with rheumatoid arthritis aged ≥50 years with ≥1 cardiovascular risk factor: results from a phase 3b/4 randomised study of tofacitinib vs tumour necrosis factor inhibitors. Ann Rheum Dis 2022;81(Suppl 1):358–9.

[122] Charles-Schoeman C, Fleischmann R, Mysler E, Greenwald M, Ytterberg SR, Koch GG, et al. Risk of venous thromboembolism with tofacitinib versus tumor necrosis factor inhibitors in cardiovascular risk-enriched rheumatoid arthritis patients. Arthritis Rheumatol 2024;76(8):1218–29.

[123] Sandborn WJ, Panés J, Sands BE, Reinisch W, Su C, Lawendy N, et al. Venous thromboembolic events in the tofacitinib ulcerative colitis clinical development programme. Aliment Pharmacol Ther 2019;50(10):1068–76.

[124] Gouverneur A, Avouac J, Prati C, Cracowski JL, Schaeverbeke T, Pariente A, et al. JAK inhibitors and risk of major adverse cardiovascular events or venous thromboembolism: a self-controlled case series study. Eur J Clin Pharmacol 2022;78(12):1981–90.

[125] Rubbert-Roth A, Kakehasi AM, Takeuchi T, Schmalzing M, Palac H, Coombs D, et al. Malignancy in the upadacitinib clinical trials for rheumatoid arthritis, psoriatic arthritis, ankylosing spondylitis, and non-radiographic axial spondyloarthritis. Rheumatol Ther 2024;11(1):97–112.

[126] Meudec L, Richebé P, Pascaud J, Mariette X, Nocturne G. Janus kinase inhibitors alter NK cell phenotypes and inhibit their antitumour capacity. Rheumatology (Oxford) 2023;62(8):2855–63.

[127] Hirose W, Harigai M, Amano K, Hidaka T, Itoh K, Aoki K, et al. Real-world effectiveness and safety of tofacitinib and abatacept in patients with rheumatoid arthritis. Rheumatol Adv Pract 2022;6(3):rkac090.

[128] Bower H, Frisell T, Di Giuseppe D, Delcoigne B, Ahlenius GM, Baecklund E, et al. Impact of the COVID-19 pandemic on morbidity and mortality in patients with inflammatory joint diseases and in the general population: a nationwide Swedish cohort study. Ann Rheum Dis 2021;80(8):1086–93.

[129] Monemi S, Berber E, Sarsour K, Wang J, Lampl K, Bharucha K, et al. Incidence of gastrointestinal perforations in patients with rheumatoid arthritis treated with tocilizumab from clinical trial, postmarketing, and real-world data sources. Rheumatol Ther 2016;3(2):337–52.

[130] Guttman-Yassky E, Teixeira HD, Simpson EL, Papp KA, Pangan AL, Blauvelt A, et al. Once-daily upadacitinib versus placebo in adolescents and adults with moderate-to-severe atopic dermatitis (Measure Up 1 and Measure Up 2): results from two replicate double-blind, randomised controlled phase 3 trials. Lancet 2021;397(10290):2151–68.

[131] Katoh N, Ohya Y, Murota H, Ikeda M, Hu X, Ikeda K, et al. A phase 3 randomized, multicenter, double-blind study to evaluate the safety of upadacitinib in combination with topical corticosteroids in adolescent and adult patients with moderate-to-severe atopic dermatitis in Japan (Rising Up): an interim 24-week analysis. JAAD Int 2022;6:27–36.

[132] Reich K, Teixeira HD, de Bruin-Weller M, Bieber T, Soong W, Kabashima K, et al. Safety and efficacy of upadacitinib in combination with topical corticosteroids in adolescents and adults with moderate-to-severe atopic dermatitis (AD Up): results from a randomised, double-blind, placebo-controlled, phase 3 trial. Lancet 2021;397(10290):2169–81.

[133] Mendes-Bastos P, Ladizinski B, Guttman-Yassky E, Jiang P, Liu J, Prajapati VH, et al. Characterization of acne associated with upadacitinib treatment in patients with moderate-to-severe atopic dermatitis: a post hoc integrated analysis of 3 phase 3 randomized, double-blind, placebo-controlled trials. J Am Acad Dermatol 2022;87(4):784–91.

[134] Wollenberg A, Kircik L, Simpson E, Brinker D, Katoh N, Rueda MJ, et al. Pooled analysis of baricitinib tolerability in patients with atopic dermatitis in relation to acne, headache, and gastrointestinal events from 8 clinical trials. Dermatitis 2023;34(4):308–14.

[135] Loftus Jr. EV, Panés J, Lacerda AP, Peyrin-Biroulet L, D'Haens G, Panaccione R, et al. Upadacitinib induction and maintenance therapy for Crohn's disease. N Engl J Med 2023;388(21):1966–80.

[136] Danese S, Vermeire S, Zhou W, Pangan AL, Siffledeen J, Greenbloom S, et al. Upadacitinib as induction and maintenance therapy for moderately to severely active ulcerative colitis: results from three phase 3, multicentre, double-blind, randomised trials. Lancet 2022;399(10341):2113–28.

[137] Armstrong AW, Gooderham M, Warren RB, Papp KA, Strober B, Thaçi D, et al. Deucravacitinib versus placebo and apremilast in moderate to severe plaque psoriasis: efficacy and safety results from the 52-week, randomized, double-blinded, placebo-controlled phase 3 POETYK PSO-1 trial. J Am Acad Dermatol 2023;88(1):29–39.

[138] Mease PJ, Deodhar AA, van der Heijde D, Behrens F, Kivitz AJ, Neal J, et al. Efficacy and safety of selective TYK2 inhibitor, deucravacitinib, in a phase II trial in psoriatic arthritis. Ann Rheum Dis 2022;81(6):815–22.

[139] Morand E, Pike M, Merrill JT, van Vollenhoven R, Werth VP, Hobar C, et al. Deucravacitinib, a tyrosine kinase 2 inhibitor, in systemic lupus erythematosus: a phase II, randomized, double-blind, placebo-controlled trial. Arthritis Rheumatol 2023;75(2):242–52.

[140] Strober B, Thaçi D, Sofen H, Kircik L, Gordon KB, Foley P, et al. Deucravacitinib versus placebo and apremilast in moderate to severe plaque psoriasis: efficacy and safety results from the 52-week, randomized, double-blinded, phase 3 program for evaluation of TYK2 inhibitor psoriasis second trial. J Am Acad Dermatol 2023;88(1):40–51.

[141] King B, Mesinkovska N, Mirmirani P, Bruce S, Kempers S, Guttman-Yassky E, et al. Phase 2 randomized, dose-ranging trial of CTP-543, a selective Janus kinase inhibitor, in moderate-to-severe alopecia areata. J Am Acad Dermatol 2022;87(2):306–13.

[142] Papp K, Pariser D, Catlin M, Wierz G, Ball G, Akinlade B, et al. A phase 2a randomized, double-blind, placebo-controlled, sequential dose-escalation study to evaluate the efficacy and safety of ASP015K, a novel Janus kinase inhibitor, in patients with moderate-to-severe psoriasis. Br J Dermatol 2015;173(3):767–76.

[143] Robinson MF, Damjanov N, Stamenkovic B, Radunovic G, Kivitz A, Cox L, et al. Efficacy and safety of PF-06651600 (ritlecitinib), a novel JAK3/TEC inhibitor, in patients with moderate-to-severe rheumatoid arthritis and an inadequate response to methotrexate. Arthritis Rheumatol 2020;72 (10):1621–31.
[144] Ezzedine K, Peeva E, Yamaguchi Y, Cox LA, Banerjee A, Han G, et al. Efficacy and safety of oral ritlecitinib for the treatment of active nonsegmental vitiligo: a randomized phase 2b clinical trial. J Am Acad Dermatol 2023;88 (2):395–403.
[145] Rosmarin D, Passeron T, Pandya AG, Grimes P, Harris JE, Desai SR, et al. Two phase 3, randomized, controlled trials of ruxolitinib cream for vitiligo. N Engl J Med 2022;387(16):1445–55.
[146] Russell MD, Dey M, Flint J, Davie P, Allen A, Crossley A, et al. British Society for Rheumatology guideline on prescribing drugs in pregnancy and breastfeeding: immunomodulatory anti-rheumatic drugs and corticosteroids. Rheumatology (Oxford) 2023;62(4):e48–88.
[147] Mahadevan U, Chaparro M, Segovia Medina M, Kulisek N, Guo X, Wu J, et al. P956 pregnancy outcomes after maternal or paternal exposure in the tofacitinib ulcerative colitis clinical programme. J Crohn Colitis 2024;18 (Suppl 1):i1735–6.
[148] Westhovens R, Rigby WFC, van der Heijde D, Ching DWT, Stohl W, Kay J, et al. Filgotinib in combination with methotrexate or as monotherapy versus methotrexate monotherapy in patients with active rheumatoid arthritis and limited or no prior exposure to methotrexate: the phase 3, randomised controlled FINCH 3 trial. Ann Rheum Dis 2021;80(6):727–38.
[149] Harigai M, Winthrop K, Takeuchi T, Hsieh TY, Chen YM, Smolen JS, et al. Evaluation of hepatitis B virus in clinical trials of baricitinib in rheumatoid arthritis. RMD Open 2020;6(1):e001095.
[150] Akinlade B, Guttman-Yassky E, de Bruin-Weller M, Simpson EL, Blauvelt A, Cork MJ, et al. Conjunctivitis in dupilumab clinical trials. Br J Dermatol 2019;181(3):459–73 Sep.
[151] Blauvelt A, Teixeira HD, Simpson EL, Costanzo A, De Bruin-Weller M, Barbarot S, et al. Efficacy and safety of upadacitinib vs dupilumab in adults with moderate-to-severe atopic dermatitis: a randomized clinical trial. JAMA Dermatol 2021;157(9):1047–55 Sep 1.
[152] Gelato F, Mastorino L, Quaglino P, Cavaliere G, Ortoncelli M, Ribero S. Ocular adverse events in patients with atopic dermatitis treated with upadacitinib: a real-life experience. Dermatitis 2023;34(5):445–7.
[153] Hansen KE, Mortezavi M, Nagy E, Wang C, Connell CA, Radi Z, et al. Fracture in clinical studies of tofacitinib in rheumatoid arthritis. Ther Adv Musculoskelet Dis 2022;14 1759720X221142346.
[154] Simon D, Minopoulou I, Kemenes S, Bayat S, Tascilar K, Mutlu MY, et al. Baricitinib improves bone properties and biomechanics in patients with rheumatoid arthritis: results of the prospective interventional BARE BONE trial. Arthritis Rheumatol 2023;75(11):1923–34.
[155] Balsa A, Wassenberg S, Tanaka Y, Tournadre A, Orzechowski HD, Rajendran V, et al. Effect of filgotinib on body mass index (BMI) and effect of baseline BMI on the efficacy and safety of filgotinib in rheumatoid arthritis. Rheumatol Ther 2023;10(6):1555–74.
[156] Kivitz AJ, Cohen S, Keystone E, van Vollenhoven RF, Haraoui B, Kaine J, et al. A pooled analysis of the safety of tofacitinib as monotherapy or in combination with background conventional synthetic disease-modifying antirheumatic drugs in a phase 3 rheumatoid arthritis population. Semin Arthritis Rheum 2018;48(3):406–15.
[157] Fleischmann R, Wollenhaupt J, Cohen S, Smolen JS, Dahl P, Iikuni N, et al. SAT0247 Impact of glucocorticoids on efficacy and safety of tofacitinib with and without methotrexate and adalimumab with methotrexate for rheumatoid arthritis: results from a phase 3b/4 randomised trial. Ann Rheum Dis 2018;77(Suppl 2):985–6.
[158] Mori S, Ueki Y, Ishiwada N. Impact of Janus kinase inhibitors on antibody response to 13-valent pneumococcal conjugate vaccine in patients with rheumatoid arthritis. Mod Rheumatol 2023;33(2):312–7.
[159] Calabrese LH, Abud-Mendoza C, Lindsey SM, Lee SH, Tatulych S, Takiya L, et al. Live zoster vaccine in patients with rheumatoid arthritis treated with tofacitinib with or without methotrexate, or adalimumab with methotrexate: a post hoc analysis of data from a phase IIIb/IV randomized study. Arthritis Care Res (Hoboken) 2020;72(3):353–9.
[160] Syversen SW, Jyssum I, Tveter AT, Tran TT, Sexton J, Provan SA, et al. Immunogenicity and safety of standard and third-dose SARS-CoV-2 vaccination in patients receiving immunosuppressive therapy. Arthritis Rheumatol 2022;74(8):1321–32.
[161] Winthrop KL, Bingham III CO, Komocsar WJ, Bradley J, Issa M, Klar R, et al. Evaluation of pneumococcal and tetanus vaccine responses in patients with rheumatoid arthritis receiving baricitinib: results from a long-term extension trial substudy. Arthritis Res Ther 2019;21(1):102.
[162] Winthrop K, Vargas JI, Drescher E, Garcia C, Friedman A, Hendrickson B, et al. Evaluation of response to 13-valent conjugated pneumococcal vaccination in patients with rheumatoid arthritis receiving upadacitinib: results from a phase 2 open-label extension study. RMD Open 2022;8(1): e002110.
[163] Winthrop K, Klaff J, Liu Y, Garcia CG, Mysler E, Wells AF, et al. OP0225 evaluation of response to adjuvanted recombinant zoster vaccination in patients with rheumatoid arthritis receiving upadacitinib: results from a randomized trial sub-study. Ann Rheum Dis 2023;82(Suppl 1):148.
[164] Venerito V, Stefanizzi P, Cantarini L, Lavista M, Galeone MG, Di Lorenzo A, et al. Immunogenicity and safety of adjuvanted recombinant zoster vaccine in rheumatoid arthritis patients on anti-cellular biologic agents or JAK inhibitors: a prospective observational study. Int J Mol Sci 2023;24(8):6967.
[165] Esteban-Vazquez A, Steiner M, Castañeda E, Andreu-Vazquez C, Thiussard IJ, Somodevilla A, et al. The real-world study of immunogenicity and safety of the adjuvant recombinant vaccine against varicella zoster virus in patients with immune-mediated inflammatory diseases treated with Janus kinase inhibitors. Vaccines (Basel) 2023;11(10):1610.
[166] Pons-Bas A, Rosas J, Pons-Canet L, Senabre-Gallego JM, Soler GS, Bernal JA, et al. AB1774-HPR safety of the recombinant herpes zoster vaccine in patients with rheumatoid arthritis treated with JAKi drugs. Ann Rheum Dis 2023;82(Suppl 1):2121.
[167] Lal H, Cunningham AL, Godeaux O, Chlibek R, Diez-Domingo J, Hwang SJ, et al. Efficacy of an adjuvanted herpes zoster subunit vaccine in older adults. N Engl J Med 2015;372(22):2087–96.
[168] Cunningham AL, Lal H, Kovac M, Chlibek R, Hwang SJ, Diez-Domingo J, et al. Efficacy of the herpes zoster subunit vaccine in adults 70 years of age or older. N Engl J Med 2016;375(11):1019–32.
[169] Cunningham AL, Heineman TC, Lal H, Godeaux O, Chlibek R, Hwang SJ, et al. Immune responses to a recombinant glycoprotein E herpes zoster vaccine in adults aged 50 years or older. J Infect Dis 2018;217(11):1750–60.
[170] Wieske L, van Dam KPJ, Steenhuis M, Stalman EW, Kummer LYL, van Kempen ZLE, et al. Humoral responses after second and third SARS-CoV-2 vaccination in patients with immune-mediated inflammatory disorders on immunosuppressants: a cohort study. Lancet Rheumatol 2022;4(5): e338–50.
[171] Whelan MG, Santacroce L, Masto L, Qian G, Kowalski E, Vanni K, et al. Predictors of low spike antibody response in patients with systemic rheumatic disease after an initial course of COVID-19 vaccination. Clin Rheumatol 2023;42(6):1695–700.
[172] Seror R, Camus M, Salmon JH, Roux C, Dernis E, Basch A, et al. Do JAK inhibitors affect immune response to COVID-19 vaccination? Data from the MAJIK-SFR Registry. Lancet Rheumatol 2022;4(1):e8–11.
[173] Gladman DD, Charles-Schoeman C, McInnes IB, Veale DJ, Thiers B, Nurmohamed M, et al. Changes in lipid levels and incidence of cardiovascular events following tofacitinib treatment in patients with psoriatic arthritis: a pooled analysis across phase III and long-term extension studies. Arthritis Care Res (Hoboken) 2019;71(10):1387–95.
[174] Charles-Schoeman C, Fleischmann R, Davignon J, Schwartz H, Turner SM, Beysen C, et al. Potential mechanisms leading to the abnormal lipid profile in patients with rheumatoid arthritis versus healthy volunteers and reversal by tofacitinib. Arthritis Rheumatol 2015;67(3):616–25.
[175] Charles-Schoeman C, Gonzalez-Gay MA, Kaplan I, Boy M, Geier J, Luo Z, et al. Effects of tofacitinib and other DMARDs on lipid profiles in rheumatoid arthritis: implications for the rheumatologist. Semin Arthritis Rheum 2016;46(1):71–80.
[176] Taylor PC, Kremer JM, Emery P, Zuckerman SH, Ruotolo G, Zhong J, et al. Lipid profile and effect of statin treatment in pooled phase II and phase III baricitinib studies. Ann Rheum Dis 2018;77(7):988–95.
[177] Sands BE, Colombel JF, Ha C, Farnier M, Armuzzi A, Quirk D, et al. Lipid profiles in patients with ulcerative colitis receiving tofacitinib-implications for cardiovascular risk and patient management. Inflamm Bowel Dis 2021;27(6):797–808.
[178] Sands BE, Taub PR, Armuzzi A, Friedman GS, Moscariello M, Lawendy N, et al. Tofacitinib treatment is associated with modest and reversible increases in serum lipids in patients with ulcerative colitis. Clin Gastroenterol Hepatol 2020;18(1) 123−32.e3.
[179] McInnes IB, Kim HY, Lee SH, Mandel D, Song YW, Connell CA, et al. Open-label tofacitinib and double-blind atorvastatin in rheumatoid arthritis patients: a randomised study. Ann Rheum Dis 2014;73(1):124–31.
[180] Panaccione R, Isaacs JD, Chen LA, Wang W, Marren A, Kwok K, et al. Characterization of creatine kinase levels in tofacitinib-treated patients with ulcerative colitis: results from clinical trials. Dig Dis Sci 2021;66 (8):2732–43.
[181] Charles-Schoeman C, Giles JT, Lane NE, Choy E, Furst DE, Vencovsky J, et al. Impact of upadacitinib on laboratory parameters and related adverse events in patients with RA: integrated data up to 6.5 years. Rheumatol Ther 2024;11(1):157–75.

[182] Tuttle KR, Brosius III FC, Adler SG, Kretzler M, Mehta RL, Tumlin JA, et al. JAK1/JAK2 inhibition by baricitinib in diabetic kidney disease: results from a phase 2 randomized controlled clinical trial. Nephrol Dial Transplant 2018;33(11):1950–9.

[183] Favalli EG, Buch MH, Galloway J, Constantin A, Durez P, Van Hoek P, et al. AB0454 safety of filgotinib in patients with RA: laboratory analysis results from a long-term extension study. Ann Rheum Dis 2023;82(Suppl 1):1417–8.

[184] Kay J, Harigai M, Rancourt J, Dickson C, Melby T, Issa M, et al. Changes in selected haematological parameters associated with JAK1/JAK2 inhibition observed in patients with rheumatoid arthritis treated with baricitinib. RMD Open 2020;6(3):e001370.

[185] McInnes IB, Anderson JK, Magrey M, Merola JF, Liu Y, Kishimoto M, et al. Trial of upadacitinib and adalimumab for psoriatic arthritis. N Engl J Med 2021;384(13):1227–39.

[186] Loveikyte R, de Haas A, Oortwijn A, Eskens B, Jamoul C, Muller K, et al. P393 effect of filgotinib on anaemia in patients with ulcerative colitis in SELECTION. J Crohns Colitis 2023;17(Suppl 1):i525–7.

[187] Gottenberg JE, Burmester GR, Van Beneden K, Watson C, Seghers I, Rajendran V, et al. POS0513 safety of filgotinib in patients with rheumatoid arthritis: analysis of lymphocytes in the long-term extension FINCH 4 study. Ann Rheum Dis 2022;81(Suppl 1):512–3.

[188] Fleischmann RM, Thaçi D, Gooderham M, Strober B, Korman NJ, Banerjee S, et al. POS1040 safety of deucravacitinib, an oral, selective tyrosine kinase 2 inhibitor: as assessed by laboratory parameters − results from a phase 2 trial in psoriatic arthritis and 2 phase 3 trials in psoriasis. Ann Rheum Dis 2022;81(Suppl 1):835–6.

[189] Morand E, Merola JF, Tanaka Y, Gladman D, Fleischmann R. TYK2: an emerging therapeutic target in rheumatic disease. Nat Rev Rheumatol 2024;20(4):232–40.

[190] Strober B, Blauvelt A, Warren RB, Papp KA, Armstrong AW, Gordon KB, et al. Deucravacitinib in moderate-to-severe plaque psoriasis: pooled safety and tolerability over 52 weeks from two phase 3 trials (POETYK PSO-1 and PSO-2). J Eur Acad Dermatol Venereol 2024;38(8):1543–54.

[191] Dougados M, Soubrier M, Antunez A, Balint P, Balsa A, Buch MH, et al. Prevalence of comorbidities in rheumatoid arthritis and evaluation of their monitoring: results of an international, cross-sectional study (COMORA). Ann Rheum Dis 2014;73(1):62–8.

[192] Radner H, Yoshida K, Hmamouchi I, Dougados M, Smolen JS, Solomon DH. Treatment patterns of multimorbid patients with rheumatoid arthritis: results from an international cross-sectional study. J Rheumatol 2015;42 (7):1099–104.

[193] Dougados M. Comorbidities in rheumatoid arthritis. Curr Opin Rheumatol 2016;28(3):282–8.

[194] Giles J, Charles-Schoeman C, Buch M, Dougados M, Szekanecz Z, Ytterberg S, et al. POS0520 association between baseline statin treatment and major adverse cardiovascular events in patients with rheumatoid arthritis: a post hoc analysis of ORAL Surveillance. Ann Rheum Dis 2022;81 (Suppl 1):518–9.

Ann Rheum Dis 84 (2025) 716−725

Contents lists available at ScienceDirect

Annals of the Rheumatic Diseases

journal homepage: https://www.sciencedirect.com/journal/annals-of-the-rheumatic-diseases

Rheumatoid arthritis

Do newly approved drugs have a worse observed safety profile than once established? A study on time trends in risks of key safety outcomes with immunomodulatory drugs against rheumatoid arthritis

Viktor Molander[1,2,*], Hannah Bower[1], Thomas Frisell[1], Johan Askling[1,2]

[1] *Clinical Epidemiology Division, Department of Medicine Solna, Karolinska Institutet, Stockholm, Sweden*
[2] *Rheumatology, Theme Inflammation and Ageing, Karolinska University Hospital, Stockholm, Sweden*

ARTICLE INFO

Article history:
Received 24 August 2024
Received in revised form 29 October 2024
Accepted 2 December 2024

ABSTRACT

Objectives: To investigate rates of key safety outcomes in patients with rheumatoid arthritis (RA) initiating biologic/targeted synthetic disease-modifying antirheumatic drugs (b/tsDMARDs) and in reference cohorts, presented over time since the market entry of each b/tsDMARD class and over calendar period at treatment start.
Methods: This was a nationwide register-based cohort study conducted from 2006 to 2022. From the Swedish Rheumatology Quality Register and national registers, we identified treatment initiators of b/tsDMARDs (n = 33,550 initiations), an early bionaive RA cohort (n = 16,011), and a matched general population cohort (n = 111,074). The main outcome was first of either major adverse cardiovascular event, venous thromboembolism, cancer, or serious infection. We stratified rates by time since market entry of each b/tsDMARD class at treatment start, and by calendar year of treatment start. We calculated incidence rates (IRs) and hazard ratios (HRs) using Cox regression and adjusted for patient characteristics.
Results: Overall, 5862 events were observed in the b/tsDMARD initiator cohort. b/tsDMARD treatments initiated >5 (vs <2) years since market entry of that class were associated with lower outcome rates (unadjusted HR = 0.74; 95% CI = 0.67-0.81). This association was attenuated once adjusting for patient characteristics (adjusted HR = 0.93; 95% CI = 0.84-1.03). By contrast, during our study period, adjusted rates declined (adjusted HR = 0.74 and 95% CI = 0.69-0.80 for b/tsDMARDs initiated 2016-2021 vs 2006-2010), despite a constant rate in the background population.
Conclusions: Modest channelling makes the safety profile of b/tsDMARDs appear worse when new on the market. Declining incidences of typical RA comorbidities in b/tsDMARD initiators during recent years suggest that the bar defining an "acceptable" safety profile for new b/tsDMARDs for use in RA should be lower(ed).

*Correspondence to Dr Viktor Molander, Clinical Epidemiology Division, Karolinska University Hospital Solna, T2:02, 171 76 Stockholm, Sweden.
E-mail address: viktor.molander@ki.se (V. Molander).

Handling editor Josef S. Smolen.

https://doi.org/10.1016/j.ard.2025.01.020

WHAT IS ALREADY KNOWN ON THIS TOPIC

- Concerns regarding increased risks of cardiovascular, thromboembolic, malignant, and infectious adverse effects of the most recently approved class of antirheumatic drugs (Janus kinase inhibitors [JAKis]) limit their clinical use.
- Recently approved drugs are more likely to be prescribed to difficult-to-treat patients with rheumatoid arthritis (RA) with higher risks for comorbidities. Conversely, an increasing use of immunomodulatory antirheumatic drugs might lower the average *a priori* risk of safety events. Such channelling might make newly approved drugs appear to have a worse safety profile than established drugs. The magnitude of such an effect on the observed safety rates with time from approval remains poorly quantified.

WHAT THIS STUDY ADDS

- We found that the observed rate of a combined safety outcome (first of: major adverse cardiovascular event [MACE], venous thromboembolism, cancer, or serious infection) was ~25% higher during the first years after market entry compared with thereafter, an effect that could be readily explained by changing patient characteristics.
- We noted a more marked decline in rates of the composite safety outcome among biologic/targeted synthetic disease-modifying antirheumatic drug (b/tsDMARD) initiators over calendar time but not in the general population.

HOW THIS STUDY MIGHT AFFECT RESEARCH, PRACTICE OR POLICY

- Our results provide a quantification of the strength of channelling due to "new on the market" on the observed rates (~25% higher) of key safety outcomes with b/tsDMARDs as used during the first 2 vs later years since their market entry.
- Our finding of a secular trend towards declining rates of the same safety outcomes over calendar time exclusively in patients starting b/tsDMARDs suggests that with (on average) healthier patients selected for treatment, the bar that defines "acceptable" rates of safety outcomes of new and future antirheumatic drugs might be lower than that used during the approval of existing b/tsDMARDs.

INTRODUCTION

Individuals with rheumatoid arthritis (RA) are at increased risk of several comorbidities, including major adverse cardiovascular events (MACEs) [1−3], venous thromboembolism (VTE) [4−6], and cancers such as lung cancer and lymphoma [7,8], compared with individuals without RA. These risks vary with RA disease activity and general health status and may be impacted positively or negatively by antirheumatic drugs. The rates of such RA comorbidities constitute an important part of the "safety profile" of biologic/targeted synthetic disease-modifying antirheumatic drugs (b/tsDMARDs). For instance, in recent years, there have been concerns regarding an increased risk of these outcomes in patients with RA treated with Janus kinase inhibitors (JAKis). Such signals were initially detected in data from the clinical development programmes as a numerical increase of VTE for baricitinib and upadacitinib versus placebo [9] and (for tofacitinib) were strengthened by results from the ORAL Surveillance Safety Trial [10]. These findings have resulted in warnings for tofacitinib from the European Medicines Agency (EMA) and the US Food and Drug Administration (FDA) [11,12], which were later extended to the entire class of JAKis [13,14]. To date, data from observational studies based on patients treated in clinical practice are scarce, mainly because of limitations in follow-up time. However, studies on MACEs and solid noncutaneous cancer have not replicated the results from the ORAL Surveillance trial [15−17], whereas results from studies on VTE with JAKis have been mixed [18−21].

Because of the association between RA and RA disease activity, and the risk of MACE, VTE, and certain cancers, evaluation of any causal effect between a specific drug class and these outcomes using observational designs is nontrivial, as opposed to randomised trials, such as ORAL Surveillance, for which the generalisability of the results to other patient populations is instead the challenge (calling for the said observational studies). For reasons related to lack of experience with the drug, and as a general risk minimisation measure, drugs from a new class are likely to be predominantly prescribed to "difficult to treat" patients with RA, thereby adding a correlation to a higher burden of comorbidities and of RA disease activity. The impact of such selective use of newer treatments in clinical practice on the observed risks for key safety outcomes is not well quantified but may constitute an important reason behind "safety signals" appearing in observational studies with new drugs once available in clinical practice.

In an era of rapid drug development and safety concerns such as those exemplified by JAKis, there is a need to better understand the impact of any such new-on-the-market channelling on the observed rates of safety outcomes in clinical practice. Therefore, we aimed to investigate if the observed rates of key safety outcomes (here: MACE, VTE, cancer, and serious infection) in patients with RA initiating different classes of b/tsDMARDs differ by time since market entry of the first drug in that class of b/tsDMARD. For contextualisation, we put these rates in relation to any changes in the rate of the same outcomes over calendar time of treatment start (instead of time since market entry) and rates among b/tsDMARD-naive patients with RA and in the general population.

METHODS

Study design

We conducted a nationwide register-based cohort study using prospectively recorded data from Swedish registers.

Setting

In Sweden, health care and prescriptions are publicly funded with an annual threshold of payment of €125 and €250, respectively. The vast majority of patients with RA are treated by rheumatologists at public hospital-based clinics.

Use of drugs approved by EMA and the Swedish Medical Products Agency is at the discretion of the individual physician, with guidelines issued by the Swedish Society for Rheumatology largely compliant with those issued by European Alliance of Associations for Rheumatology (EULAR) [22,23].

Data sources

For this study, we used data from the following Swedish data sources: the Swedish Rheumatology Quality Register (SRQ), the National Patient Register, the Prescribed Drug Register (PDR), the Cause of Death Register, the National Cancer Register, the Swedish Population Register, and the Longitudinal database for insurance and labour market studies (LISA). Supplemental Table S1 provides detailed description of each of these registers.

Through personal identification numbers issued to all Swedish residents, individual-level data from these registers were linked together.

Study population

We identified all b/tsDMARD initiations (first ever per b/tsDMARD class) between January 1, 2006, and December 31, 2021, among all patients with RA aged ≥18 years registered in SRQ. We also identified all first methotrexate initiations in bionaive patients with early RA, defined as time from RA diagnosis to methotrexate start less than 2 years. In addition, we included a matched general population comparator cohort; for each individual with RA who contributed data on a b/tsDMARD initiation, we matched 5 individuals without RA by age, sex (male or female), and residential area at the time of RA diagnosis of the index patient.

Exposure

b/tsDMARDs were categorised into the following drug class categories: tumour necrosis factor inhibitors (TNFis: etanercept, infliximab, adalimumab, golimumab, and certolizumab pegol), rituximab, interleukin 6 inhibitors (IL6is) (tocilizumab and sarilumab), abatacept, and JAKis (tofacitinib, baricitinib, upadacitinib and filgotinib). Of note, “exposure” was not the drug but aspects of time. We stratified b/tsDMARDs (overall and by class) by time since market entry of the b/tsDMARD class under study at treatment start (<2 years, 2-5 years, and >5 years). Treatment initiations remained in these categories irrespective of the duration of the treatment in question. For each drug class, we defined market entry as the date when the first drug in that class became available for prescription in Sweden (with RA as the approved indication) according to data from EMA and the Swedish Medical Products Agency (Supplemental Table S2). In addition, we also stratified by the calendar year of treatment initiation (2006-2010, 2011-2015, and 2016-2021).

Each patient could contribute one (the first) treatment episode to each b/tsDMARD class. For instance, a patient starting tocilizumab as a first ever b/tsDMARD in 2017, followed by baricitinib in 2020, contributed both episodes—the first to the IL6i class (with the treatment in question assigned to the “>5 years” since market entry category) and the second to the JAKi class (with the treatment in question assigned to the “2-5 years” since market entry category).

Outcome

The main outcomes were MACE, VTE, cancer, and serious (here: hospitalised) infection. We used a time to first event analysis from January 1, 2006, to December 31, 2022, and thereby allowed for a minimum of 1 year of follow-up data. First, we combined the 4 outcomes into a composite outcome (henceforth referred to as the “composite safety outcome”), defined as the first occurrence of any of the individual outcomes during follow-up. Second, we assessed the 4 outcomes individually. Individuals with a history of the outcome in question were included. Supplemental Table S3 provides the definition of outcomes and other covariates included.

Follow-up

Start of follow-up for the b/tsDMARD initiator cohorts and the methotrexate-initiator cohort was defined as the date of treatment start recorded in SRQ, with the additional requirement of at least one dispensation of the same drug in the PDR (not applicable to intravenous biologic DMARDs because these are provided in the hospital). Start of follow-up for the general population cohort was the date that the corresponding index b/tsDMARD patient initiated his/her first exposure-defining therapy. We used an on-drug approach, ie, follow-up ended at the recorded date of treatment discontinuation. To minimise informative right censoring, b/tsDMARD treatment episodes were censored 60 days after the registered date of treatment discontinuation.

End of follow-up was thus defined as either of (1) first record of any outcome (for analyses of the composite safety outcome) or (2) first record per outcome (for analyses of the individual outcomes) *or* 60 days after discontinuation of treatment, death, emigration, or end of study period.

Treatment discontinuation was defined as either of (1) registered date of discontinuation in the SRQ; (2) start of alternative b/tsDMARD in SRQ; or (3) date of filled prescription for alternative b/tsDMARD in PDR, whichever came first. Switch from an originator to biosimilar was considered the same treatment episode, as was restarting the same treatment within 90 days after discontinuation (180 days for rituximab) if no other b/tsDMARD was initiated in between.

Statistical analyses

We calculated crude incidence rates (IRs) for all cohorts and outcomes, separately by time since market entry of the b/tsDMARD class under study at treatment start (<2 years, 2-5 years, and >5 years), and by the calendar year of treatment initiation (2006-2010, 2011-2015, and 2016-2021).

Hazard ratios (HRs) comparing rates (by time since market entry and by calendar year) were estimated for the b/tsDMARD cohorts (overall and for each drug class) using Cox proportional hazards regression, both crude (HR1, ie, as observed) as well as adjusted for age, sex, and line of treatment (HR2), and additionally in a fully adjusted model, ie, a model adjusted for RA disease characteristics, comorbidities, comedications, and socioeconomic variables (HR3); see Supplemental Table S4 for details. We used a missing indicator for variables with missing data (see Supplemental Table S5 for the proportion missing for the 5 variables in HR3). Further statistical analyses are described in the online supplement.

Sensitivity analyses

Since the TNFi cohort was only represented in the “>5 years” category when stratifying on time since market entry (Swedish market entry in 1999 and study start in 2006), and since 55% of all b/tsDMARD treatment initiations were TNFis, we performed a sensitivity analysis in which TNFi was excluded from the overall b/tsDMARD cohort. In addition, since hospitalisation for infections comprised 61% of all events of the composite safety outcome, we performed a sensitivity analysis in which the composite safety outcome only included MACE, VTE, and cancer. We also used a Cox model where we combined the two 3-level exposures (time since market entry and calendar time period) into 1 variable, with 9 categories.

Data management and analyses were performed using SAS Enterprise Guide V.7.1 (SAS Institute) and Stata V.15 (StataCorp LLC), respectively.

Table 1
Characteristics at treatment start among 33,550 initiations of b/tsDMARD treatments in Swedish patients with RA from 2006 to 2021

	Years since market entry (of the b/tsDMARD class) at treatment start			Calendar period of treatment start		
	<2 y	2-5 y	>5 y	2006-2010	2011-2015	2016-2021
b/tsDMARD treatment initiations, n	2289	4116	27,145	8045	10,505	15,000
Individuals, n	2044	3713	21,468	7029	8766	11,915
Follow-up (y), median (IQR)	2.3 (0.7-4.7)	2.1 (0.9-4.4)	2.2 (0.8-5.1)	2.9 (0.9-8.6)	2.4 (0.8-7.1)	1.8 (0.8-3.6)
Age at treatment start (y), median (IQR)	60 (52-69)	61 (52-69)	59 (49-68)	59 (49-66)	60 (49-68)	60 (50-70)
Females (%)	81%	78%	76%	76%	76%	78%
Ever smoker (%)	22%	21%	25%	23%	29%	23%
RA duration (y), median (IQR)	13 (7-22)	12 (6-21)	8 (3-16)	9 (3-18)	8 (3-17)	9 (3-18)
No. of previous biologics, median (IQR)	2.0 (1.0-3.0)	2.0 (1.0-3.0)	0.0 (0.0-1.0)	0.0 (0.0-1.0)	0.0 (0.0-1.0)	0.0 (0.0-2.0)
Seropositive (RF and/or CCP2 positive) (%)	82%	82%	80%	82%	81%	80%
DAS28CRP, median (IQR)	4.9 (4.1-5.7)	4.8 (3.9-5.5)	4.5 (3.7-5.3)	4.9 (4.1-5.6)	4.6 (3.8-5.4)	4.3 (3.5-5.0)
CRP mg/L, median (IQR)	10 (4-29)	10 (4-27)	8 (3-20)	12 (5-29)	9 (3-23)	6 (2-16)
HAQ, median (IQR)	1.4 (0.9-1.9)	1.2 (0.9-1.8)	1.0 (0.6-1.5)	1.1 (0.8-1.6)	1.1 (0.8-1.6)	1.0 (0.5-1.5)
Comorbidities [a]						
Venous thromboembolism	4%	3%	2%	2%	3%	3%
Coronary heart disease	8%	8%	5%	6%	5%	5%
Hypertension	21%	22%	18%	15%	19%	20%
Hypercholesterolemia	4%	4%	4%	3%	4%	4%
Cerebrovascular disease	2%	2%	2%	2%	2%	2%
Cancer (other than NMSC)	5%	6%	4%	4%	5%	5%
Serious infection	18%	17%	10%	12%	12%	11%
Chronic kidney disease	2%	2%	1%	1%	1%	2%
COPD and asthma	17%	19%	16%	13%	16%	18%
Diabetes	9%	11%	9%	8%	9%	10%
Coagulopathy	1%	1%	0%	0%	1%	0%

b/tsDMARD, biologic/targeted synthetic disease-modifying antirheumatic drug; CCP2, cyclic citrullinated peptide 2; COPD, chronic obstructive pulmonary disease; CRP, C-reactive protein; DAS28CRP, disease activity score 28 C-reactive protein; HAQ, health assessment questionnaire; NMSC, nonmelanoma skin cancer; RA, rheumatoid arthritis; RF, rheumatoid factor.

[a] Registered within 5 years before treatment initiation, unless otherwise stated.

RESULTS

Table 1 presents baseline characteristics for the b/tsDMARD cohort, by time since market entry at treatment start and by calendar period at treatment start. Overall, 23,326 individuals with RA contributed to 33,550 b/tsDMARD initiations. Of all b/tsDMARD initiations included in our study, 6.8% occurred during the first 2 years after market entry of the drug class in question, whereas 81% occurred >5 years after market entry. Supplemental Tables S6 and S7 present additional baseline characteristics for these 2 stratifications. In general, the proportions of comorbidities were relatively similar for initiations of established vs recently approved drug classes (with the exception of prior serious infection, which was markedly lower for use of established drug classes), and for treatments initiated 2006-2010 vs 2016-2021, but along each time axis, the disease activity at treatment start declined. Supplemental Table S8 presents baseline characteristics for individual b/tsDMARDs as well as for the methotrexate cohort and the matched general population cohort.

Composite safety outcome by time since market entry at treatment start

Table 2 presents the number of events and IRs of the composite safety outcome for b/tsDMARDs overall and by drug class. Overall, there were 5862 composite safety events in the b/tsDMARD cohort, with a corresponding crude IR of 56 (95% CI = 55-58) per 1000 person-years (PYs). The IR was 47 (95% CI = 45-48) per 1000 PYs for the methotrexate cohort and 29 (95% CI = 29-30) per 1000 PYs for the general population cohort.

Table 2 also presents the number of events, IRs, and HRs for the composite safety outcome by time since drug class market entry at treatment start (<2 years, 2-5 years, and >5 years), both overall and by separate b/tsDMARD classes. For b/tsDMARDs overall, and using <2 years as reference, the unadjusted HR was 1.03 (95% CI = 0.92-1.15) for 2 to 5 years since market entry, and 0.74 (95% CI = 0.67-0.81) for >5 years since market entry. When using a fully adjusted model, the corresponding HRs were 0.99 (95% CI = 0.89-1.11) and 0.93 (95% CI = 0.84-1.03), respectively. Figure 1 visualises these rates by time since treatment start, both crude as well as estimated age- and sex-standardised, and Supplemental Figures S1 and S2 visualise the corresponding rates for separate b/tsDMARD classes.

Composite safety outcome by calendar period

Figure 2 presents the observed 1-year rates of the composite safety outcome for the overall b/tsDMARD cohort, the methotrexate cohort, and the general population cohort by calendar year of treatment start. There was a decrease in the observed crude rate of the composite outcome during the second half of the study period for the b/tsDMARD cohort, whereas the corresponding rates for the methotrexate cohort and the general population cohort remained more stable. Figure 3 visualises the smoothed crude 1-year rates of the composite safety outcome for each b/tsDMARD class separately. A decrease in rates during the latter half of the study period was also observed for the individual drug classes. In addition, different drug classes had somewhat varying initial (ie, soon after approval) estimated rates, and these differences lasted throughout the study period.

Rates and HRs for the composite safety outcome stratified by calendar period at treatment start are presented in Table 3 and visually depicted in Figure 4 and (for separate b/tsDMARDs) in Supplemental Figure S3. For b/tsDMARDs overall, using 2006-2010 as reference, the unadjusted HR was 0.93 (95% CI = 0.87-

Table 2

Number of events, time at risk, crude incidence rates and hazard ratios for composite safety outcome, stratified by time since market entry of b/tsDMARD class at treatment start

	Obs, N	PYs at risk	Events, N	Crude IR/1000 PYs (95% CI)	HR1[a] (95% CI)	HR2[b] (95% CI)	HR3[c] (95% CI)
All b/tsDMARD	33,550	103,802	5862	56 (55-58)			
<2 y	2289	7042	503	71 (65-78)	1 (ref)	1 (ref)	1 (ref)
2-5 y	4116	12,233	900	74 (69-79)	1.03 (0.92-1.15)	1.01 (0.90-1.13)	0.99 (0.89-1.11)
>5 y	27,145	84,527	4459	53 (52-54)	0.74 (0.67-0.81)	0.83 (0.76-0.92)	0.93 (0.84-1.03)
MTX	16,011	75,694	3548	47 (45-48)			
Gen.pop.	111,074	822,604	24,246	29 (29-30)			
	Obs, N	PYs at risk	Events, N	Crude IR/1000 PYs (95% CI)	HR1[a] (95% CI)	HR2[b] (95% CI)	HR3[c] (95% CI)
TNFi	18,254	61,603	2826	46 (44-48)			
<2 y	0	0	0	0	n/a[d]	n/a	n/a
2-5 y	0	0	0	0	n/a	n/a	n/a
>5 y	18,254	61,603	2826	46 (44-48)	n/a	n/a	n/a
RTX	5277	18,051	1509	83 (79-88)			
<2 y	458	1908	167	88 (75-102)	1 (ref)	1 (ref)	1 (ref)
2-5 y	1290	5220	466	89 (82-98)	1.02 (0.86-1.22)	0.93 (0.78-1.11)	0.99 (0.82-1.19)
>5 y	3529	10,924	876	80 (75-86)	0.88 (0.74-1.04)	0.77 (0.65-0.92)	0.83 (0.69-1.00)
IL6i	3356	9141	503	55 (50-60)			
<2 y	443	1709	100	59 (48-71)	1 (ref)	1 (ref)	1 (ref)
2-5 y	798	2286	161	57 (49-66)	0.94 (0.73-1.22)	0.96 (0.74-1.23)	0.96 (0.74-1.26)
>5 y	2115	4606	242	53 (46-60)	0.81 (0.63-1.03)	0.78 (0.61-0.99)	0.82 (0.62-1.08)
Abatacept	4035	9912	703	71 (66-76)			
<2 y	240	787	57	72 (56-94)	1 (ref)	1 (ref)	1 (ref)
2-5 y	548	1731	131	76 (64-90)	1.00 (0.73-1.37)	0.97 (0.71-1.33)	1.04 (0.76-1.44)
>5 y	3247	7394	515	70 (64-76)	0.85 (0.64-1.12)	0.74 (0.56-1.98)	0.93 (0.68-1.25)
JAKi	2628	5095	321	63 (56-70)			
<2 y	1148	2638	179	68 (59-79)	1 (ref)	1 (ref)	1 (ref)
2-5 y	1480	2457	142	58 (49-68)	0.78 (0.62-0.98)	0.80 (0.63-1.00)	0.78 (0.60-1.01)
>5 y	0	0	0	0	n/a	n/a	n/a

b/tsDMARD, biologic/targeted synthetic disease-modifying antirheumatic drug; Gen. pop., general population; HR, hazard ratio; IL6i, interleukin 6 inhibitor; IR, incidence rate; JAKi, Janus kinase inhibitor; MTX, methotrexate; n/a, not applicable; Obs, observations; PY, person-year; ref, reference; RTX, rituximab; TNFi, tumour necrosis factor inhibitor.

[a] HR1 from unadjusted Cox regression model.

[b] HR2 adjusted for age, sex, and line of therapy.

[c] HR3 further adjusted for rheumatoid arthritis (RA) disease variables, comorbidities, comedications, and socioeconomic variables.

[d] Calculation of HRs was not applicable due to no observations in 1 or several time categories for that specific drug class.

0.99) for 2011-2015 and 0.82 (95% CI = 0.77-0.88) for 2016-2021. In the fully adjusted model, the corresponding HRs were 0.87 (95% CI = 0.82-0.93) and 0.74 (95% CI = 0.69-0.80), respectively.

Analyses by outcome type (MACE, VTE, cancer, and serious infection)

As displayed in Table 4, there were in total of 1397 MACE events, corresponding to IR 12 (95% CI = 12-13) per 1000 PYs; 663 VTE events, corresponding to IR 5.8 (95% CI = 5.3-6.2); 1139 cancer events, corresponding to IR 12 (95% CI = 11-12); and 3592 serious infection events, corresponding to IR 33 (95% CI = 32-34). For MACE, cancer, and serious infection, the HR fell below 1 with increasing calendar time, whereas for VTE, the unadjusted HR was 1.12 (95% CI = 0.91-1.38) for 2016-2021 vs 2006-2010 and remained so after adjustment. These findings are further visualised in Supplemental Figures S4 and S5 (by time since market entry) and S6 and S7 (by calendar period).

The observed 1-year rates for b/tsDMARDs overall, the methotrexate cohort, and the general population cohort are visualised per separate outcome in Supplemental Figure S8.

Sensitivity analyses

When using a stratified Cox model conditioning the HR on b/tsDMARD drug class, ie, comparing within each b/tsDMARD class, the unadjusted stratified HR for established vs recently approved drug classes was largely similar to that of the main analysis (stratified HR = 0.82; 95% CI = 0.73-0.91 vs not stratified HR = 0.74; 95% CI = 0.67-0.81) and remained similar after adjusting (Supplemental Table S9).

When combining the 2 exposure variables into 1, the decrease in unadjusted HRs for established vs recently approved drug classes was more pronounced in the first two-thirds of the study period. However, once adjusted, this decrease was only observed in the last third of the study period (Supplemental Table S10).

When excluding TNFis from the overall b/tsDMARD cohort, the unadjusted HR for the risk of the composite safety outcome increased from 0.74 (95% CI = 0.67-0.81) to 0.98 (95% CI = 0.88-1.08, not stratified) and 0.82 (95% CI = 0.73-0.91, stratified) for established vs recently approved drug classes. The fully adjusted (not stratified) HRs remained very similar (HR = 0.92; 95% CI = 0.82-1.02) to the original fully adjusted analyses (HR = 0.93; 95% CI = 0.84-1.03). A similar increase towards 1 in the unadjusted HRs for the individual outcomes

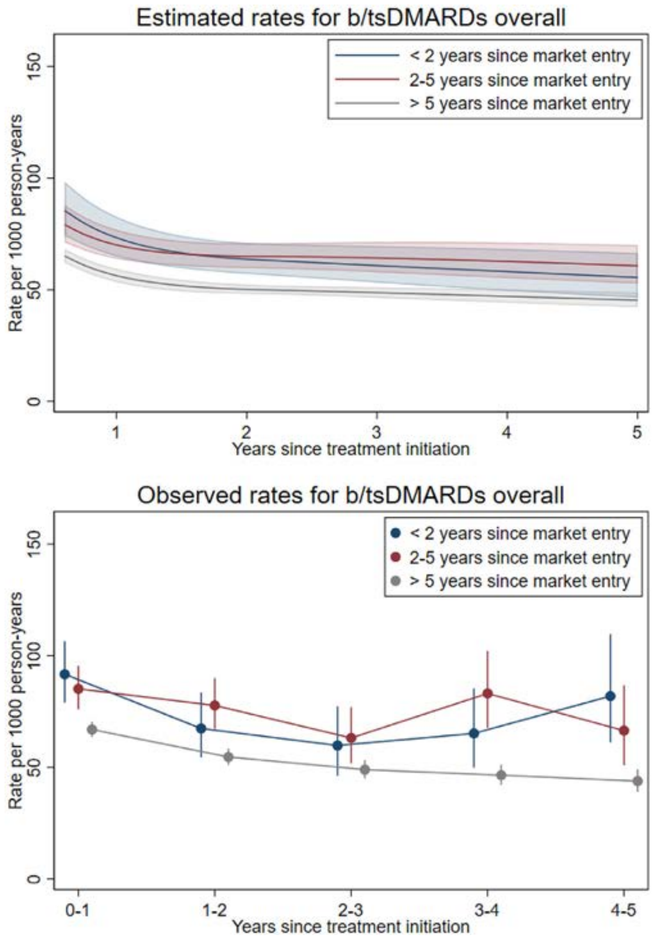

Figure 1. Rates of composite safety outcome for biologic/targeted synthetic disease-modifying antirheumatic drugs (b/tsDMARDs) overall in Swedish patients with rheumatoid arthritis (RA), stratified by time since drug class market entry at treatment start. Upper panel presents estimated age- and sex-standardised rates from a flexible parametric survival model (similar to a Cox model), and lower panel presents the observed rates.

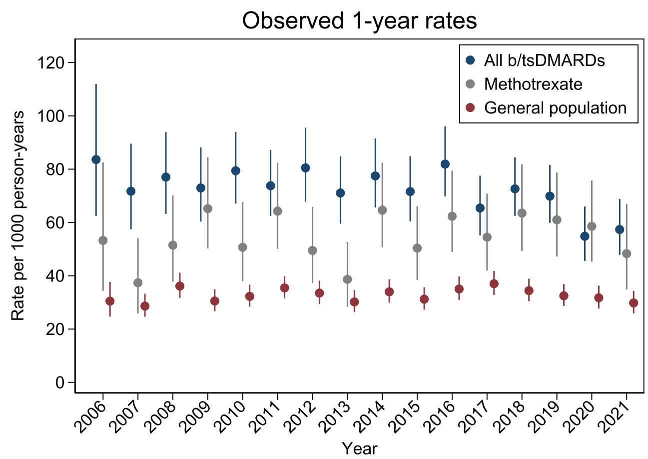

Figure 2. Observed 1-year rates of the composite safety outcome per calendar year at treatment start for biologic/targeted synthetic disease-modifying antirheumatic drugs (b/tsDMARDs) overall, the methotrexate cohort, and the matched general population cohort.

was also observed. For analyses by calendar period of treatment start, results from analyses excluding TNFis were similar to the main analysis (Supplemental Tables S11-S13).

When excluding serious infection from the composite safety outcome, the overall unadjusted HR for the risk of the composite

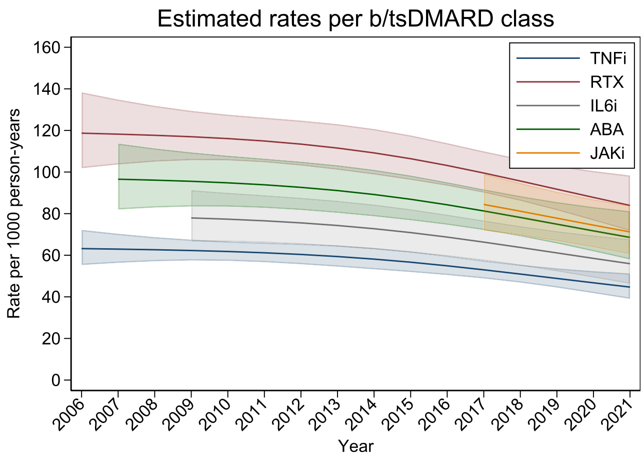

Figure 3. Smoothed crude 1-year rates of the composite safety outcome for each b/tsDMARD class in Swedish patients with rheumatoid arthritis (RA). Rates estimated using Poisson regression with log-person-time offset. ABA, abatacept; b/tsDMARD, biologic/targeted synthetic disease-modifying antirheumatic drug; IL6i, interleukin 6 inhibitor; JAKi, Janus kinase inhibitor; RTX, rituximab; TNFi, tumour necrosis factor inhibitor.

safety outcome for established vs recently approved drug classes went from 0.74 (95% CI = 0.67-0.81) to 0.93 (95% CI = 0.81-1.08). This change vs the main analysis was confined to rituximab and JAKis, where unadjusted HRs went from <1 to >1, although these data were statistically nonsignificant. The pattern of a decrease in rates by calendar time period was somewhat reduced when excluding serious infection from the composite outcome (Supplemental Tables S14 and S15).

DISCUSSION

In this nationwide cohort study including 33,550 b/tsDMARD initiations and 5862 composite safety events (first of MACE, VTE, cancer, or serious infection), we made the following observations: (1) there was a limited decline in the observed rates of the composite safety outcome going from treatments initiated within 2 years of market entry to treatments with the very same drug class but initiated ≥5 years since its market entry; (2) this difference disappeared after adjusting for RA disease variables, comorbidities, comedication, and socioeconomic variables; (3) there was a decrease in rates of the composite safety outcome during the study period for b/tsDMARDs overall, which remained after adjustment for the same variables; and (4) the same rates remained stable during the study period in bionaive early RA methotrexate users and in the general population.

To the best of our knowledge, this is the first study to investigate the impact of channelling bias specifically on the observed risks of safety outcomes with use of individual b/tsDMARDs when established vs when recently approved on the market. A previous study from our research group published in 2018 using an RA cohort overlapping with ours (albeit less updated) investigated (and confirmed that) patient characteristics influence the choice of biologic DMARD but did not investigate any time-axis trends [24].

Since the clinically observed ("crude" unadjusted) risks represent the net effect of measured or unmeasured confounding and any causal drug-specific effect(s), we chose to present our main results as crude or adjusted/standardised for age and sex only. Assuming that the biological properties of the drugs under study have remained constant, a perfect adjustment for all

Table 3

Number of events, time at risk, crude incidence rates, and hazard ratios for composite safety outcome, overall, and by b/tsDMARD treatment cohorts, stratified by calendar period at treatment start

	Obs, N	PYs at risk	Events, N	Crude IR/1000 PYs (95% CI)	HR1[a] (95% CI)	HR2[b] (95% CI)	HR3[c] (95% CI)
All b/tsDMARD	33,550	103,802	5862	56 (55-58)			
2006-2010	8045	34,721	2040	59 (56-61)	1 (ref)	1 (ref)	1 (ref)
2011-2015	10,505	36,310	2031	56 (54-58)	0.93 (0.87-0.99)	0.85 (0.80-0.91)	0.87 (0.82-0.93)
2016-2021	15,000	32,770	1791	55 (52-57)	0.82 (0.77-0.88)	0.70 (0.66-0.75)	0.74 (0.69-0.80)
MTX	16,011	75,694	3548	47 (45-48)			
Gen. pop.	111,074	822,604	24,246	29 (29-30)			
	Obs, N	PYs at risk	Events, N	Crude IR/1000 PYs (95% CI)	HR1[a] (95% CI)	HR2[b] (95% CI)	HR3[c] (95% CI)
TNFi	18,254	61,603	2826	46 (44-48)			
2006-2010	5586	25,217	1263	50 (47-53)	1 (ref)	1 (ref)	1 (ref)
2011-2015	5507	19,501	849	44 (41-47)	0.83 (0.78-0.93)	0.82 (0.75-0.90)	0.86 (0.78-0.95)
2016-2021	7161	16,885	714	42 (39-46)	0.78 (0.70-0.85)	0.69 (0.63-0.76)	0.74 (0.66-0.83)
RTX	5277	18,051	1509	83 (79-88)			
2006-2010	1537	6225	556	89 (82-97)	1 (ref)	1 (ref)	1 (ref)
2011-2015	2012	7653	621	81 (75-88)	0.90 (0.80-1.02)	0.86 (0.76-0.97)	0.90 (0.79-1.01)
2016-2021	1728	4172	332	80 (71-89)	0.80 (0.70-0.92)	0.71 (0.62-0.82)	0.72 (0.61-0.84)
IL6i	3356	9141	503	55 (50-60)			
2006-2010	428	1657	95	57 (47-70)	1 (ref)	1 (ref)	1 (ref)
2011-2015	1406	4633	257	55 (49-63)	0.93 (0.73-1.18)	0.93 (0.73-1.18)	0.95 (0.73-1.22)
2016-2021	1522	2851	151	53 (45-62)	0.80 (0.61-1.05)	0.74 (0.57-0.98)	0.77 (0.57-1.05)
Abatacept	4035	9912	703	71 (66-76)			
2006-2010	494	1623	126	78 (65-92)	1 (ref)	1 (ref)	1 (ref)
2011-2015	1580	4523	304	67 (60-75)	0.82 (0.67-1.01)	0.76 (0.62-0.94)	0.84 (0.67-1.06)
2016-2021	1961	3767	273	72 (64-82)	0.80 (0.64-0.99)	0.65 (0.52-0.81)	0.75 (0.59-0.97)
JAKi	2628	5095	321	63 (56-70)			
2006-2010	0	0	0	0	n/a[d]	n/a	n/a
2011-2015	0	0	0	0	n/a	n/a	n/a
2016-2021	2628	5095	321	63 (56-70)	n/a	n/a	n/a

b/tsDMARD, biologic/targeted synthetic disease-modifying antirheumatic drug; Gen. pop., general population; HR, hazard ratio; IL6i, interleukin 6 inhibitor; IR, incidence rate; JAKi, Janus kinase inhibitor; MTX, methotrexate; n/a, not applicable; Obs, observations; PY, person-year; ref, reference; RTX, rituximab; TNFi, tumour necrosis factor inhibitor.

[a] HR1 from unadjusted Cox regression model.

[b] HR2 adjusted for age, sex, and line of therapy.

[c] HR3 further adjusted for rheumatoid arthritis (RA) disease variables, comorbidities, comedications, and socioeconomic variables.

[d] Calculation of HRs not applicable due to no observations in 1 or several time categories for that specific drug class.

known and unknown confounders would completely nullify the effect we wished to quantify. Following further adjustment for relevant confounders, our HR for the risk of the composite safety outcome for drugs used when established vs recently approved shifted from 0.74 (95% CI = 0.67-0.81) to 0.93 (95% CI = 0.84-1.03). This shift in point estimate indicates that (1) there is indeed some confounding by indication (by measurable factors) that changes with time since market approval; (2) adjustment for confounders available in our registers handle this issue to a large extent; and therefore (3) any (to us) unmeasured confounding is likely to have a negligible effect on the rate of the observed safety outcomes. Importantly, again, this reasoning assumes no difference in (“true”) rates of safety outcome depending on the time that a given drug class has been on the market. The baseline characteristics demonstrate a limited although consistent decline in several comorbidities and comedications, as well as in disease activity, with use of drugs when recently approved vs later, which is in line with our main finding. Exclusion of TNFis from the b/tsDMARD cohort removed some of the observed effect (in models not conditioned on b/tsDMARD class but not in models comparing within each b/tsDMARD class), which may be explained by lower rates in the TNFi group that generally also reflected past rather than recent calendar time initiations.

Although our analyses by individual drug class where somewhat limited due to lack of power and no observations in certain time strata for TNFis and JAKis, HRs were generally very similar to those for b/tsDMARDs overall.

Regarding secular trends, we noted a general decrease in the overall rate of the composite safety outcome during the last third of the study period compared with the first third (overall HR 0.82), for all b/tsDMARD cohorts but neither for the methotrexate cohort nor for the general population comparator cohort. In contrast to the often-marked impact of adjustment for relevant patient characteristics in the analysis for established vs recently approved drug classes, adjusting for confounders had less impact on the results by calendar period at treatment start.

The same observation was made in the analyses restricted to individual b/tsDMARD classes, with the exception of JAKis (only treatment starts in the last third of the study period). When excluding serious infection from the composite safety outcome, the finding of decreasing rates during the study period was generally diminished, which is expected since serious infection is a proxy for general frailty and contributed to more than 60% of all composite safety events. We also noted that different drug classes had varying rates early after market entry, such that rituximab had the highest rates and TNFis the lowest. This might simply be an effect of rituximab increasing the risk of

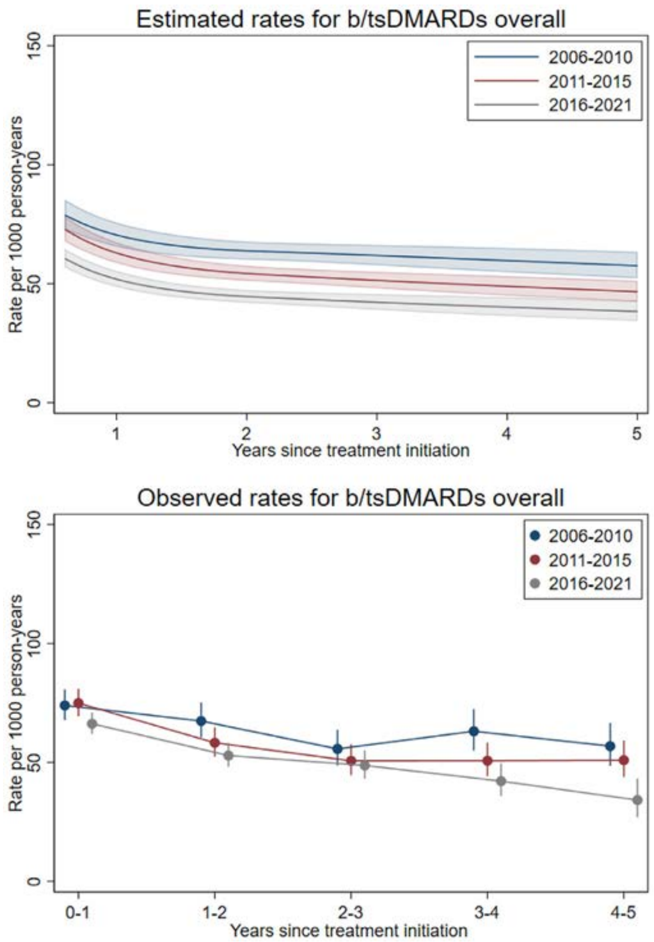

Figure 4. Rates of composite safety outcome for biologic/targeted synthetic disease-modifying antirheumatic drugs (b/tsDMARDs) overall in Swedish patients with rheumatoid arthritis (RA), stratified by calendar period at treatment start. Upper panel presents estimated age- and sex-standardised rates from a flexible parametric model (similar to a Cox model), and lower panel presents observed rates.

serious infections relative to other b/tsDMARDs. In addition, rituximab was preferred over other b/tsDMARDs for patients with a history of malignancy (ie, frail patients) during the majority of the study period.

Variations in the rate of safety events over calendar time may have several explanations. In the case of JAKis, safety signals and warnings from authorities are likely to influence the rate of prescription, as illustrated by an ecological study from the United Kingdom [25]. In addition, such warnings are likely to introduce channelling towards patients with low risk of the outcome in question, as indicated in a French observational study that noticed a decrease in the proportion of patients with a history of VTE initiating tofacitinib and baricitinib after vs before EMA's warning in 2019 [26]. The fact that the rates for the composite safety outcome were stable for the general population during the study period suggests that the decline in rates are specific for the RA cohort, which might reflect an increasing overall health of people with RA (about to start a b/tsDMARD) over time.

We also performed analyses for the separate outcomes, ie, MACE, VTE, cancer, and serious infection. Interestingly, and opposite to other outcomes, we noted an increase in VTE rates over calendar time for b/tsDMARD users (although not statistically significant). In addition, the adjusted HR for the risk of VTE for established vs recently approved drug classes was 0.63 (95% CI = 0.49-0.81), ie, a higher risk if the drug was used within 2 years since market entry, which might partially be driven by JAKis. However, it was beyond the scope of this study to disentangle any causal associations between individual drugs or classes of b/tsDMARD and the safety outcomes under study. For MACE, cancer, and serious infection, the incidence decreased over calendar time periods, and these findings remained in the fully adjusted analyses, which is likely to be explained by an overall increase in health of the RA population over time.

In addition to our main result, we also estimated HRs for the overall b/tsDMARD cohort from a conditioned (by drug class) Cox model to allow for an overall estimate without the assumption of equal underlying rates between drug classes. In this analysis, the unadjusted HR was similar to the main results, both for early vs later use of drugs in a class as well as with increasing calendar period, supporting the robustness of our results.

The potential impact of depletion of susceptibles on our results needs to be addressed and may be one explanation for the general pattern of an immediate decrease in rates during the first year after treatment initiation, as observed in all exposure (time-)categories. However, to impact our result of decreasing rates with time since market entry and with calendar year, the impact of depletion of susceptibles would need to vary between these time categories, ie, if the baseline risk of the outcomes under study over time of follow-up varied across our exposure categories.

Data from the SRQ show that the mean number of previous b/tsDMARDs for patients initiating a b/tsDMARD increased from 0.2 in 2006 to 1.2 in 2021. During the same time period, the proportion of the entire Swedish RA population treated with any b/tsDMARD has more than doubled and was ~50% in 2021. Thus, when interpreting our results, it is important to consider that the population under study is not static and that some of our observed effects emanate from selection of patients to new(-est) drugs, whereas others stem from (an increasing) selection of previously b/tsDMARD-naive patients to established drugs (here: TNFis).

This study has certain limitations. Although the registers used in our study allow for information on many relevant covariates, we lack information on certain potential confounders such as body mass index, physical activity, and blood pressure. Some of the variables included in our fully adjusted model had missing data, such as smoking and disease activity. On the other hand, previous studies from our group have shown minimal changes in results when applying multiple imputation for missing variables [18]. The so far relatively short follow-up time for JAKis in Sweden limits the analyses and conclusions regarding this specific drug class. Given our study design, we are unable to separate the impact of channelling from a true interaction between a certain drug class and some specific patient characteristic, although the latter is unlikely to have any major impact on our results.

This study also has certain strengths. We used data from the SRQ, which include more than 85% of all Swedish patients with RA treated by rheumatologists, linked to prospectively collected data from national registers with high internal validity and coverage. This allowed for low selection bias and the collection of safety outcomes independent of the exposure status. These registers also enabled us to compare our finding for the b/tsDMARD cohorts to a methotrexate-treated bionaive early RA cohort as well as a matched general population comparator cohort. Further, exposure validity was strengthened by qualifying exposure on a reported treatment start in combination of a dispensation of the same drug.

In conclusion, we found a 25% decrease in observed rates of a composite safety outcome (first of MACE, VTE, cancer, or serious infection) for b/tsDMARD classes when established vs recently approved. This difference disappeared after adjustment

Table 4

Overall number of events, time at risk, crude incidence rates, and hazard ratios for MACE, VTE, cancer, and serious infection, stratified by time since market entry of b/tsDMARD class at treatment start (upper half) and by calendar period at treatment start (lower half)

	Obs, N	PYs at risk	Events, N	Crude IR/1000 PYs (95% CI)	HR1[a] (95% CI)	HR2[b] (95% CI)	HR3[c] (95% CI)
MACE	33,550	114,098	1397	12 (12-13)			
<2 y	2289	8047	105	13 (11-16)	1 (ref)	1 (ref)	1 (ref)
2-5 y	4116	13,897	235	17 (15-19)	1.31 (1.03-1.64)	1.26 (1.00-1.59)	1.25 (1.00-1.58)
>5 y	27,145	92,154	1057	11 (11-12)	0.89 (0.73-1.09)	1.01 (0.82-1.25)	1.13 (0.91-1.40)
VTE	33,550	115,298	663	5.8 (5.3-6.2)			
<2 y	2289	8087	66	8.2 (6.4-10)	1 (ref)	1 (ref)	1 (ref)
2-5 y	4116	14,107	114	8.1 (6.7-9.7)	0.99 (0.73-1.34)	0.96 (0.71-1.31)	0.98 (0.72-1.33)
>5 y	27,145	93,104	483	5.2 (4.7-5.7)	0.63 (0.49-0.81)	0.68 (0.51-0.90)	0.74 (0.56-0.99)
Cancer	33,550	115,106	1339	12 (11-12)			
<2 y	2289	8109	98	12 (9.9-15)	1 (ref)	1 (ref)	1 (ref)
2-5 y	4116	14,084	185	13 (11-15)	1.09 (0.85-1.39)	1.04 (0.81-1.33)	1.02 (0.80-1.32)
>5 y	27,145	92,913	1056	11 (11-12)	0.95 (0.77-1.16)	1.00 (0.80-1.24)	1.01 (0.81-1.27)
Infection	33,550	108,544	3592	33 (32-34)			
<2 y	2289	7377	344	47 (42-52)	1 (ref)	1 (ref)	1 (ref)
2-5 y	4116	13,026	571	44 (40-48)	0.94 (0.82-1.08)	0.93 (0.81-1.06)	0.90 (0.79-1.03)
>5 y	27,145	88,141	2677	30 (29-32)	0.65 (0.58-0.73)	0.76 (0.67-0.85)	0.86 (0.76-0.97)
	Obs, N	PYs at risk	Events, N	Crude IR/1000 PYs (95% CI)	HR1[a] (95% CI)	HR2[b] (95% CI)	HR3[c] (95% CI)
MACE	33,550	114,098	1397	12 (12-13)			
2006-2010	8045	39,457	541	14 (13-15)	1 (ref)	1 (ref)	1 (ref)
2011-2015	10,505	39,859	490	12 (11-13)	0.92 (0.81-1.05)	0.83 (0.73-0.94)	0.83 (0.73-0.95)
2016-2021	15,000	34,782	366	11 (9-12)	0.81 (0.70-0.94)	0.66 (0.57-0.76)	0.65 (0.55-0.76)
VTE	33,550	115,298	663	5.8 (5.3-6.2)			
2006-2010	8045	40,142	199	4.9 (4.3-5.7)	1 (ref)	1 (ref)	1 (ref)
2011-2015	10,505	40,201	238	5.9 (5.2-6.7)	1.17 (0.96-1.42)	1.09 (0.90-1.33)	1.11 (0.91-1.37)
2016-2021	15,000	34,956	226	6.5 (5.7-7.4)	1.12 (0.91-1.38)	1.00 (0.81-1.23)	1.10 (0.87-1.39)
Cancer	33,550	115,106	1339	12 (11-12)			
2006-2010	8045	39,997	498	12 (11-14)	1 (ref)	1 (ref)	1 (ref)
2011-2015	10,505	40,271	467	12 (11-13)	0.94 (0.83-1.07)	0.90 (0.79-1.02)	0.90 (0.78-1.03)
2016-2021	15,000	34,838	374	11 (10-12)	0.90 (0.78-1.04)	0.83 (0.71-0.96)	0.82 (0.69-0.96)
Infection	33,550	108,544	3592	33 (32-34)			
2006-2010	8045	36,811	1275	35 (33-37)	1 (ref)	1 (ref)	1 (ref)
2011-2015	10,505	38,026	1236	33 (31-34)	0.89 (0.82-0.97)	0.81 (0.75-0.88)	0.84 (0.77-0.91)
2016-2021	15,000	33,706	1081	32 (30-34)	0.77 (0.71-0.84)	0.65 (0.60-0.71)	0.71 (0.65-0.79)

b/tsDMARD, biologic/targeted synthetic disease-modifying antirheumatic drug; HR, hazard ratio; IR, incidence rate; MACE, major adverse cardiovascular event; Obs, observations; PY, person-year; ref, reference; VTE, venous thromboembolism.

[a] HR1 from unadjusted Cox regression model.

[b] HR2 adjusted for age, sex, and line of therapy.

[c] HR3 adjusted for rheumatoid arthritis (RA) disease variables, comorbidities, comedications, and socioeconomic variables.

for confounders, suggesting that channelling is behind this observation. We also noted a trend towards declining rates of the composite safety outcome over calendar time, suggesting that the bar defining "acceptable" rates of safety outcomes of new and future antirheumatic drugs should be lower than that used for the past approval of existing b/tsDMARDs.

Competing interests

Karolinska Institutet, with JA as principal investigator, has or has had research agreements with AbbVie, Astra-Zeneca, BMS, Eli Lilly, Galapagos, MSD, Pfizer, Roche, Samsung Bioepis, Sanofi, and UCB, mainly in the context of safety monitoring of biologics via ARTIS/Swedish Biologics Register.

Acknowledgements

We would like to thank all rheumatologists and patients with RA in Sweden for persistently entering data into the Swedish Rheumatology Quality Register (SRQ), as well as rheumatology nurses and staff at the SRQ office for their work with further increasing the coverage of the register.

Contributors

All authors participated in the design of the study and drafting of the study protocol before the analyses. VM and HB conducted the statistical analyses. VM drafted the first version of the manuscript. All authors contributed to interpretation of the results and the critical revision of the manuscript for important intellectual content. VM is guarantor for the study.

Funding

This study has received funding from the Swedish Research Council (individual project- and ERA-PerMed grants), the Swedish Heart Lung Foundation, the Swedish Cancer Society, Nordforsk, Vinnova, Horizon EU (the SPIDERR, SUEEZE and STRATAFIT projects) and the Karolinska Institutet Region Stockholm funds (ALF).

Patient consent for publication

See ethics approval.

Ethics approval

This study involves human participants and was approved by Regional Ethics Committee, Stockholm, Sweden (Dnr 2015/1844-31/2). Informed consent for this study was, in accordance with Swedish law, not required from the Ethics Committee.

Provenance and peer review

Peer reviewed.

Patient and public involvement

Patients or the public were not involved in the study design, or conduct, or reporting, or dissemination plans of our research but contributed data through patient-reported data in the Swedish Rheumatology Quality Register.

Supplementary materials

Supplementary material associated with this article can be found in the online version at doi:10.1016/j.ard.2025.01.020.

REFERENCES

[1] England BR, Thiele GM, Anderson DR, Mikuls TR. Increased cardiovascular risk in rheumatoid arthritis: mechanisms and implications. BMJ 2018;361:k1036.
[2] Kremers HM, Crowson CS, Therneau TM, Roger VL, Gabriel SE. High ten-year risk of cardiovascular disease in newly diagnosed rheumatoid arthritis patients: a population-based cohort study. Arthritis Rheum 2008;58(8):2268–74.
[3] Delcoigne B, Ljung L, Provan SA, Glintborg B, Hetland ML, Grøn KL, et al. Short-term, intermediate-term and long-term risks of acute coronary syndrome in cohorts of patients with RA starting biologic DMARDs: results from four Nordic countries. Ann Rheum Dis 2022;81(6):789–97.
[4] Kim SC, Schneeweiss S, Liu J, Solomon DH. Risk of venous thromboembolism in patients with rheumatoid arthritis. Arthritis Care Res (Hoboken) 2013;65(10):1600–7.
[5] Molander V, Bower H, Frisell T, Askling J. Risk of venous thromboembolism in rheumatoid arthritis, and its association with disease activity: a nationwide cohort study from Sweden. Ann Rheum Dis 2021;80(2):169–75.
[6] Choi HK, Rho YH, Zhu Y, Cea-Soriano L, Aviña-Zubieta JA, Zhang Y. The risk of pulmonary embolism and deep vein thrombosis in rheumatoid arthritis: a UK population-based outpatient cohort study. Ann Rheum Dis 2013;72(7):1182–7.
[7] Zintzaras E, Voulgarelis M, Moutsopoulos HM. The risk of lymphoma development in autoimmune diseases: a meta-analysis. Arch Intern Med 2005;165(20):2337–44.
[8] Wu X, Peng H, Wen Y, Cai X, Li C, Zhong R, et al. Rheumatoid arthritis and risk of lung cancer: meta-analysis and Mendelian randomization study. Semin Arthritis Rheum 2021;51(3):565–75.
[9] Xie W, Huang Y, Xiao S, Sun X, Fan Y, Zhang Z. Impact of Janus kinase inhibitors on risk of cardiovascular events in patients with rheumatoid arthritis: systematic review and meta-analysis of randomised controlled trials. Ann Rheum Dis 2019;78(8):1048–54.
[10] Ytterberg SR, Bhatt DL, Mikuls TR, Koch GG, Fleischmann R, Rivas JL, et al. Cardiovascular and cancer risk with tofacitinib in rheumatoid arthritis. N Engl J Med 2022;386(4):316–26.
[11] US Food and Drug Administration. Safety trial finds risk of blood clots in the lungs and death with higher dose of tofacitinib (Xeljanz, Xeljanz XR) in rheumatoid arthritis patients; FDA to investigate. Available from: https://www.fda.gov/drugs/drug-safety-and-availability/safety-trial-finds-risk-blood-clots-lungs-and-death-higher-dose-tofacitinib-xeljanz-xeljanz-xr [Accessed 8 Oct 2024].
[12] European Medicines Agency. Increased risk of blood clots in lungs and death with higher dose of Xeljanz (tofacitinib) for rheumatoid arthritis. Available from: https://www.ema.europa.eu/en/documents/press-release/increased-risk-blood-clots-lungs-and-death-higher-dose-xeljanz-tofacitinib-rheumatoid-arthritis_en.pdf [Accessed 8 Oct 2024].
[13] US Food and Drug Administration. FDA requires warnings about increased risk of serious heart-related events, cancer, blood clots, and death for JAK inhibitors that treat certain chronic inflammatory conditions. Available: https://www.fda.gov/drugs/drug-safety-and-availability/fda-requires-warnings-about-increased-risk-serious-heart-related-events-cancer-blood-clots-and-death [Accessed 8 Oct 2024].
[14] European Medicines Agency. EMA recommends measures to minimise risk of serious side effects with Janus kinase inhibitors for chronic inflammatory disorders. Available from: https://www.ema.europa.eu/en/news/ema-recommends-measures-minimise-risk-serious-side-effects-janus-kinase-inhibitors-chronic-inflammatory-disorders [Accessed 8 Oct 2024].
[15] Bower H, Frisell T, di Giuseppe D, Delcoigne B, Askling J. Comparative cardiovascular safety with Janus kinase inhibitors and biological disease-modifying antirheumatic drugs as used in clinical practice: an observational cohort study from Sweden in patients with rheumatoid arthritis. RMD Open 2023;9(4):e003630.
[16] Huss V, Bower H, Hellgren K, Frisell T, Askling J, ARTIS group. Cancer risks with JAKi and biological disease-modifying antirheumatic drugs in patients with rheumatoid arthritis or psoriatic arthritis: a national real-world cohort study. Ann Rheum Dis 2023;82(7):911–9.
[17] Westermann R, Cordtz RL, Duch K, Mellemkjaer L, Hetland ML, Burden AM, et al. Cancer risk in patients with rheumatoid arthritis treated with Janus kinase inhibitors: a nationwide Danish register-based cohort study. Rheumatology (Oxford) 2024;63(1):93–102.
[18] Molander V, Bower H, Frisell T, Delcoigne B, Di Giuseppe D, Askling J, ARTIS study group. Venous thromboembolism with JAK inhibitors and other immune-modulatory drugs: a Swedish comparative safety study among patients with rheumatoid arthritis. Ann Rheum Dis 2023;82(2):189–97.
[19] Hoisnard L, Pina Vegas L, Dray-Spira R, Weill A, Zureik M, Sbidian E. Risk of major adverse cardiovascular and venous thromboembolism events in patients with rheumatoid arthritis exposed to JAK inhibitors versus adalimumab: a nationwide cohort study. Ann Rheum Dis 2023;82(2):182–8.
[20] Desai RJ, Pawar A, Khosrow-Khavar F, Weinblatt ME, Kim SC. Risk of venous thromboembolism associated with tofacitinib in patients with rheumatoid arthritis: a population-based cohort study. Rheumatology (Oxford) 2021;61(1):121–30.
[21] Salinas CA, Louder A, Polinski J, Zhang TC, Bower H, Phillips S, et al. Evaluation of VTE, MACE, and serious infections among patients with RA treated with baricitinib compared to TNFi: a multi-database study of patients in routine care using disease registries and claims databases. Rheumatol Ther 2023;10(1):201–23.
[22] Svensk Reumatologisk Förening. Guidelines for treatment of rheumatoid arthritis, Swedish Society for Rheumatology. Available from: https://riktlinjer.svenskreumatologi.se/wp-content/uploads/2022/03/riktlinjer-for-lakemedelsbehandling-vid-ra_2024_till-styrelsen.docx [Accessed 8 Oct 2024].
[23] Smolen JS, Landewé RBM, Bergstra SA, Kerschbaumer A, Sepriano A, Aletaha D, et al. EULAR recommendations for the management of rheumatoid arthritis with synthetic and biological disease-modifying antirheumatic drugs: 2022 update. Ann Rheum Dis 2023;82(1):3–18.
[24] Frisell T, Baecklund E, Bengtsson K, Di Giuseppe D, Forsblad-D'Elia H, Askling J, ARTIS study group. Patient characteristics influence the choice of biological drug in RA, and will make non-TNFi biologics appear more harmful than TNFi biologics. Ann Rheum Dis 2018;77(5):650–7.
[25] Russell MD, Yang Z, Walter B, Alveyn E, Bechman K, Miracle A, et al. The influence of safety warnings on the prescribing of JAK inhibitors. Lancet Rheumatol 2024;6(3):e138–9.
[26] Philippoteaux C, Deprez V, Nottez A, Cailliau E, Houvenagel E, Deprez X, et al. Characteristics of patients treated with JAK inhibitors in rheumatoid arthritis before versus after VTE risk warnings. J Clin Med 2022;12(1):207.

Ann Rheum Dis 84 (2025) 726−745

Contents lists available at ScienceDirect

Annals of the Rheumatic Diseases

journal homepage: https://www.sciencedirect.com/journal/annals-of-the-rheumatic-diseases

Rheumatoid arthritis

Generation of cytotoxic aptamers specifically targeting fibroblast-like synoviocytes by CSCT-SELEX for treatment of rheumatoid arthritis

Fang Qiu[1,2], Duoli Xie[1,2], Hongzhen Chen[1], Zhuqian Wang[1,2], Jie Huang[1,2], Chunhao Cao[1,2], Yiying Liang[3], Xu Yang[4], Dong-Yi He[5], Xuekun Fu[1,*], Aiping Lu[2,6,7,*], Chao Liang[1,2,8,*]

[1] *Department of Systems Biology, School of Life Sciences, Southern University of Science and Technology, Shenzhen, China*

[2] *Institute of Integrated Bioinfomedicine and Translational Science (IBTS), School of Chinese Medicine, Hong Kong Baptist University, Hong Kong SAR, China*

[3] *LingGene Biotech Co., Ltd, Shenzhen, China*

[4] *Department of Computational Biology, St Jude Children's Research Hospital, Memphis, TN, USA*

[5] *Department of Rheumatology, Shanghai Guanghua Hospital of Integrative Medicine, Shanghai University of Traditional Chinese Medicine, Shanghai, China*

[6] *Guangdong-Hong Kong-Macau Joint Lab on Chinese Medicine and Immune Disease Research, Guangzhou, China*

[7] *Shanghai University of Traditional Chinese Medicine, Shanghai, China*

[8] *State Key Laboratory of Proteomics, National Center for Protein Sciences (Beijing), Beijing Institute of Lifeomics, Beijing, China*

ARTICLE INFO

Article history:
Received 22 January 2024
Accepted 21 August 2024

Keywords:
Rheumatoid Arthritis
Fibroblasts
Inflammation
Therapeutics
Arthritis
Experimental

ABSTRACT

Objectives: Rheumatoid arthritis (RA) is an autoimmune disease characterised by aggressive fibroblast-like synoviocytes (FLSs). Very few RA patients-derived FLSs (RA-FLSs)-specific surface signatures have been identified, and there is currently no approved targeted therapy for RA-FLSs. This study aimed to screen therapeutic aptamers with cell-targeting and cytotoxic properties against RA-FLSs and to uncover the molecular targets and mechanism of action of the screened aptamers.

Methods: We developed a cell-specific and cytotoxic systematic evolution of ligands by exponential enrichment (CSCT-SELEX) method to screen the therapeutic aptamers without prior knowledge of the surface signatures of RA-FLSs. The molecular targets and mechanisms of action of the screened aptamers were determined by pull-down assays and RNA sequencing. The therapeutic efficacy of the screened aptamers was examined in arthritic mouse models.

Results: We obtained an aptamer SAPT8 that selectively recognised and killed RA-FLSs. The molecular target of SAPT8 was nucleolin (NCL), a shuttling protein overexpressed on the surface and involved in the tumor-like transformation of RA-FLSs. Mechanistically, SAPT8 interacted with the surface NCL and was internalised to achieve lysosomal degradation of NCL, leading to the upregulation of proapoptotic p53 and downregulation of antiapoptotic B-cell lymphoma 2 (Bcl-2) in RA-FLSs. When administrated systemically to arthritic mice, SAPT8 accumulated in the inflamed FLSs of joints. SAPT8 monotherapy or its combination with tumour necrosis factor (TNF)-targeted biologics was shown to relieve arthritis in mouse models.

*Correspondence to Dr. Xuekun Fu; Prof. Aiping Lu; Dr. Chao Liang.

E-mail addresses: fuxk@mail.sustech.edu.cn (X. Fu), aipinglu@hkbu.edu.hk (A. Lu), liangc@sustech.edu.cn (C. Liang).

Handling editor Josef S. Smolen.

FQ and DX contributed equally.

https://doi.org/10.1136/ard-2024-225565

Conclusions: CSCT-SELEX could be a promising strategy for developing cell-targeting and cytotoxic aptamers. SAPT8 aptamer selectively ablates RA-FLSs via modulating NCL-p53/Bcl-2 signalling, representing a potential alternative or complementary therapy for RA.

WHAT IS ALREADY KNOWN ON THIS TOPIC

- Fibroblast-like synoviocytes (FLSs)-directed therapies have long been suggested as an alternative or complementary approach to the current immunosuppressive agents for rheumatoid arthritis (RA).
- Cadherin-11 (CDH11) has been identified as a surface target for developing selective anti-FLS therapy, while antibodies against CDH11 fail to display therapeutic effects for patients with RA.
- A primary obstacle is that molecular events driving pathological transformation of FLSs in RA are poorly understood, and few FLSs-specific surface targets have been identified.

WHAT THIS STUDY ADDS

- This study presents a cell-specific and cytotoxic systematic evolution of ligands by exponential enrichment (CSCT-SELEX) technology to screen aptamers with cell-targeting and cytotoxic properties without prior knowledge of cell surface signatures.
- The SAPT8 aptamer generated by CSCT-SELEX selectively ablates inflamed FLSs and relieves arthritis symptoms in mouse models after monotherapy or combined therapy with an anti-tumour necrosis factor (TNF) agent.
- Nucleolin (NCL) is identified as the specific target of SAPT8 on the surface of inflamed FLSs, and SAPT8 induces lysosomal degradation of NCL to modulate p53/B-cell lymphoma 2 signalling.

HOW THIS STUDY MIGHT AFFECT RESEARCH, PRACTICE OR POLICY

- CSCT-SELEX is a promising technology for identifying therapeutic aptamers and surface molecular targets for disease cells.
- The SAPT8 aptamer targeting RA patients-derived FLSs (RA-FLSs) represents an alternative or complementary therapy to the current immunosuppressive agents for RA.
- NCL offers potential as a molecular target on the surface of RA-FLSs for developing FLSs-directed therapies for RA.

INTRODUCTION

Rheumatoid arthritis (RA) is a systemic, autoimmune, peripheral polyarthritis that primarily involves the small joints of feet and hands [1]. It is characterised by chronic inflammation, synovial hyperplasia, pannus formation and destruction of bone and cartilage [2]. Currently, the aetiology of RA remains unclear, and numerous genetic and environmental factors have been reported to be associated with an increased risk of RA [3]. Pathophysiology of RA involves the overactivation of immune cells such as T cells, B cells and macrophages and the release of large numbers of inflammatory mediators, such as interleukin 6 (IL-6), IL-1β, tumour necrosis factor-α (TNF-α) and matrix metalloproteinases (MMPs) [4−8]. Significant progress in RA management has been made in the last decades, since the introduction of diverse synthetic and biologic disease-modifying antirheumatic drugs (DMARDs) [9]. Despite this, still a considerable proportion of patients with RA do not respond adequately to the currently available therapies [10], and there is an urgent need for new treatment options for RA.

The commonly used DMARDs are immunosuppressive agents that prevent the excessive activation of immune response in RA [11]. However, it is now widely considered that an immunosuppressive strategy is not sufficient to completely halt RA progression because non-immune cells have also been suggested to play critical roles in RA development besides the innate and adaptive immune systems, particularly the fibroblast-like synoviocytes (FLSs) [10]. FLSs, also known as synovial fibroblasts, are highly specialised mesenchymal cells that populate the intimal lining of synovium [12]. The normal function of FLSs is to maintain the homeostasis of the diarthrodial joints by producing extracellular matrix components and synovial fluid, thereby lubricating and nourishing cartilage surfaces [11]. In RA, however, FLSs are activated to undergo phenotypic transformation into tumour-like cells [13] and produce many inflammatory mediators, leading to growing synovial pannus that invade adjacent cartilage and bone [14]. Thus, RA patients-derived FLSs (RA-FLSs)-directed therapies have long been suggested as a potentially alternative or complementary approach to the current DMARDs-based immune-directed therapies in RA [12−14].

Depressingly, no clinically available therapy selectively ablates RA-FLSs until now [10]. So far, only cadherin-11 (CDH11), a major cell surface adhesion molecule that acts as a critical regulator of synovial lining formation [15], has been extensively tested as a potential target for developing selective anti-RA-FLSs therapy [16], even though a monoclonal antibody against CDH11 fails to display sufficient efficacy in treating RA in a clinical trial [10]. Recently, another emerging RA-FLSs-specific cell surface molecular target is receptor tyrosine phosphatase sigma (PTPRS), while efforts to target it remain in their infancy [16,17]. A primary obstacle to developing selective anti-RA-FLSs therapies is that molecular events that drive the tumour-like transformation of RA-FLSs are poorly understood, and very few RA-FLSs-specific cell surface molecular signatures have been identified [18]. We wonder whether it is possible to design a high-throughput screening strategy to develop selective anti-RA-FLS therapies without prior knowledge of RA-FLSs-specific cell surface molecular signatures.

Keeping the above idea in mind, we think of aptamer technology [19]. Aptamers are single-stranded DNA (ssDNA) or RNA, which can fold into unique three-dimensional structures and specifically recognise a variety of targets, including organic molecules, peptides, proteins and even whole cells [20−22]. They can be screened by an in vitro high-throughput procedure called the systematic evolution of ligands by exponential enrichment (SELEX) [23]. Besides being widely employed as navigation tools in nanotechnology [24], aptamers are emerging as a new class of nucleic acid drugs with affinity and specificity, rivalling that of antibodies [20]. When carried out against whole cells, the SELEX is specified as cell-SELEX [25], a counterselection strategy to screen aptamers that only interact with target cells but not control cells [20]. The unique advantage of cell-SELEX is that the process can generate aptamers without any prior knowledge of specific molecular signatures expressed on the cell surface of target cells and also enables the identification of previously unknown cell surface molecular signatures [26]. This advantage of cell-SELEX seems to fit in with our idea of developing selective anti-RA-FLS therapies without prior knowledge of RA-FLSs-specific cell surface molecular signatures. However, in most cases, cell-SELEX only generates cell-targeting aptamers [27], but barely produces therapeutic aptamers exhibiting functional impacts on target cells [28]. Thus, cell-SELEX could not guarantee the identification of desired aptamers that selectively ablate RA-FLSs.

In our study, we develop a cell-specific and cytotoxic SELEX (CSCT-SELEX) strategy to screen aptamers with both cell-targeting and cytotoxic properties without any prior knowledge of molecular signatures specifically expressed on the cell surface of target cells. By CSCT-SELEX, we obtained two aptamers (SAPT4 and SAPT8) that display specific binding with RA-FLSs and proapoptotic potential against RA-FLSs. We further show that SAPT4 and SAPT8 also specifically recognise and kill a human synovial cell line SW982 and FLSs from arthritic rat and mouse models in vitro. Mechanistically, we failed to identify the target of SAPT4, but we discovered that the molecular target of SAPT8 is nucleolin (NCL), which is specifically expressed on the cell surface of RA-FLSs. NCL has been reported to act as an RNA-binding protein that controls gene expression by regulating either mRNA stability or translation [27]. Interestingly, NCL has been shown to shuttle from the nucleus to the cell membrane to facilitate resistance to apoptosis and the growth of tumours [29]. However, NCL is rarely studied in RA. Here, we reveal the pathogenic role of NCL in the tumour-like transformation of RA-FLSs. We find that SAPT8 recognises and ablates RA-FLSs via targeting and degrading NCL in a lysosome-dependent manner. SAPT8 modulates the expression of NCL target genes, including proapoptotic p53 and antiapoptotic B-cell lymphoma 2 (Bcl-2) [30], leading to inhibited tumour-like phenotypes of RA-FLSs. Our in vivo study shows the obvious accumulation of SAPT8 in FLSs of arthritic mice and the desired therapeutic effects of SAPT8 monotherapy or SAPT8 in combination therapy with a TNF-targeted biological DMARD for treating arthritis.

In summary, this study provides a new type of SELEX, that is, CSCT-SELEX, which would be a promising strategy for screening aptamers possessing both cell-targeting and cytotoxic properties without prior knowledge of cell surface molecular signatures. By CSCT-SELEX, we obtain an aptamer SAPT8 that selectively ablates RA-FLSs via modulating NCL-p53/Bcl-2 signalling, representing a potential alternative or complementary therapy to the current DMARDs for RA.

RESULTS

Development of CSCT-SELEX to generate RA-FLSs-specific and cytotoxic aptamers

We developed a new SELEX strategy, called cell-specific and cytotoxic SELEX (CSCT-SELEX), to screen cytotoxic aptamers specifically targeting RA-FLSs. The CSCT-SELEX was a tandem process consisting of a cell-specific SELEX (CS-SELEX) module followed by a cytotoxic SELEX (CT-SELEX) module (figure 1A). Briefly, CS-SELEX was performed using a random ssDNA library and included multiple rounds of positive selection and negative selection, which was similar with that of the traditional cell-SELEX [31,32]. RA-FLSs, characterised by high expression of fibroblastic biomarkers THY1 and vimentin[33,34] as well as absence of a macrophage marker CD68 [35] (online supplemental figure S1A,B), were employed as target cells in the positive selection (figure 1A), and human monocytic THP-1 cells and osteoblastic hFOB 1.19 cells were used as control cells in the negative selection (figure 1A). Via the CS-SELEX, ssDNA sequences specifically recognising RA-FLSs could be enriched, and interfering sequences bound with the common cell surface molecular signatures between target cells and control cells could be removed (figure 1A). Then, the CT-SELEX was initiated using the ssDNA enriched pool that exhibited the strongest binding ability with RA-FLSs in the CS-SELEX module (figure 1A). The CT-SELEX module was an iterative process via treating RA-FLSs with the enriched ssDNA pools and collecting apoptotic cells rather than live cells for isolating proapoptotic aptamers (figure 1A).

During CS-SELEX, we monitored the binding ability of the enriched ssDNA pools with target cells (RA-FLSs) and control cells (THP-1 and hFOB 1.19 cells). After incubation with Cy3-labelled enriched pools from increasing rounds of CS-SELEX, the mean fluorescence intensity (MFI) of RA-FLSs was gradually enhanced, whereas there was no obvious improvement in MFI of THP-1 and hFOB 1.19 cells (figure 1B). We also examined the proapoptotic capacity of the enriched pools from the CT-SELEX on RA-FLSs. Apoptotic cells of RA-FLSs were increased after incubation with the enriched pools from the increasing rounds of the CT-SELEX (figure 1C). After the whole CSCT-SELEX, we sequenced the enriched ssDNA and chose the most enriched eight aptamer candidates (SAPT1-8) for further characteristics (online supplemental table S1). Among the candidates, SAPT4 and SAPT8 not only showed good binding with RA-FLSs (figure 1D) but also had proapoptotic capacity against RA-FLSs (figure 1E and online supplemental figure S1C). Notably, the binding ability and proapoptotic capacity of SAPT8 against RA-FLSs were better than those of SAPT4 (figure 1D,E and online supplemental figure S1C). Both SAPT4 and SAPT8 displayed time-dependent and concentration-dependent binding with RA-FLSs (figure 1F,G). The equilibrium dissociation constants (K_d) of SAPT4 and SAPT8 with RA-FLSs were 101.7±29.6 and 71.2±15.0 nM, respectively (figure 1H). Neither SAPT4 nor SAPT8 could bind with THP-1 and hFOB 1.19 cells (online supplemental figure S1D). We observed no obvious binding between SAPT4 or SAPT8 with a human normal skin fibroblast cell line BJ (online supplemental figure S1D). We obtained minimally activated FLSs from individuals who suffered from an anterior cruciate ligament injury (ACLI), that is, ACLI-FLSs. SAPT8 only showed marginal binding with ACLI-FLSs (online supplemental figure S1D). Neither SAPT4 nor SAPT8 induced apoptosis of THP-1 cells, hFOB 1.19 cells, BJ cells and ACLI-FLSs (online supplemental figure S1E). Both SAPT4 and SAPT8 showed good serum stability for at least 24 hours (online supplemental figure S1F). The predicted secondary structures of SAPT4 and SAPT8 are shown in figure 1I.

SAPT4 and SAPT8 inhibit tumour-like phenotypes of RA-FLSs and SW982 in vitro

Besides apoptosis resistance, RA-FLSs also acquire other tumour-like phenotypes, such as hyperproliferation and increased invasion and migration [36,37]. We examined whether SAPT4 and SAPT8 had inhibitory effects on these phenotypes of RA-FLSs in vitro. We incubated RA-FLSs with phosphate buffered saline (PBS), a negative control (NC) sequence, SAPT4 or SAPT8 and performed Cell Counting Kit-8 (CCK-8), colony formation, transwell and wound healing assays. CCK-8 and colony formation assays demonstrated that both SAPT4 and SAPT8 inhibited cell viability and proliferation of RA-FLSs when compared with PBS or NC (figure 2A,B). Transwell assays

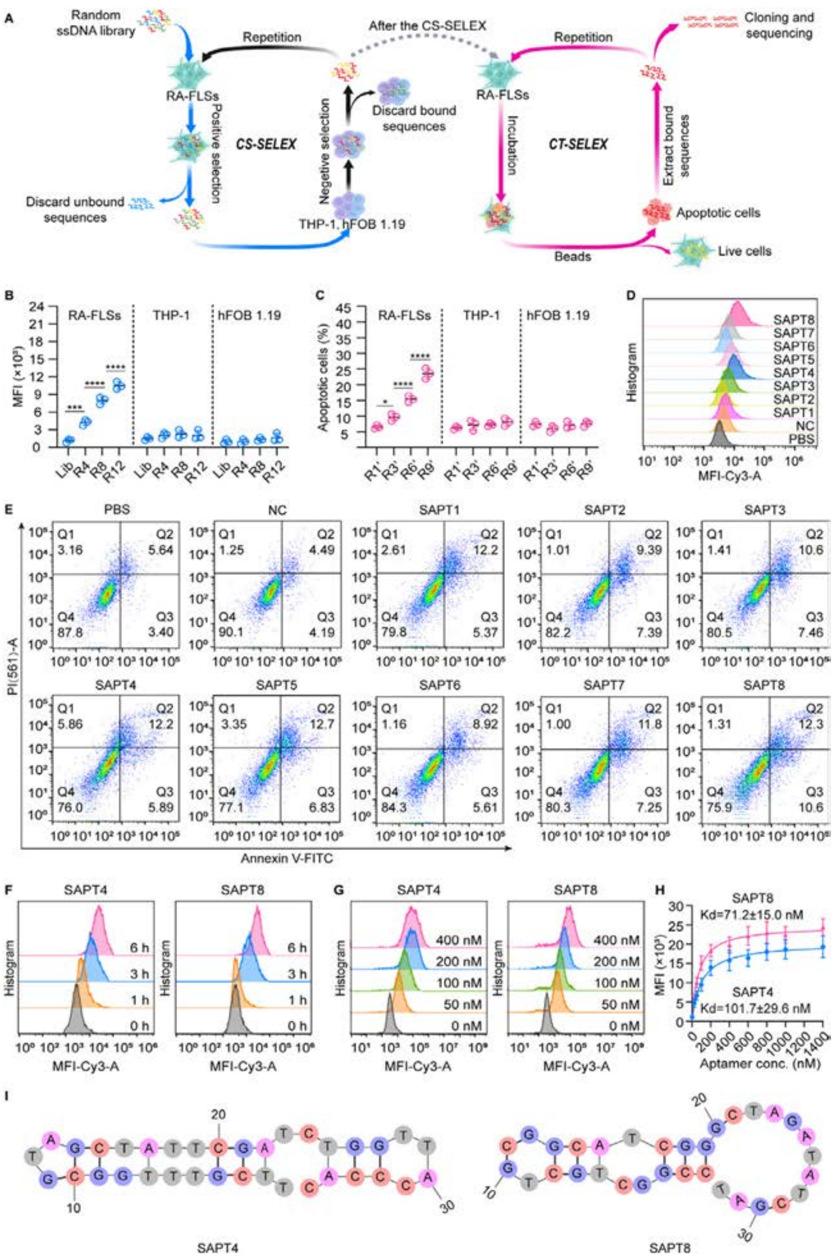

Figure 1. Generation of rheumatoid arthritis patients-derived fibroblast-like synoviocytes (RA-FLSs)-specific and cytotoxic aptamers by cell-specific and cytotoxic systematic evolution of ligands by exponential enrichment (CSCT-SELEX). (A) Workflow of the CSCT-SELEX. Briefly, the CSCT-SELEX was a tandem process consisting of a cell-specific SELEX (CS-SELEX) module followed by a cytotoxic SELEX (CT-SELEX) module. The CS-SELEX module included multiple rounds of positive selection against target cells (RA-FLSs) and negative selection against control cells (a human monocytic cell line THP-1 and a human osteoblastic cell line hFOB 1.19) using an initial random single-stranded DNA (ssDNA) library. After the CS-SELEX, the CT-SELEX module was conducted using the enriched ssDNA pool that exhibited the strongest binding ability with RA-FLSs in the CS-SELEX module. The CT-SELEX module was an iterative process via treating RA-FLSs with the enriched ssDNA pools and collecting apoptotic cells rather than live cells for isolating proapoptotic aptamers. (B) Mean fluorescence intensity (MFI) of RA-FLSs, THP-1 and hFOB 1.19 cells after incubation with the enriched ssDNA pools from the CS-SELEX module, as determined by a microplate reader. The cells were incubated with 200 nM Cy3-labelled ssDNA library (Lib) or the enriched ssDNA pools from the 4th round (R4), the 8th round (R8) and the 12th round (R12) of CS-SELEX for 3 hours. (C) Percentage of apoptotic cells of RA-FLSs after treatment with the enriched ssDNA pools from the CT-SELEX module, as determined by the annexin V-coated magnetic beads. The RA-FLSs were daily treated with 400 nM ssDNA enrichment pools from the first round (R1′), the third round (R3′), the sixth round (R6′) and the ninth round (R9′) of CT-SELEX for 3 days. (D) Binding of RA-FLSs with 200 nM Cy3-labelled negative control (NC) or the most enriched eight aptamer candidates (SAPT1-8) from CSCT-SELEX after incubation for 3 hours, as determined by flow cytometry. (E) Apoptosis of RA-FLSs after daily treatment with phosphate buffered saline (PBS), 400 nM NC or SAPT1-8 for 4 days, as determined by flow cytometry. (F) Binding of RA-FLSs with 200 nM Cy3-labelled SAPT4 or SAPT8 at different time points (0, 1, 3 and 6 hours). (G) Binding of RA-FLSs with Cy3-labelled SAPT4 or SAPT8 at different concentrations (0, 50, 100, 200 or 400 nM) for 3 hours. (H) Binding curves of SAPT4 or SAPT8 with RA-FLSs. The cells were incubated with increasing concentrations (conc.) of Cy3-labelled SAPT4 or SAPT8 for 3 hours. The equilibrium dissociation constants (K_d) were calculated by nonlinear fitting analysis. Data from three (B−G) or six (H) independent biological replicates were represented as mean±standard deviation (SD) and statistical significance was calculated by the one-way analysis of variance with a post hoc test. *p<0.05, ***p<0.001, ****p<0.0001. (I) Secondary structures of SAPT4 and SAPT8 predicted by the RNAstructure software.

showed that both SAPT4 and SAPT8 reduced invasion and migration of RA-FLSs (figure 2C,D). Wound healing assay confirmed the inhibitory effects of both SAPT4 and SAPT8 on RA-FLSs migration (figure 2E). RA-FLSs are also activated to produce a range of inflammatory mediators, such as IL-1β and MMPs [38]. When treated with SAPT4 or SAPT8, RA-FLSs had lower expression of IL-1β and MMP3 than the cells treated with NC or PBS (figure 2F). Notably, the inhibitory effects of SAPT8 on these phenotypes of RA-FLSs were superior to those of SAPT4 (figure 2A−F). We also tested the in vitro binding ability and therapeutic effects of SAPT4 and SAPT8 against a human synovial cell line SW982. We observed that both SAPT4 and SAPT8 bound with SW982 cells (online supplemental figure S2A), induced apoptosis and decreased viability, proliferation, invasion and migration of SW982 cells in vitro (online supplemental figure S2B−G). Consistently, SAPT8 also displayed better therapeutic effects on SW982 cells than SAPT4 (online supplemental figure S2A−G).

SAPT4 and SAPT8 suppress aggressive phenotypes of FLSs from arthritic rats and mice in vitro

We established rat and mouse models with collagen-induced arthritis (CIA) and isolated CIA rat FLSs (CIA-RFLSs) and CIA mouse FLSs (CIA-MFLSs), respectively.[39,40] CIA-RFLSs characterised by excessive expression of both THY1 and vimentin and absence of CD68 (online supplemental figure S3A) were incubated with PBS, NC, SAPT4 or SAPT8. SAPT4 or SAPT8 had strong binding ability with CIA-RFLSs (online supplemental figure S3B). Dramatic apoptosis was observed in CIA-RFLSs after treatment with SAPT4 or SAPT8 (online supplemental figure S3C). The viability, proliferation, invasion

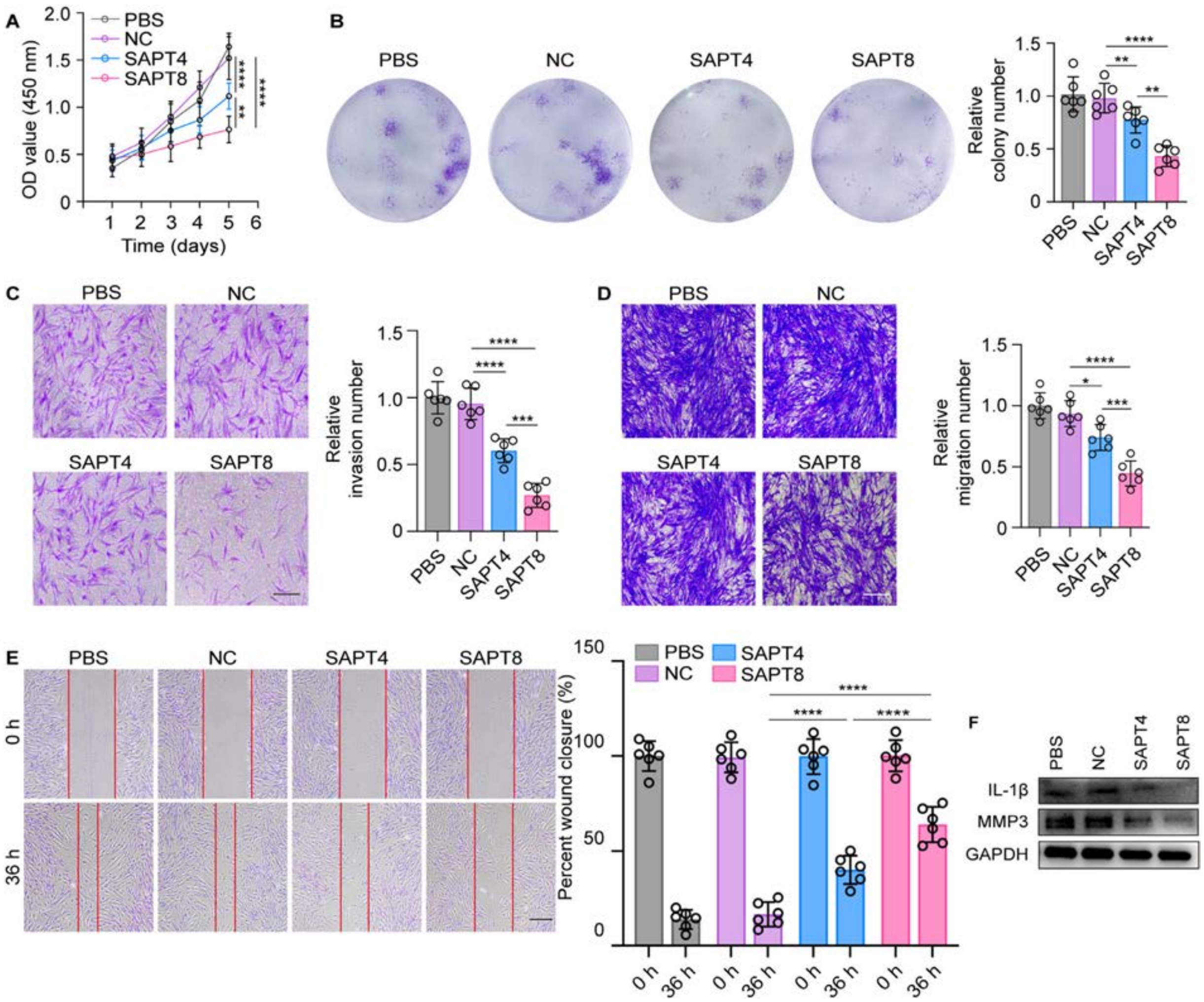

Figure 2. Effects of SAPT4 and SAPT8 on rheumatoid arthritis patients-derived fibroblast-like synoviocytes (RA-FLSs) in vitro. (A) Viability of RA-FLSs after daily treatment with phosphate buffered saline (PBS) or 400 nM negative control (NC), SAPT4 or SAPT8 for 5 days as determined by Cell Counting Kit-8 assays. (B) Colony formation of RA-FLSs after daily treatment with PBS or 400 nM NC, SAPT4 or SAPT8 for 13 days. (C) Invasion of RA-FLSs after daily treatment with PBS or 400 nM NC, SAPT4 or SAPT8 for 2 days, as determined by transwell assays. Scale bars = 200 μm. (D) Migration of RA-FLSs after daily treatment with PBS or 400 nM NC, SAPT4 or SAPT8 for 2 days, as determined by transwell assays. Scale bars = 200 μm. (E) Wound healing assays of RA-FLSs after treatment with PBS or 400 nM NC, SAPT4 or SAPT8 for 36 hours. Scale bars = 200 μm. (F) Protein expression of interleukin (IL)-1β and MMP3 in RA-FLSs after treatment with PBS or 400 nM NC, SAPT4 or SAPT8 for 24 hours, as determined by western blotting. Data from six independent biological replicates were represented as mean±standard deviation (SD) and statistical significance was calculated by the two-way analysis of variance (ANOVA) (A) or the one-way ANOVA (B–E) with a post hoc test. *$p<0.05$, **$p < 0.01$, ***$p<0.001$, ****$p<0.0001$. OD, optical density.

and migration of CIA-RFLSs were suppressed by SAPT4 or SAPT8 (online supplemental figure SD–H). There were better binding ability and therapeutic effects of SAPT8 than SAPT4 against CIA-RFLSs (online supplemental figure S3B–H). In addition, SAPT4 or SAPT8 also showed good binding ability with CIA-MFLSs that displayed positive expression of both THY1 and vimentin and negative expression of CD68 (online supplemental figure S4A,B), while they could not recognise non-CIA-MFLSs, including healthy mouse FLSs (H-MFLSs), a mouse osteoblast-like cell line MC3T3-E1, a mouse macrophage-like cell line RAW 264.7, a mouse fibroblastic cell line L929 and a mouse chondrogenic cell line ATDC5 (online supplemental figure S4B,C). No apoptosis was observed for H-MFLSs incubated with SAPT4 or SAPT8 (online supplemental figure S4D), whereas apoptosis of CIA-MFLSs was induced after treatment with SAPT4 or SAPT8 when compared with PBS or NC (online supplemental figure S4E). Cell viability, proliferation, invasion and migration of CIA-MFLSs were decreased by SAPT4 or SAPT8 (online supplemental figure S4F–J). SAPT8 had stronger binding ability with CIA-MFLSs and better inhibitory effects on tumour-like phenotypes of CIA-MFLSs (online supplemental figure S4B, E–J).

NCL is identified as the cell surface target of SAPT8 on RA-FLSs

To identify the cell surface targets of SAPT4 and SAPT8, we conducted a pull-down assay using streptavidin-coated beads after incubating membrane proteins of RA-FLSs with PBS or biotin-labelled NC, SAPT4 or SAPT8. The beads, along with the captured proteins, were eluted and separated by sodium dodecyl sulfate-polyacrylamide gel electrophoresis (SDS-PAGE). Silver staining demonstrated that SAPT8 specifically interacted with a protein that had a molecular weight between 100 and 130 kDa, whereas none of any specific protein was captured by SAPT4, when compared with NC or PBS (figure 3A). Next, we performed liquid chromatography-tandem mass spectrometry (LC-MS/MS) analysis to identify the SAPT8-captured protein. Among the 100 candidate proteins identified by LC-MS/MS (online supplemental table S2), NCL attracted our attention, as it had been reported to have a predicted molecular weight of 76.6 kDa and an

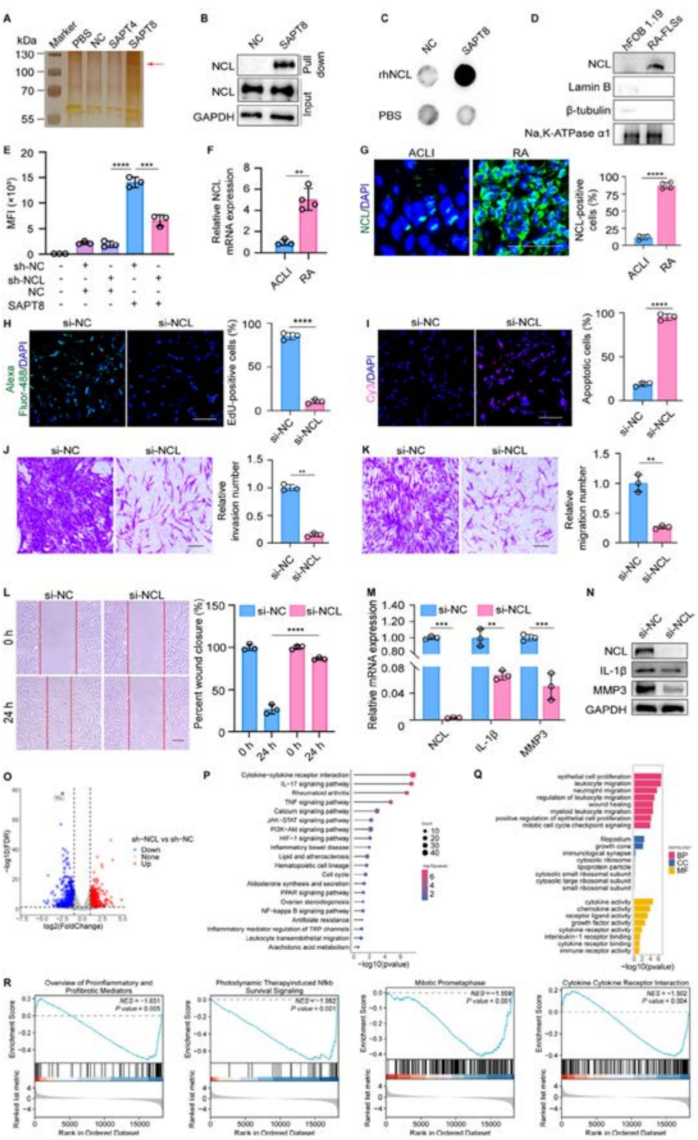

Figure 3. Identification of the target proteins of SAPT8. (A) Pull-down assays of SAPT4-interacting or SAPT8-interacting proteins. The membrane proteins of rheumatoid arthritis patients-derived fibroblast-like synoviocytes (RA-FLSs) were incubated with phosphate buffered saline (PBS) or 1 μM biotin-labelled negative control (NC), SAPT4 or SAPT8 for 6 hours before the addition of streptavidin-coated beads. The NC-interacting, SAPT4-interacting or SAPT8-interacting proteins were separated on sodium dodecyl sulfate-polyacrylamide gel electrophoresis, followed by silver staining. The arrow showed the protein band of interest, which was collected for liquid chromatography-tandem mass spectrometry analysis. (B) The interaction between SAPT8 and nucleolin (NCL) in RA-FLSs detected by pull-down assay followed by western blotting. (C) Analysis of direct interaction between SAPT8 and NCL by dot blotting. 20 ng recombinant human NCL (rhNCL) was immobilised on a nitrocellulose membrane and then incubated with 1 μM biotin-labelled NC or SAPT8 before the addition of horseradish peroxidase (HRP)-conjugated streptavidin. (D) Expression of NCL on the surface of RA-FLSs or hFOB 1.19 cells. (E) MFI of RA-FLSs transfected with siRNA targeting NCL (si-NCL) or negative control siRNA (si-NC) after incubation with 200 nM NC or SAPT8 for 3 hour. (F) Relative mRNA level of NCL in synovial tissues from knee joints of individuals with anterior cruciate ligament injury (ACLI) (n = 3) or patients with RA (n = 4). (G) Immunofluorescence staining of NCL (green) on sections of the synovial tissues. Cell nuclei were counterstained with 4',6-diamidino-2-phenylindole (DAPI) (blue). Scale bars = 50 μm. (H) Proliferation of RA-FLSs after transfection with si-NC or si-NCL for 48 hours, as measured by 5-ethynyl-2′-deoxyuridine (EdU) staining. Scale bars = 100 μm. (I) Apoptosis of RA-FLSs after transfection with si-NC or si-NCL, as measured by terminal deoxynucleotidyl transferase 2′-deoxyuridine 5′-triphosphate (dUTP) nick end labelling (TUNEL) staining. Scale bars = 100 μm. (J) Invasion of RA-FLSs after transfection with si-NC or si-NCL. Scale bars = 200 μm. (K) Migration of RA-FLSs after transfection with si-NC or si-NCL. Scale bars = 200 μm. (L) Wound healing assays of RA-FLSs after transfection with si-NC or si-NCL. Scale bars = 200 μm. (M) Relative mRNA levels of NCL, IL-1β and MMP3 in RA-FLSs after transfection with si-NC or si-NCL. (N) Protein levels of NCL, IL-1β and MMP3 in RA-FLSs after transfection with si-NC or si-NCL. (O) Volcano plot of differentially expressed genes between RA-FLSs infected with lentivirus vector expressing shRNA targeting NCL (sh-NCL) and RA-FLSs infected with lentivirus vector expressing negative control shRNA (sh-NC), as determined by RNA sequencing. Red: upregulated genes, blue: downregulated genes, grey: non-differentially expressed genes. (P) Kyoto Encyclopedia of Genes and Genomes pathway analysis of the downregulated genes in NCL-silenced RA-FLSs. (Q) Gene ontology (GO) enrichment analysis of molecular function (MF), cellular components (CC) and biological processes (BP) for the downregulated genes in NCL-silenced RA-FLSs. (R) Gene set enrichment analysis of inflammation and survival-related signalling in NCL-silenced RA-FLSs. Data from three independent biological replicates were represented as mean±standard deviation (SD) and statistical significance was calculated by the one-way analysis of variance with a post hoc test (E) or the two-tailed Student's t-test (F–M). **p<0.01, ***p<0.001, ****p<0.0001.

observed molecular weight of 100–110 kDa [41,42], which were consistent with our silver staining and LC-MS/MS results. We further verified that NCL could be captured by SAPT8 in a pull-down assay followed by western blotting (figure 3B). We performed a dot blotting assay and showed a direct interaction between SAPT8 and recombinant human NCL (rhNCL) (figure 3C). Previously, no study revealed the presence of NCL on the surface of RA-FLSs. We isolated membrane proteins of hFOB 1.19 cells and RA-FLSs and observed the high level of NCL on surface of RA-FLSs rather than on surface of hFOB 1.19 cells (figure 3D). We performed gene silencing of NCL in RA-FLSs and found that there was decreased binding of SAPT8 with NCL-silenced RA-FLSs (figure 3E), suggesting that NCL was the cell surface target of SAPT8 on RA-FLSs.

NCL plays a pathological role in the tumour-like transformation of RA-FLSs

Until now, NCL has been found to be a multifunctional shuttling protein present in the nucleus, cytoplasm and on the surface of tumour cells [43]. The cell surface NCL contributes to resistance to apoptosis and the growth of tumour cells [43]. To date, no study demonstrates the pathological role of NCL in RA-FLSs. We examined the expression of NCL in synovial tissues of patients with RA and synovial tissues of individuals with ACLI. There was higher mRNA and protein expression of NCL in synovial tissues of patients with RA when compared with those of individuals with ACLI (figure 3F,G). We manipulated NCL expression in RA-FLSs in vitro. The siRNA targeting NCL (si-NCL) significantly inhibited proliferation and promoted apoptosis of RA-FLSs when compared with the NC siRNA (si-NC), as determined by 5-ethynyl-2′-deoxyuridine (EdU) staining and terminal deoxynucleotidyl transferase 2‘-deoxyuridine 5‘-triphosphate (dUTP) nick end labelling (TUNEL) staining, respectively (figure 3H,I). Invasion and migration of RA-FLSs were decreased by the si-NCL rather than the si-NC (figure 3L). The si-NCL reduced the mRNA and protein expression of IL-1β and MMP3 (figure 3M,N). We constructed lentiviral vectors expressing short hairpin RNA targeting NCL (sh-NCL) or NC shRNA (sh-NC) and performed RNA sequencing in RA-FLSs infected with lentiviral particles. The volcano plot showed significant downregulation of NCL in RA-FLSs treated with sh-NCL and numerous differentially expressed genes (DEGs) between NCL-silenced RA-FLSs and RA-FLSs transduced with sh-NC (figure 3O). Kyoto Encyclopedia of Genes and Genomes (KEGG) pathway analysis revealed that sh-NCL downregulated a series of immune-associated pathways in RA-FLSs, such as IL-17, TNF, nuclear factor kappa-light-chain-enhancer of activated B cells (NF-κB) and janus kinase-signal transducers and activators of transcription (JAK-STAT) (figure 3P). Gene Ontology (GO) enrichment analysis demonstrated that biological events including cell proliferation, migration and inflammatory response were suppressed in RA-FLSs treated with sh-NCL (figure 3Q). Gene set enrichment analysis (GSEA) confirmed that the downregulated genes in RA-FLSs treated with sh-NCL were mainly involved in inflammation and survival of RA-FLSs (figure 3R). We also overexpressed NCL in RA-FLSs. The overexpression of NCL enhanced proliferation and suppressed apoptosis of RA-FLSs (online supplemental figure S5A,B). Invasion and migration of RA-FLSs and expression of IL-1β and MMP3 in RA-FLSs were boosted after overexpression of NCL (online supplemental figure S5C–G). These results suggested that NCL played a critical role in the activation and tumour-like transformation of RA-FLSs.

SAPT8 interacts with NCL and modulates NCL-p53/Bcl-2 signalling in RA-FLSs

To explore how SAPT8 inhibits activation and tumour-like transformation of RA-FLSs via targeting NCL, we examined the mRNA and protein levels of NCL in RA-FLSs after treatment with PBS, NC or SAPT8. Compared with PBS or NC, SAPT8 had no effect on mRNA expression of NCL (figure 4A), but SAPT8 significantly decreased the protein level of NCL (figure 4B). Bcl-2 and p53 are the two most studied target genes of NCL that are involved in resistance to apoptosis and growth of tumour cells [30]. NCL interacts with the p53 mRNA 5′ untranslated region (5′-UTR) and prevents its translation, whereas NCL stabilises Bcl-2 mRNA by binding to the 3′-UTR and protecting it from nuclease degradation, thus allowing tumour cells to avoid apoptosis.[27,30] We showed that SAPT8 increased the expression of p53 and reduced the level of Bcl-2 (figure 4B). We examined the subcellular distribution of SAPT8 in RA-FLSs and observed both the cell surface and intracellular localisation of SAPT8, suggesting that SAPT8 could enter RA-FLSs via targeting cell surface NCL (figure 4C). To determine the endocytic pathways of SAPT8, we incubated RA-FLSs with SAPT8 with or without the presence of an inhibitor of macropinocytosis (amiloride hydrochloride), an inhibitor of clathrin-mediated endocytosis (chlorpromazine (CPZ)) or an inhibitor of caveolae-dependent endocytosis (genistein (GNT)) [44]. Both CPZ and GNT decreased cellular uptake of SAPT8 (figure 4D), demonstrating that SAPT8 entered RA-FLSs via both clathrin-dependent and caveolae-dependent endocytic pathways. It is generally accepted that endocytosis via caveolae or clathrin directs the receptor-ligand complex to lysosomal and/or proteasomal degradation.[45,46] We found that SAPT8 was colocalised with a lysosome tracker in RA-FLSs (figure 4E). We examined whether SAPT8 modulated the levels of NCL as well as its target genes Bcl-2 and p53 in a proteasome-dependent or lysosome-dependent manner. We treated the RA-FLSs with SAPT8 with or without the presence of a proteasome inhibitor MG132 or lysosomal inhibitors bafilomycin A1 (Baf A1) and chloroquine (CQ) [47]. MG132 had no effect on SAPT8-induced alteration of NCL, Bcl-2 and p53, whereas Baf A1/CQ reversed SAPT8-induced degradation of NCL, a decrease of Bcl-2 and an increase of p53 in RA-FLSs (figure 4F), suggesting that SAPT8 specifically induced lysosomal degradation of NCL and subsequently altered the expression of p53 and Bcl-2 in RA-FLSs.

To make sure that SAPT8-induced lysosomal degradation of NCL and alteration of p53/Bcl-2 signalling was the dominant mechanism of action for its inhibitory effects on RA-FLSs, we performed NCL gene silencing in RA-FLSs and then incubated these cells with NC and SAPT8. SAPT8 could not induce apoptosis of the NCL-silenced RA-FLSs and was also unable to inhibit proliferation, invasion and migration of the RA-FLSs (online supplemental figure S6A–D), suggesting that SAPT8 exerted therapeutic effects on RA-FLSs in an NCL-dependent manner. Besides the SAPT8 identified in our study, AS1411 has already been well-known as an aptamer that specifically recognises NCL on the surface of tumour cells [48,49]. We found that AS1411 also recognised RA-FLSs and competed with SAPT8 for binding with RA-FLSs (figure 4G). Unlike the role of SAPT8 in mediating the lysosomal degradation of NCL, AS1411 mainly inhibits activation (phosphorylation) of NCL rather than affects the expression of NCL [48]. Moreover, it is worth noting that even though AS1411 at nanomolar concentrations could recognise NCL, micromolar concentrations of AS1411 are typically required to inhibit NCL phosphorylation and display therapeutic effects [50–52]. We confirmed that the protein levels of NCL, p53 and Bcl-2 were not changed in RA-FLSs after treatment with nanomolar AS1411, while nanomolar AS1411 rescued SAPT8-induced degradation of NCL and alteration of Bcl-2 and p53 (figure 4H). Cellular uptake and lysosomal localisation of SAPT8 were also decreased after the addition of nanomolar AS1411 (figure 4I). Consistently, we also demonstrated that nanomolar AS1411 had no effect on tumour-like phenotypes of RA-FLSs (figure 4J–M), whereas it reversed SAPT8-induced suppression of the tumour-like phenotypes of RA-FLSs (figure 4J–M). In addition, we examined whether AS1411 at micromolar concentrations could display therapeutic effects on RA-FLSs. Our results showed that AS1411 at a concentration of 5 μM reduced the level of phosphorylated NCL (online supplemental figure S7A) and inhibited the tumour-like phenotypes of RA-FLSs (online supplemental figure S7B–E). In addition to AS1411, iSN04 is another newly identified aptamer targeting NCL [42,53]. We showed that iSN04 also could bind with RA-FLSs (online supplemental figure S8A). Like AS1411, iSN04 did not induce the degradation of NCL but decreased the phosphorylation of NCL and inhibited the phenotypes of RA-FLSs (online supplemental figure S8B–F). However, iSN04 was less potent than AS1411 as we demonstrated that iSN04 only exhibited therapeutic effects at a concentration of 10 μM (online supplemental figure S8B–F), which was much higher than the effective concentration of AS1411 (5 μM).

SAPT8 is selectively accumulated in FLSs of CIA mice in vivo

SAPT8, on the one hand, displayed stronger binding ability with RA-FLSs, SW982, CIA-MFLSs and CIA-RFLSs, as well as better inhibitory effects on the tumour-like transformation of these FLSs than SAPT4; on the other hand, the mechanism of action of SAPT8 was also clearly interpreted. We thus chose SAPT8 for in vivo studies. To examine the tissue and cellular accumulation of SAPT8, CIA mice were administrated with Cy3-labelled NC or SAPT8 by tail-vein injection, and the in vivo and ex vivo fluorescence distribution was evaluated. The whole-body biophotonic imaging demonstrated stronger fluorescence intensity of SAPT8 in the inflamed paws, whereas only a few fluorescence signals

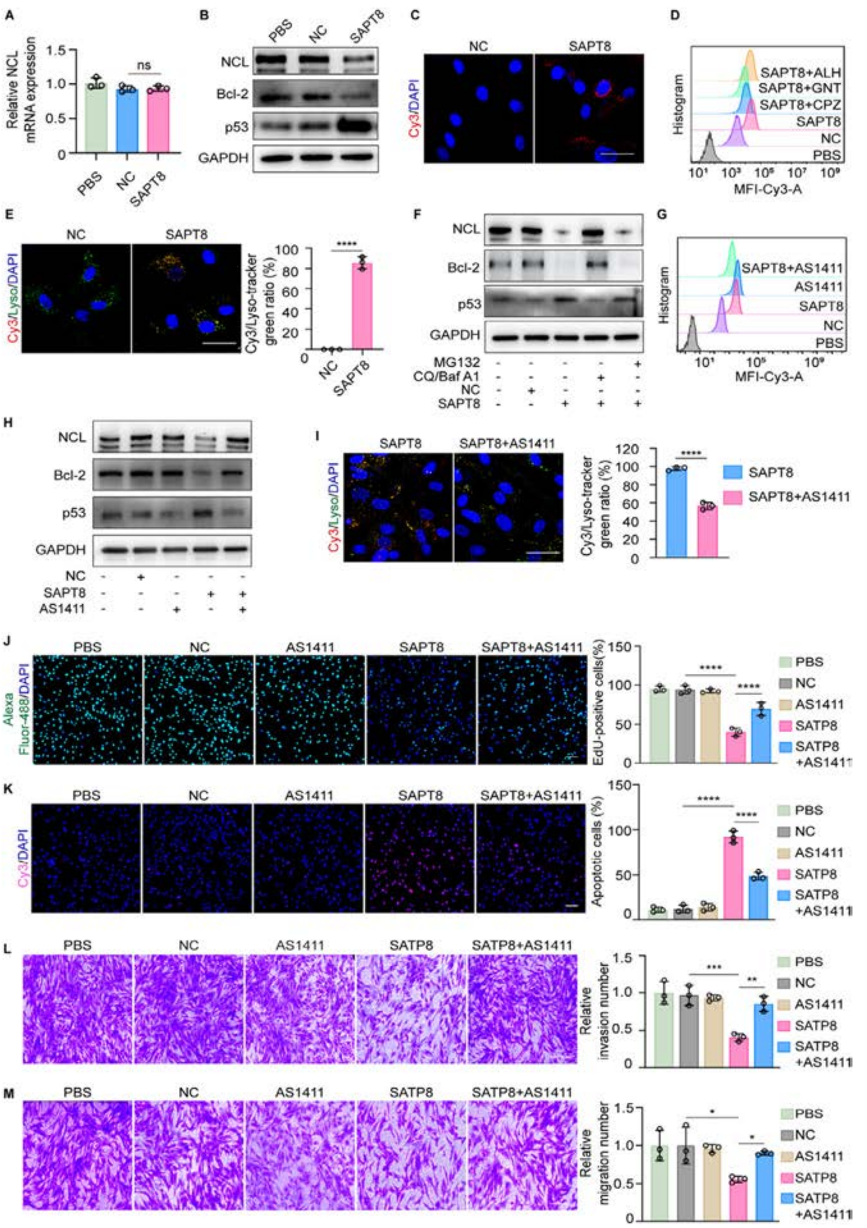

Figure 4. Mechanism of action of SAPT8. (A) Relative mRNA level of nucleolin (NCL) in rheumatoid arthritis patients-derived fibroblast-like synoviocytes (RA-FLSs) after treatment with phosphate buffered saline (PBS) or 400 nM negative control (NC) or SAPT8 for 24 hours. (B) Protein expression of NCL, B-cell lymphoma 2 (Bcl-2) and p53 in RA-FLSs after treatment with PBS, 400 nM NC or SAPT8 for 24 hours. (C) Subcellular distribution of SAPT8 in RA-FLSs. RA-FLSs were treated with 200 nM Cy3-labelled NC or SAPT8 for 6 hours. (D) Binding of SAPT8 with RA-FLSs with or without the presence of different inhibitors of endocytic pathways. RA-FLSs were incubated with amiloride hydrochloride (ALH, an inhibitor of macropinocytosis), chlorpromazine (CPZ, an inhibitor of clathrin-mediated endocytosis) or genistein (GNT, an inhibitor of caveolae-mediated endocytosis) for 1 hour and then treated with PBS or 200 nM Cy3-labelled NC or SAPT8 for 3 hours. (E) Colocalisation of SAPT8 with the lysosome in RA-FLSs. RA-FLSs were incubated with 200 nM Cy3-labelled NC or SAPT8 (red) for 6 hours before the addition of a lysosome tracker (green). Scale bars = 100 µm. (F) Protein expression of NCL, Bcl-2 and p53 in RA-FLSs after treatment with 400 nM NC or SAPT8 for 24 hours, with or without the presence of a proteasome inhibitor MG132 or lysosomal inhibitors chloroquine and bafilomycin A1 (CQ/Baf A1). (G) Binding of SATP8 with RA-FLSs with or without the presence of AS1411. RA-FLSs were incubated with 200 nM Cy3-labelled NC, SAPT8, AS1411 or SAPT8 with the presence of 800 nM AS1411 for 3 hours. (H) Protein expression of NCL, Bcl-2 and p53 in RA-FLSs after treatment with 400 nM NC or SAPT8 for 24 hours, with or without the presence of 800 nM AS1411. (I) Colocalisation of SAPT8 with lysosome in RA-FLSs with or without the presence of 800 nM AS1411. (J) Proliferation of RA-FLSs after treatment with 400 nM NC or SAPT8 for 4 days, with or without the presence of 800 nM AS1411, as measured by 5-ethynyl-2′-deoxyuridine (EdU) staining. Scale bars = 100 µm. (K) Apoptosis of RA-FLSs after treatment with 400 nM NC or SAPT8 for 4 days, with or without the presence of 800 nM AS1411, as measured by terminal deoxynucleotidyl transferase 2′-deoxyuridine 5′-triphosphate (dUTP) nick end labelling (TUNEL) staining. Scale bars = 100 µm. (L) Invasion of RA-FLSs after treatment with 400 nM NC or SAPT8 for 48 hours, with or without the presence of 800 nM AS1411. Scale bars = 200 µm. (M) Migration of RA-FLSs after treatment with 400 nM NC or SAPT8 for 48 hours, with or without the presence of 800 nM AS1411. Scale bars = 200 µm. Fluorescence images were captured by a confocal microscope. Data from three independent biological replicates were represented as mean±standard deviation (SD) and statistical significance was calculated by the one-way analysis of variance with a post hoc test (A and J–M) or the two-tailed Student's t-test (E,I). ns, no significance, *p<0.05, **p<0.01, ***p<0.001, ****p<0.0001.

were observed in the inflamed paws of mice injected with NC (figure 5A). Then, the mice were sacrificed, and major organs (heart, liver, spleen, lung and kidney), as well as synovial tissues and hind paws, were harvested and visualised ex vivo. Both NC and SAPT8 displayed no obvious fluorescence signals in the heart, liver, spleen, lung and kidney (figure 5B). The fluorescence signals of SAPT8 in synovial tissues and hind paws were much stronger when compared with those of NC (figure 5B). We performed immunofluorescent staining to detect THY1-positive or vimentin-positive FLSs at the inflamed paws and investigated whether there was selective cellular accumulation of SAPT8 within CIA-MFLSs in vivo. Confocal imaging showed that fluorescence signals were highly aggregated in the CIA-MFLSs of mice injected with SAPT8, whereas signals were hardly observed in the CIA-MFLSs of mice injected with NC (figure 5C,D).

SAPT8 monotherapy or SAPT8 combined with anti-TNF etanercept attenuates CIA in mice

CIA mice were intravenously injected with PBS, NC, SAPT8, biologic anti-TNF etanercept, a combination of NC with etanercept or a combination of SAPT8 with etanercept two times per week (figure 6A). After the treatment, arthritic scoring showed that SAPT8 dramatically impeded the progression of CIA when compared with NC or PBS (figure 6B). Microcomputerised tomography (μCT) scans demonstrated that CIA mice treated with SAPT8 showed reduced bone erosion and a lower ratio of bone surface to bone volume (BV) of ankle joints than the mice treated with NC or PBS (figure 6C,D). Histological analysis by H&E and safranin O/fast green (SO/FG) staining showed that SAPT8 caused a notable inhibition of synovial hyperplasia, bone erosion and cartilage destruction (figure 6E and online

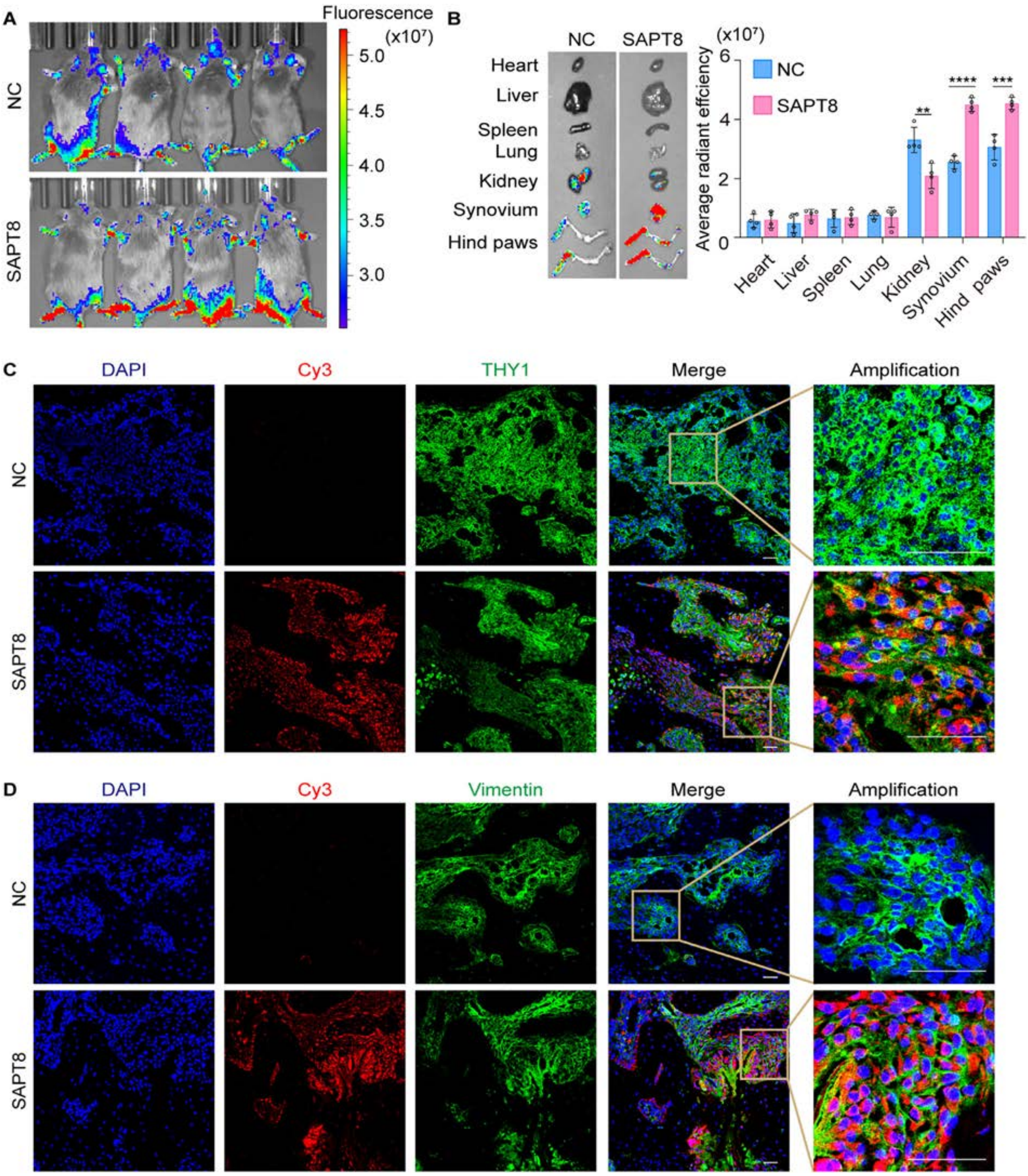

Figure 5. Tissue and cellular distribution of SAPT8 in collagen-induced arthritis (CIA) mice. (A) The global fluorescence signal of Cy3-labelled negative control (NC) or SAPT8 in mice with CIA as determined by the in vivo imaging system. CIA mice were treated with 5 mg/kg Cy3-labelled NC or SAPT8 by tail-vein injection for 24 hours. (B) Ex vivo fluorescence of the major organs (heart, liver, spleen, lung and kidney), synovial tissues and hind paws of the CIA mice treated with Cy3-labelled NC or SAPT8 for 24 hours. n = 4 mice per treatment group. Data were represented as mean±standard deviation (SD) and statistical significance was calculated with the two-tailed Student's t-test. **p<0.01, ***p<0.001, ****p<0.0001. (C,D) Fluorescence images showing the cellular distribution of Cy3-labelled NC or SAPT8 (red) on sections of the inflamed hind paws of CIA mice as determined by confocal microscopy. Immunofluorescence staining of THY1 (green, (C) or vimentin (green, (D) indicated the fibroblast-like synoviocytes in the inflamed hind paws. Cell nuclei were counterstained with 4',6-diamidino-2-phenylindole (DAPI) (blue). Scale bars = 50 μm.

supplemental figure S9A). Quantitation of synovitis score, bone erosion and cartilage erosion on H&E-stained and SO/FG-stained sections consistently demonstrated the good therapeutic effects of SAPT8 in CIA mice (figure 6F−H). Immunofluorescence staining demonstrated that SAPT8 significantly increased p53 level and decreased expression of NCL, Bcl-2, IL-6, IL-1β, MMP3 and cyclooxygenase-2 (COX-2, a key mediator of inflammatory pain [54,55]) (figure 6I and online supplemental figure S9B−G). TUNEL assay showed that SAPT8 induced apoptosis of synovial tissues (figure 6J). Furthermore, we evaluated the therapeutic efficacy of the combination of SAPT8 with etanercept in the CIA mice. The combination of SAPT8 with etanercept more significantly relieved CIA when compared with the monotherapy using SAPT8 or etanercept or a combination of NC with etanercept (figure 6B−J and online supplemental figure S9A−G). In addition, we examined the hepatotoxicity of SAPT8 monotherapy and SAPT8 in combined therapy with etanercept. Blood biochemical assays

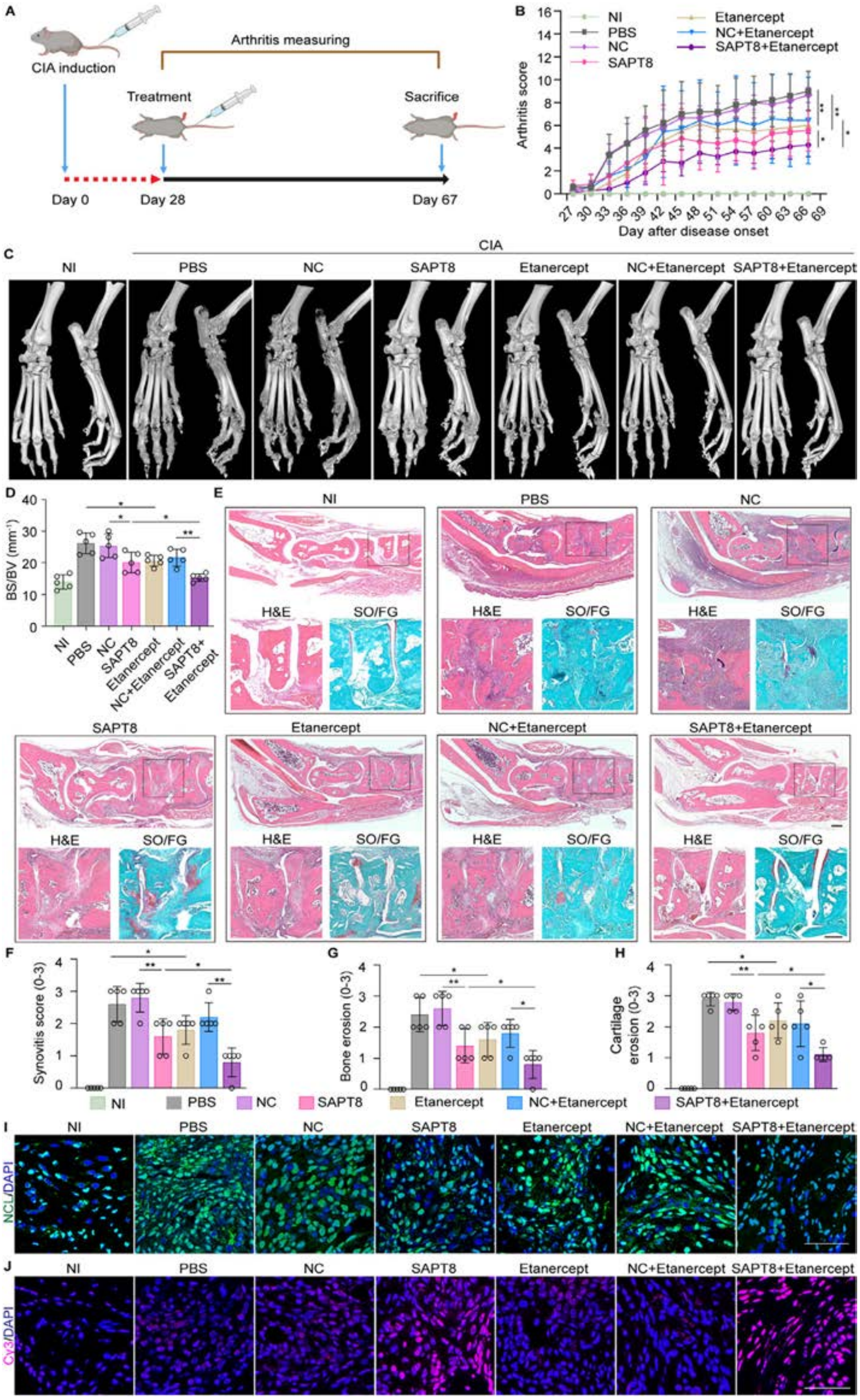

Figure 6. Therapeutic effects of SAPT8 with or without the presence of an anti-tumour necrosis factor (anti-TNF) etanercept in collagen-induced arthritis (CIA) mice. (A) Flowchart for experimental design in CIA mice. Briefly, mice were immunised with bovine type II collagen for 28 days to establish CIA. Then, the CIA mice were systemically administered with phosphate buffered saline (PBS), negative control (NC), SAPT8, etanercept, a combination of NC with etanercept (NC + etanercept) or a combination of SAPT8 with etanercept (SAPT8 + etanercept) two times per week for 39 days. NC or SAPT8 was intravenously injected at a dosage of 30 mg/kg, and etanercept was intraperitoneally administrated at a dosage of 5 mg/kg. (B) Arthritis scoring of paws from non-immunised (NI) mice or CIA mice in different treatment groups. (C) Representative microcomputerised tomography (μCT) images of the hind paws (dorsal and lateral view) from mice in each treatment group. (D) The ratio of bone surface to bone volume (BS/BV) of ankle joints as measured by μCT. (E) Representative images of H&E staining and SO/FG staining on sections of the hind paws (lateral view) from mice in each treatment group. Scale bars = 500 µm. Quantification of synovitis score (F), bone erosion (G) and cartilage erosion (H). (I) Immunofluorescence staining of NCL on sections of the hind paws. Scale bars = 50 µm. (J) Apoptosis of synovial tissues on sections of the hind paws as determined by terminal deoxynucleotidyl transferase 2'-deoxyuridine 5'-triphosphate (dUTP) nick end labelling (TUNEL) assay. Scale bars = 50 µm. n = 5 mice per treatment group. Data were represented as mean±standard deviation (SD) and statistical significance was calculated by the two-way analysis of variance (ANOVA) (B) or the one-way ANOVA (D and F–H) with a post hoc test. *p<0.05, **p<0.01.

demonstrated that the CIA mice treated with SAPT8 or a combination of SAPT8 with Etanercept had no obvious changes in liver function parameters including alanine aminotransferase (ALT), aspartate aminotransferase (AST), albumin (ALB) and total protein (TP), when compared with other treatment groups (online supplemental figure S9H).

SAPT8 recognises osteoarthritis (OA)-FLSs and relieves destabilisation of the medial meniscus (DMM)-induced OA in mice

Unlike RA, OA, characterised by cartilage deterioration, osteophyte formation and synovial pannus, is not an autoimmune disease. However, it is the most common degenerative joint disease [56]. Pathogenesis of OA is complex and also not fully understood [57]. Increasing evidence indicates that FLSs are activated in all stages of OA and contribute to the progression of OA [58]. It has been proposed that FLSs-targeted therapeutic strategies in OA may possibly prevent cartilage breakdown while alleviating other symptoms [59]. We showed that mRNA and protein expression of NCL in synovial tissues from OA patients was higher when compared with the synovial tissues of individuals with an ACLI (online supplemental figure S10A–B). OA-FLSs were isolated and characterised by high expression of THY1 and vimentin as well as the absence of CD68 (online supplemental figure S10C). SAPT8 also recognised OA-

FLSs with good affinity (online supplemental figure S10D). SAPT8 modulated NCL-p53/Bcl-2 signalling and demonstrated inhibitory effects on the aggressive phenotype of OA-FLSs in vitro (online supplemental figure S10E−I). We conducted the surgical DMM to induce OA in mice and administrated the mice with PBS, NC or SAPT8 by intra-articular injection two times per week (online supplemental figure S11A). μCT scans showed that DMM mice treated with SAPT8 had less osteophyte formation and lower BV of calcified meniscus and synovium than the mice treated with PBS or NC (online supplemental figure S11B −D). H&E and SO/FG staining of joint sections demonstrated that synovial hyperplasia, bone erosion and cartilage erosion were significantly reduced in DMM mice treated with SAPT8 (online supplemental figure S11E−F). Quantitative analysis of synovitis score, Osteoarthritis Research Society International Score, and cartilage area consistently suggested the protective effects of SAPT8 on DMM-induced OA mice (online supplemental figure S11G−I). There were decreased NCL expression and increased apoptotic cells in synovial tissues of DMM mice treated with SAPT8 (online supplemental figure S11J and K). The level of p53 was higher, but levels of Bcl-2, IL-6, IL-1β, MMP3 and COX-2 were lower in synovial tissues of DMM mice treated with SAPT8 than those in synovial tissues of DMM mice treated with PBS or NC (online supplemental figure S12A−F). Blood biochemical assays demonstrated no obvious change in liver function parameters, including ALT, AST, ALB and TP, in OA mice treated with SAPT8 when compared with the mice treated with PBS or NC (online supplemental figure S12G).

DISCUSSION

RA remains an unmet clinical challenge despite a variety of immunomodulatory therapies are available [18]. During RA, FLSs, as the dominant non-immune cells of synovial tissues, are activated and suggested to be not just ‘passive responders’ but ‘imprinted aggressors’ in the joint microenvironment [12]. RA-FLSs acquire a series of aggressive phenotypes, which are like those of the tumour cells, and transform from a friend to a foe [60]. RA-FLSs play critical roles in many pathogenic events of RA. They break down the extracellular matrix by producing MMPs, directly invade and digest articular cartilage, promote bone erosion and enhance inflammation through the secretion of inflammatory mediators [61]. In addition to the DMARDs-based immune therapies, exploring RA-FLSs targeted therapies has been highlighted for RA treatment [11]. However, therapies targeting RA-FLSs have been hampered because of the lack of RA-FLSs-specific cell surface molecular signatures [16]. In our study, we made a breakthrough in developing selective anti-RA-FLSs therapies without prior knowledge of RA-FLSs-specific surface signatures and identified a previously undiscovered molecular target for developing FLSs-directed therapies.

The ideal anti-FLS therapies have been proposed to be cell-specific and capable of interrupting one or more tumour-like phenotypes of RA-FLSs [18]. To date, therapeutics have been developed to target the only two available cell surface molecular targets, CDH11 and PTPRS, to block adhesion and migration and invasion of RA-FLSs, respectively [18]. However, no therapies specifically inducing apoptosis of RA-FLSs have been reported. Here, we addressed this issue using nucleic acid aptamers. We developed a novel CSCT-SELEX method for de novo screening of cytotoxic aptamers without prior knowledge of RA-FLSs-specific cell surface molecular signatures. Compared with the conventional cell-SELEX that only ensured the identification of cell-targeting aptamers, the CSCT-SELEX was designed to juggle the cell specificity and cytotoxicity of the aptamers against target cells via a CS-SELEX module in tandem with a CT-SELEX module. Monocytes are circulating leukocytes important in immune defence and stay for a relatively long time in circulation [62,63]. We chose monocytes as one type of control cell in our CSCT-SELEX to eliminate the non-specific binding between aptamers and monocytes after in vivo administration of the selected aptamers in CIA mice. Additionally, osteoblasts are key cells involved in bone formation and joint repair [64]. We chose osteoblasts as another type of control cell to minimise the influence of aptamers on osteoblasts in the joint microenvironment of CIA mice. Further, both were cell lines that could be easily obtained. Initially, our intention was to use normal joint FLSs from healthy individuals as non-RA-FLSs for the negative selection of the CSCT-SELEX to ensure the selectivity of the screened aptamers for RA-FLSs. This choice was predicated on the understanding that normal joint FLSs are the progenitors from which the aggressive RA-FLSs derive. However, CTCX-SELEX involved iterative cycles of selection, amplification and incubation to isolate aptamers. Each cycle consisted of repeated washing and eluting steps and required a tremendous number of target or NC cells. Regrettably, we encountered difficulties in acquiring sufficient human normal joint samples and thus were unable to proceed with using these cells as NCs. Besides the normal joint FLSs, a broader range of readily accessible non-RA fibroblasts, such as those from skin punch biopsies, immortalised fibroblast lines or iPSC-derived fibroblasts, could also serve as alternative NC cells for CSCT-SELEX due to their fibroblastic characteristics similar to RA-FLSs. Although these non-RA fibroblasts were not employed as NC cells during our CSCT-SELEX, we did investigate the binding specificity of our selected aptamers to both a human normal skin fibroblastic cell line (BJ) and a mouse fibroblastic cell line (L929). The results indicated that our aptamers did not bind to BJ or L929 cells, demonstrating their high selectivity for RA-FLSs. This selectivity is likely due to the specific expression of the target molecules of the aptamers on the surface of RA-FLSs, rather than on the non-RA fibroblasts, such as NCL for the SAPT8 aptamer [65,66].

Although both SAPT4 and SAPT8 met our expectations as cell-specific and cytotoxic aptamers against RA-FLSs, we noticed that SAPT8 displayed advantages over SAPT4 regardless of the binding affinity and the proapoptotic capacity. We speculated that they might recognise different molecular signatures on the surface of the RA-FLSs. Then, we isolated membrane proteins of RA-FLSs and tried to identify the molecular targets of both SAPT4 and SAPT8 by pull-down assays. Interestingly, no protein was captured by SAPT4, while a specific protein with an observed molecular weight between 100 and 130 kDa was captured by SAPT8. Thus, we continued to identify the protein target of SAPT8 by mass spectrometry and interpreted the mechanism of action of SAPT8. Regarding the mechanism of action of SAPT4, we did not obtain a clue from the pull-down assay. However, it has been reported that the potential molecular targets of aptamers include not only proteins but also lipids or saccharides on the surface of the target cells [67,68]. We raised a bold hypothesis that the target molecules of SAPT4 might be lipids or saccharides, which could not be identified by our pull-down assays. Nevertheless, we did attempt to prove this hypothesis and interpret the mechanism of action of SAPT4 since the characterisation of lipids or saccharides was not our expertise. By LC-MS/MS analysis and experimental verification, the protein target of SAPT8 was proven to be NCL, which has been reported to be a ubiquitous expressed nucleolar protein primarily involved in the synthesis and maturation of ribosomes [66], but it also serves as a specific shuttling protein between nucleus and membrane of various tumour cells [43]. Previously, the surface expression of NCL on RA-FLSs was not reported and the pathologic role of NCL in RA-FLSs was also not characterised. Here, we revealed the presence of NCL on the surface of RA-FLSs and demonstrated that NCL conferred resistance to apoptosis and promoted migration, invasion and proliferation of RA-FLSs. These results suggested that NCL was a new surface molecular target for developing FLSs-directed therapies.

Mechanistically, we found that SAPT8 not only interacted with NCL but also decreased the protein level rather than the mRNA level of NCL in RA-FLSs. The most studied target genes of NCL are proapoptotic p53 and antiapoptotic Bcl-2 [30]. NCL interacts with p53 mRNA 5′-UTR and prevents its translation, whereas NCL stabilises Bcl-2 mRNA by binding to the 3′-UTR and protecting it from nuclease degradation [27,30]. Both p53 and Bcl-2 are suggested to be key regulators involved in the tumour-like transformation of RA-FLSs [27,30]. We demonstrated that SAPT8 targeted NCL to upregulate p53 expression and downregulate Bcl-2 level, providing a reasonable explanation for the proapoptotic capacity of SAPT8 against inflamed FLSs. Furthermore, it was interesting to see that SAPT8 could be internalised via both clathrin-mediated and caveolae-mediated endocytic pathways and enter the lysosome of RA-FLSs, suggesting that SAPT8 might carry NCL into the lysosome for degradation. Consistently, inhibition of lysosomal activity of RA-FLSs diminished the SAPT8-induced degradation of NCL protein, and blockage of SAPT8-NCL interaction by AS1411 reversed the SAPT8-induced suppression of tumour-like phenotypes of RA-FLSs, validating that SAPT8 acted as a lysosomal degrader of NCL to modulate NCL-p53/Bcl-2 signalling and display anti-RA-FLSs potential. As NCL shuttles between the nucleus, the cytoplasm and the cell surface of RA-FLSs, we speculated that, once the SAPT8-mediated elimination of surface NCL happens, intracellular NCL would be retranslocated onto the surface of RA-FLSs and excessive free SAPT8 in the extracellular environment would then bind with new NCL on the surface of RA-FLSs and induce a new cycle of NCL degradation until the exhaustion of extracellular SAPT8. This possibly explained the SAPT8-induced overall degradation of NCL in RA-FLSs as observed in this study. Besides our SAPT8, AS1411 and iSN04 were previously reported to be aptamers targeting NCL [42,43,53]. However, unlike the SAPT8, we demonstrated that neither AS1411 nor iSN04 triggered the degradation of NCL, while they decreased the NCL phosphorylation in RA-FLSs. Based on all our results, we could easily find that SAPT8 at nanomolar concentration was enough to inhibit the aggressive phenotypes of RA-FLSs, but micromolar AS1411 or iSN04 were required to exhibit therapeutic effects on RA-FLSs. Moreover, we also observed that iSN04 was less potent than AS1411 since iSN04 only showed effects at a concentration of 10 μM, whereas the effective concentration of AS1411 was 5 μM. The underlying reasons for the varied mechanisms of action and differential therapeutic efficacies among SAPT8, AS1411 and iSN04 remain to be elucidated. As NCL is an established cell surface molecular target for a variety of tumours and AS1411 targeting NCL has been tested for antitumour therapy [43], we propose that SAPT8 may also be used for antitumour therapy, which needs to be further confirmed in future studies. The aptamer-induced lysosomal degradation of target proteins was not merely seen in our study. A previous study identified an aptamer that was shown to target and facilitate the lysosomal degradation of an oncoprotein ErbB-2, thus retarding the tumorigenic growth of gastric cancer [69].

When applied SAPT8 in CIA mice, we observed the selective accumulation of SAPT8 in FLSs both at tissue and cellular levels, which was consistent with the good binding ability and specificity of SAPT8 with CIA-MFLSs in vitro. After periodic administration, SAPT8 monotherapy effectively decreased NCL expression and induced cell apoptosis of synovial tissues, leading to inhibited synovial hyperplasia, bone erosion and cartilage destruction in CIA mice. Moreover, combined therapy using SAPT8 and an anti-TNF biological DMARD synergistically alleviates the disease progression of CIA in mice. These results supported the currently popular theory that RA-FLSs-directed therapies could be a potentially alternative or complementary approach to the current DMARDs-based immune-directed therapies [12−14]. Besides RA, OA is also characterised by synovial hyperplasia, bone erosion and cartilage destruction, even though it has a very different aetiology from RA [70]. OA is a degenerative joint disease with a still-evolving concept of pathophysiology from being viewed as a cartilage-limited destruction to a multifactorial chronic disease that affects the whole joint [71]. FLSs have been recognised to play a critical role in the pathophysiology of OA and are suggested to be cellular targets for OA treatment [72]. In our study, we found that OA patients also had enhanced expression of NCL in synovial tissues, and intra-articular injection of SAPT8 reduced NCL expression, induced cell apoptosis of synovial tissues and displayed protective effects on DMM-induced OA mice. These studies demonstrated the broad prospects of SAPT8 in treating a variety of joint diseases featuring synovial hyperplasia or synovitis.

As SAPT8 was a cytotoxic aptamer selected for specifically targeting RA-FLSs, it was necessary to evaluate the side effects of SAPT8 on normal tissues in vivo. In CIA mice, we showed that there was no obvious accumulation of SAPT8 in the heart, liver, spleen and lung and less distribution of SAPT8 in the kidney. Liver function parameters, such as ALT, AST, ALB and TP, were in normal ranges in CIA mice systemically treated with SAPT8 monotherapy or SAPT8 in a combined therapy with an anti-TNF biological DMARD. Local administration of SAPT8 also showed a good safety profile in DMM-induced OA mice. These could be attributed to the excellent specificity and binding affinity of SAPT8 with inflamed FLSs and reflect the huge advantage of our proposed CSCT-SELEX strategy in developing cytotoxic aptamers specifically killing target cells but without damaging normal cells. This advantage of CSCT-SELEX will also benefit the screening of new types of cytotoxic drugs for treating other prevalent diseases, especially tumours. Traditional cytotoxic drugs, also known as chemotherapeutics, are medications that drive cells into apoptosis, thus causing the arrest of cancers or other non-malignant diseases, such as RA, multiple sclerosis and lupus [73,74]. Most of them are small molecular drugs that interfere with DNA synthesis, or produce chemical damage to DNA, leading to cell death. However, they are not specific to diseased cells and kill all dividing cells including healthy cells, leading to severe side effects, such as nausea and vomiting, and a narrow therapeutic window [75,76]. The current leading-edge solution is to conjugate the cytotoxic drugs with monoclonal antibodies against the specific antigens on the surface of tumour cells, that is, antibody-drug conjugates (ADCs), to achieve the tumour-selective delivery of the cytotoxic drugs [77]. However, ADCs have limited solid tumour permeability due to their large molecular weights, and the complexity of payload pharmacokinetics and insufficient release can also affect the efficacy of ADCs [78]. The CSCT-SELEX strategy developed in our study could directly confer the cell-targeting ability to the cytotoxic aptamers, which may address the limitation of ADCs.

There are also a few limitations of our study. Even though we proved that NCL was expressed on the surface of RA-FLSs and cell surface NCL contributed to the tumour-like phenotypes of RA-FLSs, we still know nothing about how NCL shuttles from the nucleus to the cell surface of RA-FLSs. The same question was also an unaddressed challenge in tumours although the surface expression of NCL on tumours has been discovered for decades [30]. Second, the efficacy of nucleic acid therapies can be limited by unwanted nuclease-mediated degradation. Nucleic acid drugs are always designed to enhance their pharmacokinetic properties in vivo via chemical modifications, such as PS linkage, 2′-OMe, 2′-MOE, 2′-F and LNA [79]. In our study, as we saw the excellent stability of SAPT8 in a serum degradation test in vitro, we directly performed the proof-of-concept study to determine the therapeutic efficacy of unmodified SAPT8 in arthritic animal models. In the future, SAPT8 should be extensively modified before commercialization and entering clinical trials. Although we observed that SAPT8 decreased the expression of COX-2, a key mediator involved in inflammatory pain, in arthritic mice at the end of SAPT8 aptamer treatment, it should be worth exploring whether the induction of apoptosis of RA-FLSs by SAPT8 could potentially lead to temporary increased pain in future studies.

In conclusion, CSCT-SELEX is a promising strategy for generating cell-specific and cytotoxic aptamers. SAPT8, selected by CSCT-SELEX, could be an aptamer drug selectively killing RA-FLSs, which may be a potential alternative or complementary approach to the current DMARDs-based immune-directed therapies. NCL is a newly identified molecular target on the surface of RA-FLSs and will pave the way for developing diverse FLSs-directed therapies for treating arthritis.

MATERIALS AND METHODS

Cell culture

RA-FLSs, OA-FLSs and ACLI-FLSs were isolated from synovial tissues of patients with RA, OA and ACLI, respectively [80,81]. H-MFLSs, CIA-MFLSs and CIA-RFLSs were isolated from synovial tissues of healthy mice, CIA mice and CIA rats, respectively [39]. The human synovial cell line SW982 (HTB-93), human monocytic cell line THP-1 (TIB-202), human osteoblastic cell line hFOB 1.19 (CRL-3602), human normal skin fibroblast cell line BJ (CRL-2522), mouse osteoblast-like cell line MC3T3-E1 (CRL-2593), mouse macrophage-like cell line RAW 264.7 (TIB-71), mouse fibroblast cell line L929 (CCL-1) and human embryonic kidney cell line 293 T cells (CRL-3216) were obtained from American Type Culture Collection. The mouse chondrogenic cell line ATDC5 (CVCL_3894) was obtained from the Type Culture Collection of the Chinese Academy of Sciences. RA-FLSs, OA-FLSs and ACLI-FLSs were cultured in Dulbecco's Modified Eagle Medium (DMEM, Corning, USA) supplemented with 20% fetal bovine serum (FBS). H-MFLSs, CIA-MFLSs, CIA-RFLSs, BJ cells, RAW 264.7 cells and 293 T cells were cultured in DMEM medium supplemented with 10% FBS. SW982 cells were cultured in Leibovitz's L-15 medium (Corning, USA) supplemented with 10% FBS. THP-1 cells were cultured in RPMI-1640 medium supplemented with 10% FBS. hFOB 1.19 cells were cultured in DMEM/Ham's F12 (Thermo Fisher, USA) medium supplemented with 10% FBS, 2.5 mM L-glutamine, and 300 μg/mL G418 (Beyotime, China). MC3T3-E1 cells were cultured in Alpha MEM medium (Corning, USA) supplemented with 10% FBS. L929 cells were cultured in EMEM medium (Corning, USA) supplemented with 10% FBS. ATDC5 cells were cultured in DMEM/F12 supplemented with 10% FBS. All media were supplemented with 1% penicillin−streptomycin. All cells were negative for mycoplasma and maintained at a 37°C humid atmosphere with 5% CO_2.

Random ssDNA library and primers

The initial ssDNA library contained a central randomised sequence of 35 nucleotides flanked by two 20-nt primer hybridisation sites: 5′-TGAGAATATGTAGACGATCC-(35N)-CGGAGCTTCAAGATGATCTG-3′, the forward primer: 5′-TGAGAATATGTAGACGATCC-3′, the reverse primer: 5′-CAGATCATCTTGAAGCTCCG-3′. The ssDNA library, primers and all ssDNA aptamer candidates were synthesised by Sangon Biotech (Shanghai, China).

CSCT-SELEX procedure

The CSCT-SELEX consisted of a CS-SELEX module followed by a CT-SELEX module. The CS-SELEX was based on the traditional cell-SELEX with some modifications [25]. During CS-SELEX, RA-FLSs were employed as target cells in the positive selection, and THP-1 and hFOB 1.19 cells were used as control cells in the negative selection. We used the FLSs from patients who shared some similar features (such as gender and age) and comparable levels of indices for the severity of RA (such as CRP and ESR), and we characterised them with equivalent expression of molecular markers, including THY1 and vimentin, and used them at uniform passages in a specific experiment. For the first round of CS-SELEX, a 10 nmol random ssDNA library was dissolved in 400 μL binding buffer containing 4.5 g/L glucose, 0.1 mg/mL yeast tRNA, 5 mM $MgCl_2$ and 1 mg/mL bovine serum albumin (BSA) in Dulbecco's PBS (DPBS). After denaturing at 95°C for 5 min and rapid cooling on ice for 10 min, the ssDNA library was incubated with 1×10^6 RA-FLSs for 3 hours at 37°C. Then, the cells were centrifuged and washed with 500 μL washing buffer containing 4.5 g/L glucose and 5 mM $MgCl_2$ in DPBS to remove unbound sequences. The bound sequences were recovered by heating the cell-DNA complex at 95°C and PCR amplified to create a new pool. PCR was conducted using unlabelled forward primers and biotin-labelled reverse primers (5 min at 95°C, 10−20 cycles of 30 s at 95°C, 30 s at 55°C and 30 s at 72°C, followed by 5 min at 72°C). After denaturing in an alkaline condition (0.1 M NaOH), the sense ssDNA strand was separated from the biotinylated antisense ssDNA strand by Streptavidin Sepharose High-Performance Beads (GE Healthcare, UK), desalted and lyophilised for the next round of selection. From the third round of CS-SELEX, negative selection was carried out to filter out sequences that might bind to the molecules existing on the surface of both target cells and control cells prior to the positive selection. 200 pmol enriched ssDNA pool dissolved in 400 μL binding buffer was incubated with 5×10^6 control cells (THP-1 and hFOB 1.19 cells) for 3 hours at 37°C. The unbound ssDNA was collected and used for positive selection with RA-FLSs. To acquire aptamers with high affinity and specificity, the wash strength was enhanced gradually by increasing the volume of washing buffer (from 0.5 to 5 mL) and the number of washes (from three to five). The progress of the CS-SELEX was monitored by a microplate reader (PerkinElmer, EnSpire, USA). Briefly, the enriched ssDNA pools from the 4th round (R4), the 8th round (R8) and the 12th round (R12) were PCR-amplified using Cy3-labelled forward and biotin-labelled reverse primers before obtaining the sense ssDNA strand by alkaline denaturation and subsequent streptavidin-coated magnetic beads separation. The enriched ssDNA pools with Cy3 labelling were then incubated with 5×10^5 RA-FLSs, THP-1 cells or hFOB 1.19 cells for 3 hours at 37°C before determining the MFI of the cells using the microplate reader (PerkinElmer, EnSpire, USA).

After 12 rounds of CS-SELEX, CT-SELEX was started using the enriched ssDNA pool that exhibited the highest binding ability with RA-FLSs from the CS-SELEX module as the initial pool. 1000 nM enriched ssDNA pool was heated at 95°C for 5 min, chilled on ice for 10 min and then incubated with 5×10^6 RA-FLSs for 3 days. During the incubation, the medium containing 1000 nM enriched ssDNA pool was changed every day. After the incubation, apoptotic RA-FLSs were collected using an Annexin V MicroBead Kit (Miltenyi Biotec, USA) and resuspended in 400 µL binding buffer. The apoptotic cell-associated sequences were recovered by heating the apoptotic cell-DNA complex at 95°C. PCR was conducted using unlabelled forward primers and biotin-labelled reverse primers (5 min at 95°C, 10−20 cycles of 30 s at 95°C, 30 s at 55°C and 30 s at 72°C, followed by 5 min at 72°C). After denaturing in an alkaline condition (0.1 M NaOH), the sense ssDNA was separated from the biotinylated antisense ssDNA strand by Streptavidin Sepharose High-Performance Beads (GE Healthcare, UK), desalted and lyophilised for the next round of selection. The progress of the CT-SELEX was monitored by the annexin V-coated magnetic beads. Briefly, 5×10^6 RA-FLSs were daily treated with 400 nM enriched ssDNA pools from the first round (R1′), the third round (R3′), the sixth round (R6′) and the ninth round (R9′) of CT-SELEX for 3 days. The percentage of apoptotic RA-FLSs was determined by the Annexin V MicroBead Kit (Miltenyi Biotec, USA). After the CT-SELEX, the enriched ssDNA pool with the highest proapoptotic ability was PCR-amplified using unlabelled primers and cloned into *Escherichia coli* by using the TA cloning kit (Invitrogen, USA). Cloned sequences were sequenced to identify individual aptamer candidates by Sangon Biotech (Shanghai, China).

Binding assays by flow cytometry

RA-FLSs (6×10^4 per well), ACLI-FLSs (6×10^4 per well), CIA-MFLSs (5×10^4 per well), CIA-RFLSs (3×10^4 per well), SW982 cells (4×10^4 per well), hFOB 1.19 cells (5×10^4 per well), MC3T3-E1 cells (4×10^4 per well), RAW 264.7 cells (6×10^4 per well), L929 cells (4×10^4 per well), ATDC5 cells (3×10^4 per well), H-MFLSs (5.5×10^4 per well), BJ cells (4×10^4 per well) or OA-FLSs (5×10^4 per well) were seeded in six-well plates and allowed to adhere for 24 hours. THP-1 cells (6×10^4 per well) were maintained in six-well plates for 24 hours. After different treatments in each study, the adherent cells were digested with 0.25% trypsin −EDTA (Thermo Fisher, USA) and washed with PBS. Fluorescence signals were detected by a flow cytometer (BD, FACSCanto SORP, USA) and data were analysed by FlowJo software. To measure the equilibrium dissociation constant (K_d), RA-FLSs (6×10^4 per well) were treated with increasing concentrations of Cy3-labelled aptamers. The K_d value of the interaction between aptamers and RA-FLSs was determined by fitting the dependence of fluorescence intensity using Prism GraphPad V.9 software with the equation $Y = B_{max}X/(K_d + X)$, where X was the aptamer concentration; Y was MFI of X; and B_{max} was maximum MFI [82].

Serum stability assay

Aptamers were incubated with 50% FBS in the medium for 0, 1, 3, 6, 12 and 24 hours at 37°C. Subsequently, the samples were mixed with DNA loading dye and subjected to non-denaturing PAGE for 2 hours at 100 V. The gel was stained with 4S Gelblue (Sangon Biotech, China) for 15 min at room temperature and then visualised under ultraviolet light [83].

Apoptosis analysis by flow cytometry

RA-FLSs (3×10^4 per well), CIA-MFLSs (2×10^4 per well), CIA-RFLSs (2×10^4 per well), SW982 cells (3×10^4 per well), BJ cells (4×10^4 per well) or OA-FLSs (3.5×10^4 per well) were seeded in six-well plates and allowed to adhere for 24 hours. After different treatments in each study, the cells were digested with 0.25% trypsin−EDTA and washed with PBS. An Annexin V-FITC Apoptosis Detection Kit (Beyotime, China) was used to stain apoptotic cells. Flow cytometry was performed to detect apoptotic cells and data were analysed by FlowJo software [84].

TUNEL assay

After different treatments in each study, RA-FLSs and joint tissue sections were fixed in 4% formalin for 10 min and incubated with Cy3-labelled dUTP and terminal deoxynucleotidyl transferase enzyme mixture from a One Step TUNEL Apoptosis Assay Kit (Beyotime, China) for 1 hour at room temperature. Cell nuclei were counterstained with DAPI (Thermo Fisher, USA), and apoptotic cells were imaged using a confocal fluorescence microscope (Zeiss, LSM980, DE) [85].

CCK-8 assay

RA-FLSs (2×10^3 per well), CIA-MFLSs (1×10^3 per well), CIA-RFLSs (1×10^3 per well) or SW982 cells (1×10^3 per well) were seeded in 96-well plates and allowed to adhere for 24 hours. After different treatments in each study, proliferation of the cells was measured using CCK-8 according to the manufacturer's instructions (MedChemExpress, MCE, USA). The cells were washed with PBS, and 10 µL CCK-8 solution and 90 µL complete medium were added to each well. Plates were detected by a microplate reader at 450 nm [86].

Colony formation assay

RA-FLSs (2×10^3 per well), CIA-MFLSs (800 per well), CIA-RFLSs (500 per well), SW982 cells (1×10^3 per well) or OA-FLSs (3×10^3 per well) were seeded in six-well plates and allowed to adhere for 24 hours. After different treatments in each study, the cells were fixed in 4% formalin for 20 min and stained with crystal violet (Aladdin, China) for 30 min at room temperature [80]. Digital images of the colonies were obtained using a camera. The number of colonies was counted using ImageJ software.

Transwell migration and invasion assays

To examine cell migration, 200 µL serum-free medium containing RA-FLSs (8×10^3 per well), CIA-MFLSs (6×10^3 per well), CIA-RFLSs (8×10^3 per well), SW982 cells (1×10^4 per well) or OA-FLSs (8.5×10^3 per well) were directly seeded in 24-well transwell inserts with a pore size of 8.0 µm (Corning, New York, USA). To determine cell invasion, the upper chambers were coated with a solution of matrigel at a concentration of 1.25 mg/mL (20 µL per well) before cell seeding. Then, 600 µL medium containing 20% FBS was added to the lower chamber. After different treatments in each study, non-migrated cells were removed by cotton swabs, and cells that migrated to the lower face of the upper chamber were fixed in 4% formalin for 20 min and stained with crystal violet for 30 min at room temperature [87]. The chambers were washed with PBS and air dried. Photographs were obtained by an inverted microscope (NanoZoomer S60, Japan), and the number of migrated cells was quantitated using ImageJ software [87].

Wound healing assay

RA-FLSs, CIA-MFLSs, CIA-RFLSs or SW982 cells were seeded in six-well plates and cultured until cells became more than 90% confluent. Subsequently, the cells were scratched uniformly with 200 μL sterile pipette tips, and floating cells and cell debris were washed off with culture medium. After different treatments in each study, wound healing was captured by the inverted microscope, and the area of the wound gap was calculated and recorded using ImageJ software [77].

Western blotting

RA-FLSs or OA-FLSs, after different treatments in each study, were lysed in lysis buffer (50 mM Tris-HCl (pH 7.4), 150 mM NaCl, 1% Triton X-100, 2 mM EDTA and 10% glycerol) containing protease inhibitor cocktails (Sigma, USA). The total protein concentration of each cell sample was evaluated by a bicinchoninic acid assay. The proteins in each cell sample were separated by SDS-PAGE and transferred to a polyvinylidene fluoride membrane (Millipore, Massachusetts, USA) using a transfer apparatus (Bio-Rad, Trans-Blot Turbo, USA). After blocking, the membranes were reacted with primary antibodies at 4°C overnight. Subsequently, the membranes were washed and reacted with the corresponding horseradish peroxidase (HRP)-conjugated secondary antibodies for 1 hour at room temperature. The membranes were probed by using an Enhanced Chemiluminescence ECL Kit (ABclonal, China) and visualised with a chemiluminescence imaging system (Tanon, Multi5200, China) [83]. The primary antibodies were as follows: anti-NCL antibody (14574, Cell Signaling Technology, CST, USA), anti-Bcl-2 antibody (ab182858, Abcam, UK), anti-p53 antibody (ab26, Abcam, UK), anti-IL-1β antibody (ab254360, Abcam, UK), anti-MMP3 antibody (ab52915, Abcam, UK) and anti-GAPDH antibody (AC002, Abclonal, China).

Pull-down assay by aptamers

Membrane proteins of RA-FLSs were extracted using a Minute Plasma Membrane Protein Isolation Kit (Invent Biotechnologies, USA) and incubated with biotin-labelled aptamers at 4°C for 6 hours. The Streptavidin Sepharose High-Performance Beads (GE Healthcare, UK) were added to the mixture of membrane proteins and aptamers and incubated overnight at 4°C. The beads were washed and heated to elute the captured proteins. The captured proteins were separated by SDS-PAGE gel. After silver staining of the gel using a Pierce Silver Stain for Mass Spectrometry Kit (Thermo, USA), the specific band of protein captured by aptamer was excised for digestion and analysed by LC-MS/MS in BGI Genomics. A MASCOT database search was used to assign possible protein candidates to the MS results [88].

Dot blotting assay

The rhNCL protein (MCE, USA) was diluted into 10 μg/mL and spotted (2 μL/dot) onto a nitrocellulose membrane. The membrane was dried naturally, blocked with 5% non-fat dry milk for 2 hours at room temperature and incubated with biotin-labelled aptamer overnight at 4°C. Subsequently, the membrane was washed, incubated with HRP-labelled streptavidin (MCE, USA) for 1 hour at room temperature and probed by using an Enhanced Chemiluminescence ECL Kit (ABclonal, China) and visualised with a chemiluminescence imaging system (Tanon, Multi5200, China) [82].

Real-time PCR

Total RNA was extracted using the TransZol Up Plus kit (TransGen, China). cDNA was synthesised using the PrimeScript RT Master Mix (Takara, Japan). Real-time PCR was performed on a CFX 96 Touch Real-Time PCR System (Bio-Rad, USA), with SYBR Green qPCR Master Mix from TransGen Biotech. Data were normalised to the expression levels of the housekeeping gene GAPDH and expressed as mean±SEM. Results were calculated as fold change compared with the expression level of each gene in control samples using the comparative threshold cycle (Ct) method with the formula $2^{(-\wedge\wedge Ct)}$ [83]. Primer sequences are listed in online supplemental table S3.

Gene silencing by siRNA

RA-FLSs were seeded in six-well plates and allowed to adhere for 24 hours. According to the manufacturer's instructions, the cells were transfected at a final concentration of 20 nM siRNA using Lipofectamine RNAiMAX Reagent (Thermo Fisher, USA). The sequences of siRNA are listed in online supplemental table S4.

Lentivirus production and transduction

Lentivirus production and transduction were performed as previously described [89]. Briefly, 1 mg of desired plasmids, 0.75 mg psPAX2 and 0.25 mg pMD2.G were cotransfected into 293 T cells using Effectene transfection reagent (Qiagen, Germany). The culture medium was replenished at 12 hours post transfection. Subsequently, the supernatant was collected at 48 and 72 hours. For transduction, RA-FLSs (5×10^4 per well) were seeded in six-well plates and allowed to adhere for 24 hours. The lentivirus solutions with 8 μg/mL polybrene (Sigma-Aldrich, USA) were added to the cells. The culture medium was changed at 36 hours post transfection, and antibiotic selection was started at 72 hours post transfection with 2 μg/mL puromycin (Beyotime, China) in the medium. The targeted gene expression on RA-FLSs was measured at 4 days after adding antibiotic selection. The information on plasmids used in this study is listed in online supplemental table S5.

EdU proliferation assay

Cell proliferation was determined using a BeyoClick EdU Cell Proliferation Kit with Alexa Fluor 488 (Beyotime, China). Briefly, RA-FLSs (1×10^4 cells per well) were seeded in confocal plates and allowed to adhere for 24 hours. After different treatments in each study, 50 μL EdU was added into the cells and incubated at 37°C. The cells were fixed in 4% formalin for 10 min, permeabilized with 0.2% Triton X-100 for 10 min, and blocked with 5% BSA in PBS for 1 hour. A staining cocktail including 430 μL click reaction buffer, 50 μL click additive solution, 1 μL Alexa Fluor 488 and 20 μL $CuSO_4$ were added into the cells for 30 min. Finally, the cells were counterstained with

DAPI, and images were acquired using a confocal fluorescence microscope [90].

RNA sequencing analysis

RNA sequencing was performed in Sangon Biotech (Shanghai, China). Raw sequencing reads were subjected to a comprehensive quality check using FastQC (V.0.11.9). Cleaned reads were aligned to a reference genome. Postalignment data management, including sorting of alignment files, index construction and alignment efficiency statistics, was performed using SAMtools [91] (V.1.10). Gene expression levels were determined using featureCounts [92] (V.2.0.1), which assigned reads to genes or transcripts to generate counts for each feature. Normalisation of gene expression across sh-NCL and sh-NC datasets was executed using the DESeq V.2 package [93]. DEGs between sh-NCL and sh-NC groups were identified based on criteria of p value<0.05 and $|\log_2 FC|>1$. DEGs visualisation was achieved using volcano plots (ggplot V.2 package) and heatmaps (pheatmap package). DEGs were subjected to GO and KEGG pathway enrichment analyses via the clusterProfiler R package [94,95]. Only pathways with a p value less than 0.05 were considered for significant enrichment. Differences in biological processes between si-NCL and si-NC groups were explored using GSEA [96]. Analysis was based on the 'c2.cp.all.v2022.1.Hs.symbols.gmt' gene set from MSigDB, with pathways holding a false discovery rate<0.25 regarded as significantly enriched.

Collection of human samples

Synovial tissues of RA and OA patients were collected during joint replacement surgery and synovial tissues of ACLI patients were collected during ACL reconstruction surgery. The collected synovial tissues were preserved in liquid nitrogen. The synovial tissues were detected for positive expression of fibroblastic biomarkers THY1 and vimentin [33,34], as well as the absence of a macrophage marker CD68 [35]. The clinical characteristics of patients are shown in online supplemental table S6.

CIA rat model

Male SD rats (170–190 g of weight) were purchased from the Chinese University of Hong Kong and kept with free access to food and water under standard temperature conditions (22°C) and a 12 hours light/dark cycle. The CIA rat model was established as follows [97]. Briefly, bovine type II collagen (Chondrex, USA) was emulsified in an equal volume of Incomplete Freund's adjuvant (Chondrex, USA). The rats were immunised subcutaneously at the base of the tail with 200 µL emulsion containing 200 µg collagen. Booster immunisation was administered on day 7 with a 100 µL injection of the same emulsion as the first time. Arthritis severity was evaluated by clinical arthritic scores, which were performed by two independent, blinded observers. Scoring was performed with a 0–4 scale, where 0 = no swelling or erythema; 1 = slight swelling and/or erythema; 2 = low-to-moderate oedema; 3 = pronounced oedema with limited joint usage; and 4 = excess oedema with joint rigidity. Each paw was graded, and the maximum possible score was 16 for each rat. A rat with a score of one or above was regarded as arthritic.

CIA mouse model

Male DBA/1 mice aged 8–10 weeks were from the Gempharmatech and kept with free access to food and water under standard temperature conditions (22°C) and a 12 hours light/dark cycle. CIA mouse model was established as follows [98]. Briefly, bovine type II collagen (Chondrex, USA) was emulsified in an equal volume of Complete Freund's adjuvant (Chondrex, USA). The mice were immunised with a single subcutaneous injection at the base of the tail with 100 µL emulsion containing 100 µg collagen and 2 mg/mL *Mycobacterium tuberculosis*. Arthritis severity was evaluated by clinical arthritic scores, which were performed by two independent, blinded observers. Scoring was performed with a 0–4 scale, where 0 = normal; 1 = redness and/or swelling in one joint; 2 = redness and/or swelling in more than one joint; 3 = redness and/or swelling in the entire paw; and 4 = deformity and/or ankylosis. Each paw was graded, and the maximum possible score was 16 for each mouse. A mouse with a score of one or above was regarded as arthritic.

DMM mouse model

Male C57BL/6J mice aged 6–8 weeks were purchased from the Gempharmatech and kept with free access to food and water under standard temperature conditions (22°C) and a 12 hours light/dark cycle. DMM surgery was conducted in the right knees in C57BL/6 mice for the establishment of the OA model [99]. Briefly, a mouse was anaesthetised using a 2.5% avertin with a dosage of 250 mg/kg body weight via intraperitoneal injection. The medial meniscotibial ligament of the right knee joint of each mouse was transected. The sham-operated controls underwent the same surgery except that the meniscotibial ligament was not cut.

In vivo fluorescence imaging

Cy3-labelled NC or SATP8 was intravenously given to the CIA mice via the tail vein. An in vivo imaging system Spectrum imaging system (PerkinElmer, USA) was used to examine the fluorescence of NC and SAPT8. The quantification of fluorescence was analysed via Living Image V.4.4 software (Caliper Life Sciences, USA) [100].

µCT analysis

The joints were fixed in 10% formalin (Solarbio, China) and then transferred to 70% ethanol. Scanning was performed at a Skyscan scanner 1276 high-resolution µCT scanner (Bruker, Germany) with a voxel size of 10 µm, at 60 kVp/100 µAmp. The images were reconstructed to generate three-dimensional (3D) images using NRecon software (Bruker, Germany) and Date Viewer (Bruker, Germany). The µCT data were processed using CTAn software (Bruker, Germany) and images were generated using CTVOX software (Bruker, Germany). Bone erosion was quantified as previously described [99]. Scanned images were processed using the same thresholds to keep the 3D structural rendering of each sample.

Histological analysis

The joints were fixed, decalcified, dehydrated and embedded in paraffin. A series of sections (5 µm thick) was stained with H&E and SO/FG (Solarbio, China) using standard protocols according to the manufacturer's instructions. The specimens were independently viewed and analysed by two pathologists under a light microscope (NanoZoomer S60, Japan). The histopathological scoring was performed as previously described [16,99].

Immunofluorescent staining

Tissue sections were subjected to deparaffinization using xylene, rehydrated and antigen retrieval. The sections were permeabilised with 0.2% Triton X-100 for 10 min, blocked with 5% BSA in PBS for 1 hour and incubated with primary antibodies anti-NCL (14574, CST, USA), anti-Bcl-2 antibody (ab182858, Abcam, UK), anti-p53 antibody (ab26, Abcam, UK), anti-IL-6 (ab233551, Abcam, UK), anti-IL-1β (ab254360, Abcam, UK), anti-MMP3 (ab52915, Abcam, UK) and anti-COX2 (ab179800, Abcam, UK) at 4°C overnight. After washing, the sections were incubated with anti-mouse Alexa Fluor 488 (ab150113, Abcam, UK) or anti-rabbit Alexa Fluor 488 (ab150077, Abcam, UK) for 1 hour at room temperature. Finally, the sections were counterstained with DAPI, and images were acquired using a confocal fluorescence microscope [99].

Serum biochemical assays

Blood samples were collected from mice after treatment via hepatic portal vein puncture. Serum was collected via centrifugation of blood samples in 12 000×*g* at 4°C for 30 min. Serum biochemical parameters, including ALT, AST, ALB and TP, were analysed by an MS-480 Automatic Biochemistry Analyzer (Medicalsystem Biotechnology, China) [101].

Statistical analysis

All numerical data are expressed as the mean±SD. Statistical differences among multiple independent groups were analysed by the one-way analysis of variance (ANOVA) with a post hoc test. Statistical differences between two independent groups were determined by the two-tailed Student's t-test. Statistical differences between the groups that were defined by two categorical factors were analysed by the two-way ANOVA with a post hoc test. All statistical analyses were performed with GraphPad Prism V.9 software. $P<0.05$ was considered statistically significant. We chose the representative images based on the average level of the data for each group. For the in vivo experiments, the sample size was predetermined by a power calculation. The mice were grouped randomly and blindly by researchers. The mice in poor body condition before the experiments were excluded.

Acknowledgments

The authors acknowledge the assistance of the Southern University of Science and Technology Core Research Facilities, the Microscope and Imaging Center and the Experimental Animal Center of the Southern University of Science and Technology. Schematic diagram of CTCS-SELEX was created with BioRender.com.

Contributors

CL, AL and XF are guarantors for all content. CL, AL, and XF supervised and revised the manuscript. FQ and DX performed the major research and wrote the paper with equal contributions. HC, ZW, JH, CC, YL and XY provided the technical support and professional expertise. All authors contributed to the article and approved the submitted version.

Funding

This work is supported by the National Natural Science Foundation Council of China (82172386 and 81922081 to CL and 82100943 to XF), the 2020 Guangdong Provincial Science and Technology Innovation Strategy Special Fund (Guangdong-Hong Kong-Macau Joint Lab) (2020B1212030006 to AL), the Guangdong Basic and Applied Basic Research Foundation (2022A1515012164 to CL), the Science, Technology, and Innovation Commission of Shenzhen (JCYJ20210324104201005 to CL), the Shenzhen Medical Research Fund (A2303061 to XF), the Hong Kong General Research Fund (12102722 to AL), the Hong Kong RGC Theme-based Research Scheme (T12-201/20-R to AL) and Shenzhen LingGene Biotech.

Competing interests

Shenzhen LingGene Biotech has a patent application related to this work.

Patient and public involvement

Patients and/or the public were not involved in the design, or conduct, or reporting, or dissemination plans of this research.

Patient consent for publication

Not applicable.

Ethics approval

All the clinical procedures were approved by the committees of clinical ethics in the Shanghai Guanghua Hospital of Integrative Medicine, Shanghai University of Traditional Chinese Medicine. We obtained informed consent from the participants. The protocols of animal experiments were approved by the Institutional Animal Care and Use Committee of the Southern University of Science and Technology (SUSTech-JY202302087, SUSTech-JY20241003) and the Committees of Animal Ethics and Experimental Safety of the Hong Kong Baptist University (REC/21-22/0151). We complied with all relevant ethical regulations for animal testing and research.

Data availability statement

Data are available in a public, open access repository. Data are available on reasonable request. Data are available in a public, open access repository. The RNA sequencing data have been uploaded to Gene Expression Omnibus platform with the accession number GSE268214.

Supplemental material

Supplementary material associated with this article can be found in the online version at doi:10.1136/ard-2024-225565.

Orcid

Xuekun Fu: http://orcid.org/0000-0002-8208-9939
Chao Liang: http://orcid.org/0000-0002-5617-3483

REFERENCES

[1] Huang J, Fu X, Chen X, et al. Promising Therapeutic Targets for Treatment of Rheumatoid Arthritis. Front Immunol 2021;12:686155. doi: 10.3389/fimmu.2021.686155.

[2] Smolen JS, Aletaha D, McInnes IB. Rheumatoid arthritis. The Lancet 2016;388:2023–38. doi: 10.1016/S0140-6736(16)30173-8.

[3] Klareskog L, Catrina AI, Paget S. Rheumatoid arthritis. The Lancet 2009;373:659–72. doi: 10.1016/S0140-6736(09)60008-8.

[4] Looney RJ. B cell-targeted therapy for rheumatoid arthritis: an update on the evidence. Drugs (Abingdon Engl) 2006;66:625–39. doi: 10.2165/00003495-200666050-00004.

[5] Ma Y, Pope RM. The role of macrophages in rheumatoid arthritis. Curr Pharm Des 2005;11:569–80. doi: 10.2174/1381612053381927.

[6] Yasuda T. Cartilage destruction by matrix degradation products. Mod Rheumatol 2006;16:197–205. doi: 10.1007/s10165-006-0490-6.

[7] Furst DE, Emery P. Rheumatoid arthritis pathophysiology: update on emerging cytokine and cytokine-associated cell targets. Rheumatol (Oxford) 2014;53:1560–9. doi: 10.1093/rheumatology/ket414.

[8] Skapenko A, Leipe J, Lipsky PE, et al. The role of the T cell in autoimmune inflammation. Arthritis Res Ther 2005;7:1–11. doi: 10.1186/ar1703.

[9] Alivernini S, Firestein GS, McInnes IB. The pathogenesis of rheumatoid arthritis. Immunity 2022;55:2255–70. doi: 10.1016/j.immuni.2022.11.009.

[10] Németh T, Nagy G, Pap T. Synovial fibroblasts as potential drug targets in rheumatoid arthritis, where do we stand and where shall we go? Ann Rheum Dis 2022;81:1055–64. doi: 10.1136/annrheumdis-2021-222021.

[11] Nygaard G, Firestein GS. Restoring synovial homeostasis in rheumatoid arthritis by targeting fibroblast-like synoviocytes. Nat Rev Rheumatol 2020;16:316–33. doi: 10.1038/s41584-020-0413-5.

[12] Bottini N, Firestein GS. Duality of fibroblast-like synoviocytes in RA: passive responders and imprinted aggressors. Nat Rev Rheumatol 2013;9:24–33. doi: 10.1038/nrrheum.2012.190.

[13] Chu CQ. Fibroblasts in Rheumatoid Arthritis. N Engl J Med 2020;383:1679–81. doi: 10.1056/NEJMcibr2024718.

[14] Singh V, Naldi A, Soliman S, et al. A large-scale Boolean model of the rheumatoid arthritis fibroblast-like synoviocytes predicts drug synergies in the arthritic joint. NPJ Syst Biol Appl 2023;9:33. doi: 10.1038/s41540-023-00294-5.

[15] Lee DM, Kiener HP, Agarwal SK, et al. Cadherin-11 in synovial lining formation and pathology in arthritis. Science 2007;315:1006–10. doi: 10.1126/science.1137306.

[16] Svensson MND, Zoccheddu M, Yang S, et al. Synoviocyte-targeted therapy synergizes with TNF inhibition in arthritis reversal. Sci Adv 2020;6:eaba4353. doi: 10.1126/sciadv.aba4353.

[17] Pratt AG, Siebert S, Cole M, et al. Targeting synovial fibroblast proliferation in rheumatoid arthritis (TRAFIC): an open-label, dose-finding, phase 1b trial. Lancet Rheumatol 2021;3:e337–46. doi: 10.1016/S2665-9913(21)00061-8.

[18] Chu CQ. Highlights of Strategies Targeting Fibroblasts for Novel Therapies for Rheumatoid Arthritis. Front Med (Lausanne) 2022;9:846300. doi: 10.3389/fmed.2022.846300.

[19] Mayer G, Ahmed MSL, Dolf A, et al. Fluorescence-activated cell sorting for aptamer SELEX with cell mixtures. Nat Protoc 2010;5:1993–2004. doi: 10.1038/nprot.2010.163.

[20] Zhou J, Rossi J. Aptamers as targeted therapeutics: current potential and challenges. Nat Rev Drug Discov 2017;16:181–202. doi: 10.1038/nrd.2016.199.

[21] Chang D, Wang Z, Flynn CD, et al. A high-dimensional microfluidic approach for selection of aptamers with programmable binding affinities. Nat Chem 2023;15:773–80. doi: 10.1038/s41557-023-01207-z.

[22] Kacherovsky N, Cardle II, Cheng EL, et al. Traceless aptamer-mediated isolation of $CD8^+$ T cells for chimeric antigen receptor T-cell therapy. Nat Biomed Eng 2019;3:783–95. doi: 10.1038/s41551-019-0411-6.

[23] Keefe AD, Pai S, Ellington A. Aptamers as therapeutics. Nat Rev Drug Discov 2010;9:537–50. doi: 10.1038/nrd3141.

[24] Lin N, Wu L, Xu X, et al. Aptamer Generated by Cell-SELEX for Specific Targeting of Human Glioma Cells. ACS Appl Mater Interfaces 2021;13:9306–15. doi: 10.1021/acsami.0c11878.

[25] Shangguan D, Li Y, Tang Z, et al. Aptamers evolved from live cells as effective molecular probes for cancer study. Proc Natl Acad Sci U S A 2006;103:11838–43. doi: 10.1073/pnas.0602615103.

[26] Sefah K, Shangguan D, Xiong X, et al. Development of DNA aptamers using Cell-SELEX. Nat Protoc 2010;5:1169–85. doi: 10.1038/nprot.2010.66.

[27] Zhang X, Xiao S, Rameau RD, et al. Nucleolin phosphorylation regulates PARN deadenylase activity during cellular stress response. RNA Biol 2018;15:251–60. doi: 10.1080/15476286.2017.1408764.

[28] Shigdar S, Agnello L, Fedele M, et al. Profiling Cancer Cells by Cell-SELEX: use of Aptamers for Discovery of Actionable Biomarkers and Therapeutic Applications Thereof. Pharmaceutics 2021;14:28. doi: 10.3390/pharmaceutics14010028.

[29] Fu X, Liang C, Li F, et al. The Rules and Functions of Nucleocytoplasmic Shuttling Proteins. Int J Mol Sci 2018;19:1445. doi: 10.3390/ijms19051445.

[30] Yangngam S, Prasopsiri J, Hatthakarnkul P, et al. Cellular localization of nucleolin determines the prognosis in cancers: a meta-analysis. J Mol Med (Berl) 2022;100:1145–57. doi: 10.1007/s00109-022-02228-w.

[31] Santana-Viera L, Dassie JP, Rosàs-Lapeña M, et al. Combination of protein and cell internalization SELEX identifies a potential RNA therapeutic and delivery platform to treat EphA2-expressing tumors. Mol Ther Nucleic Acids 2023;32:758–72. doi: 10.1016/j.omtn.2023.05.003.

[32] Earnest KG, McConnell EM, Hassan EM, et al. Development and characterization of a DNA aptamer for MLL-AF9 expressing acute myeloid leukemia cells using whole cell-SELEX. Sci Rep 2021;11:19174. doi: 10.1038/s41598-021-98676-4.

[33] Bi X, Guo XH, Mo BY, et al. LncRNA PICSAR promotes cell proliferation, migration and invasion of fibroblast-like synoviocytes by sponging miRNA-4701-5p in rheumatoid arthritis. EBioMedicine 2019;50:408–20 S2352-3964(19)30773-X doi:10.1016/j.ebiom.2019.11.024.

[34] Tu J, Chen W, Fang Y, et al. PU.1 promotes development of rheumatoid arthritis via repressing FLT3 in macrophages and fibroblast-like synoviocytes. Ann Rheum Dis 2023;82:198–211. doi: 10.1136/ard-2022-222708.

[35] Glehr M, Breisach M, Walzer S, et al. The influence of resveratrol on the synovial expression of matrix metalloproteinases and receptor activator of NF-kappaB ligand in rheumatoid arthritis fibroblast-like synoviocytes. Z Naturforsch C J Biosci 2013;68:336–42. doi: 10.5560/ZNC.2013.68c0336.

[36] Hu Z, Chen J, Wang M, et al. Rheumatoid arthritis fibroblast-like synoviocytes maintain tumor-like biological characteristics through ciRS-7-dependent regulation of miR-7. Mol Biol Rep 2022;49:8473–83. doi: 10.1007/s11033-022-07666-w.

[37] Lee S, Choi E, Chae S, et al. Identification of MYH9 as a key regulator for synoviocyte migration and invasion through secretome profiling. Ann Rheum Dis 2023;82:1035–48. doi: 10.1136/ard-2022-223625.

[38] Tolboom TCA, Pieterman E, van der Laan WH, et al. Invasive properties of fibroblast-like synoviocytes: correlation with growth characteristics and expression of MMP-1, MMP-3, and MMP-10. Ann Rheum Dis 2002;61:975–80. doi: 10.1136/ard.61.11.975.

[39] Zhao J, Ouyang Q, Hu Z, et al. A protocol for the culture and isolation of murine synovial fibroblasts. Biomed Rep 2016;5:171–5. doi: 10.3892/br.2016.708.

[40] Yang Y, Dong Q, Li R. Matrine induces the apoptosis of fibroblast-like synoviocytes derived from rats with collagen-induced arthritis by suppressing the activation of the JAK/STAT signaling pathway. Int J Mol Med 2017;39:307–16. doi: 10.3892/ijmm.2016.2843.

[41] Jia W, Yao Z, Zhao J, et al. New perspectives of physiological and pathological functions of nucleolin (NCL). Life Sci 2017;186:1–10. doi: 10.1016/j.lfs.2017.07.025.

[42] Shinji S, Umezawa K, Nihashi Y, et al. Identification of the Myogenetic Oligodeoxynucleotides (myoDNs) That Promote Differentiation of Skeletal Muscle Myoblasts by Targeting Nucleolin. Front Cell Dev Biol 2020;8:616706. doi: 10.3389/fcell.2020.616706.

[43] Farin K, Di Segni A, Mor A, et al. Structure-function analysis of nucleolin and ErbB receptors interactions. PLoS ONE 2009;4:e6128. doi: 10.1371/journal.pone.0006128.

[44] Rennick JJ, Johnston APR, Parton RG. Key principles and methods for studying the endocytosis of biological and nanoparticle therapeutics. Nat Nanotechnol 2021;16:266–76. doi: 10.1038/s41565-021-00858-8.

[45] Yoon S, Rossi JJ. Aptamers: uptake mechanisms and intracellular applications. Adv Drug Deliv Rev 2018;134:22–35. doi: 10.1016/j.addr.2018.07.003.

[46] Jin M, Park J, Lee S, et al. Hantaan Virus Enters Cells by Clathrin-Dependent Receptor-Mediated Endocytosis. Virol (Auckl) 2002;294:60–9. doi: 10.1006/viro.2001.1303.

[47] Wu Y, Lin B, Lu Y, et al. Frontispiece: aptamer−LYTACs for Targeted Degradation of Extracellular and Membrane Proteins. Angew Chem Int Ed 2023;62. doi: 10.1002/anie.202381561.

[48] Iturriaga-Goyon E, Vivanco-Rojas O, Magaña-Guerrero FS, et al. AS1411 Nucleolin-Specific Binding Aptamers Reduce Pathological Angiogenesis through Inhibition of Nucleolin Phosphorylation. Int J Mol Sci 2021;22:13150. doi: 10.3390/ijms222313150.

[49] Zhang L, Li L, Wang X, et al. Development of a novel PROTAC using the nucleic acid aptamer as a targeting ligand for tumor selective degradation of nucleolin. Mol Ther Nucleic Acids 2022;30:66–79. doi: 10.1016/j.omtn.2022.09.008.
[50] Shum KT, Zhou J, Rossi JJ. Nucleic Acid Aptamers as Potential Therapeutic and Diagnostic Agents for Lymphoma. J Cancer Ther 2013;4:872–90. doi: 10.4236/jct.2013.44099.
[51] Nimjee SM, White RR, Becker RC, et al. Aptamers as Therapeutics. Annu Rev Pharmacol Toxicol 2017;57:61–79. doi: 10.1146/annurev-pharmtox-010716-104558.
[52] Malik MT, O'Toole MG, Casson LK, et al. AS1411-conjugated gold nanospheres and their potential for breast cancer therapy. Oncotarget 2015;6:22270–81. doi: 10.18632/oncotarget.4207.
[53] Yamamoto M, Miyoshi M, Morioka K, et al. Anti-nucleolin aptamer, iSN04, inhibits the inflammatory responses in C2C12 myoblasts by modulating the β-catenin/NF-κB signaling pathway. Biochem Biophys Res Commun 2023;664:1–8. doi: 10.1016/j.bbrc.2023.04.098.
[54] Kamei D, Yamakawa K, Takegoshi Y, et al. Reduced pain hypersensitivity and inflammation in mice lacking microsomal prostaglandin e synthase-1. J Biol Chem 2004;279:33684–95. doi: 10.1074/jbc.M400199200.
[55] Tu M, Yang M, Yu N, et al. Inhibition of cyclooxygenase-2 activity in subchondral bone modifies a subtype of osteoarthritis. Bone Res 2019;7:29. doi: 10.1038/s41413-019-0071-x.
[56] Sanchez-Lopez E, Coras R, Torres A, et al. Synovial inflammation in osteoarthritis progression. Nat Rev Rheumatol 2022;18:258–75. doi: 10.1038/s41584-022-00749-9.
[57] Hügle T, Geurts J. What drives osteoarthritis?-synovial versus subchondral bone pathology. Rheumatol (Oxford) 2017;56:1461–71. doi: 10.1093/rheumatology/kew389.
[58] Mathiessen A, Conaghan PG. Synovitis in osteoarthritis: current understanding with therapeutic implications. Arthritis Res Ther 2017;19:18. doi: 10.1186/s13075-017-1229-9.
[59] Han D, Fang Y, Tan X, et al. The emerging role of fibroblast-like synoviocytes-mediated synovitis in osteoarthritis: an update. J Cell Mol Med 2020;24:9518–32. doi: 10.1111/jcmm.15669.
[60] Mousavi MJ, Karami J, Aslani S, et al. Transformation of fibroblast-like synoviocytes in rheumatoid arthritis; from a friend to foe. Auto Immun Highlights 2021;12:3. doi: 10.1186/s13317-020-00145-x.
[61] Bartok B, Firestein GS. Fibroblast-like synoviocytes: key effector cells in rheumatoid arthritis. Immunol Rev 2010;233:233–55. doi: 10.1111/j.0105-2896.2009.00859.x.
[62] Kratofil RM, Kubes P, Deniset JF. Monocyte Conversion During Inflammation and Injury. Arterioscler Thromb Vasc Biol 2017;37:35–42. doi: 10.1161/ATVBAHA.116.308198.
[63] Wolf AA, Yáñez A, Barman PK, et al. The Ontogeny of Monocyte Subsets. Front Immunol 2019;10:1642. doi: 10.3389/fimmu.2019.01642.
[64] Mizoguchi T, Ono N. The diverse origin of bone-forming osteoblasts. J Bone Miner Res 2021;36:1432–47. doi: 10.1002/jbmr.4410.
[65] Brignole C, Bensa V, Fonseca NA, et al. Cell surface Nucleolin represents a novel cellular target for neuroblastoma therapy. J Exp Clin Cancer Res 2021;40:180. doi: 10.1186/s13046-021-01993-9.
[66] Hovanessian AG, Soundaramourty C, El Khoury D, et al. Surface expressed nucleolin is constantly induced in tumor cells to mediate calcium-dependent ligand internalization. PLoS ONE 2010;5:e15787. doi: 10.1371/journal.pone.0015787.
[67] Li H, Liu J, Xiao X, et al. A Novel Aptamer LL4A Specifically Targets Vemurafenib-Resistant Melanoma through Binding to the CD63 Protein. Mol Ther Nucleic Acids 2019;18:727–38. doi: 10.1016/j.omtn.2019.10.005.
[68] Kelly L, Maier KE, Yan A, et al. A comparative analysis of cell surface targeting aptamers. Nat Commun 2021;12:6275. doi: 10.1038/s41467-021-26463-w.
[69] Mahlknecht G, Maron R, Mancini M, et al. Aptamer to ErbB-2/HER2 enhances degradation of the target and inhibits tumorigenic growth. Proc Natl Acad Sci U S A 2013;110:8170–5. doi: 10.1073/pnas.1302594110.
[70] MacDonald IJ, Huang CC, Liu SC, et al. Targeting CCN Proteins in Rheumatoid Arthritis and Osteoarthritis. Int J Mol Sci 2021;22:4340. doi: 10.3390/ijms22094340.
[71] Martel-Pelletier J, Barr AJ, Cicuttini FM, et al. Osteoarthritis. Nat Rev Dis Primers 2016;2:16072. doi: 10.1038/nrdp.2016.72.
[72] Nanus DE, Badoume A, Wijesinghe SN, et al. Synovial tissue from sites of joint pain in knee osteoarthritis patients exhibits a differential phenotype with distinct fibroblast subsets. EBioMedicine 2021;72:103618. doi: 10.1016/j.ebiom.2021.103618.
[73] Manfredi S. The 'old' cytotoxic drugs, the basis of anti-cancer treatments. Therapie 2022;77:251–5. doi: 10.1016/j.therap.2021.11.006.
[74] Brogan PA, Dillon MJ. The use of immunosuppressive and cytotoxic drugs in non-malignant disease. Arch Dis Child 2000;83:259–64. doi: 10.1136/adc.83.3.259.
[75] Muth CC. Chemotherapy and Hair Loss. JAMA 2017;317:656. doi: 10.1001/jama.2016.21266.
[76] Chari RVJ. Targeted cancer therapy: conferring specificity to cytotoxic drugs. Acc Chem Res 2008;41:98–107. doi: 10.1021/ar700108g.
[77] He L, Luan H, He J, et al. Shikonin attenuates rheumatoid arthritis by targeting SOCS1/JAK/STAT signaling pathway of fibroblast like synoviocytes. Chin Med 2021;16:96. doi: 10.1186/s13020-021-00510-6.
[78] Tsuchikama K, An Z. Antibody-drug conjugates: recent advances in conjugation and linker chemistries. Protein Cell 2018;9:33–46. doi: 10.1007/s13238-016-0323-0.
[79] Egli M, Manoharan M. Chemistry, structure and function of approved oligonucleotide therapeutics. Nucleic Acids Res 2023;51:2529–73. doi: 10.1093/nar/gkad067.
[80] Zhou X, Xie D, Huang J, et al. Therapeutic Effects of (5R)-5-Hydroxytriptolide on Fibroblast-Like Synoviocytes in Rheumatoid Arthritis via lncRNA WAKMAR2/miR-4478/E2F1/p53 Axis. Front Immunol 2021;12:605616. doi: 10.3389/fimmu.2021.605616.
[81] Wu J, Feng Z, Chen L, et al. TNF antagonist sensitizes synovial fibroblasts to ferroptotic cell death in collagen-induced arthritis mouse models. Nat Commun 2022;13:676. doi: 10.1038/s41467-021-27948-4.
[82] Wu G, Liu C, Cao B, et al. Connective tissue growth factor-targeting DNA aptamer suppresses pannus formation as diagnostics and therapeutics for rheumatoid arthritis. Front Immunol 2022;13:934061. doi: 10.3389/fimmu.2022.934061.
[83] Ueki R, Uchida S, Kanda N, et al. A chemically unmodified agonistic DNA with growth factor functionality for in vivo therapeutic application. Sci Adv 2020;6. doi: 10.1126/sciadv.aay2801.
[84] Hong P, Liu QW, Xie Y, et al. Echinatin suppresses esophageal cancer tumor growth and invasion through inducing AKT/mTOR-dependent autophagy and apoptosis. Cell Death Dis 2020;11:524. doi: 10.1038/s41419-020-2730-7.
[85] Little CB, Barai A, Burkhardt D, et al. Matrix metalloproteinase 13-deficient mice are resistant to osteoarthritic cartilage erosion but not chondrocyte hypertrophy or osteophyte development. Arthritis Rheum 2009;60:3723–33. doi: 10.1002/art.25002.
[86] Liang C, Li F, Wang L, et al. Tumor cell-targeted delivery of CRISPR/Cas9 by aptamer-functionalized lipopolymer for therapeutic genome editing of VEGFA in osteosarcoma. Biomaterials 2017;147:68–85. doi: 10.1016/j.biomaterials.2017.09.015.
[87] Sun X, Xie L, Qiu S, et al. Elucidation of CKAP4-remodeled cell mechanics in driving metastasis of bladder cancer through aptamer-based target discovery. Proc Natl Acad Sci U S A 2022;119. doi: 10.1073/pnas.2110500119.
[88] Nahlé S, Quirion L, Boulais J, et al. Defining the interactomes of proteins involved in cytoskeletal dynamics using high-throughput proximity-dependent biotinylation in cellulo. STAR Protoc 2022;3:101075. doi: 10.1016/j.xpro.2021.101075.
[89] Guan M, Qu L, Tan W, et al. Hepatocyte nuclear factor-4 alpha regulates liver triglyceride metabolism in part through secreted phospholipase A_2 GXIIB. Hepatology 2011;53:458–66. doi: 10.1002/hep.24066.
[90] Su J, Liang H, Yao W, et al. MiR-143 and MiR-145 regulate IGF1R to suppress cell proliferation in colorectal cancer. PLoS ONE 2014;9:e114420. doi: 10.1371/journal.pone.0114420.
[91] Li H, Handsaker B, Wysoker A, et al. The Sequence Alignment/Map format and SAMtools. Bioinformatics 2009;25:2078–9. doi: 10.1093/bioinformatics/btp352.
[92] Liao Y, Smyth GK, Shi W. featureCounts: an efficient general purpose program for assigning sequence reads to genomic features. Bioinformatics 2014;30:923–30. doi: 10.1093/bioinformatics/btt656.
[93] Love MI, Huber W, Anders S. Moderated estimation of fold change and dispersion for rna-seq data with deseq2. Genome biology 2014 [Preprint] doi:10.1101/002832.
[94] Gene Ontology C. Gene Ontology Consortium: going forward. Nucleic Acids Res 2015;43:D1049–56. doi: 10.1093/nar/gku1179.
[95] Kanehisa M, Goto S. KEGG: kyoto encyclopedia of genes and genomes. Nucleic Acids Res 2000;28:27–30. doi: 10.1093/nar/28.1.27.
[96] Subramanian A, Tamayo P, Mootha VK, et al. Gene set enrichment analysis: a knowledge-based approach for interpreting genome-wide expression profiles. Proc Natl Acad Sci U S A 2005;102:15545–50. doi: 10.1073/pnas.0506580102.
[97] Guo Q, Zheng K, Fan D, et al. Wu-Tou Decoction in Rheumatoid Arthritis: integrating Network Pharmacology and In Vivo Pharmacological Evaluation. Front Pharmacol 2017;8:230. doi: 10.3389/fphar.2017.00230.

[98] Liang C, Li J, Lu C, et al. HIF1α inhibition facilitates Leflunomide-AHR-CRP signaling to attenuate bone erosion in CRP-aberrant rheumatoid arthritis. Nat Commun 2019;10:4579. doi: 10.1038/s41467-019-12163-z.

[99] Wu X, Lai Y, Chen S, et al. Kindlin-2 preserves integrity of the articular cartilage to protect against osteoarthritis. Nat Aging 2022;2:332–47. doi: 10.1038/s43587-021-00165-w.

[100] Liu Y, Peng C, Zhang H, et al. DNA aptamer S11e recognizes fibrosarcoma and acts as a tumor suppressor. Bioact Mater 2022;12:278–91. doi: 10.1016/j.bioactmat.2021.10.011.

[101] Li F, Lu J, Liu J, et al. A water-soluble nucleolin aptamer-paclitaxel conjugate for tumor-specific targeting in ovarian cancer. Nat Commun 2017;8:1390. doi: 10.1038/s41467-017-01565-6.

Ann Rheum Dis 84 (2025) 746−759

Contents lists available at ScienceDirect

Annals of the Rheumatic Diseases

journal homepage: https://www.sciencedirect.com/journal/annals-of-the-rheumatic-diseases

Sjögren's syndrome

m6A RNA methylation controls salivary gland epithelial cell function and has a protective role in Sjögren's disease

Frederic Truffinet[1,a], Alejandro Arco-Hierves[1,2,a], Hosnia Shalabi[1], Juliette Pascaud[1], Paul Mazet[1], Elodie Rivière[3], Sacha E. Silva-Saffar[1], Lucilla Fabbri[4,5], Sophie Leboucher[6], Laetitia Besse[7], Cedric Messaoudi[7], Aurore Attina[8], Alexandre David[8,9], Stephan Vagner[4,5], Gaetane Nocturne[1,10], Xavier Mariette[1,10], Rami Bechara[1,*]

[1] *Université Paris-Saclay, Inserm, CEA, Center for Immunology of Viral, Auto-immune, Hematological and Bacterial diseases (IMVA-HB/IDMIT), Inserm U1184, Le Kremlin-Bicetre, France*

[2] *Fondation Arthritis, Neuilly Sur Seine, France*

[3] *UMR 1125, Sorbonne Paris Nord University, AP-HP, GHUPSSD, Department of Rheumatology, INSERM, Bobigny, France*

[4] *Institut Curie, PSL Research University, CNRS UMR 3348, INSERM U1278, Orsay, France*

[5] *Université Paris-Saclay, CNRS UMR 3348, INSERM U1278, Orsay, France*

[6] *Histology Platform, Institut Curie, PSL Research University, Université Paris-Saclay, Orsay, France*

[7] *Multimodal Imaging Center, Institut Curie, CNRS UAR2016, INSERM US43, PSL Research University, Université Paris-Saclay, Orsay, France*

[8] *PPC, IRBM, INM, Univ Montpellier, CHU Montpellier, INSERM CNRS, Montpellier, France*

[9] *IRCM, Univ Montpellier, ICM, INSERM, Montpellier, France*

[10] *Hôpitaux de Paris, Hôpital Bicêtre, Department of Rheumatology, APHP, Le Kremlin Bicêtre, France*

ARTICLE INFO

Article history:
Received 5 June 2024
Accepted 23 August 2024

Keywords:
Autoimmune Diseases
Cytokines
Inflammation
Sjogren's Syndrome
Autoimmunity

ABSTRACT

Objectives: The RNA epitranscriptomic modification known as *N6*-methyladenosine (m^{6}A) represents a novel mechanism of gene regulation that is poorly understood in human autoimmune diseases. Our research explores the role of this RNA m^{6}A modification in salivary gland epithelial cells (SGEC) and its impact on the pathogenesis of Sjögren's disease (SjD).

Methods: SGECs from SjD patients and controls were analysed for m^{6}A writers METTL3 and METTL14 expression using RNA-seq, quantitative PCR and immunohistochemistry. Functional assays assessed the impact of *METTL3* knockdown or pharmacological inhibition on proinflammatory gene expression and immune cell interactions (using transwell and coculture systems). Mechanistic studies examined METTL3-mediated m^{6}A modifications in double-stranded RNA (dsRNA) formation through immunofluorescence. Unsupervised clustering identified patterns of interferon activation in salivary glands and their correlation with m^{6}A writers.

Results: METTL3 and METTL14 were elevated in SGEC from SjD patients in comparison to controls. Paradoxically, inhibiting METTL3 increased proinflammatory gene expression, enhancing SGEC's ability to attract immune cells and activate B cells. Conversely, inhibiting the eraser FTO had the opposite effect. METTL3-mediated m^{6}A modifications prevented dsRNA formation and

* **Correspondence to** Dr. Rami Bechara.

E-mail address: rami.bechara@universite-paris-saclay.fr (R. Bechara).

Handling editor Josef S. Smolen.

FT and AA-H contributed equally.

[a] Co-first authors.

https://doi.org/10.1136/ard-2024-226224

IFN signalling activation. SGEC from SjD showed insufficient *METTL3* upregulation compared with controls in response to inflammatory triggers, indicating a limited capacity to regulate the inflammatory response. SjD patients with elevated disease activity and higher interferon signature exhibit reduced *METTL3* expression.

Conclusions: Impairment of m^{6}A modifications in SGEC in response to inflammatory triggers favour the formation of dsRNA, potentially amplifying the interferon loop and contributing to SjD pathogenesis.

WHAT IS ALREADY KNOWN ON THIS TOPIC

- Salivary gland epithelial cells (SGECs) play a pivotal role in the pathogenesis of Sjögren's disease (SjD), acting as both targets of autoimmunity and contributors to inflammatory responses.
- Recent research has shed light on the importance of post-transcriptional mRNA modifications, specifically *N6*-methyladenosine (m^{6}A) RNA methylation, in gene regulation. However, the involvement of RNA m^{6}A modifications in SGEC function and in human autoimmune diseases, particularly SjD pathology, was previously unexplored.

WHAT THIS STUDY ADDS

- The m^{6}A RNA methylation pathway serves as a negative feedback mechanism on Poly(I:C) and interferon signalling in SGECs, thus limiting excessive inflammation in salivary glands.
- METTL3 deficiency in SGEC during inflammation results in abnormal production of endogenous double-stranded RNA, contributing to SjD pathogenesis.
- SjD patients exhibit insufficient upregulation of *METTL3* in SGEC in response to inflammatory triggers, indicating a limited capacity to regulate the inflammatory response.
- SjD patients with elevated disease activity and high IFN signature show reduced expression of *METTL3*, indicating its potential as a biomarker for disease prognosis and stratification.

HOW THIS STUDY MIGHT AFFECT RESEARCH, PRACTICE OR POLICY

- Understanding how m^{6}A modifications impact SGEC function may pave the way for the development of targeted therapies for SjD, focusing on maintaining SGEC integrity, decreasing the crosstalk between SGEC and immune cells and enhancing salivary gland function.
- The expression levels of m^{6}A writers could serve as valuable biomarkers for predicting disease prognosis and stratifying SjD patients.

INTRODUCTION

Sjögren's disease (SjD) is a prototypic systemic autoimmune disease affecting 0.1% of the population and characterised by the dysfunction of salivary and lachrymal glands, along with numerous systemic complications [1,2]. Although this process is mediated by autoreactive B and T cells, proinflammatory triggers maintain a feed-forward process that sustains inflammation, resulting in gland hypofunction and pathology [1,3−8]. Therefore, understanding the mechanisms that drive abnormal immune cell responses is essential to develop the next generation of therapeutics and interventions. The salivary gland epithelial cells (SGECs) are an important—yet still not well understood—contributor to B cell and T cell activation and SjD pathology [3,9].

Several lines of evidence support that SGEC are not only the target of autoimmunity but may also play an active role in SjD pathogenesis [10]. First, SGECs express a plethora of immune receptors, which activation by immune triggers causes the upregulation of chemokines and cytokines implicated in immune cell recruitment and activation [8 10−15]. Of those, CXCL10 and IL-7 maintain SGEC-T cell crosstalk [3,9,16−19] and BAFF, encoded by *TNFSF13B*, participates in B cell activation [6,9,20−22]. Production of these molecules is highly dependent on the expression of type I and type II Interferons (IFNs) [1,7,23,24]. Indeed, SGECs from SjD patients are characterised by a dominant IFN signature [4,23,25] and a high responsiveness to TLR3 signalling [26]. Moreover, SGECs express costimulatory molecules [27,28] and may present autoantigen to immune cells [29,30]. Expression of these costimulatory molecules is further upregulated by cytokines derived from immune cells [13,28]. Last, SGEC's continuous activation by environmental triggers, cytokines or immune complexes, leads to the expression of pro-apoptotic proteins (eg, Fas receptor), causing tissue damage [31−35]. Unless interrupted, this vicious circle drives persistent inflammation, SGEC damage and gland hypofunction [10]. Hence, targeting a regulator of proinflammatory signalling pathways is in principle an effective strategy to limit SGEC damage. Achieving this goal will require a better understanding of the molecular pathways and mechanisms that promote proinflammatory trigger-induced SGEC activation.

From the initial sensing of immune insults by SGEC, through the upregulation of IFN-gene signature and resolution of inflammation, each step of immune signalling is rigorously regulated. Whereas regulation at the level of gene transcription is well established, post-transcriptional control of mRNA is also a vital component in the regulation of immune responses [36]. As such, proper regulation of RNA is crucial for maintaining a coordinated immune response. Recently, several immune mRNAs were shown to carry a methylation at the *N6* position of adenosine, *N6*-methyladenosine (m^{6}A) modifications [37−42]. m^{6}A is added to specific RNA by methyltransferase enzymes termed 'writers' (eg, METTL3, METTL14). METTL3 acts as the catalytic component, directly catalysing the methylation of the adenosine base at the m^{6}A site. METTL14 while not directly involved in the catalytic process, plays a crucial role in the complex by stabilising METTL3 and enhancing the specificity and efficiency of the m^{6}A methylation process. This modification can be reversed by demethylases 'erasers' (eg, FTO (Fat mass and obesity-associated protein), ALKBH5). Diverse 'readers' (proteins of the YTH domains or IGF2BP family) can bind to m^{6}A directly or to sequence structures influenced by this modification. The consequences of m^{6}A marks are myriad, impacting RNA stabilisation, translation, etc [43]. However, the immunological ramifications of these m^{6}A marks have been largely overlooked, and to date, nothing is known regarding the role of m^{6}A machinery in SGEC function. Therefore, this study aims to dissect the role of RNA m^{6}A modifications in influencing SGEC response to inflammation and SjD pathogenesis.

METHODS

Patients

Minor salivary gland (MSG) biopsies were obtained from consecutive patients referred for suspected SjD to the Rheumatology

Table 1
Characteristics of the patients included in the study

	SjD (n = 38)	Control (n = 50)
Median age (min–max)	50 (22–78)	54 (26–81)
Female sex, n (%)	36 (95)	48 (96)
Pathological Schirmer, n (%)*	25 (65.7)	20 (40)
Pathological salivary flow, n (%)†	12 (31.5)	15 (30)
Focus score ≥1, n (%)	26 (68.4)	0 (0)
Anti-SSA +, n (%)	27 (71)	0 (0)

SJD, Sjögren's disease.
* Pathological Schirmer: result ⩽ 5 mm in 5 min.
† Pathological salivary flow: salivary flow ⩽ 0.10 mL/min.

Department of Bicêtre Hospital, a tertiary reference centre for systemic autoimmune diseases. SjD was defined according to the 2016 American College of Rheumatology/European League Against Rheumatism criteria, and controls were patients presenting sicca symptoms without anti-Ro/SSA (Sjögren's syndrome-related antigen A) or anti-La/SSB antibodies and with normal or subnormal MSGs (eg, focus score of <1). MSG biopsies were used for immunohistochemistry (IHC), quantitative PCR (qPCR) analysis of sorted cells, m^6A quantification, two-dimensional cell culture and coculture experiments. The characteristics of the patients and controls included in the study are presented in table 1. Epithelial cell isolation and sorting as well as culture, stimulation and transfection are detailed in online supplemental materials. Patients or the public were not involved in the design, conduct, reporting or dissemination plans of our research.

Western blotting analysis

Immunoblots were performed from whole cell lysate of cells prepared using RIPA buffer (Thermo Fisher Scientific) supplemented with protease and phosphatase inhibitors (Roche). Protein samples were resolved on NuPAGE 4%–12% Bis-Tris gels with MOPS buffer (Thermo Fisher Scientific) and then transferred to 0.45 µm nitrocellulose membrane (Thermo Fisher Scientific). After saturation in Tris-buffered saline buffer supplemented with 5% powdered milk, the membranes were incubated with antibodies overnight at 4°C with agitations.

Incucyte live imaging

Cells were seeded into 96-well plates. After 24 hours, cells were treated with STM2457 at 1 µM or 10 µM or with DMSO, in triplicates. Cell proliferation, measured by the percentage of cell confluence, was continuously imaged on an IncuCyte videomicroscope system for the indicated time.

Nucleoside modification analysis by liquid chromatography–mass spectrometry

200 nanograms of RNA were decapped with 5 U of RppH (New England Biolabs) for 2 hours at 37 °C and were subsequently digested to single nucleotides with 1 U of Nuclease P1 (Sigma) for 2 hours at 42 °C. Nucleotides were then dephosphorylated into nucleosides with 1 U of Alkaline phosphatase (AP) for 2 hours at 37 °C. The sample was filtered (0.22 µm pore size, 4 mm diameter, Millipore) and 10 µL of the solution was analysed by liquid chromatography–mass spectrometry (LC-MS/MS).

Isolation of B cells for coculture experiments

Peripheral mononuclear cells were isolated from residual blood of apheresis from healthy subjects (French blood donors) by Ficoll gradient separation. B lymphocytes were isolated by CD19 magnetic bead positive selection according to the manufacturer's instructions (CD19 Microbeads human and Fc-Block, Miltenyi Biotec) to achieve a purity of greater than 80% as assessed by FACS analysis (percentage of $CD20^+$ cells).

SGECs and B cell cocultures

SGECs were pretreated or not with STM2457 or FB23-2 at 10 µM for 16 hours before being washed and cocultured with allogeneic B cells for 5 days. B cells, either cultured alone or in conjunction with SGECs, were cultured in 2 mL RPMI-1640 supplemented with 10% heat-inactivated fetal bovine serum and 1X penicillin-streptomycin. Additionally, Poly(I:C) at a concentration of 10 µg/mL was added to the medium where indicated. After 5 days of coculture, B cells were harvested for immunostaining and flow cytometry analysis.

Transwell-based chemotaxis assay

SGECs were pretreated with DMSO or STM2457 at 10 µM for 16 hours then stimulated with Poly(I:C) at 10 µg/mL for 6 hours. Transwell assays were performed with 5 µm pore-sized inserts (10107341; Inserts in 24-well plates, Fisher Scientific). PBMCs were placed in the upper chamber, and SGECs in the lower compartment in 0.6 mL of RPMI-1640 supplemented with 10% heat-inactivated fetal bovine serum, and penicillin-streptomycin (1X). After 16 hours, cells were harvested for immunostaining.

qPCR and RNAseq

RNA from MSG was isolated with NucleoSpin RNA Plus (Macherey Nagel). RNA from SGEC was isolated with QIAshredder columns (Qiagen) and GeneJET RNA purification kit (ThermoScientific). Complementary DNA was synthesised by RT^2 First Strand kit (Qiagen). Real-time qPCR was performed with SYBR Green FastMix ROX (BioRad) on a CFX (BioRad), normalised to Gapdh. Primers were from QuantiTect Primer Assays or RT2 qPCR primer assay (QIAGEN). RNASeq and bioinformatic analysis are detailed in online supplemental materials.

IHC, immunofluorescence and double-stranded RNA staining

Slides were incubated with primary antibodies for METTL3, METTL14 and EpCAM overnight at 4°C. Biotinylated IgG (H + L) and ImmPRESS-AP Polymer IgG are used as secondary antibodies, and the visualisation is done using an HRP-conjugated ABC system with DAB as the chromogen. Red AP Substrate Kit (Vector Labs SK-5100) is used for detection. Finally, the sections are counterstained with haematoxylin and mounted with an aqueous mounting medium. Cells grown coverslips were fixed with 4% PFA then permeabilised with 0.5% Triton X for 10 min and stained with the double-stranded RNA (dsRNA)-specific antibody J2 (Jena Bioscience), according to the supplier's recommendations.

Quantification of cytokine production

Human CXCL10 ELISA assays were performed on culture supernatants of SGEC and measured in duplicate, according to the manufacturer's instructions (R&D Systems, Minneapolis). CXCL9, CXCL11, APRIL and IFNβ were quantified using MSD multiplex assay, following manufacturer's instructions (Meso Scale Discovery, Gaithersburg, Maryland, USA).

Statistics

One-way analysis of variance with post hoc Tukey's analysis or Student's t-test was used to assess statistical significance, with $p<0.05$ considered significant. Data were analysed on Graphpad Prism. Each symbol represents one donor unless indicated. *p<0.05, **<0.01, ***<0.001, ****<0.0001.

RESULTS

The m^{6}A writers METTL3 and METTL14 are increased in SGEC from SjD

To assess whether m^{6}A regulators were differentially expressed in SGEC from SjD patients versus controls, we retrieved RNA-seq data from SGEC that were sorted from MSG biopsies of 5 SjD patients and four controls [9]. We noticed a significant increase in *METTL14* expression (component of the m^{6}A writer complex) among the differentially expressed genes between SjD and controls (figure 1A,B). This finding was further validated by qPCR performed on SGEC-sorted cells (figure 1C).

While *METTL3* mRNA levels were not significantly different between the two groups (figure 1A−C), our IHC analysis on MSG biopsies revealed an increased number of METTL3$^+$ EpCAM$^+$ cells and METTL14$^+$ EpCAM$^+$ in the salivary glands (SGs) of SjD patients compared with controls (figure 1D,E). Furthermore, flow cytometry on dissociated SGs confirmed that EpCAM+cells from SjD patients express higher levels of METTL3 protein compared with controls (figure 1F; online supplemental figure S1). The discrepancy between *METTL3* mRNA and protein levels might be due to post-transcriptional regulatory mechanisms that influence protein stability, translation efficiency or degradation rates, which are not reflected in mRNA expression alone. In addition, we found a modest enrichment in m^{6}A modification in RNAs purified from MSG of SjD versus controls (figure 1G). While the low input material limited our ability to conduct more extensive analyses, these findings still provide valuable insights. Of note, we did not observe any differences in other RNA-related modifications, such as 2′-O-methylcytosine, 2′-O-methyladenosine and 2′-O-methylguanosine (figure 1G).

METTL3 and METTL14 inhibit CXCL10 expression in SGEC, counteracted by FTO

The impact of m^{6}A methyltransferases on SGEC response to proinflammatory stimuli remains unexplored. To elucidate the biological roles of METTL3 and METTL14 in this context, we transduced SGEC with lentivirus-expressing shRNAs targeting these two enzymes. Our investigation focused on examining the effects of *METTL3* and *METTL14* depletion on Poly(I:C) or IFN-stimulated SGEC. These two stimuli were chosen considering the elevated IFN levels in SjD and the shared transcriptomic signatures between Poly(I:C)-activated SGEC and SjD glands, characterised by an increase in *CXCL10* expression (online supplemental figure S2). Knockdown of *METTL3* and *METTL14* was efficient (figure 2A) and led to Poly(I:C) or IFNα/γ-mediated upregulation of *CXCL10* expression (figure 2B; online supplemental figure S3A).

To ascertain whether this effect was mediated by the m^{6}A catalytic activity of METTL3, we employed a pharmacological inhibitor targeting its catalytic function, STM2457. While we used STM2457 at non-toxic concentration (online supplemental figure S3B), the proliferation of SGEC 48 hours post-treatment was decreased in a concentration-dependent manner (online supplemental figure S3C). Inhibition of METTL3 catalytic activity led to a dose-dependent increase in Poly(I:C) or IFN-induced *CXCL10* expression, contrasting with the effects of STM2120, a structurally related molecule to STM2457, but 1000-fold less active (figure 2C; online supplemental figure S3D). Consistent results were observed at the protein level (figure 2D). While *METTL3* depletion increased *CXCL10* expression, inhibition of the FTO activity with FB23-2 led to the opposite effect, underscoring the dynamic nature as well as the importance of the m^{6}A pathway (figure 2E,F).

Given that SGECs primarily consist of acinar and ductal cells, we investigated the impact of METTL3 on proliferation and *CXCL10* expression in both cell types (online supplemental figure S3E,F). Our findings revealed a concentration-dependent reduction in proliferation in ductal cells (NS-SV-TT-DC) following METTL3 inhibition with STM2457 while no significant effect was observed in acinar cells (NS-SV-TT-AC) (online supplemental figure S3E). Additionally, loss of METTL3 catalytic activity resulted in increased *CXCL10* expression in both cell types (online supplemental figure S3F). These results highlight the crucial role of METTL3 catalytic function in sustaining ductal cell proliferation and inhibiting *CXCL10* expression in both acinar and ductal.

METTL3 inhibits SGEC-intrinsic interferon response

We next thought to understand the transcriptional impact of targeting the catalytic domain of METTL3 in SGEC. Therefore, we employed RNA sequencing to analyse the transcription response following Poly(I:C) stimulation in the presence or absence of STM2457. Comparison of unstimulated and Poly(I:C)-stimulated SGEC revealed the upregulation of numerous genes, predominantly established targets of IFN gene signalling (eg, *CXCL10, CXCL9, CXCL11, IFIT1, ISG15, TNFSF13B*) (figure 3A). Treatment of SGEC with STM2457 alone induced alterations of the transcriptome, which overlapped with the effects of Poly(I:C) treatment, suggesting that STM2457 induces a cellular state mimicking the Poly(I:C)-induced response (figure 3B). Additionally, Poly(I:C) treatment induced changes in the transcriptional response of SGEC pretreated with STM2457 (figure 3C). Specifically, inhibition of METTL3 augmented the upregulation of *CXCL10, CXCL9* and *CXCL11* (figure 3C) as well as boosted the antigen presenting capacity of SGEC evaluated by an increase in the expression of *CD86, HLA-DRA and HLA-DQA1* (online supplemental figure S3G). Differential gene expression and gene ontology analysis revealed that the predominant transcriptional programmes induced in Poly(I:C)-treated SGEC following METTL3 inhibition were associated with IFN and Jak-STAT signalling pathways (figure 3D). Real-time PCR analysis confirmed that inhibition of METTL3 with STM2457 or the second-generation METTL3 inhibitor, STM3006, markedly enhanced the Poly(I:C) or IFNα-mediated upregulation of selected target genes after 24 hours of stimulation (figure 3E; online supplemental figure S4A,B). Western blot analysis of interferon-stimulated genes (ISGs) confirmed increased IFN activation and ISGs such as IFIT1 and ISG15 in SGEC treated with METTL3 inhibitor (figure 3F). Furthermore, secretion of IFNβ, APRIL and the chemokines CXCL9 and CXCL11 was increased in

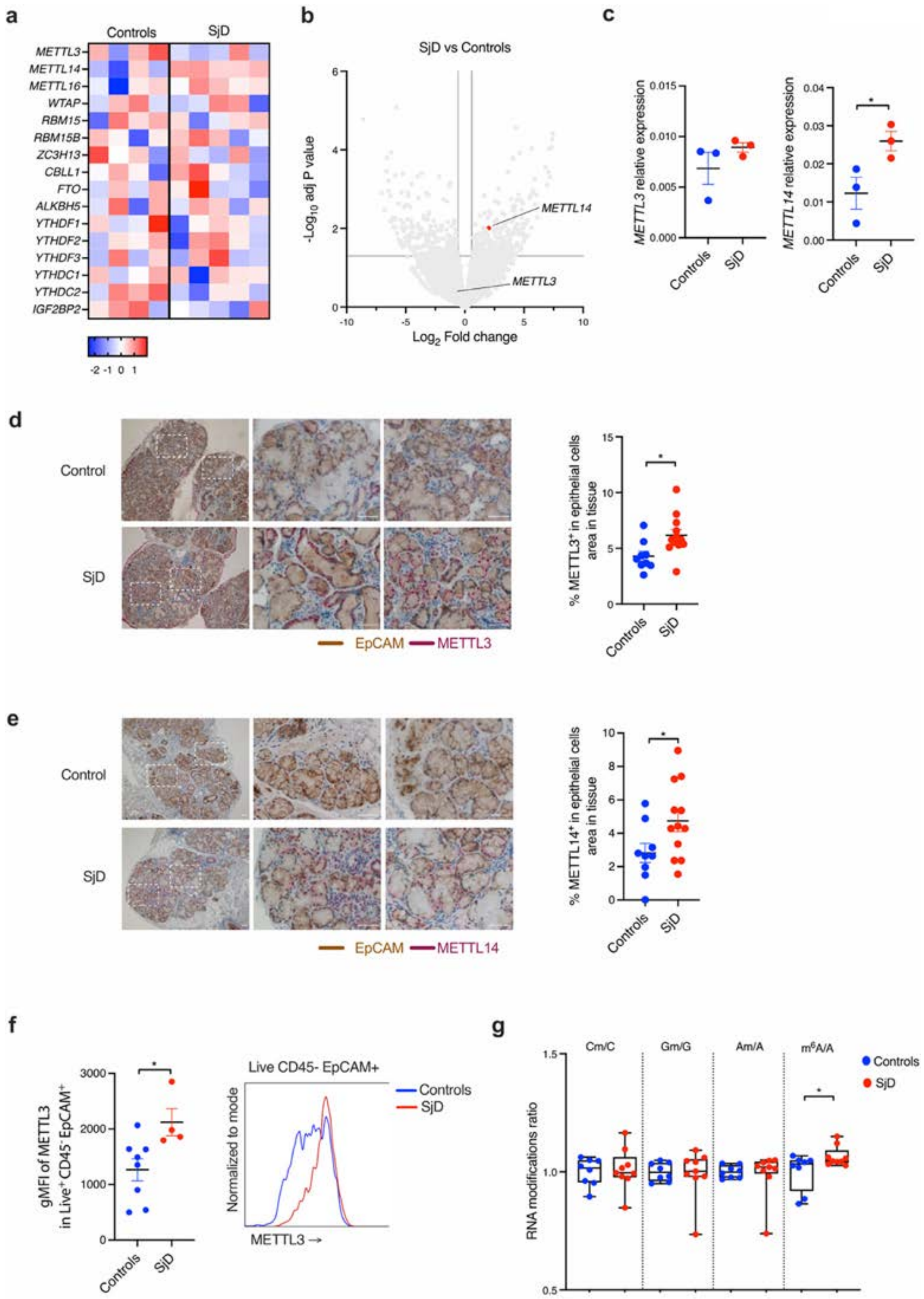

Figure 1. Levels of m^{6}A methyltransferases METTL3 and METTL14 are increased in SjD salivary gland epithelial cells. (A) RNA-seq was performed in Rivière *et al* [9]. Heatmap of the m^{6}A machinery extracted from sorted SGECs from SjD (n = 5) and controls (n = 4). (B) Volcano plots showing the transcriptional response of sorted SGEC in SjD versus controls. Cut-off for significance adj. p<0.05 and Log2FC of >0.58 or <−0.58. (C) Indicated mRNAs were assessed by qPCR in SGECs sorted from three SjD patients and three controls. Each symbol represents one individual. Data show relative expression±SEM. (D, E) Left: Representative images of IHC-stained MSG sections of control and SjD patients (scale 50 µm). Right: Slides were scored for METTL3 and METTL14 expression from SjD (n = 12) and controls (n = 9). Each symbol represents one individual. Bars show mean±SEM. (F) Salivary glands from SjD patients and control were enzymatically dissociated. The expression of METTL3 in Live CD45- EpCAM + cells was detected by flow cytometry. Each symbol represents one individual. Bars show mean±SEM. (G) Liquid chromatography−mass spectrometry (LC/MS-MS) nucleoside modification analysis. Total RNAs from MSG of SjD (n = 9) and controls (n = 8) were purified and were subjected to digestion. Samples were then subjected to LC/MS-MS quantification. Each type of RNA methylation was normalised to non-methylated nucleotide base (A or G or C). Each symbol represents one individual. *p<0.05, by unpaired t-test. A, adenosine; C, cytosine; G, guanosine; IHC, immunohistochemistry; mA, 2'-O-methyladenosine; m^{6}A: 6-methyladenosine; mC, 2′-O-methylcytosine; mG, 2′-O-methylguanosine; SGECs, salivary gland epithelial cells; SJD, Sjögren's disease.

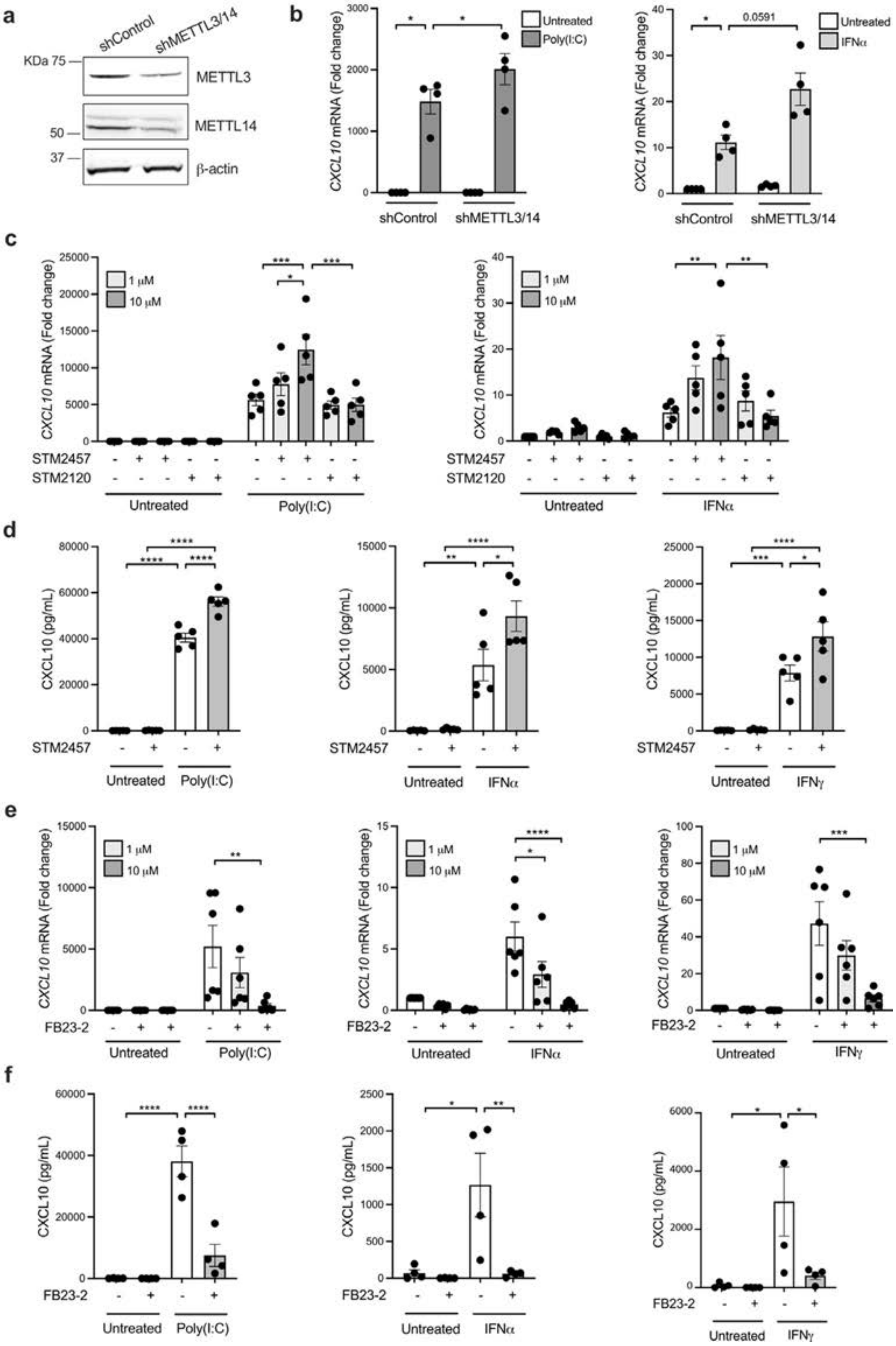

Figure 2. METTL3 and METTL14 inhibition enhances CXCL10 expression in SGEC, whereas FTO exerts the opposite effect. (A) SGECs were transfected with lentiviruses targeting *METTL3* and *METTL14* or scrambled control. METTL3, METTL14 and β-actin expression was assessed by WB. Data are shown as representative of three independent experiments. (B) SGECs were transfected with lentiviruses targeting *METTL3* and *METTL14* or scrambled control, treated±Poly(I:C) or IFNα for 24 hours and *CXCL10* assessed by qPCR. Data are normalised to untreated samples with control lentiviruses, from four independent experiments±SEM. (C) SGECs were pretreated with STM2457 or STM2120 for 6 hours, then stimulated±Poly(I:C) or IFNα for 24 hours and *CXCL10* was assessed by qPCR. Data are normalised to untreated samples, from five independent experiments±SEM. (D) SGECs were pretreated with STM2457 for 6 hours, then stimulated±Poly(I:C) or IFNα or IFNγ for 24 hours and CXCL10 in conditioned supernatants was assessed by ELISA. Data are shown as pg/mL±SEM from five independent experiments. (E) SGEC was pretreated with FB23-2 for 6 hours, then stimulated±Poly(I:C) or IFNα or IFNγ for 24 hours and *CXCL10* was assessed by qPCR. Data are normalised to untreated samples, from five independent experiments±SEM. (F) SGECs were pretreated with FB23-2 for 6 hours, then stimulated±Poly(I:C) or IFNα or IFNγ for 24 hours and CXCL10 in conditioned supernatants was assessed by ELISA. Data are shown as pg/mL±SEM from four independent experiments. *p<0.05, **p<0.01, ***p<0.001, ****p<0.0001 by ANOVA with post hoc Tukey's test. ANOVA, analysis of variance; qPCR, quantitative PCR; SGEC, salivary gland epithelial cell.

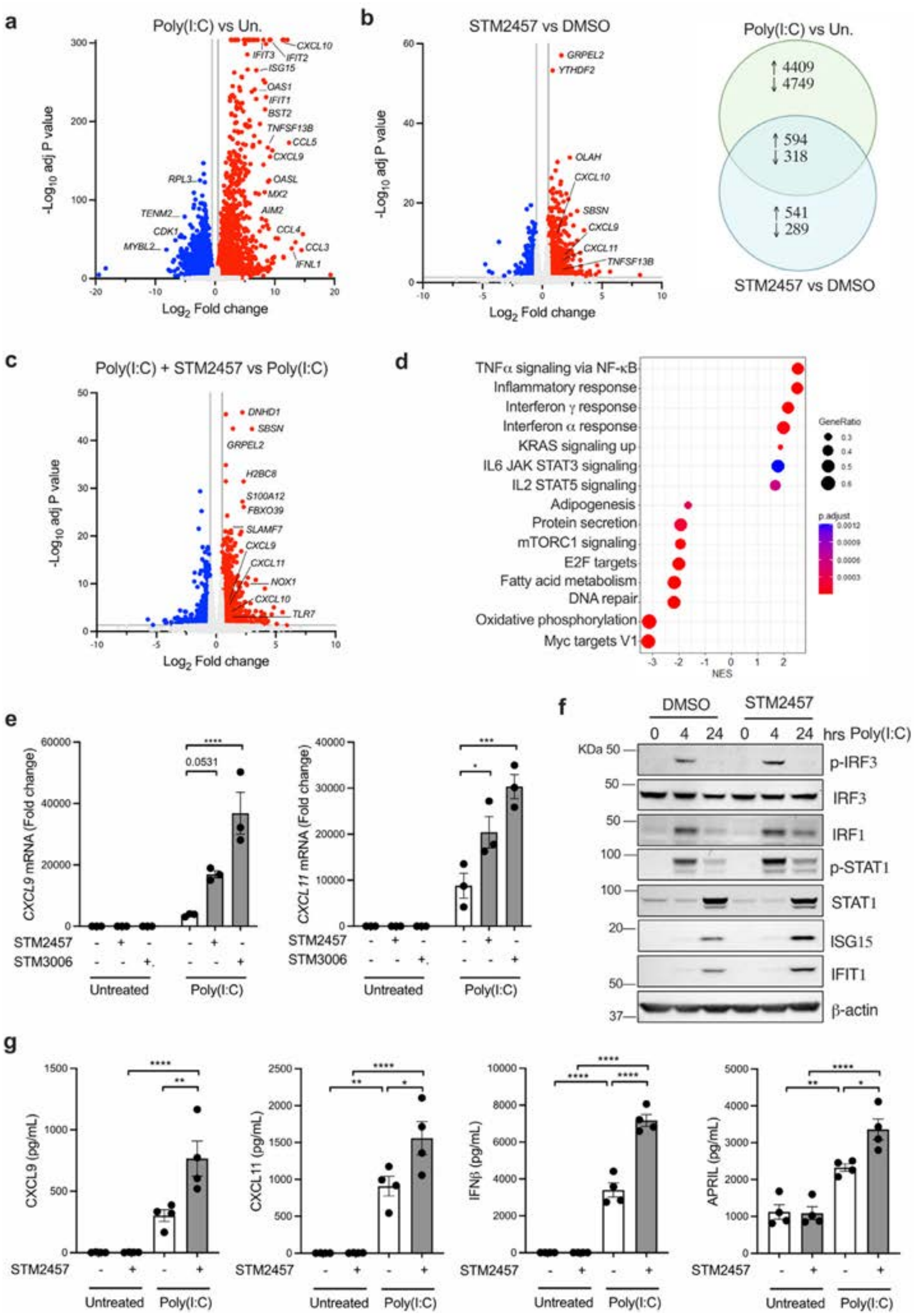

Figure 3. METTL3 inhibition induces an IFN signature in SGEC. (A) SGECs were pretreated with STM2457 for 6 hours, then stimulated±Poly(I:C) for 24 hours. RNA-seq (n = 4) was performed on the Illumina platform. Volcano plots showing the transcriptional response induced by Poly(I:C) versus untreated. In red and blue are selected transcripts that were significantly changed (adj. $p<0.05$ and Log2 FC>0.5 or <−0.5; based on four experiments). (B) Left, SGECs were pretreated with STM2457. RNA-seq (n = 4) was performed on the Illumina platform. Volcano plots showing the transcriptional response induced by STM2457 versus DMSO. In red and blue are selected transcripts that were significantly changed (adj. $p<0.05$ and Log2 FC>0.5 or <−0.5; based on four experiments). Right, Diagram indicates the intersection between transcripts that are differentially expressed in Poly(I:C) versus untreated in comparison to STM2457 versus DMSO. (C) SGECs were pretreated with STM2457 for 6 hours, then stimulated±Poly(I:C) for 24 hours. RNA-seq (n = 4) was performed on the Illumina platform. Volcano plots showing the transcriptional response induced by Poly(I:C)±STM2457. In red and blue are selected transcripts that were significantly changed (adj. $p<0.05$ and Log2 FC>0.5 or <−0.5; based on four experiments). (D) Gene set enrichment analysis of Poly(I:C) + STM2457 versus Poly(I:C). (E) SGECs were pretreated with STM2457 or STM3006 for 6 hours, then stimulated±Poly(I:C) and indicated transcripts were assessed by qPCR. Data are normalised to untreated samples, from three independent experiments±SEM. (F) SGECs were pretreated with STM2457 for 6 hours, then stimulated±Poly(I:C) for 24 hours. p-IRF3, IRF3, IRF1, p-STAT1, STAT1, ISG15, IFIT1 and β-actin were assessed in cell extracts by immunoblotting. Blots are representative of three independent experiments. (G) SGECs were pretreated with STM2457 for 6 hours, then stimulated±Poly(I:C) for 24 hours. CXCL9, CXCL11, IFNβ and APRIL in conditioned supernatants were assessed by MSD. Data are shown as pg/mL±SEM from four experiments. *$p<0.05$, **$p<0.01$, ***$p<0.001$, ****$p<0.0001$ by ANOVA with post hoc Tukey's test. ANOVA, analysis of variance; qPCR, quantitative PCR; SGEC, salivary gland epithelial cell.

SGEC treated with METTL3 inhibitor (figure 3G; online supplemental figure S4C). Altogether, these data demonstrated that METTL3 catalytic activity leads to the general inhibition of IFN transcriptional responses in SGEC.

METTL3 activity prevents dsRNA formation in SGEC

Recent investigations have demonstrated that mammalian cells may accumulate endogenous dsRNAs in instances where various cellular processes become dysregulated [44,45]. One notable mechanism underlying the formation of these immunogenic dsRNA structures involves the defective installation of m^6A modifications [44,45]. To ascertain whether METTL3-mediated m^6A modification prevents dsRNA formation, SGECs were pretreated with STM2457, followed by IFNα stimulation for 24 hours. Using the anti-J2 antibody (specific for dsRNA), we assessed dsRNA formation via immunofluorescence, confirming increased dsRNA formation on catalytic inhibition of METTL3, particularly notable on SGEC activation (figure 4A). Additionally, we observed increased dsRNA formation in NS-SV-TT-AC cells using flow cytometry when METTL3 was inhibited (figure 4B), consistent with previously published findings on these cell lines [44].

Recent reports have highlighted mitochondrial dysfunction and accumulation of mt-dsRNA in SjD patients [46]. To probe the role of mt-dsRNAs in STM2457-induced upregulation of *CXCL10*, we depleted mt-dsRNAs using 2 C′-methyladenosine (2 CM), an inhibitor of POLRMT. Pretreatment with 2 CM led to a significant decrease in *CXCL10* expression (figure 4C), suggesting that METTL3-mediated suppression of IFN responses partly involves

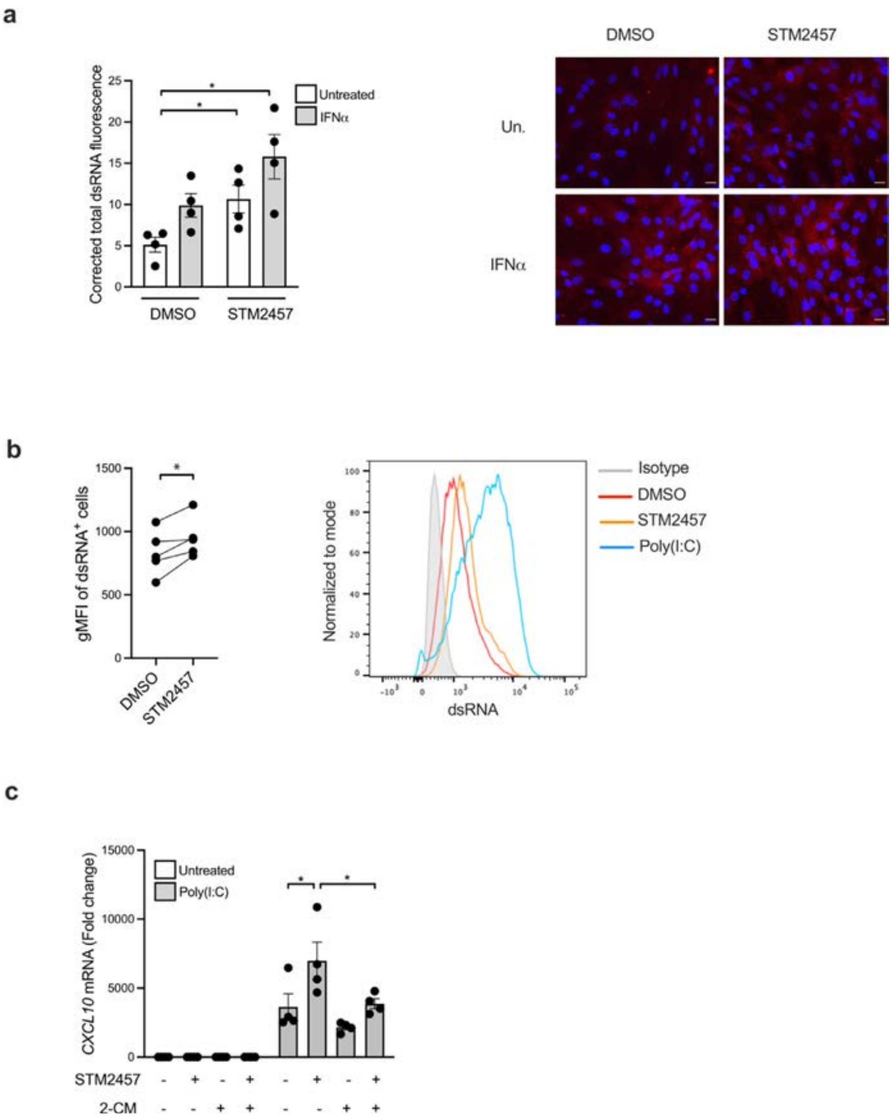

Figure 4. METTL3 inhibition induces the formation of dsRNA in SGEC.(A) Left; SGECs were pretreated with STM2457 for 6 hours, then stimulated±IFNα for 24 hours. Formation of dsRNA was assessed using anti-J2 antibody. Data are shown as corrected total cell fluorescence (CTCF)±SEM from four independent experiments, quantified by ImageJ. CTCF = integrated density −(area of selected cell×mean fluorescence of background readings). Right, representative IF image of dsRNA. Scale bar = 20 µm (B) NS-SV-TT-AC cells were treated with STM2457 for 24 hours and dsRNA was assessed by flow cytometry using anti-J2 antibody using geometric MFI. Representative FACS plot is shown. (C) SGECs were pretreated with 2-CM±STM2457 for 6 hours, then stimulated±Poly(I:C) for 24 hours and *CXCL10* was assessed by qPCR. Data are normalised to untreated samples, from four independent experiments±SEM *p<0.05 by ANOVA with post hoc Tukey's test. ANOVA, analysis of variance; dsRNA, double-stranded RNA; MFI, mean fluorescence intensity; SGEC, salivary gland epithelial cell.

downregulation of mt-dsRNAs. Collectively, these findings illustrate that catalytic inhibition of METTL3 results in dsRNA accumulation and subsequent activation of IFN responses.

METTL3 inhibition enhances SGEC-mediated immune cell recruitment and B cell activation

Given the observed rise in SGEC activation and chemokine release after METTL3 inhibition, our aim was to investigate whether this inhibition within SGEC could influence immune cell recruitment. SGECs were pretreated with STM2457 (10 µM), with or without Poly(I:C) stimulation for 24 hours, followed by washing and placement in the lower compartment of a transwell chamber migration assay (figure 5A; online supplemental figure S5A). PBMCs were introduced into the upper compartment, and their migration was evaluated by flow cytometry (figure 5A). Notably, there was an increase in immune cell recruitment, particularly of CD4 + T cells, CD8 + T cells, NK cells and B cells on METTL3 inhibition in Poly(I:C)-treated SGEC (figure 5B), suggesting that METTL3 inhibition in SGEC triggered immune cell attraction.

B cells play a pivotal role in SjD pathogenesis [47]. Thus, we proceeded to examine how modulating the m^{6}A pathway in SGEC affected B cell survival and activation using a 5-day coculture model. SGECs were pretreated with STM2457 (10 µM) or FB23-2 (10 µM) for 24 hours, then washed before coculturing with allogeneic B cells, with or without Poly(I:C) stimulation (figure 5C). No mismatch occurred because we used isolated B cells, thereby avoiding T-cell-mediated allogenic reactions. As previously shown [9], the presence of SGEC augmented B cell survival and even more in presence of Poly(I:C) (figure 5D; online supplemental figure S5B). This effect seemed unaffected by STM2457 pretreatment of SGEC (figure 5D; online supplemental figure S5B). However, inhibition of FTO by FB23-2 in SGEC decreased B cell survival (figure 5D; online supplemental figure S5B).

Furthermore, B-cell activation post cocultures with SGEC was examined by flow cytometry. As previously shown [9], Poly(I:C) stimulation led to a significant elevation in the mean fluorescence intensity of CD38 on B cells (online supplemental figure S5C). During Poly(I:C) stimulation, pretreatment of SGEC with STM2457 further intensified B cell activation (figure 5E; online supplemental figure S5C). Conversely, pretreatment with FB23-2 reduced B cell activation (figure 5E; online supplemental figure S5C). In summary, these results confirm that METTL3 inhibition increases immune cell recruitment and B cell activation by SGEC in the context of an IFN environment.

Insufficient METTL3 upregulation in SGEC from SjD patients on Poly(I:C) activation

In the light of the established regulatory role of METTL3 in dampening inflammation in SGEC, the upregulation of METTL3

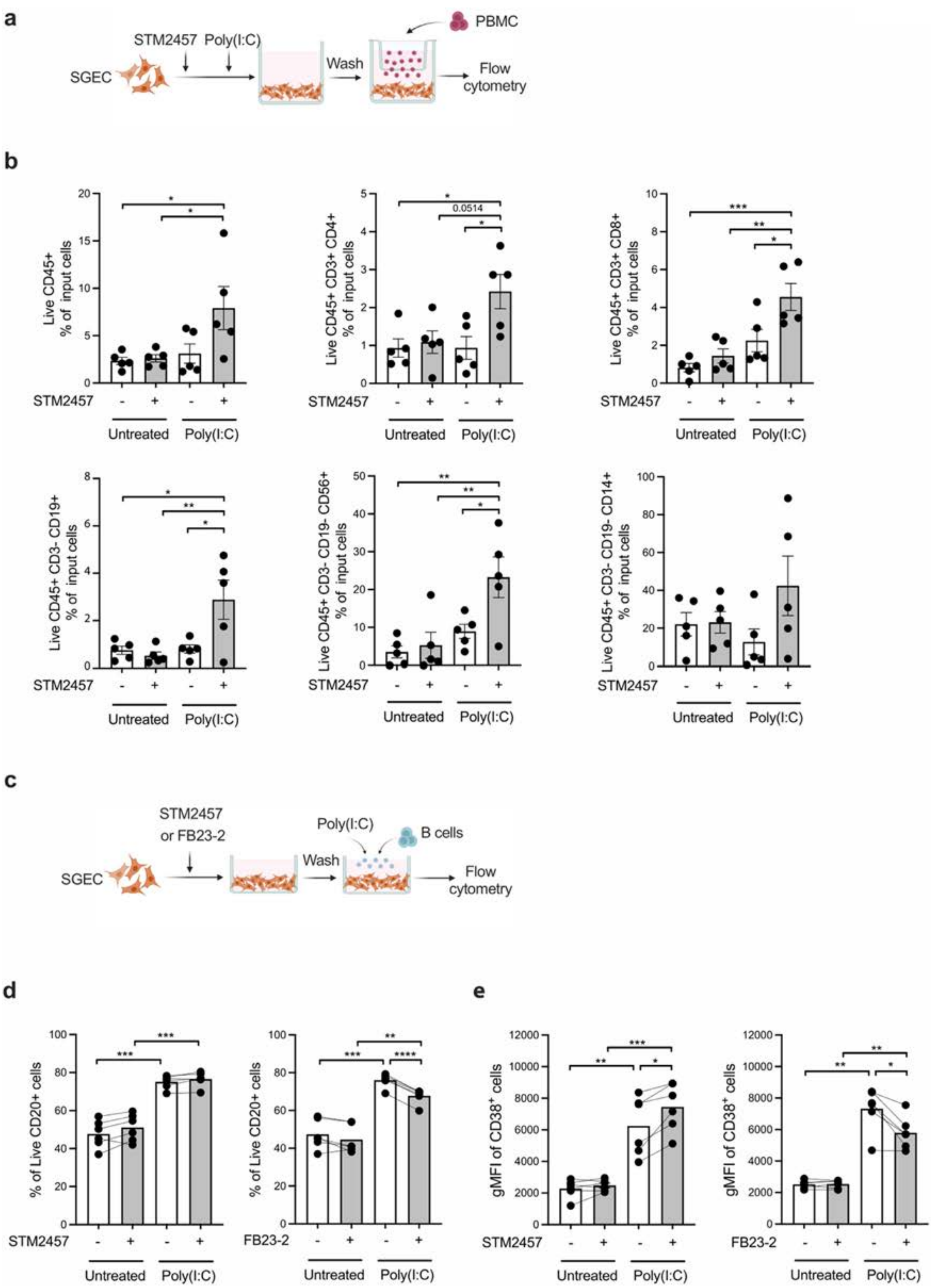

Figure 5. METTL3 inhibition enhances the recruitment of immune cells by SGEC and activates B cells. (A) Chemotactic response of PBMC to SGECs that were pretreated with STM2457 for 16 hours, then stimulated±Poly(I:C) for 6 hours before being washed and placed in the low compartment of transwell for 16 hours. (B) Percentage of live immune cells that migrated to the lower compartment in the transwell assay. Data are shown mean±SEM from five independent experiments. (C) Coculture of allogeneic CD19 + B cells, isolated from PBMC, and SGEC that were pretreated with STM2457 or FB23-2 for 16 hours, then washed before being stimulated±Poly(I:C) for 5 days. (D) Percentage of live B cells on day 5, cocultured with DMSO or STM2457 or FB23-2-treated SGECs with or without Poly(I:C) stimulation. Data are shown mean±SEM from six independent experiments. (E) geometric MFI (gMFI) of CD38 in B cells on day 5, cocultured with DMSO or STM2457 or FB23-2-treated SGECs with or without Poly(I:C) stimulation. Data are shown mean±SEM from six independent experiments. *p<0.05, **p<0.01, ***p<0.001, ****p<0.0001 by ANOVA with post hoc Tukey's test. ANOVA, analysis of variance; MFI, mean fluorescence intensity; SGECs, salivary gland epithelial cells.

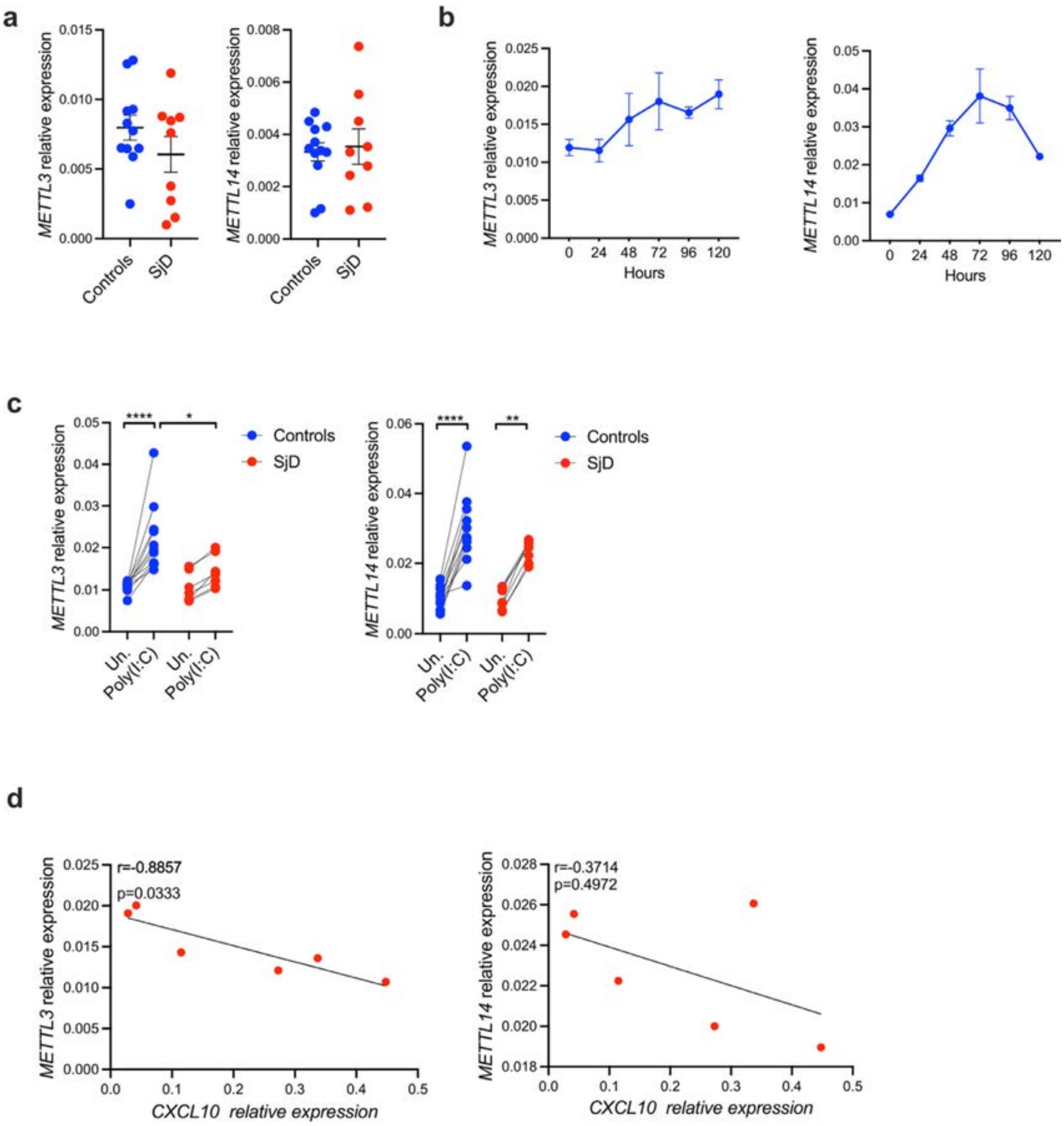

Figure 6. SGEC stimulated with Poly(I:C) upregulate METTL3 and METTL14 expression. (A) Indicated mRNAs were assessed by qPCR in SGECs cultured from 9 SjD patients and 11 controls. Each symbol represents one individual. Data show relative expression±SEM. (B) SGECs were stimulated±Poly(I:C) for the indicated time and *METTL3/14* transcripts were assessed by qPCR. Data are normalised to untreated samples. (C) Indicated mRNAs were assessed by qPCR in SGECs±Poly(I:C) for 24 hours, cultured from nine SjD patients and eight controls. Each symbol represents one individual. (D) Indicated mRNAs were assessed by qPCR in SGECs±Poly(I:C) for 5 days, cultured from 7 SjD patients and 11 controls. Each symbol represents one individual. *p<0.05, **p<0.01, ****p<0.0001 by ANOVA with post hoc Tukey's test. (E) Correlation between *METTL3/METTL14* and *CXCL10* expression in primary cultured SGECs from SjD (n = 6). *p<0.05 by Spearman analysis. ANOVA, analysis of variance; qPCR, quantitative PCR; SGECs, salivary gland epithelial cells.

observed in SjD patients compared with controls may appear counterintuitive. Hence, we investigated whether subjecting SGEC isolated from both SjD patients and controls to identical immune triggers would result in differential expressions of *METTL3* and *METTL14*. Interestingly, *METTL3* and *METTL14* were not differentially expressed in cultured SGECs from SjD and controls without any stimulation (figure 6A). We then investigated whether inflammatory triggers increase *METTL3* and *METTL14* expression in primary SGEC cultured in vitro. Poly(I:C)-stimulated SGEC increased the expression of both m^{6}A writers in a time-dependent manner (figure 6B). These findings suggest that the abnormal increase in *METTL3* and *METTL14* observed in SGEC from SjD is the consequence of a proinflammatory microenvironment present in the glandular epithelia. We then cultured SGECs from SjD patients and controls and stimulated them with Poly(I:C) for 24 hours (figure 6C) and 5 days (figure 6D). While a comparable increase in *METTL14* expression was noted in both SGEC groups (figure 6C,D), SGEC from SjD patients failed to upregulate *METTL3* to the same extent as SGEC from controls after 5 days of stimulation (figure 6D). Moreover, *METTL3* mRNA expression negatively correlated with the expression of *CXCL10* in SGEC from SjD patients (figure 6E). This insufficient *METTL3* upregulation after Poly(I:C) stimulation could lead to dsRNA accumulation, potentially amplifying IFN pathways and subsequent immune cell activation, thereby playing a pivotal role in SjD pathogenesis.

To further elucidate the association between m^{6}A writers and the IFN pathway in MSG of SjD patients, we examined RNAseq data from four studies (GSE23117 [48], GSE154926 [49], GSE157159 [50], GSE173808[51]). Unsupervised clustering revealed two distinct clusters among SjD patients based on their patterns of IFN type I and type II activation (figure 7A,B). Cluster A exhibited increased IFN pathway activation while cluster B showed attenuated IFN pathway activation (figure 7C). Notably,

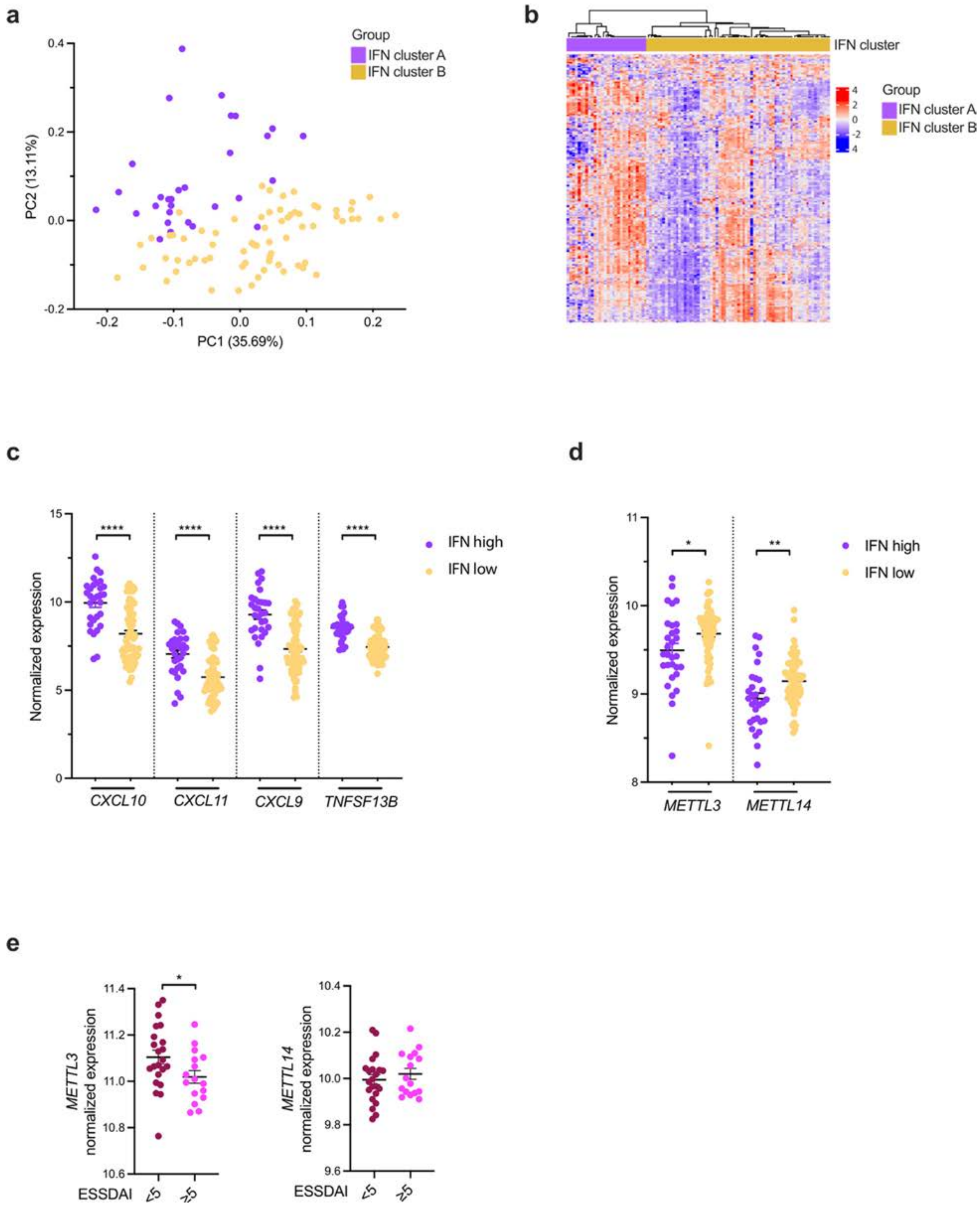

Figure 7. METTL3 expression associated with MSG IFN response and disease activity. (A) PCA analysis was conducted on transcriptomic data obtained from MSG of 99 SjD patients and clusters were established based on interferon α and γ signalling from GSEA. (B) Heatmap showing two clusters A and B based on interferon α and γ signalling from GSEA. (C, D) Normalised expression of indicated transcripts between cluster A (IFN high) and B (IFN low). (E) *METTL3* and *METTL14* normalised expression in MSG of SjD stratified based on EULAR Sjögren's Syndrome Disease Activity Index (ESSDAI) score. Each symbol represents one individual. *p<0.05, **p<0.01, ****p<0.0001 by unpaired t-test. EULAR, European Alliance of Associations for Rheumatology; SjD, Sjögren's disease.

METTL3 and *METTL14* expression was decreased in cluster A, aligning with their suppressive role on the IFN pathway (figure 7D).

Prompted by these findings, we explored whether SjD patients with elevated disease activity would exhibit reduced *METTL3* expression. Indeed, on analysing RNAseq data from GSE173808, we found that SjD patients with higher disease activity (Sjögren's Syndrome Disease Activity Index ≥5) demonstrated a significant reduction in *METTL3* expression (figure 7E). In conclusion, our findings underscore the significance of

METTL3 dysregulation in SjD pathogenesis, highlighting its potential role in promoting IFN activation and immune dysregulation in SGEC.

DISCUSSION

In this study, we demonstrated that the m^{6}A RNA methylation pathway provides a negative feedback mechanism on Poly (I:C) and IFN signalling in SGEC, thereby preventing excessive and harmful inflammation within SG (online supplemental figure S6). However, this protective effect appears to be insufficient in SjD patients. While levels of METTL3 and METTL14 are increased in ex vivo SGEC from SjD patients compared with controls, our in vitro experiments demonstrated that SGEC from controls exhibit greater responsiveness and more effectively upregulate *METTL3* when exposed to Poly(I:C). A deficiency in METTL3 expression during inflammation could result in the aberrant production of endogenous dsRNA. Therefore, the insufficient upregulation of METTL3 in SGEC may contribute to SjD pathogenesis, highlighting the importance of further investigating the m^{6}A epitranscriptomic mark in target cells of autoimmune diseases.

We present multiple lines of evidence confirming METTL3's role in downregulating the activation status of SGEC through the m^{6}A pathway. Initially, silencing *METTL3/14* in primary SGEC increased CXCL10 expression. Furthermore, inhibiting the catalytic function of METTL3 increased IFN signalling while inhibiting FTO led to the opposite phenotype. Our investigation extended to include acinar and ductal SG cell lines, demonstrating consistent behaviour across various salivary epithelial cell types. Finally, we report that METTL3 inhibition in SGEC boosted their ability to recruit immune cells and activate B cells.

To begin to dissect the mechanism involved in the protective role of METTL3 in SGEC, we considered recent findings reporting increased accumulation of intracellular dsRNA on METTL3 depletion.[44,45] Consistent with these findings, METTL3 inhibition triggered the formation of dsRNAs, and hence the activation of IFN signalling. This dsRNA, possibly originating from mitochondrial RNA, can activate pattern recognition receptors such as RIG-I, MDA5 and TLR3, which are known to trigger the production of type I IFN via IRF3 signalling pathway. Therefore, METTL3 could be considered as a safeguard against the formation of dsRNA. A deficiency in METTL3 expression during inflammation could result in the aberrant production of endogenous dsRNA. In line with these observations, dsRNA levels are reported to be elevated in the tears and saliva of SjD patients [46]. Moreover, mitochondrial dsRNA depletion decreased IFN signalling in salivary epithelial cell lines [46]. Additional investigations are required to ascertain whether the m^{6}A pathway specifically affects the formation or elimination of mitochondrial dsRNA or other subtypes of dsRNA in SGEC.

Further studies are also warranted to identify m^{6}A-modified transcripts in SGEC and whether this m^{6}A signature is different in SGEC of SjD versus controls. For instance, deletion of *METTL3/14* in fibroblasts increases the mRNA stability of *Ifnb* on viral infection [42,52]. Moreover, depletion of m^{6}A methyltransferases increased the stability of transcripts associated with the IFN−γ−Stat1−Irf1 pathway in colorectal carcinoma [53]. Hence, the current body of work leaves open the possibility that METTL3 inhibition might induce potent SGEC-intrinsic interferon response through complementary mechanisms that are independent of the formation of dsRNA. Collectively, the interplay between METTL3/14 inhibition and the activation of the Jak/STAT pathway could be mediated by both direct m^{6}A-mediated effects on IFN transcripts and indirect mechanisms involving dsRNA-mediated Jak-STAT activation.

We found that METTL3 and METTL14 expression was markedly elevated in SGEC from SjD compared with control. While *METTL3* transcripts were not significantly different between SjD and controls, its protein expression is elevated, which could be attributed to post-transcriptional regulation or increased protein stability in the disease context. For example, enhanced translation of *METTL3* mRNA or reduced degradation of the METTL3 protein, possibly driven by disease-specific signalling pathways, might contribute to this elevation. The involvement of microRNAs, RNA-binding proteins or other regulatory factors could also play a role in stabilising METTL3 protein specifically in the inflamed environment of SjD.

Although the increase in METTL3 expression in SjD versus controls may seem counterintuitive given its role in restricting inflammation, it is likely that the increased levels reflect the ongoing inflammatory milieu found in diseased SGEC. Interestingly, on stimulation with Poly(I:C), in vitro cultured SGEC from SjD patients displayed a reduced capacity to efficiently upregulate METTL3. This implies an inherent activation state of these cells, which may elucidate earlier observations indicating that SGECs from SjD patients promote increased survival and activation of B cells compared with those from controls [9]. Indeed, SGEC from SjD patients may exhibit an altered cellular phenotype compared with healthy controls, potentially due to chronic inflammation or epigenetic alterations. Therefore, it is possible that SjD-associated epigenetic modifications hinder the transcriptional upregulation of METTL3 on stimulation.

We methodically examined the relationship between the expression of m^{6}A writers and the IFN response across diverse cohorts of patients with SjD. We observed that a reduced IFN response correlated with higher expression of m^{6}A methyltransferases, whereas an elevated IFN phenotype was associated with decreased *METTL3/14* expression. Additionally, SjD patients with increased disease activity exhibited lower levels of *METTL3*. These findings suggest the potential utility of the RNA methylation pathway in stratifying SjD patients and as a possible biomarker for disease prognosis.

In summary, our findings indicate that RNA m^{6}A methylation serves as a protective mechanism in SGECs, preventing the amplification of IFN signalling and maintaining it at an optimal level to promote homoeostasis. We propose that this pathway may be impaired in SjD, resulting in sustained IFN response. Given that several autoimmune diseases exhibit increased activity in the IFN pathway, it is important to explore how the dysregulation of RNA m^{6}A methylation, as observed in SjD, serves as a protective mechanism against IFN upregulation. This investigation should extend to the target cells involved in other autoimmune conditions. Based on these results, we suggest that therapeutic enhancement of METTL3-mediated m^{6}A modifications in SjD patients could potentially preserve SGEC integrity during disease progression and improve salivary function and disease activity.

Acknowledgments

We thank Dr Yaara Ofir-Rosenfeld and STORM Therapeutics for providing METTL3 inhibitors and for helpful comments. We are grateful to Dr Nihal Altan-Bonnet for NS-SV-TT-AC and NS-SV-TT-DC cell lines. We thank Pr. Salima Hacein-Bey-Abina and Dr Pascale Chretien for providing access to the MSD platform.

Contributors

Conceptualisation: RB, AA-H and FT; Methodology: FT, AA-H, HS, JP, PM, ER, SE-S-S, LF, SL, LB, CM, AD, SV, GN, XM and RB; Investigation: FT, AA-H, HS, JP, PM, ER, SE-S-S, LF, SL, LB, CM and RB; Writing−original draft: RB; Writing−review and editing: AA-H, FT, HS, JP, PM, ER, SE-S-S, LF, SL, LB, CM, AD, SV, GN and XM; Funding acquisition: RB; Supervision, RB. RB was responsible for the overall content as the guarantor. All authors reviewed and approved of the final manuscript.

Funding

This work received funding from the ANR-JCJC Program (ANR-22-CE15-0031) by the French National Research Agency, the France 2030 program (ANR-11-IDEX-0003) from the OI HEALTHI initiative at Université Paris-Saclay and the UPS IDEX AAP TECHNICS 2023 (R23097LL) grant from the HEADS Graduate School at Université Paris-Saclay and from FRM for the project PREMSS (R23073LL). AA-H is the recipient of a PhD fellowship from Arthritis Foundation Courtin, Arthritis R&D (CIFRE 2023/005). HS is the recipient of the M2 fellowship from OI HEALTHI at Université Paris-Saclay (IDEX HTI 2021-06).

Competing interests

XM received an honorarium for consultancy advice on Sjögren's disease from Argenx, BMS, GSK, Novartis and Otsuka. The rest of the authors declare that they have no relevant conflicts of interest.

Patient and public involvement

Patients and/or the public were not involved in the design, or conduct, or reporting, or dissemination plans of this research.

Patient consent for publication

Not applicable.

Ethics approval

This study involves human participants and our centre has obtained approval from the local APHP ethics committee for this project (AP-HP210093, No IDRCB: 2020-A00509-30), and informed consent will be obtained from all patients and control subjects. Participants gave informed consent to participate in the study before taking part.

Data availability statement

Data are available in a public, open access repository. Data are available on reasonable request. NS-SV-TT-AC and NS-SV-TT-DC cells are available by MTA from the National Heart, Lung and Blood Institute (NHLBI) and the National Institute of Dental and Craniofacial Research (NIDCR). STM2457, STM2120 and STM3006 are under MTA from STORM THERAPEUTICS LTD. All other reagents are commercially available. RNAseq data generated in this study are available on reasonable request, rami.bechara@universite-paris-saclay.fr. RNAseq data from these studies GSE23117 (48), GSE154926 (49), GSE157159 (50), GSE173808 (51) are publicly available.

Supplementary materials

Supplementary material associated with this article can be found in the online version at doi:10.1136/ard-2024-226224.

Orcid

Elodie Rivière: http://orcid.org/0000-0003-1010-3081
Lucilla Fabbri: http://orcid.org/0000-0003-2928-3983
Laetitia Besse: http://orcid.org/0000-0001-5031-652X
Alexandre David: http://orcid.org/0000-0003-3365-1339
Stephan Vagner: http://orcid.org/0000-0003-1452-7164
Gaetane Nocturne: http://orcid.org/0000-0001-6809-0733
Xavier Mariette: http://orcid.org/0000-0002-4244-5417
Rami Bechara: http://orcid.org/0000-0002-1611-0242

REFERENCES

[1] Nocturne G, Mariette X. Advances in understanding the pathogenesis of primary Sjögren's syndrome. Nat Rev Rheumatol 2013;9:544–56. doi: 10.1038/nrrheum.2013.110.

[2] Mariette X, Criswell LA. Primary Sjögren's Syndrome. N Engl J Med 2018;378:931–9. doi: 10.1056/NEJMcp1702514.

[3] Rivière E, Pascaud J, Virone A, et al. Interleukin-7/Interferon Axis Drives T Cell and Salivary Gland Epithelial Cell Interactions in Sjögren's Syndrome. Arthritis Rheumatol 2021;73:631–40. doi: 10.1002/art.41558.

[4] Nezos A, Gravani F, Tassidou A, et al. Type I and II interferon signatures in Sjogren's syndrome pathogenesis: Contributions in distinct clinical phenotypes and Sjogren's related lymphomagenesis. J Autoimmun 2015;63:47–58. doi: 10.1016/j.jaut.2015.07.002.

[5] Bikker A, van Woerkom JM, Kruize AA, et al. Increased expression of interleukin-7 in labial salivary glands of patients with primary Sjögren's syndrome correlates with increased inflammation. Arthritis Rheum 2010;62:969–77. doi: 10.1002/art.27318.

[6] Daridon C, Devauchelle V, Hutin P, et al. Aberrant expression of BAFF by B lymphocytes infiltrating the salivary glands of patients with primary Sjögren's syndrome. Arthritis Rheum 2007;56:1134–44. doi: 10.1002/art.22458.

[7] Ittah M, Miceli-Richard C, Eric Gottenberg J, et al. B cell-activating factor of the tumor necrosis factor family (BAFF) is expressed under stimulation by interferon in salivary gland epithelial cells in primary Sjögren's syndrome. Arthritis Res Ther 2006;8:R51. doi: 10.1186/ar1912.

[8] Amft N, Bowman SJ. Chemokines and cell trafficking in Sjögren's syndrome. Scand J Immunol 2001;54:62–9. doi: 10.1046/j.1365-3083.2001.00970.x.

[9] Rivière E, Pascaud J, Tchitchek N, et al. Salivary gland epithelial cells from patients with Sjögren's syndrome induce B-lymphocyte survival and activation. Ann Rheum Dis 2020;79:1468–77. doi: 10.1136/annrheumdis-2019-216588.

[10] Verstappen GM, Pringle S, Bootsma H, et al. Epithelial-immune cell interplay in primary Sjögren syndrome salivary gland pathogenesis. Nat Rev Rheumatol 2021;17:333–48. doi: 10.1038/s41584-021-00605-2.

[11] Boumba D, Skopouli FN, Moutsopoulos HM. Cytokine mRNA expression in the labial salivary gland tissues from patients with primary Sjögren's syndrome. Br J Rheumatol 1995;34:326–33. doi: 10.1093/rheumatology/34.4.326.

[12] Fox RI, Kang HI, Ando D, et al. Cytokine mRNA expression in salivary gland biopsies of Sjögren's syndrome. J Immunol 1994;152:5532–9.

[13] Spachidou MP, Bourazopoulou E, Maratheftis CI, et al. Expression of functional Toll-like receptors by salivary gland epithelial cells: increased mRNA expression in cells derived from patients with primary Sjögren's syndrome. Clin Exp Immunol 2007;147:497–503. doi: 10.1111/j.1365-2249.2006.03311.x.

[14] Xanthou G, Polihronis M, Tzioufas AG, et al. "Lymphoid" chemokine messenger RNA expression by epithelial cells in the chronic inflammatory lesion of the salivary glands of Sjögren's syndrome patients: possible participation in lymphoid structure formation. Arthritis Rheum 2001;44:408–18 10.1002/1529-0131(200102)44:2<408::AID-ANR60>3.0.CO;2-0.

[15] Ogawa N, Ping L, Zhenjun L, et al. Involvement of the interferon-gamma-induced T cell-attracting chemokines, interferon-gamma-inducible 10-kd protein (CXCL10) and monokine induced by interferon-gamma (CXCL9), in the salivary gland lesions of patients with Sjögren's syndrome. Arthritis Rheum 2002;46:2730–41. doi: 10.1002/art.10577.

[16] Carrette F, Surh CD. IL-7 signaling and CD127 receptor regulation in the control of T cell homeostasis. Semin Immunol 2012;24:209–17. doi: 10.1016/j.smim.2012.04.010.
[17] Bikker A, Kruize AA, Wenting M, et al. Increased interleukin (IL)-7Rα expression in salivary glands of patients with primary Sjogren's syndrome is restricted to T cells and correlates with IL-7 expression, lymphocyte numbers and activity. Ann Rheum Dis 2012;71:1027–33. doi: 10.1136/annrheumdis-2011-200744.
[18] Jin JO, Kawai T, Cha S, et al. Interleukin-7 enhances the Th1 response to promote the development of Sjögren's syndrome-like autoimmune exocrinopathy in mice. Arthritis Rheum 2013;65:2132–42. doi: 10.1002/art.38007.
[19] Wang X, Shaalan A, Liefers S, et al. Dysregulation of NF-kB in glandular epithelial cells results in Sjögren's-like features. PLoS ONE 2018;13:e0200212. doi: 10.1371/journal.pone.0200212.
[20] Ittah M, Miceli-Richard C, Gottenberg J-E, et al. Viruses induce high expression of BAFF by salivary gland epithelial cells through TLR- and type-I IFN-dependent and -independent pathways. Eur J Immunol 2008;38:1058–64. doi: 10.1002/eji.200738013.
[21] Batten M, Groom J, Cachero TG, et al. BAFF mediates survival of peripheral immature B lymphocytes. J Exp Med 2000;192:1453–66. doi: 10.1084/jem.192.10.1453.
[22] Mackay F, Schneider P. Cracking the BAFF code. Nat Rev Immunol 2009;9:491–502. doi: 10.1038/nri2572.
[23] Gottenberg J-E, Cagnard N, Lucchesi C, et al. Activation of IFN pathways and plasmacytoid dendritic cell recruitment in target organs of primary Sjögren's syndrome. Proc Natl Acad Sci U S A 2006;103:2770–5. doi: 10.1073/pnas.0510837103.
[24] Lee J, Lee J, Kwok S-K, et al. JAK-1 Inhibition Suppresses Interferon-Induced BAFF Production in Human Salivary Gland: Potential Therapeutic Strategy for Primary Sjögren's Syndrome. Arthritis Rheumatol 2018;70:2057–66. doi: 10.1002/art.40589.
[25] Soret P, Le Dantec C, Desvaux E, et al. A new molecular classification to drive precision treatment strategies in primary Sjögren's syndrome. Nat Commun 2021;12:3523. doi: 10.1038/s41467-021-23472-7.
[26] Manoussakis MN, Spachidou MP, Maratheftis CI. Salivary epithelial cells from Sjogren's syndrome patients are highly sensitive to anoikis induced by TLR-3 ligation. J Autoimmun 2010;35:212–8. doi: 10.1016/j.jaut.2010.06.010.
[27] Dimitriou ID, Kapsogeorgou EK, Moutsopoulos HM, et al. CD40 on salivary gland epithelial cells: high constitutive expression by cultured cells from Sjögren's syndrome patients indicating their intrinsic activation. Clin Exp Immunol 2002;127:386–92. doi: 10.1046/j.1365-2249.2002.01752.x.
[28] Kapsogeorgou EK, Moutsopoulos HM, Manoussakis MN. Functional expression of a costimulatory B7.2 (CD86) protein on human salivary gland epithelial cells that interacts with the CD28 receptor, but has reduced binding to CTLA4. J Immunol 2001;166:3107–13. doi: 10.4049/jimmunol.166.5.3107.
[29] Kapsogeorgou EK, Abu-Helu RF, Moutsopoulos HM, et al. Salivary gland epithelial cell exosomes: A source of autoantigenic ribonucleoproteins. Arthritis Rheum 2005;52:1517–21. doi: 10.1002/art.21005.
[30] Tsunawaki S, Nakamura S, Ohyama Y, et al. Possible function of salivary gland epithelial cells as nonprofessional antigen-presenting cells in the development of Sjögren's syndrome. J Rheumatol 2002;29:1884–96.
[31] Katsiougiannis S, Tenta R, Skopouli FN. Activation of AMP-activated protein kinase by adiponectin rescues salivary gland epithelial cells from spontaneous and interferon-gamma-induced apoptosis. Arthritis Rheum 2010;62:414–9. doi: 10.1002/art.27239.
[32] Polihronis M, Tapinos NI, Theocharis SE, et al. Modes of epithelial cell death and repair in Sjögren's syndrome (SS). Clin Exp Immunol 1998;114:485–90. doi: 10.1046/j.1365-2249.1998.00705.x.
[33] Abu-Helu RF, Dimitriou ID, Kapsogeorgou EK, et al. Induction of salivary gland epithelial cell injury in Sjogren's syndrome: in vitro assessment of T cell-derived cytokines and Fas protein expression. J Autoimmun 2001;17:141–53. doi: 10.1006/jaut.2001.0524.
[34] Ping L, Ogawa N, Sugai S. Novel role of CD40 in Fas-dependent apoptosis of cultured salivary epithelial cells from patients with Sjögren's syndrome. Arthritis Rheum 2005;52:573–81. doi: 10.1002/art.20789.
[35] Ewert P, Aguilera S, Alliende C, et al. Disruption of tight junction structure in salivary glands from Sjögren's syndrome patients is linked to proinflammatory cytokine exposure. Arthritis Rheum 2010;62:1280–9. doi: 10.1002/art.27362.
[36] Bechara R, Vagner S, Mariette X. Post-transcriptional checkpoints in autoimmunity. Nat Rev Rheumatol 2023;19:486–502. doi: 10.1038/s41584-023-00980-y.
[37] Zhou J, Zhang X, Hu J, et al. m(6)A demethylase ALKBH5 controls CD4(+) T cell pathogenicity and promotes autoimmunity. Sci Adv 2021;7. doi: 10.1126/sciadv.abg0470.
[38] Tong J, Cao G, Zhang T, et al. m6A mRNA methylation sustains Treg suppressive functions. Cell Res 2018;28:253–6. doi: 10.1038/cr.2018.7.
[39] Li H-B, Tong J, Zhu S, et al. m6A mRNA methylation controls T cell homeostasis by targeting the IL-7/STAT5/SOCS pathways. Nat New Biol 2017;548:338–42. doi: 10.1038/nature23450.
[40] Bechara R, Amatya N, Bailey RD, et al. The m6A reader IMP2 directs autoimmune inflammation through an IL-17- and TNFα-dependent C/EBP transcription factor axis. Sci Immunol 2021;6:eabd1287. doi: 10.1126/sciimmunol.abd1287.
[41] McFadden MJ, Horner SM. N6-Methyladenosine Regulates Host Responses to Viral Infection. Trends Biochem Sci 2021;46:366–77. doi: 10.1016/j.tibs.2020.11.008.
[42] Winkler R, Gillis E, Lasman L, et al. Publisher Correction: m6A modification controls the innate immune response to infection by targeting type I interferons. Nat Immunol 2019;20:173–82. doi: 10.1038/s41590-019-0314-4.
[43] Bechara R, Gaffen SL. (m6)A' stands for 'autoimmunity': reading, writing, and erasing RNA modifications during inflammation. Trends Immunol 2021;42:1073–6. doi: 10.1016/j.it.2021.10.002.
[44] Guirguis AA, Ofir-Rosenfeld Y, Knezevic K, et al. Inhibition of METTL3 Results in a Cell-Intrinsic Interferon Response That Enhances Antitumor Immunity. Cancer Discov 2023;13:2228–47. doi: 10.1158/2159-8290.CD-23-0007.
[45] Gao Y, Vasic R, Song Y, et al. m6A Modification Prevents Formation of Endogenous Double-Stranded RNAs and Deleterious Innate Immune Responses during Hematopoietic Development. Immunity 2020;52:1007–21. doi: 10.1016/j.immuni.2020.05.003.
[46] Yoon J, Lee M, Ali AA, et al. Mitochondrial double-stranded RNAs as a pivotal mediator in the pathogenesis of Sjögren's syndrome. Mol Ther Nucleic Acids 2022;30:257–69. doi: 10.1016/j.omtn.2022.09.020.
[47] Nocturne G, Mariette X. B cells in the pathogenesis of primary Sjögren syndrome. Nat Rev Rheumatol 2018;14:133–45. doi: 10.1038/nrrheum.2018.1.
[48] Greenwell-Wild T, Moutsopoulos NM, Gliozzi M, et al. Chitinases in the salivary glands and circulation of patients with Sjögren's syndrome: macrophage harbingers of disease severity. Arthritis Rheum 2011;63:3103–15. doi: 10.1002/art.30465.
[49] Chiorini JA, Mo Y, Pranzatelli TJ, et al. Bulk RNA sequencing in minor salivary glands of brazilian patients with primary sjögren's syndrome (SS) and healthy volunteers. GEO; 2021.
[50] Oyelakin A, Horeth E, Song E-AC, et al. Transcriptomic and Network Analysis of Minor Salivary Glands of Patients With Primary Sjögren's Syndrome. Front Immunol 2020;11:606268. doi: 10.3389/fimmu.2020.606268.
[51] Verstappen GM, Gao L, Pringle S, et al. The Transcriptome of Paired Major and Minor Salivary Gland Tissue in Patients With Primary Sjögren's Syndrome. Front Immunol 2021;12:681941. doi: 10.3389/fimmu.2021.681941.
[52] Rubio RM, Depledge DP, Bianco C, et al. RNA m6A modification enzymes shape innate responses to DNA by regulating interferon β. Genes Dev 2018;32:1472–84. doi: 10.1101/gad.319475.118.
[53] Wang L, Hui H, Agrawal K, et al. m6A RNA methyltransferases METTL3/14 regulate immune responses to anti-PD-1 therapy. EMBO J 2020;39:e104514. doi: 10.15252/embj.2020104514.

Ann Rheum Dis 84 (2025) 760−766

Contents lists available at ScienceDirect

Annals of the Rheumatic Diseases

journal homepage: https://www.sciencedirect.com/journal/annals-of-the-rheumatic-diseases

Systemic lupus erythematosus

Risk of HPV-associated precancer and cancer in women with systemic lupus erythematosus

Kanwal Zahid Siddiqi[1,2], Louise Baandrup[1,3,4], Louise Diederichsen[2], Rasmus Hertzum-Larsen[1], Henrik Christian Bidstrup Leffers[2], Søren Jacobsen[2,4], Susanne Krüger Kjær[1,4,5,*]

[1] *Unit of Virus, Lifestyle and Genes, Danish Cancer Institute, Copenhagen, Denmark*
[2] *Copenhagen Center for Autoimmune Connective Tissue Diseases, Rigshospitalet, University of Copenhagen, Copenhagen, Denmark*
[3] *Department of Pathology, Zealand University Hospital, Roskilde, Denmark*
[4] *Department of Clinical Medicine, University of Copenhagen, Copenhagen, Denmark*
[5] *Juliane Marie Centre, Rigshospitalet, University of Copenhagen, Copenhagen, Denmark*

ARTICLE INFO

Article history:
Received 3 October 2024
Received in revised form 16 November 2024
Accepted 21 November 2024

ABSTRACT

Objectives: We aimed to compare the occurrence of human papillomavirus (HPV)-associated precancer and cancer in a nationwide cohort of women with systemic lupus erythematosus (SLE) with general female population rates.
Methods: In the nationwide Patient Registry, we identified all women in Denmark with a first diagnosis of SLE recorded during 1996-2021 (N = 5092). The cohort was followed up in nationwide registries for HPV-associated precancer and cancer until 2022. Standardised incidence ratios (SIRs) were computed with 95% CIs overall and stratified by age at SLE diagnosis and follow-up time.
Results: Compared with general population rates, women with SLE had increased rates of cervical (SIR, 2.3; 95% CI, 2.0-2.7), vaginal (SIR, 4.3; 95% CI, 1.1-9.5), vulvar (SIR, 3.7; 95% CI, 2.3-5.5), and anal (SIR, 4.3; 95% CI, 1.7-8.1) precancers. Increased cancer rates were observed for cervix, anus, and oropharynx, but only the SIR for oropharyngeal cancer was near statistical significance (SIR, 2.5; 95% CI, 0.9-4.9). The increased SIRs for precancers and cancers sustained throughout follow-up and were higher in women diagnosed with SLE at age <50 years compared with ≥50 years, but CIs were overlapping.
Conclusions: Women in this nationwide SLE cohort had twice the risk of cervical precancer (vs the general population) and up to 5-fold increased risk of the individual noncervical anogenital precancers. Rates of oropharyngeal cancer and the anogenital cancers were not statistically significantly increased; however, estimates were based on few cases.

INTRODUCTION

Systemic lupus erythematosus (SLE) is a chronic multiorgan autoimmune disease affecting primarily women. The aetiology of SLE involves a complex interplay between genetic predispositions and environmental factors [1]. Patients with SLE typically experience periods of flare and remission, cumulatively resulting in disease and therapy-related organ damage [2]. The cornerstone of SLE treatment is currently immunosuppressive therapy [3].

* **Correspondence to** Prof Susanne Krüger Kjær, Unit of Virus, Lifestyle and Genes; Danish Cancer Institute, Copenhagen, Denmark.

E-mail address: susanne@cancer.dk (S.K. Kjær).

SJ and SKK contributed equally to this work.

Handling editor Josef S. Smolen.

https://doi.org/10.1016/j.ard.2025.01.026

WHAT IS ALREADY KNOWN ON THIS TOPIC

- Patients with systemic lupus erythematosus (SLE) have impaired clearance of human papillomavirus (HPV) resulting in increased persistence of infection. Previous data on the risk of HPV-associated neoplasia in patients with SLE have mostly focused on cervical precancer and cancer, and till date, no study has investigated the risk of noncervical anogenital precancers in SLE.

WHAT THIS STUDY ADDS

- In this nationwide cohort of women with SLE, we found increased rates of high-grades of cervical (SIR, 2.3; 95% CI, 2.0-2.7), vaginal (SIR, 4.3; 95% CI, 1.1-9.5), vulvar (SIR, 3.7; 95% CI, 2.3-5.5), and anal (SIR, 4.3; 95% CI, 1.7-8.1) precancers. Regarding HPV-associated cancers, increased rates were observed for cervix, anus, and oropharynx; however, only rates for oropharynx were near statistical significance (SIR, 2.5; 95% CI, 0.9-4.9).

HOW THIS STUDY MIGHT AFFECT RESEARCH, PRACTICE OR POLICY

- This study demonstrates that women with SLE represent a patient group at high risk of both cervical and noncervical HPV-associated precancers and cancers. Our data support adherence to preventive screening programmes among women with SLE for HPV-associated precancers and cancers.

As the life expectancy of patients with SLE increases [4], late-onset comorbidities including malignancies contribute to an increasing burden of multimorbidity in patients with SLE [5]. Previous studies have suggested that the overall risk of cancer is increased in patients with SLE, especially for cancers associated with oncogenic viruses [6,7].

Persistent infection with oncogenic types of human papillomavirus (HPV) causes virtually all cervical precancers and cancers and is also a major risk factor for oropharyngeal cancer and noncervical anogenital cancers and their immediate precursor lesions [8,9]. The host immune response and the oncogenic potential of the infecting HPV type may contribute to the persistence of infection and its progression to precancer and invasion [9]. Impaired innate and cellular immune responses, due to immunologic aberrations associated with SLE and therapy-related immunosuppression, may impair clearance of HPV infection and result in persistent HPV infections and an increased carcinogenic risk in patients with SLE [10,11].

Several studies have reported significantly increased relative risks of cervical precancers in patients with SLE [12]. In countries with well-organised cervical cancer screening, however, the relative risk of cervical cancer in women with SLE appears to be approximately the same as the general population [6,13]. Regarding the noncervical HPV-associated cancers, some studies have suggested that patients with SLE are predisposed to cancers of the anus [6,14], vagina/vulva [6,13,15,16], and oropharynx [6,7,17,18]. To our knowledge, no previous study has examined the association between SLE and risk of noncervical HPV-associated anogenital precancers.

The present study aimed (1) to compare the occurrence of HPV-associated anogenital cancer and precancer and oropharyngeal cancer in a nationwide cohort of women with SLE relative to the general female population and (2) to examine these risks by age, length of follow-up since SLE diagnosis, and periods before and after implementation of HPV vaccination in Denmark.

METHODS

Study cohort

The study cohort comprised all women with at least 1 recording of an SLE diagnosis in the Danish National Patient Register during a 26-year study period (1996-2021). The Patient Registry contains nationwide information of all somatic hospitalisations since 1978 and all outpatient consultations since 1995 [19,20]. The SLE diagnosis was based on the International Classification of Diseases (ICD) 8th revision (ICD-8) code (73419) from 1977 until 1993, and ICD 10th revision (ICD-10) codes (M32.1, M32.8, and M32.9) from 1994 onwards. For all women, we retrieved their full history in the Patient Registry. If a woman was registered with SLE on several occasions, only the first occurrence was used, and if this was before 1996, the woman was not included in the cohort.

Follow-up and identification of precancerous lesions and cancers

Since 1968, all residents in Denmark have been assigned a unique personal identification number. The personal identification number is incorporated in all health registries and is a key identifier enabling individual-level linkage of information between registries.

Our study cohort was linked to the nationwide Danish Pathology Registry to retrieve information on HPV-associated precancerous lesions. The registry holds information on all cytologic and histologic diagnoses performed at all pathology departments in Denmark since 1997 [21]. The Pathology Registry uses a Danish version of the Systemised Nomenclature of Medicine (SNOMED) based on codes for topography and morphology. HPV-associated lesions were identified by SNOMED topography codes corresponding to cervix, vagina, vulva, and anus and SNOMED morphology codes corresponding to cervical intraepithelial neoplasia (CIN) grade 2-3 or adenocarcinoma in situ (AIS) for cervix and high-grade intraepithelial lesion (HSIL) for the remaining sites.

Information on HPV-associated cancer occurrence in our study cohort was obtained by linkage to the nationwide and population-based Danish Cancer Registry. The registry has collected information on incident cancer cases in Denmark since 1943 [22]. Reporting of cancers to the registry is considered 95% to 98% complete since 1943, although reporting first became mandatory in 1987 [23,24]. All cancers since 1978 are coded according to ICD-10 and the Third Oncology version (ICD-O-3). HPV-associated cancers included cervical squamous cell carcinomas and adenocarcinomas and vulvar, vaginal, anal, and oropharyngeal squamous cell carcinomas.

The women in the study cohort were followed up for all subsequent diagnoses of HPV-associated precancerous lesions and cancer from date of first SLE diagnosis until the date of death, emigration, or December 31, 2021, whichever occurred first. Information on migration and death was obtained from the Civil Registration System [25]. The Civil Registration System was established in 1968, and all persons alive and living in Denmark are registered with information on name, gender (defined as male or female), date of birth, and continuously updated information on vital status and place of residence [26].

Statistical analysis

To evaluate the risk of HPV-associated precancerous lesions and cancer following a diagnosis of SLE, standardised incidence ratios (SIRs) with 95% CIs were estimated in log-linear Poisson models with number of observed cases in 5-year age and calendar-year periods as the outcome, and the logarithm of number of women-years of follow-up times the corresponding age-specific and calendar-year specific incidence rates in the general Danish female population as offset. SIRs were stratified according to length of follow-up (<1 year, 1-4 years, and ≥5 years) since the SLE diagnosis, and separate analysis of women diagnosed with SLE at age <50 years and ≥50 years, respectively, was performed, as some studies have shown that SLE diagnosed at early age is often more severe [27,28]. Owing to the rarity of vulvar and vaginal HSIL, these lesions were merged in stratified analyses. Regarding cancers, vulvar and vaginal cases were merged in overall analyses, and stratified analyses were only performed for all HPV-associated cancers combined. Finally, we divided our study period into pre-HPV vaccine era (<2012) and post-HPV vaccine era (≥2012) to study whether the associations between SLE and HPV-associated precancer and cancer were the same in these 2 periods.

We performed 2 separate sensitivity analyses. First, to reduce potential diagnostic misclassification, we restricted our cohort to women who had 2 or more hospital contacts with SLE, and the first contact served as date of diagnosis. Second, we excluded cases with previous diagnosis of cancer (except non-melanoma skin cancer) on the same day or before the SLE diagnosis.

Owing to data protection rules at Statistics Denmark, we are not allowed to provide the exact number when the number of observed cases is between 1 and 4. All statistical data analyses were carried out using R 4.1 (R Core Team 2021) [29].

Patient and public involvement

Patients and the public were not involved in this study any way.

RESULTS

The study included 5092 women with a first-time registration of SLE during 1996-2021. The median age at diagnosis was 45.7 years. The number of women-years that the women in our cohort were followed varied between outcomes and ranged from 64,228 women-years for CIN2-3 to 67,665 women-years for anal cancer.

Risk of HPV-associated precancerous lesions

Table 1 shows SIRs of HPV-associated precancerous lesions in women with SLE. Compared with rates in the general female population, women with SLE had more than twice the risk of CIN2-3 and AIS (SIR, 2.3; 95% CI, 2.0-2.7). The risks of the non-cervical precancers were also increased in women with SLE with over 4-fold increased rate of vaginal HSIL (SIR, 4.3; 95% CI, 1.1-9.5) and anal HSIL (SIR, 4.3; 95% CI, 1.7-8.1) and over 3-fold increased rate of vulvar HSIL (SIR, 3.7; 95% CI, 2.3-5.5).

In Table 2, SIRs of HPV-associated precancerous lesions in women with SLE according to age at SLE diagnosis and length of follow-up are displayed. For all lesions, the highest SIR was observed in women diagnosed with SLE at younger age compared with that in those at older age. Regarding CIN2-3 and AIS, women diagnosed with SLE at <50 years of age had a nearly 3-fold higher rate compared with the female background population (SIR, 2.6; 95% CI, 2.2-3.0), whereas the SIR was 0.8 (95% CI, 0.3-1.4) in women diagnosed with SLE at age ≥50 years. Similarly, the SIR of vulvar and vaginal HSIL was higher in women diagnosed with SLE at age <50 years (SIR, 4.4; 95% CI, 2.5-6.8), whereas in women who were diagnosed after age 50 years, the SIR was 2.7 (95% CI, 1.1-5.0). All observed cases of anal HSIL occurred in women diagnosed with SLE at younger ages.

Regarding follow-up time, the increased rate of all precancerous lesions remained elevated ≥5 years after the SLE diagnosis (CIN2-3 and AIS: SIR, 2.4; 95% CI, 2.0-2.9; vulvar and vaginal HSIL: SIR, 2.9; 95% CI, 1.5-4.8; anal HSIL: SIR, 6.6; 95% CI, 2.6-12.5).

Risk of HPV-associated cancer

Table 3 shows SIRs for HPV-associated cancers in women with SLE. Compared with rates in the general female population, women with SLE had an increased rate of all HPV-associated cancers combined (SIR, 1.7; 95% CI, 1.1-2.5). For individual HPV-associated cancers, the rate of oropharyngeal cancer was over 2-fold increased (SIR, 2.5; 95% CI, 0.9-4.9) in women with SLE. Women with SLE also had increased rates of cervical cancer (SIR, 1.6; 95% CI, 0.8-2.7) and anal cancer (SIR, 1.8; 95% CI,

Table 1
SIRs of HPV-associated precancers among women with systemic lupus erythematosus

Variables	Observed	Expected	SIR	95% CI
Cervical precancer (CIN2-3 and AIS)	167	71.7	2.3	2.0-2.7
Vulvar HSIL	<25	<10	3.7	2.3-5.5
Vaginal HSIL	<5	<5	4.3	1.1-9.5
Anal HSIL	7	1.6	4.3	1.7-8.1

AIS, adenocarcinoma in situ; CIN, cervical intraepithelial neoplasia; HPV, human papillomavirus virus; HSIL, high-grade intraepithelial lesion; SIR, standardised incidence ratio.

Table 2
SIRs of HPV-associated precancers among women with SLE by age at diagnosis and length of follow-up

Variables	Observed	Expected	SIR	95% CI
Age at SLE diagnosis (y)				
Cervical precancer (CIN2-3 and AIS)				
<50	159	61.6	2.6	2.2-3.0
≥50	8	10.2	0.8	0.3-1.4
Vulvar or vaginal HSIL				
<50	16	3.7	4.4	2.5-6.8
≥50	7	2.6	2.7	1.1-5.0
Anal HSIL				
<50	7	0.9	7.7	3.0-14.5
≥50	0	—	—	—
Length of follow-up (y)				
Cervical precancer (CIN2-3 and AIS)				
<1	23	7.5	3.0	1.9-4.4
1-4	49	25.0	2.0	1.4-2.5
≥5	95	39.2	2.4	2.0-2.9
Vulvar or vaginal HSIL				
<1	<5	<5	2.2	0.0-8.5
1-4	<15	<5	5.8	2.8-10.0
≥5	<15	<5	2.9	1.5-4.8
Anal HSIL				
<1	0	—	—	—
1-4	0	—	—	—
≥5	7	1.1	6.6	2.6-12.5

AIS, adenocarcinoma in situ; CIN, cervical intraepithelial neoplasia; HPV, human papillomavirus virus; HSIL, high-grade intraepithelial lesion; SIR, standardised incidence ratio; SLE, systemic lupus erythematosus.

Table 3
SIRs of HPV-associated cancers among women with systemic lupus erythematosus

Variables	Observed	Expected	SIR	95% CI
All HPV-associated cancers combined	25	14.5	1.7	1.1-2.5
Cervical SCC and AC	12	7.4	1.6	0.8-2.7
Vulvar or vaginal SCC	<5	<5	1.1	0.2-2.7
Anal SCC	<5	<5	1.8	0.5-4.0
Oropharyngeal SCC	6	2.4	2.5	0.9-4.9

AC, adenocarcinoma; HPV, human papillomavirus virus; SCC, squamous cell carcinoma; SIR, standardised incidence ratio.

0.5-4.0), although not statistically significant. The rate of vulvar and vaginal cancer (SIR, 1.1; 95% CI, 0.2-2.7) was similar for women with SLE and females in the general population.

Table 4 shows SIRs of all HPV-associated cancers combined in women with SLE according to age at diagnosis and length of follow-up. In age-stratified analysis, the rate of HPV-associated cancer was highest in women diagnosed with SLE at age <50 years (SIR, 1.9; 95% CI, 1.0-3.1) compared with ≥50 years (SIR, 1.6; 95% CI, 0.8-2.6). Regarding follow-up, the SIR of HPV-associated cancers combined remained increased ≥5 years after the SLE diagnosis (SIR, 1.8; 95% CI, 1.1-2.8).

Pre-HPV and post-HPV vaccine era

Table 5 shows SIRs of HPV-associated precancerous lesions, and all HPV-associated cancers combined stratified according to pre-HPV vaccine era (<2012) and post-HPV vaccine era (≥2012). The SIRs of precancerous lesions were similar in the 2 periods, with SIRs for CIN2-3 and AIS being 2.0 (95% CI, 1.5-2.5) and 2.6 (95% CI, 2.1-3.1) in the pre-HPV and post-HPV vaccine era, respectively. Regarding all HPV-associated cancers combined, the SIRs were likewise similar for pre-HPV vaccine era (SIR, 1.5; 95% CI, 0.6-2.8) and post-HPV vaccine era (SIR, 1.9; 95% CI, 1.1-2.9).

The sensitivity analyses with restriction to women with minimum 2 hospital contacts with SLE included 3974 women. The associations were similar to the main analysis, but SIRs tended to be slightly higher with wider CIs (Supplemental Tables S1 and S2). Exclusion of women with diagnosis of cancer concurrent with or before SLE diagnosis revealed similar SIR estimates as found in the analyses including all women with SLE (data not shown).

DISCUSSION

In this Danish nationwide cohort study of more than 5000 women with SLE, we found that they had a more than 2 times increased risk of cervical high-grade precancer and an even higher risk of the noncervical HPV-associated precancers compared with the general female population. The overall rate of HPV-associated cancers was 1.7 times higher than background population rates. Our data reflect women of a country with organised cervical cancer screening and show a moderately, nonsignificantly elevated risk of cervical cancer in women with SLE compared with the background female population. Among the noncervical HPV-associated cancers, oropharyngeal cancer was the one associated with the highest increase in risk among women with SLE.

Table 4
SIRs of all HPV-associated cancers combined among women with SLE by age at diagnosis and length of follow-up

Variables	Observed	Expected	SIR	95% CI
Age at SLE diagnosis (y)				
<50	14	7.3	1.9	1.0-3.1
≥50	11	7.1	1.6	0.8-2.6
Length of follow-up (y)				
<1	<5	<5	0.9	0.0-3.4
1-4	<10	<5	1.7	0.7-3.2
≥5	17	9.2	1.8	1.1-2.8

HPV, human papillomavirus virus; SIR, standardised incidence ratio; SLE, systemic lupus erythematosus.

The observed 2 times higher incidence than expected of cervical high-grade precancer in women with SLE is line with previous reports from Denmark consisting of a small clinic-based study [6] and data from the Danish Pathology Registry covering the period 2008-2010 [30]. Moreover, a Swedish nationwide cohort study showed a nearly 2-fold elevated relative risk of CIN2-3 in women with SLE (hazard ratio, 1.95; 95% CI, 1.43-2.65) [31], and a US study [32] of more than 14,000 women with SLE reported an hazard ratio of 1.7 (95% CI, 1.2-2.3) for the association with CIN2-3 or cervical cancer compared with a control group of women hospitalised with hypertension. In contrast to these rather similar risk estimates, a meta-analysis [12] of 7 smaller studies reported that women with SLE had an almost 9-fold increased risk of cervical HSIL with a wide CI (pooled odds ratio, 8.7; 95% CI, 3.7-20.0). There may be several reasons explaining differences across studies. Most of the studies in the meta-analysis were undertaken in countries where cervical cancer screening is not systematically offered to the entire population [33] as it is in Denmark and Sweden [34], and there are also global differences in HPV prevalence [35]. Socioeconomic status may also play a role [36]. The US study [32] was based on claims data from 2 commercial US health plans, which primarily insure working adults and their family members, and findings may not be generalisable to the entire population.

We found that the risk of cervical cancer among women with SLE was only moderately increased and not statistically significant. In line with this, a multisite international cohort study including nearly 15,000 women with SLE from primarily North America and Europe reported a SIR for cervical cancer of 1.27 (95% CI, 0.78-1.93) [13], and country-specific data from Denmark [6], Finland [37], Sweden [38], and United States [32] have also suggested that patients with SLE have no substantially increased cervical cancer risk. It is plausible that these findings could be attributed to the benefit of the cervical cancer screening programmes in these countries. This hypothesis would require that women with SLE attend such screening programmes with a higher participation rate than the female background population, which has been shown, for example, in a US SLE cohort [39]. In contrast to this, clinic-based data from a highly specialised rheumatology department in the United Kingdom including 595 patients with SLE showed that the women in the cohort had 4-fold increased risk of cervical cancer compared with the background female population [14]. Similar magnitude of cervical cancer risk in women with SLE has been reported from Korea [17], whereas more moderately elevated risk was observed in Taiwan [18] and Israel [40].

To our knowledge, we are the first to investigate the association between SLE and the noncervical HPV-associated precancers. Nearly all anal precancers are associated with HPV, whereas the HPV-attributable fraction of vulvar and vaginal precancerous lesions is slightly lower [41]. We found that the risk of HSIL at all these anogenital sites increased in women with SLE compared with the background female population, with

Table 5

SIRs of HPV-associated precancers and all cancers combined among women with systemic lupus erythematosus according to prevaccine and postvaccine era

	Prevaccine era (<2012)				Postvaccine era (≥2012)			
Variables	Observed	Expected	SIR	95% CI	Observed	Expected	SIR	95% CI
Cervical precancer (CIN2-3 and AIS)	54	27.3	2.0	1.5-2.5	110	43.1	2.6	2.1-3.1
Vulvar and vaginal HSIL	7	1.8	3.8	1.5-7.2	15	4.2	3.6	2.0-5.6
Anal HSIL	0	—	—	—	7	1.0	6.8	2.7-12.7
All HPV-associated cancers combined	7	4.8	1.5	0.6-2.8	17	9.0	1.9	1.1-2.9

AIS, adenocarcinoma in situ; CIN, cervical intraepithelial neoplasia; HPV, human papillomavirus; HSIL, high-grade intraepithelial lesion; SIR, standardised incidence ratio.

SIRs being even higher than for cervical precancerous lesions although CIs were wider because of the rarer occurrence of noncervical anogenital precancers. The corresponding cancers were also rare both in our SLE cohort and in the background female population. The SIR was statistically nonsignificantly increased for anal cancer, of which 90% are estimated to be caused by HPV [41]. The HPV-attributable fraction of vulvar and vaginal cancer is approximately 30% and 70%, respectively [41], and we found no increased risk for these cancers among women with SLE. Two studies originating from Denmark and United Kingdom previously reported on the association between SLE and anal cancer, respectively [6,14]. Both studies reported a markedly increased risk based on data from highly specialised rheumatology departments, potentially making them prone to selection bias due to a higher number of patients with SLE with severe disease. Our risk estimate for vulvar/vaginal cancer was not increased, but it was based on very few cases and the CI was wide. Recent data from Finland [37] and from the international multicenter SLE cohort mentioned earlier [13] reported an elevated SIR for vaginal/vulvar cancer and vaginal cancer, respectively, but with wide CIs including 1. The multicenter study found a statistically significantly elevated SIR for vulvar cancer [13], and 2 large-scaled studies reporting on vulvar/vaginal cancers observed that women with SLE had statistically significantly increased risk of these 2 cancer types [6,15,16]. Thus, the current literature points toward an elevated relative risk of the noncervical HPV-associated cancers in patients with SLE.

Regarding oropharyngeal cancer, our data showed that women with SLE had a nearly 3 times increased risk when compared with the female background population, and this is in accordance with previous data from Denmark [7] and Asia [15,42,43]. The Asian studies originated from Korea [17,42] and Taiwan [18,43] and all reported approximately a doubling of oropharyngeal cancer risk in patients with SLE compared with background population rates.

The observed findings of increased rates for HPV-associated precancerous lesions and for all cancers combined among women with SLE did not appear to be due to surveillance bias as risk was elevated throughout more than 5 years after the SLE diagnosis. This also seems plausible as gynaecologic examination is rarely involved in the diagnosis of SLE [44]. We also observed that the increased risks were higher for women diagnosed with SLE before the age of 50 years. Some studies have shown that SLE diagnosed at early age is often more severe, which could suggest that SLE disease severity is a contributing factor to the persistence of HPV infection [27,28]. Our findings thus emphasise the failure to clear HPV infections in SLE that could be caused by the treatment or the underlying disease. Use of immunosuppressives may be associated with an increased risk of cervical precancerous lesions and cancer in women with SLE, however, most previous results have not been statistically significant [32,45–47].

In our study, we also examined whether there were any differences in the association between SLE and HPV-associated precancer and cancer before and after implementation of HPV vaccination. Denmark introduced the vaccine in the childhood vaccination programme to 12-year-old girls in 2009 with simultaneous catch-up vaccination of young women up to the age of 27 years, and HPV vaccine effectiveness at the population level against cervical lesions has already been documented [48]. In this study, we observed no variation in SIRs according to pre-HPV and post-HPV vaccine era, suggesting that women with SLE had vaccination rates similar to the background female population. Any evaluation of the potential effect of HPV vaccination in women with SLE would require individual-level information on HPV vaccination status and separate analyses for vaccinated and unvaccinated women with SLE. We linked our cohort to 2 nationwide Danish registries with complete vaccination information [49,50] and found that only 13% of the women with SLE in our study cohort had received the HPV vaccine making analyses of HPV vaccine effectiveness in this patient group impossible.

Our study has several strengths. It is the first to report HPV-associated precancerous lesions for noncervical anogenital sites using data derived from high-quality nationwide registries in women with SLE and with virtually complete follow-up. However, we also had some limitations. Except for age and calendar year of diagnosis, we were not able to consider other potential confounders, such as body mass index, smoking, immunosuppressive therapy, screening attendance, and sexual habits, which could possibly have influenced the association between SLE and subsequent HPV-associated precancerous lesions and cancer.

In conclusion, this study is the first nationwide cohort study to show that women with SLE are at increased risk of developing not only cervical but also noncervical HPV-associated precancerous lesions. Regarding HPV-associated cancers, oropharyngeal cancer was the one associated with the strongest increase in risk. These findings could reflect that Danish women with SLE might have higher cervical cancer screening rates than the background female population and benefit from the screening programme in regard to not only cervical cancer but potentially also the noncervical anogenital cancers. Overall, our study findings are in alignment with a hypothesis of reduced ability to clear HPV infections in patients with SLE and supports close monitoring of women with SLE for HPV-associated precancerous lesions and cancer. More research is needed to fully uncover the biological mechanisms explaining the association between SLE disease-specific manifestations and increased risk of HPV-associated precancerous lesions and cancer.

Competing interests

SKK has received speaker fee from MSD and research grant through her research institution from Merck. SJ has participated

on a data safety monitoring advisory board for Lundbeck Pharma. All other authors report no conflicts of interest.

Contributors

KZS and LB were responsible for conceptualisation, methodology, investigation, and writing the original draft. LD, HCBL, and SJ conceived the study and reviewed and edited the manuscript. RH-L performed the methodology, software, and analyses. SKK was responsible for conceptualisation, funding, methodology, investigation, review and editing of the manuscript, and supervision. SKK is the guarantor.

Funding

This work was supported by grants from the University of Copenhagen (Department of Clinical Medicine) and the Independent Research Fund Denmark (0134-00473B).

Patient consent for publication

Not applicable.

Ethics approval

The study used exclusively register data and did not need ethical approval. In agreement with the General Data Protection Regulation, the project is registered in the Danish Cancer Society's internal list of projects dealing with personalised data (journal number: 2019-DCRC-0094).

Provenance and peer review

Not commissioned; externally peer reviewed.

Data availability statement

All data related to the project are stored at the Danish Cancer Institute's project database at Statistics Denmark (project number 704874) where all statistical analyses were performed. The data are available after application to and permission from Statistic Denmark. Further information is available from the corresponding author upon request.

Supplementary materials

Supplementary material associated with this article can be found in the online version at doi:10.1016/j.ard.2025.01.026.

REFERENCES

[1] Kaul A, Gordon C, Crow MK, Touma Z, Urowitz MB, van Vollenhoven R, et al. Systemic lupus erythematosus. Nat Rev Dis Primers 2016;2:16039. doi: 10.1038/nrdp.2016.39.

[2] Bertsias GK, Cervera R, Boumpas DT. Systemic lupus erythematosus: pathogenesis and clinical features. In: Bijlsma JWJ, Hachulla E, editors. Eular textbook on rheumatic diseases. London: BMJ; 2012. p. 476–505.

[3] Faurschou M, Starklint H, Halberg P, Jacobsen S. Prognostic factors in lupus nephritis: diagnostic and therapeutic delay increases the risk of terminal renal failure. J Rheumatol 2006;33(8):1563–9.

[4] Urowitz MB, Gladman DD, Abu-Shakra M, Farewell VT. Mortality studies in systemic lupus erythematosus. Results from a single center. III. Improved survival over 24 years. J Rheumatol 1997;24(6):1061–5.

[5] Lerang K, Gilboe IM, Steinar Thelle D, Gran JT. Mortality and years of potential life loss in systemic lupus erythematosus: a population-based cohort study. Lupus 2014;23(14):1546–52. doi: 10.1177/0961203314551083.

[6] Dreyer L, Faurschou M, Mogensen M, Jacobsen S. High incidence of potentially virus-induced malignancies in systemic lupus erythematosus: a long-term followup study in a Danish cohort. Arthritis Rheum 2011;63(10):3032–7. doi: 10.1002/art.30483.

[7] Westermann R, Zobbe K, Cordtz R, Haugaard JH, Dreyer L. Increased cancer risk in patients with cutaneous lupus erythematosus and systemic lupus erythematosus compared with the general population: a Danish nationwide cohort study. Lupus 2021;30(5):752–61. doi: 10.1177/0961203321990106.

[8] Ryerson AB, Peters ES, Coughlin SS, Chen VW, Gillison ML, Reichman ME, et al. Burden of potentially human papillomavirus-associated cancers of the oropharynx and oral cavity in the US, 1998-2003. Cancer 2008;113(10 Suppl):2901–9. doi: 10.1002/cncr.23745.

[9] Schiffman M, Kjaer SK. Chapter 2: natural history of anogenital human papillomavirus infection and neoplasia. J Natl Cancer Inst Monogr 2003(31):14–9. doi: 10.1093/oxfordjournals.jncimonographs.a003476.

[10] Garcia-Pineres AJ, Hildesheim A, Herrero R, Trivett M, Williams M, Atmetlla I, et al. Persistent human papillomavirus infection is associated with a generalized decrease in immune responsiveness in older women. Cancer Res 2006;66(22):11070–6. doi: 10.1158/0008-5472.CAN-06-2034.

[11] Sasagawa T, Takagi H, Makinoda S. Immune responses against human papillomavirus (HPV) infection and evasion of host defense in cervical cancer. J Infect Chemother 2012;18(6):807–15. doi: 10.1007/s10156-012-0485-5.

[12] Zard E, Arnaud L, Mathian A, Chakhtoura Z, Hie M, Touraine P. Increased risk of high grade cervical squamous intraepithelial lesions in systemic lupus erythematosus: a meta-analysis of the literature. Autoimmun Rev 2014;13(7):730–5. doi: 10.1016/j.autrev.2014.03.001.

[13] Bernatsky S, Ramsey-Goldman R, Labrecque J, Joseph L, Boivin JF, Petri M, et al. Cancer risk in systemic lupus: an updated international multi-centre cohort study. J Autoimmun 2013;42:130–5. doi: 10.1016/j.jaut.2012.12.009.

[14] Dey D, Kenu E, Isenberg DA. Cancer complicating systemic lupus erythematosus — a dichotomy emerging from a nested case-control study. Lupus 2013;22(9):919–27. doi: 10.1177/0961203313497118.

[15] Chen YJ, Chang YT, Wang CB, Wu CY. Malignancy in systemic lupus erythematosus: a nationwide cohort study in Taiwan. Am J Med 2010;123(12):1150.e1–. doi: 10.1016/j.amjmed.2010.08.006.

[16] Parikh-Patel A, White RH, Allen M, Cress R. Risk of cancer among rheumatoid arthritis patients in California. Cancer Causes Control 2009;20(6):1001–10. doi: 10.1007/s10552-009-9298-y.

[17] Bae EH, Lim SY, Han KD, Jung JH, Choi HS, Kim CS, et al. Systemic lupus erythematosus is a risk factor for cancer: a nationwide population-based study in Korea. Lupus 2019;28(3):317–23. doi: 10.1177/0961203319826672.

[18] Yu KH, Kuo CF, Huang LH, Huang WK, See LC. Cancer risk in patients with inflammatory systemic autoimmune rheumatic diseases: a nationwide population-based dynamic cohort study in Taiwan. Medicine (Baltimore) 2016;95(18):e3540. doi: 10.1097/MD.0000000000003540.

[19] Lynge E, Sandegaard JL, Rebolj M. The Danish National Patient Register. Scand J Public Health 2011;39(7 Suppl):30–3. doi: 10.1177/1403494811401482.

[20] Andersen TF, Madsen M, Jorgensen J, Mellemkjoer L, Olsen JH. The Danish National Hospital Register. A valuable source of data for modern health sciences. Dan Med Bull 1999;46(3):263–8.

[21] Bjerregaard B, Larsen OB. The Danish Pathology Register. Scand J Public Health 2011;39(7 Suppl):72–4. doi: 10.1177/1403494810393563.

[22] The Danish Cancer Registry [Internet]. 2022 Available from: https://sundhedsdatastyrelsen.dk/da/registre-og-services/om-de-nationale-sundhedsregistre/sygdomme-laegemidler-og-behandlinger/cancerregisteret.

[23] Storm HH. Completeness of cancer registration in Denmark 1943-1966 and efficacy of record linkage procedures. Int J Epidemiol 1988;17(1):44–9. doi: 10.1093/ije/17.1.44.

[24] Storm HH, Michelsen EV, Clemmensen IH, Pihl J. The Danish Cancer Registry — history, content, quality and use. Dan Med Bull 1997;44(5):535–9.

[25] The Civil Registration System [Internet]. 2022. Available from: http://www.cpr.dk.

[26] Pedersen CB. The Danish Civil Registration System. Scand J Public Health 2011;39(7 Suppl):22–5. doi: 10.1177/1403494810387965.

[27] Ambrose N, Morgan TA, Galloway J, Ionnoau Y, Beresford MW, Isenberg DA, UK JSLE Study Group. Differences in disease phenotype and severity in SLE across age groups. Lupus 2016;25(14):1542–50. doi: 10.1177/0961203316644333.

[28] Merola JF, Bermas B, Lu B, Karlson EW, Massarotti E, Schur PH, et al. Clinical manifestations and survival among adults with (SLE) according to age at diagnosis. Lupus 2014;23(8):778–84. doi: 10.1177/0961203314526291.

[29] R Core Team. R: a language and environment for statistical computing. Vienna, Austria: R Foundation for Statistical Computing; 2020.

[30] Dugue PA, Lynge E, Rebolj M. Increased risk of high-grade squamous intraepithelial lesions in systemic lupus erythematosus: additional data from Denmark. Autoimmun Rev 2014;13(12):1241–2. doi: 10.1016/j.autrev.2014.08.004.
[31] Wadstrom H, Arkema EV, Sjowall C, Askling J, Simard JF. Cervical neoplasia in systemic lupus erythematosus: a nationwide study. Rheumatology 2017;56(4):613–9. doi: 10.1093/rheumatology/kew459.
[32] Kim SC, Glynn RJ, Giovannucci E, Hernández-Díaz S, Liu J, Feldman S, et al. Risk of high-grade cervical dysplasia and cervical cancer in women with systemic inflammatory diseases: a population-based cohort study. Ann Rheum Dis 2015;74(7):1360–7. doi: 10.1136/annrheumdis-2013-204993.
[33] Bruni L, Serrano B, Roura E, Alemany L, Cowan M, Herrero R, et al. Cervical cancer screening programmes and age-specific coverage estimates for 202 countries and territories worldwide: a review and synthetic analysis. Lancet Glob Health 2022;10(8):e1115–e27. doi: 10.1016/S2214-109X(22)00241-8.
[34] Pedersen K, Fogelberg S, Thamsborg LH, Clements M, Nygård M, Kristiansen IS, et al. An overview of cervical cancer epidemiology and prevention in Scandinavia. Acta Obstet Gynecol Scand 2018;97(7):795–807. doi: 10.1111/aogs.13313.
[35] Forman D, de Martel C, Lacey CJ, Soerjomataram I, Lortet-Tieulent J, Bruni L, et al. Global burden of human papillomavirus and related diseases. Vaccine 2012;30(Suppl 5):F12–23. doi: 10.1016/j.vaccine.2012.07.055.
[36] Douglas E, Waller J, Duffy SW, Wardle J. Socioeconomic inequalities in breast and cervical screening coverage in England: are we closing the gap? J Med Screen 2016;23(2):98–103. doi: 10.1177/0969141315600192.
[37] Tallbacka KR, Pettersson T, Pukkala E. Increased incidence of cancer in systemic lupus erythematosus: a Finnish cohort study with more than 25 years of follow-up. Scand J Rheumatol 2018;47(6):461–4. doi: 10.1080/03009742.2017.1384054.
[38] Bjornadal L, Lofstrom B, Yin L, Lundberg IE, Ekbom A. Increased cancer incidence in a Swedish cohort of patients with systemic lupus erythematosus. Scand J Rheumatol 2002;31(2):66–71. doi: 10.1080/03009740252937568.
[39] Bruera S, Lei X, Zogala R, Pundole X, Zhao H, Giordano SH, et al. Cervical cancer screening in women with systemic lupus erythematosus. Arthritis Care Res (Hoboken) 2021;73(12):1796–803. doi: 10.1002/acr.24414.
[40] Azrielant S, Tiosano S, Watad A, Mahroum N, Whitby A, Comaneshter D, et al. Correlation between systemic lupus erythematosus and malignancies: a cross-sectional population-based study. Immunol Res 2017;65(2):464–9. doi: 10.1007/s12026-016-8885-8.
[41] Serrano B, de Sanjose S, Tous S, Quiros B, Muñoz N, Bosch X, et al. Human papillomavirus genotype attribution for HPVs 6, 11, 16, 18, 31, 33, 45, 52 and 58 in female anogenital lesions. Eur J Cancer 2015;51(13):1732–41. doi: 10.1016/j.ejca.2015.06.001.
[42] Han JY, Kim H, Jung SY, Jang EJ, Cho SK, Sung YK. Increased risk of malignancy in patients with systemic lupus erythematosus: population-based cohort study in Korea. Arthritis Res Ther 2021;23(1):270. doi: 10.1186/s13075-021-02648-y.
[43] Chang SL, Hsu HT, Weng SF, Lin YS. Impact of head and neck malignancies on risk factors and survival in systemic lupus erythematosus. Acta Otolaryngol 2013;133(10):1088–95. doi: 10.3109/00016489.2013.800228.
[44] Johnson SR, Brinks R, Costenbader KH, Daikh D, Mosca M, Ramsey-Goldman R, et al. Performance of the 2019 EULAR/ACR classification criteria for systemic lupus erythematosus in early disease, across sexes and ethnicities. Ann Rheum Dis 2020;79(10):1333–9. doi: 10.1136/annrheumdis-2020-217162.
[45] Feldman CH, Liu J, Feldman S, Solomon DH, Kim SC. Risk of high-grade cervical dysplasia and cervical cancer in women with systemic lupus erythematosus receiving immunosuppressive drugs. Lupus 2017;26(7):682–9. doi: 10.1177/0961203316672928.
[46] Blumenfeld Z, Lorber M, Yoffe N, Scharf Y. Systemic lupus erythematosus: predisposition for uterine cervical dysplasia. Lupus 1994;3(1):59–61. doi: 10.1177/096120339400300112.
[47] Ognenovski VM, Marder W, Somers EC, Johnston CM, Farrehi JG, Selvaggi SM, et al. Increased incidence of cervical intraepithelial neoplasia in women with systemic lupus erythematosus treated with intravenous cyclophosphamide. J Rheumatol 2004;31(9):1763–7.
[48] Ring LL, Munk C, Galanakis M, Tota JE, Thomsen LT, Kjaer SK. Incidence of cervical precancerous lesions and cervical cancer in Denmark from 2000 to 2019: Population impact of multi-cohort vaccination against human papillomavirus infection. Int J Cancer 2023;152(7):1320–7. doi: 10.1002/ijc.34328.
[49] Andersen JS, Olivarius Nde F, Krasnik A. The Danish National Health Service Register. Scand J Public Health 2011;39(7 Suppl):34–7. doi: 10.1177/1403494810394718.
[50] Kildemoes HW, Sorensen HT, Hallas J. The Danish National Prescription Registry. Scand J Public Health 2011;39(7 Suppl):38–41. doi: 10.1177/1403494810394717.

Ann Rheum Dis 84 (2025) 767−776

Contents lists available at ScienceDirect

Annals of the Rheumatic Diseases

journal homepage: https://www.sciencedirect.com/journal/annals-of-the-rheumatic-diseases

Systemic lupus erythematosus

Reduced organ damage accumulation in adult patients with SLE on anifrolumab plus standard of care compared to real-world external controls

Zahi Touma[1,2,*], Ian N. Bruce[3,4], Richard Furie[5], Eric Morand[6], Raj Tummala[7], Shelly Chandran[8], Gabriel Abreu[9], Jacob Knagenhjelm[9], Kellyn Arnold[10], Hopin Lee[10], Eleanor Ralphs[10], Aleksandr Bedenkov[11], Danuta Kielar[11], Miina Waratani[11]

[1] *Schroeder Arthritis Institute, Krembil Research Institute, University Health Network, Toronto, ON, Canada*
[2] *University of Toronto Lupus Clinic, Centre for Prognosis Studies in Rheumatic Diseases, Toronto Western Hospital, Toronto, ON, Canada*
[3] *Centre for Musculoskeletal Research, Faculty of Biology, Medicine and Health, University of Manchester, Manchester, UK*
[4] *Centre for Public Health, Faculty of Medicine, Health and Life Sciences, Queens University Belfast, Belfast, UK*
[5] *Division of Rheumatology, Zucker School of Medicine at HofstraNorthwell Health, Great Neck, NY, USA*
[6] *Centre for Inflammatory Diseases, Monash University, Melbourne, VIC, Australia*
[7] *AstraZeneca, BioPharmaceuticals R&D, Gaithersburg, MD, USA*
[8] *AstraZeneca, Medical and Scientific Affairs, R&I, Mississauga, ON, Canada*
[9] *AstraZeneca, BioPharmaceuticals R&D, Gothenburg, Sweden*
[10] *IQVIA, Europe, Middle East, and Africa (EMEA) Real World Methods and Evidence Generation, London, UK*
[11] *AstraZeneca, BioPharmaceuticals Medical, Cambridge, UK*

A R T I C L E I N F O

Article history:
Received 8 October 2024
Received in revised form 22 November 2024
Accepted 28 November 2024

A B S T R A C T

Objectives: Anifrolumab is approved for the treatment of systemic lupus erythematosus (SLE). We aimed to determine if anifrolumab plus standard of care (SOC) was associated with reduced organ damage accumulation in adult patients with moderately to severely active SLE compared to real-world (RW) external controls from the University of Toronto Lupus Clinic (UTLC) cohort who received SOC only.

Methods: Patients who initiated 300 mg anifrolumab in the TULIP (Treatment of Uncontrolled Lupus via the Interferon Pathway) trials were included in the anifrolumab arm; key eligibility criteria were applied to the UTLC to create the RW SOC arm. Propensity score and censoring weighting were used to account for baseline confounding and loss to follow-up. The primary endpoint was change in Systemic Lupus International Collaborating Clinics/American College of Rheumatology Damage Index (SDI) score from baseline to week 208, and the secondary endpoint was time to first SDI score increase.

Results: 354 patients were included in the anifrolumab arm, and 561 patients were included in the RW SOC arm. Following weighting, mean change in SDI was 0.416 points lower (95% CI: −0.582, −0.249; $P < .001$) in the anifrolumab arm than in the RW SOC arm. Patients in the anifrolumab arm were 59.9% less likely (hazard ratio: 0.401; 95% CI: 0.213, 0.753, $P = .005$) to experience an increase in SDI within 208 weeks.

*Correspondence to** Dr Zahi Touma, Toronto Western Hospital, Toronto, Ontario, Canada.
E-mail address: Zahi.Touma@uhn.ca (Z. Touma).
Handling editor Josef S. Smolen.

https://doi.org/10.1016/j.ard.2025.01.025

Conclusions: Patients who received anifrolumab accumulated significantly less organ damage after 208 weeks than patients who received RW SOC. The addition of anifrolumab to SOC is effective at preventing and/or delaying organ damage in patients with moderately to severely active SLE.

WHAT IS ALREADY KNOWN ON THIS TOPIC

- Patients with systemic lupus erythematosus (SLE) typically accumulate irreversible organ damage due to uncontrolled disease activity, disease flares, and long-term glucocorticoid treatment.
- The accumulation of organ damage is associated with multimorbidity, increased health care costs, and increased mortality.
- Anifrolumab has previously been demonstrated to be effective for controlling disease activity while simultaneously reducing the dose of glucocorticoids; however, its long-term effectiveness for preventing organ damage requires further elucidation.

WHAT THIS STUDY ADDS

- This study demonstrates that anifrolumab plus standard of care (SOC) is effective at reducing organ damage accumulation and prolonging time to organ damage progression compared to SOC alone over 4 years.

HOW THIS STUDY MIGHT AFFECT RESEARCH, PRACTICE OR POLICY

- These results support the use of anifrolumab plus SOC as a safe and effective long-term treatment for SLE, which may assist clinicians in determining the appropriate treatment for patients with SLE.

INTRODUCTION

Systemic lupus erythematosus (SLE) is an autoimmune disease that can lead to widespread inflammation and tissue damage in the affected organs [1]. Treatment for SLE aims to achieve remission or low disease activity and prevention of disease flares. Conventional standard of care (SOC) consists primarily of antimalarials, glucocorticoids, immunosuppressants, and nonsteroidal anti-inflammatory drugs [2]. However, numerous studies have demonstrated that irreversible organ damage accrual in SLE is linked to uncontrolled disease activity, disease flares, and long-term glucocorticoid treatment [3−5]. Early diagnosis and treatment with advanced therapies to reduce disease activity and reliance on glucocorticoids is recommended to prevent organ damage accrual in patients with SLE [6].

Type 1 interferons (T1IFNs) play an important role in the pathogenesis of SLE, and T1IFN antagonists have demonstrated efficacy for the treatment of SLE [7,8]. Anifrolumab is a human immunoglobulin G1 kappa monoclonal antibody that inhibits the biologic activity of T1IFNs by binding to the common T1IFN receptor. Anifrolumab has been evaluated in 2 separate 52-week phase 3, randomised, double-blind trials known as the TULIP (Treatment of Uncontrolled Lupus via the Interferon Pathway) trials (ClinicalTrials.gov identifiers: NCT02446912 and NCT02446899) [9,10]. In TULIP-2, the efficacy of anifrolumab compared to placebo after 1 year of treatment was demonstrated using the British Isles Lupus Assessment Group (BILAG)-based Composite Lupus Assessment (BICLA) response criterion, in patients with moderate to severely active SLE receiving SOC treatment [8,11]; these findings were supported by TULIP-1 [12]. A 3-year long-term extension (LTE) of the trials also supported the long-term safety, tolerability, and efficacy of anifrolumab (ClinicalTrials.gov identifier: NCT02794285) [13,14]. Anifrolumab has been approved for use in over 50 countries, including United States, Europe, Canada, Australia, and Japan [15−17].

Although anifrolumab has been shown to reduce disease activity and promote reduction of glucocorticoids [14,18,19], its long-term effectiveness for preventing organ damage compared to SOC requires further elucidation. Patients who received placebo in TULIP-1 or -2 were randomised at a 4:1 ratio to switch to anifrolumab plus SOC in the LTE study, and there was a high dropout rate in the placebo arm. Of the 368 patients allocated to the placebo arm in TULIP-1 or -2, 270 (73.4%) completed the initial year-long study, and only 54 (14.7%) completed the LTE study while still receiving placebo. In comparison, 361 patients were allocated to receive 300 mg of anifrolumab in TULIP-1 or -2, 296 (82.0%) completed the initial year-long study, and 178 (49.3%) completed the LTE study while still receiving anifrolumab [8,18,19]. Previous analyses found that mean Systemic Lupus International Collaborating Clinics/American College of Rheumatology Damage Index (SDI) score remained stable across treatment arms in the LTE study [14]. However, the high attrition rate in the placebo arm and the discrepancy in completion rates across arms prevented accurate analysis of the long-term impact of anifrolumab on damage accrual directly in the trial dataset, resulting in the need for alternative forms of evidence generation. It is also of interest to understand how changes in organ damage observed in the TULIP trials among patients who received anifrolumab compared to real-world (RW) evidence.

In this study, we estimated the effectiveness of anifrolumab on preventing organ damage over 4 years in adult patients with moderately to severely active SLE using a RW external control arm from the University of Toronto Lupus Clinic (UTLC). We also estimated the effectiveness of anifrolumab on prolonging time to organ damage progression.

METHODS

Study design

This was a retrospective study that compared patients who initiated 300 mg of anifrolumab while receiving stable SOC treatment in TULIP-1 and -2 (ie, the ‘anifrolumab arm’) to external controls in the UTLC who received RW SOC (ie, the ‘RW SOC arm’).

Patients in the anifrolumab arm were indexed at anifrolumab initiation and were followed until the earliest of death, loss to follow-up, or week 208 assessment in the LTE study. Patients in the RW SOC arm were indexed at the first instance of meeting all eligibility criteria in which they were receiving ≥1 eligible SOC treatment (their ‘index assessment’) between January 1, 1995, and December 31, 2023 [20]; they were followed until the earliest of death, loss to follow-up, or December 31, 2023.

Data sources

This study used data from the TULIP trials (-1, -2, and LTE) and from the UTLC. The TULIP trials were conducted between

2015 and 2021. TULIP-1 evaluated the efficacy and safety of 2 doses of anifrolumab (150 mg and 300 mg) vs placebo [9], while TULIP-2 evaluated the efficacy and safety of 300 mg of anifrolumab vs placebo [10], both after 52 weeks of treatment. Patients who initiated 300 mg of anifrolumab in TULIP-1 or -2 were able to continue receiving treatment in the LTE study for up to 156 additional weeks (ie, 3 years) [13]. Across all trials, patients were assessed every 4 weeks according to a standardised protocol that included demographic, clinical, laboratory, and treatment measurements.

The UTLC was established in 1970 in Toronto, Ontario, Canada and has since enrolled patients with SLE as part of a prospective cohort study [21]. Patients are typically assessed every 3 to 4 months according to a standardised protocol that includes demographic, clinical, laboratory, and treatment measurements.

Patient selection

All eligible patients who initiated 300 mg of anifrolumab in TULIP-1 or -2 were included in the anifrolumab arm (regardless of subsequent enrolment in the LTE study). Patients in the UTLC were included in the RW SOC arm if they met key eligibility criteria from TULIP-1 and -2. Inclusion criteria (evaluated at index) were: aged 18 to 70; weight ≥40.0 kg; diagnosis of SLE ≥24 weeks prior using ≥4 of the 11 modified American College of Rheumatology classification criteria, with ≥1 positive antinuclear antibody test, anti-dsDNA antibodies, or elevated anti-Smith antibody; Systemic Lupus Erythematosus Disease Activity Index 2000 (SLEDAI-2K) ≥6 points; no record of current pregnancy; and valid measurement of SDI score. Exclusion criteria (evaluated at index) were: glucocorticoid dose >40 mg/d (oral prednisone equivalent); current receipt of any biologic agent or within 4 weeks prior; record of prior malignancy, except skin malignancy ≥1 year prior; record of persistent, new, or recurrent nephrotic syndrome, chronic dialysis, or renal transplant; or serum creatinine >2.0 mg/dL.

Treatment strategies

The active exposure was 300 mg of anifrolumab, delivered intravenously every 4 weeks, in combination with SOC. Eligible SOC included glucocorticoids, antimalarials, and immunosuppressants. Patients were not allowed to initiate new antimalarials or immunosuppressants, and dosage was required to remain stable through week 52. Between weeks 8 to 40, glucocorticoid dose tapering to ≤7.5 mg/d was attempted in all patients with a baseline dose of ≥10 mg/d.

The comparison exposure was RW SOC, delivered according to standard clinical practice in the UTLC. Eligible SOC included glucocorticoids, antimalarials, and immunosuppressants, without restriction on dosage or length of treatment.

Outcomes

We used SDI score to assess irreversible damage across 12 organ systems. SDI is a validated measure that has been used in clinical trials and RWD analyses [3,21−23]; its score can range from 0 to 46 points [24]. In TULIP-1 and -2, SDI was assessed at weeks 0, 24, and 52; in the LTE study, SDI was assessed at weeks 104, 156, and 208. In the UTLC, SDI has been assessed prospectively on an annual basis since 1995 [21].

The primary study endpoint was change in SDI from index date to week 208. The value of SDI at week 208 was derived in study participants with ≥208 weeks of follow-up. For patients in the anifrolumab arm, SDI at week 208 was used if available; otherwise, since SDI values cannot decrease over time, its value was imputed by carrying forward the most recently recorded value. For patients in the RW SOC arm, SDI at week 208 was used if available; otherwise, its value was imputed using linear interpolation from the closest values recorded before and after. For study participants with <208 weeks of follow-up, SDI at week 208 was considered missing due to loss to follow-up.

The secondary study endpoint was time to first SDI progression, defined as the time from index date to the first observed increase in SDI.

Baseline and confounding variables

Operational definitions of variables were harmonised across the TULIP trials and UTLC. In TULIP, baseline characteristics were recorded at randomisation or during a screening visit within 30 days before randomisation. In UTLC, baseline characteristics were recorded at the initial assessment performed upon enrolment or during the index assessment.

Baseline confounders were selected following consultation with clinical experts and a relevant study [22]. The following characteristics (evaluated at index) were considered: age; SLE duration (y); gender (as recorded); race; SLEDAI-2K score; SDI score; proteinuria; glucocorticoid use; glucocorticoid dose (mg/d, oral prednisone equivalent); antimalarial use; immunosuppressant use; high blood pressure (BP) or hypertension; and history of smoking.

The following baseline variables were also described: year of diagnosis; age at diagnosis; year of index; body mass index (BMI) at index; and serum creatinine level at index (mg/dL).

Statistical analysis

Baseline variables were described stratified by treatment arm. Continuous variables were described as mean (SD) and median (Q1, Q3), and categorical variables were described as counts and percentages. After assessing missingness patterns, missing values for baseline confounders were imputed using a 2-stage approach. First, where available, values recorded within 3 months before or after index were used for direct imputation, followed by multiple imputation.

Comparative analyses estimated the relative average treatment effect of initiating 300 mg of anifrolumab plus SOC compared to receiving RW SOC. To allow the estimated treatment effect to be generalisable to patients represented by the RW SOC arm, the average treatment effect in the control (ATC) was chosen as the primary estimand. Standardised mortality ratio weighting (SMRW) based on propensity scores was used to adjust for baseline confounding [25,26]. Standardised mean differences (SMDs) were used to assess baseline imbalance before and after SMRW [27,28]. Inverse probability of censoring weighting (IPCW) was used to account for possibly informative loss to follow-up [29].

Mean change in SDI from index to week 208 was calculated separately in each weighted treatment arm. The mean difference in change in SDI from index to week 208 between the anifrolumab and RW SOC arms was then estimated using a weighted linear regression model, which was additionally adjusted for variables that remained imbalanced (SMD ≥0.2) after SMRW. The point estimate and corresponding 95% CI and P value were estimated. As sensitivity analyses, the average treatment effect in the treated (ATT) was estimated using the same methods, and the average treatment effect in the overlap (ATO) population was estimated using 1:1 nearest-neighbour matching with

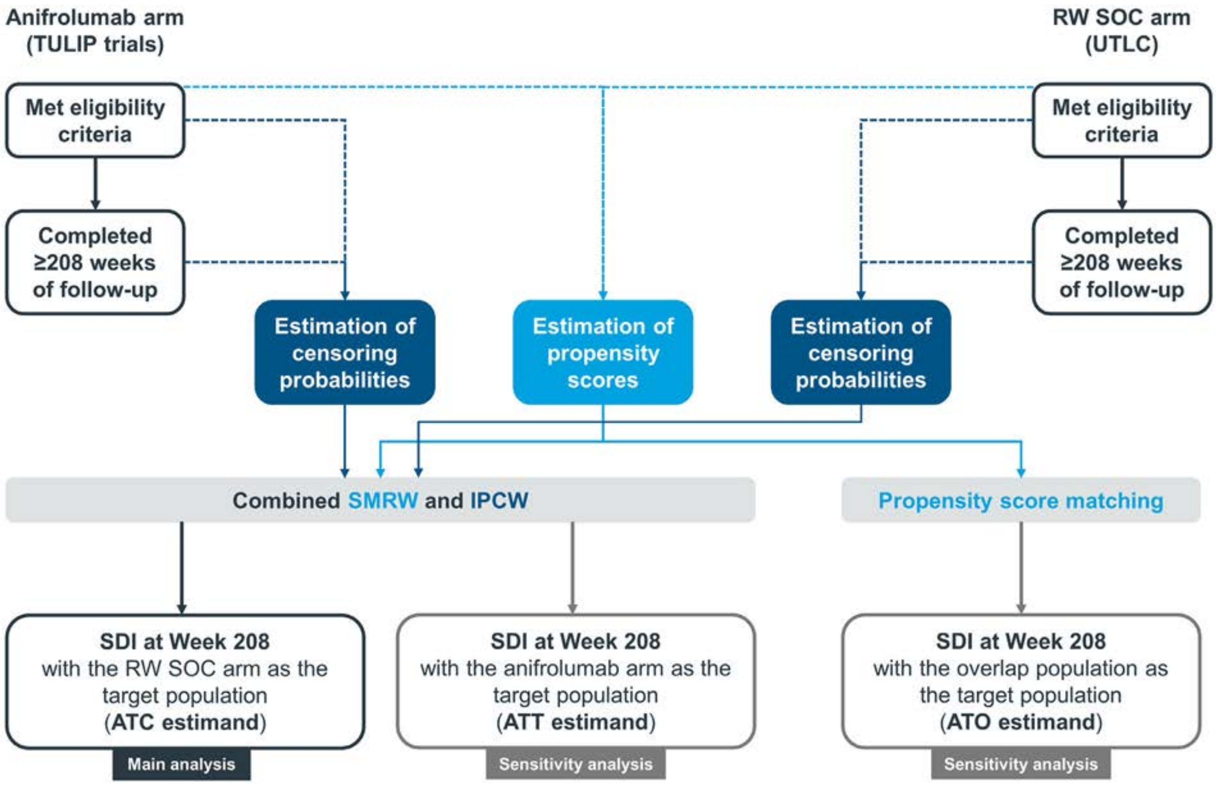

Figure 1. Diagram summarising methodology for primary study endpoint (SDI score at Week 208). ATC/ATO/ATT, average treatment effect in the control/overlap/treated population; IPCW, inverse probability of censoring weighting; RW, real-world; SOC, standard of care; SDI, Systemic Lupus International Collaborating Clinics/American College of Rheumatology Damage Index; SMRW, standardised mortality ratio weighting; TULIP, Treatment of Uncontrolled Lupus via the Interferon Pathway; UTLC, University of Toronto Lupus Clinic.

replacement. For the ATO, patients in the anifrolumab arm with ≥208 weeks of follow-up were matched to patients in the RW SOC arm with ≥208 weeks of follow-up, and no IPCW was performed. Statistical analyses for the primary objective are summarised in Figure 1.

The average treatment effect on time to first SDI increase was estimated using a Cox regression model. Death, loss to follow-up, 208 weeks post-index, and end of study period were treated as censoring events. The estimated hazard rate in each treatment arm was reported along with the comparative hazard ratio (HR), with corresponding 95% CI and P value. The survival function for each treatment group was depicted using a weighted Kaplan-Meier plot, and median survival time with 95% CI was reported.

As sensitivity analyses, all primary analyses (ATC estimand) were repeated with an indexing period in the RW SOC arm restricted to January 1, 2005 to December 31, 2023. To better understand which components of SDI drove observed increases, a post hoc analysis was also conducted in patients with ≥208 weeks of follow-up to summarise organ damage accrual within each component between index and week 208. Methodological details are provided in Supplemental Materials. All analyses were conducted using R, version 4.1.2 [30].

Patient and public involvement

There was no patient or public involvement in this study.

RESULTS

354 patients from TULIP-1 and -2 were included in the anifrolumab arm, of whom 175 completed 208 weeks of follow-up. 561 patients from the UTLC were included in the RW SOC arm, of whom 345 completed 208 weeks of follow-up.

Baseline characteristics are presented in Table 1. Compared to patients in the anifrolumab arm, patients in the RW SOC arm were generally younger at SLE diagnosis (median age: 25 vs 31 years) and at index (median age: 31 vs 42 years), were less likely to be White (48.1% vs 64.7%), had lower disease activity at index (median SLEDAI-2K: 8 vs 10 points), and were more likely to have had proteinuria at index (39.6% vs 4.8%). SOC treatments received at index also differed, with patients in the RW SOC arm more likely to be receiving glucocorticoids (96.4% vs 81.4%), antimalarials (72.2% vs 67.5%), and immunosuppressants (61.9% vs 48.0%) than patients in the anifrolumab arm. Median baseline glucocorticoid dose was also higher in the RW SOC arm than in the anifrolumab arm (12.5 vs 10.0 mg/d). Gender, SDI, high BP or hypertension, and smoking history were similar between treatment arms.

The amount of missing baseline data was low across both treatment arms, with only race, BMI, high BP or hypertension, and smoking history having missing values. Visual inspection of missingness patterns and Little's test indicated that data were not missing completely at random ($P < .01$).

Following SMRW (ATC estimand), the 2 treatment arms were adequately balanced with respect to all baseline confounding variables except SLEDAI-2K score (SMD: −0.21) and proteinuria (SMD: −0.22) (Table 2). Adequate balance was also achieved for all confounding variables when targeting the ATT estimand (results in Supplemental Table S1).

Mean change in SDI from index to week 208 was 0.162 in the weighted anifrolumab arm and 0.587 in the weighted RW SOC arm (Table 3). After additionally adjusting for SLEDAI-2K score and proteinuria, the mean change in SDI from index to week 208 was 0.416 points lower (95% CI: −0.582, −0.249; $P < .001$) in the weighted anifrolumab arm than in the RW SOC arm (ATC). The sensitivity analysis that considered the ATT

Table 1
Baseline characteristics by treatment arm

Variable	Level	Anifrolumab arm (N = 354)		RW SOC arm (N = 561)	
		N	%	N	%
Year of diagnosis	pre-1970	0	0.00%	0	0.00%
	1970-1979	3	0.85%	6	1.07%
	1980-1989	17	4.80%	23	4.10%
	1990-1999	50	14.12%	181	32.26%
	2000-2009	117	33.05%	234	41.71%
	2010-2019	167	47.18%	117	20.86%
	2020-present	0	0.00%	0	0.00%
Age at diagnosis (y)	Mean (SD)	32.60 (11.95)		27.31 (12.04)	
	Median (Q1, Q3)	31.00 (23.00, 41.00)		25.00 (18.00, 35.00)	
Year of index	1995-1999	0	0.00%	46	8.20%
	2000-2004	0	0.00%	116	20.68%
	2005-2009	0	0.00%	129	22.99%
	2010-2014	0	0.00%	122	21.75%
	2015-2019	354	100%	126	22.46%
	2020-present	0	0.00%	22	3.92%
Age at index[a] (y)	Mean (SD)	42.57 (11.97)		34.09 (12.16)	
	Median (Q1, Q3)	42.00 (34.00, 50.00)		31.00 (24.00, 43.00)	
SLE duration at index (y)[a]	Mean (SD)	9.58 (8.59)		6.78 (6.46)	
	Median (Q1, Q3)	7.00 (3.00, 15.00)		4.77 (1.60, 9.54)	
Gender[a]	Male	27	7.63%	65	11.59%
	Female	327	92.37%	496	88.41%
Race[a]	White	229	64.69%	270	48.13%
	Black	46	12.99%	121	21.57%
	Native North American	4	1.13%	6	1.07%
	Other	67	18.93%	155	27.63%
	Missing	8	2.26%	9	1.60%
BMI at index	<18.5	8	2.26%	15	2.67%
	≥18.5 and <25	145	40.96%	148	26.38%
	≥25 and <30	77	21.75%	82	14.62%
	≥30 and <35	76	21.47%	44	7.84%
	≥35	48	13.56%	10	1.78%
	Missing	0	0.00%	262	46.70%
SLEDAI-2K score at index[a]	Mean (SD)	11.38 (3.82)		10.36 (4.90)	
	Median (Q1, Q3)	10.00 (8.00, 13.00)		8.00 (6.00, 12.00)	
SDI score at index[a]	0	241	68.08%	358	63.81%
	1	59	16.67%	118	21.03%
	≥2	54	15.25%	85	15.15%
Serum creatinine level at index (mg/dL)	<0.5	20	5.65%	21	3.74%
	≥0.5 and <1.2	323	91.24%	505	90.02%
	≥1.2 and ≤2	11	3.11%	35	6.24%
Proteinuria at index[a]	Yes	17	4.80%	222	39.57%
	No	337	95.20%	339	60.43%
Glucocorticoid use at index[a]	Yes	288	81.36%	541	96.43%
	No	66	18.64%	20	3.57%
Glucocorticoid dose at index (mg/d)[a]	Mean (SD)	8.98 (7.31)		14.66 (10.16)	
	Median (Q1, Q3)	10.00 (5.00, 10,00)		12.50 (7.50, 20.00)	
Antimalarial use at index[a]	Yes	239	67.51%	405	72.19%
	No	115	32.49%	156	27.81%
Immunosuppressant use at index[a]	Yes	170	48.02%	347	61.85%
	No	184	51.98%	214	38.15%
High BP or hypertension at index[a]	Yes	114	32.20%	167	29.77%
	No	225	63.56%	393	70.05%
	Missing	15	4.24%	1	0.18%
History of smoking at index[a]	Yes	79	22.32%	120	21.39%
	No	260	73.45%	430	76.65%
	Missing	15	4.24%	11	1.96%

BMI, body mass index; BP, blood pressure; Q1/Q3, first/third quartile; RW SOC, real-world standard of care; SDI, Systemic Lupus International Collaborating Clinics/American College of Rheumatology Damage Index; SLE, systemic lupus erythematosus; SLEDAI-2K, Systemic Lupus Erythematosus Disease Activity Index 2000.

[a] Denotes confounding variable.

(−0.337; 95% CI: −0.524, −0.150; $P < .001$) was consistent with ATC results. Propensity score matching in the subgroup of patients with ≥208 weeks of follow-up also favoured treatment with anifrolumab (−0.370; 95% CI: −0.578, −0.163; $P = .002$) (all results in Table 3).

In post hoc analyses, the largest increases in SDI were observed in the musculoskeletal, ocular, and renal systems (Supplemental Table S5 and Fig S2), with the largest single-component increases observed in avascular necrosis (41 and 0 points accrued in the RW SOC and anifrolumab arms, respectively), cataracts (28 and 7 points accrued, respectively), and end-stage renal disease (15 and 0 points accrued, respectively).

Patients in the anifrolumab arm were 59.9% less likely (HR: 0.401; 95% CI: 0.213, 0.753; $P = .005$) to experience an

Table 2
Baseline confounders pre- and post-SMRW (ATC estimand)

Variable	Level	Standardised mean difference	
		Pre-SMRW	Post-SMRW
Age at index	Mean	0.70	−0.09
Age at index, squared	Mean	0.69	−0.08
SLE duration at index	Mean	0.43	0.04
Gender	Male	−0.12	−0.13
Race	White	0.33	0.13
	Black	−0.20	0.01
	Native North American	<0.01	0.07
	Other	−0.19	−0.17
SLEDAI-2K score at index	6-10 points	−0.26	−0.21
SDI score at index	0	0.09	<0.01
	1	−0.11	−0.02
	≥2	<0.01	0.02
Proteinuria at index	Yes	−0.71	−0.22
Glucocorticoid use at index	Yes	−0.81	−0.02
Glucocorticoid dose at index	<5	0.38	−0.09
	≥5 and ≤7.5	0.12	−0.11
	>7.5 and ≤10	0.28	−0.04
	>10 and ≤20	−0.27	0.08
	>20 and ≤40	−0.37	0.12
Antimalarial use at index	Yes	−0.10	0.13
Immunosuppressant use at index	Yes	−0.28	−0.03
High BP or hypertension at index	Yes	0.08	−0.13
History of smoking at index	Yes	0.03	0.05

ATC, average treatment effect in the control population; BP, blood pressure; SDI, Systemic Lupus International Collaborating Clinics/American College of Rheumatology Damage Index; SLE, systemic lupus erythematosus; SLEDAI-2K, Systemic Lupus Erythematosus Disease Activity Index 2000; SMRW, standardised mortality ratio weighting.
Note that the values in this table were obtained following imputation for missing variables.

increase in SDI score within 208 weeks than patients in the RW SOC arm (Fig 2). Early separation of the weighted Kaplan-Meier curves was observed, with an estimated 96% of patients in the anifrolumab arm (95% CI: 92%, 99%) not experiencing organ damage progression by week 52 compared to 89% of patients in the RW SOC arm (95% CI: 86%, 92%).

When the indexing period in the RW SOC arm was restricted to January 1, 2005 to December 31, 2023, 362 patients from the UTLC were included in the RW SOC arm. Results are presented in Supplemental Materials, including baseline characteristics (Supplemental Table S2) and covariate balance following SMRW (Supplemental Table S3). The mean change in SDI from index to week 208 was 0.270 points lower (95% CI: −0.429, −0.112; $P < .001$) in the weighted anifrolumab arm compared to the RW SOC arm (Supplemental Table S4). Patients in the anifrolumab arm were 41.0% less likely (HR: 0.590; 95% CI: 0.290, 1.200; $P = .138$) to experience an increase in SDI within 208 weeks than patients in the RW SOC arm (Supplemental Fig S1).

DISCUSSION

The accumulation of organ damage in patients with SLE is associated with numerous unfavourable outcomes, including multimorbidity, increased health care costs, and ultimately, increased mortality [31−35]. A recent systematic review and meta-analysis estimated that the standardised mortality ratio for patients with SLE was 2.87 times higher relative to the general population [36]. It has also been estimated that a 1-point increase in SDI is associated with a 34% increase in the relative rate of death [33]. These figures highlight the importance of controlling disease activity and reducing consumption of glucocorticoids for preventing organ damage, improving prognosis, and enhancing quality of life in patients with SLE, and are recommended strategies by the European Alliance of Associations for Rheumatology [2].

The connection between low disease activity and reduced organ damage accrual has been demonstrated in many studies [3,37−40]. Longer periods spent in Lupus Low Disease Activity State (LLDAS) or remission are associated with greater reductions in disease flare rates and organ damage accrual. Indeed, a recent study found that *any* duration of sustained LLDAS or remission >3 months was associated with reduced organ damage accrual, with increasingly longer periods of sustained LLDAS corresponding to increasingly protective associations [40]. Glucocorticoids—although a mainstay of SLE management—have also been linked to irreversible organ damage in this population [3−5,41,42].

Previous analyses of TULIP trial data have demonstrated the effectiveness of anifrolumab for controlling disease activity while simultaneously reducing glucocorticoids [14]. A post hoc analysis of TULIP-1 and -2 found that anifrolumab was

Table 3
Estimated difference between treatment arms in change in SDI score between index and 208 weeks post-index (all estimands)

Analysis	Methods			Anifrolumab arm		RW SOC arm		Estimated mean difference in change in SDI[b] (95% CI)	*P*
	Confounding adjustment	Informative censoring adjustment	Estimand	N	Mean change in SDI[a]	N	Mean change in SDI[a]		
Primary	SMRW	IPCW	ATC	354	0.162	561	0.587	−0.416 (−0.582, −0.249)	< .001
Sensitivity	SMRW	IPCW	ATT	354	0.224	561	0.561	−0.337 (−0.524, −0.150)	< .001
	Propensity score matching[c]	n/a	ATO	116	0.201	116	0.571	−0.370 (−0.578, −0.163)	.002

ATC/ATO/ATT, average treatment effect in the control/overlap/treated population; IPCW, inverse probability of censoring weighting; n/a, not applicable; RW SOC, real-world standard of care; SDI, Systemic Lupus International Collaborating Clinics/American College of Rheumatology Damage Index; SMRW, standardised mortality ratio weighting.
[a] Estimated following weighting for confounding and/or informative censoring, as specified in methods.
[b] Estimated following weighting for confounding and/or informative censoring, as specified in methods, and direct adjustment for baseline variables which remained imbalanced.
[c] 1:1 nearest-neighbour matching with replacement.

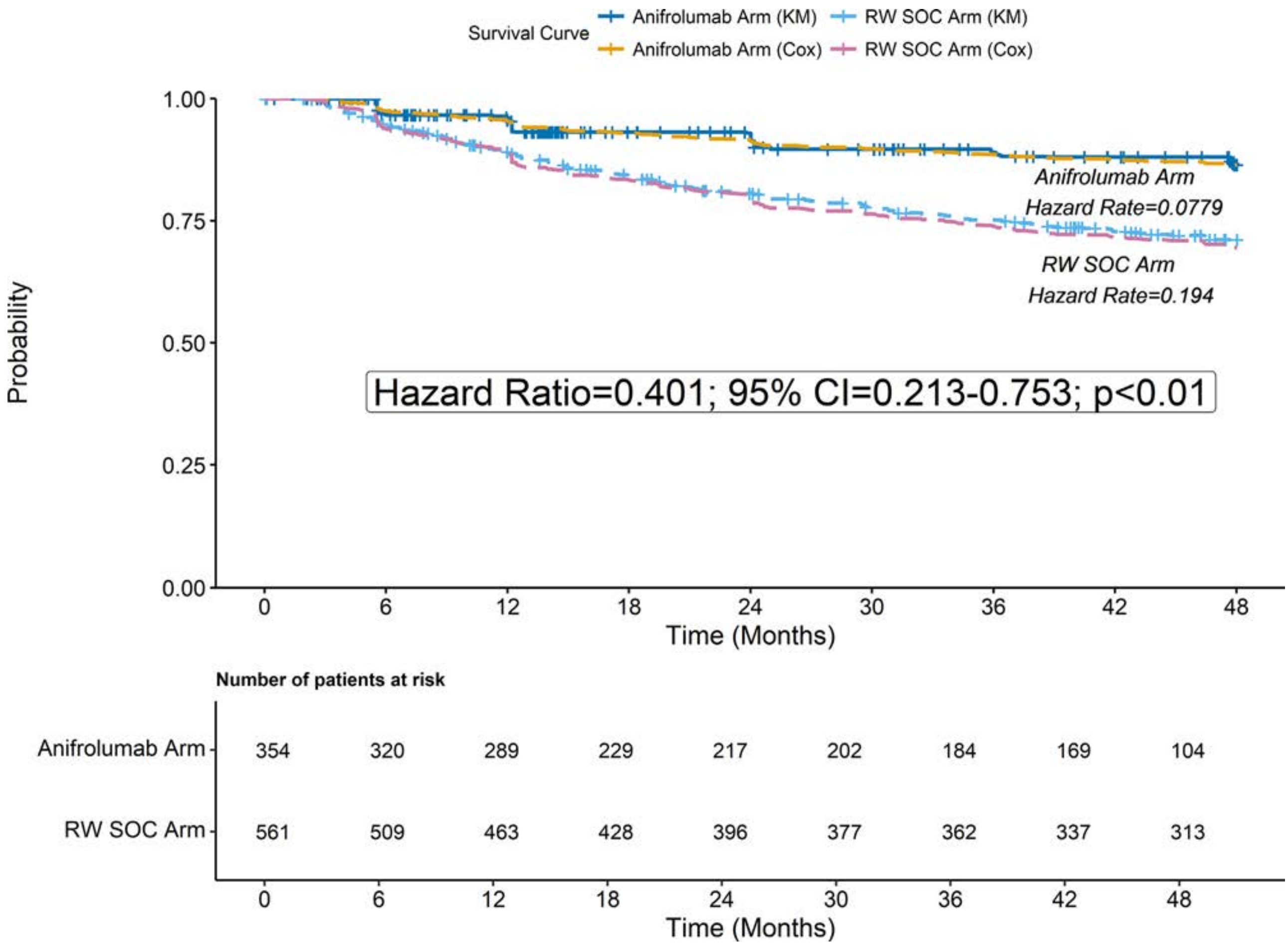

Figure 2. Kaplan-Meier curves for time to organ damage progression by treatment arm, with estimated hazard rates from fitted Cox models (ATC estimand). ATC, average treatment effect in the control population; KM, Kaplan-Meier; RW, real-world; SOC, standard of care.

associated with earlier attainment of LLDAS (HR: 1.76; 95% CI: 1.25, 2.30; $P < .001$), increased cumulative time in LLDAS (mean: 2.40 months vs 1.40 months, $P < .001$), and higher likelihood of sustained LLDAS ($P < .001$) than placebo [43]. Analyses of TULIP LTE data also found that 30.3% of patients treated with anifrolumab achieved disease remission by 4 years compared to 18.3% of patients in the placebo arm ($P = .06$) [18]. In TULIP-1 and -2, sustained glucocorticoid tapering was achieved by 51% of patients treated with anifrolumab plus SOC compared to 32% of patients treated with SOC alone ($P < .001$) [19]. However, no studies have previously demonstrated the effectiveness of anifrolumab for preventing long-term organ damage.

We used a RW external control arm to evaluate the effect of anifrolumab plus SOC in the TULIP-1 and -2 trials compared to RW SOC on long-term organ damage. After accounting for differences in baseline patient characteristics, including baseline SDI, our results suggest that anifrolumab plus SOC reduces organ damage accumulation in patients with moderately to severely active SLE. Over 4 years of follow-up, SDI increased by an average of 0.587 points in the RW SOC arm compared to 0.162 points in the anifrolumab arm, resulting in 0.416 fewer points of organ damage, on average, for patients who initiated 300 mg of anifrolumab in TULIP-1 and -2. Treatment with anifrolumab plus SOC was also associated with a 59.9% decreased risk of organ damage progression up to 4 years. Our results were consistent across 3 estimands (ie, ATT, ATC, and ATO), corresponding analytical methods (ie, propensity score weighting and matching), and inclusion period in the RW SOC arm, demonstrating robustness of study results.

The results of our study are also consistent with a previous external control arm study using the UTLC, which found that treatment with belimumab plus SOC was associated with a 0.424-point reduction in organ damage after 5 years (95% CI: −0.667, −0.201) and a 60.9% decreased risk of organ damage progression up to 5 years compared to RW SOC [22].

There are likely several mechanisms through which anifrolumab plus SOC reduces organ damage accumulation compared to RW SOC. The effects estimated in this study therefore represent a combination of causal pathways, including the direct effect of anifrolumab on controlling disease activity and its indirect effect on glucocorticoid reduction, as well as the effect of SOC restrictions imposed by the TULIP trial protocols (eg, no new antimalarials or immunosuppressants). Indeed, post hoc analyses revealed large increases in avascular necrosis and cataracts in the RW SOC arm during follow-up, both of which are linked to glucocorticoids [5]. Results should therefore be interpreted as estimates for the effect of the anifrolumab plus SOC *regimen* rather than the effect of anifrolumab alone.

Our study design and analysis were guided by the target trial emulation framework, which is increasingly used and recommended for external control studies as it provides a structured framework to help avoid common biases that typically affect analyses of RW data [44,45]. We applied key eligibility criteria from TULIP-1 and -2 to patients in the UTLC cohort to minimise selection bias, and we used propensity score weighting to minimise baseline confounding and retain a larger analytical sample than comparable matching methods. We also used censoring weighting to correct for loss to follow-up rather than conducting a complete-case analysis, which is prone to survivorship bias due to patients who responded well to treatment being more likely to remain in the study. We used data from a high-quality RW cohort which has been used for numerous other studies in SLE [3,21,22,46,47]. Loss to follow-up from the UTLC has previously been shown to be low and not influence overall outcomes [46,48]; we also observed low amounts of missing data for the variables used in this study.

The estimated average treatment effect represents a clinically meaningful reduction in organ damage given the known rate of damage accrual in patients with SLE and the association of increased damage with poorer health-related quality of life and higher mortality [49]. A study of 2054 patients in the Hopkins' Lupus Cohort found that SDI increased at a rate of only 0.13 points per year [50], while a study of 4106 patients in the Asia-Pacific Lupus Collaboration cohort found that only 20% of patients with established disease developed new organ damage over a mean follow-up time of 2.6 years [51].

While key sources of bias were minimised through appropriate design and analysis, we acknowledge that the use of propensity score methods cannot replace a randomised trial, and our study has several limitations. Differential outcome misclassification could affect results due to the combination of trial and RW data sources. However, given that SDI changes slowly over time and patients in both treatment cohorts were expected to have a recording of SDI approximately once per year, significant bias is not expected. Changes in SOC over time could also affect study results, with the most notable change being the introduction of mycophenolate mofetil in the early 2000s and biologic agents since 2020 [2,52]. For this reason, we conducted sensitivity analyses in which we restricted the inclusion period for the RW SOC arm to January 1, 2005. We also excluded RW patients who received any biologic agents within 4 weeks prior to their index date but acknowledge that patients could have received them during follow-up. Finally, while the anifrolumab and RW SOC arms were balanced at baseline, balance was not guaranteed during follow-up. Our censoring models considered only baseline covariates, but loss to follow-up could also be influenced by post-baseline factors including disease activity.

We also acknowledge that more proactive attention to glucocorticoid sparing has been a feature of more recent SLE management guidelines [2], which may have influenced results. Indeed, glucocorticoid tapering in patients with a baseline dose of ≥10 mg/d was a feature of TULIP-1 and -2, although this only affected approximately 25% of patients. There have also been temporal improvements in the screening and management of key comorbidities, such as hypertension, hyperlipidaemia, and bone protection, such that we cannot completely exclude the possibility of residual confounding. Further analyses are planned to evaluate the effects of anifrolumab on daily and cumulative glucocorticoid dose.

CONCLUSION

Compared to an external control group, we observed clinically and statistically significantly lower organ damage accrual after 4 years in patients who initiated anifrolumab in the TULIP-1 and -2 trials, as well as a longer time to first organ damage progression. In addition to the proven effectiveness of anifrolumab for controlling disease activity, attaining LLDAS and remission, and enabling glucocorticoid tapering, this study shows that anifrolumab is effective for preventing long-term organ damage compared to RW SOC. The results of our study therefore support the benefit of adding anifrolumab to SOC for minimising long-term organ damage in patients with SLE.

Competing interests

ZT does not have any conflicts of interest to disclose. INB received research grants from AstraZeneca and Janssen; received consulting fees from AstraZeneca, GSK, Eli Lilly, Takeda, Dragonfly Therapeutics, and Janssen; and received speaker fees from AstraZeneca, GSK, and Janssen. RF received grants or contracts to his institution from AstraZeneca; received consulting fees, payment or honoraria, and support for attending meetings and/or travel from AstraZeneca; and participated in data safety monitoring or advisory boards for AstraZeneca. EM received research grants to his institution from AbbVie, Amgen, AstraZeneca, Biogen, BMS, EMD Serono, Eli Lilly, Janssen, GSK, Genentech, Novartis, Takeda, and UCB; received consulting fees from AbbVie, Alpine, AstraZeneca, Biogen, BMS, Dragonfly, EMD Serono, GSK, Gilead, Janssen, Novartis, Remegen, Roche, Takeda, and UCB; received honoraria from AstraZeneca, BMS, EMD Serono, and Roche; received support for attending meetings and/or travel from EMD Serono and Roche; has WO2022074123A1, WO2021184080A1, WO2023044530A1, WO2021094378A1, and WO2023057369A2 patents planned, issued or pending; participated in advisory boards for Dragonfly; held/holds the Board Director position in Rare Voices Australia and Exosome Biosciences; and owns stock or stock options of Dragonfly Therapeutics. RT is a former employee of and received stock or stock options from AstraZeneca. SC is an employee and owns stock or stock options of AstraZeneca. GA is an employee, owns stock or stock options of AstraZeneca; and has other financial interests from AstraZeneca. JK is an employee and owns stock or stock options of AstraZeneca. KA is an employee of IQVIA Ltd. HL is an employee of IQVIA Ltd. ER is an employee of IQVIA Ltd., which is contracted and funded by AstraZeneca to develop the content of the manuscript. AB is an employee and owns stock or stock options of AstraZeneca. DK is an employee and owns stock or stock options of AstraZeneca. MW is an employee and owns stock or stock options of AstraZeneca.

Acknowledgements

The authors wish to acknowledge Zheyuan Yang and Tarana Mehdikhanova for their support in programming and analysis, and Nelly Ly for her support in study design (all IQVIA).

Contributors

RT, SC, GA, JK, AB, DK, and MW were involved in study conceptualisation. ZT contributed to data acquisition. ZT, RT, SC, GA, JK, KA, HL, ER, and MW were involved in study design and methodology. KA, HL, and ER were involved in the analysis. KA, HL, and MW were involved in writing the original draft, and all authors were involved in reviewing and editing the manuscript. MW is responsible for the overall content as guarantor.

Funding

This study was funded by AstraZeneca.

Patient consent for publication

Patient consent was not required as this study involved secondary use of anonymised data.

Ethics approval

This study was approved by The University Health Network Research Ethics Board and Ontario Personal Health Information Protection Act [reference number 24-5028].

Provenance and peer review

Not commissioned; externally peer reviewed.

Data availability statement

Data underlying the findings described in this manuscript may be obtained in accordance with AstraZeneca's data sharing policy described at: https://astrazenecagrouptrials.pharmacm.com/ST/Submission/Disclosure.

Supplementary materials

Supplementary material associated with this article can be found in the online version at doi:10.1016/j.ard.2025.01.025.

REFERENCES

[1] Centers for Disease Control and Prevention. Systemic lupus erythematosus (SLE) [Internet]. Centers for Disease Control and Prevention; 2023. Available from: https://www.cdc.gov/lupus/about/index.html.

[2] Fanouriakis A, Kostopoulou M, Andersen J, Aringer M, Arnaud L, Bae SC, et al. EULAR recommendations for the management of systemic lupus erythematosus: 2023 update. Ann Rheum Dis 2024;83(1):15–29.

[3] Urowitz MB, Gladman DD, Ibañez D, Su J, Mursleen S, Sayani A, et al. Effect of disease activity on organ damage progression in systemic lupus erythematosus: University of Toronto Lupus Clinic cohort. J Rheumatol 2021;48(1):67–73.

[4] Durcan L, O'Dwyer T, Petri M. Management strategies and future directions for systemic lupus erythematosus in adults. Lancet 2019;393(10188):2332–43.

[5] Ruiz-Arruza I, Ugarte A, Cabezas-Rodriguez I, Medina JA, Moran MA. Ruiz-Irastorza G. Glucocorticoids and irreversible damage in patients with systemic lupus erythematosus. Rheumatology 2014;53(8):1470–6.

[6] Chan J, Walters GD, Puri P, Jiang SH. Safety and efficacy of biological agents in the treatment of systemic lupus erythematosus (SLE). BMC Rheumatol 2023;7(1):37.

[7] Furie R, Khamashta M, Merrill JT, Werth VP, Kalunian K, Brohawn P, et al. Anifrolumab, an anti−interferon-α receptor monoclonal antibody, in moderate-to-severe systemic lupus erythematosus. Arthritis Rheumatol 2017;69(2):376–86.

[8] Morand EF, Furie R, Tanaka Y, Bruce IN, Askanase AD, Richez C, et al. Trial of anifrolumab in active systemic lupus erythematosus. N Engl J Med 2020;382(3):211–21.

[9] ClinicalTrials.gov. Efficacy and Safety of Two Doses of Anifrolumab Compared to Placebo in Adult Subjects With Active Systemic Lupus Erythematosus [Internet]. Bethesda (MD): National Library of Medicine; 2022. [cited 2023 Jan 1]. Available from: https://clinicaltrials.gov/study/NCT02446912.

[10] ClinicalTrials.gov. Efficacy and Safety of Anifrolumab Compared to Placebo in Adult Subjects With Active Systemic Lupus Erythematosus [Internet]. National Library of Medicine; 2022. [cited 2023 Jan 1]. Available from: https://clinicaltrials.gov/study/NCT02446899.

[11] AstraZeneca. Anifrolumab Phase III trial meets primary endpoint in systemic lupus erythematosus [Internet]. AstraZeneca; 2019. [cited 2023 Oct 6]. Available from: https://www.astrazeneca.com/media-centre/press-releases/2019/anifrolumab-phase-iii-trial-meets-primary-endpoint-in-systemic-lupus-erythematosus-29082019.html.

[12] Furie RA, Morand EF, Bruce IN, Manzi S, Kalunian KC, Vital EM, et al. Type I interferon inhibitor anifrolumab in active systemic lupus erythematosus (TULIP-1): a randomised, controlled, phase 3 trial. Lancet Rheumatol 2019;1(4):e208–19.

[13] ClinicalTrials.gov. Long-term Safety of Anifrolumab in Adult Subjects With Active Systemic Lupus Erythematosus (TULIP SLE LTE) [Internet]. National Library of Medicine; 2022. [cited 2023 Jan 1]. Available from: https://clinicaltrials.gov/study/NCT02794285.

[14] Kalunian KC, Furie R, Morand EF, Bruce IN, Manzi S, Tanaka Y, et al. A randomized, placebo-controlled phase III extension trial of the long-term safety and tolerability of anifrolumab in active systemic lupus erythematosus. Arthritis Rheumatol 2023;75(2):253–65.

[15] AstraZeneca. Saphnelo (anifrolumab) approved in the US for moderate to severe systemic lupus erythematosus [Internet]. AstraZeneca; 2021. [cited 2023 Dec 13]. Available from: https://www.astrazeneca.com/media-centre/press-releases/2021/saphnelo-approved-in-the-us-for-sle.html.

[16] AstraZeneca. Saphnelo approved in the EU for the treatment of moderate to severe systemic lupus erythematosus [Internet]. AstraZeneca; 2022. [cited 2023 Dec 13]. Available from: https://www.astrazeneca.com/media-centre/press-releases/2022/saphnelo-approved-in-eu-for-sle.html.

[17] AstraZeneca. Saphnelo approved in Japan for systemic lupus erythematosus [Internet]. AstraZeneca; 2021. [cited 2023 Dec 13]. Available from: https://www.astrazeneca.com/media-centre/press-releases/2021/saphnelo-approved-in-japan-for-sle.html.

[18] van Vollenhoven R, Morand E, Furie R, Kalunian K, Tummala R, Abreu G, et al. LBO1 DORIS remission in patients with SLE treated with anifrolumab or placebo during the 4-year TULIP-LTE trial: post hoc analysis. Lupus Sci Med 2024;11(Suppl 1):A169–70.

[19] Bruce IN, van Vollenhoven RF, Morand EF, Furie RA, Manzi S, White WB, et al. Sustained glucocorticoid tapering in the phase 3 trials of anifrolumab: a post hoc analysis of the TULIP-1 and TULIP-2 trials. Rheumatology (Oxford) 2023;62(4):1526–34.

[20] Hatswell AJ, Deighton K, Snider JT, Brookhart MA, Faghmous I, Patel AR. Approaches to selecting "time zero" in external control arms with multiple potential entry points: a simulation study of 8 approaches. Med Decis Making 2022;42(7):893–905.

[21] Gladman DD, Urowitz MB, Rahman P, Ibañez D, Tam LS. Accrual of organ damage over time in patients with systemic lupus erythematosus. J Rheumatol 2003;30(9):1955–9.

[22] Urowitz MB, Ohsfeldt RL, Wielage RC, Kelton KA, Asukai Y, Ramachandran S. Organ damage in patients treated with belimumab versus standard of care: a propensity score-matched comparative analysis. Ann Rheum Dis 2019;78(3):372–9.

[23] Gladman DD, Urowitz MB, Goldsmith CH, Fortin P, Ginzler E, Gordon C, et al. The reliability of the Systemic Lupus International Collaborating Clinics/American College of Rheumatology damage index in patients with systemic lupus erythematosus. Arthritis Rheum 1997;40(5):809–13.

[24] Gladman D, Ginzler E, Goldsmith C, Fortin P, Liang M, Urowitz M, et al. The development and initial validation of the Systemic Lupus International Collaborating Clinics/American College of Rheumatology damage index for systemic lupus erythematosus. Arthritis Rheum 1996;39(3):363–9.

[25] Greifer N, Stuart EA. Choosing the Causal Estimand for Propensity Score Analysis of Observational Studies [Internet]. 2023 [cited 2024 Jan 24]. Available from: http://arxiv.org/abs/2106.10577

[26] Desai RJ, Franklin JM. Alternative approaches for confounding adjustment in observational studies using weighting based on the propensity score: a primer for practitioners. BMJ 2019;367:l5657.

[27] Austin PC. The relative ability of different propensity score methods to balance measured covariates between treated and untreated subjects in observational studies. Med Decis Making 2009;29(6):661–77.

[28] Cohen J. Statistical power analysis for the behavioural sciences. 2nd ed. New York: Lawrence Erlbaum Associates; 1988. p. 567.

[29] Seaman SR, White IR. Review of inverse probability weighting for dealing with missing data. Stat Methods Med Res 2013;22(3):278–95.

[30] R Core Team. The R Project for Statistical Computing [Internet]. Vienna, Austria: R Foundation for Statistical Computing; 2021. Available from: https://www.R-project.org/.

[31] Figueroa-Parra G, Meade-Aguilar JA, Hulshizer CA, Gunderson TM, Chamberlain AM, Thanarajasingam U, et al. Multimorbidity in systemic lupus erythematosus in a population-based cohort: the Lupus Midwest Network. Rheumatology 2024;63(11):3056–64.

[32] Bell CF, Ajmera MR, Meyers J. An evaluation of costs associated with overall organ damage in patients with systemic lupus erythematosus in the United States. Lupus 2022;31(2):202–11.

[33] Murimi-Worstell IB, Lin DH, Nab H, Kan HJ, Onasanya O, Tierce JC, et al. Association between organ damage and mortality in systemic lupus erythematosus: a systematic review and meta-analysis. BMJ Open 2020;10(5):e031850.

[34] Segura BT, Bernstein BS, McDonnell T, Wincup C, Ripoll VM, Giles I, et al. Damage accrual and mortality over long-term follow-up in 300 patients with systemic lupus erythematosus in a multi-ethnic British cohort. Rheumatology (Oxford) 2020;59(3):524–33.
[35] Keeling SO, Vandermeer B, Medina J, Chatterley T, Nevskaya T, Pope J, et al. Measuring disease activity and damage with validated metrics: a systematic review on mortality and damage in systemic lupus erythematosus. J Rheumatol 2018;45(10):1448–61.
[36] Lee YH, Song GG. Mortality in patients with systemic lupus erythematosus: a meta-analysis of overall and cause-specific effects. Lupus 2024;33(3):929–37.
[37] Parra Sánchez AR, van Vollenhoven RF, Morand EF, Bruce IN, Kandane-Rathnayake R, Weiss G, et al. Targeting DORIS remission and LLDAS in SLE: a review. Rheumatol Ther 2023;10(6):1459–77.
[38] Golder V, Kandane-Rathnayake R, Huq M, Nim HT, Louthrenoo W, Luo SF, et al. Lupus low disease activity state as a treatment endpoint for systemic lupus erythematosus: a prospective validation study. Lancet Rheumatol 2019;1(2):e95–102.
[39] Tsang-A-Sjoe MWP, Bultink IEM, Heslinga M, Voskuyl AE. Both prolonged remission and Lupus Low Disease Activity State are associated with reduced damage accrual in systemic lupus erythematosus. Rheumatology 2017;56(1):121–8.
[40] Golder V, Kandane-Rathnayake R, Li N, Louthrenoo W, Chen YH, Cho J, et al. Association of sustained lupus low disease activity state with improved outcomes in systemic lupus erythematosus: a multinational prospective cohort study. Lancet Rheumatol 2024;6(8):e528–36.
[41] González LA, Santamaría-Alza Y, Alarcón GS. Organ damage in systemic lupus erythematosus. Rev Colomb Reumatol 2021;28(Suppl 1):66–81.
[42] Touma Z, Kayaniyil S, Parackal A, Bonilla D, Su J, Qian C, et al. Unfavorable outcomes associated with glucocorticoid use in current standard-of-care management of systemic lupus erythematosus in Canada. ACR Open Rheumatol 2024;6(9):531–9.
[43] Morand EF, Abreu G, Furie RA, Golder V, Tummala R. Lupus low disease activity state attainment in the phase 3 TULIP trials of anifrolumab in active systemic lupus erythematosus. Ann Rheum Dis 2023;82(5):639–45.
[44] Hernán MA, Robins JM. Using big data to emulate a target trial when a randomized trial is not available. Am J Epidemiol 2016;183(8):758–64.
[45] National Institute for Health and Care Excellence (NICE). NICE real-world evidence framework. Corporate document [ECD9] [Internet]. 2022 Jun 23 [cited 2023 Aug 23]. Available from: https://www.nice.org.uk/corporate/ecd9/chapter/overview
[46] Urowitz MB, Gladman DD, Tom BDM, Ibañez D, Farewell VT. Changing patterns in mortality and disease outcomes for patients with systemic lupus erythematosus. J Rheumatol 2008;35(11):2152–8.
[47] Mai L, Asaduzzaman A, Noamani B, Fortin PR, Gladman DD, Touma Z, et al. The baseline interferon signature predicts disease severity over the subsequent 5 years in systemic lupus erythematosus. Arthritis Res Ther 2021;23(1):29.
[48] Gladman DD, Koh DR, Urowitz MB, Farewell VT. Lost-to-follow-up study in systemic lupus erythematosus (SLE). Lupus 2000;9(5):363–7.
[49] Bruce IN, O'Keeffe AG, Farewell V, Hanly JG, Manzi S, Su L, et al. Factors associated with damage accrual in patients with systemic lupus erythematosus: results from the Systemic Lupus International Collaborating Clinics (SLICC) Inception Cohort. Ann Rheum Dis 2015;74(9):1706–13.
[50] Petri M, Purvey S, Fang H, Magder LS. Predictors of organ damage in systemic lupus erythematosus: the Hopkins lupus cohort. Arthritis Rheum 2012;64(12):4021–8.
[51] Golder V, Kandane-Rathnayake R, Louthrenoo W, Chen YH, Cho J, Lateef A, et al. Comparison of attainment and protective effects of lupus low disease activity state in patients with newly diagnosed versus established systemic lupus erythematosus. J Rheumatol 2024;51(8):790–7.
[52] Basta F, Fasola F, Triantafyllias K, Schwarting A. Systemic lupus erythematosus (SLE) therapy: the old and the new. Rheumatol Ther 2020;7(3):433–46.

Ann Rheum Dis 84 (2025) 777–788

Contents lists available at ScienceDirect

Annals of the Rheumatic Diseases

journal homepage: https://www.sciencedirect.com/journal/annals-of-the-rheumatic-diseases

Systemic lupus erythematosus

LLDAS and remission attainment with anifrolumab treatment in patients with systemic lupus erythematosus: results from the TULIP and long-term extension randomised controlled trials☆

Eric F. Morand[1], Ronald van Vollenhoven[2], Richard A. Furie[3], Kenneth C. Kalunian[4], Susan Manzi[5], Gabriel Abreu[6], Raj Tummala[7,†], Elizabeth A. Duncan[7,†], Hussein Al-Mossawi[8,†], Catharina Lindholm[6,*]

[1] *Sub-Faculty of Clinical and Molecular Medicine, Monash University, Melbourne, VIC, Australia*
[2] *Department of Rheumatology and Clinical Immunology, Amsterdam University Medical Centers, Amsterdam, The Netherlands*
[3] *Donald and Barbara Zucker School of Medicine, Hofstra University/Northwell Health, Great Neck, NY, USA*
[4] *Division of Rheumatology, Allergy, and Immunology, University of California San Diego, La Jolla, CA, USA*
[5] *Lupus Center of Excellence, Autoimmunity Institute, Allegheny Health Network, Pittsburgh, PA, USA*
[6] *BioPharmaceuticals R&D, AstraZeneca, Gothenburg, Sweden*
[7] *BioPharmaceuticals R&D, AstraZeneca, Gaithersburg, MD, USA*
[8] *BioPharmaceuticals R&D, AstraZeneca, Cambridge, UK*

ARTICLE INFO

Article history:
Received 15 July 2024
Received in revised form 25 November 2024
Accepted 28 November 2024

ABSTRACT

Objectives: To investigate the long-term impact of anifrolumab versus placebo on lupus low disease activity state (LLDAS) and definition of remission in systemic lupus erythematosus (DORIS) attainment in patients with systemic lupus erythematosus (SLE).

Methods: This post hoc analysis included patients with moderate to severe SLE who were randomly assigned to receive intravenous anifrolumab 300 mg or placebo (once every 4 weeks) in the 52-week, phase 3 TULIP-1/TULIP-2 trials and continued with the same treatment in the 3-year long-term extension. LLDAS/DORIS rates over time were analysed using a stratified Cochran-Mantel-Haenszel approach and logistic regression. Time to first LLDAS/DORIS was estimated using Cox regression. Cumulative time and percentage of time in LLDAS/DORIS were assessed using an analysis of covariance. All *P* values are nominal.

Results: This analysis included 369 patients (anifrolumab n = 257, placebo n = 112). After 4 years of treatment (at Week 208), 36.9% of anifrolumab-treated patients versus 17.1% of placebo-treated patients were in LLDAS (odds ratio [OR], 2.7; 95% CI, 1.3-5.5; *P* = .0081); 30.3% versus 18.3% were in DORIS (OR, 1.9; 95% CI, 1.0-3.9; *P* = .0663). Time to first LLDAS and DORIS favoured anifrolumab versus placebo (LLDAS: hazard ratio, 1.56; 95% CI, 1.18-2.09; *P* = .0024; DORIS: hazard ratio, 1.50; 95% CI, 1.04-2.22; *P* = .0373). Cumulative time in LLDAS

***Correspondence to** Dr. Catharina Lindholm.
E-mail address: catharina.lindholm@astrazeneca.com (C. Lindholm).

EFM and RvV share first authorship.

Handling editor Josef S. Smolen.

☆ Parts of this work have been previously presented at the American College of Rheumatology Convergence 2023 Congress (van Vollenhoven R, et al. Arthritis Rheumatol. 2023;75(suppl 9)), European Alliance of Associations for Rheumatology 2023 (Morand EF, et al. Ann Rheum Dis. 2023;82:33-4.) and 2024 (Morand E, et al. Ann Rheum Dis. 2024;83:1813) Congresses, Congress of Clinical Rheumatology-East 2024 (encore), and the European Lupus Society (SLEuro) 2024 Congress.

† Affiliation at the time of study initiation.

https://doi.org/10.1016/j.ard.2025.01.016

and DORIS was greater with anifrolumab than that with placebo (P = .0004 and P = .0032, respectively).

Conclusions: LLDAS and DORIS remission, which are associated with favourable outcomes such as reduced damage and mortality in patients with SLE, are attainable and sustainable treatment targets with long-term anifrolumab treatment.

WHAT IS ALREADY KNOWN ON THIS TOPIC

- The treat-to-target endpoints lupus low disease activity state (LLDAS) and remission defined by the definition of remission in systemic lupus erythematosus (DORIS) group are associated with improved long-term outcomes in patients with systemic lupus erythematosus (SLE), including reduced damage accrual and mortality and improved health-related quality of life.
- Attainment of LLDAS and DORIS remission with standard therapy is infrequent in most cohort studies, indicating the need for improved treatments to increase attainment of these protective states.
- The 52-week phase 3 TULIP-1 and TULIP-2 trials supported the approval of the type I interferon receptor-blocking monoclonal antibody anifrolumab for patients with moderate to severe SLE; post hoc analyses of these trials demonstrated higher frequencies of LLDAS and remission attainment in patients with SLE treated with anifrolumab compared with those in patients treated with standard therapy alone.

WHAT THIS STUDY ADDS

- A long-term extension trial of anifrolumab facilitated analyses of LLDAS and DORIS remission attainment rates in patients treated with either anifrolumab or placebo for up to 4 years; anifrolumab treatment was associated with increased rates of LLDAS and DORIS remission, and faster and more sustained attainment of both states, compared with placebo, in patients with moderate to severe disease who were receiving standard therapy at the start of the TULIP-1 or TULIP-2 trials.

HOW THIS STUDY MIGHT AFFECT RESEARCH, PRACTICE OR POLICY

- These data suggest that anifrolumab addition to standard therapy results in greater likelihoods of achieving LLDAS or DORIS remission, which are treat-to-target endpoints that are associated with many long-term benefits in patients with SLE.

INTRODUCTION

Recent advances in understanding systemic lupus erythematosus (SLE) pathophysiology have enabled the development of new treatment options [1]. Despite emerging treatments, uncontrolled disease activity and excess glucocorticoid exposure lead to organ damage accrual, poor quality of life, and increased mortality in patients with SLE [2–5].

Treat-to-target (T2T) approaches, whereby clinicians and patients collaborate to set treatment targets and tightly monitor responses to enable treatment adaptions, are increasingly recommended to improve outcomes in SLE [6–9]. T2T has improved outcomes for patients with hypertension, diabetes, and autoimmune diseases such as rheumatoid arthritis [10,11]. The introduction of T2T as a potential strategy in SLE has underlined the need for quantifiable T2T endpoints, such as remission as defined by the definition of remission in systemic lupus erythematosus (DORIS) group and the lupus low disease activity state (LLDAS), in order to implement T2T in practice [7–9,12].

DORIS remission requires a clinical Systemic Lupus Erythematosus Disease Activity Index 2000 (SLEDAI-2K) score of 0 and Physician Global Assessment (PGA; range, 0-3) of <0.5 in patients who may be receiving antimalarials, glucocorticoids (prednisolone equivalent) ≤5 mg/d, and/or stable immunosuppressants, including biologics [8]. DORIS remission is associated with reduced organ damage and mortality and improved health-related quality of life in patients with SLE [4,13,14]. While remission remains the ultimate SLE treatment goal [9], remission attainment rates are generally low among patients with SLE [15–17], highlighting the need for more attainable treatment targets [6].

LLDAS is an intentionally more attainable outcome than DORIS remission because it includes more pragmatic thresholds for both disease activity (total SLEDAI-2K ≤4 without major organ involvement, no new SLEDAI-2K disease activity, and PGA ≤1) and glucocorticoid dosing (prednisone or equivalent ≤7.5 mg/d). As with DORIS remission, LLDAS permits standard immunosuppressant dosing, including approved biologics and antimalarials [18]. Similar to DORIS, LLDAS is associated with positive outcomes in patients with SLE, including protection from flares, organ damage, and mortality [4,18,19]. Both DORIS remission and LLDAS are recommended in the 2023 EULAR SLE treatment guidelines [9] as treatment goals in an SLE T2T approach.

Anifrolumab is one of the only two biologic treatments approved for patients with moderate to severe SLE [1,9,20,21]. It is a fully human, IgG1κ monoclonal antibody that targets the type I interferon receptor α subunit 1 [22]. The efficacy of anifrolumab was demonstrated in the randomised placebo-controlled TULIP-2 trial [23]. In a post hoc analysis of data from the phase 3 TULIP-1 and TULIP-2 trials, anifrolumab treatment in addition to standard therapy was associated with more frequent attainment of LLDAS and DORIS remission over 1 year compared with that by placebo [24]. Patients who completed treatment in the 1-year TULIP trials could reconsent to participate in a 3-year placebo-controlled long-term extension (LTE) trial [25]. Given that longer durations of LLDAS and DORIS remission are associated with increased protection from organ damage [19,26], in this study, we aimed to investigate the long-term impact of anifrolumab compared with that of placebo, on LLDAS and DORIS attainment over the 4-year TULIP plus LTE period.

METHODS

Study design and patients

The study design, methods, procedures, and inclusion and exclusion criteria of the TULIP-1 (NCT02446912), TULIP-2 (NCT02446899), and the LTE (NCT02794285) trials have been previously described in detail [23,25,27]. In brief, patients aged 18 to 70 years with SLE (according to the American College of Rheumatology [ACR] 1997 classification criteria) who had moderate to severe disease activity despite standard therapy and completed the 52-week double-blind treatment in the TULIP-1/

TULIP-2 trials could reconsent to participate in the randomised, placebo-controlled, double-blind, 3-year LTE.

During the TULIP-1/TULIP-2 trials, patients receiving a glucocorticoid dosage ≥10 mg/d were required to attempt to taper dosage to ≤7.5 mg/d from Weeks 8 to 40; stable glucocorticoid dosages were required from Weeks 40 to 52 [23,24,27]. Tapering of glucocorticoid dosage was also encouraged in TULIP-1/TULIP-2 for patients receiving glucocorticoid dosages of <10 mg/d at baseline. During the LTE, tapering of glucocorticoid was encouraged; modification of standard immunosuppressant doses was also allowed to reflect real-world practice [25].

In this study, we chiefly analysed data from patients who were randomly assigned to receive intravenous anifrolumab 300 mg or placebo (once every 4 weeks) in the TULIP-1 or TULIP-2 trials and who continued with the same treatment in the LTE trial (known as the LTE population) [25].

LLDAS and DORIS definitions

LLDAS was defined as all of the following items [19]: SLEDAI-2K ≤4 without major organ involvement (central nervous, vascular, renal, cardiovascular, and respiratory systems), no new SLEDAI-2K disease activity compared with the previous assessment, PGA (0-3) ≤1, prednisone or equivalent ≤7.5 mg/d, standard maintenance immunosuppressant doses, no use of restricted medications (during the TULIP-1/TULIP-2 periods only), and no premature discontinuation of investigational product (IP); antimalarials were permitted.

DORIS remission was defined as all of the following items [8]: total clinical SLEDAI-2K score (sum of all SLEDAI-2K items except for increased DNA binding and low complement) of 0, PGA (0-3) <0.5, prednisone/equivalent dosage ≤5 mg/d, stable maintenance dosages of immunosuppressants, no restricted medications (TULIP-1/TULIP-2 only), and no premature IP discontinuation; antimalarials were permitted.

Outcome assessments

LLDAS and DORIS attainment were assessed post hoc for the 4-year TULIP + LTE period. We analysed baseline disease characteristics and SLE treatments among patients with or without ≥1 attainment of LLDAS or DORIS remission, agnostic to the treatment group.

In analyses by treatment group (anifrolumab 300 mg vs placebo), we assessed the proportions of patients attaining LLDAS or DORIS over time, as well as the individual criteria defining attainment of these targets. To capture the transitions through LLDAS and DORIS remission over time, patients in LLDAS without DORIS and in DORIS remission regardless of LLDAS were also visualised individually and as proportions over time.

We evaluated the median time to first LLDAS or DORIS (defined as the date of the visit when LLDAS or DORIS remission was attained minus the date of first IP administration), cumulative time in LLDAS or DORIS, percentage of time spent in LLDAS or DORIS, and the proportion of patients in LLDAS or DORIS for thresholds of ≥20%, ≥50%, or ≥70% of the TULIP + LTE period.

In addition to the aforementioned analyses using the published DORIS definition [8], we also assessed attainment over time by treatment group of more stringent remission criteria in which patients were considered responders if they met the DORIS remission disease activity cutoffs plus had a glucocorticoid (prednisone or equivalent) dosage of 0 mg/d or had no immunosuppressant use.

The average time spent in LLDAS or DORIS was compared, agnostic to treatment, between patients who did and those who did not accrue new organ damage over the treatment period. New damage accrual was defined as any increase from baseline in Systemic Lupus International Collaborating Clinics/ACR Damage Index.

Statistical analysis

Baseline disease characteristics and SLE-related treatments for patients who attained LLDAS or DORIS were summarised using descriptive statistics. For all subsequent analyses, patients who discontinued IP prematurely and/or withdrew from the study due to lack of efficacy and/or disease worsening were considered nonresponders from that visit onwards. Patients who discontinued IP prematurely and/or withdrew from the study due to any other reasons were excluded from the analyses from that visit onwards. Missing SLEDAI-2K items and/or PGA data were imputed during the TULIP-1/TULIP-2 trials, carrying forward the last observation for only the first missing visit; any values that remained missing resulted in nonresponse.

The proportion of patients with LLDAS or DORIS attainment (adjusted percentages and nominal P values) over time were derived from a stratified Cochran-Mantel-Haenszel (CMH) approach, with stratification factors of SLEDAI-2K score at screening (<10 vs ≥10), Day 1 glucocorticoid dosage (<10 vs ≥10 mg/d prednisone or equivalent), interferon gene signature (IFNGS) status at screening (high vs low) [20,23,27], and TULIP study for the pooled analysis (TULIP-1 vs TULIP-2); odds ratios (ORs), 95% confidence intervals (CIs), and corresponding nominal P values were calculated using logistic regression with the same stratification factors as for the CMH approach. The proportions of patients meeting each DORIS/LLDAS criteria used observed data and excluded patients up to and including Week 52 who discontinued due to reasons other than SLE worsening/lack of efficacy. Transitions between LLDAS and DORIS attainment over time overall and per-patient were analysed as observed data.

Treatment group comparisons of time to first LLDAS/DORIS (hazard ratios [HR], 95% CIs, nominal P values) were estimated using a Cox regression model with covariates of treatment group, SLEDAI-2K score at screening, Day 1 glucocorticoid dosage, IFNGS status at screening, and TULIP study. Median times to first LLDAS/DORIS were analysed using summary statistics and the Kaplan-Meier method. Cumulative time and percentage of time spent in LLDAS or DORIS were analysed using an analysis of covariance with stratification factors the same as for the CMH approach. The proportions of patients who spent ≥20%, ≥50%, or ≥70% time in LLDAS or DORIS were calculated using a stratified CMH approach (adjusted percentages) and logistic regression (ORs, 95% CIs, and corresponding nominal P values) using the CMH stratification factors described previously. Time spent in LLDAS/DORIS by new damage accrual was analysed descriptively.

RESULTS

Among patients who completed treatment in the TULIP trials, 369 continued with the same treatment in the 3-year LTE (anifrolumab 300 mg, n = 257; placebo, n = 112) (Supplemental Fig S1) [25].

Baseline patient characteristics agnostic to treatment group

We compared baseline disease characteristics and SLE-related treatments in patients who attained LLDAS/DORIS at least once (n = 260) versus those who did not attain LLDAS/DORIS

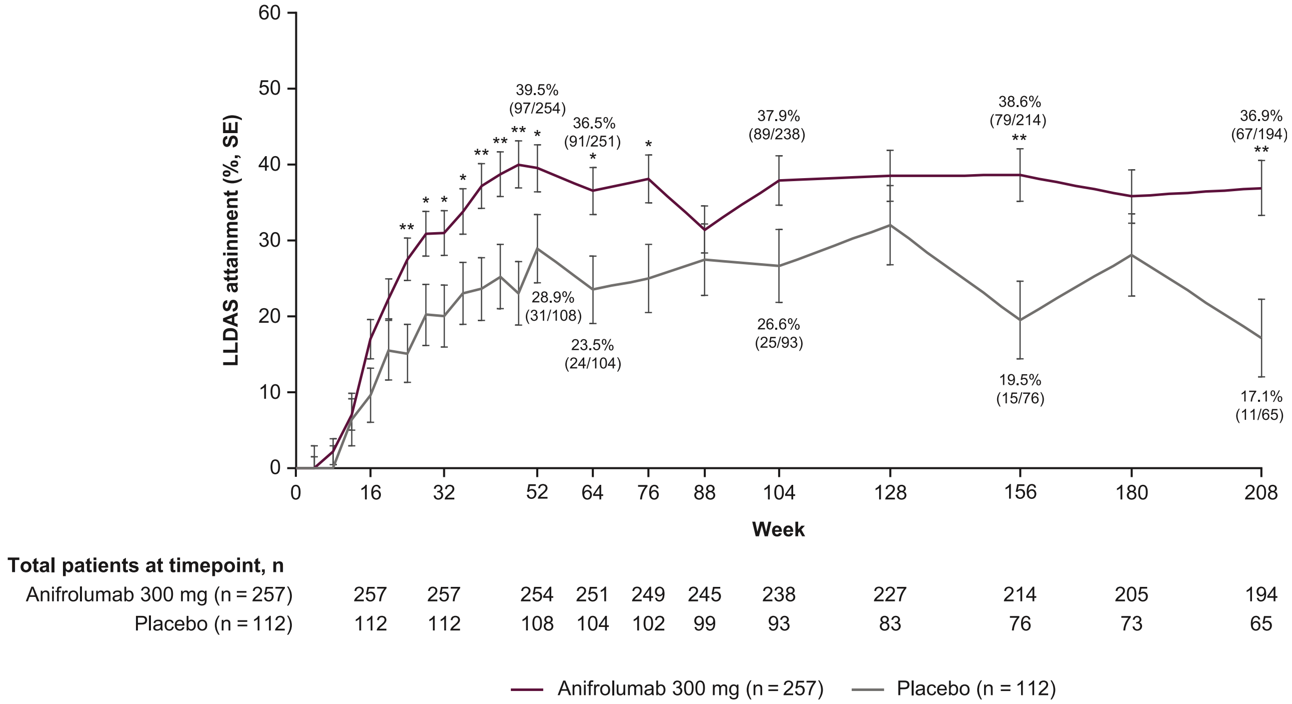

Figure 1. LLDAS attainment during 4 years of treatment. LLDAS attainment was defined as all of the following: SLEDAI-2K ≤4 without major organ involvement, no new SLEDAI-2K disease activity compared with the previous assessment, PGA (0-3) ≤1, prednisone or equivalent ≤7.5 mg/d, standard immunosuppressant dosing (LTE period only), no use of restricted medications (TULIP-1/TULIP-2 period only), and no premature discontinuation of IP. Patients who discontinued IP prematurely and/or withdrew from the study due to lack of efficacy and/or disease worsening were considered nonresponders from that visit onwards. Patients who discontinued IP and/or withdrew for any other reasons were excluded from the analyses from that visit onwards. LLDAS attainment rates (adjusted percentages) and nominal *P* values were calculated using a stratified CMH approach, with stratification factors SLEDAI-2K score at screening, Day 1 glucocorticoid dose, type I IFNGS test result at screening, and TULIP study (TULIP-1 vs TULIP-2). Missing SLEDAI-2K items and/or missing PGA data were imputed during the TULIP-1 and TULIP-2 trials, carrying forward the last observation for only the first missing visit. Any values that remained missing resulted in nonresponse. The nominal *P* values are different from the text, which reports *P* values from the respective logistic regression using the same stratification factors as for the CMH approach. Nominal *P*: **P* < .05, ***P* < .01. Reproduced with permission from Lupus Low Disease Activity State Attainment in the Phase 3 Placebo-controlled TULIP Long-term Extension Trial of Anifrolumab. Presented at EULAR 2023. CMH, Cochran-Mantel-Haenszel; IFNGS, interferon gene signature; IP, investigational product; LLDAS, lupus low disease activity state; LTE, long-term extension; PGA, Physician Global Assessment; SE, standard error; SLEDAI-2K, Systemic Lupus Erythematosus Disease Activity Index 2000.

(n = 109) during the TULIP + LTE treatment period, agnostic to study treatment (Supplemental Table S1). Generally, baseline clinical variables, IFNGS status, and serologies (anti−double-stranded DNA antibodies, antinuclear antibodies, and complement C3) did not differ between patients who did and did not achieve LLDAS or DORIS remission. However, mean standard deviation (SD) baseline global British Isles Lupus Assessment Group and total PGA scores were slightly lower in patients who attained LLDAS/DORIS versus those who did not (British Isles Lupus Assessment Group: 18.7 [5.19] vs 19.9 [6.04]; PGA: 1.72 [0.417] vs 1.86 [0.400]). The proportion of patients with SLEDAI-2K score ≥10 at baseline was slightly lower in LLDAS/DORIS responders versus nonresponders (68.1% [177/260] vs 76.1% [83/109]).

There was a trend towards less baseline glucocorticoid use in patients with versus without LLDAS/DORIS attainment. For example, a lower proportion of LLDAS/DORIS responders were receiving a baseline glucocorticoid dosage of ≥10 mg/d compared with LLDAS/DORIS nonresponders (46.9% [122/260] vs 56.0% [61/109]). Antimalarial and immunosuppressant use were generally comparable between the groups.

Baseline demographics and patient characteristics by treatment group

Demographics and patient characteristics at TULIP baseline were generally balanced across treatment groups, as previously described [25]. The mean (SD) total SLEDAI-2K and PGA scores were similar between treatment groups at baseline (SLEDAI-2K: anifrolumab 11.2 [3.7] vs placebo 11.3 [3.6]; PGA: anifrolumab 1.8 [0.4] vs placebo 1.8 [0.4]) [25]. Similar proportions of patients were receiving glucocorticoids at baseline in both treatment groups (anifrolumab: 80.9% [208/257]; placebo: 82.1% [92/112]) [25]. In general, similar proportions of patients were receiving immunosuppressants in the anifrolumab and placebo groups [25].

LLDAS and DORIS attainment over time with anifrolumab versus placebo

We next assessed LLDAS and DORIS attainment rates over time in the anifrolumab 300-mg and placebo treatment groups in the overall LTE population (n = 257 and n = 112, respectively). Overall, LLDAS attainment rates increased from TULIP baseline to Week 52 and remained relatively stable throughout the 3-year LTE period in each treatment group (Fig 1). At Week 64, 36.5% of the anifrolumab group and 23.5% of the placebo group were in LLDAS (OR, 1.9; 95% CI, 1.1-3.2; nominal *P* = .0185). Attainment of LLDAS also favoured anifrolumab versus placebo at Week 208 (36.9% vs 17.1%; OR, 2.7; 95% CI, 1.3-5.5; nominal *P* = .0081).

As with LLDAS, DORIS remission attainment rates increased from TULIP baseline to Week 208 in each treatment group in the overall LTE population (Fig 2). However, at Week 64, 19.7% of patients receiving anifrolumab achieved DORIS remission versus 9.9% with placebo (OR, 2.3; 95% CI 1.1-4.8; nominal *P* = .0225). A similar trend favouring anifrolumab compared

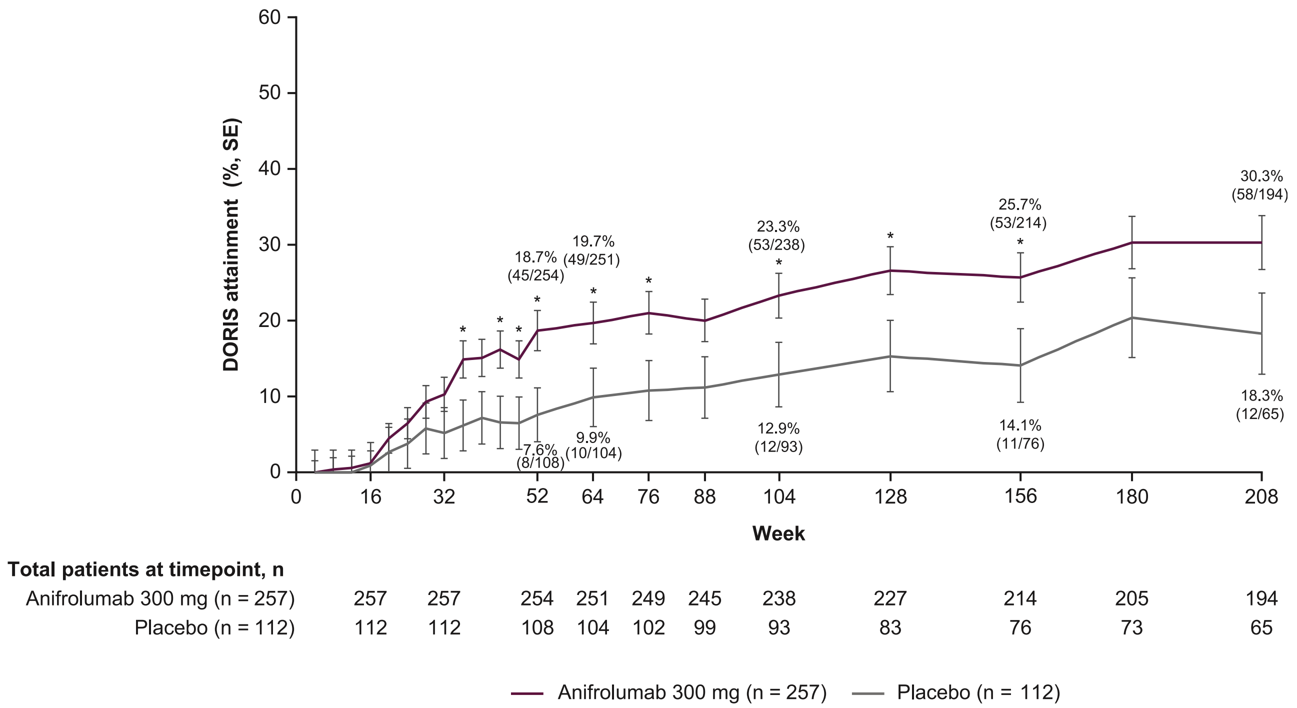

Figure 2. DORIS remission attainment during 4 years of treatment. DORIS attainment was defined as all of the following: total clinical SLEDAI-2K score of 0 (sum of all SLEDAI-2K items except increased DNA binding and low complement), PGA (0-3) <0.5, prednisone/equivalent dosage ≤5 mg/d, stable maintenance immunosuppressant doses, no use of restricted medications (TULIP-1 and TULIP-2 period only), and no premature discontinuation of IP; antimalarials were allowed. Patients who discontinued IP prematurely and/or withdrew from the study due to lack of efficacy and/or disease worsening were considered nonresponders from that visit onward. Patients who discontinued IP and/or withdrew for any other reasons were excluded from the analyses from that visit onward. DORIS attainment rates (adjusted percentages) and nominal *P* values were calculated using a stratified CMH approach, with stratification factors of SLEDAI-2K at screening, Day 1 glucocorticoid dosage, type I interferon gene signature at screening, and TULIP study (TULIP-1 vs TULIP-2). Missing SLEDAI-2K items (resulting in missing clinical SLEDAI-2K) and/or missing PGA data were imputed during the TULIP-1 and TULIP-2 trials, carrying forward the last observation for only the first missing visit. Any values that remained missing resulted in nonresponse. The nominal *P* values are different from the text, which reports *P* values from the respective logistic regression using the same stratification factors as for the CMH approach. Nominal *P*: **P* < .05. Reproduced with permission from van Vollenhoven et al. Lupus Sci Med. 2024;11(Suppl 1):A1−A185 with permission from BMJ Publishing Group Ltd. CMH, Cochran-Mantel-Haenszel; DORIS, definition of remission in systemic lupus erythematosus; IP, investigational product; LTE, long-term extension; PGA, Physician Global Assessment; SLE, systemic lupus erythematosus; SE, standard error; SLEDAI-2K, Systemic Lupus Erythematosus Disease Activity Index 2000.

with placebo was seen up to Week 208 (anifrolumab: 30.3%, placebo: 18.3%; OR, 1.9; 95% CI, 1.0-3.9; nominal *P* = .0663).

When evaluating the individual items, failure to meet the LLDAS criteria [19] at Week 52 was driven by not achieving a SLEDAI-2K score ≤4, with other domains of LLDAS more frequently met including attaining a glucocorticoid dosage ≤7.5 mg/d and no new SLEDAI-2K disease activity (Supplemental Table S2). At Week 208, a similar pattern was seen, but the proportion of patients with no new SLEDAI-2K activity decreased compared with that at Week 52. The largest percentage difference between anifrolumab and placebo was seen for attainment of PGA ≤1 at both Weeks 52 and 208. At both Weeks 52 and 208, failure to meet the DORIS remission criteria [8] was driven by failure to attain the clinical SLEDAI-2K of 0 requirement, while the domains met most frequently were attaining a glucocorticoid dosage ≤5 mg/d and PGA <0.5 in both treatment groups. Proportions of patients attaining all individual DORIS remission criteria increased from Weeks 52 to 208 (Supplemental Table S2). The largest percentage difference between anifrolumab and placebo was seen for attainment of PGA <0.5 at Week 52 and for clinical SLEDAI of 0 at Week 208.

Transitions to LLDAS and DORIS over time

LLDAS and DORIS remission are concentrically more stringent states of response [28]. Therefore, with few exceptions, patients in DORIS remission also meet the definition of LLDAS attainment, whereas a proportion of patients in LLDAS are not in remission [28]. To assess this in the context of this study, the proportions of patients who were in LLDAS but not DORIS remission, DORIS remission regardless of LLDAS, or no LLDAS/DORIS response were visualised over time (Fig 3). From baseline to Week 52, the proportion of patients in LLDAS was consistently higher than that in DORIS in both treatment groups (Fig 3A). From Weeks 64 to 208, the proportion of patients in LLDAS but not remission tended to decrease while the proportion of patients attaining DORIS tended to increase. By the end of the LTE, there were more patients in DORIS remission than patients in LLDAS without DORIS remission.

Analysis of patient-level data over time revealed that the transition from high disease activity to LLDAS, and then to DORIS thresholds, occurred earlier and was more sustained in anifrolumab-treated patients compared with patients receiving placebo, who also had higher rates of discontinuation (Fig 3B).

Time course of LLDAS and DORIS remission attainment

Time to first attainment of LLDAS favoured anifrolumab over placebo (HR, 1.56; 95% CI, 1.18-2.09; nominal *P* = .0024). The Kaplan-Meier analysis showed that 50% of anifrolumab-treated patients attained LLDAS at 9.9 months, compared with 20.2 months in the placebo group (Supplemental Fig S2). Among

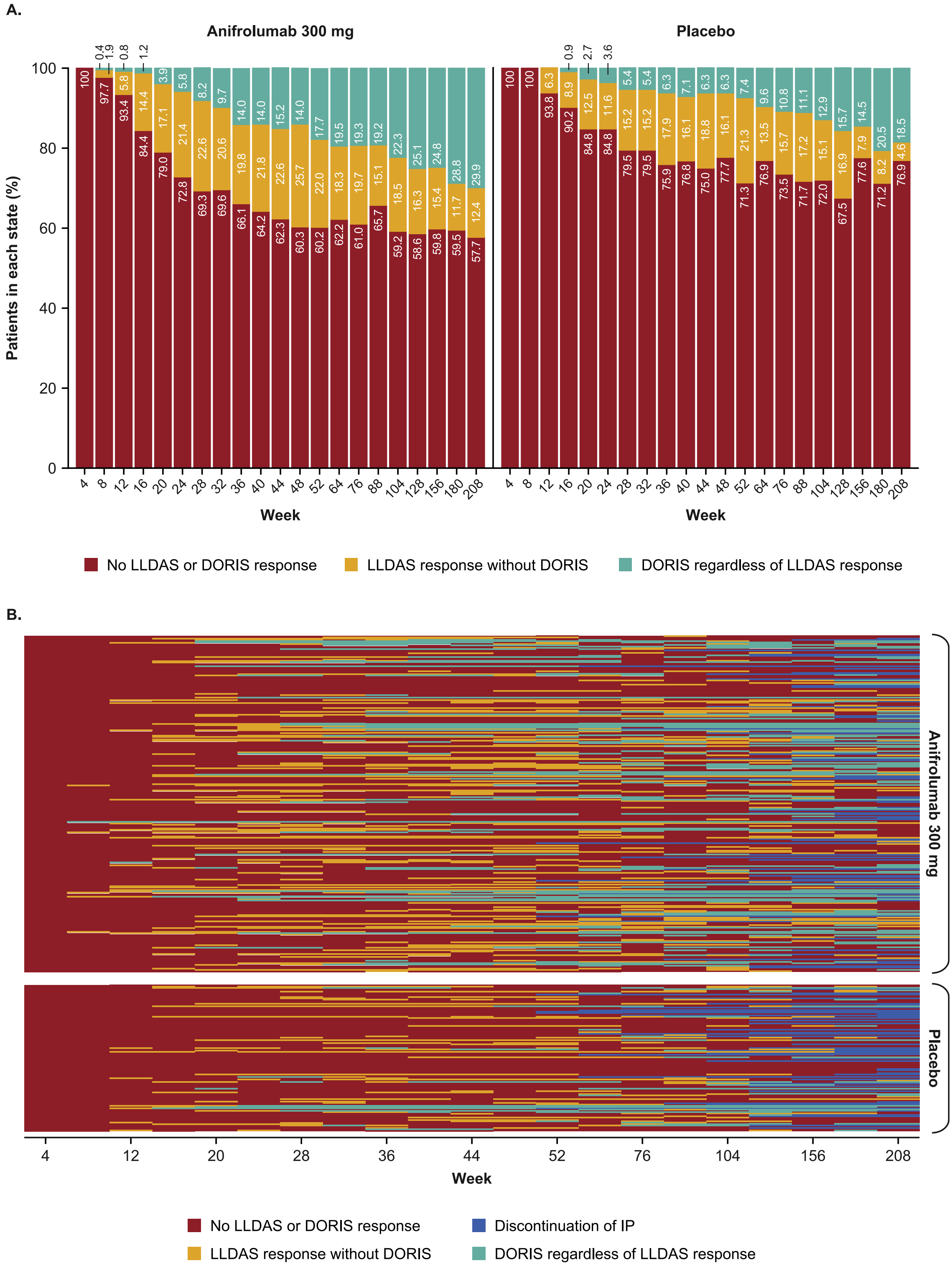

Figure 3. (A) Proportions of patients who attained LLDAS without DORIS remission, DORIS remission, discontinued IP, or no response, and (B) patient-level data of patients transitioning from high disease activity to LLDAS without DORIS remission, DORIS remission, or IP discontinuation during the 4-year TULIP + LTE period. LLDAS attainment was defined as all of the following: SLEDAI-2K ≤4 without major organ involvement, no new SLEDAI-2K disease activity compared with the previous assessment, PGA (0-3) ≤1, prednisone or equivalent ≤7.5 mg/d, standard immunosuppressant dosing (LTE period only), no use of restricted medications (TULIP-1/TULIP-2 period only), and no premature discontinuation of IP. DORIS attainment was defined as all of the following: total clinical SLEDAI-2K score of 0 (sum of all SLEDAI-2K items except increased DNA binding and low complement), PGA (0-3) <0.5, prednisone/equivalent dosage ≤5 mg/d, stable maintenance immunosuppressant doses, no use of restricted medications (TULIP-1 and TULIP-2 period only), and no premature discontinuation of IP; antimalarials were allowed. Patients who discontinued IP prematurely and/or withdrew from the study due to lack of efficacy and/or disease worsening were considered nonresponders from that visit onwards. Patients who discontinued IP and/or withdrew for any other reasons were excluded from the analyses from that visit onwards. Missing SLEDAI-2K items (resulting in missing clinical SLEDAI-2K) and/or missing PGA data were imputed during the TULIP-1 and TULIP-2 trials, carrying forward the last observation for only the first missing visit. Any values that remained missing resulted in nonresponse. Discontinuation of IP indicates discontinuations due to reasons other than worsening/lack of efficacy only. DORIS, definition of remission in systemic lupus erythematosus; IP, investigational product; LLDAS, lupus low disease activity state; LTE, long-term extension; PGA, Physician Global Assessment; SLEDAI-2K, Systemic Lupus Erythematosus Disease Activity Index 2000.

Table
Time in LLDAS and DORIS remission during the 4-year TULIP plus LTE period

Assessment	Anifrolumab 300 mg (n = 257)	Placebo (n = 112)	LS mean difference (95% CI); nominal *P*
	LS mean ± SE		
Time in LLDAS[a,b]			
Cumulative time (mo)	13.98 ± 1.010	8.72 ± 1.392	5.26 (2.34-8.17); .0004
Percentage of time	30.71 ± 2.109	20.71 ± 2.909	10.01 (3.92-16.09); .0013
Time in DORIS[a,b]			
Cumulative time (mo)	7.33 ± 0.886	3.47 ± 1.222	3.86 (1.30-6.41); .0032
Percentage of time	15.75 ± 1.858	7.60 ± 2.562	8.15 (2.79-13.51); .0030

CI, confidence interval; DORIS, definition of remission in systemic lupus erythematosus; IFNGS, interferon gene signature; IP, investigational product; LLDAS, lupus low disease activity state; LS, least squares; LTE, long-term extension; mo, months; PGA, Physician Global Assessment; SE, standard error; SLEDAI-2K, Systemic Lupus Erythematosus Disease Activity Index 2000.

LLDAS attainment was defined as all of the following: SLEDAI-2K ≤4 without major organ involvement, no new SLEDAI-2K disease activity compared with the previous assessment, PGA (0-3) ≤1, prednisone or equivalent ≤7.5 mg/d, standard immunosuppressant dosing (LTE period only), no use of restricted medications (TULIP-1/TULIP-2 period only), and no premature discontinuation of IP. DORIS attainment was defined as all the following: total clinical SLEDAI-2K score of 0 (sum of all SLEDAI-2K items except increased DNA binding and low complement,), PGA (0-3) <0.5, prednisone/equivalent dosage ≤5 mg/d, stable maintenance immunosuppressant doses, no use of restricted medications (TULIP-1 and TULIP-2 period only), and no premature discontinuation of IP; antimalarials were allowed. Patients who discontinued IP prematurely and/or withdrew from the study due to lack of efficacy and/or disease worsening were considered nonresponders from that visit onwards. Patients who discontinued IP and/or withdrew for any other reasons were excluded from the analyses from that visit onwards. Cumulative time (months) and percentage of time spent in LLDAS or DORIS were analysed using an analysis of covariance with stratification factors SLEDAI-2K score at screening, Day 1 glucocorticoid dosage, type I IFNGS test result at screening, and TULIP study (TULIP-1 vs TULIP-2).

[a] Time spent in LLDAS or DORIS was calculated as the number of days between a visit with attained LLDAS or DORIS and the corresponding succeeding visit (with Week 208 as the upper limit), or discontinuation of IP, whichever came first.

[b] Missing SLEDAI-2K items (resulting in missing clinical SLEDAI-2K) and/or missing PGA data were imputed during the TULIP-1 and TULIP-2 trials, carrying forward the last observation for only the first missing visit. Any values that remained missing resulted in nonresponse.

those attaining LLDAS at least once during the 4 years of treatment, the median time to LLDAS was 7.3 and 7.4 months with anifrolumab and placebo, respectively.

Time to first attainment of DORIS remission also favoured anifrolumab over placebo (HR, 1.50; 95% CI, 1.04-2.22; nominal *P* = .0373). For the Kaplan-Meier analysis of DORIS remission, we used a threshold of 25% attainment rate because less than 50% of patients in the placebo group attained DORIS during the 4-year treatment period. The analysis showed that 25% of anifrolumab-treated patients attained DORIS at 14.8 months, compared with 20.6 months in the placebo group (Supplemental Fig S3). For reference, 50% of anifrolumab-treated patients attained DORIS at 48.4 months. Among those attaining DORIS at least once during the 4-year TULIP + LTE period, the median time to DORIS was 12.2 and 15.0 months with anifrolumab and placebo, respectively.

Cumulative time spent in LLDAS was greater in anifrolumab-treated patients than that with placebo (least squares mean [SE] anifrolumab: 13.98 [1.010] months; placebo: 8.72 [1.392] months; nominal *P* = .0004) (Table). Similarly, anifrolumab-treated patients spent more time in DORIS remission than placebo patients (anifrolumab: 7.33 [0.886] months; placebo: 3.47 [1.222] months; nominal *P* = .0032) (Table). Accordingly, a greater percentage of time was spent in LLDAS by patients receiving anifrolumab compared with those receiving placebo (least squares mean [SE]: 30.71% [2.109] vs 20.71% [2.909]; nominal *P* = .0013) (Table). Similar results were observed for DORIS remission (anifrolumab: 15.75% [1.858]; placebo: 7.60% [2.562]; nominal *P* = .0030).

When specific thresholds of time in LLDAS or DORIS remission were considered, more patients spent ≥20% of time in LLDAS with anifrolumab than those with placebo (54.0% vs 35.0%; OR, 2.1; 95% CI, 1.3-3.4; nominal *P* = .0014) (Fig 4). Similarly, at the thresholds of ≥20% and ≥50%, more patients spent time in DORIS remission with anifrolumab than those with placebo (≥20%: 29.5% vs 13.7%; OR, 2.7; 95% CI, 1.5-5.0; nominal *P* = .0016; ≥50%: 15.8% vs 5.7%; OR, 3.2; 95% CI, 1.3-7.8; nominal *P* = .0120) (Fig 5).

Although the primary goal was to compare patients treated with placebo with those treated with anifrolumab throughout the TULIP-1/TULIP-2 and LTE trials, we also analysed attainment of LLDAS and DORIS remission in patients who were randomised to placebo in TULIP-1/TULIP-2 and subsequently randomised to anifrolumab in the LTE (Weeks 52-208). In the group of patients who crossed over from placebo to anifrolumab at Week 52, attainment of LLDAS and DORIS remission progressively increased, separating from the attainment of these states in patients who received placebo throughout TULIP and the LTE. The LLDAS attainment rate was similar from Week 102 onwards in patients who received anifrolumab throughout both trials (Supplemental Fig S4A); the rate of DORIS remission attainment was similar from Week 180 onwards (Supplemental Fig S4B).

Remission with additional requirements for glucocorticoid withdrawal/no use of immunosuppressants

When analysing the proportions of patients achieving remission who were also able to withdraw from glucocorticoids, at Week 52, a numerically greater proportion of patients attained remission off glucocorticoids with anifrolumab versus placebo (8.1% vs 1.9%; OR, 4.7; 95% CI, 1.1-20.8; nominal *P* = .0427) (Supplemental Fig S5). Similar trends were observed at Week 208 (19.1% vs 8.3%; OR, 3.1; 95% CI, 1.1-8.4; nominal *P* = .0280). Irrespective of DORIS or LLDAS attainment, a numerically higher proportion of patients with anifrolumab versus placebo were able to taper glucocorticoid dosage from ≥7.5 mg/d at baseline to ≤5 mg/d (58.2% [39/67] vs 47.8% [11/23]), or completely withdraw from glucocorticoids (22.4% [15/67] vs 8.7% [2/23]), by week 208 (Supplemental Fig S6).

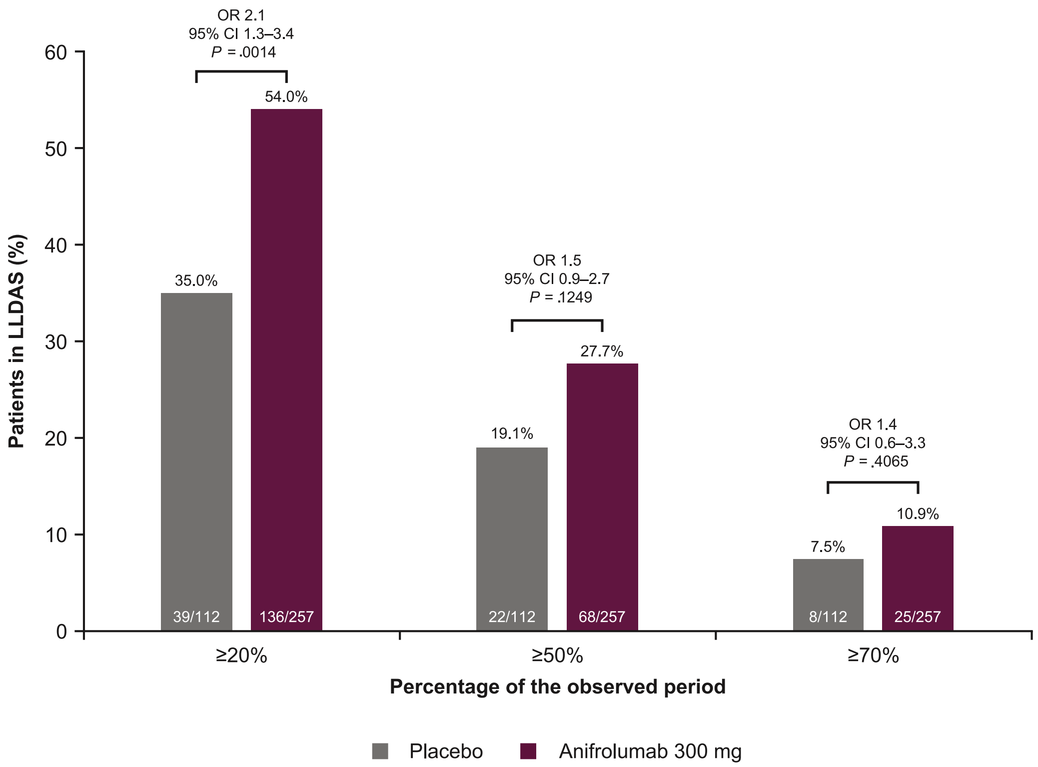

Figure 4. Percentages of patients attaining LLDAS for at least 20%, 50%, or 70% of observed time from Week 0 to Week 208. LLDAS attainment was defined as all of the following: SLEDAI-2K ≤4 without major organ involvement, no new SLEDAI-2K disease activity compared with the previous assessment, PGA (0-3) ≤1, prednisone or equivalent ≤7.5 mg/d, standard immunosuppressant dosing (LTE period only), no use of restricted medications (TULIP-1/TULIP-2 period only), and no premature discontinuation of IP. Patients who discontinued IP prematurely and/or withdrew from the study due to lack of efficacy and/or disease worsening were considered nonresponders from that visit onwards. Patients who discontinued IP and/or withdrew for any other reasons were excluded from the analyses from that visit onwards. The number of days spent in LLDAS constituted the sum of the number of days between the visits with attained LLDAS and the corresponding succeeding visits, with Week 208 as the upper limit, or IP discontinuation, whichever came first. The percentage (adjusted) of time in LLDAS was calculated using a stratified Cochran-Mantel-Haenszel approach, with stratification factors SLEDAI-2K score at screening, Day 1 glucocorticoid dose, type I IFNGS test result at screening, and TULIP study (TULIP-1 vs TULIP-2). ORs, 95% CIs, and corresponding nominal *P* values were calculated using a logistic regression with the above-described stratification factors. Missing SLEDAI-2K items and/or missing PGA data were imputed during the TULIP-1 and TULIP-2 trials, carrying forward the last observation for only the first missing visit. Any values that remained missing resulted in nonresponse. *P* values are nominal. CI, confidence interval; IFNGS, interferon gene signature; IP, investigational product; LLDAS, lupus low disease activity state; OR, odds ratio; PGA, Physician Global Assessment; SLEDAI-2K, Systemic Lupus Erythematosus Disease Activity Index 2000.

When analysing the proportions of patients achieving remission who were not receiving immunosuppressants, at week 52, a greater proportion of anifrolumab-treated patients attained remission off immunosuppressants compared with placebo (9.5% vs 2.1%; OR, 5.9; 95% CI, 1.4-25.8; nominal *P* = .0183) (Supplemental Fig S7). Similar trends were seen at Week 208 (anifrolumab: 16.8%; placebo: 6.5%; OR, 3.3; 95% CI, 1.1-9.7, nominal *P* = .0325).

Time spent in LLDAS or DORIS remission by new organ damage accrual, agnostic to treatment group assignment

We analysed time spent in LLDAS or DORIS in patients with no new organ damage (n = 293) and those who accrued new organ damage during the study (n = 76). Patients with no new damage spent numerically more time (months [SE]) in LLDAS than those who accrued new damage (12.54 [0.807] vs 9.55 [1.299]); this equated to 27.95% (1.673) vs 21.26% (2.791) of the study duration in LLDAS.

Similarly, patients with no new damage spent more time (months [SE]) in DORIS than those who accrued new damage (7.17 [0.716] vs 3.81 [0.932] months); this equated to 15.44% [1.497] vs 8.40% [2.023] of the study duration in DORIS.

DISCUSSION

Insufficient efficacy of SLE treatments poses challenges for controlling disease activity [29], leaving patients at risk for organ damage, poor quality of life, and mortality [3,4,30]. LLDAS and DORIS remission constitute measurable, achievable treatment targets associated with reduced glucocorticoid use, protection from flares and organ damage, improved health-related quality of life, and reduced risk of mortality [4,6,9,13,19,26,31,32]. In the EULAR 2023 SLE treatment guidelines, DORIS remission [8] is described as the ultimate treatment goal in a T2T approach, followed by LLDAS [18] if remission is not attainable [9]. These target states are associated with meaningful changes in biomarkers of immune activation [33], supporting the biological validity of the associations of these clinically based definitions with improved long-term outcome. In this post hoc analysis, we investigated the long-term attainment of LLDAS and DORIS remission comparing anifrolumab versus placebo alongside standard therapy in patients from the TULIP-1/TULIP-2 and LTE trials. We found that, compared with placebo, anifrolumab treatment was associated with more frequent and more sustained attainment of both LLDAS and DORIS remission for up to 4 years of treatment. By the end of the LTE period, 36.9% of anifrolumab-treated patients were in LLDAS and 30.3% were in DORIS remission.

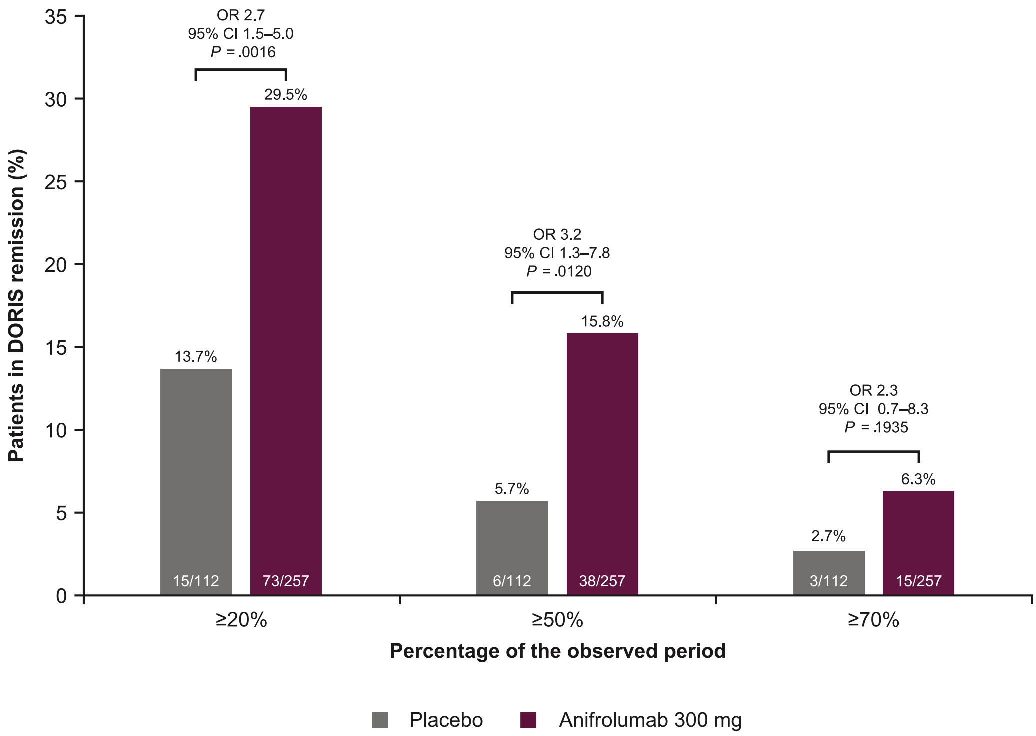

Figure 5. Percentages of patients attaining DORIS remission for at least 20%, 50%, or 70% of observed time from Week 0 to Week 208. DORIS attainment was defined as all of the following: total clinical SLEDAI-2K score of 0 (sum of all SLEDAI-2K items except increased DNA binding and low complement), PGA (0-3) <0.5, prednisone/equivalent dosage ≤5 mg/d, stable maintenance immunosuppressant doses, no use of restricted medications (TULIP-1 and TULIP-2 period only), and no premature discontinuation of IP; antimalarials were allowed. Patients who discontinued IP prematurely and/or withdrew from the study due to lack of efficacy and/or disease worsening were considered nonresponders from that visit onwards. Patients who discontinued due to any other reason were excluded from the analyses. Patients who discontinued IP and/or withdrew for any other reasons were excluded from the analyses from that visit onwards. The number of days spent in DORIS constituted the sum of the number of days between the visits with attained DORIS remission and the corresponding succeeding visits, with Week 208 as the upper limit, or IP discontinuation, whichever came first. The percentage (adjusted) of time in DORIS was calculated using a stratified Cochran-Mantel-Haenszel approach, with stratification factors SLEDAI-2K score at screening, Day 1 glucocorticoid dose, type I IFNGS test result at screening, and TULIP study (TULIP-1 vs TULIP-2). ORs, 95% CIs, and corresponding nominal *P* values were based on a logistic regression using the above-described stratification factors. Missing SLEDAI-2K items (resulting in missing clinical SLEDAI-2K) and/or missing PGA data were imputed during the TULIP-1 and TULIP-2 trials, carrying forward the last observation for only the first missing visit. Any values that remained missing resulted in nonresponse. *P* values are nominal. DORIS, definition of remission in systemic lupus erythematosus; IFNGS, interferon gene signature; IP, investigational product; LTE, long-term extension; OR, odds ratio; PGA, Physician Global Assessment; SLEDAI-2K, Systemic Lupus Erythematosus Disease Activity Index 2000.

Given that an overlap between LLDAS and remission attainment was previously reported, and that both endpoints associate with the same long-term benefits [4,13,14], some experts suggest that separate definitions of LLDAS and DORIS remission may be redundant [34,35]. In fact, LLDAS was intentionally designed as a less stringent state than remission, but in which remission would be concentric, such that the 2 metrics represent stepwise states of deeper T2T outcomes [28]. In this post hoc analysis, we observed a shorter time to first LLDAS versus first DORIS in patients receiving anifrolumab, higher rates of LLDAS attainment than those of DORIS remission at most time points, and more overall time spent by patients in LLDAS than that by patients in DORIS remission. These results align with findings from post hoc analyses of belimumab trials, in which approximately half of the patients in LLDAS at any time point were not in remission [13]. We also observed higher rates of LLDAS (without DORIS) attainment than DORIS remission from baseline to Week 52, after which many patients in LLDAS transitioned to DORIS remission by the end of the trial; this finding suggests that patients in LLDAS after 1 year of treatment with anifrolumab could still have additional benefit and reach DORIS with further treatment. Our findings therefore support that LLDAS and DORIS remission are stepwise states and support the use of both LLDAS and DORIS as clinical trial endpoints and treatment targets in real-world practice [6,9].

Accumulating evidence supports the association between time spent in LLDAS or DORIS remission and the extent of clinical benefit [6,36]. For example, longer periods spent in LLDAS or DORIS remission have been associated not only with greater reductions in flare rates and organ damage accrual, [6,19,26,36] but also with lower rates of adverse events, hospitalisations, and mortality [37]. Furthermore, earlier attainment of LLDAS is associated with improved outcomes across a range of variables, including flares and glucocorticoid exposure [38]. In this study, independent of treatment group assignment, patients with no new damage accrual spent almost twice as much time in DORIS remission than patients with new damage, supporting an association between DORIS attainment and protection from organ damage in a clinical trial setting. In this study, anifrolumab treatment was associated with more time in LLDAS and DORIS remission compared with placebo, as measured using multiple analytical methods (percentage of time and cumulative time). Recent work demonstrates that even periods as short as 3 months of sustained LLDAS or DORIS remission are protective [36]. Although unmet need remains, as evidenced by the proportions of patients who achieved neither LLDAS nor DORIS, our results suggest the potential for a protective effect of long-term anifrolumab treatment against adverse outcomes through attainment of LLDAS and DORIS remission [16].

Long-term use of glucocorticoids and immunosuppressants can induce detrimental outcomes for patients with SLE, including cardiovascular events, serious infections, and organ damage accrual [39−43]. As such, the 2023 EULAR guidelines recommend the gradual tapering of glucocorticoids to a maintenance dosage of 5 mg/d or less, and tapering of immunosuppressants, if withdrawal is not possible [9]. The updated recommended glucocorticoid maintenance dosage of ≤5 mg/d [9] is stricter than the LLDAS criteria that allow up to 7.5 mg/d [18]. However, a recent study has shown that changing the glucocorticoid threshold from ≤7.5 to ≤5 mg/d in LLDAS had no effect on protective associations (ie, when all other criterion of LLDAS were met, this change in glucocorticoid threshold alone made no difference) [44]. In this study, anifrolumab treatment was associated with numerically higher rates of attainment of modified definitions of remission requiring complete withdrawal of glucocorticoids or no use of immunosuppressants, compared with placebo. Regardless of DORIS remission/LLDAS attainment, numerically more patients were able to taper glucocorticoids to ≤5 mg/d, or completely withdraw glucocorticoids, with anifrolumab than with standard therapy alone. Therefore, our findings suggest that anifrolumab may be a valid T2T treatment option targeting disease activity control with concurrent glucocorticoid and/or immunosuppressant reduction.

This study has both strengths and limitations. The studies from which the data are drawn used a rigorous randomised placebo-controlled trial design with long-term prospective data collection and prespecified LLDAS and DORIS remission domains. The inclusion of a placebo group ensured the ability to investigate the long-term impact of anifrolumab treatment alongside standard therapy. However, our findings were derived from post hoc analyses and should be confirmed through formal T2T trials. We observed a higher attainment of DORIS versus LLDAS in the placebo group at Week 208. This finding may relate to the individual SLEDAI-2K components included in the DORIS versus LLDAS definitions, such as the exclusion of increased DNA binding and low complement from SLEDAI-2K when analysing DORIS. Because of the long duration of the TULIP + LTE period, discontinuation rates across treatment groups reduced the overall sample size. Survival bias during the LTE is possible because there was no imputation performed for patients with IP discontinuation; however, these imputations would more likely favour placebo than anifrolumab because discontinuation rates were higher in the placebo group [25].

In conclusion, the results of this post hoc analysis of the 4-year TULIP plus LTE trial periods show that LLDAS and DORIS remission are achievable and realistic treatment targets over time with anifrolumab, with higher long-term attainment rates compared with standard therapy alone. These findings, combined with the glucocorticoid-sparing capacity of anifrolumab [25], may lead to reduced damage accrual and mortality. Our results support the potential of anifrolumab to provide long-term benefits in patients with SLE.

Competing interests

EFM received research grants to his institution from AbbVie, Amgen, AstraZeneca, Biogen, BMS, EMD Serono, Eli Lilly, Janssen, GSK, Genentech, Novartis, Takeda, and UCB; received consulting fees from AbbVie, AstraZeneca, Biogen, BMS, EMD Serono, GSK, Gilead, and Novartis; received honoraria from AstraZeneca, EMD Serono, and Roche; received support for attending meetings and/or travel from EMD Serono and Roche; has WO2022074123A1, WO2021184080A1, WO2023044530A1, WO2021094378A1, and WO2023057369A2 patents planned, issued, or pending; has participated in advisory boards for EMD Serono, Janssen, BMS, Takeda, Biogen, GSK, and DragonFly; held/holds the Board Director position in Rare Voices Australia and Exosome Biosciences; and owns stock or stock options of Dragonfly Tx. RvV received grant support to his institution from Bristol Myers Squibb; received support for educational programmes to his institution from AstraZeneca, Galapagos, MSD, Novartis, Pfizer, Roche, Sanofi, and UCB; received consultancy fees (institutional and/or personal honoraria) from AbbVie, AstraZeneca, Biogen, Bristol Myers Squibb, Galapagos, GSK, Janssen, Pfizer, RemeGen, and UCB; and received speaking fees (institutional and/or personal honoraria) from AbbVie, AstraZeneca, Bristol Myers Squibb, Galapagos, GSK, Janssen, Pfizer, and UCB. RAF received consulting fees, payment or honoraria, and support for attending meetings and/or travel from AstraZeneca and participated in Data Safety Monitoring or Advisory Boards for AstraZeneca. KCK has received consulting fees from AstraZeneca. SM received research grants from AbbVie, Amgen, AstraZeneca, Bristol Myers Squibb, Cartesian, and HGS/GSK; served as consultant for AstraZeneca, Eli Lilly, Exagen Diagnostics Inc, GSK, and UCB Advisory Boards; served as advisory consultant for Cartesian; has patents planned, issued or pending for Exagen Diagnostics, Inc (assignees: Allegheny Singer Research Institute, University of Pittsburgh); held/holds royalties for Exagen Diagnostics Inc; participated in a Data Safety Monitoring Board for NIAID; and served as Board Chair of the Lupus Foundation of America. GA is an employee of AstraZeneca. RT is a former employee of AstraZeneca. CL is an employee of AstraZeneca. EAD is a former employee and owns stocks of AstraZeneca. HA-M is a former employee of AstraZeneca; holds leadership or fiduciary roles in Immunocore; and owns stock or stock options in AstraZeneca and Immunocore.

Acknowledgements

We thank the investigators, research staff, health care providers, and especially the patients who participated in the TULIP-1/TULIP-2 and LTE trials. The views expressed in this publication are those of the author(s). Medical writing support was provided by Vasileios Stamou, PhD, and Rosie Butler, PhD, of JK Associates, Inc, part of Avalere Health, and funded by AstraZeneca.

Contributors

All authors were involved in analysing and interpreting data, drafting the article, or revising it critically for important intellectual content. All authors approved the final version to be published. EFM, RvV, RAF, KCK, GA, RT, and CL conceived or designed the study. EFM, RAF, KCK, RT, and CL performed data acquisition. All authors are accountable for all aspects of this work. EFM and RvV contributed equally to this paper. CL is the guarantor.

Funding

This study was funded by AstraZeneca.

Patient consent for publication

All patients provided informed consent for the publication of results from the TULIP-1, TULIP-2, and LTE trials. Neither patients nor the public was involved in the design, conduct, reporting, or dissemination plans of this research.

Ethics approval

The TULIP-1/TULIP-2 and LTE trials were conducted according to the principles of the Declaration of Helsinki and the International Conference on Harmonisation Guidance for Good Clinical Practice [20,23,25,27]. Informed consent was provided by all patients before taking part in all 3 trials. The trials obtained ethics approval from the ethics committee or institutional review board at each study center [20,23,25,27].

Data availability statement

Data underlying the findings described in this manuscript may be obtained in accordance with AstraZeneca's data sharing policy described at https://astrazenecagrouptrials.pharmacm.com/ST/Submission/Disclosure. Reuse is permitted only with permission from AstraZeneca.

Supplementary materials

Supplementary material associated with this article can be found in the online version at doi:10.1016/j.ard.2025.01.016.

REFERENCES

[1] Venturelli V, Isenberg DA. Targeted therapy for SLE-what works, what doesn't, what's next. J Clin Med 2023;12:3198. doi: 10.3390/jcm12093198.
[2] Al Sawah S, Zhang X, Zhu B, Magder LS, Foster SA, Iikuni N, et al. Effect of corticosteroid use by dose on the risk of developing organ damage over time in systemic lupus erythematosus-the Hopkins Lupus Cohort. Lupus Sci Med 2015;2:e000066. doi: 10.1136/lupus-2014-000066.
[3] Chaigne B, Chizzolini C, Perneger T, Trendelenburg M, Huynh-Do U, Dayer E, et al. Impact of disease activity on health-related quality of life in systemic lupus erythematosus—a cross-sectional analysis of the Swiss Systemic Lupus Erythematosus Cohort Study (SSCS). BMC Immunol 2017;18:17. doi: 10.1186/s12865-017-0200-5.
[4] Kandane-Rathnayake R, Golder V, Louthrenoo W, Chen YH, Cho J, Lateef A, et al. Lupus low disease activity state and remission and risk of mortality in patients with systemic lupus erythematosus: a prospective, multinational, longitudinal cohort study. Lancet Rheumatol 2022;4:e822–30. doi: 10.1016/S2665-9913(22)00304-6.
[5] Urowitz MB, Gladman DD, Ibañez D, Su J, Mursleen S, Sayani A, et al. Effect of disease activity on organ damage progression in systemic lupus erythematosus: University of Toronto Lupus Clinic Cohort. J Rheumatol 2021;48:67–73. doi: 10.3899/jrheum.190259.
[6] Parra Sánchez AR, van Vollenhoven RF, Morand EF, Bruce IN, Kandane-Rathnayake R, Weiss G, et al. Targeting DORIS remission and LLDAS in SLE: a review. Rheumatol Ther 2023;10:1459–77. doi: 10.1007/s40744-023-00601-w.
[7] Parra Sánchez AR, Voskuyl AE, van Vollenhoven RF. Treat-to-target in systemic lupus erythematosus: advancing towards its implementation. Nat Rev Rheumatol 2022;18:146–57. doi: 10.1038/s41584-021-00739-3.
[8] van Vollenhoven RF, Bertsias G, Doria A, Isenberg D, Morand E, Petri MA, et al. 2021 DORIS definition of remission in SLE: final recommendations from an international task force. Lupus Sci Med 2021;8:e000538. doi: 10.1136/lupus-2021-000538.
[9] Fanouriakis A, Kostopoulou M, Andersen J, Aringer M, Arnaud L, Bae SC, et al. EULAR recommendations for the management of systemic lupus erythematosus: 2023 update. Ann Rheum Dis 2024;83:15–29. doi: 10.1136/ard-2023-224762.
[10] Atar D, Birkeland KI, Uhlig T. 'Treat to target': moving targets from hypertension, hyperlipidaemia and diabetes to rheumatoid arthritis. Ann Rheum Dis 2010;69:629–30. doi: 10.1136/ard.2010.128462.
[11] van Vollenhoven R. Treat-to-target in rheumatoid arthritis—are we there yet? Nat Rev Rheumatol 2019;15:180–6. doi: 10.1038/s41584-019-0170-5.
[12] Doria A, Gatto M, Zen M, Iaccarino L, Punzi L. Optimizing outcome in SLE: treating-to-target and definition of treatment goals. Autoimmun Rev 2014;13:770–7. doi: 10.1016/j.autrev.2014.01.055.
[13] Emamikia S, Oon S, Gomez A, Lindblom J, Borg A, Enman Y, et al. Impact of remission and low disease activity on health-related quality of life in patients with systemic lupus erythematosus. Rheumatology (Oxford) 2022;61:4752–62. doi: 10.1093/rheumatology/keac185.
[14] Ugarte-Gil MF, Gamboa-Cardenas RV, Reátegui-Sokolova C, Pimentel-Quiroz VR, Medina M, Elera-Fitzcarrald C, et al. LLDAS (lupus low disease activity state) and/or remission are associated with less damage accrual in patients with systemic lupus erythematosus from a primarily Mestizo population: data from the Almenara Lupus Cohort. Lupus Sci Med 2022;9:e000616. doi: 10.1136/lupus-2021-000616.
[15] Gao D, Hao Y, Mu L, Xie W, Fan Y, Ji L, et al. Frequencies and predictors of the lupus low disease activity state and remission in treatment-naive patients with systemic lupus erythematosus. Rheumatology (Oxford) 2020;59:3400–7. doi: 10.1093/rheumatology/keaa120.
[16] Petri M, Magder LS. Comparison of remission and lupus low disease activity state in damage prevention in a United States Systemic Lupus Erythematosus Cohort. Arthritis Rheumatol 2018;70:1790–5. doi: 10.1002/art.40571.
[17] Tani C, Vagelli R, Stagnaro C, Carli L, Mosca M. Remission and low disease activity in systemic lupus erythematosus: an achievable goal even with fewer steroids? Real-life data from a monocentric cohort. Lupus Sci Med 2018;5:e000234. doi: 10.1136/lupus-2017-000234.
[18] Franklyn K, Lau CS, Navarra SV, Louthrenoo W, Lateef A, Hamijoyo L, et al. Definition and initial validation of a lupus low disease activity state (LLDAS). Ann Rheum Dis 2016;75:1615–21. doi: 10.1136/annrheumdis-2015-207726.
[19] Golder V, Kandane-Rathnayake R, Huq M, Nim HT, Louthrenoo W, Luo SF, et al. Lupus low disease activity state as a treatment endpoint for systemic lupus erythematosus: a prospective validation study. Lancet Rheumatol 2019;1:e95–102. doi: 10.1016/S2665-9913(19)30037-2.
[20] AstraZeneca. SAPHNELO (anifrolumab) Prescribing Information. 2023. https://www.accessdata.fda.gov/drugsatfda_docs/label/2023/761123s003lbl.pdf. (accessed 12 June 2024).
[21] GlaxoSmithKline. BENLYSTA (belimumab) Prescribing Information. 2018. https://www.accessdata.fda.gov/drugsatfda_docs/label/2018/125370s062%2C761043s002lbl.pdf. (accessed 12 June 2024).
[22] Riggs JM, Hanna RN, Rajan B, Zerrouki K, Karnell JL, Sagar D, et al. Characterisation of anifrolumab, a fully human anti-interferon receptor antagonist antibody for the treatment of systemic lupus erythematosus. Lupus Sci Med 2018;5:e000261. doi: 10.1136/lupus-2018-000261.
[23] Morand EF, Furie R, Tanaka Y, Bruce IN, Askanase AD, Richez C, et al. Trial of anifrolumab in active systemic lupus erythematosus. N Engl J Med 2020;382:211–21. doi: 10.1056/NEJMoa1912196.
[24] Morand EF, Abreu G, Furie RA, Golder V, Tummala R. Lupus low disease activity state attainment in the phase 3 TULIP trials of anifrolumab in active systemic lupus erythematosus. Ann Rheum Dis 2023;82:639–45. doi: 10.1136/ard-2022-222748.
[25] Kalunian KC, Furie R, Morand EF, Bruce IN, Manzi S, Tanaka Y, et al. A randomized, placebo-controlled phase III extension trial of the long-term safety and tolerability of anifrolumab in active systemic lupus erythematosus. Arthritis Rheumatol 2023;75:253–65. doi: 10.1002/art.42392.
[26] Tsang-A-Sjoe MW, Bultink IE, Heslinga M, Voskuyl AE. Both prolonged remission and lupus low disease activity state are associated with reduced damage accrual in systemic lupus erythematosus. Rheumatology (Oxford) 2017;56:121–8. doi: 10.1093/rheumatology/kew377.
[27] Furie RA, Morand EF, Bruce IN, Manzi S, Kalunian KC, Vital EM, et al. Type I interferon inhibitor anifrolumab in active systemic lupus erythematosus (TULIP-1): a randomised, controlled, phase 3 trial. Lancet Rheumatol 2019;1:e208–19. doi: 10.1016/S2665-9913(19)30076-1.
[28] Golder V, Tsang-A-Sjoe MW. Treatment targets in SLE: remission and low disease activity state. Rheumatology (Oxford) 2020;59:v19–28. doi: 10.1093/rheumatology/keaa420.
[29] Basta F, Fasola F, Triantafyllias K, Schwarting A. Systemic lupus erythematosus (SLE) therapy: the old and the new. Rheumatol Ther 2020;7:433–46. doi: 10.1007/s40744-020-00212-9.
[30] Arnaud L, Tektonidou MG. Long-term outcomes in systemic lupus erythematosus: trends over time and major contributors. Rheumatology (Oxford) 2020;59:v29–38. doi: 10.1093/rheumatology/keaa382.
[31] Hao Y, Oon S, Ji L, Gao D, Fan Y, Geng Y, et al. Determinants and protective associations of the lupus low disease activity state in a prospective Chinese cohort. Clin Rheumatol 2022;41:357–66. doi: 10.1007/s10067-021-05940-z.
[32] Ugarte-Gil MF, Hanly J, Urowitz M, Gordon C, Bae SC, Romero-Diaz J, et al. Remission and low disease activity (LDA) prevent damage accrual in patients with systemic lupus erythematosus: results from the Systemic Lupus International Collaborating Clinics (SLICC) inception cohort. Ann Rheum Dis 2022;81:1541–8. doi: 10.1136/ard-2022-222487.
[33] Parodis I, Lindblom J, Barturen G, Ortega-Castro R, Cervera R, Pers JO, et al. Molecular characterisation of lupus low disease activity state (LLDAS) and

DORIS remission by whole-blood transcriptome-based pathways in a pan-European systemic lupus erythematosus cohort. Ann Rheum Dis 2024; 83:889–900. doi: 10.1136/ard-2023-224795.
[34] Zen M, Iaccarino L, Gatto M, Saccon F, Larosa M, Ghirardello A, et al. Lupus low disease activity state is associated with a decrease in damage progression in Caucasian patients with SLE, but overlaps with remission. Ann Rheum Dis 2018;77:104–10. doi: 10.1136/annrheumdis-2017-211613.
[35] Zen M, Gatto M, Doria A. Defining the targets in SLE management: insights and unmet gaps. Ann Rheum Dis 2022;81:1483–5. doi: 10.1136/ard-2022-222991.
[36] Golder V, Kandane-Rathnayake R, Li N, Louthrenoo W, Chen YH, Cho J, et al. Association of sustained lupus low disease activity state with improved outcomes in systemic lupus erythematosus: a multinational prospective cohort study. Lancet Rheumatol 2024;6:e528–36. doi: 10.1016/S2665-9913(24)00121-8.
[37] Pitsigavdaki S, Nikoloudaki M, Garantziotis P, Silvagni E, Repa A, Marangoni A, et al. Pragmatic targets for moderate/severe SLE and their implications for clinical care and trial design: sustained DORIS or LLDAS for at least 6 months is sufficient while their attainment for at least 24 months ensures high specificity for damage-free progression. Ann Rheum Dis 2024;83:464–74. doi: 10.1136/ard-2023-224919.
[38] Kikuchi J, Hanaoka H, Saito S, Oshige T, Hiramoto K, Kaneko Y, et al. Lupus low disease activity state within 12 months is associated with favourable outcomes in severely active systemic lupus erythematosus. Rheumatology (Oxford) 2022;61:3777–91. doi: 10.1093/rheumatology/keac002.
[39] Apostolopoulos D, Kandane-Rathnayake R, Louthrenoo W, Luo SF, Wu YJ, Lateef A, et al. Factors associated with damage accrual in patients with systemic lupus erythematosus with no clinical or serological disease activity: a multicentre cohort study. Lancet Rheumatol 2020;2:e24–30. doi: 10.1016/S2665-9913(19)30105-5.
[40] Apostolopoulos D, Kandane-Rathnayake R, Raghunath S, Hoi A, Nikpour M, Morand EF. Independent association of glucocorticoids with damage accrual in SLE. Lupus Sci Med 2016;3:e000157. doi: 10.1136/lupus-2016-000157.
[41] He J, Li Z. Dilemma of immunosuppression and infection risk in systemic lupus erythematosus. Rheumatology (Oxford) 2023;62:i22–9. doi: 10.1093/rheumatology/keac678.
[42] Paredes-Ruiz D, Ruiz-Irastorza G, Amoura Z. Systemic lupus erythematosus and glucocorticoids: a never-ending story? Best Pract Res Clin Rheumatol 2023;37:101873. doi: 10.1016/j.berh.2023.101873.
[43] Stojan G, Petri M. The risk benefit ratio of glucocorticoids in SLE: have things changed over the past 40 years? Curr Treatm Opt Rheumatol 2017;3:164–72. doi: 10.1007/s40674-017-0069-8.
[44] Kandane-Rathnayake R, Golder V, Hoi A, Louthrenoo W, Chen YH, Cho J, et al. OPO124 Impact of glucocorticoid dose threshold in definition of lupus low disease activity state. Ann Rheum Dis 2024;83:156–7. doi: 10.1136/annrheumdis-2024-eular.2742.

Ann Rheum Dis 84 (2025) 789−797

Contents lists available at ScienceDirect

Annals of the Rheumatic Diseases

journal homepage: https://www.sciencedirect.com/journal/annals-of-the-rheumatic-diseases

Systemic lupus erythematosus

Genetic burden of lupus increases the risk of transition from normal to preclinical autoimmune conditions via antinuclear antibody development

Sehwan Chun[1,†], So-Young Bang[2,3,4,†], Ayeong Kwon[1], Chan Young Kim[1], Soojin Cha[3,4], Young-Chang Kwon[3,4], Young Bin Joo[2,3], Soo-Kyung Cho[2,3], Chan-Bum Choi[2,3], Yoon-Kyoung Sung[2,3], Ji-Young Han[5], Tae-Hwan Kim[2,3], Jae-Bum Jun[2,3], Dae Hyun Yoo[2,3], Hye-Soon Lee[2,3,4], Kwangwoo Kim[1,6,*], Sang-Cheol Bae[2,3,4,**]

[1] *Department of Biology, Kyung Hee University, Seoul, Republic of Korea*
[2] *Department of Rheumatology, Hanyang University Hospital for Rheumatic Diseases, Seoul, Republic of Korea*
[3] *Hanyang University Institute for Rheumatology Research, Seoul, Republic of Korea*
[4] *Hanyang Institute of Bioscience and Biotechnology, Seoul, Republic of Korea*
[5] *Department of Periodontology, Division of Dentistry, Hanyang University, College of Medicine, Seoul, Republic of Korea*
[6] *Department of Biomedical and Pharmaceutical Sciences, Kyung Hee University, Seoul, Republic of Korea*

A R T I C L E I N F O

Article history:
Received 14 May 2024
Received in revised form 4 December 2024
Accepted 5 December 2024

A B S T R A C T

Objectives: This study aimed to investigate the association between the genetic burden of systemic lupus erythematosus (SLE) and the loss of tolerance to self-nuclear antigens in the preclinical stage.
Methods: We analysed genetic data from 349 Korean individuals who tested positive for autoantibodies in the preclinical stage, along with 33,596 healthy controls and 2057 patients with SLE. Genome-wide and pathway-specific polygenic risk scores (PRSs) of SLE were calculated based on 180 known non-human leukocyte antigen (non-HLA) SLE loci, *HLA-DRB1* classical alleles, and predefined immune-related pathways to subsequently correlate with clinical phenotypes, particularly the presence of antinuclear antibodies (ANAs) at various titre thresholds.
Results: Individuals with preclinical autoimmune conditions exhibited significantly higher SLE PRSs than healthy controls ($P = 2.99 \times 10^{-5}$), with a significantly upward trend between ANA titres and PRS ($P = 1.12 \times 10^{-3}$). Stratification analysis revealed that preclinical-stage individuals with PRSs exceeding the means of age- and sex-matched PRSs among patients with SLE were at a significantly higher risk of ANA development (odds ratio = 2.25; $P = 8.12 \times 10^{-3}$ at a dilution factor of 1:80). Pathway-specific PRS analysis identified the significant enrichment of SLE-risk effects in nine pathways, such as signalling related to reactive oxygen species production, T cell receptor, B cell receptor, and cytokines, in ANA-positive preclinical individuals ($P_{adjusted} < 0.05$).
Conclusions: Our findings illustrate that the genetic burden of SLE may lead to a crucial transition from normal to preclinical autoimmune conditions prior to the pathogenic stage by increasing the susceptibility to and levels of ANAs.

* **Correspondence to** Dr. Kwangwoo Kim.
** **Correspondence to** Dr. Sang-Cheol Bae.
E-mail addresses: kkim@khu.ac.kr (K. Kim), scbae@hanyang.ac.kr (S.-C. Bae).
Handling editor Josef S. Smolen.
† SC and S-YB contributed equally.

https://doi.org/10.1016/j.ard.2025.01.015

WHAT IS ALREADY KNOWN ON THIS TOPIC

- The aetiology of systemic lupus erythematosus (SLE) involves numerous genetic variants (~200 identified loci) and environmental factors, collectively inducing systemic inflammatory conditions.
- The clinical course of SLE progresses through various stages, including a preclinical phase where autoantigen-specific lymphocytes and autoantibodies such as antinuclear antibody (ANA) may exist without symptoms.
- Despite advances in genome-wide association studies identifying genetic loci associated with SLE, the association between the genetic burden of SLE and the progression to an ANA-producing preclinical stage has never been thoroughly investigated.

WHAT THIS STUDY ADDS

- This study presents the distribution of the polygenic risk score (PRS) of SLE in healthy controls, patients with SLE, and individuals in the preclinical autoimmunity stage.
- The genetic burden of SLE significantly increases the susceptibility to and levels of ANAs in the general population, resulting in a crucial shift from normal to preclinical autoimmune conditions.
- This study identifies the biological pathways that enrich the genetic burden of SLE in ANA-positive individuals in preclinical stages, suggesting the crucial role of these pathways in ANA development.

HOW THIS STUDY MIGHT AFFECT RESEARCH, PRACTICE, OR POLICY

- The findings can serve as a basis for investigating into the genetic architecture that shapes the preclinical phases of autoimmune diseases, suggesting that genetic effects contributing to disease risk operate throughout the entire course of the diseases.
- The identification of ANA-related pathways in this study will encourage further research on the mechanisms underlying immune dysregulation associated with ANA development.

INTRODUCTION

Systemic lupus erythematosus (SLE) is a complex and chronic autoimmune disorder that predominantly affects women in their young reproductive years, leading to manifestations in patients resulting from an aberrant immune response, causing extensive damage to multiple organs and systems throughout the body [1]. Its serological hallmark is the detection of antinuclear antibodies (ANAs). Specific ANA staining patterns and levels are crucial serological diagnostic markers for identifying individuals with an autoimmune disease [2]. The production of ANAs and the subsequent deposition of ANA-mediated immune complexes in patients with SLE can cause chronic inflammation, tissue damage, and a spectrum of clinical symptoms, ranging from skin rashes to severe lupus nephritis [3].

Autoimmune diseases typically progress through stages over time and exhibit highly heterogeneous progression rates among individuals [4]. The development of SLE possibly involves a preclinical phase in which affected individuals may possess autoantigen-specific lymphocytes and autoantibodies such as ANAs but remain asymptomatic [3,5]. The subsequent progression to a pathogenic stage observed in patients with SLE entails a shift from nonpathogenic to pathogenic autoreactive immune responses, occurring over a variable timeframe that extends up to several years [6].

The aetiology of SLE has been well documented for its diverse factors that increase the liability to disease and manifestations. However, the risk factors causing the transition from a healthy condition to a preclinical autoimmune stage have been poorly studied. As SLE-risk factors likely contribute to triggering a systemic inflammatory condition, it is plausible that the preclinical stage producing ANAs may be shaped by SLE-risk factors, encompassing genetic backgrounds, including specific alleles in the major histocompatibility complex (MHC) region and other numerous non-MHC variants, as well as environmental factors such as smoking, obesity, UV light, hormonal exposure, and infection [5–8]. Furthermore, these environmental factors may interact to trigger systemic inflammation and autoimmunity, activating signalling cascades involving genes associated with autoimmune diseases. For instance, smoking can increase the risk of autoimmune diseases by interacting with genetic factors like the human leukocyte antigen (HLA) haplotype [9,10]. UV radiation can exacerbate autoimmune conditions by inducing apoptosis, which exposes self-antigens and stimulates autoantigen-specific B cells influenced by SLE-associated genes [10]. Infections may also trigger autoimmunity through the epigenetic regulation of SLE-associated genes and interactions with pattern recognition receptors such as toll-like receptors associated with autoimmune diseases [10,11].

Advances in genome-wide association studies (GWASs) have remarkably enhanced our understanding of genetic aetiology in SLE. Recent studies, including large-scale GWAS meta-analyses and sophisticated fine-mapping approaches with functional annotations, have identified and characterized ~200 SLE-associated genetic loci [12].

HLA-DRB1 in the MHC region has been predominantly acknowledged for its significant genetic associations with SLE [7,12]. Specifically, *HLA-DRB1* amino acid positions 11, 13, and 26 (or 37) in the epitope-binding groove explain the majority of MHC associations in SLE and the known associations of classical alleles such as HLA-DRB1*03:01 and HLA-DRB1*15:01 [13–15].

The known associations in non-MHC SLE-risk loci are mostly attributed to non-coding common variants with modest effect sizes. These variants are expected to regulate the expression of neighbouring SLE-risk genes in allele-specific manners and consequently act on the regulatory elements of disease-relevant cell types [12]. The genes implicated by SLE GWASs are involved in crucial immune processes related to interferon pathway regulation, lymphocyte signalling, reactive oxygen species (ROS) production, and apoptotic cell and immune complex clearance; thus, they potentially lead to aberrant immune responses in SLE [7,12].

The identified SLE GWAS variants can be utilized to assess an individual's genetic burden of SLE by accounting for their cumulative effects. The polygenic risk score (PRS), calculated based on the number and effect size of multiple risk alleles in both MHC and non-MHC loci [13,16–18], offers a quantitative measure, that can be used to comprehensively evaluate an individual's genetic predisposition and provide valuable insight beyond a single variant. PRS of SLE may serve as a crucial predictive index for the progression of SLE as well as its development. In our previous research, we found that SLE PRS was higher in childhood-onset SLE compared to adult-onset and late-onset SLE. It was also significantly associated with the number of SLE manifestations, anti-Smith (anti-Sm) antibody production and severe lupus nephritis subtypes [19]. However, we cannot exclude the possibility that genetic factors or their effect sizes may change throughout the course of disease development and progression. For instance, our previous GWAS identified 2 novel loci associated with childhood-onset SLE [20].

In this study, we investigated the association between the genetic burden of SLE and the progression to an ANA-producing preclinical stage, a facet that has been overlooked in previous SLE genetic association studies focusing on genetic differences between healthy controls and patients with fully developed SLE. This study involves estimating SLE PRSs from the genetic data of autoantibody-positive individuals in preclinical phases, as well as a substantial number of general healthy controls and patients with SLE to reveal the association between the PRS of SLE and the emergence, levels, and specific staining patterns of ANAs.

METHOD

Study design and participants

This study conducted analyses on three separate cohorts composed of unrelated Korean subjects. The first cohort consisted of 33,596 healthy control participants in a general Korean population sourced from the National Biobank of Korean National Institute of Health. The cohort of patients with SLE (known as the BAE SLE Cohort) included 2,057 participants recruited from Hanyang University Hospital for Rheumatic Diseases [21]. The preclinical-phase cohort, assembled in the Study of Preclinical Autoantibody-positive Rheumatic diseases (SPAR), consisted of 349 individuals in the preclinical autoimmunity phase, recruited from Hanyang University by rheumatologists.

All patients with SLE were ANA-positive and met either the American College of Rheumatology (ACR) revised criteria for SLE, as updated in 1997 [22], or the 2012 Systemic Lupus International Collaborating Clinics (SLICC) criteria [23] for SLE classification. Clinical information, such as sex, age of onset, and clinical manifestations, was collected.

Individuals in the preclinical-phase cohort were enrolled starting from September 2012 and consisted of those who tested positive for any of the following autoantibodies: ANA, rheumatoid factor (RF), or anti−cyclic citrullinated peptide (anti-CCP) autoantibody. The titres and staining patterns of ANAs were determined via indirect immunofluorescence assays with a human epithelial cell line (HEp-2) [24] at the time of enrollment at a single centre, Hanyang University Hospital. The staining patterns of ANAs classified based on the International Consensus on ANA Patterns (ICAP) [25]. Rheumatologists with over 10 years of experience examined these individuals and, if they were in the preclinical stages without overt clinical manifestations of autoimmune, liver-associated, or rheumatic diseases, enrolled them in the preclinical cohort and followed them. The detailed demographic and clinical characteristics of individuals in the preclinical-phase cohort are provided in Table 1. This study was approved by the Institutional Review Board of Hanyang University (HYG-12-005-16 and HYG-16-129-15), and all participants provided written informed consent for their participation in this study. Patients and the public were not involved in the design, conduct, reporting, or dissemination plans of this research.

Genetic data

Genome-wide variant data were acquired using a Korea Biobank Array, known as K-CHIP, which was specifically designed to capture genetic variants prevalent among the Korean population, thus ensuring sufficient coverage for the Korean genetic architecture [26]. The genetic data of patients with SLE and healthy controls were described in our previous GWAS [27], whereas the genetic data of the preclinical autoimmunity cohort were newly generated.

Table 1
Clinical characteristics of individuals in the preclinical-phase cohort

	Preclinical individuals (n = 349)
Age (years), mean (SD)	45.13 (11.07)
Female, n (%)	320 (91.69%)
Family history of SLE, n (%)	10 (2.87%)
BMI (kg/m^2), mean (SD)	22.41 (3.84)
Ever-smoker, n (%)	49 (14.04%)
Alcohol consumption (none, 0 g/d), n (%)	148 (42.41%)
Follow-up duration (years), mean (SD)	7.01 (5.36)
ANA negativity,[a] n	109
	Preclinical ANA-positive individuals (n = 240)
ANA positivity,[b] n	
Titre positive at ≥1:80	240
Titre positive at ≥1:160	196
Titre positive at ≥1:320	135
ANA patterns,[c] n	
Nuclear (AC-1 to AC-14)	224
Speckled (AC-4, AC-5)	98
Homogeneous (AC-1)	18
Cytoplasmic (AC-15 to AC-23)	27
Mitotic (AC-24 to AC-28)	1

ANA, antinuclear antibody; BMI, body mass index; SLE, systemic lupus erythematosus.

[a] These individuals were negative for ANA at a titre of 1:80 but positive for either rheumatoid factor (RF) (61.5%) or anti−cyclic citrullinated peptide (anti-CCP) antibodies (18.3%), or both (20.2%).

[b] The numbers of the ANA-positive individuals are based on three different positivity thresholds (≥1:80, ≥1:160, and ≥1:320). Consequently, an individual with a high ANA titre could be counted as positive under multiple thresholds.

[c] ANA staining patterns were classified based on the International Consensus on ANA Patterns (ICAP) nomenclature for individuals who tested positive for ANAs at a dilution factor of 1:80. It is possible for an individual to exhibit multiple ANA staining patterns. Twelve individuals with ANA titres of ≥1:80 exhibited mixed patterns, with 11 showing both nuclear and cytoplasmic patterns, and one showing nuclear and mitotic patterns simultaneously.

After the genetic data from all three phenotypic cohorts were merged, quality control (QC) procedures were performed, excluding variants with genotype missing rates <5%, minor allele frequencies (MAFs) <0.5%, and *P* values for Hardy−Weinberg equilibrium (HWE) $<10^{-10}$ for SLE cases and 10^{-6} for controls. Additionally, the samples with outlying heterozygosity rates, cryptic relatedness, and discrepancies in genetically imputed and self-reported sex were removed. Principal component analysis (PCA) revealed no outlier, indicating a highly homogeneous genetic background among study subjects. After the QC procedures, 463,188 variants in 36,009 individuals (33,596 controls, 2,057 with SLE, and 349 with preclinical autoimmune conditions) were subjected to whole-genome imputation analysis. Genotype imputation was performed using the Michigan Imputation Server with Eagle v2.4, Minimac4, and the 1000 Genomes Project Phase 3 v5 imputation reference panel [28]. Post-imputation QC retained the variants with imputation accuracy values (rsq) >0.3, MAFs >0.5%, and *P* values for HWE $>10^{-10}$ for SLE cases and 10^{-6} for controls. The dosage of two-field *HLA-DRB1* classical alleles was imputed using the Michigan Imputation Server with a multi-ethnic HLA imputation reference panel [29].

Calculation of PRSs for SLE

We compiled all known SLE variants that had previously surpassed the genome-wide significance threshold of *P* value of

5×10^{-8} in recent genome-wide association meta-analysis studies [12,27]. A total of 190 non-MHC SLE susceptibility loci were defined after merging the known SLE variants within a 300 kb distance around each variant. The most significantly SLE-associated variant in each non-MHC susceptibility locus and the two-field classical alleles of *HLA-DRB1* were selected for PRS calculation. Among non-MHC lead variants, 180 variants (=174 biallelic variants in autosome and six in chromosome X) were present on the quality-checked imputed data. The reported effect sizes of non-MHC variants and HLA-DRB1 amino acid haplotypes on SLE are shown in Supplemental Tables S1 and S2. The effect sizes of two-field classical *HLA-DRB1* alleles were previously estimated based on an amino acid haplotype model comprising residues at amino acid positions 11, 13, and 26 [13].

To quantify the cumulative genetic risk of SLE in an individual, the PRS was calculated as the sum of products between the imputed dosage of each SLE-risk allele in the individual and its reported effect size on SLE, as previously described [19]. Specifically, the PRS of an individual was computed using the following equation:

$$PRS = \sum_{i=1}^{213} \beta_i D_i$$

where we used the individual's allelic dosages (D) and the reported effect sizes (β) of each of the 213 alleles, consisting of 180 non-MHC SLE-risk alleles and 33 *HLA-DRB1* classical alleles. For individuals (3.9%) lacking one or two copies of *HLA-DRB1* classical alleles, possibly due to imputation uncertainty, we inferred the missing fraction of PRS as the average PRS per copy from nonmissing *HLA-DRB1* alleles in the individual's phenotypic group; in this way, it compensated for the deflation caused by the absence of *HLA-DRB1* alleles.

PRS association analysis

To assess the association between PRS and the phenotype of interest, we conducted tests to compare PRS levels among phenotypic groups using analysis of covariance (ANCOVA) or logistic regression, adjusting for the first four genomic principal components. Additionally, we employed a one-sided Jonckheere−Terpstra test to identify any upward trend between PRS and ANA titres in individuals in the preclinical phase.

Stratification analysis was performed by dividing the preclinical samples into two groups: high- and low-PRS groups. Considering previous studies that reported significantly higher PRSs for SLE in male patients compared to female patients, and in those with an early onset compared to a late onset [1,3], our initial step involved creating a linear regression model to predict PRS from age of SLE onset, sex, and the top four principal components in patients with SLE. We then predicted the PRS using age, sex, and principal components of each individual in the preclinical autoimmunity phase, employing the linear regression model developed from patients with SLE. This allowed us to assess if their actual PRSs were higher or less than those of sex-matched patients with SLE who developed the disease at the same age. We classified preclinical individuals into high-PRS groups (those with higher observed PRSs than predicted PRSs) and low-PRS groups (those with lower observed PRSs).

Pathway-specific PRS analysis

Pathway-specific PRSs were calculated to gauge the degree of genetic risk for SLE from genetic variants within and around genes involved in the pathway of interest. Specifically, each SLE-associated variant (listed in Supplemental Tables S1 and S2) was assigned to the gene members of the pathway as long as the variant was located within ±100 kb of the gene. Given that the pathway k comprises m gene members, the formulation for the pathway-specific PRS, denoted as PRS_k, is expressed as follows:

$$PRS_k = \sum_{j=1}^{m} \sum_{i=1}^{213} \beta_i D_i I_{i,j,k}$$

$$I_{i,j,k} = \begin{cases} 1, & \textit{if allele } i \textit{ is within } \pm 100 \textit{ kb of gene } j \textit{ in pathway } k. \\ 0, & \textit{otherwise} \end{cases}$$

where β_i represents the effect size of allele i, and D_i is the allelic dosage of allele i. $I_{i,j,k}$ is an indicator function to ascertain whether each allele i is associated with gene j within pathway k based on the specified proximity criterion. If allele i is located within ±100 kb of gene j in pathway k, it is considered to be associated with gene j, and the indicator function $I_{i,j,k}$ takes the value of 1. Otherwise, $I_{i,j,k}$ is set to 0.

The pathway-specific PRSs were calculated across the 100 precurated immune pathways with at least 10 gene members. These pathways are the subordinate pathways of the immune system (Reactome ID: R-HSA-168256) [30], thus ensuring a comprehensive analysis within the only likely relevant pathological context.

Differences in pathway-specific PRS between controls and ANA-positive preclinical individuals at a dilution factor of 1:160 were assessed using linear regression adjusting for the first four principal components. We then applied the false discovery rate (FDR) correction, setting the threshold at 0.05.

RESULTS

Characteristics of the preclinical cohort with autoimmune conditions

The demographic and clinical characteristics of 349 individuals in the preclinical-phase cohort are provided in Table 1. The mean age at enrollment was 45.13 years, and 14.4% of the cohort were ever-smokers. These individuals tested positive for at least 1 of the following autoantibodies: ANA (n = 240), anti-CCP antibodies (n = 141), and RF (n = 259). The immunofluorescent staining patterns of ANAs, including SLE-associated homogeneous and speckled patterns, were determined for ANA-positive individuals. Among ANA-positive individuals, 98 individuals exhibited a speckled pattern, and 18 individuals showed a homogeneous pattern. ANA-negative individuals (n = 109) tested positive for either anti-CCP antibodies or RF, or both (Supplemental Fig S1), which are more relevant to rheumatoid arthritis (RA). The majority of individuals in the preclinical phase were females (91.7%), and 10 individuals (2.9%) reported a positive family history of SLE in first-degree relatives.

High PRS of SLE in preclinical ANA-positive individuals

We estimated the SLE PRS of 349 preclinical individuals with autoimmunity, 2057 patients with SLE, and 33,596 healthy controls (Fig 1A). The pairwise comparison of the PRS revealed that PRSs in the preclinical-phase group were significantly higher than those in the healthy control group ($P = 2.99 \times 10^{-5}$) and lower than those in the SLE group ($P = 2.86 \times 10^{-58}$; Fig 2A). Additionally, when stratifying the preclinical-phase group according to ANA titres, we observed that the PRS significantly

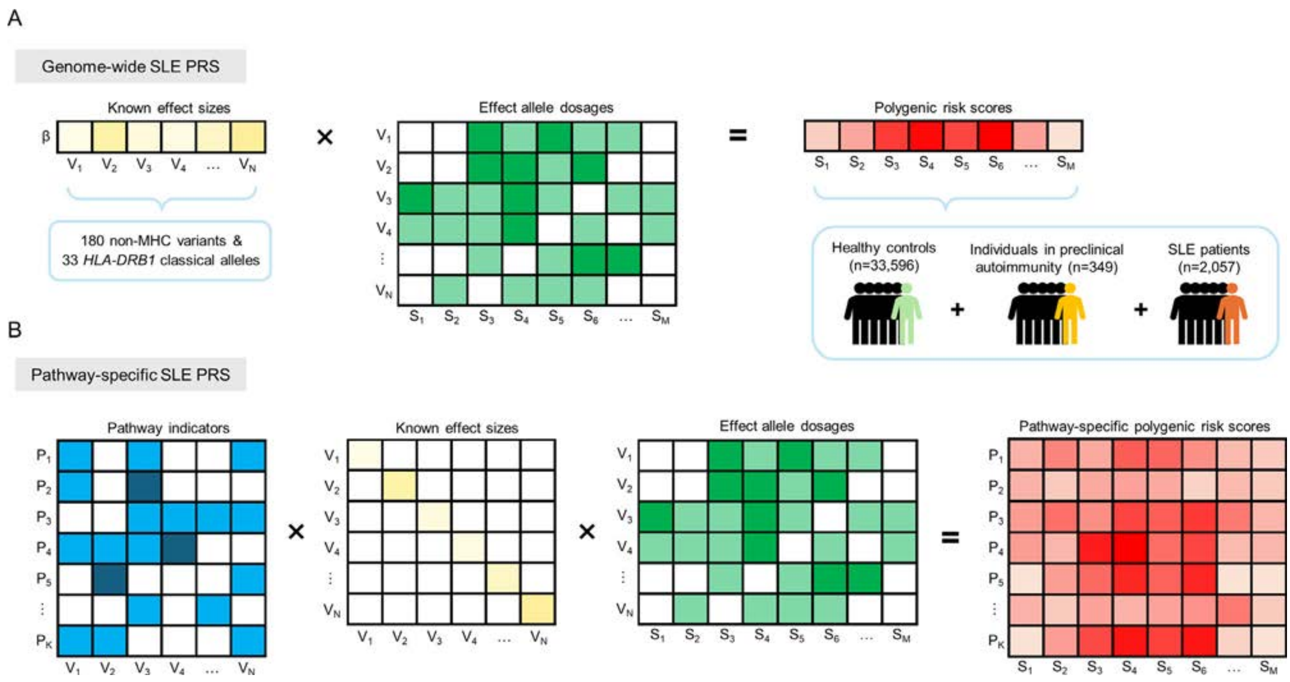

Figure 1. Assessment of systemic lupus erythematosus (SLE) genetic burden using polygenic risk scores (PRSs) derived from known SLE variants. (A) This study illustrated the SLE PRS of participants (from S_1 to S_M), encompassing 33,596 healthy controls, 349 individuals in the preclinical phase, and 2,057 patients with SLE. This PRS is derived from a multiplication operation between a vector of reported effect sizes and a matrix representing individual-level effect allele dosages for SLE variants (from V_1 to V_N), which includes 180 non−major histocompatibility complex (MHC) alleles and 33 *HLA-DRB1* classical alleles. (B) Similarly, pathway-specific PRSs are presented as a product of three matrices: a matrix of pathway indicators, a diagonal matrix of known effect sizes, and a matrix of individuals' allele dosages. The matrix of pathway indicators determines whether each allele is associated with any pathways (from P_1 to P_k) based on genes in proximity to the allele (for further details, refer to the Methods section).

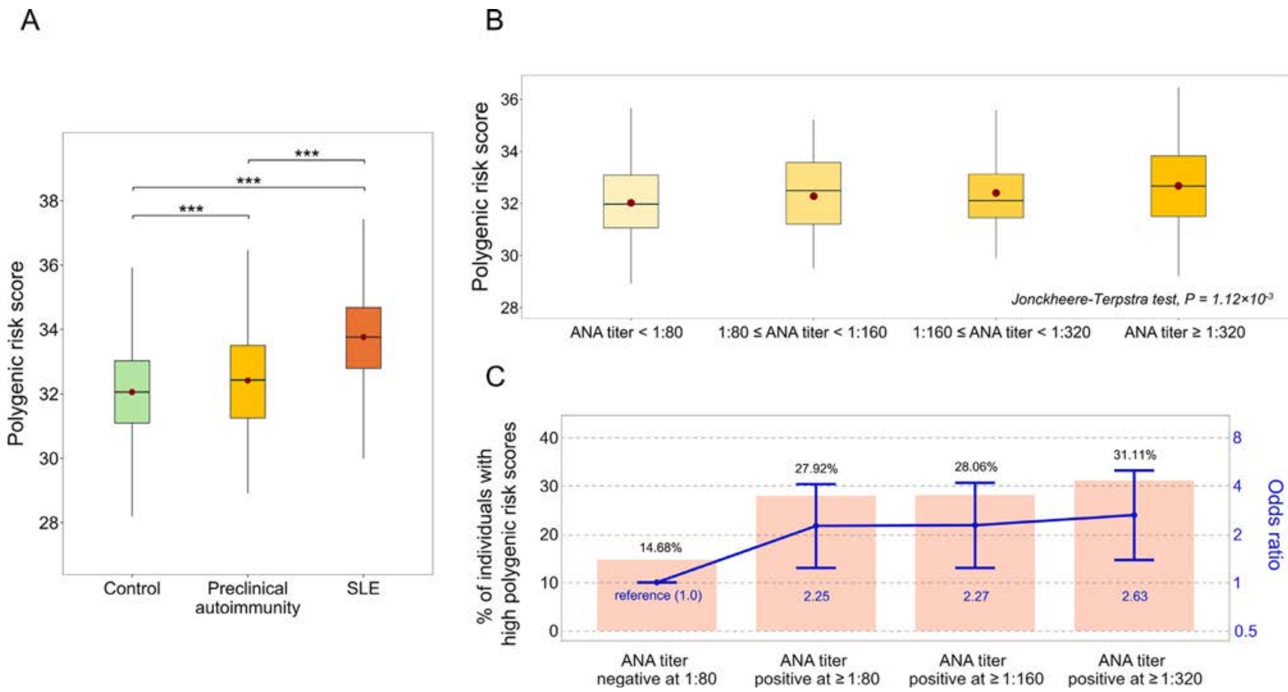

Figure 2. High polygenic risk scores (PRSs) among preclinical-phase individuals with seropositivity and high titres of antinuclear antibodies (ANAs). (A) The boxplot presents the distribution of systemic lupus erythematosus (SLE) PRSs in healthy controls, individuals with preclinical autoimmunity (ANA, rheumatoid factor [RF], or anti−cyclic citrullinated peptide [anti-CCP] antibody positivity), and patients with SLE. *** indicates $P \leq 2.99 \times 10^{-5}$. (B) The distribution of the SLE PRS of individuals in the preclinical phase, stratified by ANA titres, exhibits a positively increasing trend between SLE PRSs and ANA titres, as observed in a one-sided Jonckheere−Terpstra test. (C) Preclinical individuals were stratified into high- and low-PRS subgroups. The bar plot displays the proportion of high-PRS preclinical individuals at various ANA titre thresholds. The line graph represented by a blue line depicts the trend of odds ratios of having a high PRS in different ANA titre−stratified groups compared to the reference group who tested negative for ANAs at a dilution factor of 1:80. The error bars on the line plot represent the 95% CI for each odds ratio.

Table 2

Association between a high PRS of SLE and the risk of ANA seropositivity in the preclinical-phase cohort

	High-PRS group[a] (n = 83)	Low-PRS group (n = 266)	OR (95% CI)	*P* value
ANA titre negative at 1:80	16	93	1.00 (reference)	
ANA titre positive at ≥1:80	67	173	2.25 (1.23-4.10)	7.10×10^{-3}
ANA titre positive at ≥1:160	55	141	2.27 (1.23-4.19)	8.04×10^{-3}
ANA titre positive at ≥1:320	42	93	2.63 (1.38-5.00)	2.72×10^{-3}

ANA, antinuclear antibody; OR, odds ratio; PRS, polygenic risk score; SLE, systemic lupus erythematosus.

[a] Individuals in the high-PRS group have PRSs exceeding the average PRS of same-sex patients with SLE diagnosed at the individuals' age.

and gradually increased, progressing from the ANA-negative subgroup (defined as negative at a dilution factor of 1:80) to the low- to high-titre ANA subgroups ($P = 1.12 \times 10^{-3}$ in a one-sided Jonckheere−Terpstra test; Fig 2B). Notably, the mean PRS of ANA-negative individuals with autoimmune conditions was not statistically different from that of the control group ($P = 0.823$).

We defined ANA positivity/negativity at three different dilution factors (1:80, 1:160, and 1:320) and compared SLE PRSs between ANA-negative and ANA-positive subgroups defined at each dilution factor. As expected, the PRS was significantly higher in the ANA-positive subgroup compared to the ANA-negative subgroup ($P = 3.24 \times 10^{-3}$ at 1:80, $P = 3.20 \times 10^{-3}$ at 1:160, and $P = 3.15 \times 10^{-3}$ at 1:320; Supplemental Fig S2).

We stratified the individuals in the preclinical-phase cohort into high- and low-PRS subgroups based on the distribution of PRSs in patients with SLE while considering sex and age (as described in Methods). In brief, an individual in the high-PRS group had a PRS exceeding the mean PRS of same-sex patients with SLE who developed the disease at the preclinical-phase individual's age, despite not yet having a clinical diagnosis of SLE. A total of 83 individuals (23.8%) were categorized as the high-PRS subgroup. We observed substantial odds ratios (ORs), indicating over two-fold increase in the odds of ANA positivity when individuals belonged to the high-PRS group (eg, OR = 2.25; $P = 7.10 \times 10^{-3}$ based on ANA test results at the 1:80 dilution factor; Fig 2C and Table 2).

Collectively, these results strongly indicated that the presence and quantity of ANA were strongly linked to a genetic predisposition from SLE-risk variants. It is noteworthy that, in contrast, the positivity for the other autoantibodies less relevant to SLE, such as anti-CCP antibodies and RF, was not significantly associated with SLE PRS ($P = 0.531$ and $P = 0.525$, respectively; Supplemental Fig S3). The lack of PRS associations with these autoantibodies consistently reinforced the ANA-specific loss of immune tolerance driven by the genetic burden of SLE.

In our subsequent analysis, we investigated the association between SLE PRS and ANA staining patterns, particularly homogeneous and speckled patterns that have previously been associated with SLE [31] in preclinical ANA-positive individuals. We found that the mean PRS was higher in the group with homogeneous or speckled ANA patterns than in the group without these patterns, particularly at higher ANA titres; however, the difference in the mean PRS did not reach statistical significance possibly because of the limited size of ANA-positive individuals (Supplemental Table S3).

Individuals with a family history of SLE are prone to harbouring numerous SLE-risk variants and may share nongenetic SLE-risk factors with affected family members [32]. This shared genetic and environmental context could collectively increase the risk of ANA development. In this regard, we performed a sensitivity analysis to reassess the associations between ANAs and SLE PRS in individuals in the preclinical phase, excluding 10 individuals with a family history of SLE. We verified that removing these individuals from the analysis did not change the significance of the observed associations (Supplemental Table S4).

Additionally, we note that some of the reported effect sizes used in PRS calculation were derived from previous SLE GWAS meta-analyses using non-Korean datasets and our Korean datasets, with substantial overlap in the patients with SLE and healthy controls included in this study. To ensure no systemic bias from using effect sizes partially contributed by our subjects in PRS calculation, we repeated the analyses using PRS derived from non-Korean effect sizes. The results confirmed that our key findings remained consistent and reliable, as detailed in the online supplemental information.

Pathways highlighted by pathway-specific PRSs in ANA-positive individuals

To understand the genetic aetiology associated with the development of ANAs at the pathway level, we computed the pathway-specific PRSs of SLE based on SLE-risk alleles in proximity to genes involved in the predefined Reactome pathways (Fig 1B). We examined the deviation of pathway-specific PRSs between general healthy controls and preclinical individuals testing positive for ANAs at a dilution factor of 1:160.

We identified nine pathways that showed significant enrichment of pathway-specific PRS in ANA-positive individuals compared to general healthy controls (FDR-corrected $P < 0.05$; Fig 3 and Supplemental Table S5). These pathways included the *adaptive immune system* (R-HSA-1280218), *ROS and reactive nitrogen species (RNS) production in phagocytes* (R-HSA-1222556), *antigen processing-cross presentation* (R-HSA-1236975), *signalling by the B cell receptor* (BCR; R-HSA-983705), *downstream T cell receptor (TCR) signalling* (R-HSA-202424), *cytokine signalling in the immune system* (R-HSA-1280215), *MHC class II antigen presentation* (R-HSA-2132295), *downstream signalling events of BCR* (R-HSA-1168372), and *TCR signalling* (R-HAS-202403).

Among these pathways, *adaptive immune system* and *cytokine signalling in the immune system* had large gene sizes (n > 700). Although the contribution of SLE variants (n = 36 and 51, respectively) in the two pathways to the PRS enrichment was weak or modest, they collectively made significant differences in pathway-specific PRSs between the ANA-positive preclinical cohort and the control group. In contrast, the seven other significant pathways with moderate gene sizes (n = 36 to 159) had relatively large per-gene PRS differences between the ANA-positive preclinical cohort and the control group (Fig 3).

The pathway-specific PRSs for these nine pathways were derived from 106 genes adjacent to SLE-risk variants. Among these 106 genes, 16 commonly participated in three or more of these pathways. Therefore, they could have potential key roles in ANA development before the onset of SLE and in the complex genetic network involved in ANA development. The most

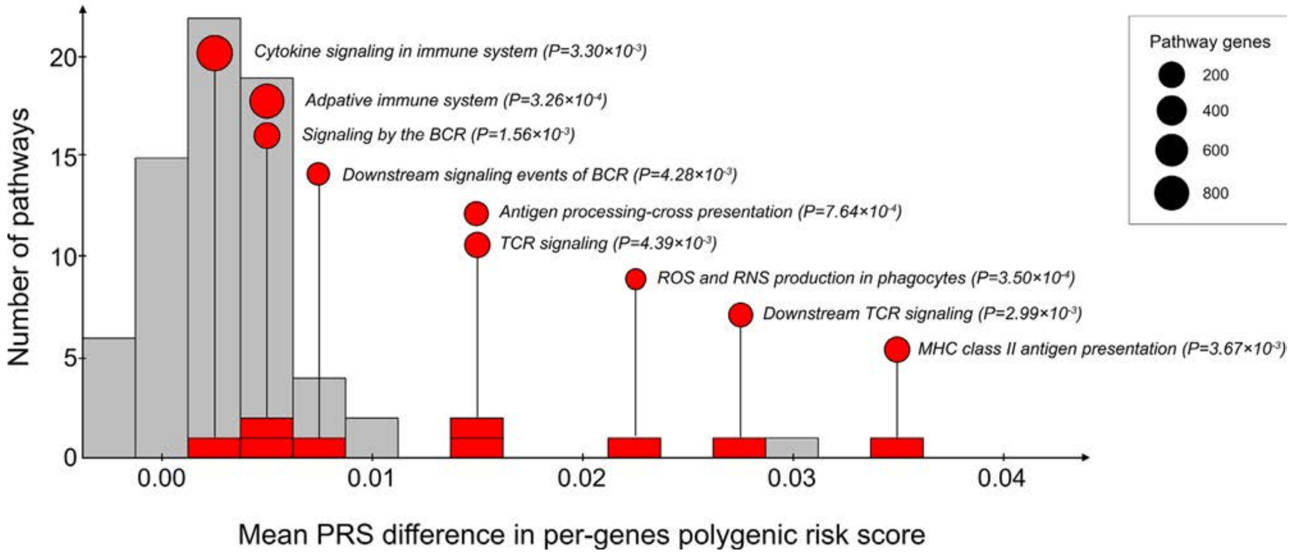

Figure 3. Nine pathways with significantly higher pathway-specific polygenic risk scores (PRSs) among antinuclear antibody (ANA)−positive preclinical individuals. In the histogram, nine pathways with significantly higher pathway-specific PRSs are highlighted in red, and their false discovery rate (FDR)−corrected *P* values and pathway names are displayed; insignificant pathways are shown in grey. The x-axis represents the mean difference in pathway-specific PRSs, normalized by the number of genes used for pathway-specific PRS calculation, between ANA-positive preclinical individuals and general healthy controls. The y-axis indicates the number of pathways in each bin of PRS differences. Only pathways with at least three genes associated with systemic lupus erythematosus (SLE) variants are included in the figure. BCR, B cell receptor; MHC, major histocompatibility complex; RNS, reactive nitrogen species; ROS, reactive oxygen species; TCR, T cell receptor.

frequently associated genes were *IKBKB* and *PSMB6*, observed seven times each across the pathways, followed by *SKP1, HLA-DRB1*, and *HRAS*, appearing six five, and four times, respectively. Additionally, *CSK, GRAP2, GRB2, HRAS, LYN, NCF1, NCF2, NFATC1, PRKCB, RASGRP1, RASGRP3*, and *VAV1* were identified three times each.

DISCUSSION

This study was the first to illustrate that the genetic burden of SLE increased the susceptibility to the development of ANAs, a crucial transition point from normal to an autoimmune condition prior to a pathogenic stage. We obtained genome-wide variant data from large-scale Korean cohorts with a genetically homogeneous background [27]. As the genetic data were generated by the same version of a GWAS array [26] and subsequently subjected to QC and imputation steps, we could minimize the batch effect and the differences in imputation quality. Additionally, all individuals with preclinical autoimmune conditions were recruited into a prospective cohort and followed up annually at a single medical centre, where they were examined for their clinical characteristics by using an identical, well-curated protocol conducted by rheumatologists.

The genetic analysis from the preclinical autoimmune cohort, increasingly emphasized in SLE research [3−5], offered us a unique opportunity to explore genetic predispositions involved in the early stages of the disease. The association with PRS for SLE was specific to the risk of ANA development but not to other autoantibodies that are relatively less relevant to SLE. This emphasizes that ANA-specific genetic risk is highly enriched in SLE-risk variants.

The analysis of PRS-based stratification revealed that individuals in the preclinical stage with high PRSs faced a markedly elevated risk of ANA development, with an OR of 2.25 ($P = 8.12 \times 10^{-3}$; at a dilution factor of 1:80), compared to low-PRS preclinical individuals. In this stratification analysis, we attempted to dichotomize preclinical individuals into high- and low-PRS subgroups based on their predicted PRSs from those among the same-sex patients who developed SLE at the same age. Adjustment for demographic factors is important in a PRS-stratified analysis because the impact of genetic burden in a liability threshold trait model can vary among individuals depending on their nongenetic characteristics. We could identify preclinical individuals with high PRSs, which were even higher than the predicted PRSs in matched patients with SLE, offering a more tailored view of an individual's risk. The increased prevalence of ANA across the high-PRS subgroup, compared to their low-PRS counterparts, further verified the association between the genetic burden of SLE and the susceptibility to ANA development.

Another important point we addressed in our genetic analysis was the confounding effect arising from a familial history of SLE, particularly the effect of SLE-risk environmental exposures that were shared with the affected family members [32]. To mitigate any concerns regarding the influence of family history on the observed genetic associations, we conducted a sensitivity analysis excluding 10 individuals with a family history of SLE and found that the association between ANA development and PRS for SLE was robust.

The average PRS of the preclinical autoimmunity cohort with high-titre ANAs was not as high as that of the patients with SLE. This finding might indicate that not all SLE-risk variants confer the risk of ANA development, motivating for us to stratify the genome-wide PRS for SLE according to the specific biological pathways. We identified nine pathways with significantly higher PRSs in the ANA-positive preclinical group than in the general healthy controls.

Regarding ROS and RNS production, these free radicals are highly reactive and endogenously formed by redox processes in the mitochondria or endoplasmic reticulum. The importance of ROS has been well recognized because these molecules are used not only for pathogen killing but also for controlling the cell cycle, apoptosis, and other signal transduction [33−35]. An abnormal level of oxidative stress is involved in SLE pathogenesis, leading to immune cell dysfunction and autoantigen production [36]. The SLE-risk variants that contributed to the genetic burden of SLE in this pathway were located near *NCF1* and *NCF2*, which encode components of the neutrophilic nicotinamide adenine dinucleotide phosphate (NADPH) oxidase (NOX2) strongly associated with neutrophil extracellular trap formation (NETosis) [36,37].

The variant rs117026326 at *NCF1* is strongly associated with multiple autoimmune diseases, including SLE [27,38,39]. This variant is in a high linkage disequilibrium (LD) with the *NCF1* p. Arg90His (rs201802880) variant [40]. His90 encoded by an SLE-risk allele not only decreases ROS production but also increases the expression of the regulatory genes of type I interferon, contributing to a modified immune response [41,42]. Notably, the number of ANA-positive autoreactive B cells increases in His90 knock-in mice [43]. Similarly, rs13306575 (or R395W), a protein-altering variant located in exon 14 of *NCF2* [27], likely disrupts the stable structure formation between NCF2 and NCF4 by breaking the bridge necessary for their interaction; consequently, the efficiency in ROS production decreases [44]. Furthermore, this variant reduces the expression of NCF2 and NCF4 in neutrophils [45].

Our study had limitations. First, the follow-up duration of our preclinical autoimmune cohort was insufficient to analyse disease courses, including transitions to disease onset (not limited to SLE). Second, the new emergence of additional antibody positivity over time remains unknown. These limitations underscore the essential need for longitudinal clinical data from the preclinical cohort to understand the progression from preclinical autoimmunity to the development of autoimmune diseases in terms of the genetic burden of SLE. Lastly, the pathway-specific PRS relied on genes near SLE-risk variants, assumed to be causal. This proximity-based approach may include genes not directly involved in disease pathogenesis, introducing bias and potentially inflating pathway-specific PRS enrichment in ANA-positive preclinical individuals. The complexity and heterogeneity of SLE loci make it difficult to identify definitive causal genes based solely on lead variants without extensive experimental validation. Therefore, we suggest interpreting these findings with caution, as future studies based on the functional validation of implicated genes may lead to clearer understanding of the underlying biological mechanisms.

In summary, this pioneering study demonstrates that the genetic burden of SLE significantly increases the susceptibility to and levels of ANAs in the general population, making a crucial shift from normal to asymptomatic autoimmune conditions. Our findings enhance our understanding of the genetic aetiopathology of SLE, providing new insights into biological pathways during transition to preclinical stages and offering opportunities for the development of personalized medicine for SLE.

Competing interests

All authors declare they have no competing interests.

Contributors

S-YB, H-SL, KK, and S-CB designed the study. S-YB, S Cha, Y-CK, YBJ, S-KC, C-BC, Y-KS, J-YH, T-HK, J-BJ, DHY, H-SL, and S-CB recruited and characterized preclinical autoimmune individuals and patients with SLE. S-YB, H-SL, KK, and S-CB obtained genetic data. S Chun led the genetic analysis, assisted by AK and CYK. S Chun, S-YB, KK, and S-CB wrote the manuscript. All authors reviewed and approved the manuscript. S-CB serves as the guarantor of the study.

Funding

This research was supported by Basic Science Research Program through the National Research Foundation of Korea (NRF; 2021R1A6A1A03038899, 2022R1A2C2006073, and 2022R1A2C2092164) and the National Research Facilities and Equipment Center (NFEC) grant (NFEC 2023R1A6C101A009).

Patient consent for publication

All participants, including patients with SLE and individuals in the preclinical phase, provided their written informed consent before enrollment.

Ethics approval

The study received ethical approval from the Institutional Review Board (IRB) of Hanyang University in Korea (HYG-12-005-16 and HYG-16-129-15).

Provenance and peer review

Not commissioned; externally peer reviewed.

Data availability statement

Data are available on reasonable request.

Supplementary materials

Supplementary material associated with this article can be found in the online version at doi:10.1016/j.ard.2025.01.015.

REFERENCES

[1] Barber MRW, Drenkard C, Falasinnu T, Hoi A, Mak A, Kow NY, et al. Global epidemiology of systemic lupus erythematosus. Nat Rev Rheumatol 2021;17 (9):515–32. doi: 10.1038/s41584-021-00668-1.

[2] Pisetsky DS, Lipsky PE. New insights into the role of antinuclear antibodies in systemic lupus erythematosus. Nat Rev Rheumatol 2020;16(10):565–79. doi: 10.1038/s41584-020-0480-7.

[3] Fanouriakis A, Tziolos N, Bertsias G, Boumpas DT. Update on the diagnosis and management of systemic lupus erythematosus. Ann Rheum Dis 2021;80 (1):14–25. doi: 10.1136/annrheumdis-2020-218272.

[4] Bieber K, Hundt JE, Yu X, Ehlers M, Petersen F, Karsten CM, et al. Autoimmune pre-disease. Autoimmun Rev 2023;22(2):103236. doi: 10.1016/j.autrev.2022.103236.

[5] Choi MY, Costenbader KH. Understanding the concept of pre-clinical autoimmunity: prediction and prevention of systemic lupus erythematosus: identifying risk factors and developing strategies against disease development. Front Immunol 2022;13:890522. doi: 10.3389/fimmu.2022.890522.

[6] Arbuckle MR, McClain MT, Rubertone MV, Scofield RH, Dennis GJ, James JA, et al. Development of autoantibodies before the clinical onset of systemic lupus erythematosus. N Engl J Med 2003;349(16):1526–33. doi: 10.1056/NEJMoa021933.

[7] Kwon YC, Chun S, Kim K, Mak A. Update on the genetics of systemic lupus erythematosus: genome-wide association studies and beyond. Cells 2019;8 (10):1180. doi: 10.3390/cells8101180.

[8] Crow MK. Pathogenesis of systemic lupus erythematosus: risks, mechanisms and therapeutic targets. Ann Rheum Dis 2023;82(8):999–1014. doi: 10.1136/ard-2022-223741.

[9] Kim K, Jiang X, Cui J, Lu B, Costenbader KH, Sparks JA, et al. Interactions between amino acid-defined major histocompatibility complex class II variants and smoking in seropositive rheumatoid arthritis. Arthritis Rheumatol 2015;67(10):2611–23. doi: 10.1002/art.39228.

[10] Wahren-Herlenius M, Dörner T. Immunopathogenic mechanisms of systemic autoimmune disease. Lancet 2013;382(9894):819–31. doi: 10.1016/S0140-6736(13)60954-X.
[11] Harley JB, Chen X, Pujato M, Miller D, Maddox A, Forney C, et al. Transcription factors operate across disease loci, with EBNA2 implicated in autoimmunity. Nat Genet 2018;50(5):699–707. doi: 10.1038/s41588-018-0102-3.
[12] Ha E, Bae SC, Kim K. Recent advances in understanding the genetic basis of systemic lupus erythematosus. Semin Immunopathol 2022;44(1):29–46. doi: 10.1007/s00281-021-00900-w.
[13] Kim K, Bang SY, Lee HS, Okada Y, Han B, Saw WY, et al. The HLA-DRβ1 amino acid positions 11-13-26 explain the majority of SLE-MHC associations. Nat Commun 2014;5:5902. doi: 10.1038/ncomms6902.
[14] Molineros JE, Looger LL, Kim K, Okada Y, Terao C, Sun C, et al. Amino acid signatures of HLA class-I and II molecules are strongly associated with SLE susceptibility and autoantibody production in Eastern Asians. PLoS Genet 2019;15(4):e1008092. doi: 10.1371/journal.pgen.1008092.
[15] Sun C, Molineros JE, Looger LL, Zhou XJ, Kim K, Okada Y, et al. High-density genotyping of immune-related loci identifies new SLE risk variants in individuals with Asian ancestry. Nat Genet 2016;48(3):323–30. doi: 10.1038/ng.3496.
[16] Horton R, Wilming L, Rand V, Lovering RC, Bruford EA, Khodiyar VK, et al. Gene map of the extended human MHC. Nat Rev Genet 2004;5(12):889–99. doi: 10.1038/nrg1489.
[17] Torkamani A, Wineinger NE, Topol EJ. The personal and clinical utility of polygenic risk scores. Nat Rev Genet 2018;19(9):581–90. doi: 10.1038/s41576-018-0018-x.
[18] Lambert SA, Abraham G, Inouye M. Towards clinical utility of polygenic risk scores. Hum Mol Genet 2019;28(R2):R133–42. doi: 10.1093/hmg/ddz187.
[19] Kwon YC, Ha E, Kwon HH, Park DJ, Shin JM, Joo YB, et al. Higher genetic risk loads confer more diverse manifestations and higher risk of lupus nephritis in systemic lupus erythematosus. Arthritis Rheumatol 2023;75(9):1566–72. doi: 10.1002/art.42516.
[20] Joo YB, Lim J, Tsao BP, Nath SK, Kim K, Bae SC. Genetic variants in systemic lupus erythematosus susceptibility loci, XKR6 and GLT1D1 are associated with childhood-onset SLE in a Korean cohort. Sci Rep 2018;8(1):9962. doi: 10.1038/s41598-018-28128-z.
[21] Joo YB, Bae SC. Assessment of clinical manifestations, disease activity and organ damage in 996 Korean patients with systemic lupus erythematosus: comparison with other Asian populations. Int J Rheum Dis 2015;18(2):117–28. doi: 10.1111/1756-185X.12462.
[22] Hochberg MC. Updating the American College of Rheumatology revised criteria for the classification of systemic lupus erythematosus. Arthritis Rheum 1997;40(9):1725. doi: 10.1002/art.1780400928.
[23] Petri M, Orbai AM, Alarcón GS, et al. Derivation and validation of the Systemic Lupus International Collaborating Clinics classification criteria for systemic lupus erythematosus. Arthritis Rheum 2012;64(8):2677–86. doi: 10.1002/art.34473.
[24] Choi MY, Clarke AE, Urowitz M, Hanly J, St-Pierre Y, Gordon C, et al. Longitudinal analysis of ANA in the Systemic Lupus International Collaborating Clinics (SLICC) Inception Cohort. Ann Rheum Dis 2022;81(8):1143–50. doi: 10.1136/annrheumdis-2022-222168.
[25] Agmon-Levin N, Damoiseaux J, Kallenberg C, Sack U, Witte T, Herold M, et al. International recommendations for the assessment of autoantibodies to cellular antigens referred to as anti-nuclear antibodies. Ann Rheum Dis 2014;73(1):17–23. doi: 10.1136/annrheumdis-2013-203863.
[26] Moon S, Kim YJ, Han S, Hwang MY, Shin DM, Park MY, et al. The Korea biobank array: design and identification of coding variants associated with blood biochemical traits. Sci Rep 2019;9(1):1382. doi: 10.1038/s41598-018-37832-9.
[27] Yin X, Kim K, Suetsugu H, Bang SY, Wen L, Koido M, et al. Meta-analysis of 208370 East Asians identifies 113 susceptibility loci for systemic lupus erythematosus. Ann Rheum Dis 2021;80(5):632–40. doi: 10.1136/annrheumdis-2020-219209.
[28] Das S, Forer L, Schönherr S, Sidore C, Locke AE, Kwong A, et al. Next-generation genotype imputation service and methods. Nat Genet 2016;48(10):1284–7. doi: 10.1038/ng.3656.
[29] Luo Y, Kanai M, Choi W, Li X, Sakaue S, Yamamoto K, et al. A high-resolution HLA reference panel capturing global population diversity enables multi-ancestry fine-mapping in HIV host response. Nat Genet 2021;53(10):1504–16. doi: 10.1038/s41588-021-00935-7.
[30] Gillespie M, Jassal B, Stephan R, Milacic M, Rothfels K, Senff-Ribeiro A, et al. The reactome pathway knowledgebase 2022. Nucleic Acids Res 2022;50(D1):D687–92. doi: 10.1093/nar/gkab1028.
[31] Al-Mughales JA. Anti-nuclear antibodies patterns in patients with systemic lupus erythematosus and their correlation with other diagnostic immunological parameters. Front Immunol 2022;13:850759. doi: 10.3389/fimmu.2022.850759.
[32] Cooper GS, Dooley MA, Treadwell EL, St Clair EW, Gilkeson GS. Risk factors for development of systemic lupus erythematosus: allergies, infections, and family history. J Clin Epidemiol 2002;55(10):982–9. doi: 10.1016/s0895-4356(02)00429-8.
[33] Li H, Zhou X, Huang Y, Liao B, Cheng L, Ren B. Reactive oxygen species in pathogen clearance: the killing mechanisms, the adaption response, and the side effects. Front Microbiol 2020;11:622534. doi: 10.3389/fmicb.2020.622534.
[34] Verbon EH, Post JA, Boonstra J. The influence of reactive oxygen species on cell cycle progression in mammalian cells. Gene 2012;511(1):1–6. doi: 10.1016/j.gene.2012.08.038.
[35] Redza-Dutordoir M, Averill-Bates DA. Activation of apoptosis signalling pathways by reactive oxygen species. Biochim Biophys Acta 2016;1863(12):2977–92. doi: 10.1016/j.bbamcr.2016.09.012.
[36] Yan Z, Chen Q, Xia Y. Oxidative stress contributes to inflammatory and cellular damage in systemic lupus erythematosus: cellular markers and molecular mechanism. J Inflamm Res 2023;16:453–65. doi: 10.2147/JIR.S399284.
[37] Vorobjeva NV, Chernyak BV. NETosis: molecular mechanisms, role in physiology and pathology. Biochemistry (Mosc) 2020;85(10):1178–90. doi: 10.1134/S0006297920100065.
[38] Li Y, Zhang K, Chen H, Sun F, Xu J, Wu Z, et al. A genome-wide association study in Han Chinese identifies a susceptibility locus for primary Sjogren's syndrome at 7q11.23. Nat Genet 2013;45(11):1361–5. doi: 10.1038/ng.2779.
[39] Liu C, Yan S, Chen H, Wu Z, Li L, Cheng L, et al. Association of GTF2I, NFKB1, and TYK2 regional polymorphisms with systemic sclerosis in a Chinese Han population. Front Immunol 2021;12:640083. doi: 10.3389/fimmu.2021.640083.
[40] Zhao J, Ma J, Deng Y, Kelly JA, Kim K, Bang SY, et al. A missense variant in NCF1 is associated with susceptibility to multiple autoimmune diseases. Nat Genet 2017;49(3):433–7. doi: 10.1038/ng.3782.
[41] Olsson LM, Johansson ÅC, Gullstrand B, Jönsen A, Saevarsdottir S, Rönnblom L, et al. A single nucleotide polymorphism in the NCF1 gene leading to reduced oxidative burst is associated with systemic lupus erythematosus. Ann Rheum Dis 2017;76(9):1607–13. doi: 10.1136/annrheumdis-2017-211287.
[42] Kelkka T, Kienhöfer D, Hoffmann M, Linja M, Wing K, Sareila O, et al. Reactive oxygen species deficiency induces autoimmunity with type 1 interferon signature. Antioxid Redox Signal 2014;21(16):2231–45. doi: 10.1089/ars.2013.5828.
[43] Geng L, Zhao J, Deng Y, Molano I, Xu X, Xu L, et al. Human SLE variant NCF1-R90H promotes kidney damage and murine lupus through enhanced Tfh2 responses induced by defective efferocytosis of macrophages. Ann Rheum Dis 2022;81(2):255–67. doi: 10.1136/annrheumdis-2021-220793.
[44] Kim-Howard X, Sun C, Molineros JE, Maiti AK, Chandru H, Adler A, et al. Allelic heterogeneity in NCF2 associated with systemic lupus erythematosus (SLE) susceptibility across four ethnic populations. Hum Mol Genet 2014;23(6):1656–68. doi: 10.1093/hmg/ddt532.
[45] Song Z, Yoo D-G, Idol RA, Barbu EA, Jacob CO, Dinauer MC. Lupus-associated NCF2 variant p.R395W in the NADPH oxidase 2 complex results in a reduced production of reactive oxygen species by myeloid cells. Front Lupus 2023;1:1186641. doi: 10.3389/flupu.2023.1186641.

Ann Rheum Dis 84 (2025) 798−809

Contents lists available at ScienceDirect

Annals of the Rheumatic Diseases

journal homepage: https://www.sciencedirect.com/journal/annals-of-the-rheumatic-diseases

Systemic sclerosis

Dysfunctional KLRB1$^+$CD8$^+$ T-cell responses are generated in chronically inflamed systemic sclerosis skin

Alyxzandria M. Gaydosik[1], Tracy Tabib[1,2], Jishnu Das[2], Adriana Larregina[3], Robert Lafyatis[1], Patrizia Fuschiotti[1,*]

[1] *Department of Medicine, Division of Rheumatology and Clinical Immunology, University of Pittsburgh School of Medicine, Pittsburgh, PA, USA*
[2] *Center for Systems Immunology, Departments of Immunology and Computational & Systems Biology, University of Pittsburgh School of Medicine, Pittsburgh, PA, USA*
[3] *Department of Dermatology, University of Pittsburgh School of Medicine, Pittsburgh, PA, USA*

A R T I C L E I N F O

Article history:
Received 18 September 2024
Received in revised form 21 November 2024
Accepted 22 November 2024

A B S T R A C T

Objectives: To analyse the immune mechanisms of diffuse cutaneous systemic sclerosis (dcSSc) skin disease focusing on CD8$^+$ T-cell responses in the affected skin of patients because chronic inflammation, vasculopathy, and extensive cutaneous fibrosis are prominent features of dcSSc skin disease, causing pain and disability in patients, with no effective therapy.
Methods: Single-cell transcriptomics and epigenomics were applied to well-characterised patient skin samples to identify transcriptomes and key regulators of skin-resident CD8$^+$ T-cell subsets. Multicolor immunofluorescence miscoscopy was used to validate molecular findings. *Ex vivo* skin explant assays were used to functionally characterise dysfunctional CD8$^+$ T-cell subsets on nonlesional autologous skin.
Results: We identified 2 major developmentally connected CD8$^+$ T-cell subpopulations that were expanded in SSc skin lesions compared with healthy control skin. The first was a heterogeneous subset of effector-memory CD8$^+$KLRB1$^+$IL7R$^+$ cells characterised by increased cytolytic and Tc2/Tc17 effector functions that appear to induce tissue damage and fibrosis in early-stage dcSSc skin lesions. The second, found primarily in patients with late-stage disease, was an exhausted CD8$^+$KLRG1$^+$IL7R$^-$ subset that exhibited transcriptional features of long-lived effector cells, likely contributing to chronic inflammation. Significantly, both subsets were also expanded in other benign dermatoses, implicating these cell populations in the pathogenesis of chronic human skin inflammation.
Conclusions: This study provides new insight into core regulatory programmes modulating skin-resident CD8$^+$ T-cell plasticity and identifies distinct CD8$^+$ T-cell subpopulations that contribute to initiation and chronicity of inflammatory responses in systemic sclerosis skin lesions. These findings reveal prospective molecular targets for new therapeutic strategies against this incurable disease.

* **Correspondence to** Dr Patrizia Fuschiotti, Department of Medicine, Division of Rheumatology and Clinical Immunology, University of Pittsburgh School of Medicine, Pittsburgh, PA.

E-mail address: paf23@pitt.edu (P. Fuschiotti).

Handling editor Josef S. Smolen.

https://doi.org/10.1016/j.ard.2025.01.022

WHAT IS ALREADY KNOWN ON THIS TOPIC

- Skin involvement strongly affects the quality of life of patients with early diffuse cutaneous systemic sclerosis (dcSSc).
- There is no effective disease-modifying treatment and only limited understanding of the underlying mechanisms of pathogenesis.

WHAT THIS STUDY ADDS

- Single-cell multiomics reveal the expansion of 2 developmentally connected skin-resident CD8$^+$ T-cell subpopulations in the lesional skin of patients with dcSSc, which are involved with initiation (CD8$^+$KLRB1$^+$IL7R$^+$ cells) and chronicity (CD8$^+$KLRG1$^+$IL7R$^-$ cells) of inflammatory responses.
- Effector-memory CD8$^+$KLRB1$^+$IL7R$^+$ cells exhibit increased cytolytic and Tc2/Tc17 effector functions that appear to directly induce tissue damage and fibrosis in early-stage dcSSc skin lesions.
- CD8$^+$KLRG1$^+$IL7R$^-$ cells are found primarily in patients with late-stage disease and exhibit an exhausted phenotype and transcriptional features of long-lived effector cells, likely contributing to chronic inflammation.
- Both subsets are also expanded in the skin of other benign dermatoses, implicating these cell populations in the pathogenesis of chronic human skin inflammation.

HOW THIS STUDY MIGHT AFFECT RESEARCH, PRACTICE OR POLICY

- Identification of the precise immune mechanisms underlying dcSSc skin disease opens avenues for the development of more effective and less toxic therapeutic agents for this currently incurable disease.

INTRODUCTION

Tissue-resident memory CD8$^+$ T cells (T$_{RM}$) are critical mediators of long-lasting immunity in nonlymphoid tissues, especially at barrier sites such as skin and mucosal surfaces [1,2]. T$_{RM}$ cells permanently reside in nonlymphoid tissue and are phenotypically distinct from recirculating memory CD8$^+$ T cells [3,4]. However, both exhibit extensive functional heterogeneity and various subsets of T$_{RM}$ CD8$^+$ cells have been identified in multiple tissues [3,5−7]. Killer cell lectin-like receptor subfamily G, member 1 (KLRG1) and interleukin (IL)7R have been used as markers to identify distinct CD8$^+$ T-cell subsets with specific effector function, migratory properties, long-term survival, and memory potential [6,8,9]. Terminally differentiated CD8$^+$KLRG1$^+$IL7R$^-$ short-lived effector cells (SLECs) are the predominant cell type during the effector phase of infection. Although CD8$^+$KLRG1$^+$IL7R$^-$ cells display limited potential to become memory cells, a fraction may persist following infection as long-lived effector cells (LLECs) with low proliferative ability [10,11]. Conversely, CD8$^+$KLRG1$^-$IL7R$^+$ memory precursor effector cells exhibit increased survival during the contraction phase and continue to differentiate into protective, long-lived memory cells.

Although T$_{RM}$ CD8$^+$ cell heterogeneity has been well-characterised in infection and cancer, diversity in chronic inflammation is less understood. In this study, we analysed CD8$^+$ T$_{RM}$ responses in chronically inflamed skin with a focus on diffuse cutaneous systemic sclerosis (dcSSc) skin disease characterised by inflammation, vasculopathy, and extensive fibrosis. Skin involvement is the predominant manifestation in dcSSc, especially in the early stages [12], causing pain and disability in patients, and the complex pathogenesis has delayed development of effective therapy. Although we previously identified profibrotic IL13-producing CD8$^+$ T cells in the blood [13,14] and skin [15] of patients, a comprehensive phenotypic and functional analysis of CD8$^+$ T-cell responses in dcSSc skin disease is lacking. Here, we have combined new droplet-based single-cell methods to establish transcriptional (scRNA-seq) [16] and epigenetic (Assay for Transposase Accessible Chromatin, snATACseq) [17,18] programmes in thousands of individual cells directly from SSc skin samples. Uncovering the cellular and molecular immune mechanisms that lead to dcSSc skin disease will reveal prospective molecular targets for developing therapeutic strategies for this incurable disease.

METHODS

We analysed skin samples from 52 patients with a confirmed diagnosis of dcSSc [19]: 25 were enrolled at the Scleroderma Clinic of UPMC and 27 were collected previously [20] (Supplemental Table S1). Disease subtype and internal organ involvement were assessed according to established criteria [19,21]. Of these samples, 27 were used for scRNAseq, 7 for snATACseq, 4 for Cellular Indexing of Transcriptomes and Epitopes by sequencing (CITE-seq), 6 for *ex vivo* skin explant assays, and 8 for validation by immunofluorescence microscopy. Controls included healthy control (HC) skin samples (n = 28) obtained at the UPMC Arthritis and Autoimmunity Center from age-matched and sex-matched donors with no history of any connective tissue disease. Human subject research protocols were approved by the University of Pittsburgh Institutional Review Board.. All participants gave written informed consent in accordance with the Declaration of Helsinki. The approved study is an observational study of skin biopsies from patients with dcSSc. Experimental procedures for droplet-based single-cell methods followed established techniques using Chromium Single Cell reagents (10× Genomics) [18,20,22] Multicolor immunofluorescence (mIF) microscopy was performed on formalin-fixed, paraffin-embedded skin samples stained using tyramide signal amplification (ThermoFisher) [20]. *Ex vivo* skin explant assays were performed as previously described [23]. See Supplemental Methods for details. Datasets analysed in this study are available in the GEO database under accession numbers GSE153760 (atopic dermatitis [AD]) [24], GSE151177 (psoriasis [PS]) [25], GSE186476 (cutaneous lupus [CL]) [26], GSE138669 (SSc) [27], and GSE182861 (HC) [28]. Microarray and snATAC-seq data are available upon reasonable request.

RESULTS

Tissue-resident long-lived CD8$^+$KLRG1$^+$IL7R$^-$ T cells contribute to persistent inflammation in dcSSc skin lesions

We analysed our previously reported scRNAseq dataset to comprehensively characterise CD8$^+$ T-cell responses in dcSSc skin samples (Fig 1A, Supplemental Table S1a) [20]. In total, we analysed 1226 CD8$^+$ T cells from 27 dcSSc (n = 964 cells) and 10 HC (n = 262 cells) skin samples [29−31]. The majority of SSc and HC CD8$^+$ T cells were skin resident (CD69$^+$ITGAE$^{+/-}$) [32], and only a small proportion of SSc CD8$^+$ T cells were recirculating (CCR7$^+$SELL$^{+/-}$) [32] (Fig 1B). While most SSc and HC CD8$^+$ T cells expressed markers of memory precursor cells (IL7R$^+$KLRG1$^-$), a considerable number of cells, mostly derived from patient samples, presented the phenotype of SLECs (KLRG1$^+$IL7R$^-$) [1,6] (Fig 1C). Using publicly available scRNAseq datasets, we showed that CD8$^+$KLRG1$^+$IL7R$^-$ cells are also found in the skin lesions of patients with other chronic inflammatory skin diseases such as AD, PS, and CL (Fig 1D,E, Supplemental Table S2). While we detected a significant increase in the proportion of

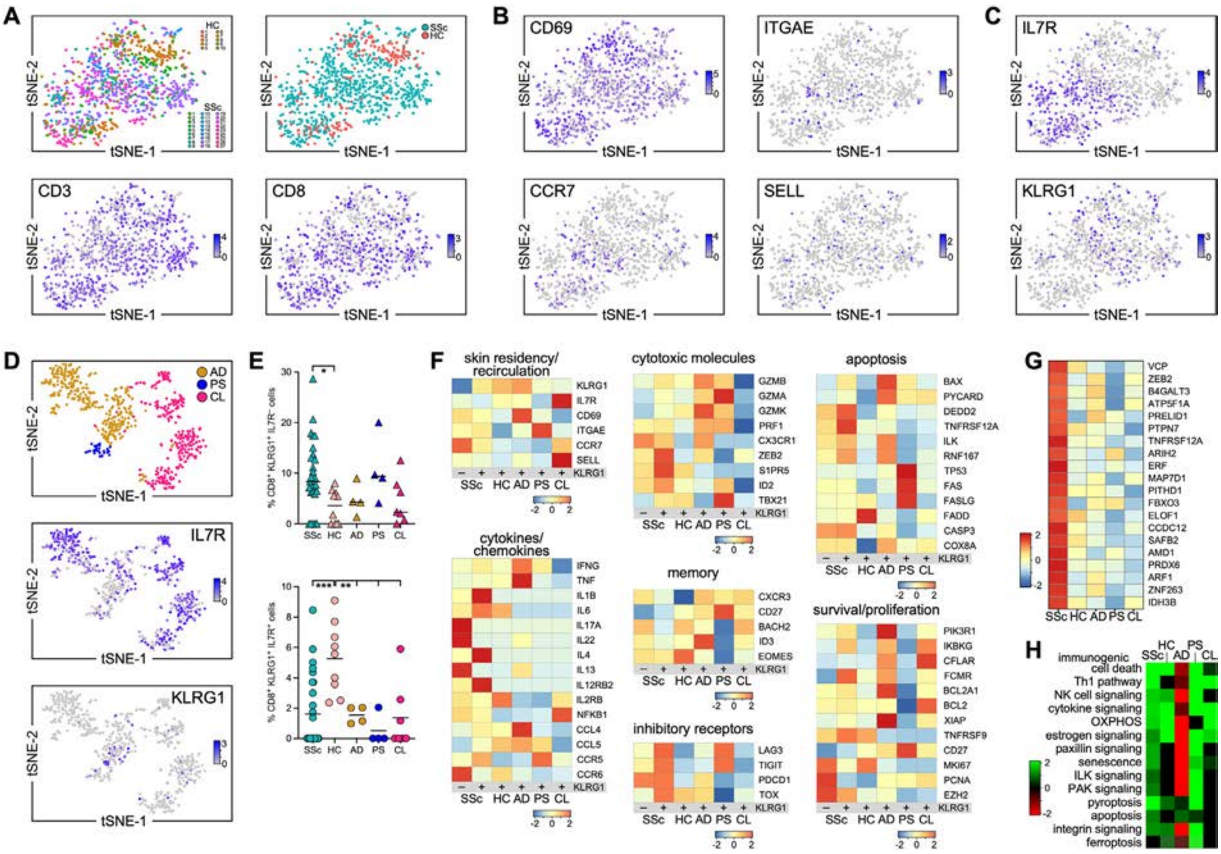

Figure 1. Transcriptional profiles of tissue-resident CD8$^+$KLRG1$^+$ T lymphocytes from progressive systemic sclerosis (SSc) skin lesions. Transcriptomes of 1226 CD8$^+$ cells (262 cells from healthy control [HC] and 964 cells from SSc skin samples) were analysed using Seurat. (A, upper) Two-dimensional t-SNE shows dimensional reduction of reads from single cells, revealing grouping in each SSc sample (n = 27) compared with all HC (n = 10) skin samples. Cells from each subject (indicated by different colours) or all patient samples combined are shown. (A, lower) Expression of CD3 and CD8 cell markers by *CD3*$^+$ cells from patient and HC skin samples. (B) t-SNE plots show expression of skin-residency marker genes. (C) Expression of *IL7R* and *KLRG1* genes by CD3$^+$CD8$^+$ cells from patient and HC skin samples. (D) Transcriptomes of 2237 CD8$^+$ cells (1428 from atopic dermatitis [AD; n = 4], 714 from cutaneous lupus [CL; n = 7], and 95 from psoriasis [PS; n = 4] samples) revealing grouping in each disease type (upper) and expression of *IL7R* and *KLRG1* genes (lower). All samples are combined and colour-coded by disease status. (E) Proportion of CD8$^+$KLRG1$^+$IL7R$^{-/+}$ cells by individual SSc, HC, AD, PS, or CL samples. Statistics by unpaired 2-tailed Student *t* test. (F) Average expression for a selection of genes associated with skin residency and various effector functions for CD8$^+$KLRG1$^+$ cells from SSc (n = 27), HC (n = 10), AD (n = 9), PS (n = 4), and CL (n = 7) skin samples. (G) Heat map shows average gene expression of CD8$^+$KLRG1$^+$ cells signature genes from SSc versus HC, AD, PS, and CL samples. Gene differential tests are described in the Methods. (H) Pathway analysis by Ingenuity (Qiagen). Highly significant examples of distinct pathways activated in each group are shown. In Ingenuity Pathway Analysis (IPA), the differential gene lists from individual samples (*P* value < .05, log fold change 0.1, minimum percentage, 10%) were run in IPA to compare each other for common pathways. Heatmap shows *z*-scores of pathways for upregulation or downregulation of pathways.

CD8$^+$KLRG1$^+$IL7R$^-$ cells in SSc compared with that in HC samples, the HC exhibited a higher proportion of CD8$^+$KLRG1$^+$IL7R$^+$ cells compared with all groups (Fig 1E). We found that CD8$^+$KLRG1$^+$IL7R$^{-/+}$ from the skin lesions of all samples exhibited a high degree of transcriptional overlap, characterised by expression of genes encoding for markers of tissue residency as well as by the expression of variable levels of proinflammatory effector mediators (Fig 1F and Supplemental Fig S1). These included chemokines (*CCL4, CCL5*, and *CCR5*), cytokines (*IFNG* and *TNF*) and markers of cytotoxicity such as granzymes (*PRF1, ID2*, and *TBX21*). Of note, we observed that SSc CD8$^+$KLRG1$^+$ cells specifically expressed *IL12RB2, IL1B*, and *IL4* compared with CD8$^+$KLRG1$^+$ cells from all other samples. No expression of T_H17 and other T_H2 cytokines was detected in CD8$^+$KLRG1$^+$ cells from any of the cohorts tested apart from AD CD8$^+$KLRG1$^+$ cells expressing IL22 and IL13. In addition to expressing markers of cytotoxicity, CD8$^+$KLRG1$^+$ cells across all samples expressed variable levels of memory markers (*CXCR3, CD27, ID3*, and *EOMES*) and of proapoptotic (*BAX, DEDD2, TNFRSF12A, FAS, FASLG*, and *CASP3*), prosurvival (*PIK3R1, FCMR, BCL2, BCL2A1, TNFRSF9*, and *XIAP*), and proliferation (*MIK67, PCNA*, and *EZH2*) genes (Fig 1F). Strikingly, SSc CD8$^+$KLRG1$^+$ cells expressed the highest levels of various inhibitory checkpoint molecules compared to CD8$^+$KLRG1$^+$ cells from all other samples and specifically expressed several genes associated with apoptosis, control of proliferation, and metabolism (Fig 1G, Supplemental Table S3a). Accordingly, we found some heterogeneity between SSc and healthy and disease control CD8$^+$KLRG1$^+$IL7R$^-$ cells in the upregulation of several processes including immunogenic cell death, apoptosis, T_H1 and NK signalling, senescence as well as paxillin, ILK, and PAK pathways (Fig 1H).

Thus, SSc CD8$^+$KLRG1$^+$IL7R$^-$ cells represent a heterogeneous exhausted cell population expressing effector and prosurvival genes that may confer a long-lived effector fate.

Increased proportions of tissue-resident effector-memory CD8$^+$KLRB1$^+$ T cells are found in the lesional skin of SSc and other chronic inflammatory skin diseases

Louvain clustering of SSc and HC CD8$^+$ T cells [29,30] yielded 4 major clusters (Fig 2A). Most cells from clusters 0 and 3 derived from SSc samples (93.8% and 92.5%, respectively), whereas

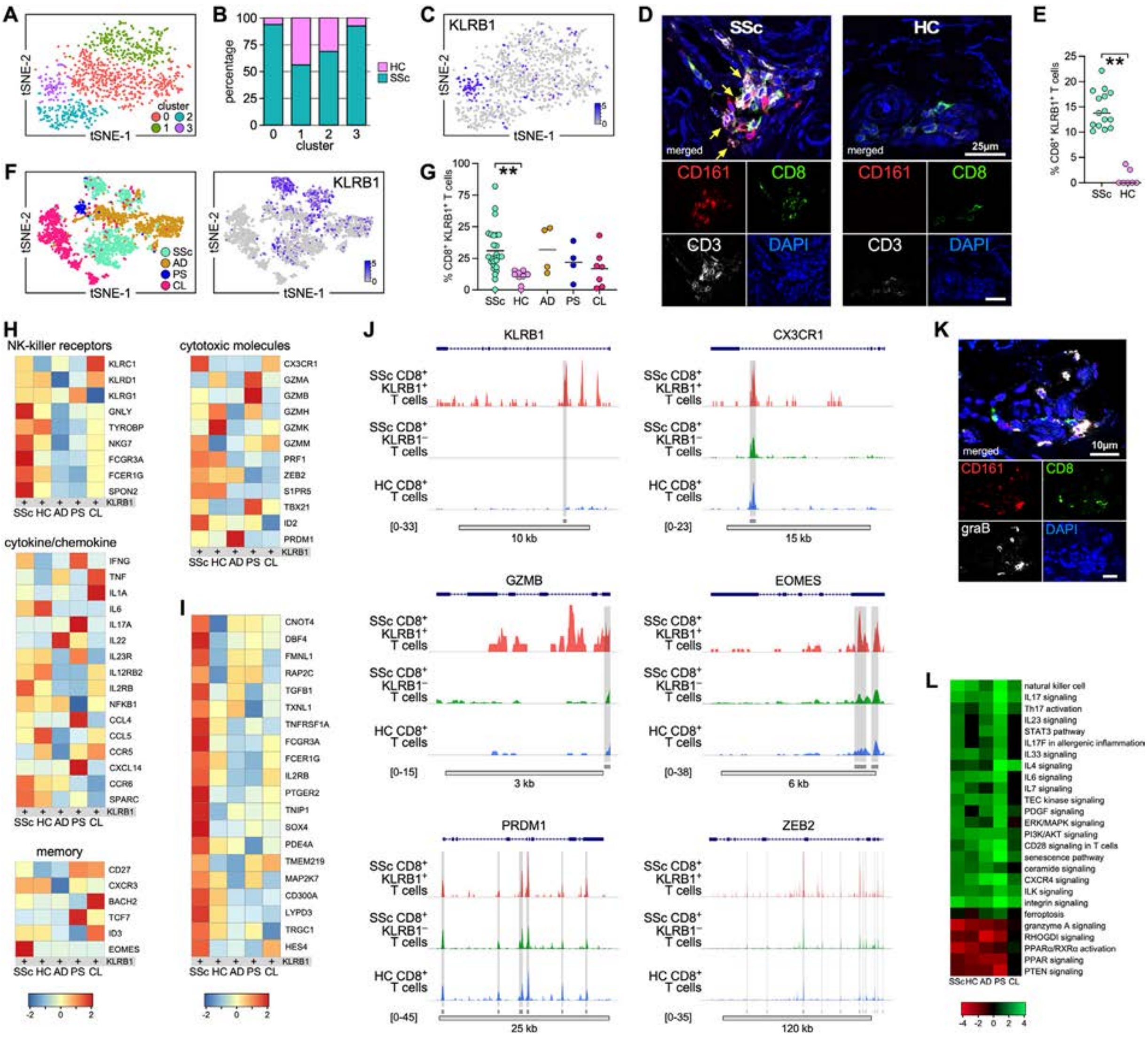

Figure 2. Characterisation of the systemic sclerosis (SSc)-specific CD8$^+$KLRB1$^+$ T-cell subset in the lesional skin of patients with active diffuse cutaneous SSc. (A) Seurat analysis identified 4 discrete CD8$^+$-cell Louvain clusters. (B) Bar plot showing the proportion of CD8$^+$ cells from SSc and healthy control (HC) skin samples within individual clusters. (C) Expression of KLRB1 from patient (n = 27) and HC (n = 10) skin samples. (D,E) Multicolor immunofluorescence microscopy staining for CD3, CD8, and KLRB1 in progressive SSc (n = 15) and HC (n = 6) skin samples. Representative examples (D) and the proportion (E) of CD3$^+$CD8$^+$KLRB1$^+$ cells are shown. Results are expressed as a percentage of positive cells out of the entire infiltrate following quantification of 8 high-power fields/sample (magnification, ×600). Error bars are mean ± SD. Statistics by unpaired 2-tailed Student *t* test. (F) Transcriptomes of 3463 CD8$^+$ cells from combined SSc, HC, atopic dermatitis (AD), psoriasis (PS), and cutaneous lupus (CL) skin samples and expression of *KLRB1* gene. (G) Proportion of CD8$^+$KLRB1$^+$ cells by individual SSc, HC, AD, PS, or CL samples. Statistics by one-way ANOVA, followed by Tukey multiple comparisons test. (H) Average expression for a selection of genes associated with skin residency and effector functions of CD8$^+$KLRB1$^+$ cells from SSc (n = 27), HC (n = 10), AD (n = 4), PS (n = 4), and CL (n = 7) skin samples. (I) Heat map shows average gene expression of CD8$^+$KLRB1$^+$ cells signature genes from SSc versus HC, AD, PS, and CL samples. Gene differential tests are described in the Methods. (J) Normalised scATACseq profiles in SSc (n = 7) CD8$^+$KLRB1$^+$, SSc CD8$^+$KLRB1$^-$, and HC (n = 5) CD8$^+$ T cells by Signac [17]. Merged coverage plots demonstrating pseudo-bulk chromatin accessibility (fragment coverage by frequency of Tn5 insertion) across 6 loci, with single-nucleus ATACseq (snATACseq) peaks depicted by grey bars. Y-axis corresponds to cell subsets. Range of normalised accessibility for fragment coverage of each gene listed on X-axis. Peaks differentially expressed by SSc CD8$^+$KLRB1$^+$ cells are highlighted in grey. (K) Representative example (×1000) of multicolor immunofluorescence microscopy (mIF) staining for CD8, KLRB1, and graB in progressive SSc (n = 7) skin samples. DAPI (4′,6-diamidino-2-phenylindole) stains nuclei. (L) Heatmap depicts highly significant ($P < .05$) examples of upregulated and downregulated pathways activated by CD8$^+$KLRB1$^+$ cells from SSc, HC, AD, PS, and CL samples, *z*-scores are shown.

clusters 1 and 2 were a mixture of cells from HC and patient samples (Fig 2B). Cells from cluster 0 showed low average *KLRG1* expression and upregulation of several genes associated with TCR signalling, NFAT activation, and T-cell exhaustion (Supplemental Fig S2A,B). In comparison, cells from cluster 3 showed highly increased average expression of killer cell lectin-like receptor subfamily B, member 1 (*KLRB1*) and upregulated JAK family kinase signalling in IL6-like cytokines as well as T_H2 and NK pathways (Fig 2C and Supplemental Fig S2A,B).

Transcriptional data were validated by mIF microscopy showing higher proportions of CD161$^+$ (encoded by *KLRB1*) CD3$^+$CD8$^+$ T cells in SSc compared to those in HC cells (Fig 2D, E). We also found an increased trend in proportions of CD8$^+$KLRB1$^+$ cells in other chronic inflammatory skin diseases (Fig 2F,G). CD8$^+$KLRB1$^+$ cells from patients and control samples presented a tissue-resident phenotype and expressed multiple memory (*IL7R, CCR7, CD27, CXCR3, BACH2, TCF7, ID3*, and *EOMES*), prosurvival (*CD27, BCL2, BCL2A1*, and *FCMR*), and proliferation (*PCNA, MIK67, EZH2*, and *XIAP*) genes (Fig 2H and Supplemental Fig S2C). Interestingly, we found that CD8$^+$KLRB1$^+$ cells from all groups expressed several NK-killer receptors (Fig 2H and Supplemental Fig S2C) and various levels of effector genes such as those encoding for inflammatory cytokines (*IFNG, TNF, IL1A, IL17A*, and *IL22*), chemokines (*CCL4, CCL5, CCR6*, and *SPARC*), and cytotoxic molecules (granzymes, *CX3CR1, ZEB2, S1PR5, TBX21, ID2*, and *PRDM1*) (Fig 2H and Supplemental Fig S2C). SSc-specific gene expression by CD8$^+$KLRB1$^+$ cells included genes associated with proinflammatory cytokine signalling (*CNOT4, PTGER2, PDE4A, TGFB1, FCER1G*, and *SOX4*) (Fig 2I, Supplemental Table S3b).

To determine whether gene expression differences between SSc CD8$^+$KLRB1$^+$ and CD8$^+$KLRB1$^-$ T-cell subsets correlated with chromatin remodelling, we determined the chromatin accessibility landscape using snATACseq with analysis by Signac [17,18]. The analysis of key effector gene loci (*CX3CR1, GZMB, EOMES, PRDM1, ZEB2, PRF1, ID2*, and *TBX21*) revealed that SSc CD8$^+$KLRB1$^+$ cells exhibited increased chromatin accessibility compared with SSc CD8$^+$KLRB1$^-$ cells or HC CD8$^+$ cells (Fig 2J and Supplemental Fig S3), indicating that chromatin remodelling in SSc CD8$^+$KLRB1$^+$ cells may explain the cytotoxic phenotype of these cells. By mIF microscopy, we validated expression of graB by CD8$^+$CD161$^+$ cells in dcSSc skin lesions (Fig 2K). Pathway analysis by Ingenuity Pathway Analysis showed that CD8$^+$KLRB1$^+$ cells from patients and control samples upregulated several pathways in common, including those associated with T-cell activation and signalling, NK signalling, T$_H$17, T$_H$2, IL7, and IL6 activation (Fig 2L).

Thus, the proportion of CD8$^+$KLRB1$^+$ cells is increased in patients with chronic inflammatory skin conditions compared to HC skin and they exhibit increased cytolytic and proinflammatory effector functions.

Cutaneous SSc CD8$^+$KLRB1$^+$ and CD8$^+$KLRG1$^+$ cells represent heterogeneous subsets of developmentally connected cells

We compared the phenotype and function of CD8$^+$KLRB1$^+$ and CD8$^+$KLRG1$^+$ cells (Fig 3A). While SSc CD8$^+$KLRB1$^+$KLRG1$^{-/+}$ cells upregulated expression of genes associated with cytotoxicity (*CX3CR1, GZMB, PRF1, ID2, ZEB2, S1PR5*, and *SATB1*) and memory (*ID3, CXCR3, IL7R, EOMES*, and *RUNX1*) phenotypes, CD8$^+$KLRG1$^+$KLRB1$^-$ cells showed increased expression of *CD27, TBX21, GZMA, GZMK, IFNG*, and *TNF*. Moreover, CD8$^+$KLRB1$^+$KLRG1$^-$ cells exhibited enhanced expression of T$_H$17 and T$_H$2 cytokines as well as of their regulators *IL23R, RORC* (T$_H$17) and *IL1RL1, IL4R*, and *GATA3* (T$_H$2). Interestingly, AD CD8$^+$KLRB1$^+$KLRG1$^-$ cells also exhibited a Tc2/Tc17 phenotype, while PS CD8$^+$KLRB1$^+$KLRG1$^-$ cells upregulated T$_H$17-related genes (Tc17), and CL CD8$^+$KLRB1$^+$ cells expressed *TNF, IL17A*, and RORC (Supplemental Fig S4). Although both SSc CD8$^+$KLRB1$^+$KLRG1$^{-/+}$ and CD8$^+$KLRB1$^+$KLRG1$^{-/+}$ subsets expressed checkpoint inhibitory receptors, the highest levels were found in CD8$^+$KLRG1$^+$KLRB1$^-$ cells which also diminished proliferation markers (Fig 3A and Supplemental Figs S1 and 2C). In agreement with the transcriptional data, SSc CD8$^+$KLRB1$^+$ and CD8$^+$KLRB1$^+$KLRG1$^+$ cells displayed enhanced open chromatin states in both effector (*CX3CR1, GZMB, PRF1*, and *EOMES*) and proinflammatory (*IL13, IL23R, IL17A*, and *IL22*) gene loci compared with SSc CD8$^+$KLRG1$^+$KLRB1$^-$ cells and HC total CD8$^+$ cells (Fig 3B and Supplemental Fig S5A,B). Significantly, we found enrichment for distinct transcription factor (TF)-binding motifs (consensus sequence specific–binding sites) in open chromatin associated with each subpopulation. Consensus binding motifs for RUNX2, GATA3, IRF3, RORC, IRF4, IRF8, and IKZF1 were found more commonly in CD8$^+$KLRB1$^+$KLRG1$^-$ cells, while consensus binding motifs for KLF14, FLI1, ETS1, ERG, and TBX21 were found more commonly in CD8$^+$KLRG1$^+$KLRB1$^-$ cells (Fig 3C,D and Supplemental Fig S5C). Commonly enriched TF motifs included NFKB1, MAF::NFE2, STAT1::STAT2, and IRF9/7 and LEF1. We did not detect TF motifs associated with cytolytic activity such as ID2, ZEB2, and S1PR5 as they are not included in the TF database, JASPAR [33], used by both Signac and ChromVar [34].

We subsequently performed an RNA velocity analysis by scVelo [35,36] to examine gene expression dynamics at the single-cell level during CD8$^+$KLRB1$^+$ and CD8$^+$KLRG1$^+$ cell differentiation. RNA velocity is the time derivative of transcript abundance, which reveals the cellular dynamics by modelling the relationship between unspliced and spliced mRNAs for each gene. The ratio between them is an indicator of the future state of mature mRNA abundance, and thus, the future state of the cell. We found a strong velocity pattern originating from CD8$^+$KLRB1$^+$ cells and proceeding to CD8$^+$KLRG1$^+$ cells (Fig 4A,B and Supplemental Fig S6), indicating that CD8$^+$KLRG1$^+$ cells derive from CD8$^+$KLRB1$^+$ cells. Trajectory analysis using Monocle [37] allowed gene expression to be examined during CD8$^+$KLRB1$^+$ and CD8$^+$KLRG1$^+$ cell differentiation (Fig 4B,C). Expression dynamics of signature genes along the pseudotime showed 2 major differentiation branches for CD8$^+$KLRB1$^+$ cells, including 1 enriched by cells expressing markers of cytotoxicity (*GZMB* and *PRF1*) and a second by cytokine-producing cells (*GATA3, IL13*, and *CCR6*). *IFNG* was produced mostly by CD8$^+$KLRG1$^+$ cells. While *GZMA* was expressed by both subsets, *GZMK* expression was confined to KLRG1$^+$ cells (Fig 4C).

Both subsets exhibited increased expression of TCR signalling genes, suggesting continuous antigenic stimulation (Supplemental Fig S5D). Although the single-cell gene expression approach employed (3′ Library kit) does not allow TCR repertoire profiling and therefore the identification of antigen-specific T lymphocyte expansion, we could, nonetheless, detect increased expression of TRBC1 or TRBC2 genes in these subsets (Supplemental Fig S5E), consistent with the occurrence of $\alpha\beta$TCR expansion. Notably, we found that the proportions of SSc CD8$^+$KLRB1$^+$ cells were increased at the earliest SSc stages, while those of CD8$^+$KLRG1$^+$ cells were increased at later stages of SSc (Fig 4D). Although we found no statistical significance, a similar trend was detected in the correlation with the extent of skin fibrosis (modified Rodnan skin score). No significant correlation was found with age and sex of patients, the type of autoantibody they expressed or treatment (Fig 4D). Thus, CD8$^+$KLRB1$^+$ cells may be involved in the early-stage of SSc skin disease, while CD8$^+$KLRG1$^+$ cells likely contribute to maintaining chronic inflammation in late-stage SSc.

A distinct subset of CD8$^+$CRT$_H$2$^+$KLRB1$^+$ cells produce T$_H$2 cytokines in SSc skin lesions

We next assessed the transcriptional profile of type-2 cytokine-producing CD8$^+$KLRB1$^+$ cells in the lesional skin of patients with early-stage dcSSc. We employed CITEseq [38] to measure transcriptome and immunophenotype simultaneously and focused on cells expressing markers of T$_H$2 cells, such as CRTH2 (encoded by *PTGDR2*) [39]. Compared to scRNA-seq, CITEseq can better differentiate between cell populations with subtle transcriptomic

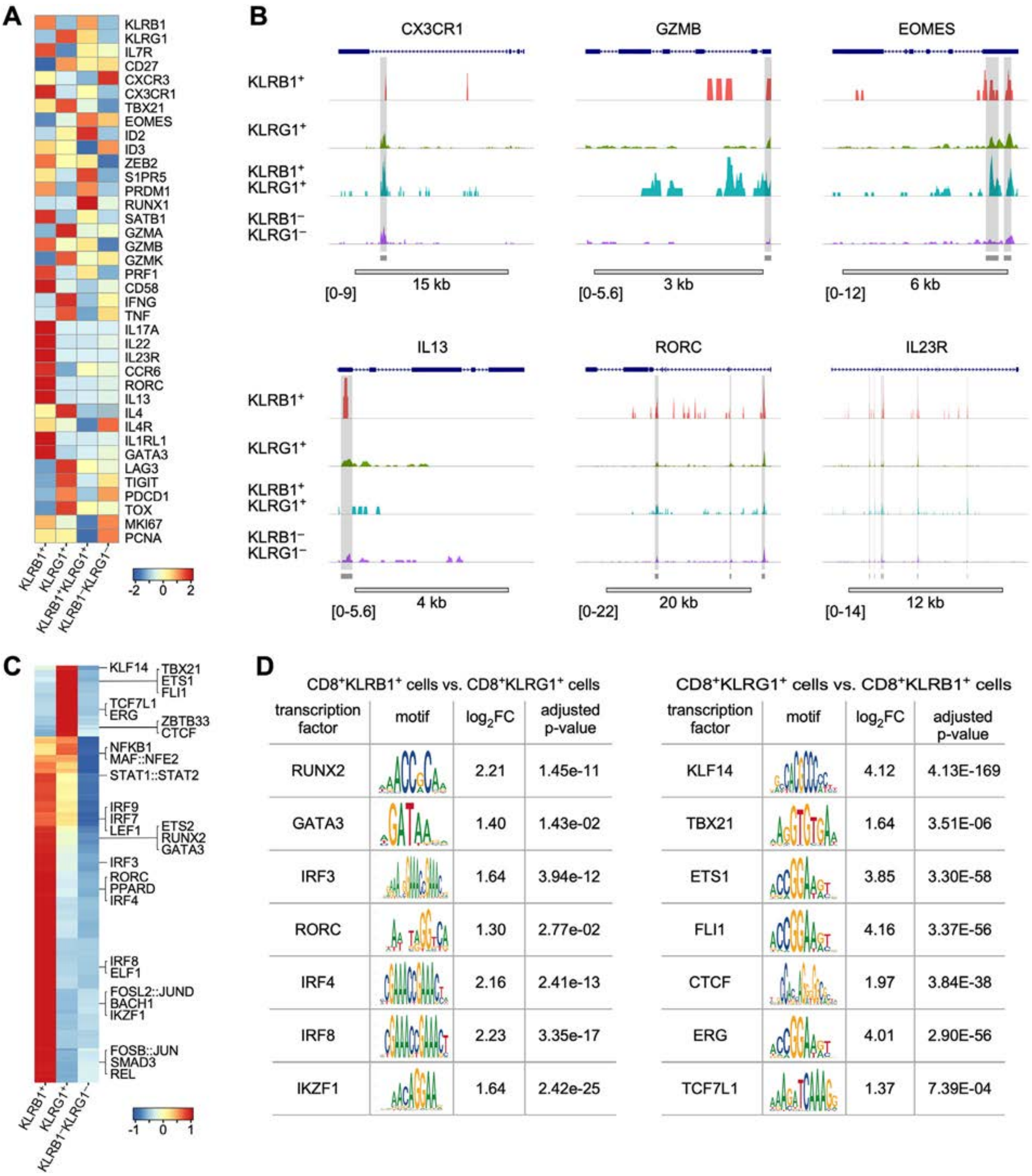

Figure 3. Comparison of CD8$^+$KLRG1$^+$ with CD8$^+$KLRB1$^+$ T cells in the lesional skin of patients with active diffuse cutaneous systemic sclerosis (SSc). (A) Heat map shows average gene expression of CD8$^+$KLRB1$^+$ and CD8$^+$KLRG1$^+$ cells signature genes from SSc samples (n = 27). Gene differential tests are described in the Methods. (B) Examples of merged coverage plots demonstrating pseudo-bulk chromatin accessibility across 6 gene loci in SSc CD8$^+$KLRB1$^+$, CD8$^+$KLRG1$^+$, CD8$^+$KLRB1$^+$KLRG1$^+$, and CD8$^+$KLRB1$^-$KLRG1$^-$ cell populations, with snATACseq peaks depicted by grey bars. (C) Heatmap by ChromVAR showing motif activity score per cell in CD8$^+$KLRB1$^+$, CD8$^+$KLRG1$^+$, and CD8$^+$KLRB1$^-$KLRG1$^-$ subsets. (D) Transcription factors with the most significantly enriched motif activity when comparing SSc CD8$^+$KLRB1$^+$ to CD8$^+$KLRG1$^+$ cells by Signac.

differences and has a lower dropout rate and better ability to detect underrepresented transcripts of key protein markers. Accordingly, while we could detect a distinct CD8$^+$ T-cell subset exhibiting increased surface expression of CRTH2 proteins, we could not detect any *PTGDR2* transcripts (Fig 5A). SSc CD8$^+$CRTH2$^+$ cells (Tc2 cells) were found to mark a subset of CD8$^+$KLRB1$^+$ cells (Fig 5B), corresponding to 38.5% of total CD8$^+$KLRB1$^+$ cells, and visualised these cells by mIF microscopy in both early and late dcSSc skin samples (Fig 5C). Focusing on the CD8$^+$KLRB1$^+$CRTH2$^+$ cells, we found that these cells expressed multiple T$_H$2 genes (*IL4R, STAT6, JAK1, STAT5A, GATA3, IL4*, and *IL13*) as well as a distinct gene expression signature, including *EPHX2, IGFBP2, DAPK2, DLG2*, and *ITCH* (Fig 5D). In contrast, CD8$^+$KLRB1$^+$CRTH2$^-$ cells displayed a T$_H$17 gene expression signature (*IL17A, IL23R, RORC*, and *CCR6*). Accordingly, at the chromatin level we found increased accessibility at several T$_H$2 (*PTGDR2, IL4R, STAT6, GATA3, IL13*, and *MAF*) gene regions in CD8$^+$KLRB1$^+$CRTH2$^+$ T cells compared with CD8$^+$KLRB1$^+$CRTH2$^-$ cells (Fig 5E and Supplemental Fig S7A). Unlike HC skin, we visualised CD8$^+$CD161$^+$IL13$^+$ cells in early dcSSc skin lesions where they appear to signal through pSTAT6 and GATA3 (Fig 5F and Supplemental Fig S7B). Finally, we showed

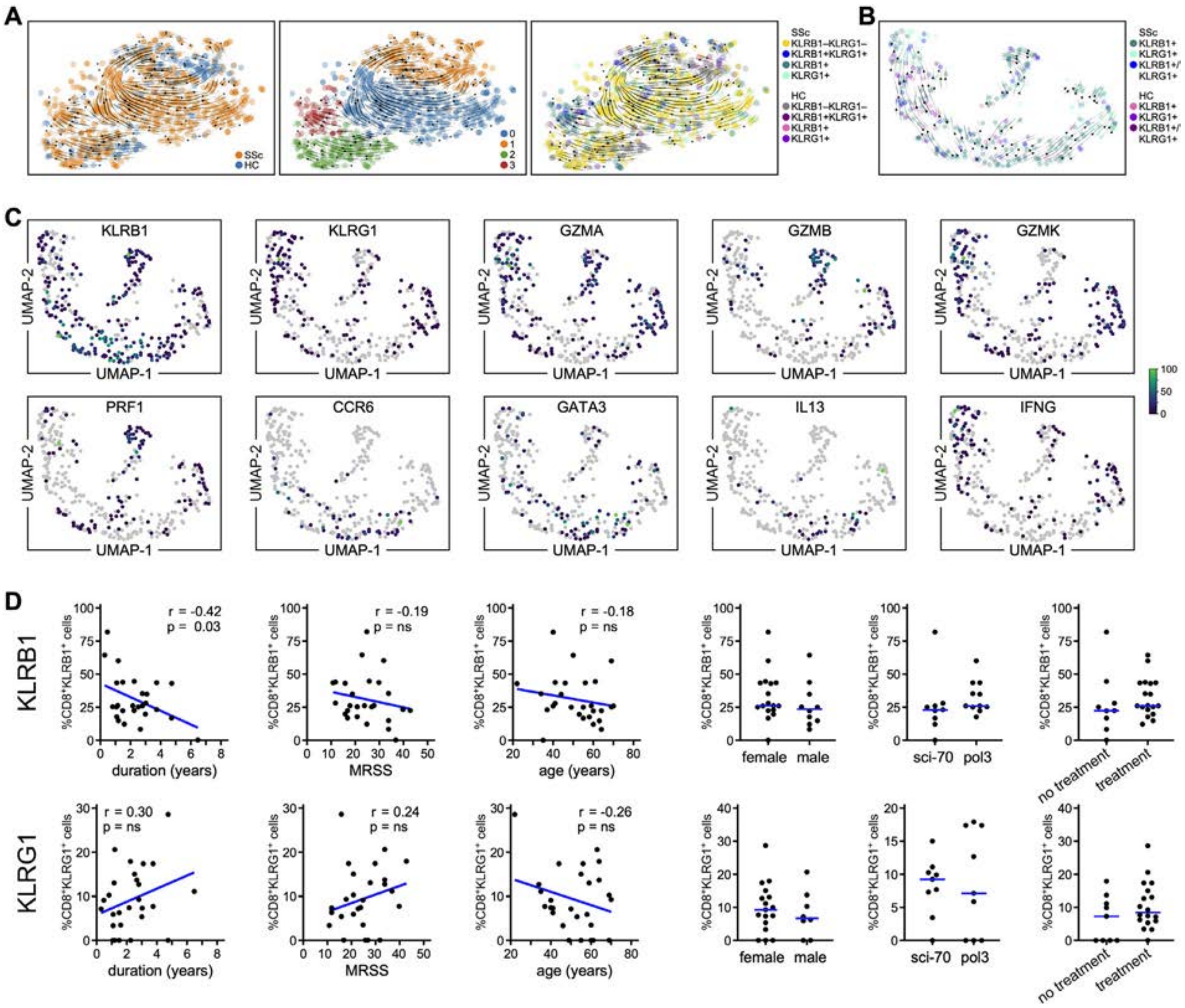

Figure 4. Dynamics of systemic sclerosis (SSc) CD8$^+$KLRB1$^+$ and CD8$^+$KLRG1$^+$ T-cell differentiation. (A) t-SNE of subset CD8$^+$ T cells coloured by health status, subcluster annotation, and assignment to KLRB1/KLRG1 expression groups with dynamic velocity stream overlaid. (B) Single-cell pseudotime trajectories of extracted KLRB1$^+$/KLRG1$^+$ CD8 T cells using Monocle 3 [37] with dynamic velocity stream overlaid. (C) Expression dynamics of signature genes along the pseudotime are shown. (D) Correlation between the frequency of CD8$^+$KLRB1$^+$ and CD8$^+$KLRG1$^+$ cells by scRNAseq and the clinical parameters of patients.

that IL13-producing CD8$^+$KLRB1$^+$ cells primarily localise in proximity of SMA$^+$ myofibroblasts, thus likely contributing to extracellular matrix (ECM) deposition (Fig 5G and Supplemental Fig S7C, D). Together, these results identify a population of CD8$^+$KLRB1$^+$CRTH2$^+$ Tc2 cells that produce profibrotic IL13, likely contributing to skin fibrosis in early dcSSc.

Cytotoxic CD8$^+$KLRB1$^+$ cells induce tissue damage in early dcSSc skin lesions

To investigate the function of CD8$^+$ T cells in dcSSc skin disease, we performed *ex vivo* skin explant assays. We isolated CD8$^+$ T cells from the lesional skin of patients with early dcSSc, cocultured them for 48 hours with autologous nonlesional [40,41] skin explants, and then performed a transcriptional analysis of explants (Fig 6A). Upregulated genes in explants after coculture included adhesion (*CEACAM5/1*), proapoptotic (*BCL2L11*), cytokine-induced (*IL13RA2, IRF6*, and *IL1A*), and metabolism (*WARS, PLA2G2F*, and *PLAUR*) genes (Fig 6A). As a control, we isolated CD8$^+$ T cells from HC skin donors and cocultured them with autologous skin explants. We compared gene expression from individual patient with SSc skin explant cocultures with those from individual HC donors as well as from HC skin explants cultured with either IL13 or TGFβ. Strikingly, we observed that CD8$^+$ T cells from several patients with SSc induced a common gene expression signature that was not induced by HC CD8$^+$ T cells on autologous skin. This signature included upregulation of several proinflammatory mediators (*SAA2, PTGS2, C3, IL1A, IL1B, IL1R2, IL13RA2, IL6ST*, and *IL36RN*), extracellular matrix proteins (*COL12A1, FN1*, and *EDN1*), and matrix metalloproteinases (*MMP1, MMP9, MMP10*, and *PLAUR*) (Fig 6B). Interestingly, some of these genes were also induced when HC skin was cultured by either TGBβ (*IL1A, IL36RN, FN1, MMP9, ITGA2, LAMC2*, and *EFNB2*) or IL13 (*C3, IL13RA2, IL36RN, TNFAIP6, CDCP1, NADP1*, and *CD274*) (Fig 6B). In agreement, Ingenuity Pathway Analysis indicated that CD8$^+$ T cells from the dcSSc lesional skin induced pathways of acute phase response, wound healing, as well as IL8, PAK, and CXCR4 signalling to the unaffected autologous skin (Fig 6C), some of which were commonly upregulated also by TGFβ and IL13 treatment but not by HC CD8$^+$ T cells on autologous skin (Fig 6C).

Focusing on SSc CD8$^+$KLRB1$^+$ cells, Connectome analysis [42] from our scRNAseq dataset predicted several ligand/receptor interactions between CD8$^+$KLRB1$^+$ cells and other cell types within the lesional skin microenvironment that appear to

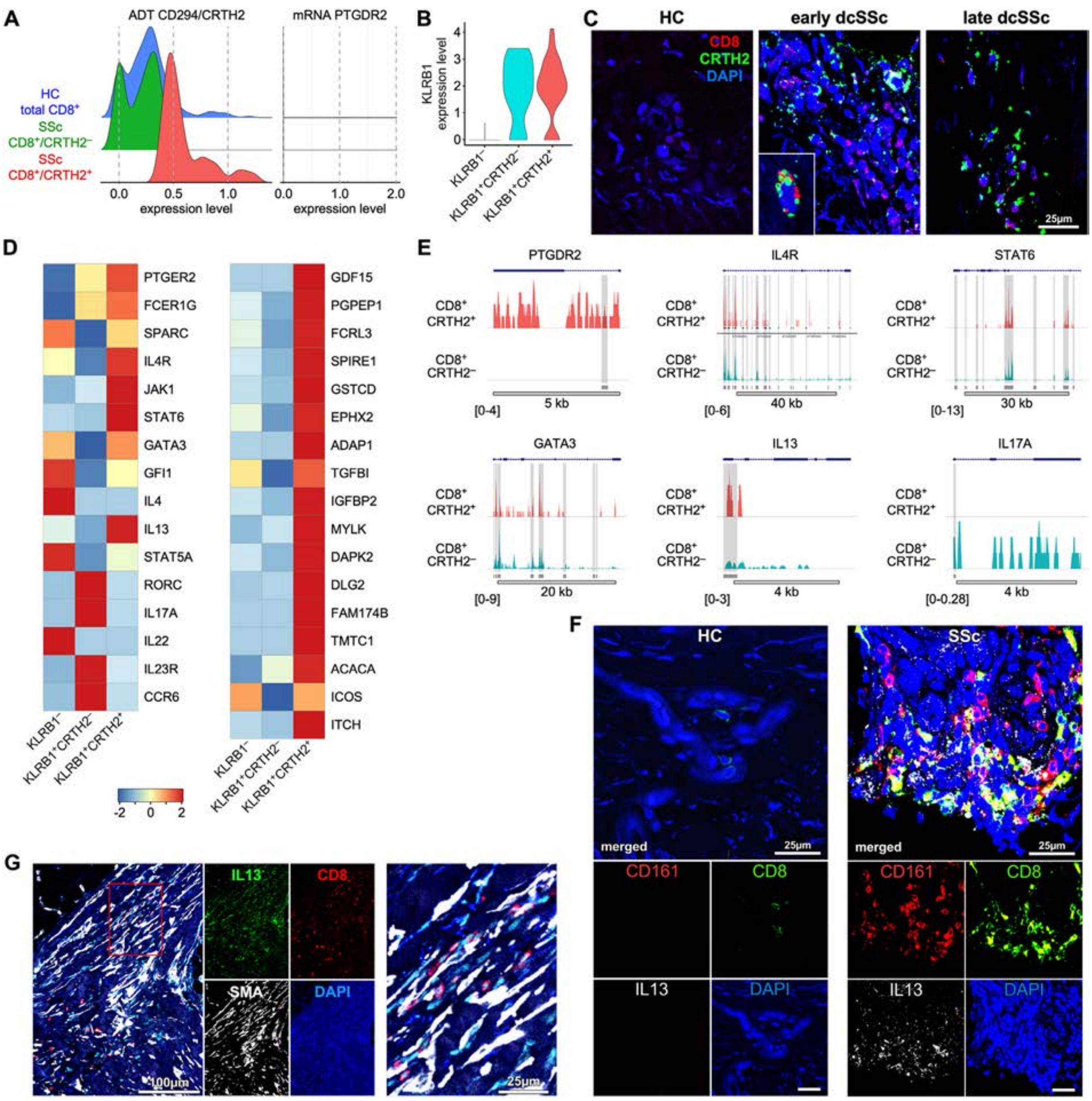

Figure 5. Characterisation of the systemic sclerosis (SSc)-specific CRTH2$^+$ T-cell subset in the lesional skin of patients with active diffuse cutaneous (dcSSc). (A) Cellular Indexing of Transcriptomes and Epitopes by sequencing (CITEseq) was used to measure immunophenotypes and transcriptomes simultaneously. Comparison between healthy control (HC; n = 4) and SSc (n = 4) for CRTH2 expression by CD8$^+$ T cells using either antibody-derived tag (ADT; CRTH2) or mRNA (*PTGDR2*, encoding for CRTH2) as described in the Methods. A representative example is shown. (B) Violin plot showing expression levels of KLRB1 by SSc CD8$^+$ T-cell subsets. (C) Multicolor immunofluorescence (mIF) microscopy visualises coexpression of CD8, CRTH2 (×600) in early (n = 3), late (n = 3) dcSSc, and HC (n = 3) skin biopsies (×600). (D) Heat maps show average gene expression by SSc CD8$^+$KLRB1$^+$CRTH2$^+$ cells from SSc samples (n = 4) in comparison with CD8$^+$KLRB1$^+$CRTH2$^-$ and CD8$^+$KLRB1$^-$ cells for signature and unique genes. Gene differential tests are described in the Methods. (E) Examples of merged coverage plots demonstrating Tn5 insertion frequency by snATAC-seq across 6 signature gene loci of SSc CD8$^+$CRTH2$^+$ and CD8$^+$CRTH2$^-$ cell populations. mIF microscopy visualises coexpression of (F) CD8, KLRB1, IL13 (×600), and (G) CD8, IL13, SMA (×200) in early dcSSc skin samples (n = 7) and HC (n = 5). DAPI (4′,6-diamidino-2-phenylindole) stains nuclei.

involve IL13, GZMB, and other proinflammatory mediators secreted by CD8$^+$KLRB1$^+$ cells (Fig 6D). Top highly significant predicted interactions included CCL5-CXCR3 and CCL5-CCR3 with B cells and CCL4-CCR5 and CCL4-CCR1 with macrophage/dendritic cells. TNF released by CD8$^+$KLRB1$^+$ cells was predicted to interact with TNRF2, TNFRSF21, and TNFRSF1A on fibroblasts, endothelial and myeloid cells. IL4 and IL13 were predicted to interact with IL4R on B cells and IL4R and IL13Rα1 on myeloid cells. IL13 was also predicted to interact with IL13Rα1 and IL13Rα2 on endothelial cells and fibroblasts, where it could contribute to ECM deposition (Fig 5G and Supplemental Fig S7C,D). IFNG-IFNGR1 and IFNG-IFNGR2 on endothelial cells, fibroblasts, and myeloid cells were also predicted. Finally, GZMB released by CD8$^+$KLRB1$^+$ cells was predicted to interact with B and endothelial cells, as well as with fibroblasts. These interactions were validated with mIF by visualising CD8$^+$KLRB1$^+$graB$^+$ cells in proximity of endothelial cells undergoing apoptosis (CD31$^+$CC3$^+$) in the perivascular areas of early dcSSc skin lesions but not in HC skin (Fig 6E,F). The cytolytic function of SSc CD8$^+$KLRB1$^+$ cells was further demonstrated by *ex vivo* skin explant assays, showing that cytotoxic peripheral blood CD8$^+$KLRB1$^+$ cells induce tissue damage [43], including endothelial cell damage in autologous nonlesional dcSSc skin (Fig 6G-J and Supplemental Fig S8). Thus,

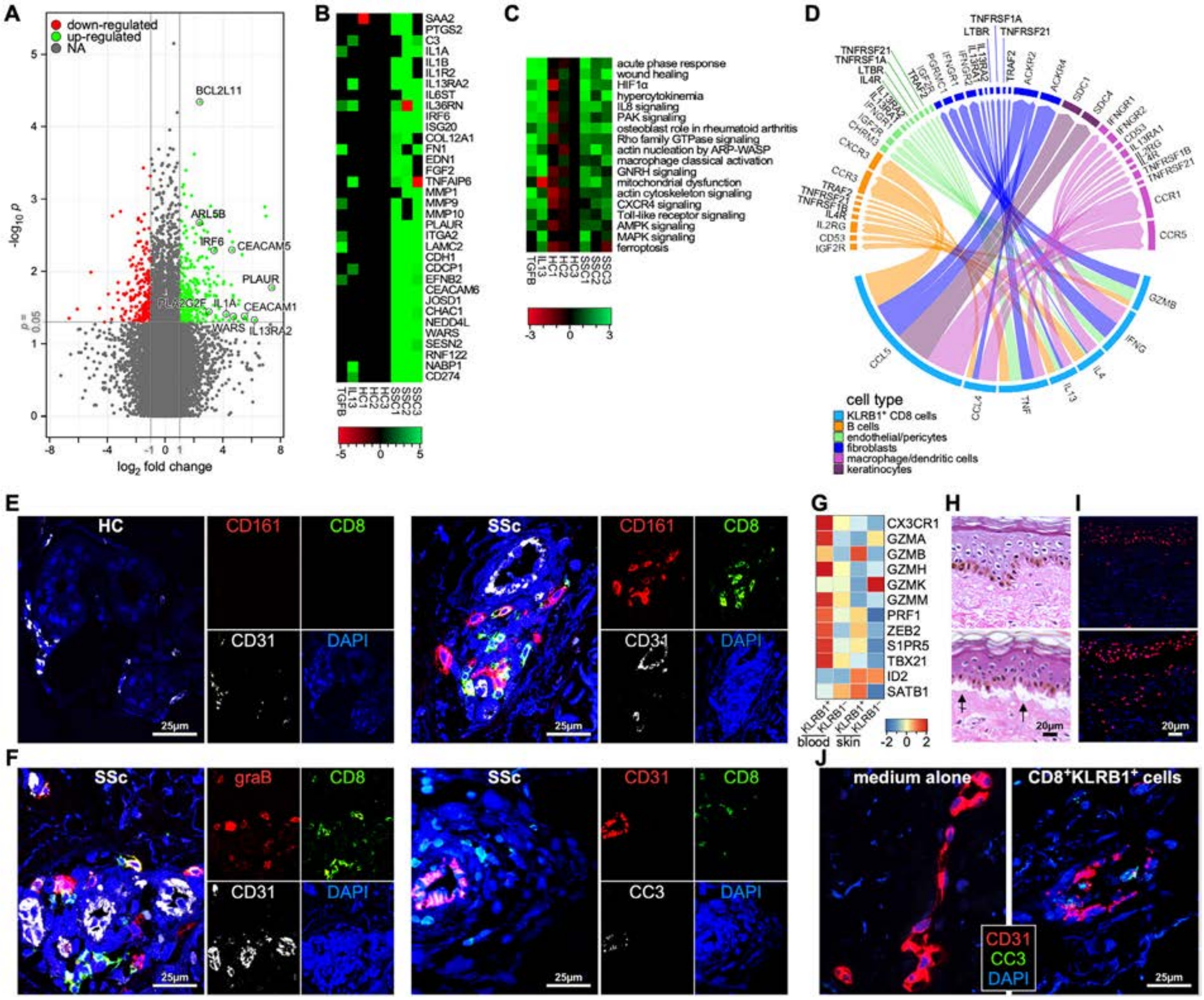

Figure 6. Establish function of CD8$^+$KLRB1$^+$ T cells in the lesional skin of patients with active diffuse cutaneous systemic sclerosis (SSc). (A-C) *Ex vivo* skin explants from the excised SSc nonlesional skin were cultured for 5 days with autologous CD8$^+$ T cells isolated from the lesional skin of patients or medium alone. Controls included HC skin cultured for 2 days with autologous skin CD8$^+$ T cells, medium alone, TGF-β, or IL13 as indicated. Microarrays by Affymetrix (Clarion D) were performed at day +2 on explants. Gene expression from each condition was compared with that from explants cultured with medium alone. Affymetrix hybridisation and data analysis were conducted following the manufacturer's instructions as described in the Methods. (A) Volcano plot shows upregulated and downregulated genes of SSc explants (n = 3) cultured with autologous CD8$^+$ cells compared with medium alone. (B) Average expression of highly significantly upregulated genes in SSc explants (n = 3) cultured with autologous CD8$^+$ cells vs culture with medium alone as well as in HC skin cultured with autologous skin CD8$^+$ cells, IL13, or TGF-β. Genes were considered differentially expressed when the fold change was ≥2 and *P* value of <.05. (C) Highly significantly upregulated pathways by Ingenuity Pathway Analysis in *ex vivo* skin explant cultures as indicated. (D) Visualisation of the CD8$^+$KLRB1$^+$ T-cell interactions with immune and stromal cells in the cutaneous microenvironment of SSc skin lesions (n = 27) by Connectome [42]. Circos plot of top 10 cell-type ligand-receptor cell-type interactions (edges) are shown. Top 10 significant CD8$^+$KLRB1$^+$ T-cell interactions in SSc (n = 27) skin samples combined. (E,F) Multicolor immunofluorescence (mIF) microscopy staining for (E) CD8, CD161 and CD31 in progressive SSc (n = 8) and HC (n = 5) skin samples and (F) CD8, graB, CD31 or CD8, CD31, and CC3 in progressive SSc (n = 8) skin samples. Representative examples are shown (×600). DAPI (4′,6-diamidino-2-phenylindole) stains nuclei. (G) Heat map shows average gene expression of SSc CD8$^+$KLRB1$^{+/-}$ cells cytotoxicity signature genes from blood versus skin samples. Gene differential tests are described in the Methods. (H-J) *Ex vivo* skin explants from nonlesional skin of patients with progressive SSc were cocultured with autologous peripheral blood CD8$^+$KLRB1$^+$ cells (bottom) or medium alone (top) for 5 days as described in the Methods. Tissue damage on explants was determined by histopathologic assessment [43] (H) and by TUNEL (I) to detect cell death-associated DNA fragmentation. Red indicates dead cells, DAPI (4′,6-diamidino-2-phenylindole) stains nuclei. (J) mIF for CD31 and CC3 to detect vascular damage in explants after coculture. Representative images at ×1000 are shown.

dcSSc CD8$^+$KLRB1$^+$ cells represent a pathogenic subset that can directly induce inflammation, tissue damage, and fibrosis in dcSSc skin disease.

DISCUSSION

While CD8 T-cell responses have been studied in the context of skin infection and cancer, their role in chronic inflammatory skin conditions is still elusive. We employed various single-cell methods to comprehensively characterise CD8 T-cell responses in human benign dermatoses with a particular focus on SSc skin disease. We identified 2 major developmentally connected tissue-resident CD8$^+$ T-cell subpopulations that are expanded in SSc skin compared with that in HC samples. These included a heterogeneous subset of effector-memory CD8$^+$KLRB1$^+$IL7R$^+$ cells characterised by increased cytolytic and Tc2/Tc17 effector functions, which appear to directly induce tissue damage and fibrosis in early-stage dcSSc skin lesions, and an exhausted CD8$^+$KLRG1$^+$IL7R$^-$ subset that shares characteristics of both short-lived effector and long-lived memory cells, likely contributing to chronic skin inflammation. While the proportion of CD8$^+$KLRG1$^+$IL7R$^-$ cells varied across benign dermatoses, that of CD8$^+$KLRB1$^+$IL7R$^+$ was increased in the lesional skin of all of them, especially SSc. Together these results provide new insight into chronic human skin inflammation pathogenesis and identify distinct CD8$^+$ T-cell subpopulations in SSc skin lesions that may contribute to initiation and chronicity of inflammatory responses.

Although CD8$^+$KLRG1$^+$IL7R$^-$ T cells are considered SLECs, a subset of LLECs with both effector and memory properties persists after resolution of acute infection and confers robust protection upon pathogen rechallenge. Similarly, we found that CD8$^+$KLRG1$^+$IL7R$^{-/+}$ cells from the lesional skin of patients with dcSSc or other chronic dermatoses exhibit a unique phenotype encompassing transcriptional features of both effector and memory T cells and are therefore reminiscent of LLECs. Unlike HC, most CD8$^+$KLRG1$^+$ cells from patient samples lacked expression of *IL7R* but exhibited increased expression of various genes associated with cytotoxicity, inflammation, survival, and apoptosis. Compared with the other groups, SSc CD8$^+$KLRG1$^+$ cells also upregulated multiple inhibitory checkpoint molecules, indicating that these cells are functionally exhausted. This agrees with previous studies showing that the persistant expression of KLRG1 by CD8$^+$ cells is associated with senescence and terminal differentiation [44−47] and importantly, senescence and senescence-associated secretory phenotype have recently been implicated in SSc pathogenesis. During chronic infection, a number of factors such as continuous local antigen stimulation, the strength of the signal received, and inflammatory cues have been identified as contributing to persistent KLRG1 expression and functional diversity of effector CD8$^+$ T cells. Consistently, we found that SSc CD8$^+$KLRG1$^+$ cells highly expressed *IL12RB2, TBX21, NFKB1*, and TCR signalling genes, which may promote intermediate levels of activating and inflammatory signals sufficient to maintain KLRG1 expression, high-level functionality, and cell survival. Accordingly, at the molecular level SSc CD8$^+$KLRG1$^+$ cells exhibited enhanced expression of TFs associated with both terminal differentiation of SLEC (*TBX21, ZEB2*, and *ID2*) as well as of memory cells (ID3 and EOMES) [10,11]. Thus, our studies indicate that skin-resident CD8$^+$KLRG1$^+$ cells from SSc and chronic inflammatory disorders comprise a heterogeneous subset of terminally differentiated cells that persist *in situ* following continuous antigenic stimulation and chronic inflammatory stimuli.

CD161 (encoded by *KLRB1*) is expressed on human NK cells and on various subsets of T cells [48,49]. CD8$^+$CD161$^+$ cells are heterogeneous including cells with stem cell-like characteristics and others characterised by distinct tissue homing and enhanced cytotoxicity against infectious agents [48,50,51]. We found that CD8$^+$CD161$^+$ T cells are expanded in the skin lesions of patients with dcSSc where they constitute a heterogeneous subset of skin-resident effector-memory cells with a prominent cytotoxic gene expression signature. A subset of SSc CD8$^+$CD161$^+$ T_{RM} cells also upregulated various Tc17-related genes. Although CD8$^+$CD161$^+$ T cells from PS and AD skin samples expressed the highest levels of *IL17A* and *IL22*, we also visualised CD8$^+$CD161$^+$ Tc17 cells in SSc skin lesions. More importantly, we identified a subset of SSc CD8$^+$KLRB1$^+$CRTH2$^+$ cells, presenting features of Tc2 cells and producing type-2 cytokines, notably IL13, which is known to contribute to ECM deposition and fibrosis. Several observations indicate that pSTAT6 and GATA3 drive differentiation of these cells in SSc skin; they show increased expression and chromatin accessibility to these TFs, as well as protein staining of pSTAT6 and GATA3 in SSc skin. The different properties of SSc CD8$^+$KLRB1$^+$ cells were reflected by differences in chromatin accessibility of key cytotoxicity-related (CX3CR1, GZMB, PRDM1, and ZEB2), Tc17-related (RORC, IL23R, IL17A, and IL22), and Tc2-related (PTGDR2, IL4R, GATA3, and IL13) gene loci. Thus, the effector functions of SSc CD8$^+$KLRB1$^+$ cells operate by both cytolytic and noncytolytic mechanisms. Significantly, CD8$^+$CD161$^+$ cells have been connected to the pathogenesis of several chronic inflammatory disorders [52,53]. While polymorphisms in *KLRB1* have been implicated in multiple sclerosis [54], none have been reported in SSc. Conversely, reduced CD161 expression by CD8$^+$ T cells was found in patients with advanced SLE disease [55], while accumulation of highly cytotoxic effector-memory CD8$^+$CD161$^-$ T cells was critical for SLE pathogenesis [56].

Comparison between SSc CD8$^+$KLRB1$^+$ and CD8$^+$KLRG1$^+$ cells indicates that they are developmentally connected, with CD8$^+$KLRG1$^+$ deriving from CD8$^+$KLRB1$^+$ cells, but highlights their different gene expression, including CD8$^+$KLRB1$^+$-specific Tc2/Tc17 signatures and proinflammatory and exhaustion programmes in CD8$^+$KLRG1$^+$ cells. Despite both subsets expressing cytolytic molecules, CD8$^+$KLRB1$^+$ cells expressed the highest levels and functional studies demonstrated their cytotoxic phenotype and ability to induce tissue damage in autologous skin. Significantly, we found that the frequency of CD8$^+$KLRB1$^+$ cells is higher in the early inflammatory stage of SSc, whereas CD8$^+$KLRG1$^+$ cells are enriched in late-stage disease, suggesting that CD8$^+$KLRB1$^+$ cells are involved in the initiation of SSc, while CD8$^+$KLRG1$^+$ cells contribute to disease perpetuation.

Our studies indicate that SSc CD8$^+$KLRB1$^+$/KLRG1$^+$ functional heterogeneity originates from developmental plasticity in response to different inflammatory stimuli in the skin and to differential states of activation rather than different effector cell precursors. Accordingly, previous studies reported that dynamic expression of key TFs regulates molecular programmes during CD8$^+$ T-cell subset differentiation and contributes to their functional plasticity [57]. Likewise, SSc CD8$^+$KLRB1$^+$ and CD8$^+$KLRG1$^+$ subsets displayed separate molecular programmes characterised by increased chromatin accessibility of distinct TF binding motifs. In CD8$^+$KLRB1$^+$ cells, these comprised motifs for TFs controlling effector functions of memory cells (RUNX2, IRF4, IRF8, and IKZF1), including Tc17 (RORC and IRF3) and Tc2 (GATA3) phenotypes. Conversely, CD8$^+$KLRG1$^+$ cells were enriched of binding motifs for various TFs regulating T-cell exhaustion such as KLF14, Fli1, ERG, TCF3, CTCF, and Tbet. Binding motifs for TFs (NFKB1, IRF7/9, STAT1, and STAT2) regulating IFN-signalling during antiviral response were enriched in both subsets.

In summary, we demonstrated that differentiation plasticity is a driving force in promoting phenotypic and functional diversity among skin-resident CD8$^+$ T cells during chronic skin inflammation. Moreover, interactions of CD8$^+$KLRB1$^+$ and CD8$^+$KLRG1$^+$ T cells with other immune and stromal cells in the lesional skin likely contribute to maintaining chronic inflammation, leading to excessive skin fibrosis.

Competing interests

The authors declare no competing financial interests.

Contributors

AMG and TT performed experiments and data analysis. RL acquired samples and collected clinical descriptions. JD and AL contributed to data analysis and interpretation. RL contributed to project development and to manuscript preparation. PF developed the project, performed experiments, analysed data, and prepared the manuscript. All authors helped reviewing the paper and approved the submission. PF is responsible for the overall content as guarantor.

Funding

This work was supported by National Institutes of Health grants: P50-AR080612 (PI: RL) and R03 AR065755 (PI: PF), and by the Pittsburgh Autoimmunity Center of Excellence in Rheumatology (PACER; to PF).

Patient consent for publication

All participants gave written informed consent in accordance with the Declaration of Helsinki. The approved study is an observational study of skin biopsies from patients with diffuse cutaneous systemic sclerosis.

Ethics approval

This study involves human participants and was approved by the University of Pittsburgh Institutional Review Board (IRB# 0409097).

Provenance and peer review

Not commissioned; externally peer reviewed.

Data availability statement

Datasets analysed in this study are available in the GEO database under accession numbers: GSE153760 (AD) [24], GSE151177 (PS) [25], GSE186476 (CL) [26], GSE138669 (SSc) [27], and GSE182861 (HC) [28]. Microarray and snATACseq data are available upon reasonable request.

Supplementary materials

Supplementary material associated with this article can be found in the online version at doi:10.1016/j.ard.2025.01.022.

Orcid

Patrizia Fuschiotti: http://orcid.org/0000-0003-1051-5262

REFERENCES

[1] Mueller SN, Gebhardt T, Carbone FR, Heath WR. Memory T cell subsets, migration patterns, and tissue residence. Ann Rev Immunol 2013;31:137–61. doi: 10.1146/annurev-immunol-032712-095954.

[2] Tokura Y, Phadungsaksawasdi P, Kurihara K, Fujiyama T, Honda T. Pathophysiology of skin resident memory T cells. Front Immunol. 2020;11:618897. doi: 10.3389/fimmu.2020.618897.

[3] Milner JJ, Toma C, He Z, Kurd NS, Nguyen QP, McDonald B, et al. Heterogenous populations of tissue-resident CD8(+) T cells are generated in response to infection and malignancy. Immunity 2020;52(5):808–824.e7. doi: 10.1016/j.immuni.2020.04.007.

[4] Szabo PA, Miron M, Farber DL. Location, location, location: tissue resident memory T cells in mice and humans. Sci Immunol 2019;4(34):eaas9673. doi: 10.1126/sciimmunol.aas9673.

[5] Kakaradov B, Arsenio J, Widjaja CE, He Z, Aigner S, Metz PJ, et al. Early transcriptional and epigenetic regulation of CD8(+) T cell differentiation revealed by single-cell RNA sequencing. Nat Immunol 2017;18(4):422–32. doi: 10.1038/ni.3688.

[6] Joshi NS, Cui W, Chandele A, Lee HK, Urso DR, Hagman J, et al. Inflammation directs memory precursor and short-lived effector CD8(+) T cell fates via the graded expression of T-bet transcription factor. Immunity 2007;27(2):281–95. doi: 10.1016/j.immuni.2007.07.010.

[7] Kurd NS, He Z, Louis TL, Milner JJ, Omilusik KD, Jin W, et al. Early precursors and molecular determinants of tissue-resident memory CD8(+) T lymphocytes revealed by single-cell RNA sequencing. Sci Immunol 2020;5(47):eaaz6894. doi: 10.1126/sciimmunol.aaz6894.

[8] Mackay LK, Rahimpour A, Ma JZ, Collins N, Stock AT, Hafon ML, et al. The developmental pathway for CD103(+)CD8+ tissue-resident memory T cells of skin. Nat Immunol 2013;14(12):1294–301. doi: 10.1038/ni.2744.

[9] Chang JT, Wherry EJ, Goldrath AW. Molecular regulation of effector and memory T cell differentiation. Nat Immunol 2014;15(12):1104–15. doi: 10.1038/ni.3031.

[10] Renkema KR, Huggins MA, Borges da Silva H, Knutson TP, Henzler CM, Hamilton SE. KLRG1(+) memory CD8 T cells combine properties of short-lived effectors and long-lived memory. J Immunol 2020;205(4):1059–69. doi: 10.4049/jimmunol.1901512.

[11] Herndler-Brandstetter D, Ishigame H, Shinnakasu R, Plajer V, Stecher C, Zhao J, et al. KLRG1(+) Effector CD8(+) T cells lose KLRG1, differentiate into all memory T cell lineages, and convey enhanced protective immunity. Immunity 2018;48(4):716–729.e8. doi: 10.1016/j.immuni.2018.03.015.

[12] Herrick AL, Assassi S, Denton CP. Skin involvement in early diffuse cutaneous systemic sclerosis: an unmet clinical need. Nat Rev Rheumatol 2022;18(5):276–85. doi: 10.1038/s41584-022-00765-9.

[13] Fuschiotti P, Larregina AT, Ho J, Feghali-Bostwick C, Medsger TA. Interleukin-13-producing CD8+ T cells mediate dermal fibrosis in patients with systemic sclerosis. Arthritis Rheum 2013;65(1):236–46. doi: 10.1002/art.37706.

[14] Hugle T, O'Reilly S, Simpson R, Kraaij MD, Bigley V, Collin M, et al. Tumor necrosis factor-costimulated T lymphocytes from patients with systemic sclerosis trigger collagen production in fibroblasts. Arthritis Rheum 2013;65(2):481–91. doi: 10.1002/art.37738.

[15] Li G, Larregina AT, Domsic RT, Stolz DB, Medsger TA, Lafyatis R, et al. Skin-resident effector memory CD8(+)CD28(-) T cells exhibit a profibrotic phenotype in patients with systemic sclerosis. J Invest Dermatol 2017;137(5):1042–50. doi: 10.1016/j.jid.2016.11.037.

[16] Macosko EZ, Basu A, Satija R, Nemesh J, Shekhar K, Goldman M, et al. Highly parallel genome-wide expression profiling of individual cells using nanoliter droplets. Cell 2015;161(5):1202–14. doi: 10.1016/j.cell.2015.05.002.

[17] Satpathy AT, Granja JM, Yost KE, Qi Y, Meschi F, McDermott GP, et al. Massively parallel single-cell chromatin landscapes of human immune cell development and intratumoral T cell exhaustion. Nat Biotechnol 2019;37(8):925–36. doi: 10.1038/s41587-019-0206-z.

[18] Stuart T, Srivastava A, Madad S, Lareau CA, Satija R. Single-cell chromatin state analysis with Signac. Nat Methods 2021;18(11):1333–41. doi: 10.1038/s41592-021-01282-5.

[19] LeRoy EC, Black C, Fleischmajer R, Jablonska S, Krieg T, Medsger TA, et al. Scleroderma (systemic sclerosis): classification, subsets and pathogenesis. J Rheumatol 1988;15(2):202–5.

[20] Gaydosik AM, Tabib T, Domsic R, Khanna D, Lafyatis R, Fuschiotti P. Single-cell transcriptome analysis identifies skin-specific T-cell responses in systemic sclerosis. Ann Rheum Dis 2021;80:1453–60. doi: 10.1136/annrheumdis-2021-220209.

[21] Medsger Jr. TA, Bombardieri S, Czirjak L, Scorza R, Della Rossa A, Bencivelli W. Assessment of disease severity and prognosis. Clin Exp Rheumatol 2003;21(3 Suppl 29):S42–6.

[22] Valenzi E, Bahudhanapati H, Tan J, Tabib T, Sullivan DI, Nouraie M, et al. Single-nucleus chromatin accessibility identifies a critical role for TWIST1 in idiopathic pulmonary fibrosis myofibroblast activity. Eur Respir J 2023;62(1):2200474. doi: 10.1183/13993003.00474-2022.

[23] Gaydosik AM, Queen DS, Trager MH, Akilov OE, Geskin LJ, Fuschiotti P. Genome-wide transcriptome analysis of the STAT6-regulated genes in advanced-stage cutaneous T-cell lymphoma. Blood 2020;136(15):1748–59. doi: 10.1182/blood.2019004725.

[24] Rojahn TB, Vorstandlechner V, Krausgruber T, Bauer WM, Alkon N, Bangert C, et al. Single-cell transcriptomics combined with interstitial fluid proteomics defines cell type-specific immune regulation in atopic dermatitis [Internet]. Gene Expression Omnibus 2020. Available from: https://www.ncbi.nlm.nih.gov/geo/query/acc.cgi?acc=GSE153760.

[25] Kim J, Krueger JG. Single-cell RNA sequencing of emigrating cells from human psoriasis skin and control normal skin. Gene Expression Omnibus; 2021. Available from: https://www.ncbi.nlm.nih.gov/geo/query/acc.cgi?acc=GSE151177.

[26] Billi AC, Ma F, Kahlenberg JM. Non-lesional and lesional lupus skin share inflammatory phenotypes that drive activation of CD16+ dendritic cells [Internet]. Gene Expression Omnibus; 2022. Available from: https://www.ncbi.nlm.nih.gov/geo/query/acc.cgi?acc=GSE186476.

[27] Tabib T, Huang M, Morse N, Papazoglou A, Behera R, Jia M, et al. Myofibroblast transcriptome indicates SFRP2+ fibroblast progenitors in systemic

sclerosis skin [Internet]. Gene Expression Omnibus 2021. Available from: https://www.ncbi.nlm.nih.gov/geo/query/acc.cgi?acc=GSE138669.

[28] Gaydosik AM, Stonesifer CJ, Geskin LJ, Fuschiotti P. Single-cell RNA sequencing unveils the clonal and transcriptional landscape of cutaneous T-cell lymphomas [Internet]. Gene Expression Omnibus 2022. Available from: https://www.ncbi.nlm.nih.gov/geo/query/acc.cgi?acc=GSE182861.

[29] Stuart T, Butler A, Hoffman P, Hafemeister C, Papalexi E, Mauck WM, et al. Comprehensive integration of single-cell data. Cell 2019;177(7):1888–1902.e21. doi: 10.1016/j.cell.2019.05.031.

[30] Satija R, Farrell JA, Gennert D, Schier AF, Regev A. Spatial reconstruction of single-cell gene expression data. Nat Biotechnol 2015;33(5):495–502. doi: 10.1038/nbt.3192.

[31] Butler A, Hoffman P, Smibert P, Papalexi E, Satija R. Integrating single-cell transcriptomic data across different conditions, technologies, and species. Nat Biotechnol 2018;36(5):411–20. doi: 10.1038/nbt.4096.

[32] Watanabe R, Gehad A, Yang C, Scott LL, Teague JE, Schlapbach C, et al. Human skin is protected by four functionally and phenotypically discrete populations of resident and recirculating memory T cells. Sci Transl Med 2015;7(279):279ra39. doi: 10.1126/scitranslmed.3010302.

[33] Fornes O, Castro-Mondragon JA, Khan A, van der Lee R, Zhang X, Richmond PA, et al. JASPAR 2020: update of the open-access database of transcription factor binding profiles. Nucleic Acids Res 2020;48(D1):D87–92. doi: 10.1093/nar/gkz1001.

[34] Schep AN, Wu B, Buenrostro JD, Greenleaf WJ. chromVAR: inferring transcription-factor-associated accessibility from single-cell epigenomic data. Nat Methods 2017;14(10):975–8. doi: 10.1038/nmeth.4401.

[35] La Manno G, Soldatov R, Zeisel A, Braun E, Hochgerner H, Petukhov V, et al. RNA velocity of single cells. Nature 2018;560(7719):494–8. doi: 10.1038/s41586-018-0414-6.

[36] Bergen V, Lange M, Peidli S, Wolf FA, Theis FJ. Generalizing RNA velocity to transient cell states through dynamical modeling. Nat Biotechnol 2020;38(12):1408–14. doi: 10.1038/s41587-020-0591-3.

[37] Trapnell C, Cacchiarelli D, Grimsby J, Pokharel P, Li S, Morse M, et al. The dynamics and regulators of cell fate decisions are revealed by pseudotemporal ordering of single cells. Nat Biotechnol 2014;32(4):381–6. doi: 10.1038/nbt.2859.

[38] Stoeckius M, Hafemeister C, Stephenson W, Houck-Loomis B, Chattopadhyay PK, Swerdlow H, et al. Simultaneous epitope and transcriptome measurement in single cells. Nat Methods 2017;14(9):865–8. doi: 10.1038/nmeth.4380.

[39] Cosmi L, Annunziato F, Galli MIG, Maggi RME, Nagata K, Romagnani S. CRTH2 is the most reliable marker for the detection of circulating human type 2 Th and type 2 T cytotoxic cells in health and disease. Eur J Immunol 2000;30(10):2972–9. doi: 10.1002/1521-4141(200010)30:10<2972::AID-IMMU2972>3.0.CO;2-#.

[40] Farina G, Lafyatis D, Lemaire R, Lafyatis R. A four-gene biomarker predicts skin disease in patients with diffuse cutaneous systemic sclerosis. Arthritis Rheum 2010;62(2):580–8. doi: 10.1002/art.27220.

[41] Saito Y, Ishikawa H. Ultrastructure of the microvasculature in skin affected by systemic scleroderma. J Dermatol 1976;3(4):127–33. doi: 10.1111/j.1346-8138.1976.tb01832.x.

[42] Raredon MSB, Yang J, Garritano J, Wang M, Kushnir D, Schupp JC, et al. Computation and visualization of cell-cell signaling topologies in single-cell systems data using Connectome. Sci Rep 2022;12(1):4187. doi: 10.1038/s41598-022-07959-x.

[43] Martins-Ribeiro A, Kizhedath A, Ahmed SS, Glassey J, Ishaq A, Freer M, et al. A human skin explant test as a novel in vitro assay for the detection of skin sensitization to aggregated monoclonal antibodies. Toxics 2024;12(5):332. doi: 10.3390/toxics12050332.

[44] Gerlach C, Moseman EA, Loughhead SM, Alvarez D, Zwijnenburg AJ, Waanders L, et al. The chemokine receptor CX3CR1 defines three antigen-experienced CD8 T cell subsets with distinct roles in immune surveillance and homeostasis. Immunity 2016;45(6):1270–84. doi: 10.1016/j.immuni.2016.10.018.

[45] Thimme R, Appay V, Koschella M, Panther E, Roth E, Hislop AD, et al. Increased expression of the NK cell receptor KLRG1 by virus-specific CD8 T cells during persistent antigen stimulation. J Virol 2005;79(18):12112–6. doi: 10.1128/JVI.79.18.12112-12116.2005.

[46] Omilusik KD, Best JA, Yu B, Goossens S, Weidemann A, Nguyen JV, et al. Transcriptional repressor ZEB2 promotes terminal differentiation of CD8+ effector and memory T cell populations during infection. J Exp Med 2015;212(12):2027–39. doi: 10.1084/jem.20150194.

[47] O'Reilly S, Tsou PS, Varga J. Senescence and tissue fibrosis: opportunities for therapeutic targeting. Trends Mol Med 2024;30:1113–25. doi: 10.1016/j.molmed.2024.05.012.

[48] Fergusson JR, Smith KE, Fleming VM, Rajoriya N, Newell EW, Simmons R, et al. CD161 defines a transcriptional and functional phenotype across distinct human T cell lineages. Cell Rep 2014;9(3):1075–88. doi: 10.1016/j.celrep.2014.09.045.

[49] Konduri V, Oyewole-Said D, Vazquez-Perez J, Weldon SA, Halpert MM, Levitt JM, et al. CD8(+)CD161(+) T-cells: cytotoxic memory cells with high therapeutic potential. Front Immunol 2020;11:613204. doi: 10.3389/fimmu.2020.613204.

[50] Turtle CJ, Swanson HM, Fujii N, Estey EH, Riddell SR. A distinct subset of self-renewing human memory CD8+ T cells survives cytotoxic chemotherapy. Immunity 2009;31(5):834–44. doi: 10.1016/j.immuni.2009.09.015.

[51] Fergusson JR, Huhn MH, Swadling L, Walker LJ, Kurioka A, Llibre A, et al. CD161(int)CD8+ T cells: a novel population of highly functional, memory CD8+ T cells enriched within the gut. Mucosal Immunol 2016;9(2):401–13. doi: 10.1038/mi.2015.69.

[52] Annibali V, Ristori G, Angelini DF, Serafini B, Mechelli R, Cannoni S, et al. CD161(high)CD8+T cells bear pathogenetic potential in multiple sclerosis. Brain 2011;134(Pt 2):542–54. doi: 10.1093/brain/awq354.

[53] Liu J, Chang HW, Huang ZM, Nakamura M, Sekhon S, Ahn R, et al. Single-cell RNA sequencing of psoriatic skin identifies pathogenic Tc17 cell subsets and reveals distinctions between CD8(+) T cells in autoimmunity and cancer. J Allergy Clin Immunol 2021;147(6):2370–80. doi: 10.1016/j.jaci.2020.11.028.

[54] International Multiple Sclerosis Genetics Consortium, Hafler DA, Compston A, Sawcer S, Lander ES, Daly MJ, De Jager PL, et al. Risk alleles for multiple sclerosis identified by a genomewide study. N Engl J Med 2007;357(9):851–62. doi: 10.1056/NEJMoa073493.

[55] Park Y, Lim J, Kim SY, Kwon GC, Koo SH, Kim J. Changes of frequency and expression level of CD161 in CD8(+) T cells and natural killer T cells in peripheral blood of patients with systemic lupus erythematosus. Microbiol Immunol 2020;64(7):532–9. doi: 10.1111/1348-0421.12798.

[56] Xiong H, Cui M, Kong N, Jing J, Xu Y, Liu X, et al. Cytotoxic CD161(-)CD8(+) T(EMRA) cells contribute to the pathogenesis of systemic lupus erythematosus. EBioMedicine 2023;90:104507. doi: 10.1016/j.ebiom.2023.104507.

[57] Giles JR, Ngiow SF, Manne S, Baxter AE, Khan O, Wang P, et al. Shared and distinct biological circuits in effector, memory and exhausted CD8(+) T cells revealed by temporal single-cell transcriptomics and epigenetics. Nat Immunol 2022;23(11):1600–13. doi: 10.1038/s41590-022-01338-4.

Ann Rheum Dis 84 (2025) 810−822

Contents lists available at ScienceDirect

Annals of the Rheumatic Diseases

journal homepage: https://www.sciencedirect.com/journal/annals-of-the-rheumatic-diseases

Systemic sclerosis

Imaging mass cytometry-based characterisation of fibroblast subsets and their cellular niches in systemic sclerosis

Aleix Rius Rigau[1,2], Minrui Liang[1,3], Veda Devakumar[4,5], Ranjana Neelagar[4,5], Alexandru-Emil Matei[4,5], Andrea-Hermina Györfi[4,5], Christina Bergmann[1,2], Tim Filla[4,5], Vladyslav Fedorchenko[1,2], Georg Schett[1,2], Jörg H.W. Distler[1,2,4,5,*], Yi-Nan Li[4,5,*]

[1] *Department of Internal Medicine 3 − Rheumatology and Clinical Immunology, Friedrich-Alexander University Erlangen-Nuremberg, Erlangen, Bayern, Germany*
[2] *Deutsches Zentrum Immuntherapie (DZI), Erlangen University Hospital, Erlangen, Bayern, Germany*
[3] *Huashan Hospital Fudan University, Shanghai, China*
[4] *Department of Rheumatology, Heinrich-Heine-Universität Düsseldorf, Düsseldorf, Nordrhein-Westfalen, Germany*
[5] *Hiller Research Center, University Hospital of Düsseldorf, Düsseldorf, Nordrhein-Westfalen, Germany*

ARTICLE INFO

Article history:
Received 28 June 2024
Accepted 6 October 2024

Keywords:
fibroblasts
scleroderma
systemic
connective tissue diseases

ABSTRACT

Objectives: Transcriptomic data demonstrated that fibroblasts are heterogeneous with functionally diverse subpopulations. Although fibroblasts are key effector cells of fibrotic diseases such as systemic sclerosis (SSc), they have not yet been characterised spatially at the cellular level. Here, we aimed to investigate fibroblast subpopulations using imaging mass cytometry (IMC) as a proteomic-based, spatially resolved omics approach.

Methods: We applied IMC to deconvolute the heterogeneity of 49 969 cells including 6501 fibroblasts at the single-cell level, to analyse their spatial distribution and to characterise their cellular niches in skin sections of patients with SSc and controls in situ.

Results: We identified 13 different subpopulations of fibroblasts in SSc and control skin, the proportion increases in five fibroblast subpopulations (myofibroblasts, FAP^{high}, $S1PR^{+}$, $Thy1^{+}$;$ADAM12^{high}$; $PU.1^{high}$ and $ADAM12^{+}$;$GLI1^{+}$ fibroblasts) and decreases in three subpopulations ($TFAM^{high}$, $PI16^{+}$; FAP^{+} and $Thy1^{+}$;$ADAM12^{low}$ fibroblasts). Several fibroblast subpopulations demonstrated spatial enrichment and altered cellular interactions in SSc. The proportion of $S1PR^{+}$-fibroblast positively correlated with more extensive skin fibrosis, whereas high numbers of $PI16^{+}$;FAP^{-}-fibroblasts were associated with milder skin fibrosis. The frequency of aberrant cellular interaction between $S1PR^{+}$ and $ADAM12^{+}$;$GLI1^{+}$-fibroblasts also positively associated with the extent of skin fibrosis in SSc.

Conclusion: Using IMC, we demonstrated profound changes in composition and localisation of the majority of fibroblast subpopulations in SSc skin. These findings may provide a rationale for specific targeting of deregulated fibroblast subpopulations in SSc. Quantification of $S1PR^{+}$-fibroblast and $PI16^{+}$;FAP^{-}-fibroblasts may offer potential for patient stratification according to severity of skin fibrosis.

*Correspondence to Dr. Yi-Nan Li; Dr. Jörg H W Distler.
E-mail addresses: Joerg.Distler@med.uni-duesseldorf.de (J.H.W. Distler), Yi-Nan.Li@med.uni-duesseldorf.de (Y.-N. Li).
Handling editor Josef S. Smolen

https://doi.org/10.1136/ard-2024-226336

WHAT IS ALREADY KNOWN ABOUT THIS SUBJECT

- Single omics data revealed that fibroblasts are a heterogenous population of cells with functionally diverse subpopulations. However, previous studies lack spatial context and did not enable a characterisation of the local microenvironment.
- In systemic sclerosis (SSc), fibroblast subpopulations have been defined based on non-spatially resolved transcriptional profiling only (single-cell RNA sequencing), but proteomic, spatially resolved omics data are not yet available.

WHAT DOES THIS STUDY ADD

- We provide the first imaging mass cytometry-based characterisation of fibroblast subpopulations in SSc and control skin.
- We identify 13 subpopulations of fibroblasts, including several new populations, 8 of which are numerically altered in SSc (5 increased and 3 decreased).
- We demonstrate alterations in the spatial distribution and cell-to-cell interactions of several fibroblast subpopulations.
- The proportion and localisation of certain fibroblast subsets are associated with the extent of skin fibrosis.

HOW MIGHT THIS IMPACT ON CLINICAL PRACTICE

- Identification and characterisation of fibroblast subsets may set the basis for selective targeting of specific, disease-promoting subpopulations.
- Certain fibroblast subpopulations and their localisation may offer potential as biomarkers for patient stratification according to the extent of skin fibrosis.

INTRODUCTION

Systemic sclerosis (SSc) is a fibrosing connective disease, which affects the skin and various internal organs [1,2]. SSc is the autoimmune disease with the highest case-specific mortality, which is predominantly caused by fibrotic tissue remodelling and fibrosis-associated end organ damage [3]. Fibroblasts are key effector cells of fibrotic tissue remodelling [2,4,5]. However, our comprehension of the fibroblast heterogeneity in both, normal and pathological conditions, is still in its early stages, and we have limited understanding of their phenotype, their local microenvironment, and their cellular interactions in situ.

Single-cell omics enable studies of cellular subpopulations at a so far unprecedented resolution. So far, predominantly non-spatially resolved single-cell RNA sequencing (scRNA-Seq) has been employed in rheumatic diseases. scRNA-Seq unravelled that fibroblasts are heterogeneous populations of cells, characterised by distinct subpopulations that differ in transcriptional profiles and functions [6,7]. scRNA-Seq data of SSc skin identified between 6 [7] and 10 [6] distinct subpopulations of fibroblasts. Each fibroblast subpopulation exhibits a specific gene expression programme indicative of specific functions of each subpopulation. However, scRNA-Seq, along with other available single-cell techniques such as flow cytometry, requires disaggregation of the tissue of interest and isolation of single cells. Thus, these techniques can neither provide information on the specific localisation of cells within the tissue nor enable characterisation of the local niches and the cellular interplay within these niches. Moreover, the recovery rates can differ among different cell populations, which may affect the results of quantification.

To overcome these limitations and to study the distribution of fibroblast subpopulations and their local microenvironment in situ, we applied imaging mass cytometry (IMC) as a spatial multiplexed protein quantification approach. IMC detects metal isotope-labelled antibodies in tissues using localisation-specific laser ablation coupled with mass spectrometry [8,9]. The use of metal tags instead of fluorescence labelling minimises signal spillover between channels, thereby allowing the simultaneous detection of around 50 metal-tagged antibodies on the same tissue slide with a subcellular resolution.

In this study, we used IMC as a spatially resolved proteomic technique to identify, quantify and characterise fibroblast subpopulations in the skin of patients with SSc, to analyse their spatial distribution and the local cellular neighbourhoods (CNs) and to investigate correlations with clinical parameters and outcome of SSc.

MATERIAL AND METHODS

Sample preparation

Formalin-fixed paraffin-embedded 5-µm skin sections from the human biopsies were prepared. As described previously, consecutive sections were used to generate a H&E staining for histopathological analysis, as well as to select the regions of interest to be analysed by IMC [10].

Statistics

The relative abundance of fibroblast subpopulations was quantified as percentage of all dermal fibroblasts. Data are presented as dot plots with the median±interquartile range (IQR). Each dot represents one biological replicate, unless indicated otherwise in the figure legend. Protein expression levels are shown as heatmaps representing the mean of the z-score-normalised values. GraphPad Prism V.9.5.1 was used to generate dot plots and to perform statistical analyses. Heatmaps were generated using the *imcRtools* R package [11]. Non-parametric Mann-Whitney U tests were applied for the comparison between two groups, if not indicated otherwise. Spearman's rank correlation analysis was performed using the *ggpubr* R package.

RESULTS

Identification of fibroblast subpopulations in SSc and healthy skin based on marker expression

To identify fibroblast subpopulations, we designed a panel of antibodies with a broad set of markers of fibroblasts along with structural markers for tissue segmentation, markers of other tissue resident cells and immune cells (online supplemental table S3), (figure 1, online supplemental figure S1). Skin samples collected from 11 patients with SSc enriched for early, clinically active disease and seven sex-matched and age-matched healthy controls were analysed by IMC and yielded a total of 49 969 single cells (patients with SSc: 27 379 cells; healthy controls: 22 590 cells). We detected 6501 fibroblasts, defined as CD45$^-$;CD31$^-$;E-cadherin$^-$;Histone3$^+$ cells after subsequent removal of vascular smooth muscle cells as αSMA^{high};SM22α^{high} cells. We further analysed the expression of specific markers and characterised their local microenvironment (figure 1).

Fibroblasts were clustered into subpopulations based on the expression levels of the following markers, all of which have been identified as markers of fibroblast subpopulations and/or are implicated in fibroblast activation [12–25]: ADAM12,

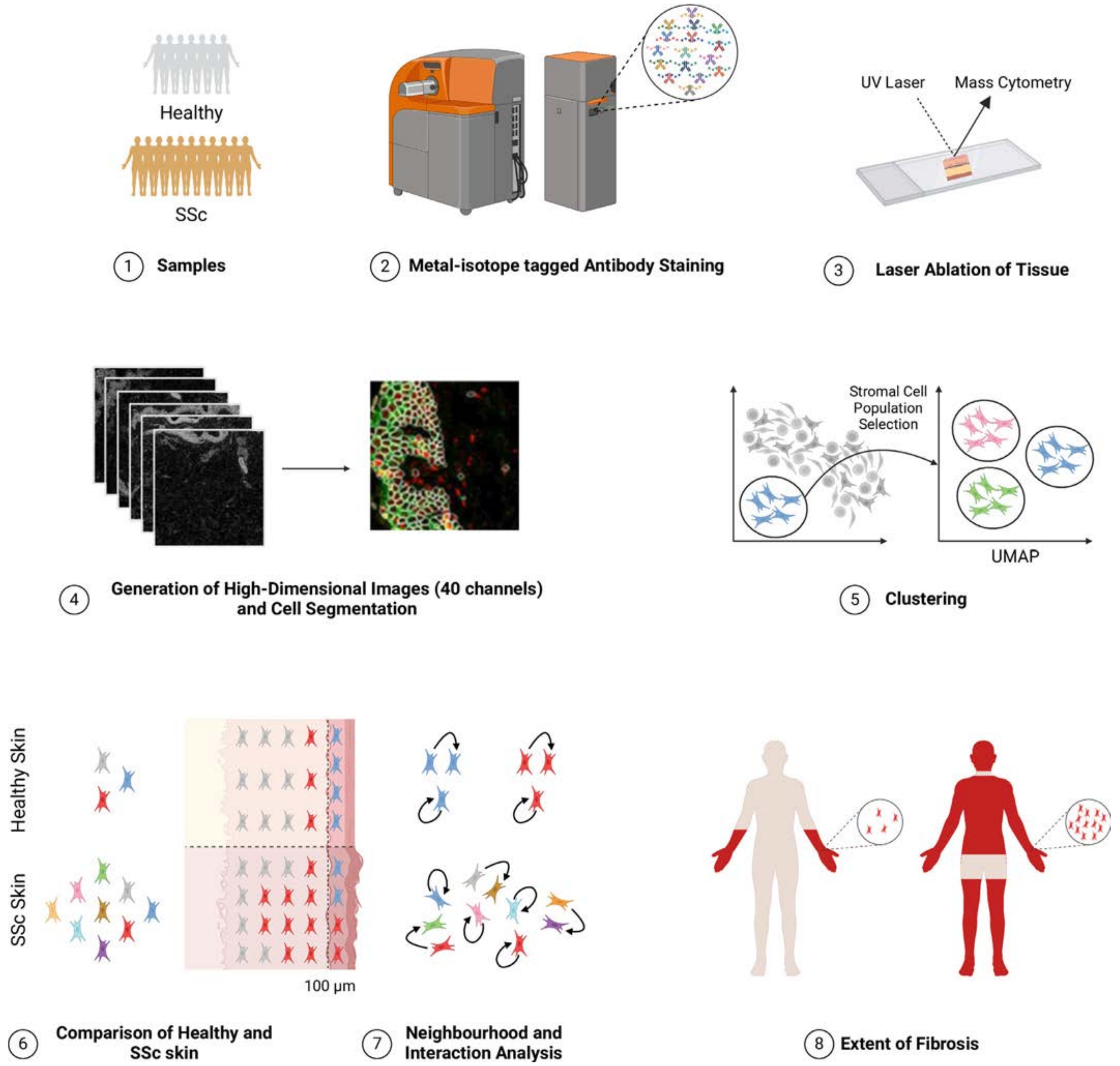

Figure 1. Graphical abstract representing the experiment and data analysis workflow. (1−2) FFPE histology samples from 11 patients with SSc and 7 healthy donors were stained with a cocktail of 36 metal-tagged antibodies and Iridium DNA intercalator after previous validation of all antibodies and building of a mass cytometry panel according to the signal intensity and predicted spillover of each antibody. (3) Samples were processed with the Hyperion IMC device. (4) The generated high-dimensional images were segmented to single-cells and the single-cell protein expression as well as their spatial coordinates obtained and exported as R object, .fcs and .csv files. (5) The fibroblasts were selected by manual gating and defined as CD45$^-$;CD31$^-$;E-cadherin$^-$;Histone 3$^+$ and unsupervised phenograph clustering was applied to all stromal cells defining 13 distinct subsets. (6) The distribution of the fibroblast subpopulations was analysed. (7) Spatial cell-to-cell interaction analysis was performed and compared between SSc and healthy donors. (8) The frequencies of fibroblasts subpopulations and interactions were correlated with the clinical phenotype and outcome of the patients with SSc. This figure was created with BioRender.com. FFPE, formalin-fixed paraffin-embedded; IMC, imaging mass cytometry; SSc, systemic sclerosis.

ADRP, αSMA, Cdh11, FAP, FSP1, GLI1, PDGFRα, PDGFRβ, PGC1α, PI16, Podoplanin, PU.1, S1PR, SM22α, SOX9, TFAM, THY1 and ZEB1.

Visualisation by dimensionality reduction with the Uniform Manifold Approximation and Projection (UMAP) algorithm demonstrated clearly distinct patterns for fibroblasts derived from skin samples of patients with SSc and healthy individuals, indicative of major phenotypic changes in fibroblast populations in SSc (figure 2A).

We defined 13 phenotypically different subpopulations of fibroblasts. Each fibroblast subset was annotated based on differential marker expression. Of those, three clusters expressed ADAM12. One of these clusters had high levels of Thy1 and PU.1, and was referred as Thy1$^+$;ADAM12^{high};PU.1^{high} fibroblasts. Another cluster expressed high levels of Thy1, but only low levels of ADAM12, and was named Thy1$^+$;ADAM12^{low} fibroblasts. The third ADAM12-expressing cluster coexpressed GLI1, and was therefore named ADAM12$^+$;GLI1$^+$ fibroblasts.

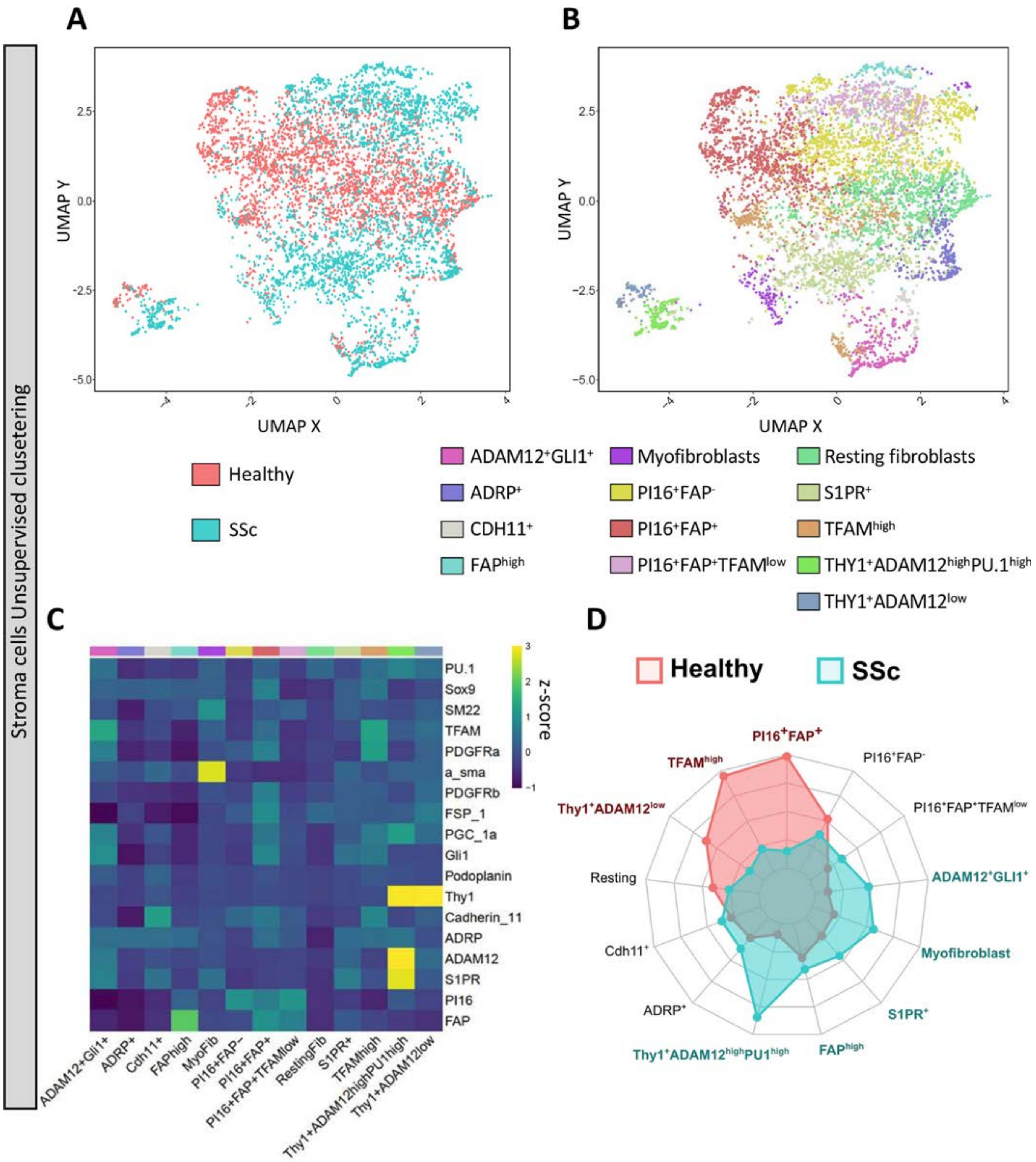

Figure 2. Identification of fibroblast subsets in SSc skin. (A, B) UMAP plots of fibroblast subsets identified in the skin of patients with SSc and healthy donors. The plots are coloured by group (SSc vs healthy; A) or by individual fibroblast subsets (B), respectively. (C) Expression heatmap of protein markers used for identification of fibroblast subsets shown as z-score. (D) Radar plots showing the changes in the frequency of the fibroblast subpopulations in SSc skin compared with healthy skin. The cell frequencies were normalised for individual subpopulations. The fibroblast subsets with significant changes in their proportions in SSc are highlighted with colour and bold font (red: decreased in SSc; blue: increased in SSc). Statistical significance was determined by the Mann-Whitney U test comparing SSc with healthy controls. P values <0.05 were considered statistically significant. SSc, systemic sclerosis; UMAP, Uniform Manifold Approximation and Projection.

Another cluster was characterised by high expression levels of S1PR (S1PR$^+$ fibroblasts). The cluster prominently expressed αSMA was annotated as myofibroblasts, whereas the cluster that exhibited high levels of FAP was identified as FAP^{high} fibroblasts. Three clusters of fibroblasts expressed PI16, but differed in the expression levels of FAP and TFAM. These fibroblasts were annotated as PI16$^+$;FAP$^-$, PI16$^+$;FAP$^+$ fibroblasts, and PI16$^+$;FAP$^+$;TFAM^{low} fibroblasts. A cluster with high PDGFRα expression also coexpressed high levels of TFAM and was therefore referred to as TFAM^{high} fibroblasts. Two other clusters were defined by the high expression levels of Cdh11$^+$ and ADRP$^+$ (Cdh11$^+$ and ADRP$^+$ fibroblasts, respectively). Another cluster was positive for PDGFRα and FSP1, but lacked the expression of activation markers, and thus was annotated as resting fibroblasts (figure 2B, C). We did not detect notable phenotypic variations within these fibroblast subpopulations across donor ethnicities or biopsy sites by IMC (online supplemental figure S2). These fibroblast subpopulations were also recovered by reanalyses of an independent scRNA-Seq dataset of SSc skin (online supplemental figure S3), thereby validating our data by an independent approach.

Shifts in fibroblast subpopulations in SSc skin

Although the overall number of fibroblasts is not altered in SSc skin compared with control skin, 8 of the 13 fibroblast subpopulations demonstrated statistically significant changes in their proportions of all fibroblasts, with upregulation of 5 and downregulation of 3 fibroblast subpopulations (figure 2, online supplemental figure S4). The subpopulations upregulated in SSc skin included well-known profibrotic populations of activated fibroblasts such as myofibroblasts and FAP^{high} fibroblasts, but also several additional subpopulations such as S1PR$^+$ fibroblasts, Thy1$^+$;ADAM12^{high};PU.1^{high} fibroblasts, and ADAM12$^+$;GLI1$^+$ fibroblasts (figure 3).

We also identified three fibroblast subpopulations that were downregulated in SSc skin compared with control skin. The proportion of TFAM^{high} fibroblasts, PI16$^+$;FAP$^+$ fibroblasts and Thy1$^+$;ADAM12^{low} fibroblasts were decreased in SSc skin compared with control skin (online supplemental figure S5). No changes in numbers between SSc skin and control skin were observed for resting fibroblasts, ADRP$^+$, PI16$^+$;FAP$^-$, PI16$^+$;FAP$^+$;TFAM^{low} and Cdh11$^+$ fibroblasts. We further confirmed our findings on the alteration in fibroblast composition in SSc using additional metrics, such as percentage of all dermal cells and cell density in the tissue (online supplemental figure S6).

These findings are consistent with previous reports of upregulation of GLI1, ADAM12 and PU.1 and downregulation of TFAM as key factors promoting the differentiation of profibrotic fibroblasts [14,16,17,24,26−30]. S1PR has previously been described as being expressed in a transforming growth factor beta (TGFβ)-dependent manner and regulating fibroblast activation [18,31].

Next, we analysed whether shifts in the proportion of fibroblast subpopulations might be attributed to proliferation or apoptosis. PI16$^+$;FAP$^+$ and TFAM^{high} fibroblasts expressed increased levels of cleaved caspase 3 in SSc, suggesting that enhanced apoptosis may contribute to the loss of these cells in SSc skin (online supplemental figure S7A). Interestingly, despite increased proportion in SSc, S1PR$^+$ fibroblasts and myofibroblasts in SSc skin expressed increased levels of cleaved caspase 3. We did not detect changes in Ki-67 expression on S1PR$^+$ fibroblasts or myofibroblasts, indicating similar proliferation rates when comparing SSc and healthy controls (online supplemental figure S7B). The FAP^{high} fibroblasts expressed reduced levels of Ki-67, suggesting decreased proliferative activity in SSc in spite of their increased abundance. Therefore, the increase of these fibroblast subpopulations in SSc is not due to proliferation and may thus be due to differentiation from precursor populations. Other fibroblast subpopulations altered numerically in SSc did not show corresponding changes in the expression levels of Ki-67 or cleaved caspase 3, suggesting that their proportions are not changed as a consequence of proliferation or apoptosis.

Altered distribution of fibroblast populations within the Dermis of patients with SSc and healthy individuals

We next aimed to characterise the intradermal distribution of the individual fibroblast populations. While some populations were equally distributed over the entire dermis, others preferentially resided in either upper or lower dermis (figure 4A and B and online supplemental figure S8). The ADAM12$^+$;GLI1$^+$ and TFAM^{high} fibroblasts were found in the upper dermis. In alignment with previous studies, most of the myofibroblasts were located in the lower dermis (figure 4B and online supplemental figure S8A)[32,33].

We further analysed alterations of the distribution of subpopulations between the upper and lower dermis in patients with SSc compared with healthy individuals (figure 4C and D). Statistical significant changes were detected in the frequencies of ADAM12$^+$;GLI1$^+$ and TFAM^{high} fibroblasts in the upper dermis of SSc skin when compared with healthy controls, but not in the lower dermis. The increased numbers of FAP^{high} fibroblasts and myofibroblasts were exclusively found in the lower dermis. In contrast, the loss of PI16$^+$;FAP$^+$ fibroblasts and the expansion of S1PR$^+$ and Thy1$^+$;ADAM12^{high};PU.1^{high} fibroblasts in SSc were found in both dermal layers.

Of note, PI16$^+$;FAP$^-$ fibroblasts did not demonstrate changes in frequencies between healthy and SSc (p value = 0.72), but they demonstrated changes in spatial distribution in SSc skin. We detected trends towards lower proportion of PI16$^+$;FAP$^-$ fibroblasts in the upper layers of the dermis and lower dermal distribution scores (p value = 0.07) in SSc compared with healthy controls. In contrast, we observed a tendency for elevated ADRP$^+$ fibroblasts in the upper dermis in SSc samples. These findings provide evidence that not only the numbers of individual fibroblast subsets are altered in SSc, but that their spatial distribution is also affected.

Local microenvironment of fibroblasts in SSc skin

As the local microenvironment can also shape the cellular phenotype, we aimed to further characterise CNs by clustering cells based on the composition of neighbouring cells [34]. This clustering approach yielded nine CNs in human skin (figure 5A). These CNs represent multicellular spatial domains, which may serve as functional units within the tissue. Indeed, some of these CNs recovered histological locations in the skin tissue. For example, the Epithelial CN identified epithelium, and the Endothelial CN identified the vascular region. Some fibroblast populations lacked specific types of neighbours and were identified as isolated cells, including well-known subsets of activated fibroblasts such as FAP^{high} fibroblasts and myofibroblasts (figure 5, online supplemental figure S9). Of interest, we found that specific fibroblast populations tended to spatially gather together in the skin. Several fibroblast populations that are downregulated in SSc skin cluster regionally: resting fibroblasts, TFAM^{high} fibroblasts and Thy1$^+$;ADAM12^{low} fibroblasts, formed the Resting CN. Another CN was primarily formed by PI16 expressing cells (PI16 CN). Of the fibroblast subsets upregulated in SSc skin, S1PR$^+$ fibroblasts formed their own CN, which consisted of almost exclusively S1PR$^+$ fibroblasts, resembling small S1PR$^+$ fibroblast foci.

We further examined the fibroblast composition in the subepithelial and vascular regions. We observed a shift in the composition of these histological CNs in SSc skin compared with healthy controls. The abundance of S1PR$^+$ fibroblasts were increased in the Endothelial CN and ADAM12$^+$;GLI1$^+$

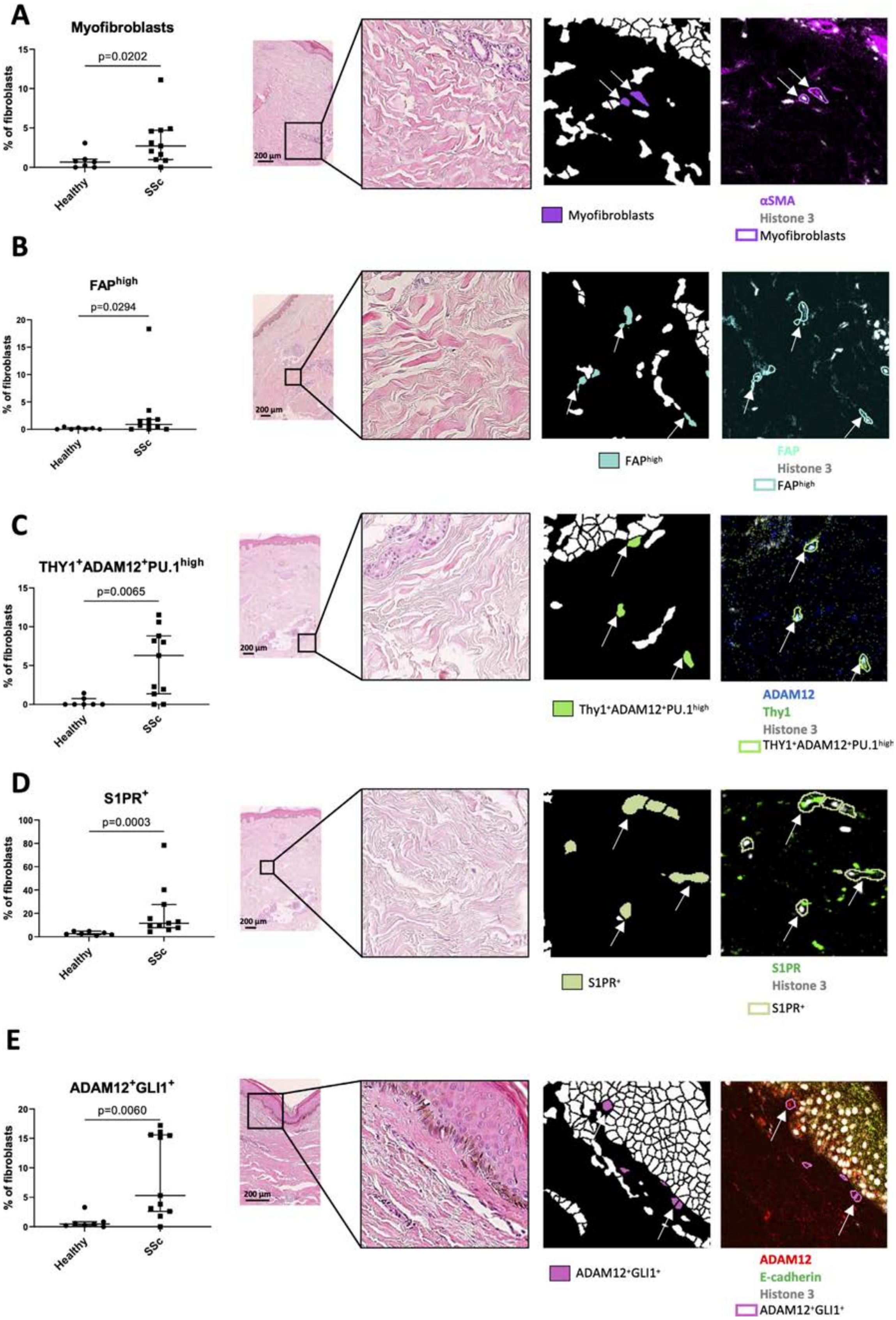

Figure 3. Alterations in the proportion of fibroblast subpopulations in SSc skin. (A−E) Representative images and quantification of fibroblast subsets enriched in SSc skin, including myofibroblast (A), FAP^{high} (B), Thy1^{+}ADAM12^{high}PU.1^{high} (C), S1PR^{+} (D) and ADAM12^{+};GLI1^{+} fibroblasts (E). Images are shown as H&E staining of a consecutive section (left), spatial distribution of selected subpopulation on the cell segmentation masks (middle) and as IMC staining with the protein expression in pseudocolours as indicated (right). Horizontal scale bars represent 200 µm. The results are shown as median±IQR and each dot represents one biological replicate (n = 7 for healthy and 11 for SSc). Statistical significance was determined by the Mann-Whitney U test. P values are indicated above the comparisons. IMC, imaging mass cytometry; SSc, systemic sclerosis.

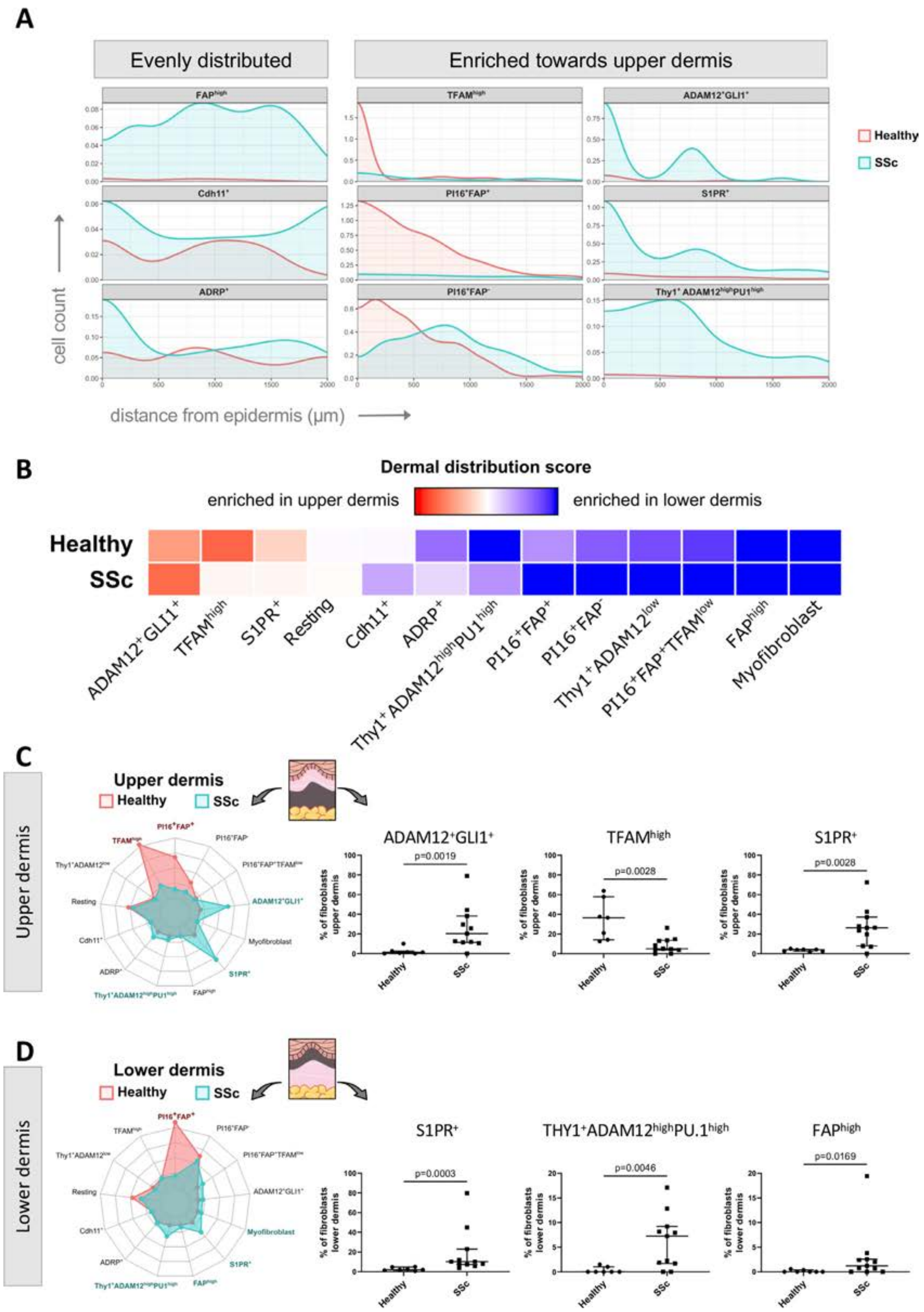

Figure 4. Spatial organisation of fibroblast subsets in the skin. (A) Distance profile of fibroblast subsets displaying the distribution of each fibroblast subset across the dermis. The distances between individual fibroblast subpopulations and the epidermis are plotted for patients with SSc and healthy donors. (B) Dermal distribution score indicating the enrichment of fibroblast subset in upper or lower dermal compartment. (C, D) Quantitative analysis of alterations in the distribution of fibroblast subsets between the upper (C) and lower (D) dermis in SSc skin compared with healthy skin. Left: radar plots showing the changes in fibroblast subpopulations in the upper and lower dermis, respectively, comparing SSc and healthy skin. The fibroblast subsets with significant changes in SSc are highlighted with colours and bold font (red: decreased in SSc; blue: increased in SSc). Right: changes in SSc skin compared with healthy skin of selected fibroblasts subpopulations shown as % of all fibroblasts in the upper dermis (C) or % of all fibroblasts in the lower dermis, respectively (D). The results are shown as median±IQR and each dot represents one biological sample (n = 7 healthy controls and 11 SSc samples). Statistical significance was determined by the Mann-Whitney U test. Significant changes are highlighted with colours and bold fonts in radar plots. P values are indicated above the comparisons. The illustration of skin components was adapted from Servier Medical Art under a CC BY 4.0 license (https://creativecommons.org/licenses/by/4.0/). SSc, systemic sclerosis.

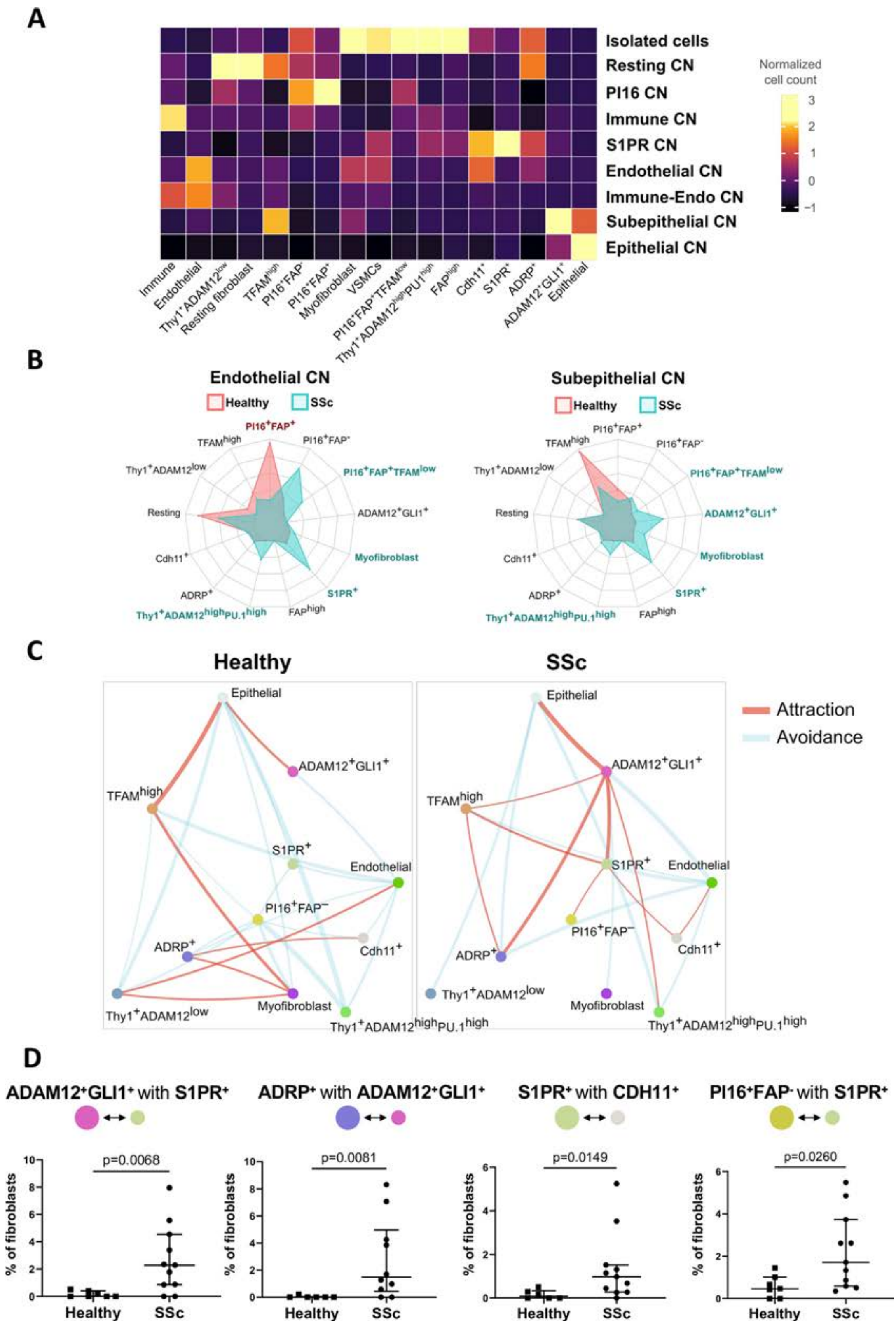

Figure 5. Cellular interaction of fibroblast subsets in SSc skin. (A) Heatmap indicating the composition of the CN. The cell frequencies were normalised individually for each fibroblast subset. (B) Radar plots showing the changes in cellular composition of Endothelial and Subepithelial CN in SSc compared with healthy controls. (C) Representative cellular interaction network visualisation showing attraction (red line) or avoidance (blue line) across cell subpopulations in samples from healthy and SSc donors. (D) Quantification of the frequencies of cells with SSc-specific cellular interactions in SSc skin. The cells with interactions were defined as cells with at least one specified partner cell residing within its local environment. The results are shown as median±IQR and each dot represents one biological replicate (n = 7 for healthy samples and 11 for SSc samples). Statistical significance was determined by the Mann-Whitney U test (B, D) and permutation test (C). Significant changes are highlighted with colours and bold fonts in radar plots (red: decreased in SSc; blue: increased in SSc). P values are indicated above the comparisons. Cellular neighbours were defined as all cells within a distance of 50 µm from the cell border. CN, cellular neighbourhoods; SSc, systemic sclerosis.

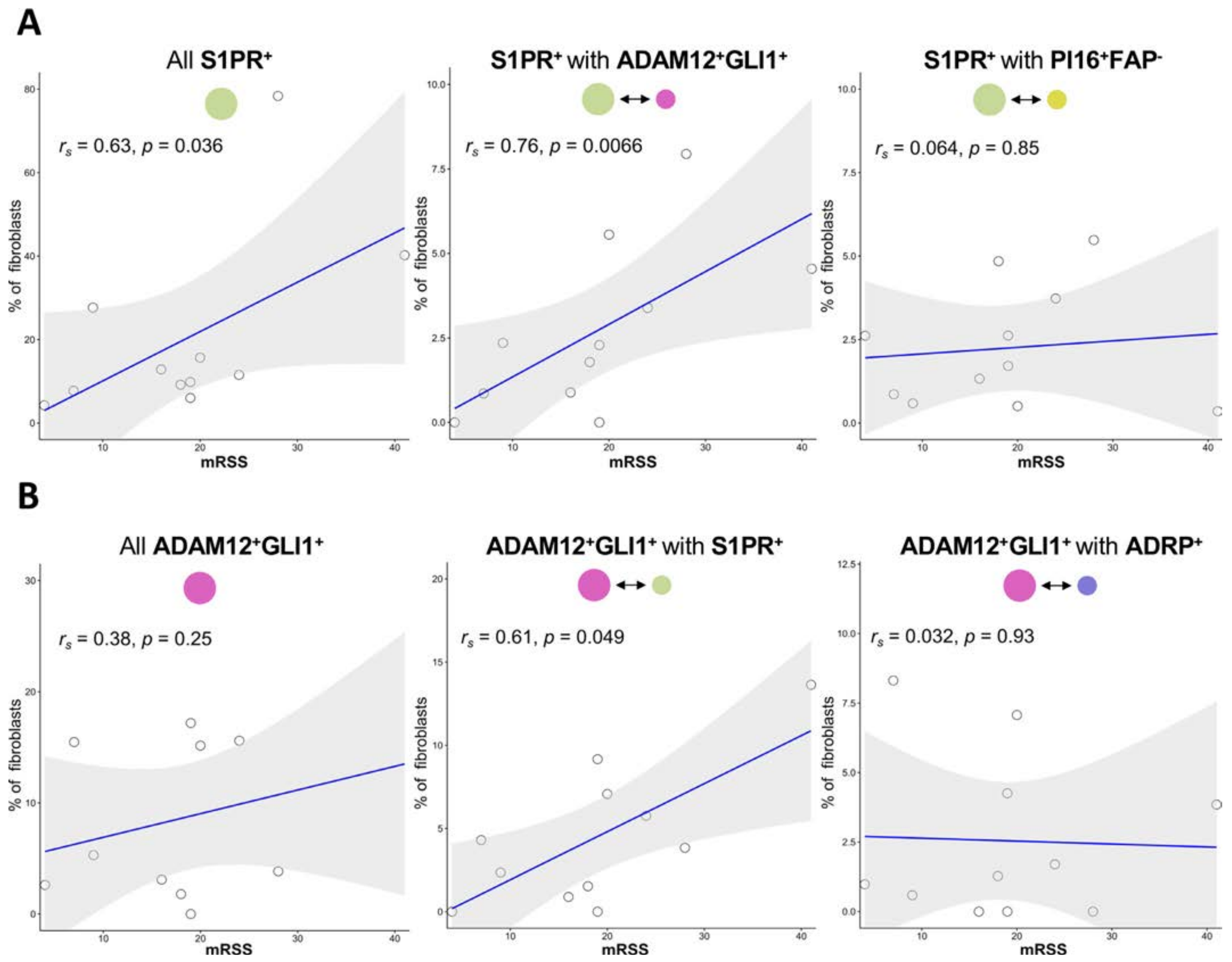

Figure 6. Association of cellular interactions across fibroblast subsets with clinical features. Spearman's rank correlation analysis on the SSc clinical outcomes, including mRSS, with the proportion of the S1PR$^+$ (A, left) and ADAM12$^+$;GLI1$^+$ fibroblasts (B, left) as well as the abundance of S1PR$^+$ (A, middle and right) and ADAM12$^+$;GLI1$^+$ fibroblasts (B, middle and right) with the indicated neighbouring fibroblast located within a distance of 50 μm from the cell border. Statistical significance was determined by Spearman's correlation analysis. Linear regression lines with the 95% CI are added to the scatter plots. The Spearman's rank correlation coefficient r_s and the p value for the correlation analysis were indicated in the plots. mRSS, modified Rodnan skin score.

fibroblasts were increased in the Subepithelial CN (figure 5, online supplemental figure S10). Consistent with previous studies, we also detected increased myofibroblasts in the Endothelial CN[32,35]. These alterations further suggest that fibroblasts may exhibit diverse functional phenotypes based on the specific CN in which they are located.

Aberrant cellular interactions are thought to contribute to the pathological phenotype of fibroblasts in SSc. We thus performed cellular interaction analysis and evaluated cellular interaction networks of fibroblasts in the skin of patients and controls with SSc. Cellular pairwise interaction analysis confirmed the topology of the subepithelial space with exclusive interaction with TFAM^{high} and ADAM12$^+$;GLI1$^+$ fibroblasts (online supplemental figure S11A). Similarly, the epithelial interaction with ADAM12$^+$;GLI1$^+$ fibroblasts was almost exclusively found in skin tissue from patients with SSc (online supplemental figure S11A and C).

Furthermore, the pairwise interaction analysis revealed distinct cellular interaction networks in SSc skin that were not detected in healthy skin samples (figure 5C). These changes in SSc include the altered interacting partners of ADAM12$^+$;GLI1$^+$ and S1PR$^+$ fibroblasts, including ADRP$^+$, TFAM^{high}, PI16$^+$;FAP$^-$ and Cdh11$^+$ fibroblasts. We also detected elevated proportions of the cells with SSc-distinct interacting partners in skin tissue from patients with SSc (figure 5D). These results provide evidence of rearrangement of the local fibroblast environment in SSc skin.

Correlation of fibroblast subsets and their cellular interactions with clinical features of SSc

We went on to investigate potential correlations of the frequencies and the localisation of fibroblast subpopulations with clinical features of SSc. We first focused on the fibrotic feature assessed by the modified Rodnan Skin Score (mRSS). The percentage of S1PR$^+$ fibroblasts in the skin was positively correlated with mRSS (figure 6A). As we noted changes in the distribution of fibroblast subsets in SSc, we further analysed whether these spatial changes might be associated with clinical phenotypes. Indeed, the proportion of S1PR$^+$ fibroblasts in the upper dermis was higher in patients with SSc with progression of skin fibrosis (defined by increase in total mRSS ≥25% from baseline to second visit within 12±2 months) as compared with patients with SSc with stable or declining mRSS (online supplemental figure S12). Together, these data suggest that accumulation of S1PR$^+$ fibroblasts are associated with a higher risk of progressive and extensive skin fibrosis.

Several associations with clinical features were also observed for PI16$^+$;FAP$^-$ fibroblasts. The total percentage of PI16$^+$;FAP$^-$ fibroblasts as well as the abundance of PI16$^+$;FAP$^-$ fibroblasts in the upper dermis were inversely correlated with the mRSS (online supplemental figure S12). Similarly, we found an inverse association between mRSS and the percentage of ADRP$^+$ fibroblasts in the upper dermis. There was no statistically significant association found between mRSS and the total number of ADRP$^+$ fibroblasts or the proportion of ADRP$^+$ fibroblasts in the lower dermis (online supplemental figure S12).

Given the profound changes in cellular interactions of SSc fibroblasts, we analysed whether the SSc-specific cellular interactions may also associate with clinical features of SSc or may even provide stronger correlations as compared with the cellular frequencies of fibroblast subsets alone. We found a stronger correlation for the mRSS and the proportion of ADAM12$^+$;GLI1$^+$ fibroblasts interacting with S1PR$^+$ fibroblasts (figure 6B). No statistically significant association was found when examining ADAM12$^+$;GLI1$^+$ cells alone or other cellular interactions, such as ADAM12$^+$;GLI1$^+$ fibroblasts with ADPR$^+$ fibroblasts. Similar findings were also detected in S1PR$^+$ fibroblasts. We noted a higher Spearman's rank correlation coefficient, when correlating the mRSS to the proportions of S1PR$^+$ fibroblasts interacting with ADAM12$^+$;GLI1$^+$ fibroblasts compared with correlating S1PR$^+$ fibroblasts alone regardless of their interaction partners (figure 6). To further validate these findings, we integrated our IMC data with recently published spatial transcriptomic datasets [32,36]. The results demonstrated that the regions with coenrichment of S1PR$^+$ fibroblasts and ADAM12$^+$;GLI1$^+$ fibroblasts expressed high levels of *COL1A1*, indicating active tissue remodelling (online supplemental figure S13).

DISCUSSION

We present herein the first spatial proteomics study on fibroblast subpopulations in SSc using IMC as a spatial proteomic technique which has not been previously employed for phenotyping of fibroblasts. We demonstrate the validity of the individual methods by cross-validating key findings of IMC by data mining of scRNA-Seq data, but also by confirming previous findings obtained by standard techniques such as immunohistochemistry including increased numbers of myofibroblasts in SSc skin compared with control skin. In contrast to spatial transcriptomics approaches such as Visium [32], IMC offers much higher resolution down to single cell level (1 μm vs 100 μm) but is limited in the number of detectable antigens. These methods provide complimentary insights and may synergize to phenotype cellular subsets at mRNA and protein level, respectively.

Quantification of the protein levels of specific markers of fibroblasts together with the spatial information enabled us to identify 13 different fibroblast subpopulations and characterise their topographical organisation in SSc and healthy skin. Besides well-known fibroblast populations such as myofibroblasts or FAP^{high} fibroblasts, we identified multiple additional subpopulations of fibroblasts with altered proportions in SSc skin. Several novel populations such as Thy1$^+$;ADAM12^{high};PU.1^{high} fibroblasts, ADAM12$^+$;GLI1$^+$ fibroblasts or TFAM^{high} fibroblasts are characterised by the expression of profibrotic transcriptional regulators in combination with a specific subset of fibroblast markers, the combination of which clearly distinguishes them from other fibroblast populations.

All fibroblast subpopulations of healthy skin are preserved in SSc skin, in line with findings from the scRNA-Seq data [6,7,37]. However, 8 out of 13 fibroblast subpopulations show statistically significant changes in frequencies, thereby highlighting the profound perturbances in the fibroblast compartment in SSc. The proportion of myofibroblasts, FAP^{high} fibroblasts, S1PR$^+$ fibroblasts, Thy1$^+$;ADAM12^{high};PU.1^{high} fibroblasts and ADAM12$^+$;GLI1$^+$ fibroblasts were increased in SSc skin. Most of those fibroblast subpopulations showed comparable proliferation between SSc skin and healthy controls with the exception of FAP^{high} fibroblasts, that proliferated to a lesser extent in SSc skin. We also did not observe reduced rates of apoptosis in any of these increased subpopulations, indicating that the number of these fibroblast subpopulations may increase in SSc due to differentiation from precursor cells. However, further experiments are required to confirm this hypothesis and to identify the molecular drivers of this differentiation.

Myofibroblasts and FAP^{high} fibroblasts have extensively been characterised as profibrotic fibroblast populations. The profibrotic effects of Thy1$^+$;ADAM12^{high};PU.1^{high} fibroblasts and ADAM12$^+$;GLI1$^+$ fibroblasts is evidenced by the upregulated expression of profibrotic transcription factors such as PU.1 and GLI1, which have been shown to stimulate the expression of profibrotic transcriptional programmes [14,28,38–40]. S1PR signalling has also been implicated in the pathogenesis of fibrosis. The expression of S1PR and its ligand S1P is induced in fibroblasts on TGFβ stimulation and inhibition of S1PR limits the release of extracellular matrix from fibroblasts [18,31]. Moreover, we demonstrate that the proportion of S1PR$^+$ fibroblasts in SSc skin is positively correlated with clinical markers of the severity of skin fibrosis such as the mRSS as a standard clinical readout for the extent of skin fibrosis and with the risk of progression of skin fibrosis.

Release of extracellular matrix is thought to be the prime function of fibroblasts. In a fibrotic disease such as SSc with excessive accumulation of extracellular matrix, one would thus at first rather expect increased numbers of fibroblasts. However, the overall number of fibroblasts is not altered in SSc skin compared with control skin. Moreover, we also demonstrate statistically significant decreases in the frequency of three populations in SSc: reduced proportion of TFAM^{high} fibroblasts, Thy1$^+$;ADAM12^{low} fibroblasts and PI16$^+$;FAP$^+$ fibroblasts. Mechanistically, two downregulated fibroblast subpopulations showed evidence of increased expression of cleaved caspase 3, but no changes in Ki-67 expression, providing evidence that removal by apoptosis, but not impaired proliferation may contribute to their numerical reduction in SSc. The finding of selective and profound downregulation of these three fibroblast subpopulations may point to homeostatic or even antifibrotic effects of TFAM^{high} fibroblasts and PI16$^+$;FAP$^+$ fibroblasts. Indeed, high expression of the mitochondrial transcription factor TFAM characterises fibroblasts with high levels of oxidative phosphorylation and low collagen release, whereas downregulation of TFAM is associated with mitochondrial damage, a consecutive switch from oxidative phosphorylation to aerobic glycolysis, upregulation of αSMA and other markers of fibroblast activation and increased release of collagen [17]. However, Thy1$^+$;ADAM12-^{low} fibroblasts and PI16$^+$;FAP$^+$ fibroblasts require further functional characterisation.

The spatial context information provided by IMC analysis enabled us to demonstrate not only profound changes in the proportions of fibroblast subpopulations, but also in their spatial distribution in SSc. Of note, even fibroblasts without changes in their frequencies between SSc and healthy across the whole skin such as PI16$^+$;FAP$^-$ fibroblasts demonstrated changes in spatial distribution in SSc skin, with redistribution to deeper layers of the dermis in SSc. The redistribution of fibroblasts by itself may have functional consequences as indicated by the associations of PI16$^+$;FAP$^-$ counts with clinical features of SSc including inverse correlations of their proportion with the mRSS. In addition to changes in the organisation of fibroblasts within the dermal layers, we also observed shifts in fibroblast composition in different histological areas, such as the vascular and epithelial regions. We detected enrichment of profibrotic fibroblasts, including S1PR$^+$ fibroblasts, Thy1$^+$;ADAM12^{high};PU.1^{high} fibroblasts and myofibroblasts in the Endothelial CN in SSc skin. These results suggest active remodelling and the formation of profibrotic fibroblasts at the perivascular sites in SSc, as shown in previous studies [35,41,42]. The CN analysis identified CNs for homeostatic fibroblasts and S1PR$^+$ fibroblasts, suggesting that the formation of these cells may be partially regulated by the local environment. Our spatial analysis discovered aberrant cellular interactions among S1PR$^+$, ADAM12$^+$;GLI1$^+$, ADRP$^+$ and PI16$^+$FAP$^-$ fibroblasts. The interaction between S1PR$^+$ and ADAM12$^+$;GLI1$^+$ fibroblasts demonstrated high associations with the extent of skin fibrosis. In contrast, the presence of ADRP$^+$ fibroblasts in the upper dermis negatively correlated with skin fibrosis, aligned with previous research on the fibrosis-resolving roles of these cells [43,44]. These findings highlight how the local environment and cellular interactions may shape the activated phenotypes and functional implications of these cells. However, further in vitro investigations are required to unravel the molecular mechanisms underlying these interactions.

While our results provide valuable insights, there are several limitations to consider. Despite taken from similar composition of gender and age, the control samples originated from the trunk and the extremities, and we had different ethical compositions. However, our correlation analysis did not detect phenotypic differences across different biopsy sites and ethnicities across the cell populations analysed in this study. Environmental factors, such as sun exposure, may influence the phenotype in the skin tissue [45]. A limitation of our study is that control biopsies were obtained mainly from non-sun exposed skin, whereas SSc biopsies were all from the distal forearm. Although we did not observed differences in the control group according to localisation, the differences in localization of the biopsied areas are a potential limitation that needs to be taken into account.

In summary, we used IMC as a spatially resolved proteomics technique to characterise fibroblast subpopulations and their spatial distribution in SSc skin. We identified new fibroblast populations and demonstrated profound changes in the abundance, localisation and cellular interactions for multiple fibroblast subpopulations. These findings may provide a rationale for specific targeting of individual fibroblast subpopulations in SSc. Moreover, the association of fibroblast counts with clinical outcomes may offer potential for patient stratification. These findings may provide a rationale for specific targeting of individual fibroblast subpopulations in SSc. Non-targeted blockage of fibroblasts may affect beneficial homeostatic or regenerative fibroblasts, also described in our previous study [37], and would increase the risk of adverse events. Our study adds to the characterisation of phenotypically and functionally distinct fibroblast populations in SSc by providing first spatially resolved proteomic data. Identification and specific targeting of profibrotic fibroblast populations increased in SSc may enable effective targeting of pathogenic populations. Moreover, the amount and the localisation of these pathogenic populations may offer potential for patient stratification. Further studies are needed to unravel the molecular mechanisms behind these interactions and may provide insights on potential strategies for inhibition of these pathological interactions.

Acknowledgments

We thank Christoph Liebel, Philipp Steinbrecher and Lukas Sokolowski for excellent technical assistance. We would also like to express our gratitude to Michael B Brenner for generously supplying the Cdh11 antibody. Our analysis was supported by a de.NBI Cloud project (Y-NL) within the German Network for Bioinformatics Infrastructure (de.NBI) and ELIXIR-DE (Forschungszentrum Jülich and W-de.NBI-001, W-de.NBI-004, W-de.NBI-008, W-de.NBI-010, W-de.NBI-013, W-de.NBI-014, W-de.NBI-016, W-de.NBI-022). We would also like to acknowledge the Bodenmiller Lab for generously sharing their expertise and assisting us in refining our analysis workflow during their IMC workshop.

Contributors

ARR, JHWD and Y-NL designed the study. ARR, ML, VD, TF, A-EM, A-HG, VF and Y-NL were involved in the acquisition and analysis of data. ARR, ML, A-EM, A-HG, TF, JHWD and Y-NL were involved in the interpretation of data. ARR, RN, JHWD and Y-NL created the original draft and data visualisation. ML, A-EM, A-HG, CB, GS, JHWD and Y-NL acquired resources and oversaw this study. All authors were involved in manuscript preparation and proofreading. ARR, JHWD and Y-NL take full responsibility for the overall content as guarantors.

Funding

The project was supported by the following grants to authors: 'Großgeräteantrag' of the German Research Foundation (DFG), INST 901095-1 FUGG / AOBJ 659788 / ID 424726560, Grants DI 1537/17-1, DI 1537/20-1, DI 1537/22-1, DI 1537/23-1 and of the German Research Foundation, SFB TR221/ project number 324392634 (B04) of the German Research Foundation, an unrestricted research grant from the Hiller-Foundation (JHWD), MA 9219/2-1 of the German Research Foundation (A-EM), grants 2021_EKEA.03 (A-EM) and 2022_EKMS.02 (A-EM) of the Else-Kröner-Fresenius-Foundation, The Edith Busch and World Scleroderma Foundation Research Grant Programme 2022-2023 (A-EM) and the Research Committee of the Medical Faculty of the Heinrich-Heine University Düsseldorf (Forschungskommission; ID 2022-18, ID 2023-33 and ID 2023-31 to A-HG, E-AM and JHWD, respectively).

Competing interests

A-HG received lecture fees from Boehringer Ingelheim and Abbvie. JHWD has consultancy relationships and/or has received research funding from AbbVie, Actelion, BMS, Celgene, Bayer Pharma, Boehringer Ingelheim, JB Therapeutics, Sanofi-Aventis, Novartis, UCB, GSK, Array Biopharma and Active Biotech in the area of potential treatments of SSc, is CEO of 4D Science and Scientific lead/Co-CEO of FibroCure. A-HG has received research founding from Boehringer Ingelheim. The project was supported by an unrestricted grant from the Hiller Foundation.

Patient and public involvement

Patients and/or the public were not involved in the design, or conduct, or reporting or dissemination plans of this research.

Patient consent for publication

Not applicable.

Ethics approval

This study involves human participants and was approved by Ethics Committee at the Faculty of Medicine of Heinrich Heine University Düsseldorf (approval number: 2022-2189_3, 2023-2561). Participants gave informed consent to participate in the study before taking part.

Supplementary materials

Supplementary material associated with this article can be found in the online version at doi:10.1136/ard-2024-226336.

Orcid

Minrui Liang: http://orcid.org/0000-0002-7650-1237
Andrea-Hermina Györfi: http://orcid.org/0000-0002-4960-3369
Christina Bergmann: http://orcid.org/0000-0001-5257-9171
Georg Schett: http://orcid.org/0000-0001-8740-9615
Jörg H.W. Distler: http://orcid.org/0000-0001-7408-9333
Yi-Nan Li: http://orcid.org/0000-0001-8934-9361

REFERENCES

[1] Denton CP, Khanna D. Systemic sclerosis. Lancet 2017;390:1685–99. doi: 10.1016/S0140-6736(17)30933-9.
[2] Distler JHW, Györfi A-H, Ramanujam M, et al. Shared and distinct mechanisms of fibrosis. Nat Rev Rheumatol 2019;15:705–30. doi: 10.1038/s41584-019-0322-7.
[3] Rosendahl A-H, Schönborn K, Krieg T. Pathophysiology of systemic sclerosis (scleroderma). Kaohsiung J Med Sci 2022;38:187–95. doi: 10.1002/kjm2.12505.
[4] Hinz B, Lagares D. Evasion of apoptosis by myofibroblasts: a hallmark of fibrotic diseases. Nat Rev Rheumatol 2020;16:11–31. doi: 10.1038/s41584-019-0324-5.
[5] Garrett SM, Baker Frost D, Feghali-Bostwick C. The mighty fibroblast and its utility in scleroderma research. J Scleroderma Relat Disord 2017;2:69–134.
[6] Gur C, Wang S-Y, Sheban F, et al. LGR5 expressing skin fibroblasts define a major cellular hub perturbed in scleroderma. Cell 2022;185:1373–88. doi: 10.1016/j.cell.2022.03.011.
[7] Tabib T, Huang M, Morse N, et al. Myofibroblast transcriptome indicates SFRP2^{hi} fibroblast progenitors in systemic sclerosis skin. Nat Commun 2021;12:4384. doi: 10.1038/s41467-021-24607-6.
[8] Bandura DR, Baranov VI, Ornatsky OI, et al. Mass Cytometry: Technique for Real Time Single Cell Multitarget Immunoassay Based on Inductively Coupled Plasma Time-of-Flight Mass Spectrometry. Anal Chem 2009;81:6813–22. doi: 10.1021/ac901049w.
[9] Chevrier S, Crowell HL, Zanotelli VRT, et al. Compensation of Signal Spillover in Suspension and Imaging Mass Cytometry. Cell Syst 2018;6:612–20. doi: 10.1016/j.cels.2018.02.010.
[10] Grönberg C, Rattik S, Tran-Manh C, et al. Combined inhibition of IL-1, IL-33 and IL-36 signalling by targeting IL1RAP ameliorates skin and lung fibrosis in preclinical models of systemic sclerosis. Ann Rheum Dis 2024;83:1156–68. doi: 10.1136/ard-2023-225158.
[11] Windhager J, Zanotelli VRT, Schulz D, et al. An end-to-end workflow for multiplexed image processing and analysis. Nat Protoc 2023;18:3565–613. doi: 10.1038/s41596-023-00881-0.
[12] Lee DM, Kiener HP, Agarwal SK, et al. Cadherin-11 in synovial lining formation and pathology in arthritis. Science 2007;315:1006–10. doi: 10.1126/science.1137306.
[13] Schneider DJ, Wu M, Le TT, et al. Cadherin-11 contributes to pulmonary fibrosis: potential role in TGF-β production and epithelial to mesenchymal transition. FASEB J 2012;26:503–12. doi: 10.1096/fj.11-186098.
[14] Kramann R, Schneider RK, DiRocco DP, et al. Perivascular Gli1+ progenitors are key contributors to injury-induced organ fibrosis. Cell Stem Cell 2015;16:51–66. doi: 10.1016/j.stem.2014.11.004.
[15] Aggarwal S, Wang Z, Rincon Fernandez Pacheco D, et al. SOX9 switch links regeneration to fibrosis at the single-cell level in mammalian kidneys. Science 2024;383:eadd6371. doi: 10.1126/science.add6371.
[16] Dulauroy S, Di Carlo SE, Langa F, et al. Lineage tracing and genetic ablation of ADAM12(+) perivascular cells identify a major source of profibrotic cells during acute tissue injury. N Med 2012;18:1262–70. doi: 10.1038/nm.2848.
[17] Zhou X, Trinh-Minh T, Tran-Manh C, et al. Impaired Mitochondrial Transcription Factor A Expression Promotes Mitochondrial Damage to Drive Fibroblast Activation and Fibrosis in Systemic Sclerosis. Arthritis Rheumatol 2022;74:871–81. doi: 10.1002/art.42033.
[18] Ko J, Chae MK, Lee JH, et al. Sphingosine-1-Phosphate Mediates Fibrosis in Orbital Fibroblasts in Graves' Orbitopathy. Invest Ophthalmol Vis Sci 2017;58:2544–53. doi: 10.1167/iovs.16-20684.
[19] Fendt BM, Hirschmann A, Bruns M, et al. Protein atlas of fibroblast specific protein 1 (FSP1)/S100A4. Histol Histopathol 2023;38:1391–401. doi: 10.14670/HH-18-621.
[20] Buechler MB, Pradhan RN, Krishnamurty AT, et al. Cross-tissue organization of the fibroblast lineage. Nat New Biol 2021;593:575–9. doi: 10.1038/s41586-021-03549-5.
[21] Singhmar P, Trinh RTP, Ma J, et al. The fibroblast-derived protein PI16 controls neuropathic pain. Proc Natl Acad Sci U S A 2020;117:5463–71. doi: 10.1073/pnas.1913444117.
[22] Yang P, Luo Q, Wang X, et al. Comprehensive Analysis of Fibroblast Activation Protein Expression in Interstitial Lung Diseases. Am J Respir Crit Care Med 2023;207:160–72. doi: 10.1164/rccm.202110-2414OC.
[23] Kamali Zonouzi S, Pezeshki PS, Razi S, et al. Cancer-associated fibroblasts in colorectal cancer. Clin Transl Oncol 2022;24:757–69. doi: 10.1007/s12094-021-02734-2.
[24] Wohlfahrt T, Rauber S, Uebe S, et al. PU.1 controls fibroblast polarization and tissue fibrosis. Nature New Biol 2019;566:344–9. doi: 10.1038/s41586-019-0896-x.
[25] Croft AP, Campos J, Jansen K, et al. Distinct fibroblast subsets drive inflammation and damage in arthritis. Nature New Biol 2019;570:246–51. doi: 10.1038/s41586-019-1263-7.
[26] Liang R, Kagwiria R, Zehender A, et al. Acyltransferase skinny hedgehog regulates TGFβ-dependent fibroblast activation in SSc. Ann Rheum Dis 2019;78:1269–73. doi: 10.1136/annrheumdis-2019-215066.
[27] Kramann R, Fleig SV, Schneider RK, et al. Pharmacological GLI2 inhibition prevents myofibroblast cell-cycle progression and reduces kidney fibrosis. J Clin Invest 2015;125:2935–51 74929 10.1172/JCI74929.
[28] Schneider RK, Mullally A, Dugourd A, et al. Gli1^{+} Mesenchymal Stromal Cells Are a Key Driver of Bone Marrow Fibrosis and an Important Cellular Therapeutic Target. Cell Stem Cell 2017;20:785–800. doi: 10.1016/j.stem.2017.03.008.
[29] Horn A, Palumbo K, Cordazzo C, et al. Hedgehog signaling controls fibroblast activation and tissue fibrosis in systemic sclerosis. Arthritis Rheum 2012;64:2724–33. doi: 10.1002/art.34444.
[30] Liang M, Dickel N, Györfi A-H, et al. Attenuation of fibroblast activation and fibrosis by adropin in systemic sclerosis. Sci Transl Med 2024;16:eadd6570. doi: 10.1126/scitranslmed.add6570.
[31] Sobel K, Menyhart K, Killer N, et al. Sphingosine 1-phosphate (S1P) receptor agonists mediate pro-fibrotic responses in normal human lung fibroblasts via S1P2 and S1P3 receptors and Smad-independent signaling. J Biol Chem 2013;288:14839–51. doi: 10.1074/jbc.M112.426726.
[32] Ma F, Tsou P-S, Gharaee-Kermani M, et al. Systems-based identification of the Hippo pathway for promoting fibrotic mesenchymal differentiation in systemic sclerosis. Nat Commun 2024;15:210. doi: 10.1038/s41467-023-44645-6.
[33] Rajkumar VS, Howell K, Csiszar K, et al. Shared expression of phenotypic markers in systemic sclerosis indicates a convergence of pericytes and fibroblasts to a myofibroblast lineage in fibrosis. Arthritis Res Ther 2005;7:R1113–23. doi: 10.1186/ar1790.
[34] Schürch CM, Bhate SS, Barlow GL, et al. Coordinated Cellular Neighborhoods Orchestrate Antitumoral Immunity at the Colorectal Cancer Invasive Front. Cell 2020;183:838. doi: 10.1016/j.cell.2020.10.021.
[35] Rius Rigau A, Li Y-N, Matei A-E, et al. Characterization of Vascular Niche in Systemic Sclerosis by Spatial Proteomics. Circ Res 2024;134:875–91. doi: 10.1161/CIRCRESAHA.123.323299.
[36] Ganier C, Mazin P, Herrera-Oropeza G, et al. Multiscale spatial mapping of cell populations across anatomical sites in healthy human skin and basal cell carcinoma. Proc Natl Acad Sci U S A 2024;121:e2313326120. doi: 10.1073/pnas.2313326120.

[37] Zhu H, Luo H, Skaug B, et al. Fibroblast Subpopulations in Systemic Sclerosis: Functional Implications of Individual Subpopulations and Correlations with Clinical Features. J Invest Dermatol 2024;144:1251–61. doi: 10.1016/j.jid.2023.09.288.

[38] Rauber S, Mohammadian H, Schmidkonz C, et al. CD200$^+$ fibroblasts form a pro-resolving mesenchymal network in arthritis. Nat Immunol 2024;25:682–92. doi: 10.1038/s41590-024-01774-4.

[39] Bergmann C, Distler JHW, Treutlein C, et al. ^{68}Ga-FAPI-04 PET-CT for molecular assessment of fibroblast activation and risk evaluation in systemic sclerosis-associated interstitial lung disease: a single-centre, pilot study. Lancet Rheumatol 2021;3:e185–94. doi: 10.1016/S2665-9913(20)30421-5.

[40] Rurik JG, Tombácz I, Yadegari A, et al. CAR T cells produced in vivo to treat cardiac injury. Science 2022;375:91–6. doi: 10.1126/science.abm0594.

[41] Manetti M, Romano E, Rosa I, et al. Endothelial-to-mesenchymal transition contributes to endothelial dysfunction and dermal fibrosis in systemic sclerosis. Ann Rheum Dis 2017;76:924–34. doi: 10.1136/annrheumdis-2016-210229.

[42] Cipriani P, Di Benedetto P, Ruscitti P, et al. Perivascular Cells in Diffuse Cutaneous Systemic Sclerosis Overexpress Activated ADAM12 and Are Involved in Myofibroblast Transdifferentiation and Development of Fibrosis. J Rheumatol 2016;43:1340–9. doi: 10.3899/jrheum.150996.

[43] Kheirollahi V, Wasnick RM, Biasin V, et al. Metformin induces lipogenic differentiation in myofibroblasts to reverse lung fibrosis. Nat Commun 2019;10:2987. doi: 10.1038/s41467-019-10839-0.

[44] Plikus MV, Guerrero-Juarez CF, Ito M, et al. Regeneration of fat cells from myofibroblasts during wound healing. Science 2017;355:748–52. doi: 10.1126/science.aai8792.

[45] Blackstone BN, Wilgus TA, Roy S, et al. Skin Biomechanics and miRNA Expression Following Chronic UVB Irradiation. Adv Wound Care 2020;9:79–89. doi: 10.1089/wound.2019.1034.

Ann Rheum Dis 84 (2025) 823−832

Contents lists available at ScienceDirect

Annals of the Rheumatic Diseases

journal homepage: https://www.sciencedirect.com/journal/annals-of-the-rheumatic-diseases

Vasculitis

The giant cell arteritis (GCA) ultrasound score (OGUS) at diagnosis and after initial treatment predicts future relapses in GCA patients: results of a multicentre prospective study

Sara Monti[1], Cristina Ponte[2,3,*], Valentin S. Schäfer[4,5], Davide Rozza[6,7], Carlo Scirè[6], Giulia Franchi[8], Alessandra Milanesi[8], Nikita Khmelinskii[2,3], Simon M. Petzinna[4,5], Greta Carrara[6], Cristina Di Nicola[6], João Eurico Fonseca[2,3], Carlomaurizio Montecucco[8], Wolfgang A. Schmidt[9], Christian Dejaco[10], Raashid A. Luqmani[11]

[1] *IRCCS Istituto Auxologico Italiano, Immunorheumatology Research Laboratory, Milan, Italy*
[2] *Department of Rheumatology, ULS Santa Maria, Centro Académico de Medicina de Lisboa, Lisbon, Portugal*
[3] *Faculdade de Medicina, Universidade de Lisboa, Lisbon, Portugal*
[4] *Department of Rheumatology, Clinic of Internal Medicine III, University Hospital Bonn, Bonn, Germany*
[5] *University of Bonn, Bonn, Germany*
[6] *Epidemiology Unit, Italian Society of Rheumatology (SIR), Milan, Italy*
[7] *University of Milano-Bicocca, Research Centre on Public Health (CESP), Monza, Italy*
[8] *Department of Internal Medicine and Therapeutics, Università di Pavia; Division of Rheumatology, Fondazione IRCCS Policlinico San Matteo, Pavia, Italy*
[9] *Immanuel Krankenhaus Berlin, Medical Center for Rheumatology Berlin-Buch, Berlin, Germany*
[10] *Department of Rheumatology, Hospital of Bruneck (ASAA-SABES), Teaching Hospital of the Paracelsius Medical University, Brunico, Italy; Department of Rheumatology and Immunology, Medical University of Graz, Graz, Austria*
[11] *Nuffield Department of Orthopaedics, Rheumatology and Musculoskeletal Science (NDORMS), University of Oxford, Oxford, UK*

A R T I C L E I N F O

Article history:
Received 29 July 2024
Received in revised form 27 November 2024
Accepted 28 November 2024

A B S T R A C T

Objectives: To test the prognostic role of ultrasonography at diagnosis of giant cell arteritis (GCA) and the change of ultrasound abnormalities during the initial weeks of follow-up for the prediction of relapse, vascular complications, or initiation of disease-modifying antirheumatic drugs (DMARDs).

Methods: Prospective, multicentre study of patients with new onset GCA undergoing serial ultrasound assessment at fixed time points. The Outcome Measures in Rheumatology (OMERACT) GCA ultrasonography score (OGUS) was used to quantify vessel wall abnormalities. Relapse was defined as recurrence of GCA-related symptoms or rise of inflammatory markers requiring treatment. A multivariable Poisson model with robust variance estimator was applied, including age, sex, large vessel GCA, glucocorticoid cumulative dose, and baseline OGUS as covariates.

*__Correspondence to__ Dr Cristina Ponte, Rheumatology Department, ULS Santa Maria, and Faculdade de Medicina, Universidade de Lisboa, Lisbon, Portugal.
E-mail address: cristinadbponte@gmail.com (C. Ponte).

Sara Monti and Cristina Ponte contributed equally.

Handling editor Josef S. Smolen.

https://doi.org/10.1016/j.ard.2025.01.018

Results: Ninety-seven patients were assessed in 849 visits. Thirty-five (36.1%) patients experienced a total of 66 relapses, with median time to relapse of 210 days (IQR, 94.5-323.5). Higher OGUS at diagnosis was associated with an increased risk of relapse within 12 months (incidence rate ratio [IRR] for each 1 point increase in OGUS: 1.85; 95% CI, 1.05-3.32). At multivariable analysis, OGUS normalisation (score <1) over the first 3 weeks was negatively associated with subsequent relapses (IRR, 0.44; 95% CI, 0.22-0.88) and predicted time to first relapse. OGUS reduction over the first 12 weeks was inversely associated with initiation of DMARDs. Ischaemic/aortic complications were rare.

Conclusions: Ultrasonography has a prognostic role in GCA and can inform risk stratification. Higher OGUS at diagnosis is associated with relapse, while a higher degree and rapidity of improvement in the first weeks are linked with lower relapse rate.

WHAT IS ALREADY KNOWN ON THIS TOPIC

- Ultrasonography of temporal and axillary arteries is a recommended tool for the diagnosis of giant cell arteritis (GCA) and is being increasingly used to monitor disease activity. The Outcome Measures in Rheumatology ultrasonography large vessel vasculitis working group has recently developed a composite ultrasonography score for GCA (OGUS) to be used as a monitoring instrument.
- Reliable prognostic markers for GCA are lacking.

WHAT THIS STUDY ADDS

- This study demonstrates for the first time, in a prospective, multicentre cohort, that ultrasonography has a prognostic role in GCA.
- Higher OGUS at the diagnosis of GCA and the rapidity and degree of improvement of OGUS during the first 3 to 6 weeks of follow-up predict the risk of future relapses.

HOW THIS STUDY MIGHT AFFECT RESEARCH, PRACTICE OR POLICY

- Based on the data of our study, ultrasonography offers the unprecedented opportunity to stratify the individual patient risk at the time of diagnosis of GCA or within the first weeks of follow-up.
- The severity and extension of disease activity measured with a feasible composite ultrasound score and the early rapidity of ultrasonography response represent novel prognostic markers of GCA that can be addressed in future research studies to guide the best therapeutic strategy, determine the intensity of follow-up, and document early response to treatment.

INTRODUCTION

Giant cell arteritis (GCA) is the most common systemic vasculitis in patients aged ≥50. GCA requires prompt treatment with high-dose glucocorticoids (GCs). Adjunctive disease-modifying antirheumatic drugs (DMARDs) are frequently used to minimise GC exposure or to manage refractory/relapsing cases [1]. Despite treatment, approximately half of patients experience a relapse [2]. To date, there are no reliable biomarkers or clinical predictors of relapse that could enable stratification of the individual risk and guide treatment decisions [1,3]. Moreover, with the expanding use of interleukin-6 inhibitors, monitoring of GCA has become a challenge given that traditional acute phase reactants become unreliable [4]. Imaging with ultrasonography of the temporal and axillary arteries is now recognised as a diagnostic modality for GCA [5]. More recently, the measurement of quantitative ultrasound data, including the intima-media thickness (IMT) and the number of sites with halos, has expanded the information that can be routinely monitored [6]. The Outcome Measures in Rheumatology (OMERACT) ultrasonography large vessel vasculitis (LVV) working group has recently published a novel ultrasonography score for GCA, the OMERACT Giant cell arteritis Ultrasonography Score (OGUS), that integrates information from the IMT of 8 vessels into a single score. OGUS was demonstrated to be feasible and has construct validity and sensitivity to change [7–10].

To date, there is no robust data supporting a prognostic role of disease extent and severity as measured by ultrasonography in predicting clinical outcomes. Similarly, we do not know whether the rapidity of response to treatment influences the long-term clinical response. Identifying predictors of relapse is crucial in a treat-to-target strategy, particularly for the implementation of the concepts of disease stratification and personalised medicine in the management of LVV [11].

In the present study, we aimed to prospectively evaluate the prognostic role of the baseline OGUS, along with its rapidity and degree of improvement in the initial weeks following the diagnosis of GCA, as predictors of future relapses (primary endpoint), the initiation of DMARD treatment, ischaemic events, and aortic aneurysms/dissections.

METHODS

Patients and data collection

Patients with a new clinical diagnosis of GCA were recruited from the Rheumatology Departments of 3 referral centres in Italy, Portugal, and Germany into a prospective, observational cohort study between March 2017 and July 2020. Diagnosis was clinically confirmed during follow-up by expert rheumatologists. The study was approved by the Pavia Ethic, Lisbon Academic Medical Centre, and Bonn Ethical committees (references E 2016 0031606, 08/17 and 097/18, respectively). All patients provided written informed consent before inclusion in the study. Patients received treatment according to standard of care in line with international recommendations. The GC regimen was not prespecified in the protocol but followed international recommendations [1,12]. The methodology from the PROgnosis of Temporal Arteritis study was applied as previously described [13]. In brief, GCA patients were recruited if they presented with a positive ultrasonography result at diagnosis, defined as the presence of an inflammatory wall thickening (halo sign) assessed qualitatively [14] at ≥1 branch of the superficial temporal (TA) and/or axillary (AX) arteries and had not received high doses of GCs (≥30 mg/d of prednisolone or equivalent) for >15 days. The initial GCA diagnosis was made by expert rheumatologists specialised in LVV, who performed both the clinical and ultrasound evaluations in accordance with the EULAR-recommended fast-track approach to this disease [1,5]. Less than

10% of patients referred to the fast-track clinics with a final diagnosis of GCA and a negative ultrasound were not eligible for the study. Large vessel (LV)-GCA was defined at diagnosis by the presence of positive ultrasound at the level of the AX. Patients were assessed clinically and by ultrasonography at baseline, weeks 1, 3, 6 and 12, and then every 3 months up to one year. Clinical follow-up continued thereafter with assessments every 3 to 4 months. At the discretion of the managing physician, computed tomography angiography, echocardiography, and chest x-ray were used to screen for the presence of aortic aneurysms during follow-up. Extra visits were scheduled in case of relapse. Relapse was defined as the recurrence of GCA-related symptoms or increased levels of acute phase reactants not otherwise explained and requiring GC/treatment increase [4]. Ultrasonographic findings were not part of the definition of relapse. The EULAR definitions for major and minor relapse were applied [1].

Patient involvement

Patients were not involved in defining the research question. Research methods and outcomes were discussed with participants, who were informed of the results of the study.

Ultrasonography methodology and OGUS calculation

Ultrasonography of the TA, with the common, parietal, and frontal branches, and the AX was performed bilaterally at each time point. The entire length of the middle and distal segments of the AX were assessed with the patient abducting the arm. Ultrasonography was conducted by a single rheumatologist at each centre (SM, CP, VS). All of them had a similar background training and levels of experience [15]. The sonographers were not blinded to the clinical data.

The presence of a halo sign, the number of sites with halos, and the maximum value of IMT measured in longitudinal view of the wall distal to the probe on greyscale images were recorded [7,14]. Colour Doppler was used to aid artery identification but was typically turned off during IMT measurement to ensure more precise values. An Esaote MyLab 7 ultrasound machine (L6-18 MHz linear probe) was used in Pavia, a GE Healthcare LOGIQ-E9 (8-18 MHz hockey stick probe) in Lisbon, and a GE Healthcare Logic S10 (18-24 MHz hockey stick probe for TA, linear 6-15 MHz for AX) in Bonn. The following technical parameters were applied: greyscale frequency of 18 MHz for TA and 13-18 MHz for AX. A pulse repetition frequency of 2.5-3.5 kHz for TA and 3-4 kHz for AX was applied, colour box-adjusted to obtain an angle steer correction to avoid perpendicularity between sound waves and artery and gain-adjusted to fill only the lumen [5,16]. The OGUS was calculated as previously described [7].

The OGUS was calculated as follows: the sum of IMT measured in every segment of the TA and AX divided by the rounded cut-off values of IMTs in each segment. The resulting value was then divided by the number of segments available [7]. Reaching OGUS <1 was referred to as OGUS normalisation because this indicates that, on average, all segments are within the normal range [7]. Importantly, OGUS <1 does not necessarily correspond to a normal (negative) ultrasound.

Statistical analysis

Patients' characteristics were reported as absolute and relative frequencies for categorical variables and mean ± SD or median and IQR for continuous ones, as appropriate.

When ascertained to be nonpathological, missing data on the IMT were imputed by values sampled from a normal random variable, upwards bounded by the IMT normal value. This occurred only if a halo was not present on ultrasound assessment. Missing visit data were imputed by within-patients means between the previous and following values for quantitative variables or last observation carried forward in case of last available visit before censoring or for categorical variables. A total of 5.4% of missing data were imputed.

A landmark definition of the exposure to the OGUS improvement or normalisation was adopted at 1, 3, 6, and 12 weeks to evaluate the rapidity of response to an OGUS change while avoiding immortal time bias. In this framework, time at risk started after the exposure was ascertained at each time point [17]. Exposure was coded as either the continuous 10% reduction in the OGUS (improvement) with respect to the baseline or as an OGUS <1. The continuous multiplicative effect of each 10% improvement of the OGUS on the risk ratio was calculated. We measured the percentage change in OGUS to differentiate the improvement effect from the starting baseline OGUS level; moreover, 10% units were set as the least numerically significant improvement that could be interpreted in relation to the starting OGUS.

Univariable and multivariable Poisson regression models with robust variance estimators were used to evaluate the association between the rapidity and degree of OGUS improvement at different time points. Multivariable models were adjusted for potential clinically relevant confounders: age, sex, baseline OGUS, cumulative GCs, and LV-GCA. Incidence rate ratios (IRRs) were calculated to provide relevant measures of the relative risk for count-type outcomes when Poisson models were applied. Time-to-event outcomes were investigated by means of Cox regression models and reported as hazard ratios (HRs) whenever the proportional hazards assumption was respected. The proportional hazards assumption was checked through visualisation of the Schoenfeld residuals and appropriate testing. Moreover, relations among covariates were inspected, and modified model specification (for example, by introducing time-varying effects) was based on clinical considerations.

Cox models with time-varying clinically relevant covariates (age, GC pulses, cumulative GC dose, DMARDs, ischaemic events, and OGUS improvement/normalisation) (referred to as longitudinal analyses) were employed to assess the overall predictors' effects on the outcomes over time, ie, the overall degree of response to an OGUS improvement during the entire follow-up period.

All analyses were made using R version 4.2.2 software (R Core Team, Foundation for Statistical Computing, 2021).

RESULTS

Population characteristics at disease onset

In total, 102 patients with GCA were included, 5 of whom were excluded due to incomplete ultrasonography data during the first weeks from diagnosis. The final population consisted of 97 patients with a confirmed diagnosis of GCA assessed in 849 visits, with a median follow-up of 388 (IQR, 331-860) days and with a median number of visits per patient of 9 (IQR, 5-11). Sixty-two (70%) patients had follow-up >12 months. The clinical presentation at disease diagnosis is shown in Table 1. Forty-two (43.3%) patients had LV-GCA. Thirty-one (31.9%) patients were on high-dose GC (>30 mg/d) when ultrasonography was conducted (for a mean of 2.1 ± 3.7 days). Overall, 33 (34%)

Table 1
Clinical presentation at disease diagnosis

Clinical characteristics at diagnosis	Patients[a] (n = 97)
Demographics	
Female sex, n (%)	58 (59.8)
Age, y, mean ± SD	77.1 ± 8.3
Symptoms at disease onset, n (%)	
Time between symptom onset and diagnosis, d, median (IQR)	12 (3-40)
Constitutional symptoms (any)	48 (49.5)
Fever (≥38°C or 100.4°F)	13 (13.4)
Weight loss (≥2 kg)	43 (44.3)
New persistent headache	68 (70.1)
New onset of vision loss (unilateral or bilateral)	21 (21.6) [b]
Stroke/transient ischaemic attack	6 (6.2)
Jaw claudication	57 (58.8)
Tongue claudication	8 (8.2)
Scalp tenderness	33 (34)
New onset of polymyalgia rheumatica	55 (56.7)
Laboratory tests at disease diagnosis; median (IQR)/mean ± SD	
ESR[d], mm/h	91 (63-100)/82±32
C-reactive protein, mg/dL	5.1 (2.5-7.8)/5.6±4
Immunosuppressive treatment at the time of baseline ultrasound	
Number of patients on high doses of GCs[c]; n (%)	31 (31.9)
Days on high-dose of GCs[c]; mean ± SD	2.1±3.7
Starting GC dose, mg/d, median (IQR)/mean ± SD	60 (50-250)/239±332
Cumulative prednisolone (or equivalent) dose, mg, median (IQR)/mean±SD	60 (0-487.5)/290±415
Treatment with intravenous methylprednisolone prior to baseline ultrasonography, n (%)	7 (7.2)

ESR, erythrocyte sedimentation rate; GC, glucocorticoid; GCA, giant cell arteritis.
[a] Italy (n = 24 patients), Portugal (n = 28 patients), Germany (n = 45 patients).
[b] Relevant proportion of patients referred to fast-track clinic by ophthalmologists due to visual loss occurring as first symptom.
[c] ≥30 mg/d of prednisolone or equivalent already received at the time of baseline ultrasound. All patients were then treated with high-dose GCs (40-60 mg/d) according to current recommendations after the baseline ultrasound, upon confirmation of the diagnosis of GCA.
[d] ESR at baseline was not performed in the German centre. There were no missing data on other parameters assessed.

patients received GC pulse therapy. TA biopsy (TAB) was performed prior to ultrasonography in 2 (1.9%) patients; one had a positive result, while the other had LV-GCA with a negative TAB. Visual symptoms (double vision, amaurosis fugax, visual loss) occurred in 36 (37.1%) patients, with permanent visual loss confirmed in 21 (21.6%).

Ultrasound findings at baseline

At baseline, all patients had ≥1 arterial segment displaying a halo with a median of 5 (IQR, 3-6) segments per patient. Ultrasound findings at baseline are depicted in Table 2. TA was involved in 93 (95.8%) patients and AX in 42 (43.3%) patients. Thirty-eight (39%) patients had both TA and AX involvement, while 4 (4.1%) had exclusive AX ultrasound positivity. Higher C-reactive protein values (>5.1 mg/dL, median value for the population) were associated with increased OGUS at baseline.

Clinical outcomes during follow-up

Relapses

During follow-up, 35 (36.1%) patients experienced ≥1 relapse, resulting in a total of 66 relapses, with a median time to relapse of 210 days (IQR, 94.5-323.5) and an overall incidence

Table 2
Ultrasound findings at baseline

Ultrasound findings at baseline	Patients (n = 97)
Number of arterial segments with halo, n (%)	
1	4 (4.1)
2	12 (12.4)
3	12 (12.4)
4	11 (11.3)
5	14 (14.4)
6	32 (33)
7	7 (7.2)
8	5 (5.2)
Temporal artery	
Common superficial TA halo, n (%)	78 (80.4)
IMT superficial TA, mm, mean ± SD	0.73 ± 0.26
Frontal branch halo, n (%)	79 (81.4)
IMT frontal branch, mm, mean ± SD	0.66 ± 0.24
Parietal branch halo, n (%)	74 (76.3)
IMT parietal branch, mm, mean ± SD	0.56 ± 0.23
Axillary artery	
Axillary artery halo, n (%)	42 (43.3)
IMT axillary artery, mm, mean ± SD	1.42 ± 0.31
OGUS	
OGUS at baseline, median (IQR)/mean ± SD	1.35 (1.11-1.70)/1.46 ± 0.5
OGUS at baseline <1, n (%)	17 (17.5)

IMT, intima-media thickness; OGUS, OMERACT Giant cell arteritis Ultrasonography Score; TA, temporal artery.

rate of 42 (95% CI, 32-53) per 100 person-years. Sixteen (16.5%) patients relapsed once, 11 (11.3%) had 2 relapses, and 8 (8.2%) had ≥3 relapses (5 patients had 3 relapses, 2 patients had 4 relapses, and 1 patient had 5 relapses). Thirty patients (30.9%) relapsed within 1 year of diagnosis. Relapse incidence rates were 29.1 (95% CI, 10.7-63.4) per 100 person-years in the group with a follow-up <12 months, and 43.9 (95% CI, 33.5-56.5) per 100 person-years after 12 months of follow-up. Details on the clinical manifestations at the time of relapse are reported in the Supplemental Material. Forty-four patients (67%) had a positive ultrasound at the time of relapse. Of these, 38 (57%) had a positive ultrasound at the level of the TA, 11 (17%) at the AX, and 5 (7%) patients had both TA and AX involvement. The mean number of halos was 2 ± 1.3.

An adjunctive DMARD during follow-up was added in 40 (41.2%) patients, with interleukin-6 inhibitor (tocilizumab [TCZ]) being the most frequently used drug, prescribed in 26 (26.8%) cases, followed by methotrexate (MTX) in 14 (14.4%). TCZ was prescribed at diagnosis in 20 patients, while 5 patients received it after a relapse. In 1 patient, TCZ was used during follow-up as part of a strategy to rapidly taper GC in the presence of severe osteoporosis. One patient was prescribed concomitant MTX in adjunction to TCZ to treat a second relapse. MTX was used to manage relapses in 11 patients; 3 patients received MTX during follow-up to spare GC because they were affected by diabetes mellitus.

Thirty-seven (38%) patients were in GC-free remission at the end of follow-up.

Visual loss and aortic complications

There was 1 new case of permanent visual loss during a relapse occurring after 45 months of follow-up (in addition to 21 patients who had permanent visual loss at presentation). Seven (7.2%) patients developed aortic aneurysms detected by computed tomography angiography after a median of 48 months (IQR, 8.5-85). One patient developed aortic dissection at 48 months of follow-up.

Table 3
Ultrasonographic changes during follow-up

Ultrasound findings during follow-up	Overall	Relapsing patients (n = 35)	Never relapsing patients (n = 62)
OGUS, median (IQR)			
Baseline	1.35 (1.11-1.70)[a]	1.47 (1.09-1.88)	1.28 (1.12-1.54)
1 wk	1.04 (0.76-1.47)	1.34 (0.80-1.66)	0.91 (0.75-1.28)
3 wk	1.03 (0.76-1.31)	1.16 (0.79-1.44)	0.96 (0.76-1.23)
6 wk	1.01 (0.82-1.21)	0.94 (0.83-1.35)	1.03 (0.83-1.15)
12 wk	0.99 (0.82-1.15)	0.98 (0.80-1.20)	1.00 (0.83-1.09)
OGUS <1, n (%)			
Baseline	17 (17.5)	5 (14.3)	12 (19.4)
1 wk	46 (47.9)	13 (37.1)	33 (54.1)
3 wk	44 (45.8)	12 (34.3)	32 (52.5)
6 wk	46 (48.9)	17 (50)	41 (78.8)
12 wk	45 (51.7)	18 (51.4)	27 (51.9)
Never reached OGUS <1	15 (15.5)	4 (11.4)	11 (17.7)
Number of sites with halo, median (IQR)			
Baseline	5 (3-6)	5 (3-6)	6 (3-6)
1 wk	2 (0-5.2)	4 (0.5-5.5)	1 (0-5)
3 wk	3 (0-5.2)	3 (0-5)	1 (0-6)
6 wk	2 (0-4)	1 (0-3)	3 (0-5)
12 wk	2 (0-4)	1 (0-3)	2 (1-5)

OGUS, OMERACT Giant cell arteritis Ultrasonography Score.
Wilcoxon test or t-test for OGUS score, chi-square test for OGUS <1, and Poisson tests for halo counts comparisons have been employed. Mean ± SD values provided in Supplemental Material (Supplemental Table S1).
[a] Baseline mean OGUS according to site (Italy: 1.29 ± 0.37; Portugal: 1.99 ± 0.52; Germany: 1.23 ± 0.24).

Ultrasound changes during follow-up

Ultrasonographic changes and information on OGUS during follow-up are presented in Table 3. Differences between patients who eventually experienced a relapse during follow-up and non-relapsing patients are presented.

Association of OGUS with clinical outcomes

Relapse risk

Baseline OGUS was associated with the risk of relapse during the subsequent 12 months with an IRR for 1-point increase in OGUS of 1.85 (95% CI, 1.05-3.32). The same was demonstrated in the adjusted longitudinal analysis in which the baseline OGUS was directly associated with the risk of relapse (HR, 2.79; 95% CI, 1.36-5.73 per 1 unit increase in baseline OGUS). Moreover, OGUS was significantly higher in patients experiencing a relapse (OGUS in relapsing vs nonrelapsing patients: test for the difference in trends, P = .004; Supplemental Fig S1). The rapidity and degree of reduction of OGUS during the first 3 to 6 weeks after diagnosis was associated with the risk of future relapse (Tables 4 and 5). At univariable analysis, the effect of a 10% reduction of OGUS at 6 weeks from diagnosis, compared to an earlier reduction, was significantly associated with the risk of relapse at 1 year (IRR, 1.24; 95% CI, 1.05-1.46). Reaching an OGUS <1 over the first 3 weeks from diagnosis, compared to a delayed improvement in OGUS, was inversely correlated with the risk of relapse over a 3-year follow-up (Table 4, Supplemental Fig S2). The Cox model confirmed that OGUS <1 within 3 weeks of follow-up was significantly associated with the time to first relapse (Supplemental Table S2).

In multivariate analysis, adjusting for potential confounders, the inverse correlation between the OGUS normalisation at weeks 1 and 3 of follow-up and the risk of future relapse was confirmed (adjusted IRR at 3 weeks, 0.44; 95% CI, 0.22-0.88) (Table 5). Moreover, in the longitudinal analysis adjusted for confounders, both a 10% improvement in OGUS and the normalisation of OGUS were confirmed to be associated with a decrease in the risk of relapse (adjusted HR, 0.67; 95% CI, 0.53-0.86 and 0.37; 95% CI, 0.17-0.81, respectively) (Table 6).

The longitudinal models for the percentage of OGUS improvement (Table 6) demonstrated that a 1-point increase in the baseline OGUS confers a 2.79-fold increase in the risk of relapse during follow-up, while the 10% improvement of OGUS at any time point compared to baseline is associated with a 33% reduction in the risk of relapse (Fig).

Initiation of adjunctive immunosuppressive treatments

Initiation of DMARDs in the first 12 months of follow-up was more common in patients with LV-GCA at diagnosis (HR in multivariable analysis: 3.38; 95% CI, 2.26-5.05). The association of the OGUS with the requirement of starting a DMARD was weak; OGUS at the time of diagnosis was not linked with the need for DMARDs, while the normalisation of OGUS over the first 12 weeks was inversely associated in the univariable analysis (IRR at 12 weeks: 0.56; 95% CI, 0.31-0.99) (Table 4). This was confirmed by Cox analysis (HR at 12 weeks: 0.79; 95% CI, 0.64-0.97) (Supplemental Table S2) but not by multivariable regression analysis (Table 5).

In longitudinal multivariable analyses (adjusted for age, sex, baseline OGUS, 10% improvement of OGUS or OGUS normalisation, GC pulses, cumulative GC dose, relapse, and LV-GCA), the associations of OGUS improvement or normalisation with the initiation of DMARDs was not statistically significant.

Ischaemic events and aortic aneurysms/dissections

Ischaemic events and aortic complications did not correlate with baseline OGUS. During follow-up, the number of ischaemic or aortic complications were too rare to allow for any statistical correlation with the ultrasonographic data.

Sensitivity analysis using single quantitative ultrasound data

We performed a sensitivity analysis to assess the effect of the single components of the OGUS and the effect of single quantitative ultrasound data (maximum IMT at the level of the TA, maximum IMT at the AX, number of halos) on the clinical outcomes

Table 4
Univariable analysis of the factors associated with the clinical outcomes

Trait	IRR for future relapse at 1 y	IRR for future relapses over 3 y	IRR for adjunctive DMARD treatment
Univariable			
Clinical and treatment characteristics			
Age (1 y older)	0.98 (0.95-1.02)	0.99 (0.95-1.02)	0.99 (0.97-1.03)
Sex (male)	0.69 (0.33-1.43)	0.92 (0.47-1.81)	1.34 (0.82-2.19)
LV-GCA	0.59 (0.27-1.29)	0.63 (0.29-1.32)	**1.96 (1.19-3.23)**
Ischaemic GCA subtype	1.16 (0.59-2.25)	0.91 (0.49-1.69)	na
PMR symptoms at onset of GCA	1.08 (0.55-2.11)	0.94 (0.51-1.72)	0.94 (0.57-1.52)
CRP at diagnosis >5.1 mg/dL[a]	1.53 (0.79-2.98)	1.14 (0.63-2.06)	1.02 (0.6-1.74)
TCZ prescribed at diagnosis	0.42 (0.13-1.34)	0.54 (0.17-1.73)	4.28 (2.86-6.41)
GC cumulative dose at baseline (effect of adjunctive 100 mg)	0.98 (0.9-1.07)	1.04 (0.96-1.13)	0.95 (0.87-1.03)
GC cumulative dose at baseline adjusted for pulses (effect of adjunctive 100 mg)	0.99 (0.89-1.1)	1.03 (0.92-1.15)	0.92 (0.84-1)
GC cumulative dose at 3 wk (effect of adjunctive 100 mg)	1 (0.99-1.02)	1.01 (0.99-1.03)	0.99 (0.98-1.01)
GC pulses	0.8 (0.37-1.75)	1.35 (0.66-2.76)	1.13 (0.68-1.88)
Ultrasound findings			
OGUS reduction by 10% at 1 wk	0.92 (0.79-1.07)	0.88 (0.76-1.01)	1.14 (0.99-1.30)
OGUS reduction by 10% at 3 wk	0.98 (0.78-1.24)	0.98 (0.78-1.24)	0.96 (0.80-1.16)
OGUS reduction by 10% at 6 wk	**1.24 (1.05-1.46)**	1.18 (0.99-1.39)	0.97 (0.83-1.14)
OGUS reduction by 10% at 12 wk	1.17 (0.95-1.45)	1.15 (0.93-1.42)	0.91 (0.79-1.05)
OGUS <1 at 1 wk	0.56 (0.28-1.12)	**0.49 (0.26-0.93)**	1.55 (0.89-2.7)
OGUS <1 at 3 wk	0.49 (0.23-1.05)	**0.44 (0.22-0.88)**	0.93 (0.54-1.61)
OGUS <1 at 6 wk	0.9 (0.47-1.72)	0.68 (0.38-1.23)	1.42 (0.81-2.48)
OGUS <1 at 12 wk	0.88 (0.45-1.72)	0.88 (0.48-1.64)	**0.56 (0.31-0.99)**

CRP, C-reactive protein; DMARD, disease-modifying antirheumatic drugs; GC, glucocorticoid; IRR, incidence rate ratio; LV-GCA, large vessel giant cell arteritis; na, not applicable; OGUS, OMERACT Giant cell arteritis Ultrasonography Score; PMR, polymyalgia rheumatica; TCZ, tocilizumab.
Univariable Poisson regression with relapse count and DMARD treatment introduction as dependent variables. Statistically significant results shown in bold.
[a] Median CRP value for the included population.

Table 5
Multivariable analysis of the factors associated with the clinical outcomes

Trait	IRR for future relapse at 1 y	IRR for future relapse over 3 y	IRR for adjunctive DMARD treatment
OGUS reduction by 10% at 1 wk	0.85 (0.7-1.04)	0.88 (0.76-1.01)	**1.16 (1.01-1.33)**
OGUS reduction by 10% at 3 wk	0.87 (0.67-1.13)	0.96 (0.81-1.15)	1.02 (0.86-1.2)
OGUS reduction by 10% at 6 wk	1.07 (0.87-1.31)	1.18 (0.99-1.39)	1.13 (0.96-1.34)
OGUS reduction by 10% at 12 wk	0.89 (0.67-1.18)	1.15 (0.93-1.42)	1.01 (0.83-1.24)
OGUS <1 at 1 wk	0.65 (0.28-1.51)	**0.49 (0.26-0.93)**	1.39 (0.72-2.7)
OGUS <1 at 3 wk	0.49 (0.19-1.31)	**0.44 (0.22-0.88)**	0.77 (0.42-1.42)
OGUS <1 at 6 wk	1.39 (0.61-3.14)	0.68 (0.38-1.23)	1.81 (0.99-3.29)
OGUS <1 at 12 wk	0.96 (0.42-2.22)	0.88 (0.48-1.64)	0.77 (0.38-1.59)

DMARD, disease-modifying antirheumatic drug; IRR, incidence rate ratio; OGUS, OMERACT Giant cell arteritis Ultrasonography Score.
Multivariable Poisson model with relapse count and DMARD treatment introduction as dependent variables. Analysis adjusted for: age, sex, baseline OGUS, cumulative glucocorticoids, large vessel giant cell arteritis. Statistically significant results shown in bold.

Table 6
Adjusted longitudinal analysis of the factors associated with the risk of relapse

Longitudinal models—10% improvement of OGUS			Longitudinal models—OGUS normalisation <1		
Relapse			Relapse		
	HR	95% CI		HR	95% CI
Age	0.98	0.94-1.02	Age	0.98	0.94-1.02
Sex (male)	0.98	0.51-1.89	Sex (male)	0.95	0.49-1.84
Baseline OGUS (effect of 1-point increase)[a]	**2.79**	**1.36-5.73**	Baseline OGUS (effect of 1-point increase)	0.85	0.44-1.65
10% improvement of OGUS (continuous)	**0.67**	**0.53-0.86**	OGUS <1	**0.37**	**0.17-0.81**
Ischaemic events	0.53	0.26-1.05	Ischaemic events	**0.45**	**0.22-0.92**
GC pulses previous visit	1.73	0.59-5.07	GC pulses previous visit	2.27	0.80-6.47
Cumulative GC (effect of adjunctive 1000 mg)	0.59	0.02-18.08	Cumulative GC (effect of adjunctive 1000 mg)	0.22	0.01-4.68
Cumulative GC (effect of adjunctive 1000 mg) (quadratic effect)	0.56	0.02-12.64	Cumulative GC (effect of adjunctive 1000 mg) (quadratic effect)	1.38	0.08-24.57
New DMARD previous visit	0.81	0.34-1.88	New DMARD previous visit	0.81	0.36-1.80
LV-GCA	0.67	0.32-1.39	[b]		

DMARD, disease-modifying antirheumatic drug; GC, glucocorticoid; HR, hazard ratio; LV-GCA, large vessel giant cell arteritis; OGUS, OMERACT Giant cell arteritis Ultrasonography Score.
Adjusted time-varying Cox models assessing the longitudinal effect of 10% improvement in the OGUS and OGUS normalisation <1 on the risk of relapse. Statistically significant results shown in bold.
[a] Baseline OGUS (effect of 0.5-point increase): HR, 1.67; 95% CI, 1.17-2.39.
[b] LV-GCA not included in OGUS normalisation model because of high collinearity with new DMARD initiation.

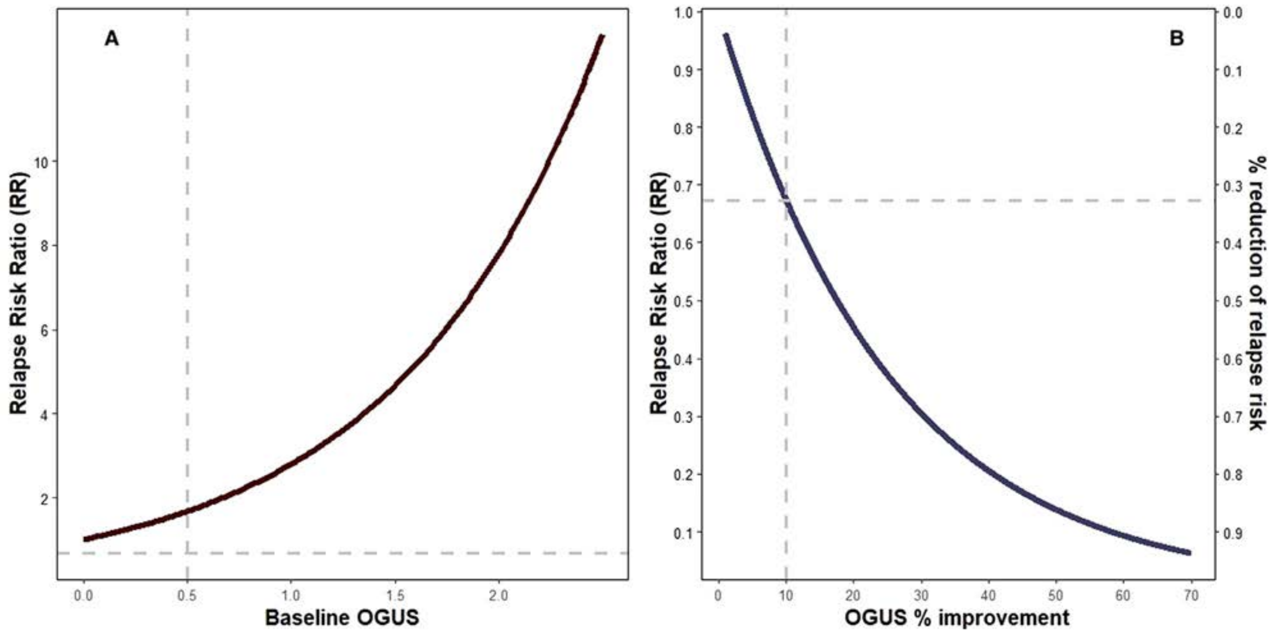

Figure. Relapse risk ratio according to each 0.5-point increase in baseline OGUS (A) and each 10% improvement in OGUS (B). OGUS, Outcome Measures in Rheumatology Giant cell arteritis Ultrasonography Score.

of interest. This analysis confirmed the association between the degree and rapidity of IMT improvement and the extension of disease measured by ultrasonography and the risk of relapse (Supplemental Material and Supplemental Tables S3 and S4).

Sensitivity analysis of the impact of TCZ prescribed at diagnosis

Patients initiating TCZ indication at diagnosis (n = 20) received the first dose after a mean of 9.5 ± 3.4 days, which therefore did not affect OGUS findings at baseline and at 1 week. The OGUS trend and rapidity of improvement from week 3 onwards did not significantly differ between patients receiving TCZ at diagnosis and patients treated with GC monotherapy (Supplemental Table S5).

DISCUSSION

This is the first study to demonstrate a prognostic role for ultrasound in GCA in a prospective international cohort of patients. We have shown that a higher OGUS at the time of diagnosis and the rapidity and degree of ultrasound improvement during the first 3 to 6 weeks of follow-up significantly predict the risk of a future relapse and time to relapse.

For each 1-point increase in the OGUS at diagnosis, the risk of relapse in the first year increases by 1.8-fold and by 2.8-fold during longer follow-up. On the other hand, a 10% improvement at any time point in the first few weeks from diagnosis confers a 32% reduction in the risk of relapse. The percentage improvement follows a multiplicative trend, meaning that a 30% improvement in OGUS would confer a 70% reduction in the risk of relapse. These results are especially relevant because they demonstrate for the first time that a noninvasive, cost-effective, repeatable imaging tool such as ultrasonography can be used for the risk stratification of patients at the time of diagnosis or shortly thereafter.

Our findings suggest a biological plausibility in which greater severity and extent of arterial involvement, indicated by a higher OGUS, likely reflects more severe disease activity, which in turn has subsequent prognostic implications. Histopathologic confirmation of such a hypothesis has been previously demonstrated, with the intensity of the transmural inflammation in TAB specimens being an independent predictor of relapse [18]. Although a direct correlation between the degree of histologic inflammatory infiltrate and the IMT size has never been assessed, the halo sign has been reported to be more frequently detectable in patients with histologic patterns showing transmural and media infiltration [19,20], and the grading of halo thickness to be higher in patients with intima hyperplasia [21]. Studies on ultrasonography, including those on quantitative ultrasonography components, have demonstrated to effectively discriminate between disease states in GCA (active vs remission) [8,13,22]. Our study confirmed that baseline OGUS was higher in patients subsequently affected by a relapse, suggesting that ultrasonography might be included as a parameter in the risk stratification of patients with GCA.

A higher OGUS may be due to larger IMT, or it may be computed in patients with a higher number of involved arterial segments displaying an IMT above the rounded normal cut-offs, and/or more extensive disease with the concomitant involvement of the AX. LV-GCA has generally been regarded as a prognostic factor increasing the risk of relapse, based on a small number of retrospective studies [18,23–25]. In our study, the presence of LV-GCA assessed by ultrasonography was not confirmed to correlate with the risk of relapse. Previous ultrasonographic studies have also questioned the role of AX positivity on ultrasonography as a predictor of the probability to attain clinical remission and found a slower rate of improvement of AX ultrasonography findings in response to treatment [8,13,26]. Further prospective studies will be needed to re-evaluate the value of LV-GCA as a risk factor for relapse. Nonetheless, as we await more studies, we adjusted our analyses for the presence of LV-GCA, and we can reasonably exclude that the prognostic role demonstrated for ultrasonography is dependent on the presence of LV-GCA. Moreover, the risk of overestimating the impact of AX involvement is counterbalanced by the design of the OGUS, scaling IMT measurements by normal cut-offs, offering the advantage of combining both TA and AX in a single score while taking into account the magnitude of changes in different vessel sizes. Finally, the sensitivity analysis performed to address the impact of the single components of ultrasonography assessment (separated TA and AX IMT and number of halos) confirmed the general results of our study and did not demonstrate a positive correlation between AX involvement and the risk of relapse but rather an association with early improvement, also at the level of the AX, with a reduction of future disease exacerbations.

Our results suggest that rather than the involvement of extracranial LVs themselves, it is the extension and severity of disease detected by ultrasonography that influences the prognosis. This is in line with the findings from Czihal et al [24] showing that patients with extensive concomitant involvement of the TA and subclavian/AX arteries at diagnosis displayed a poorer response to treatment. On the other hand, previous studies attempting to correlate quantitative ultrasonography findings or the improvement of vessel wall thickness with the risk of future relapse or treatment requirements failed; however, these studies differed from the current one because the frequency of reassessment of response was significantly less frequent or the follow-up shorter [6,27]. A recent smaller retrospective study observed a potential association of lack of OGUS improvement at 3 and 6 months of follow-up and future risk of relapse [10]. Our study shows that earlier assessment of the rapidity of improvement (first 3-6 weeks) combined with the degree (both percentage improvement and normalisation of OGUS) are key for the prognostic imaging stratification in GCA. Moreover, the identification of specific time points for ultrasonography monitoring and the demonstration of a cut-off in the OGUS (<1) associated with better outcomes improve the clinical applicability of our results and the possibility to validate the findings in future clinical trials. Future research exploring the baseline clinical factors associated with achieving an OGUS <1 could provide insights into further prognostic markers and tailored approaches to GCA.

To rule out the prognostic effect on the risk of relapse demonstrated for the early improvement of OGUS being due to the intensity of initial treatment, we corrected our analyses for the use of GC pulses, the cumulative GC dose, and in longitudinal analyses, for the use of a new DMARD. We also performed a sensitivity analysis that excluded a more rapid improvement of OGUS in patients receiving TCZ early after diagnosis. A previous clinical trial assessing the role of TCZ monotherapy preceded by 3 GC pulses (the GUSTO trial) [22] demonstrated a significant effect of pulse GC therapy on the reduction of IMT and a transient increase and slower reduction of IMT in the TCZ group, in line with a possible trend observed in our cohort. The effect of the cumulative dose of GC, even more than the number of days on GC, in reducing TA halo IMT was also reported by Ponte et al [13]. To further reduce the confounding impact of prolonged GC treatment on ultrasonography findings [28], we excluded patients who had received high-dose GCs for more than 15 days. The mean duration of GC treatment in our study was 2 days; hence, we expect a very limited impact of GC treatment on the results of our study.

Univariable analysis suggested a possible association between improvement of ultrasound findings and the requirement for DMARDs; however, this association was not confirmed after adjusting for confounders and should therefore be interpreted with caution. Since the treatment protocol was not standardised, there might have been several factors that influenced the decision to prescribe a DMARD, which were only partially captured in this study. Consequently, we cannot exclude a Type II error, and another study with a standardised treatment algorithm is needed to better investigate the predictive value of ultrasonography in regard to the use of DMARDs.

Our study failed to demonstrate an association between a higher OGUS at baseline and the risk of ischaemic events during follow-up. This is in line with previous studies with similar research questions [6,28,29] and suggests that research should focus on alternative biomarkers that might predict tissue ischaemia. Furthermore, we were unable to investigate a possible association between OGUS and the development of aneurysms and dissections because of the low number of events. Future prospective studies of large cohorts with standardised assessments for aortic dilatation are therefore required to investigate this issue.

This study has several strengths including the multicentre, international, prospective design with a prespecified fixed protocol for ultrasonography assessments during follow-up, including very early monitoring at 1, 3, and 6 weeks, which were often lacking in previous studies failing to demonstrate a prognostic role for ultrasonography [6]. There was a high number of prospective visits (849 visits) and a high number of patients (with a rare disease) [30], allowing for a careful identification of ultrasonography changes and evaluation of clinical relapses. Ultrasonography was performed using high-end equipment by experienced operators who had received similar training. A score was applied that has demonstrated good reliability, sensitivity to change, and convergent construct validity, also in comparison to other scoring systems, that allows the combination of information on both TA and AX [7,8]. Moreover, the demonstration of the prognostic value for baseline ultrasonography and degree and rapidity of improvement was consistent across several different types of statistical analyses, corrected for the most relevant confounding factors, including detailed data on GC doses.

Despite the consistency across analyses and the biological plausibility that indicates a low risk of false-positive results, we cannot exclude the possibility that a Type I error was inflated, and we acknowledge this as a potential limitation.

The study has other potential limitations to consider including the fact that the sonographers were not blinded to the clinical/ultrasonographic information, including in cases of relapse. Although ultrasound findings were not considered in the relapse definition, we cannot entirely rule out their impact on the relapse rate due to the lack of blinding. However, this approach reflects current clinical practice in fast-track clinics for the diagnosis of GCA. Different ultrasound machines were used across the 3 centres, although the ultrasound machines were always the same for the monitoring of individual patients. A few patients did not attend all scheduled visits, even though we excluded patients with insufficient follow-up data in the first weeks of follow-up. In a minority of patients, follow-up was interrupted within 12 months from diagnosis due to the COVID-19 pandemic or loss to follow-up. However, time at risk and follow-up duration were accounted for in the analyses. Moreover, the prospective ultrasonography measurement was performed in the area with the thickest IMT, which might not have captured the same level of change compared to a fixed measurement location. Interrater reliability was not assessed, but this was confirmed to be good for OGUS in an international exercise [7,31]. The results are generalisable only to patients with a positive ultrasound at diagnosis, while future studies should also investigate the value of OGUS among those who are considered to have a negative ultrasound result (but might nevertheless have minor variations of IMT during follow-up, the monitoring value of which is currently unknown). Since our study was conducted in a fast-track setting, we recruited a relatively high proportion of patients with predominant cranial disease and short symptom-to-diagnosis lag, while patients with isolated LV involvement were less numerous (4.1% with exclusive AX involvement). Patients were often referred by ophthalmology when presenting with visual symptoms, and this accounts for the relatively high frequency of visual loss in our cohort, despite the fast-track setting. TA branches were commonly involved in these patients, and we know that the IMT of the TA is usually more sensitive to change to treatment than that of the AX [13]. The prognostic value of OGUS might have been different in a population with predominant or isolated LVV, longer disease duration, and extracranial symptoms, which might occur in regular outpatient clinics outside the fast-track setting. Future studies are therefore needed to confirm the prognostic value of OGUS in different populations and settings. Moreover, the non-standardised assessment of aneurysms during follow-up in this study may have limited the number of detected cases; however, there are currently no recommendations regarding the optimal frequency of screening or the preferred imaging method [5]. Finally, while we excluded an influence of TCZ prescribed at diagnosis on the rapidity of improvement of OGUS in the first weeks of follow-up, in line with the literature [22], we cannot fully exclude that the use of TCZ might have had an influence on the prognostic value of OGUS because of the lack of power for this analysis. However, our study had an observational nature reflecting current clinical practice, and a head-to-head comparison between GC and TCZ would be needed to clarify this issue and explore the dynamics of imaging changes in patients receiving early treatment with TCZ.

In conclusion, we demonstrated for the first time that ultrasonography can be used as a prognostic tool in the management of GCA. The extent and severity of disease measured at the time of diagnosis with a simple composite ultrasonography score predicts the risk of early relapse in the subsequent year, while the rapidity and degree of ultrasonographic improvement can be used to predict long-term relapses. These findings have relevant clinical implications. Being able to address the individual patient prognosis using a noninvasive, repeatable imaging tool directly at the time of diagnosis or within the very first few weeks of follow-up would offer unprecedented chances in the future of individualising patient treatment and intensity of monitoring based on the risk stratification during the early phases of the disease.

Competing interests

NK: AstraZeneca, GSK, Novartis (honoraria); AbbVie, AstraZeneca, GSK, Lilly, Pfizer (meetings attendance). WAS: AbbVie, GlaxoSmithKline, Novartis, Sanofi (grants contracts, consulting fees, honoraria); Fresenius Kabi (consulting fees); Amgen, Bristol Myers Squibb, Chugai, Johnson & Johnson, Medac, Roche, UCB (honoraria); University of Bonn (data safety monitoring board). CD: AbbVie, Sparrow, Novartis, Sanofi, Boehringer, Pfizer, Galapago, Lilly, Janssen, Roche (consulting fees, honoraria); UCB (honoraria). RL: EPSRC, NIHR, CSL Vifor (grants or contracts); AbbVie (consulting fees); CSL Vifor, SANA, Novartis, GSK (honoraria); CSL Vifor (data safety monitoring board/advisory board).

Contributors

SM is the guarantor for the study. SM designed the study, contributed to the collection of data, and wrote the manuscript. CP contributed to the study design, collected data, contributed to manuscript writing and editing, critically revised manuscript. All authors contributed to the collection of data, and critically revised the manuscript. DR, CS, GC, and CDN performed the statistical analysis and critically revised the manuscript. CM, WS, CD, and RL supervised the work and critically revised the manuscript.

Funding

None to declare.

Patient consent for publication

All patients provided written informed consent before inclusion in the study.

Ethics approval

The study was approved by the Pavia Ethic, Lisbon Academic Medical Centre, and Bonn Ethical committees (references E 2016 0031606, 08/17 and 097/18, respectively).

Provenance and peer review

Not commissioned, externally peer-reviewed.

Data availability statement

Study protocol and raw data are accessible upon reasonable request.

Supplementary materials

Supplementary material associated with this article can be found in the online version at doi:10.1016/j.ard.2025.01.018.

REFERENCES

[1] Hellmich B, Agueda A, Monti S, Buttgereit F, de Boysson H, Brouwer E, et al. 2018 Update of the EULAR recommendations for the management of large vessel vasculitis. Ann Rheum Dis 2020;79(1):19–30.

[2] Alba MA, García-Martínez A, Prieto-González S, Tavera-Bahillo I, Corbera-Bellalta M, Planas-Rigol E, et al. Relapses in patients with giant cell arteritis: prevalence, characteristics, and associated clinical findings in a longitudinally followed cohort of 106 patients. Medicine (Baltimore) 2014;93(5):194–201.

[3] Monti S, Bartoletti A, Bellis E, Delvino P, Montecucco C. Fast-track ultrasound clinic for the diagnosis of giant cell arteritis changes the prognosis of the disease but not the risk of future relapse. Front Med (Lausanne) 2020;7:589794.

[4] Stone JH, Tuckwell K, Dimonaco S, Klearman M, Aringer M, Blockmans D, et al. Trial of tocilizumab in giant-cell arteritis. N Engl J Med 2017;377 (4):317–28.

[5] Dejaco C, Ramiro S, Bond M, Bosch P, Ponte C, Mackie SL, et al. EULAR recommendations for the use of imaging in large vessel vasculitis in clinical practice: 2023 update. Ann Rheum Dis 2024;83(6):741–51.

[6] Monti S, Ponte C, Pereira C, Manzoni F, Klersy C, Rumi F, et al. The impact of disease extent and severity detected by quantitative ultrasound analysis in the diagnosis and outcome of giant cell arteritis. Rheumatology (Oxford) 2020;59(9):2299–307.

[7] Dejaco C, Ponte C, Monti S, Rozza D, Scirè CA, Terslev L, et al. The provisional OMERACT ultrasonography score for giant cell arteritis. Ann Rheum Dis 2023;82(4):556–64.

[8] Nielsen BD, Therkildsen P, Keller KK, Gormsen LC, Hansen IT, Hauge EM. Ultrasonography in the assessment of disease activity in cranial and large-vessel giant cell arteritis: a prospective follow-up study. Rheumatology (Oxford) 2023;62(9):3084–94.

[9] Schäfer VS, Dejaco C, Karakostas P, Behning C, Brossart P, Burg LC. Follow-up ultrasound examination in patients with newly diagnosed giant cell arteritis. Rheumatology (Oxford). Published online February 2024;15. doi: 10.1093/rheumatology/keae098.

[10] Molina-Collada J, Monjo-Henry I, Fernández-Fernández E, Álvaro-Gracia JM, de Miguel E. The OMERACT Giant cell arteritis Ultrasonography Score: a potential predictive outcome to assess the risk of relapse during follow-up. Rheumatology (Oxford) 2024 Published online May 8. doi: 10.1093/rheumatology/keae260.
[11] Dejaco C, Kerschbaumer A, Aletaha D, Bond M, Hysa E, Camellino D, et al. Treat-to-target recommendations in giant cell arteritis and polymyalgia rheumatica. Ann Rheum Dis 2024;83(1):48–57.
[12] Dasgupta B, Borg FA, Hassan N, Alexander L, Barraclough K, Bourke B, et al. BSR and BHPR guidelines for the management of giant cell arteritis. Rheumatology (Oxford) 2010;49(8):1594–7.
[13] Ponte C, Monti S, Scirè CA, Delvino P, Khmelinskii N, Milanesi A, et al. Ultrasound halo sign as a potential monitoring tool for patients with giant cell arteritis: a prospective analysis. Ann Rheum Dis 2021;80(11):1475–82.
[14] Chrysidis S, Duftner C, Dejaco C, Schäfer VS, Ramiro S, Carrara G, et al. Definitions and reliability assessment of elementary ultrasound lesions in giant cell arteritis: a study from the OMERACT Large Vessel Vasculitis Ultrasound Working Group. RMD Open 2018;4(1):e000598.
[15] Monti S, Floris A, Ponte CB, Schmidt WA, Diamantopoulos AP, Pereira C, et al. The proposed role of ultrasound in the management of giant cell arteritis in routine clinical practice. Rheumatology (Oxford) 2018;57 (1):112–9.
[16] Monti S, Floris A, Ponte C, Schmidt WA, Diamantopoulos AP, Pereira C, et al. The use of ultrasound to assess giant cell arteritis: review of the current evidence and practical guide for the rheumatologist. Rheumatology (Oxford) 2018;57(2):227–35.
[17] Morgan CJ. Landmark analysis: a primer. J Nucl Cardiol 2019;26(2):391–3.
[18] Restuccia G, Boiardi L, Cavazza A, Catanoso M, Macchioni P, Muratore F, et al. Flares in biopsy-proven giant cell arteritis in northern Italy: characteristics and predictors in a long-term follow-up study. Medicine (Baltimore) 2016;95(9):e3524.
[19] Cavazza A, Muratore F, Boiardi L, Restuccia G, Pipitone N, Pazzola G, et al. Inflamed temporal artery: histologic findings in 354 biopsies, with clinical correlations. Am J Surg Pathol 2014;38(10):1360–70.
[20] Muratore F, Boiardi L, Restuccia G, Macchioni P, Pazzola G, Nicolini A, et al. Comparison between colour duplex sonography findings and different histological patterns of temporal artery. Rheumatology (Oxford) 2013;52(12):2268–74.
[21] van der Geest KSM, Wolfe K, Borg F, Sebastian A, Kayani A, Tomelleri A, et al. Ultrasonographic Halo Score in giant cell arteritis: association with intimal hyperplasia and ischaemic sight loss. Rheumatology (Oxford) 2021;60(9):4361–6.
[22] Seitz L, Christ L, Lötscher F, Scholz G, Sarbu AC, Bütikofer L, et al. Quantitative ultrasound to monitor the vascular response to tocilizumab in giant cell arteritis. Rheumatology (Oxford) 2021;60(11):5052–9.
[23] Sugihara T, Hasegawa H, Uchida HA, Yoshifuji H, Watanabe Y, Amiya E, et al. Associated factors of poor treatment outcomes in patients with giant cell arteritis: clinical implication of large vessel lesions. Arthritis Res Ther 2020;22(1):72.
[24] Czihal M, Piller A, Schroettle A, Kuhlencordt P, Bernau C, Schulze-Koops H, et al. Impact of cranial and axillary/subclavian artery involvement by color duplex sonography on response to treatment in giant cell arteritis. J Vasc Surg 2015;61(5):1285–91.
[25] de Boysson H, Liozon E, Espitia O, Daumas A, Vautier M, Lambert M, et al. Different patterns and specific outcomes of large-vessel involvements in giant cell arteritis. J Autoimmun 2019;103:102283.
[26] Haaversen ACB, Brekke LK, Kermani TA, Molberg Ø, Diamantopoulos AP. Vascular ultrasound as a follow-up tool in patients with giant cell arteritis: a prospective observational cohort study. Front Med (Lausanne) 2024;11 :1436707.
[27] Aschwanden M, Schegk E, Imfeld S, Staub D, Rottenburger C, Berger CT, et al. Vessel wall plasticity in large vessel giant cell arteritis: an ultrasound follow-up study. Rheumatology (Oxford) 2019;58(5):792–7.
[28] Ponte C, Serafim AS, Monti S, Fernandes E, Lee E, Singh S, et al. Early variation of ultrasound halo sign with treatment and relation with clinical features in patients with giant cell arteritis. Rheumatology (Oxford) 2020;59 (12):3717–26.
[29] Schmidt WA, Krause A, Schicke B, Kuchenbecker J, Gromnica-Ihle E. Do temporal artery duplex ultrasound findings correlate with ophthalmic complications in giant cell arteritis? Rheumatology (Oxford) 2009;48(4):383–5.
[30] Watts RA, Hatemi G, Burns JC, Mohammad AJ. Global epidemiology of vasculitis. Nat Rev Rheumatol 2022;18(1):22–34.
[31] Duftner C, Redlinger N, Bruyn G, Chadachan V, Chrysidis S, Correyero-Plaza M, et al. POS1430 Reliability of the OMERACT Giant cell arteritis Ultrasound Score (OGUS): results of a patient-based exercise of vascular ultrasonography experts and non-experts. Ann Rheum Dis 2024;83(Suppl 1):1091.

Ann Rheum Dis 84 (2025) 833−843

Contents lists available at ScienceDirect

Annals of the Rheumatic Diseases

journal homepage: https://www.sciencedirect.com/journal/annals-of-the-rheumatic-diseases

Vasculitis

GM-CSF drives IL-6 production by macrophages in polymyalgia rheumatica

William F. Jiemy[1], Anqi Zhang[1], Wayel H. Abdulahad[1,2], Rosanne D. Reitsema[1,3], Yannick van Sleen[1], Maria Sandovici[1], Guillermo Carvajal Alegria[4,5,6], Divi Cornec[7,8,9], Valérie Devauchelle-Pensec[7,8,9], Patrice Hemon[7,8,9], Baptiste Quéré[7,8,9], Sara Boukhlal[7,9], Caroline Roozendaal[10], Thomas Christian Kwee[11], Bhaskar Dasgupta[12], Arjan Diepstra[2], Peter Heeringa[2], Elisabeth Brouwer[1], Kornelis S.M. van der Geest[1,*]

[1] *Department of Rheumatology and Clinical Immunology, University of Groningen, University Medical Center Groningen, Groningen, The Netherlands*
[2] *Department of Pathology and Medical Biology, University of Groningen, University Medical Center Groningen, Groningen, The Netherlands*
[3] *School of Medical Sciences, Faculty of Medicine and Health, Örebro University, Örebro, Sweden*
[4] *Unité Propre de Recherche (UPR) Centre National de la Recherche Scientifique (CNRS) 4301Centre de Biophysique Moléculaire (CBM), Département NanoMédicaments et NanoSondes (NMNS), Tours, France*
[5] *Université de Tours, Unité de Formation et de Recherche (UFR) de Médecine, Tours Cedex 1, France*
[6] *Centre Hospitalier Universitaire (CHU) de Tours, Service de Rhumatologie, Tours Cedex 9, France*
[7] *Lymphocytes B, Autoimmunité et Immunothérapies (LBAI) Unité Mixte de Recherche (UMR) 1227, Institut National de la Santé et de la Recherche Médicale (INSERM), Brest, France*
[8] *Université de Bretagne Occidentale, Faculté de Médecine et Sciences de la Santé, Brest Cedex 3, France*
[9] *Centre Hospitalier Régional Universitaire (CHRU) de Brest, Service de Rhumatologie, Brest, France*
[10] *Department of Laboratory Medicine, University Medical Centre Groningen, University of Groningen, Groningen, The Netherlands*
[11] *Department of Radiology, Medical Imaging Center, University Medical Center Groningen, University of Groningen, Groningen, The Netherlands*
[12] *Department of Rheumatology, Southend University Hospital National Health Service (NHS) Foundation Trust, Westcliff-on-Sea, UK*

ARTICLE INFO

Article history:
Received 4 July 2024
Received in revised form 12 December 2024
Accepted 13 December 2024

ABSTRACT

Objectives: Insight into the immunopathology of polymyalgia rheumatica (PMR) is scarce and mainly derived from peripheral blood studies. The limited data available point towards macrophages as potential key players in PMR. This study aimed to identify the factors driving proinflammatory macrophage development and their functions in the immunopathology of PMR.
Methods: Monocyte phenotypes were investigated by flow cytometry in peripheral blood (PMR, n = 22; healthy controls, n = 20) and paired subacromial-subdeltoid (SASD) bursal fluid (PMR, n = 9). Macrophages in SASD bursa were characterised by immunohistochemistry and immunofluorescence (PMR, n = 12; controls undergoing shoulder replacement surgery, n = 10). The

*Correspondence to Dr Kornelis S M van der Geest, Department of Rheumatology and Clinical Immunology, University of Groningen, University Medical Center Groningen, HPC:AA21, Postbus 30.001, Hanzeplein 1, 9700 RB, Groningen, The Netherlands.

E-mail address: k.s.m.van.der.geest@umcg.nl (K.S.M. van der Geest).

Handling editor Prof. Josef Smolen.

William F. Jiemy and Anqi Zhang were equal contributors.

https://doi.org/10.1016/j.ard.2025.01.004

functions of cytokines expressed in PMR-affected tissue were examined using macrophage differentiation cultures (PMR, n = 7; healthy controls, n = 7).
Results: Monocytes ($CD14^{high}CD16^{-}$ and $CD14^{high}CD16^{+}$) were increased in blood of PMR patients and activated in bursal fluid. Macrophages dominated immune infiltrates in PMR-affected tissue, expressing various proinflammatory cytokines. While interleukin (IL)-6 and interferon-gamma (IFN-γ) expression was abundant in both PMR and control tissue, granulocyte-macrophage colony-stimulating factor (GM-CSF) and macrophage colony-stimulating factor (M-CSF) were significantly increased in PMR tissue. Macrophages in PMR-affected tissue showed an elevated CD206/folate receptor β ratio, reflecting a GM-CSF skewed signature. A combination of GM-CSF/M-CSF/IFN-γ significantly boosted IL-6 production *in vitro,* while limited IL-6 production was observed without GM-CSF.
Conclusions: The monocyte compartment is expanded and activated in PMR. Macrophages in PMR-affected tissue produce abundant proinflammatory cytokines such as IL-6. A network of locally expressed cytokines, including GM-CSF, M-CSF, and IFN-γ, may drive the proinflammatory functions of these macrophages. Overall, macrophages may constitute key therapeutic targets for PMR.

WHAT IS ALREADY KNOWN ON THIS TOPIC

- Polymyalgia rheumatica (PMR) is a common inflammatory disease. Insight into the immunopathology of PMR is scarce and mainly derived from peripheral blood studies, which hinders the development of urgently needed targeted therapies for PMR. Recent clinical trials have underscored the pivotal role of interleukin (IL)-6 in the pathobiology of PMR. The limited data available point towards macrophages as potential key players in the immunopathology of PMR.

WHAT THIS STUDY ADDS

- This is the first study to comprehensively investigate monocytes and macrophages in three compartments of patients with PMR: peripheral blood, bursa fluid, and bursa tissue.
- Monocytes were activated in the blood and bursa fluid of patients with PMR. Macrophages were abundant in PMR-affected bursa tissue and produced a wide array of proinflammatory cytokines, with these cells being a major source of IL-6. The number of macrophages correlated with systemic inflammation in the blood.
- Macrophage-polarising cytokines, including granulocyte-macrophage colony-stimulating factor (GM-CSF), macrophage colony-stimulating factor (M-CSF) and interferon-γ, were abundant in PMR-affected bursa tissue. The combination of these cytokines significantly upregulated IL-6 production by *in vitro* differentiated macrophages, with GM-CSF playing a particularly prominent role in this process.

HOW THIS STUDY MIGHT AFFECT RESEARCH, PRACTICE OR POLICY

- Macrophages are a key source of IL-6 in PMR-affected tissues. This study sheds light on the pathogenic functions of macrophages in PMR and identifies multiple other therapeutic targets in PMR-affected tissue.

INTRODUCTION

Polymyalgia rheumatica (PMR) is a common inflammatory rheumatic disease of individuals older than 50 years. Common symptoms include debilitating pain and stiffness of the shoulder and hip girdle and signs of systemic inflammation in the blood [1]. Imaging of the shoulders and hips may reveal (peri)articular inflammation [2]. Bursitis of the subacromial-subdeltoid (SASD) bursa is a key finding in PMR [3]. Currently, the first choice for the management of PMR is glucocorticoid treatment. However, long-term glucocorticoid treatment has severe side effects, such as osteoporosis, diabetes mellitus, hypertension, and mental problems [4]. Although novel therapies for PMR are now gradually emerging [5], the introduction of targeted therapies is limited by the absence of approval and identification of new therapeutic targets for PMR, the latter hampered by the lack of insight into the pathobiology of this disease. A better understanding of the immunopathogenesis of PMR may accelerate the selection and introduction of urgently needed glucocorticoid-sparing treatment options for patients with PMR.

Current insight into the pathobiology of PMR is primarily based on immunological studies on peripheral blood samples. The number of circulating monocytes is significantly increased in patients with PMR [6,7]. Macrophages are the predominant infiltrating cells in the glenohumeral synovium and SASD bursa in patients with PMR [8,9]. Recently, a marked interferon-gamma (IFN-γ) signature has been observed in PMR-affected bursal tissue, which was partly attributed to infiltrating $CD4^{+}$ T cells [8]. The latter finding suggests that PMR-affected tissues could be an ideal environment for the development of proinflammatory macrophages.

Macrophages are remarkably heterogeneous and exhibit distinct phenotypes and functions. Macrophages are phagocytic immune cells that present antigens to the adaptive immune system and are the main producers of proinflammatory cytokines such as interleukin (IL)-6 and granulocyte-macrophage colony-stimulating factor (GM-CSF). Although a recent report demonstrated that macrophages in PMR-affected bursa tissue produce the proinflammatory cytokine IL-6, it remains unclear whether macrophages produce other proinflammatory cytokines in PMR [10]. Overall, data on the local immunopathology of bursal inflammation in PMR remain scarce.

Macrophage heterogeneity can be driven by signals in the tissue environment. GM-CSF and macrophage colony-stimulating factor (M-CSF) skew macrophages towards the production of proinflammatory cytokines and tissue remodelling factors, respectively [11]. GM-CSF–primed macrophages upregulate CD206 expression, while M-CSF–primed macrophages increase their folate receptor β (FRβ) expression [12,13]. Although it remains unknown whether GM-CSF and M-CSF are expressed in PMR-affected tissues, these macrophage skewing factors have been found in the arterial tissue of patients with giant cell arteritis (GCA), a closely related disease that is part of the inflammatory spectrum [14]. Additionally, proinflammatory cytokines such as IFN-γ can stimulate macrophages towards proinflammatory phenotypes [15]. It remains to be elucidated which of these factors contribute to macrophage polarisation in PMR.

In the present study, we hypothesised that PMR is characterised by an activated monocyte compartment and that factors in the tissue environment drive the differentiation of proinflammatory macrophages. To address this hypothesis, we first profiled monocytes in peripheral blood and bursal fluid of patients with PMR. Furthermore, we identified and characterised macrophages in SASD bursa tissue. Lastly, we determined whether cytokines expressed in PMR-affected tissue could drive macrophage polarisation in PMR *in vitro*.

METHODS

Patients

Cryopreserved peripheral blood mononuclear cells (PBMCs) were obtained from 22 consecutive patients with newly diagnosed PMR prior to initiation of glucocorticoid treatment and from 20 age- and sex-matched healthy controls (HCs) (Supplementary Table S1; Supplementary Table S2). Here, the term 'sex' refers to the biological classification of individuals as male or female. HCs underwent medical history taking, physical examination, blood testing (including erythrocyte sedimentation rate [ESR]), and urinalysis as part of a study on healthy ageing [16–18]. Paired peripheral blood and SASD bursa fluid samples were obtained from an additional cohort of 9 patients with active PMR (5 new onset, 4 relapsing disease; Supplementary Table S3). Median disease duration for the relapsing patients who provided synovial fluid was 27 months. None of these patients received prednisolone therapy at the time of sampling, and 1 patient received either leflunomide or a placebo as part of a clinical trial (NCT03576794). Ultrasound-guided biopsies of the SASD bursa were collected from 12 consecutive patients with PMR (9 with new onset disease and 3 with relapsing disease) using a 16G or 18G core biopsy needle with a throw length of 13 to 23 mm (Argon Medical Devices) under local anaesthesia with 1% lidocaine. Median disease duration for relapsing patients who provided bursa biopsies was 58 months. Only one of these patients used prednisolone at time of sampling (2.5 mg daily), while none used disease-modifying antirheumatic drug therapy. Biopsies were dispersed in 10% formalin and paraffin-embedded. SASD bursa biopsies were also obtained from 10 control patients who underwent shoulder replacement surgery at the Université de Bretagne Occidentale, Brest, France (Supplementary Table S4). The clinical diagnosis of PMR was confirmed in all patients after 6 months of follow-up.

Flow cytometry

PBMCs of patients with PMR (n = 22) and HCs (n = 20) were stained with monoclonal antibodies or isotypes for the following surface markers: CD3, CD14, CD15, CD16, CD56, CD64, CD80, CD86, CD206, and FRβ. Similarly, paired EDTA blood and synovial fluid samples from patients with PMR (n = 9) were stained with monoclonal antibodies or isotypes for the stated surface markers. CD14 and CD16 were used to determine monocyte subsets: classical monocytes (CD14^{high}CD16^{-}), intermediate monocytes (CD14^{high}CD16^{+}), and nonclassical monocytes (CD14^{low}CD16^{high}). The gating strategy is shown in Supplementary Figure S1. Further details are provided in the Supplementary Methods.

Immunohistochemistry

Immunohistochemistry was performed to detect macrophage phenotypic markers (CD68, CD64, CD80, CD86, CD206, and FRβ) and proinflammatory cytokines (GM-CSF, M-CSF, IL-6, IL-1β, IL-12A, IL-23, IFN-γ, and tumour necrosis factor alpha [TNF-α]) (Supplementary Methods). Twelve samples of SASD bursa biopsies from PMR patients and 10 disease control samples were included. Matched isotype controls were also included. The percentage of positive cells was assessed using QuPath image analysis software version 0.4.3 [19]. Synovial inflammation was scored by a pathologist according to the synovitis score of Krenn et al [20].

Immunofluorescence imaging

To show colocalisation of macrophages with the proinflammatory cytokines, double labelling of CD68 with either GM-CSF, M-CSF, IL-6, IL-1β, IL-12A, IL-23, IFN-γ, or TNF-α was performed on SASD bursa biopsies of patients with PMR (n = 3 for each combination) (Supplementary Methods). Double staining of CD68 with MER tyrosine kinase (MerTK) was also performed on SASD bursa biopsies of patients with PMR (n = 3). Triple staining of CD68, phosphorylated(p)JAK2, and pSTAT5 was performed on SASD bursa biopsies of patients with PMR (n = 3) to investigate GM-CSF–mediated signalling.

Monocyte in vitro *culture*

Monocytes from patients with PMR (n = 7) and age- and sex-matched healthy donors (n = 7) were cultured in the presence of GM-CSF, M-CSF, or a combination of both, with or without additional activation by IFN-γ. Further details are provided in Supplementary Methods. Supernatants were collected for Luminex assay, and the cells were lysed for RNA extraction. Quantitative polymerase chain reaction (qPCR) was performed with a ViiA 7 Real-Time PCR System with Taqman probes (Thermo Scientific) targeting CD206 (*MRC1*, Hs00267207_m1) and FRβ (*FOLR2*, Hs00265255_m1). Amplification plots were analysed with QuantStudio Real-Time PCR software v1.3 (Applied Biosystems). Relative gene expression was normalised to that of β-actin (*ACTB*, Hs99999903_m1) as an internal control.

Luminex assay

Levels of IL-6, TNF-α, IL-1β, and IL-23 were assessed in the supernatant of monocyte-derived macrophages using Human premix Luminex screening assay kits (R&D Systems) according to the manufacturer's instructions and analysed on a Luminex Magpix instrument (Luminex). Supernatant levels were corrected for macrophage cell count at the time of harvesting and are expressed as nanograms per millilitre per 50,000 cells.

Statistics

Nonpaired analysis was performed using the Mann-Whitney *U* test and paired analysis using the Wilcoxon signed rank test. Correlation analysis was performed using Spearman's rank correlation coefficient. *P* values <.05 were considered statistically significant. Data were analysed with GraphPad Prism 10.0.2.

RESULTS

Circulating monocyte pool is expanded in PMR

The number of circulating monocytes was significantly higher in patients with PMR than in age- and sex-matched HCs. No correlation was observed between circulating monocyte counts and the ESR (Fig 1A) or C-reactive protein (CRP) level (Supplementary Fig S2). Percentages of $CD14^{high}CD16^{-}$ and $CD14^{high}CD16^{+}$ monocytes within total monocytes were similar between patients with PMR and HCs, whereas the frequency of $CD14^{low}CD16^{high}$ monocytes was significantly lower in patients with PMR than in HCs (Fig 1B). This imbalance was attributed to significantly increased absolute numbers of $CD14^{high}CD16^{-}$ and $CD14^{high}CD16^{+}$ monocytes (Fig 1B). The proportions of CD14/CD16-defined monocyte subsets showed no correlation with ESR or CRP (Supplementary Fig S2). No differences were observed in the frequencies of $CD80^{+}$, $CD86^{+}$, $CD206^{+}$, and $FR\beta^{+}$ monocytes. However, the proportion and per-cell surface expression (mean fluorescence intensity [MFI]) of $CD64^{+}$ monocytes were significantly higher in patients with PMR (Fig 1C), a finding consistently found across all CD14/CD16-defined monocyte subsets (Supplementary Fig S3A, B). Although CD86 was expressed by nearly all monocytes, its MFI was decreased on monocytes in PMR. CD206/FRβ ratios on total monocytes and monocyte subsets were comparable in patients with PMR and HCs (Supplementary Fig S3C). Correlations between the different cellular markers and general inflammation markers (CRP and ESR) were heterogeneous in PMR, as shown in Supplementary Figure S4. Tree plot analysis illustrated that the majority of monocytes in blood are $CD64^{+}CD206^{-}$ cells, part of which expressed FRβ (Supplementary Fig S5). These findings indicate that the circulating monocyte compartment is expanded in PMR while showing limited signs of activation.

Monocytes show signs of activation in bursa fluid

Next, we profiled monocytes in the SASD bursa fluid of patients with PMR. No difference was observed in monocyte counts between paired peripheral blood and SASD bursa fluid samples (Fig 2A). Monocyte counts in bursa fluid did not

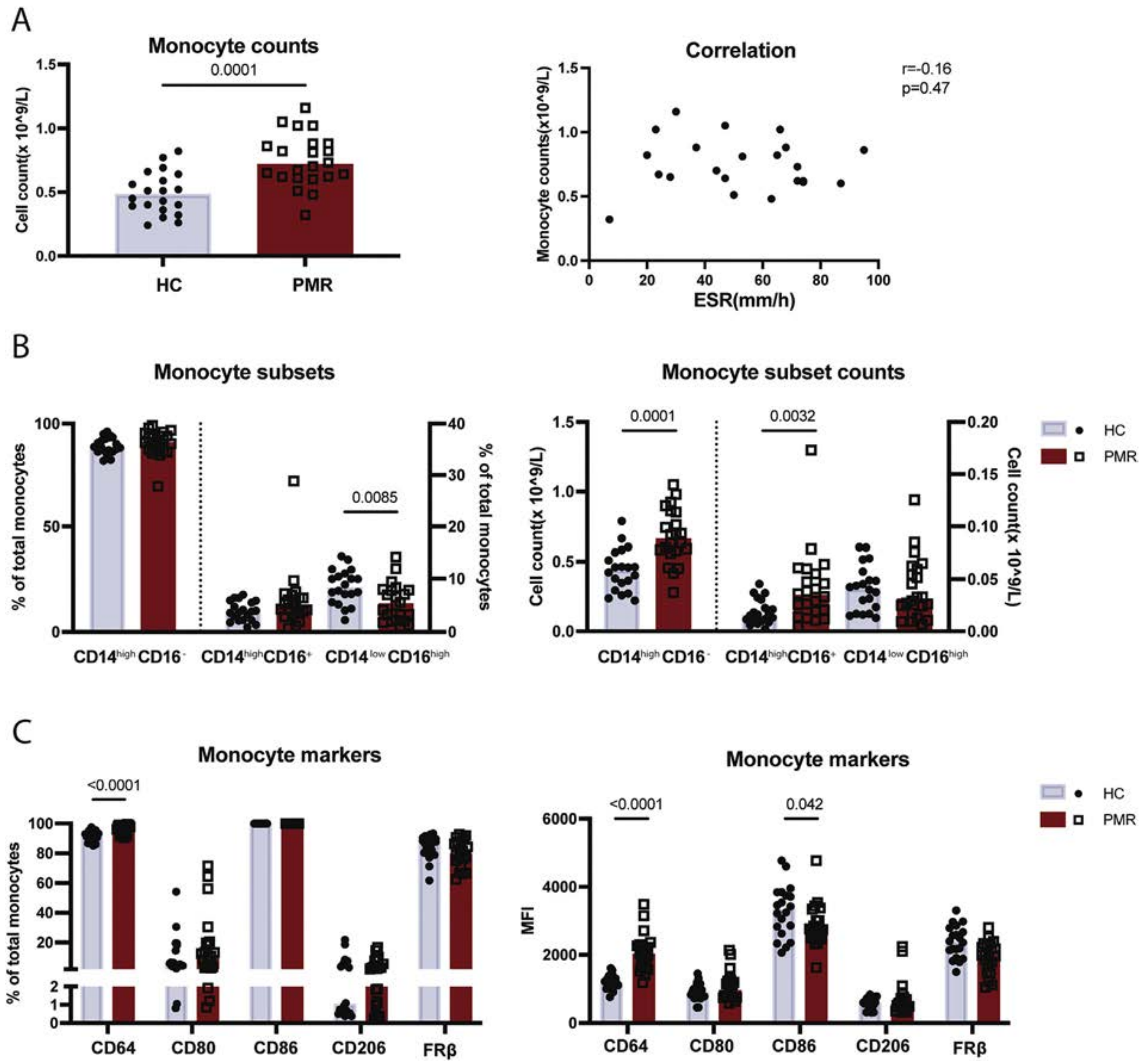

Figure 1. Monocyte counts and phenotype in peripheral blood of patients with PMR. Data are shown for patients with newly diagnosed polymyalgia rheumatica (PMR; n = 22) and healthy controls (HCs; n = 20). Differential marker expressions within monocytes were determined by flow cytometric staining of PBMCs. (A) Left: total monocyte absolute numbers in patients with PMR and HCs; right: correlation of monocyte counts and ESR levels in patients with PMR. (B) Left: proportions of monocyte subsets in patients with PMR and HCs; right: absolute numbers of monocyte subsets in patients with PMR and HCs. (C) Left: frequencies of $CD64^{+}$, $CD80^{+}$, $CD86^{+}$, $CD206^{+}$, and $FR\beta^{+}$ monocytes of patients with PMR and HCs; right: MFI of markers on total monocytes of patients with PMR and HCs. Statistical analysis was performed using the Mann-Whitney *U* test and Spearman's rank correlation coefficient. ESR, erythrocyte sedimentation rate; FRβ, folate receptor β; MFI, mean fluorescence intensity; PBMC, peripheral blood mononuclear cell.

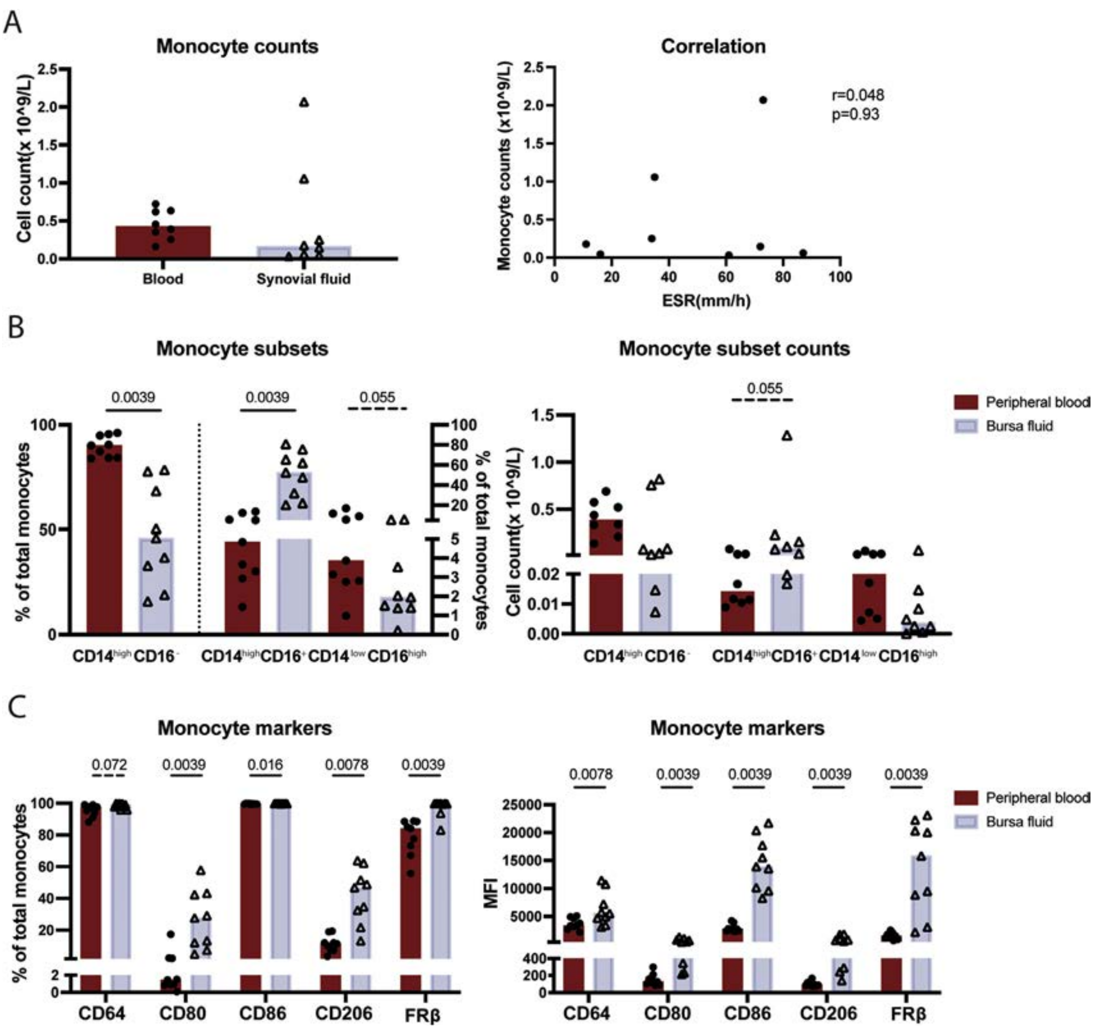

Figure 2. Monocyte counts and phenotype in paired peripheral blood and SASD bursa fluid of patients with PMR. Differential marker expressions within monocytes were determined by flow cytometric staining of full blood and bursa fluid. (A) Left: total monocyte absolute numbers in peripheral blood and bursa fluid of patients with PMR (n = 8); right: correlation of monocyte counts in bursa fluid and ESR levels in patients with PMR. (B) Left: proportions of monocyte subsets in paired peripheral blood and bursa fluid of patients with active PMR (n = 9); right: absolute numbers of monocyte subsets in paired peripheral blood and bursa fluid of patients with PMR (n = 8). (C) Left: frequencies of $CD64^+$, $CD80^+$, $CD86^+$, $CD206^+$, and $FR\beta^+$ monocytes in the two compartments of patients with active PMR; right: MFI of markers on total monocytes in two compartments of patients with active PMR. Statistical analysis was performed using the Wilcoxon signed-rank test and Spearman's rank correlation coefficient. *P* values <.05 were considered statistically significant. ESR, erythrocyte sedimentation rate; FRβ, folate receptor β; HC, healthy control; MFI, mean fluorescence intensity; PMR, polymyalgia rheumatica.

correlate with the ESR (Fig 2A) or CRP levels (data not shown). However, a significant shift in the distribution of monocyte subsets from $CD14^{high}CD16^-$ and $CD14^{low}CD16^{high}$ towards $CD14^{high}CD16^+$ was noted in the bursa fluid (Fig 2B). Phenotypic analysis revealed marked upregulation of all monocyte/macrophage markers (CD64, CD80, CD86, CD206, FRβ) in bursa fluid compared to blood (Fig 2C). This upregulation was observed among all CD14/CD16-defined monocyte subsets in bursa fluid (Supplementary Fig S6A, B). CD206/FRβ ratios on total monocytes, especially $CD14^{high}CD16^-$ and $CD14^{high}CD16^+$ monocytes, were significantly higher in bursa fluid than in blood (Supplementary Fig S6C). Tree plot analysis showed that expression of CD206 and FRβ may overlap in bursa fluid monocytes (Supplementary Fig S7). The expression of CD64 in bursa fluid correlated positively with CRP in the patients with active PMR, but no other correlations were found between the expression of monocyte markers in bursa fluid and the ESR or CRP (Supplementary Fig S8). Taken together, monocytes in bursa fluid showed a markedly activated phenotype.

Proinflammatory macrophages show a GM-CSF skewed signature in PMR bursa tissue

The median synovitis score for PMR-affected tissues was 2 (range, 0-5.5) and that for disease control tissues was 3 (range, 1-6), suggesting low-grade synovitis in both tissue types. Macrophages were equally abundant in the SASD bursa tissue of patients with PMR and controls (Fig 3A, B; Supplementary Fig S9; matched isotype controls in Supplementary Fig S10). All macrophage surface markers and proinflammatory cytokines were detected in the tissues of both groups of patients. The percentage of $CD68^+$ macrophage cells in PMR-affected tissues strongly correlated with the ESR and CRP levels in the blood (Fig 3C, D). Quantification of macrophage surface markers and proinflammatory cytokines revealed significantly higher expression of CD86, GM-CSF, M-CSF, IL-12A, and IL-23 in the PMR tissues than in the control tissues (Fig 3E). A trend towards higher IL-1β and IFN-γ expression was also found in PMR-affected tissues (Fig 3E). Scoring of the bursa tissues showed higher

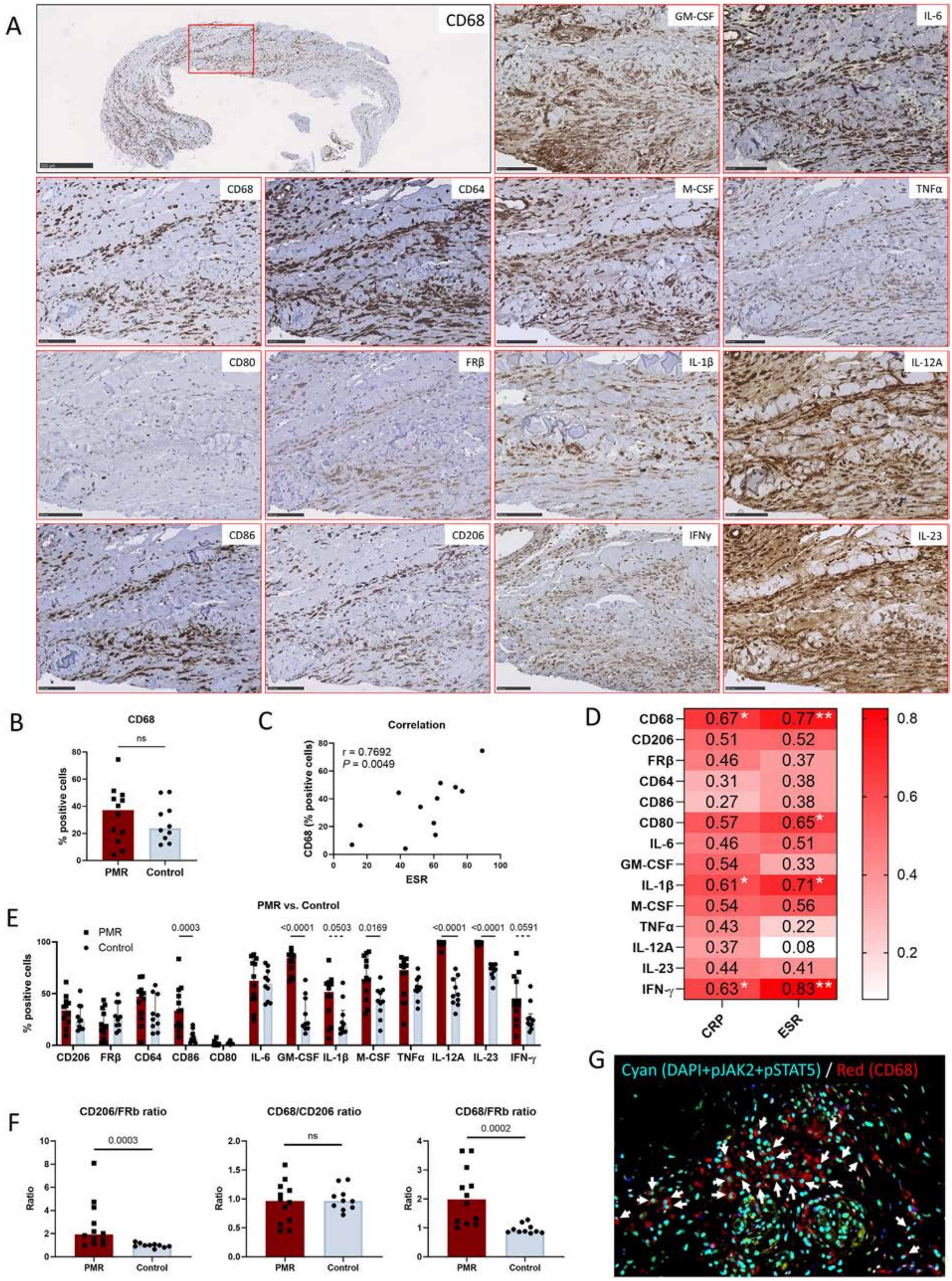

Figure 3. Macrophage phenotype in SASD bursa tissue of patients with PMR. (A) Representative immunohistochemistry stainings (consecutive sections) of PMR tissues (n = 12) for CD68, CD80, CD86, CD64, CD206, FRβ, GM-CSF, IL-1β, IL-6, IL-12A, IL-23, M-CSF, TNF-α, and IFN-γ. Black bars in IHC images represent 100 μM scale bar. (B) Comparison (quantitative score) of CD68$^+$ macrophages in bursa tissue of patiens with PMR (n = 12) and controls (n = 10). (C) Correlation of the percentages of CD68$^+$ macrophages in the tissue with the ESR in patients with PMR. (D) Correlation of each marker (percentage positive cell) with the CRP level and ESR in patients with PMR. The red shade indicates the strength of positive correlation. (E) Comparison (quantitative score) of macrophage phenotypic markers and cytokines in bursa tissue of patients with PMR (n = 12) and controls (n = 10). (F) CD206/FRβ ratio, CD68/CD206 ratio, and CD68/FRβ ratio. (G) Multiplex immunofluorescent staining of nucleus (DAPI, blue), macrophages (CD68, red), phosphorylated (p)JAK2 (green), and pSTAT5 (yellow). Colocalisation of DAPI, pJAK2, and pSTAT5 is depicted in cyan. White arrows point to macrophages positive for nuclear pJAK2 and pSTAT5. Statistical analysis was performed using the Mann-Whitney *U* test and Spearman's rank correlation coefficient. *P* values <.05 were considered statistically significant. $^*P < .05$; $^{**}P < .005$; ns, not significant. CRP, C-reactive protein; DAPI, 4',6-diamidino-2-phenylindole; ESR, erythrocyte sedimentation rate; FRβ, folate receptor β; GM-CSF, granulocyte-macrophage colony-stimulating factor; IFN-γ, interferon-gamma; IHC, immunohistochemistry; IL, interleukin; M-CSF, macrophage colony-stimulating factor; PMR, polymyalgia rheumatica; TNF-α, tumour necrosis factor alpha.

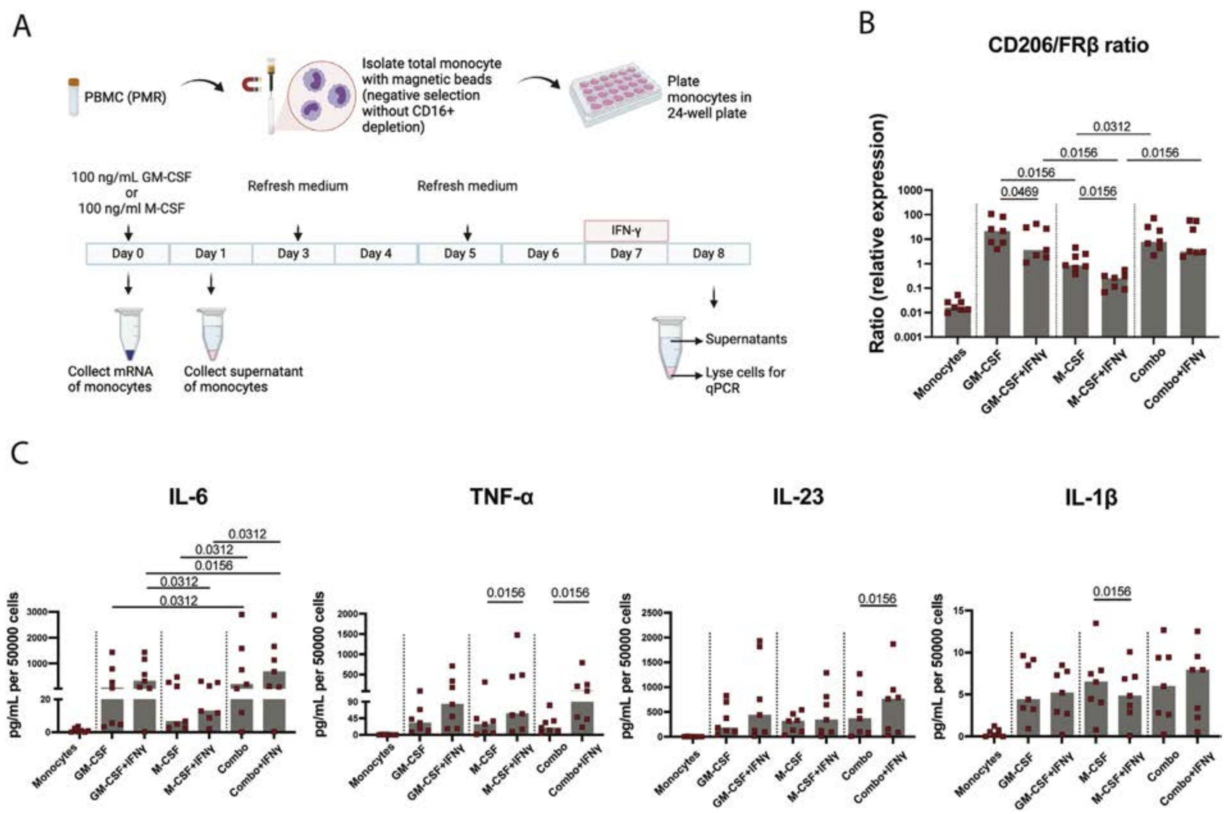

Figure 4. Differential macrophage phenotype and cytokine production driven by M-CSF, GM-CSF, and IFN-γ signals. Data are shown for patients with newly diagnosed PMR (n = 7). (A) Experimental setup for *in vitro* monocyte culture. Monocytes were differentiated into macrophages by GM-CSF, M-CSF or a combination of GM-CSF and M-CSF (Combo), with or without additional stimulation by IFN−γ. (B) qPCR analysis of CD206/FRβ ratios on cultured monocyte-derived macrophages. (C) Luminex assay (normalised per 50,000 cells) of IL-6, TNF-α, IL-23 and IL-1β in supernatants of the monocyte-derived macrophages. Statistical analysis was performed using the Wilcoxon signed-rank test. *P* values <.05 were considered statistically significant. Significance bars are shown for comparisons between monocyte-derived macrophages under different conditions; significance bars are not displayed for comparisons between macrophages and monocytes. CD206/FRβ ratio and production of all cytokines were significantly higher in macrophages than in monocytes in all groups (*P* values not shown). Graphic of experimental setup designed with BioRender.com. Combo, GM-CSF + M-CSF; FRβ, folate receptor β; GM-CSF, granulocyte-macrophage colony-stimulating factor; IFN-γ, interferon-gamma; IL, interleukin; M-CSF, macrophage colony-stimulating factor; mRNA, messenger RNA; PBMC, peripheral blood mononuclear cell; PMR, polymyalgia rheumatica; qPCR, quantitative polymerase chain reaction; TNF-α, tumour necrosis factor alpha.

expression of all markers in the bursa lining compared to nonlining bursa tissue in both PMR and control tissues (Supplementary Fig S11).

To confirm the production of proinflammatory cytokines by macrophages, correlation analyses were performed. Strong positive correlations were found between CD68$^+$ cell infiltration and IFN-γ, IL-6, GM-CSF, M-CSF, and IL-1β (Supplementary Fig S12), whereas a positive trend was found between CD68 and TNF-α and IL-23. Further immunofluorescence staining showed that indeed CD68$^+$ macrophages colocalised with IL-6, GM-CSF, M-CSF, IL-1β, TNF-α, IL-12A, IL-23, and IFN-γ (Supplementary Fig S13). Of note, these cytokines were also detected in CD68$^-$ cells.

Next, we evaluated whether macrophages in PMR-affected tissue were primarily resident macrophages (MerTK$^+$) or monocyte-derived macrophages (MerTK$^-$). Double staining of CD68 and MerTK showed MerTK expression was primarily restricted to macrophages in the lining layer, with the vast majority of macrophages in the sublining being MerTK$^-$ cells (Supplementary Fig S14). This suggests that most macrophages in bursa tissue were monocyte-derived macrophages.

Further analysis showed a significantly higher CD206/FRβ ratio in PMR-affected tissues than in control tissues (Fig 3F). Ratios between CD68 and the latter surface markers pointed towards a relatively lower expression of FRβ in PMR-affected tissues, which could indicate GM-CSF-mediated signalling. To further investigate such signalling in PMR-affected tissue, we performed multiplex staining for pJAK2 and pSTAT5. We confirmed co-expression of pJAK2 and pSTAT5 in macrophages in the PMR bursa tissue (Fig 3G; Supplementary Fig S15). Overall, these findings indicate that macrophages in PMR-affected tissues showed GM-CSF skewed signatures.

GM-CSF and IFN-γ synergistically polarise proinflammatory macrophages

Next, we determined whether the three main macrophage skewing cytokines found in PMR-affected tissue (ie, GM-CSF, M-CSF, and IFN-γ) could induce proinflammatory functions in macrophages *in vitro*. Specifically, we assessed the effects of these cytokines on the expression of CD206, FRβ, and proinflammatory cytokines by monocyte-derived macrophages from patients with PMR (Fig 4A).

GM-CSF and the combination of GM-CSF/M-CSF led monocytes of patients to differentiate into macrophages with high levels of CD206 and lower levels of FRβ, as shown by our qPCR analysis (Supplementary Fig S16). In the absence of GM-CSF, M-CSF induced elevated FRβ expression. The ratios of CD206/FRβ

were higher under skewing conditions that included GM-CSF (Fig 4B), confirming the FRβ expression-blocking capacity of GM-CSF.

Analysis of culture supernatant showed that the presence of GM-CSF (with or without IFN-γ) boosted the production of IL-6 by monocyte-derived macrophages of patients with PMR (Fig 4C). Even though M-CSF (with or without IFN-γ) showed less effect on IL-6 production, a combination of all 3 macrophage skewing cytokines (GM-CSF, M-CSF, and IFN-γ) led to the highest production of IL-6 by macrophages. The combination of macrophage skewing cytokines (GM-CSF, M-CSF, and IFN-γ) also led to increased production of TNF-α, IL-23, and IL-1β. The production of IL-12(p40) was undetectable. Overall, comparable findings were noted with monocyte-derived macrophages obtained from HCs, although macrophages from patients with PMR showed a slightly higher propensity to produce TNF-α in the presence of GM-CSF (Supplementary Fig S17).

Together, these results show that the presence of GM-CSF is important for the downregulation of FRβ and upregulation of IL-6, whereas macrophages developing in the presence of GM-CSF, M-CSF, and IFN-γ become potent producers of various proinflammatory cytokines.

DISCUSSION

This is the first study profiling monocytes/macrophages in 3 compartments (peripheral blood, bursa fluid, and bursa tissue) of patients with active PMR. We observed expansion and activation of the monocyte compartments in blood and bursa fluid, respectively. Moreover, our study reveals a cytokine network in bursa tissue driving the development of proinflammatory macrophages. GM-CSF is specifically upregulated in PMR and may underlie the pathogenic production of IL-6 in PMR.

Marked abnormalities were seen in the monocyte pool of patients with PMR, both in circulation and bursa fluid. In line with a previous study, we observed increased monocyte counts in patients with newly diagnosed PMR [6], attributed to the expansion of classical and intermediate monocytes [21]. Monocyte counts were comparable in paired peripheral blood and synovial fluid samples, but monocytes in synovial fluid were skewed from a CD14^{high}CD16^{-} towards CD14^{low}CD16^{high} phenotype. Proportion wise, CD14^{low}CD16^{high} monocytes were lower in the blood of patients with PMR, as described before in patients with GCA [6]. Interestingly, we found relatively few of these cells in the synovial fluid. Perhaps this monocyte subset is more likely to be retained in PMR-affected tissues, where these cells would differentiate into macrophages following migration from the circulation. In addition, all monocyte/macrophage lineage markers such as CD80 and CD206 were markedly upregulated in bursa fluid. This indicates that monocytes in bursa fluid were substantially activated and matured into macrophages.

High numbers of macrophages were observed in PMR-affected bursa tissue. This is in line with previous reports on bursa tissue and glenohumeral synovium [8,9]. No differences were found between PMR and disease control tissues regarding the percentages of macrophage in the tissues. However, the control SASD bursa tissues were not obtained from healthy individuals but frompatients with shoulder pathology necessitating surgery. Such pathology may also trigger bursa inflammation 22,23]. It would be interesting to make a comparison with other rheumatic inflammatory conditions, such as rheumatoid arthritis or spondyloarthritis. However, SASD bursitis is infrequent in these conditions, and we are not aware of any prior reports on the pathobiology of SASD bursitis in such conditions [23]. The majority of macrophages in PMR-affected tissue appeared to be monocyte-derived macrophages, as indicated by absence of MerTK expression [24,25]. The degree of macrophage infiltration in the tissue of patients with PMR correlated with systemic inflammatory markers CRP and ESR. This suggests that bursa tissue biopsies in our study reflect the intensity of systemic inflammation in patients with PMR.

Macrophages were a key source of proinflammatory cytokines in PMR-affected tissue. The expression levels of GM-CSF, M-CSF, IL-12, and IL-23 were significantly higher in the bursa tissue of patients with PMR than in controls. A similar trend was observed for IFN-γ and IL-1β levels. Among patients with PMR, the degree of IFN-γ and IL-1β expression in the tissue also correlated strongly with the systemic inflammatory markers CRP and ESR. IL-1β has been reported as one of the cytokines responsible for disease symptoms such as fatigue and pain [26,27]. IL-6 was abundantly expressed in PMR-affected bursa tissue, to a similar extent as in control tissue. The expression of all proinflammatory cytokines could mostly be attributed to macrophages, underscoring the importance of these cells in the immunopathology of PMR. However, other cell types in the bursa tissue, such as fibroblasts/fibroblast-like synoviocytes and endothelial cells may also express some of these cytokines [10,28−33].

GM-CSF could be a key cytokine driving macrophage development in PMR-affected bursa tissue. The ratio of CD206/FRβ was significantly higher in PMR tissues than in disease controls due to lower expression of FRβ. Macrophages skewed by either GM-CSF or M-CSF express CD206, although its expression is higher in GM-CSF skewed macrophages [28,29]. However, the presence of GM-CSF lowers the expression of FRβ regardless of the presence of M-CSF [13], as confirmed in our macrophage cultures. Furthermore, our data showed that macrophages in the tissue express pJAK2 and pSTAT5, further pointing towards GM-CSF signalling in these cells. The expression of CD206 and FRβ could indicate that the bursa tissue infiltrates are primarily composed of M2-like macrophages, which are commonly associated with anti-inflammatory properties. However, we also noted that markers of their proinflammatory M1-like macrophage counterparts (CD64, CD86) were also highly expressed by these macrophages. Overlapping expression of M1 and M2 markers has also been observed on macrophages in synovial tissue in other diseases such as rheumatoid arthritis [34]. This suggests that the conventional paradigm of M1 and M2 macrophages is not applicable to *in vivo* conditions such as PMR.

Our *in vitro* experiments demonstrated synergistic effects of macrophage-polarising cytokines (GM-CSF, M-CSF, and IFN-γ) on IL-6 expression by macrophages, with GM-CSF playing a particularly prominent role in this process. The macrophage-polarising cytokines were abundantly expressed in PMR bursa tissue. M-CSF expression can be found in the majority of tissues under homeostatic conditions. GM-CSF is often weakly expressed under homeostatic conditions but is inducible in inflammation [35]. IFN-γ is primarily expressed under inflammatory conditions, and its expression in PMR-affect bursa tissue has been partly attributed to Th1 cells [8]. Although GM-CSF and M-CSF are capable of increasing the expression of several proinflammatory cytokines, when used together, they exhibit a synergistic effect that can be enhanced even further by the addition of IFN-γ. Our macrophage cultures indicate that macrophages primarily produce IL-6 when exposed to GM-CSF. Interestingly, although IL-12(p35) was highly expressed in PMR bursa tissue, monocyte-derived macrophages produced no IL-12 *in vitro* irrespective of the conditions used. This could indicate that IL-12 production by macrophages *in vitro* may require factors other than GM-CSF, M-CSF, and IFN-γ, such as lipopolysaccharide, T cell engagement through CD40/CD40L interaction, or crucial inflammatory factors such as low molecular weight fragments of hyaluronic acid [36–38].

Our study informs on the presence of multiple targets for therapy in PMR bursa tissue. IL-6 was widely expressed in the affected tissue. Recently, the efficacy of anti-IL-6 receptor therapy in PMR has been demonstrated in 3 randomised controlled trials [39–41]. These trials have underscored the pivotal role of IL-6 in the pathobiology of PMR. Our current study adds to this understanding by identifying macrophages as a key source of IL-6 in PMR-affected tissues. Targeting IL-1β, IL-12, and IL-23 might also be of interest, but this is not yet supported by evidence from clinical trials. TNF-α and CD80/CD86 were also highly expressed in PMR-affected tissue, although therapies directed to these molecules showed no efficacy in clinical trials 42–44. This may indicate that TNF-α and CD80/CD86 only play minor roles in the complex cytokine network in PMR bursal inflammation. Targeting GM-CSF, which plays a role in upregulating IL-6 expression in macrophages, could be of interest for PMR. In a randomised phase IIb study in GCA, GM-CSF receptor blockade by mavrilimumab showed great efficacy in reducing disease activity [45]. Therapies targeting JAK2 could also be of interest in PMR as such therapies would block GM-CSF–mediated signalling [46]. A proof-of-concept clinical study showed potential of baricitinib (JAK1/2 inhibitor) in treating patients with GCA [47]. Overall, commonality with GCA-like immunopathogenesis might support the role of GM-CSF therapeutic targeting for diseases within the GCA-PMR spectrum [1].

Our study has several limitations. Although our study recruited mostly newly diagnosed, treatment-naïve patients, we were only able to obtain limited numbers of bursa fluid and tissue samples from patients that were treatment-naïve or from those that experienced limited treatment. Hence, the sample size for bursa tissue and fluid analyses was relatively small. Nevertheless, significant immunological differences were observed. Ultrasound-guided bursa biopsies are small, but the clear correlation between macrophage numbers and inflammatory markers in the blood suggests that representative tissues were evaluated. This also indicates that persisting bursal ultrasound abnormalities seen in PMR could be of importance for monitoring responses and flares. Data on cytokine expression was based immunohistochemistry analysis, and further confirmation of our findings by transcriptome analyses would be valuable. Additionally, samples were obtained from different cohorts and centres, which might have influenced the results. This, however, reflects the practical challenges of investigating the tissue pathology in PMR [23].

In conclusion, we found marked disturbances in monocyte/macrophage subpopulations, and these cells likely play an important role in the production of proinflammatory cytokines in PMR-affected tissues. A cytokine network consisting of GM-CSF, M-CSF, and IFN-γ drives the development of proinflammatory macrophages in the bursa tissue, with GM-CSF being a critical upregulator of IL-6. Our data suggests that macrophages and/or related cytokines could constitute potent targets for therapy in PMR.

Competing interests

KSMvdG reports research support from AbbVie and Siemens Healthineers, outside the submitted work. KSMvdG received personal fees from Roche, outside the submitted work. BD reports consulting fees from Roche, Chugai, Sanofi, and sponsorship grants for international meetings and workshops with Roche, Sanofi, AbbVie and GlaxoSmithKline. EB reports personal fees from Roche, outside the submitted work. EB received grants from the Dutch Arthritis Society DAS and the EU/EFPIA/Innovative Medicines Initiative 2 Joint Undertaking Immune-Image which were paid to the institution. EB received compensation from Member Board nonprofit organization ARCH (Autoimmune Research Hub) in the Netherlands, which were paid to the institution in 2023. EB received a speaker fee for a talk on GCA at a post EULAR symposium in the Netherlands in 2023. AD reports research support from Takeda. DC reports research support from Novartis, GSK, Servier, BMS, Roche-Chugai, and Astra-Zeneca. VDP received research grant and speaker fees from Novartis and support for attending meetings or travel from UCB, Lilly, and Biocon. MS received consulting fees from AbbVie which were paid to the institution. GCA received speaker fees from Roche, Lilly, BMS, and Novartis and support from Novartis. The other authors declare that the research was conducted in the absence of any commercial or financial relationships that could be construed as a potential conflict of interest.

Acknowledgements

We thank the patients who participated in our study. Part of this work was presented at the annual meeting of the European Alliance of Associations for Rheumatology and the abstract was published.

Contributors

WFJ and AZ contributed equally to this paper. WFJ, BD, EB, and KSMvdG contributed to conception or design of the work. AZ, WFJ, WHA, RDR, YvS, MS, AD, GCA, DC, VDP, PH, BQ, SB, CR, TCK, AD, PH, EB and KSMvdG contributed to acquisition of data. All authors contributed to analysis or interpretation of data. All authors were involved in drafting of the work or revising it critically for important intellectual content. All authors provided final approval of the version published. All authors agreed to be accountable for all aspects of the work in ensuring that questions related to the accuracy or integrity of any part of the work are appropriately investigated and resolved. WFJ, AZ and KSMvdG are guarantors.

Funding

The study was supported by a research grant from FOREUM Foundation for Research in Rheumatology (Career Research Grant; KSMvdG). The study was also funded by the Dutch Society for Rheumatology (Rheumatology Grant; KSMvdG), the University of Groningen (AZ), the State Scholarship Fund China (AZ), and the Mandema Stipend (KSMvdG).

Patient consent for publication

Not applicable.

Ethics approval

The study was performed in accordance with the Declaration of Helsinki. The study was approved by the Medical Ethical Committee of the UMCG (METc 2010/222 and METc 2012/375) and Brest Teaching Hospital (29BRC20.0158). All patients provided written informed consent. Participants gave informed consent to participate in the study before taking part.

Provenance and peer review

Not commissioned; externally peer reviewed.

Data availability

All relevant data are contained within the article and supplementary materials. Further inquiries can be directed to the corresponding author.

Patient and public involvement

Patients and/or the public were not involved in the design, or conduct, or reporting, or dissemination plans of this research. Advice on the feasibility and relevance of the study was obtained from patients through the Vasculitis Stichting and PMRGCAuk.

Supplementary materials

Supplementary material associated with this article can be found in the online version at doi:10.1016/j.ard.2025.01.004.

Orcid

Kornelis S.M. van der Geest: http://orcid.org/0000-0003-2798-6765

REFERENCES

[1] Tomelleri A, van der Geest KSM, Khurshid MA, Sebastian A, Coath F, Robbins D, et al. Disease stratification in GCA and PMR: state of the art and future perspectives. Nat Rev Rheumatol 2023;19(7):446–59. doi: 10.1038/s41584-023-00976-8.

[2] van der Geest KSM, van Sleen Y, Nienhuis P, Sandovici M, Westerdijk N, Glaudemans AWJM, et al. Comparison and validation of FDG-PET/CT scores for polymyalgia rheumatica. Rheumatology (Oxford) 2022;61(3):1072–82. doi: 10.1093/rheumatology/keab483.

[3] Mackie SL, Koduri G, Hill CL, Wakefield RJ, Hutchings A, Loy C, et al. Accuracy of musculoskeletal imaging for the diagnosis of polymyalgia rheumatica: systematic review. RMD Open 2015;1(1):e000100. doi: 10.1136/rmdopen-2015-000100.

[4] Floris A, Piga M, Chessa E, Congia M, Erre GL, Angioni MM, et al. Long-term glucocorticoid treatment and high relapse rate remain unresolved issues in the real-life management of polymyalgia rheumatica: a systematic literature review and meta-analysis. Clin Rheumatol 2022;41(1):19–31. doi: 10.1007/s10067-021-05819-z.

[5] Nageswaran P, Ahmed S, Tahir H. Review of phase 2/3 trials in polymyalgia rheumatica and giant cell arteritis. Expert Opin Emerg Drugs 2024;29(1):5–17. doi: 10.1080/14728214.2024.2303093.

[6] van Sleen Y, Wang Q, van der Geest KSM, Westra J, Abdulahad WH, Heeringa P, et al. Involvement of monocyte subsets in the immunopathology of giant cell arteritis. Sci Rep 2017;7(1):6553. doi: 10.1038/s41598-017-06826-4.

[7] van Sleen Y, Graver JC, Abdulahad WH, van der Geest KSM, Boots AMH, Sandovici M, et al. Leukocyte dynamics reveal a persistent myeloid dominance in giant cell arteritis and polymyalgia rheumatica. Front Immunol 2019;10:1981.

[8] Reitsema RD, Jiemy WF, Wekema L, Boots AMH, Heeringa P, Huitema MG, et al. Contribution of pathogenic T helper 1 and 17 cells to bursitis and tenosynovitis in polymyalgia rheumatica. Front Immunol 2022;13:943574. doi: 10.3389/fimmu.2022.943574.

[9] Meliconi R, Pulsatelli L, Uguccioni M, Salvarani C, Macchioni P, Melchiorri C, et al. Leukocyte infiltration in synovial tissue from the shoulder of patients with polymyalgia rheumatica. Quantitative analysis and influence of corticosteroid treatment. Arthritis Rheum 1996;39(7):1199–207. doi: 10.1002/art.1780390719.

[10] Jiemy WF, Zhang A, Boots AMH, Heeringa P, Sandovici M, Diepstra A, et al. Expression of interleukin-6 in synovial tissue of patients with polymyalgia rheumatica. Ann Rheum Dis 2023;82(3):440–2. doi: 10.1136/ard-2022-222873.

[11] Hamilton TA, Zhao C, Pavicic Jr PG, Datta S. Myeloid colony-stimulating factors as regulators of macrophage polarization. Front Immunol 2014;5:554. doi: 10.3389/fimmu.2014.00554.

[12] Kittan NA, Allen RM, Dhaliwal A, Cavassani KA, Schaller M, Gallagher KA, et al. Cytokine induced phenotypic and epigenetic signatures are key to establishing specific macrophage phenotypes. PLoS One 2013;8(10):e78045. doi: 10.1371/journal.pone.0078045.

[13] Puig-Kröger A, Sierra-Filardi E, Samaniego R, Corcuera MT, Gómez-Aguado F, et al. Folate receptor beta is expressed by tumor-associated macrophages and constitutes a marker for M2 anti-inflammatory/regulatory macrophages. Cancer Res 2009;69(24):9395–403. doi: 10.1158/0008-5472.Can-09-2050.

[14] Jiemy WF, van Sleen Y, van der Geest KS, Ten Berge HA, Abdulahad WH, Sandovici M, et al. Distinct macrophage phenotypes skewed by local granulocyte macrophage colony-stimulating factor (GM-CSF) and macrophage colony-stimulating factor (M-CSF) are associated with tissue destruction and intimal hyperplasia in giant cell arteritis. Clin Transl Immunology 2020;9(9):e1164. doi: 10.1002/cti2.1164.

[15] Wang N, Liang H, Zen K. Molecular mechanisms that influence the macrophage m1-m2 polarization balance. Front Immunol 2014;5:614. doi: 10.3389/fimmu.2014.00614.

[16] van der Geest KSM, Abdulahad WH, Teteloshvili N, Tete SM, Peters JH, Horst G, et al. Low-affinity TCR engagement drives IL-2-dependent post-thymic maintenance of naive CD4+ T cells in aged humans. Aging Cell 2015;14(5):744–53. doi: 10.1111/acel.12353.

[17] van der Geest KSM, Abdulahad WH, Tete SM, Lorencetti PG, Horst G, Bos NA, et al. Aging disturbs the balance between effector and regulatory CD4+ T cells. Exp Gerontol 2014;60:190–6. doi: 10.1016/j.exger.2014.11.005.

[18] van der Geest KSM, Lorencetti PG, Abdulahad WH, Horst G, Huitema M, Roozendaal C, et al. Aging-dependent decline of IL-10 producing B cells coincides with production of antinuclear antibodies but not rheumatoid factors. Exp Gerontol 2016;75:24–9. doi: 10.1016/j.exger.2015.12.009.

[19] Bankhead P, Loughrey MB, Fernández JA, Dombrowski Y, McArt DG, Dunne PD, et al. QuPath: open source software for digital pathology image analysis. Sci Rep 2017;7(1):16878. doi: 10.1038/s41598-017-17204-5.

[20] Krenn V, Morawietz L, Burmester GR, Kinne RW, Mueller-Ladner U, Muller B, et al. Synovitis score: discrimination between chronic low-grade and high-grade synovitis. Histopathology 2006;49(4):358–64. doi: 10.1111/j.1365-2559.2006.02508.x.

[21] Reitsema RD, Hesselink BC, Abdulahad WH, van der Geest KSM, Brouwer E, Heeringa P, et al. Aberrant phenotype of circulating antigen presenting cells in giant cell arteritis and polymyalgia rheumatica. Front Immunol 2023;14:1201575. doi: 10.3389/fimmu.2023.1201575.

[22] Precerutti M, Formica M, Bonardi M, Peroni C, Calciati F. Acromioclavicular osteoarthritis and shoulder pain: a review of the role of ultrasonography. J Ultrasound 2020;23(3):317–25. doi: 10.1007/s40477-020-00498-z.

[23] Zhang A, Brouwer E, Sandovici M, Diepstra A, Jiemy WF, van der Geest KSM. The immune pathology of bursitis in rheumatic inflammatory diseases, degenerative conditions and mechanical stress: a systematic review. Semin Arthritis Rheum 2024;68:152527. doi: 10.1016/j.semarthrit.2024.152527.

[24] Davies LC, Jenkins SJ, Allen JE, Taylor PR. Tissue-resident macrophages. Nat Immunol 2013;14(10):986–95. doi: 10.1038/ni.2705.

[25] Alivernini S, MacDonald L, Elmesmari A, Finlay S, Tolusso B, Gigante MR, et al. Distinct synovial tissue macrophage subsets regulate inflammation and remission in rheumatoid arthritis. Nat Med 2020;26(8):1295–306. doi: 10.1038/s41591-020-0939-8.

[26] Roerink ME, van der Schaaf ME, Dinarello CA, Knoop H, van der Meer JW. Interleukin-1 as a mediator of fatigue in disease: a narrative review. J Neuroinflammation 2017;14(1):16. doi: 10.1186/s12974-017-0796-7.

[27] Ren K, Torres R. Role of interleukin-1β during pain and inflammation. Brain Res Rev 2009;60(1):57–64. doi: 10.1016/j.brainresrev.2008.12.020.

[28] Lotfi N, Thome R, Rezaei N, Zhang GX, Rezaei A, Rostami A, et al. Roles of GM-CSF in the pathogenesis of autoimmune diseases: an update. Front Immunol 2019;10:1265. doi: 10.3389/fimmu.2019.01265.

[29] Hamilton JA, Filonzi EL, Ianches G. Regulation of macrophage colony-stimulating factor (M-CSF) production in cultured human synovial fibroblasts. Growth Factors 1993;9(2):157–65. doi: 10.3109/08977199309010831.

[30] Liu FL, Chen CH, Chu SJ, Chen JH, Lai JH, Sytwu HK, et al. Interleukin (IL)-23 p19 expression induced by IL-1β in human fibroblast-like synoviocytes with rheumatoid arthritis via active nuclear factor-κB and AP-1 dependent pathway. Rheumatology (Oxford) 2007;46(8):1266–73. doi: 10.1093/rheumatology/kem055.

[31] Hu SL, Chang AC, Huang CC, Tsai CH, Lin CC, Tang CH. Myostatin promotes interleukin-1β expression in rheumatoid arthritis synovial fibroblasts through inhibition of miR-21-5p. Front Immunol 2017;8:1747. doi: 10.3389/fimmu.2017.01747.

[32] Epstein Shochet G, Brook E, Israeli-Shani L, Edelstein E, Shitrit D. Fibroblast paracrine TNF-α signaling elevates integrin A5 expression in idiopathic pulmonary fibrosis (IPF). Respir Res 2017;18(1):122. doi: 10.1186/s12931-017-0606-x.

[33] Imaizumi T, Itaya H, Fujita K, Kudoh D, Kudoh S, Mori K, et al. Expression of tumor necrosis factor-α in cultured human endothelial cells stimulated with lipopolysaccharide or interleukin-1α. Arterioscler Thromb Vasc Biol 2000;20(2):410–5. doi: 10.1161/01.atv.20.2.410.

[34] Tardito S, Martinelli G, Soldano S, Paolino S, Pacini G, Patane M, et al. Macrophage M1/M2 polarization and rheumatoid arthritis: a systematic review. Autoimmun Rev 2019;18(11):102397. doi: 10.1016/j.autrev.2019.102397.

[35] Ushach I, Zlotnik A. Biological role of granulocyte macrophage colony-stimulating factor (GM-CSF) and macrophage colony-stimulating factor (M-CSF) on cells of the myeloid lineage. J Leukoc Biol 2016;100(3):481–9. doi: 10.1189/jlb.3RU0316-144R.

[36] Ma X. TNF-α and IL-12: a balancing act in macrophage functioning. Microbes Infect 2001;3(2):121–9. doi: 10.1016/S1286-4579(00)01359-9.

[37] Chand Dakal T, Dhabhai B, Agarwal D, Gupta R, Nagda G, Meena AR, et al. Mechanistic basis of co-stimulatory CD40-CD40L ligation mediated regulation of immune responses in cancer and autoimmune disorders. Immunobiology 2020;225(2):151899. doi: 10.1016/j.imbio.2019.151899.

[38] Hodge-Dufour J, Noble PW, Horton MR, Bao C, Wysoka M, Burdick MD, et al. Induction of IL-12 and chemokines by hyaluronan requires adhesion-dependent priming of resident but not elicited macrophages. J Immunol 1997;159(5):2492–500. doi: 10.4049/jimmunol.159.5.2492.

[39] Devauchelle-Pensec V, Carvajal-Alegria G, Dernis E, Richez C, Truchetet ME, Wendling D, et al. Effect of tocilizumab on disease activity in patients with active polymyalgia rheumatica receiving glucocorticoid therapy: a randomized clinical trial. JAMA 2022;328(11):1053–62. doi: 10.1001/jama.2022.15459.

[40] Bonelli M, Radner H, Kerschbaumer A, Mrak D, Durechova M, Stieger J, et al. Tocilizumab in patients with new onset polymyalgia rheumatica (PMR-SPARE): a phase 2/3 randomised controlled trial. Ann Rheum Dis 2022;81(6):838–44. doi: 10.1136/annrheumdis-2021-221126.

[41] Spiera RF, Unizony S, Warrington KJ, Sloane J, Giannelou A, Nivens MC, et al. Sarilumab for relapse of polymyalgia rheumatica during glucocorticoid taper. N Engl J Med 2023;389(14):1263–72. doi: 10.1056/NEJMoa2303452.

[42] Kreiner F, Galbo H. Effect of etanercept in polymyalgia rheumatica: a randomized controlled trial. Arthritis Res Ther 2010;12(5):R176. doi: 10.1186/ar3140.

[43] Salvarani C, Macchioni P, Manzini C, Paolazzi G, Trotta A, Manganelli P, et al. Infliximab plus prednisone or placebo plus prednisone for the initial treatment of polymyalgia rheumatica: a randomized trial. Ann Intern Med 2007;146(9):631–9. doi: 10.7326/0003-4819-146-9-200705010-00005.

[44] Saraux A, Le Henaff C, Dernis E, Carvajal-Alegria G, Tison A, Quere B, et al. Abatacept in early polymyalgia rheumatica (ALORS): a proof-of-concept, randomised, placebo-controlled, parallel-group trial. Lancet Rheumatol 2023;5(12):e728–35. doi: 10.1016/S2665-9913(23)00246-1.

[45] Cid MC, Unizony SH, Blockmans D, Brouwer E, Dagna L, Dasgupta B, et al. Efficacy and safety of mavrilimumab in giant cell arteritis: a phase 2, randomised, double-blind, placebo-controlled trial. Ann Rheum Dis 2022;81(5):653–61. doi: 10.1136/annrheumdis-2021-221865.

[46] Virtanen A, Spinelli FR, Telliez JB, O'Shea JJ, Silvennoinen O, Gadina M. JAK inhibitor selectivity: new opportunities, better drugs? Nat Rev Rheumatol 2024;20(10):649–65. doi: 10.1038/s41584-024-01153-1.

[47] Koster MJ, Crowson CS, Giblon RE, Jaquith JM, Duarte-García A, Matteson EL, et al. Baricitinib for relapsing giant cell arteritis: a prospective open-label 52-week pilot study. Ann Rheum Dis 2022;81(6):861–7. doi: 10.1136/annrheumdis-2021-221961.

Ann Rheum Dis 84 (2025) 844–855

Contents lists available at ScienceDirect

Annals of the Rheumatic Diseases

journal homepage: https://www.sciencedirect.com/journal/annals-of-the-rheumatic-diseases

Osteoarthritis

Deep learning–based clustering for endotyping and post-arthroplasty response classification using knee osteoarthritis multiomic data

Jason S. Rockel[1,2], Divya Sharma[1,3,4], Osvaldo Espin-Garcia[1,2,3,5], Katrina Hueniken[1,2,6], Amit Sandhu[1,2], Chiara Pastrello[1,2], Kala Sundararajan[1,2], Pratibha Potla[1,2], Noah Fine[1,2], Starlee S. Lively[1,2], Kim Perry[1,2], Nizar N. Mahomed[1,2,7], Khalid Syed[1,2,7], Igor Jurisica[1,2,8,9], Anthony V. Perruccio[1,2,7,10], Y. Raja Rampersaud[1,2,7], Rajiv Gandhi[1,2,7,11], Mohit Kapoor[1,2,7,11,*]

[1] *Division of Orthopaedics, Osteoarthritis Research Program, Schroeder Arthritis Institute, University Health Network, Toronto, ON, Canada*
[2] *Krembil Research Institute, University Health Network, Toronto, ON, Canada*
[3] *Department of Biostatistics, Dalla Lana School of Public Health, University of Toronto, Toronto, ON, Canada*
[4] *Department of Mathematics and Statistics, York University, Toronto, ON, Canada*
[5] *Department of Epidemiology and Biostatistics, Western University, London, ON, Canada*
[6] *Princess Margaret Cancer Centre, University Health Network, Toronto, ON, Canada*
[7] *Department of Surgery, University of Toronto, Toronto, ON, Canada*
[8] *Departments of Medical Biophysics and Computer Science, and Faculty of Dentistry, University of Toronto, Toronto, ON, Canada*
[9] *Institute of Neuroimmunology, Slovak Academy of Sciences, Bratislava, Slovakia*
[10] *Institute of Health Policy, Management and Evaluation, Dalla Lana School of Public Health, University of Toronto, Toronto, ON, Canada*
[11] *Department of Laboratory Medicine and Pathobiology, University of Toronto, Toronto, ON, Canada*

ARTICLE INFO

Article history:
Received 8 October 2024
Received in revised form 23 October 2024
Accepted 27 December 2024

ABSTRACT

Objectives: Primary knee osteoarthritis (KOA) is a heterogeneous disease with clinical and molecular contributors. Biofluids contain microRNAs and metabolites that can be measured by omic technologies. Multimodal deep learning is adept at uncovering complex relationships within multidomain data. We developed a novel multimodal deep learning framework for clustering of multiomic data from 3 subject-matched biofluids to identify distinct KOA endotypes and classify 1-year post–total knee arthroplasty (TKA) pain/function responses.

Methods: In 414 patients with KOA, subject-matched plasma, synovial fluid, and urine were analysed using microRNA sequencing or metabolomics. Integrating 4 high-dimensional datasets comprising metabolites from plasma and microRNAs from plasma, synovial fluid, or urine, a multimodal deep learning variational autoencoder architecture with K-means clustering was employed. Features influencing cluster assignment were identified and pathway analyses conducted. An integrative machine learning framework combining 4 molecular domains and a

*Correspondence to Dr. Mohit Kapoor, Schroeder Arthritis Institute, Toronto, ON, Canada.
E-mail address: mkapoor@uhnresearch.ca (M. Kapoor).

Jason S. Rockel, Divya Sharma, Osvaldo Espin-Garcia, Katrina Hueniken, Amit Sandhu, and Chiara Pastrello contributed equally as first authors.

Igor Jurisica, Anthony V. Perruccio, Y. Raja Rampersaud, Rajiv Gandhi, and Mohit Kapoor contributed equally as senior authors.

Handling editor Prof. Josef Smolen.

https://doi.org/10.1016/j.ard.2025.01.012

clinical domain was then used to classify Western Ontario and McMaster Universities Arthritis Index (WOMAC) pain/function responses after TKA within each cluster.
Results: Multimodal deep learning−based clustering of subjects across 4 domains yielded 3 distinct patient clusters. Feature signatures comprising microRNAs and metabolites across biofluids included 30, 16, and 24 features associated with clusters 1 to 3, respectively. Pathway analyses revealed distinct pathways associated with each cluster. Integration of 4 multiomic domains along with clinical data improved response classification performance, surpassing individual domain classifications alone.
Conclusions: We developed a multimodal deep learning−based clustering model capable of integrating complex multifluid, multiomic data to assist in uncovering biologically distinct patient endotypes and enhance outcome classifications to TKA surgery, which may aid in future precision medicine approaches.

WHAT IS ALREADY KNOWN ON THIS TOPIC

- Searching the PubMed database for articles published up to October 7, 2024, using the search string “osteoarthritis AND endotype AND (classify OR classification OR prediction OR predictive) AND (machine learning OR deep learning) NOT review” only uncovered 3 articles, with 2 relevant articles using machine learning approaches to identify endotypes of knee or hip osteoarthritis (OA) patients.
- With omic technologies capable of evaluating thousands of features from multiple disease-relevant biofluids, more advanced modelling techniques able to integrate multiple omic feature sets are needed.

WHAT THIS STUDY ADDS

- This study uses a large sample of patients with knee osteoarthritis (KOA) containing multiomic (miRNomics and metabolomics) molecular data from diverse patient-matched biofluids (synovial fluid, plasma and urine).
- We developed a novel multimodal deep learning and machine learning framework to seamlessly integrate these high-dimensional, multimodal data to enhance the understanding of KOA by identifying distinct patient clusters and improve classification of postsurgical pain and function responses.
- Our integrated approach goes beyond the capabilities of individual domains, providing a more comprehensive methodological approach to understand disease and treatment outcomes.
- The entire sample dataset, including multiomic measures and modelling framework, are publicly available.

HOW THIS STUDY MIGHT AFFECT RESEARCH, PRACTICE OR POLICY

- Our methodology may assist in uncovering multiple clusters of patient endotypes with unique physiologically relevant pathways, which can be evaluated in outcome classification testing, such as for pain and function responses to total knee arthroplasty (TKA) surgery.
- Integration of additional omic technology data and clinical measures will be crucial to refine endotype clustering and response classifications using this modelling approach.
- Our approach may ultimately aid joint patient−physician decision making for future precision medicine therapeutic approaches, as well as improve subject selection criteria for future clinical trials.

INTRODUCTION

Osteoarthritis (OA) is a degenerative, painful, and disabling joint disease affecting over 500 million people worldwide [1], with the knee most commonly afflicted [2]. Primary knee OA (KOA) patients are heterogeneous [3]. Risk factors of KOA include age, sex (defined as patient-reported male/female), and obesity status [2]. Mental health and persistent pain status have also been associated with KOA clinical phenotypes [4,5]. Total joint arthroplasty (TKA) is the only available therapy for patients with KOA who no longer respond to conservative management; however, up to 34% of patients with KOA that undergo TKA fail to achieve clinically relevant pain reduction [6]. Identifying those at high risk of nonresponse is of significant interest. Psychosocial and sociodemographic variables are likely insufficient to explain differences in patient outcomes to TKA [7−9]. However, it is possible that KOA heterogeneity captured by biological features may improve our ability to classify patient responses to TKA.

Biofluid microRNAs (miRNAs) and metabolites can provide highly descriptive, individualised categorisations of patients beyond clinical measures. MiRNAs epigenetically modify target RNA expression. Biofluid metabolomes represents snapshots of the metabolic activity contributed by associated cells and tissues. Advanced omic technologies can measure miRNAs (miRNomics) and metabolites (metabolomics), primarily by next-generation sequencing (NGS) and liquid chromatography-mass spectrometry/mass spectrometry (LC-MS/MS), respectively [10,11].

In a case-control study using the UK Biobank cohort, 14 distinct OA risk phenotypes were identified by multimodal machine learning (ML) using clinical factors alone [12]. The inclusion of individual proteomic, genomic or metabolomic data showed no prediction improvement of case-control status over clinical factor modelling alone [12]. In contrast, studies using individual biofluids have identified endotypes of patients with OA. Three endotypes of patients with OA (low tissue turnover, structural damage and systemic inflammation) were identified from a panel of 16 serum and urine proteins and peptides using unsupervised ML [13]. Plasma metabolomics alone uncovered multiple endotypes of patients with KOA [14,15], with some metabolite ratios able to differentiate specific endotypes of KOA subjects from control participants [14]. KOA patient biofluid miRNA signatures were also able to differentiate between slow and fast progressors [16], early and late KOA [17,18], and patients requiring TKA or not [19]. Thus, endotype data from biofluids are important for understanding KOA heterogeneity, and consequently, may be associated with patient outcomes. To our knowledge, KOA endotypes have yet to be evaluated across multiple biofluids using multiomic technologies in an integrated approach [11].

Our experience to date suggests that multi-biofluid, multiomic endotyping requires more complex modelling systems. Deep learning aids in extracting complex patterns from data.

Autoencoders are one such deep learning approach. Although standard autoencoders focus on reconstructing input data by mapping them to and from a compressed latent representation without imposing a probabilistic structure, variational autoencoders (VAEs) introduce a probabilistic framework by parameterising the latent space using distributions, such as Gaussian, rather than deterministic points. This allows VAEs to incorporate stochastic sampling during training, capturing inherent data variability and improving robustness, key attributes for clustering in high-dimensional, multimodal omic data. Integrating multimodal data from multiple sources presents challenges due to the diversity within and across data types. VAEs address this challenge by embedding diverse data domains into reduced latent dimensions, facilitating improved data clustering [20−22]. Despite the potential of VAEs, there is a lack of unified frameworks for leveraging these methods to identify clusters from multimodal data and to classify clinical responses by integrating diverse data domains. Additionally, VAEs have not been applied to investigate OA endotypes.

In this study, we developed a novel multimodal deep learning framework employing VAEs for integrative clustering using 4 high-dimensional domains of subject-matched multiomic data from synovial fluid, urine and plasma, and tested its ability to determine distinct clusters (endotypes) of a sample of patients with KOA. Leveraging these endotypes, we further developed an integrative ML framework and tested the potential of this methodology to assess pain and function responses to TKA surgery.

METHODS

Study sample

A sample of 414 patients with primary KOA who underwent TKA within the Longitudinal Evaluation in the Arthritis Program-OA cohort (University Health Network, Toronto, Ontario, Canada), as previously described [23], and who had synovial fluid (collected intraoperatively), plasma and urine (collected up to 3 months prior to surgery) available, were selected for analysis. Nonfasting blood was collected for plasma, and urine was collected at first miction. All subjects were radiographic Kellgren−Lawrence (KL) grade III/IV primary KOA, were symptomatic, and fulfilled the American College of Rheumatology clinical criteria for KOA classification [24]. Subjects completed self-reported, multidimensional questionnaires from which baseline Western Ontario and McMaster Universities Arthritis Index (WOMAC) pain and function scores were calculated, with a maximum 20 points for pain and 68 points for function, with higher scores indicative of greater pain or more disability, respectively [25]. Hospital Anxiety and Depression Scale (HADS) [26] and painDETECT [27] scores at baseline (completed within the 3 months preceding surgery), and WOMAC pain and function scores at 1 year after TKA were also calculated. Improvement in WOMAC pain and function from baseline to 1 year after TKA was calculated, and individuals were categorised as responders (>33% improvement) or nonresponders (≤33% improvement), consistent with moderately important pain change thresholds [28,29], and used in a previous report [23]. HADS depression and anxiety scores were each categorised as normal (score 0-7), borderline case (score 8-11), or definite case (score 11-21) [26]. PainDETECT neuropathic-like pain scores were used to classify subject pain as likely nociceptive (score 0-12), unclear (score 13-18), or likely neuropathic-like (score 19-38) [27]. Baseline age, sex, and weight and height (from which body mass index [BMI; kg/m^2] was calculated) were also collected. Biofluids and patient data were collected with written informed consent from each patient and Research Ethics Board approval of the University Health Network, Toronto, Ontario (REB# 07-0383-BE; 14-7592-AE).

MiRNA sequencing (miRNomics) and metabolomics

MiRNA extraction was performed using 200 μL plasma (N = 414), 100 μL synovial fluid (N = 414), and 1 mL urine (N = 414). Complementary DNA (cDNA) libraries were prepared using a protocol we previously reported [18]. NGS was conducted at the Schroeder Arthritis Institute (University Health Network, Toronto, Ontario) sequencing facility using the Illumina NextSeq550 platform. Alignment, processing, and quality assessment were performed using a previously reported pipeline [30]. Targeted metabolomics was used to profile 188 metabolites (Biocrates AbsoluteIDQ p180 kit, Biocrates Life Sciences AG) in N = 414 plasma samples at The Metabolomics Innovation Centre (Calgary, Alberta, Canada) by LC-MS/MS, as previously described [15]. Metabolite quantification and batch correction were conducted using the Absolute IDQ-coupled MetIDQ software (Biocrates). MiRNA count data and metabolite concentrations were normalised using sum normalisation, log-transformation, and Pareto scaling [31]. To stabilise variance estimates within differential expression (DE) analysis, empirical Bayes moderation techniques were applied.

OmicVAE: integrative VAE architecture for multimodal clustering

We generated a novel VAE architecture named '*omicVAE*' designed to cluster multimodal multiomic data (Fig 1). *OmicVAE* consists of a single encoder network followed by 4 individual decoder networks to perform integrative clustering combining 4 modalities: plasma metabolites, plasma miRNAs, synovial fluid miRNAs, and urine miRNAs.

The encoder network inputs concatenated multimodal multiomic data and maps them to a shared latent space representation using multiple fully connected neural network (FNN) layers with a sigmoid activation function. The encoder network's output layers parameterise the mean and variance of a Gaussian distribution representing the shared latent space. Each decoder network reconstructs its respective domain's input data from samples drawn from this latent space, using multiple FNN layers. During training, variational inference optimises the VAE's parameters. The objective function L_{total} includes the reconstruction loss (L_{rec}) and the Kullback−Leibler divergence (L_{KL}) between the learned latent distribution and a predefined prior (Equations 1-3). Minimising Kullback-Leibler divergence regularises the latent space, preventing overfitting and ensuring it remains structured and interpretable. The reconstruction loss measures the discrepancy between the input data and its reconstruction by the VAE decoder for each modality.

$$\begin{aligned} L_{rec} = {} & \frac{1}{N_{metabolites}} \sum_{i=1}^{N} \| X_{metabolites(i)} - Decoder_{metabolites(i)}(z) \|^2 \\ & + \frac{1}{N_{miRNA_{plasma}}} \sum_{i=1}^{N} \| X_{miRNA_{plasma}(i)} - Decoder_{miRNA_{plasma}(i)}(z) \|^2 \\ & + \frac{1}{N_{miRNA_{synovial}}} \sum_{i=1}^{N} \| X_{miRNA_{synovial}(i)} - Decoder_{miRNA_{synovial}(i)}(z) \|^2 \\ & + \frac{1}{N_{miRNA_{urine}}} \sum_{i=1}^{N} \| X_{miRNA_{urine}(i)} - Decoder_{miRNA_{urine}(i)}(z) \|^2 \qquad (1) \end{aligned}$$

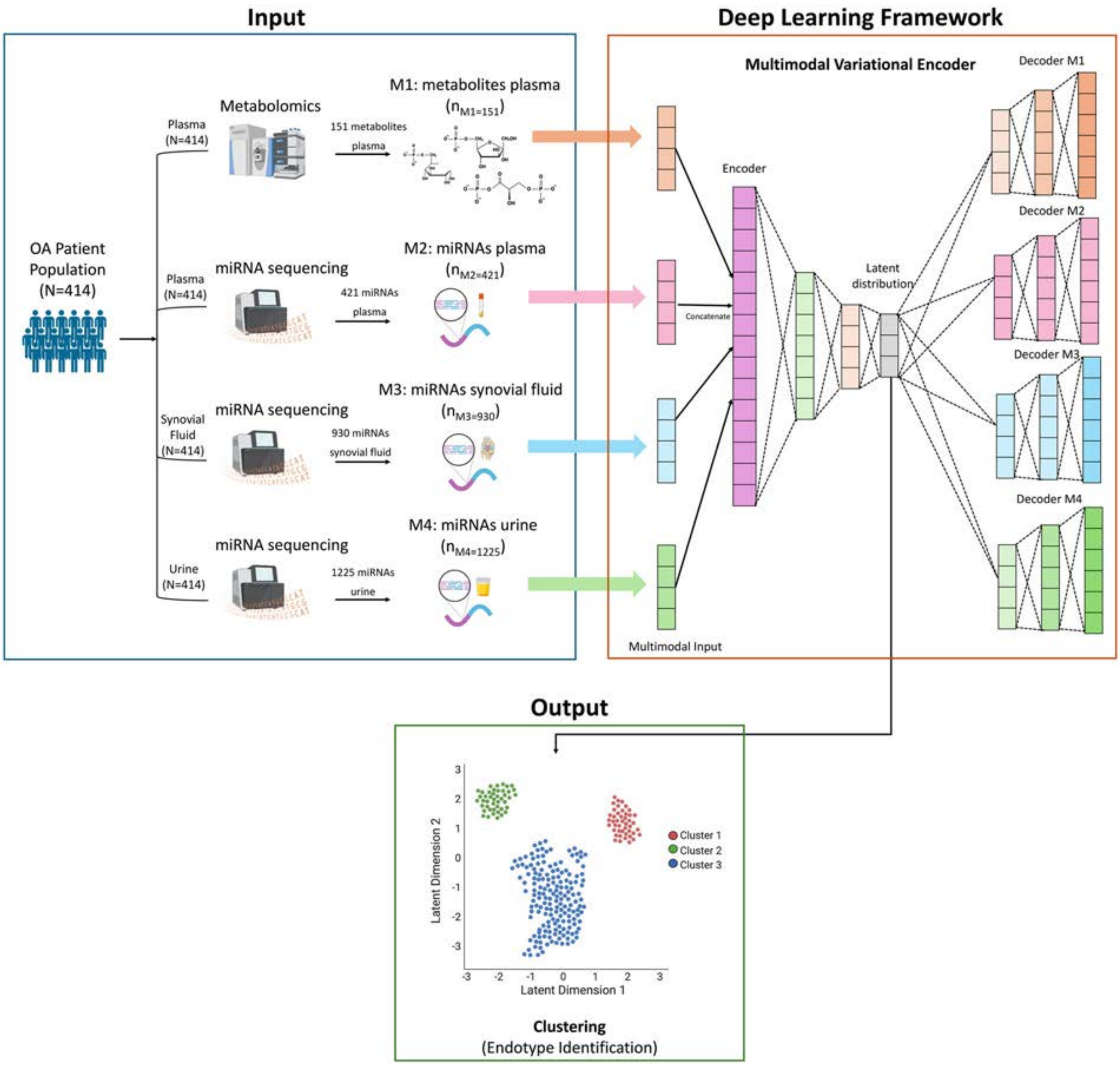

Figure 1. Overall framework for deep learning−based multimodal clustering. Deep learning framework for multimodal integration and clustering using variational autoencoder (VAE) modelling. Four individual decoders in the proposed VAE accurately identify the latent distribution within each domain (M1-M4) capturing the complex nonlinear associations within the multimodal data. K-means approach is used for identifying 3 clusters from the obtained latent distribution. 'N' represents the number of patients, and 'n_{Mx}' represents the number of features in each data domain. Created, in part, with BioRender.com. OA, osteoarthritis; miRNA, microRNA.

$$
\begin{aligned}
L_{KL} = & -\frac{1}{2}\Bigg(\left(1+\log\left(\sigma^2_{metabolites}\right)-\mu^2_{metabolites}-\sigma^2_{metabolites}\right)\\
& +\left(1+\log\left(\sigma^2_{miRNA_{plasma}}\right)-\mu^2_{miRNA_{plasma}}-\sigma^2_{miRNA_{plasma}}\right)\\
& +\left(1+\log\left(\sigma^2_{miRNA_{synovial}}\right)-\mu^2_{miRNA_{synovial}}-\sigma^2_{miRNA_{synovial}}\right)\\
& +\left(1+\log\left(\sigma^2_{miRNA_{urine}}\right)-\mu^2_{miRNA_{urine}}-\sigma^2_{miRNA_{urine}}\right)\Bigg) \qquad (2)
\end{aligned}
$$

$$L_{total} = L_{rec} + L_{KL} \qquad (3)$$

In Equations 1 to 3, i represents the samples in each modality, X is the input data, Decoder(z) is the reconstructed data, and μ and σ denote the mean and variance of the Gaussian distribution in the latent space, respectively. Once omicVAE is trained, K-means clustering on the learned latent space is used to identify distinct subpopulations within the multimodal multiomic data.

Multiomic signature identification within each cluster

We employed a comprehensive approach to identify signature features (miRNAs and/or metabolites within 3 biofluids) influencing cluster assignment within each domain. We concurrently conducted standardised mean differences (SMDs) and DE analyses for pairwise cluster comparisons (one cluster vs others), using Benjamini−Hochberg (BH) adjusted *P* values (q < 0.05) to identify statistically different features. By integrating these analyses, we identified features with both large SMDs and significant DE, capturing robust signature features distinguishing clusters.

Endotype pathway analysis

Gene targets of miRNAs per cluster were identified using the top 1% of targets per miRNA using mirDIP 5.2 (https://ophid.utoronto.ca/mirDIP) [32]. We performed pathway enrichment analysis for sets of gene targets in each cluster using pathDIP 5 (https://ophid.utoronto.ca/pathDIP) [33]. Diseases, drugs and vitamins, and genetic information processing pathway types were excluded from enrichment analysis. Only pathways with q value (BH adjusted) <0.01 were considered. Metabolite pathway enrichment analysis was not possible, so we identified pathways that included metabolites specific for each cluster for further analyses. Selected pathways specific for each cluster were visualised using NAViGaTOR 3.0.19 (https://navigator.ophid.utoronto.ca/navigatorwp) [34]. Mapping of pathways to consolidated categories in pathDIP was used to calculate the number of pathways per category. ggradar2_1.1.0 in R 4.3.0 was subsequently used to plot their distribution per cluster, scaling category pathway counts from 0% to 100%.

Integrative ML framework for classifying response

We developed a comprehensive 2-step ML framework to integrate plasma metabolite, plasma miRNA, synovial fluid miRNAs and urine miRNA domains, along with a clinical domain (consisting of age, sex, BMI, depression and anxiety categories, and neuropathic-like pain category), to classify 1-year pain and function responses (i.e., responders vs nonresponders). In the first step, we trained separate unimodal ML models for each domain to extract features classifying 1-year response. We used the *mice* (multivariate imputation by chained equations) package (version 3.14.0) in R (R Foundation for Statistical Computing, Vienna, Austria) to perform multivariate imputation by chained equations of the missing clinical data (missingness <8%). We explored various ML algorithms including logistic regression, lasso regression, ridge regression, support vector machines and random forests, selecting models based on 10-fold cross-validation performance.

In the second step, we integrated features from all domains using a Naïve Bayes meta-classifier, trained with classifiers from the unimodal models. Cross-validation was used for performance estimation and hyperparameter tuning. The final classification was generated by the meta-classifier based on integrated features. Model evaluation involved assessing the overall framework performance using area under the receiver operating characteristic curve (AUC) and analysing feature importance with mean Gini impurity metrics.

Patient and public involvement

Patients and public had no role in study design, data collection and analysis, decision to publish, or manuscript writing.

RESULTS

Endotype and signature identification using omicVAE and K-means clustering

We first sought to identify endotypes from our sample of 414 patients with KOA. The patient sample was 57% female, with a mean age (±SD) of 65.7 ± 8.7 years and BMI (±SD) of 31 ± 7.1 kg/m^2. The majority of subjects had anxiety or depression symptom scores in the normal range, and the majority had painDETECT scores indicating likely nociceptive pain. Mean baseline WOMAC pain score for the sample was 10.1 ± 3.5 points on a 20 total point scale, and baseline WOMAC function score was 34.9 ± 11.9 points on a 68 total point scale (Table 1).

After metabolomics and miRNomics analyses of plasma, synovial fluid and urine, our analytical dataset consisted of 2727 molecular features from 4 domains: 151 plasma metabolites, 421 plasma miRNAs, 930 synovial fluid miRNAs, and 1225 urine miRNAs. We then developed *omicVAE* with K-means clustering (Fig 1), which uncovered 3 clusters of patients using the 4 domains (Fig 2A). The selection of 3 clusters was informed by scree and silhouette plots (Supplementary Fig S1), which visually indicated a significant drop in explained variance (scree plot) and a peak in silhouette score at k = 3 (silhouette plot), suggesting that 3 clusters best represented the underlying data structure. Distribution of most baseline clinical, demographic and anthropometric measures were similar across clusters, except cluster 3 that had a higher proportion of subjects with depression scores in the normal range, and cluster 1 that had a higher proportion of subjects with likely neuropathic-like pain (Table 2).

Significant features associated with each cluster were identified by the intersection of DE and SMD analyses. Distinct signatures consisting of 30, 16, and 24 features for clusters 1 to 3, respectively, were identified (Fig 2B and Supplementary Table S1). Notably, each signature contained features from all 4 domains. In cluster 1, the highest mean value difference was observed for synovial fluid hsa-miR-2053. In cluster 2, synovial fluid hsa-miR-496 exhibited the highest mean value. In cluster 3, plasma hsa-miR-570-3p had the highest mean value. Thus, each cluster represents a group of subjects with a distinct endotype.

Endotype feature signatures are enriched for unique pathways

We next sought to determine if cluster endotype signatures were associated with unique physiological pathways. We first

Table 1

Summary statistics of 414 knee OA subjects at baseline undergoing total knee arthroplasty

	Full sample (N = 414)
Sex, n (%)	
Female	232 (56)
Male	182 (44)
Age (years)	
Mean (SD)	65.7 (8.4)
Median (Q1, Q3)	66 (60, 71)
BMI (kg/m^2)	
Mean (SD)	31.3 (7.0)
Median (Q1, Q3)	29.8 (26.3, 35.0)
HADS anxiety, n (%)	
Normal	301 (74)
Borderline	54 (13)
Case	50 (12)
Missing, n	9
HADS depression, n (%)	
Normal	324 (79)
Borderline	48 (12)
Case	37 (9)
Missing, n	5
painDETECT, n (%)	
Neuropathic-like	55 (13)
Nociceptive	255 (62)
Unclear	81 (20)
Missing	23 (6)
WOMAC pain at pre-TKA baseline	
Mean (SD; min, max)	10.1 (3.5; 2, 20)
Median (Q1, Q3)	10 (8, 12)
WOMAC function at pre-TKA baseline	
Mean (SD; min, max)	34.5 (11.9; 0, 67)
Median (Q1, Q3)	35 (26, 42)
Missing, n	2

BMI, body mass index; HADS, hospital anxiety and depression scale; Q, quartile; TKA, total knee arthroplasty; WOMAC, Western Ontario and McMaster Universities Arthritis Index.

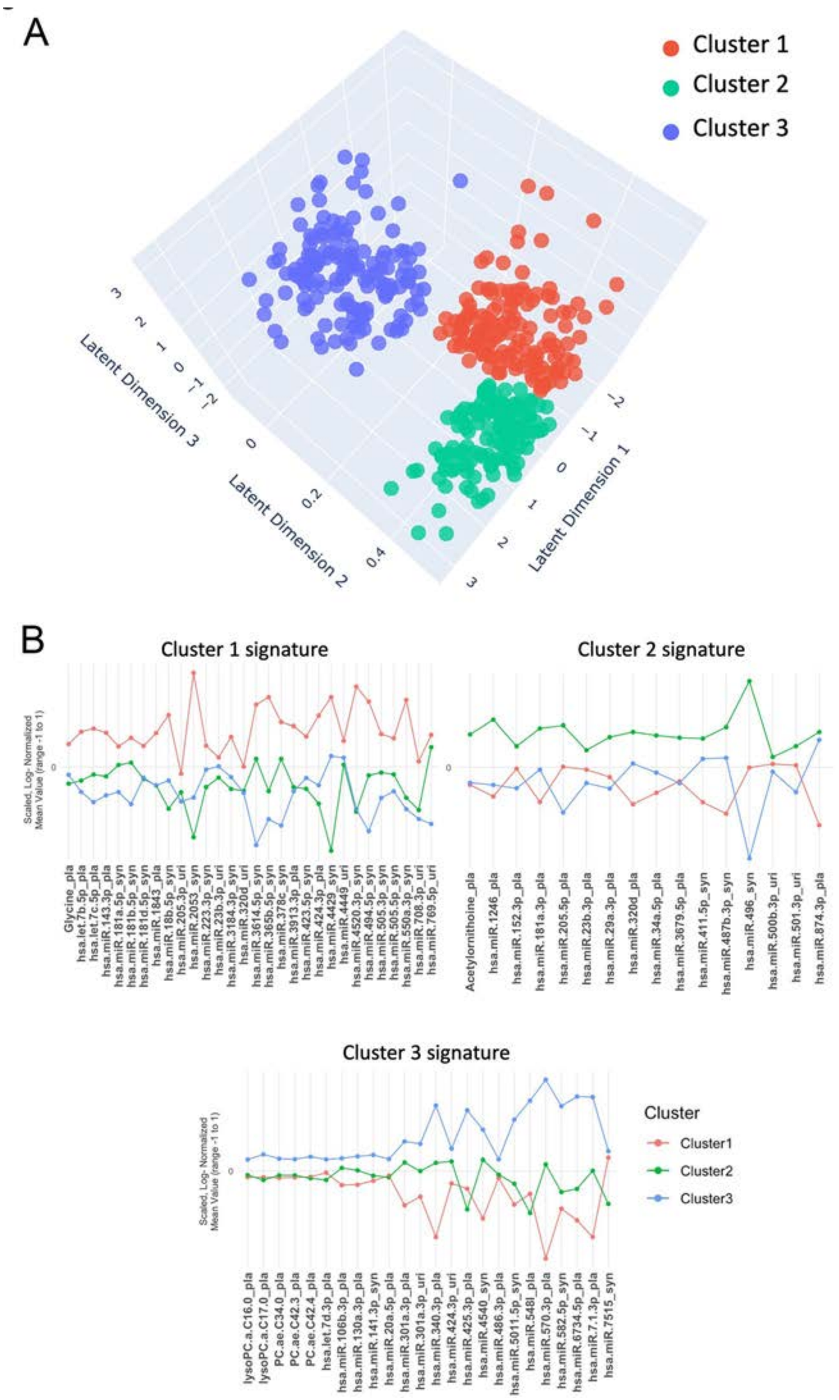

Figure 2. Integrated analysis of patient clustering and microRNA (miRNA) and metabolite feature signatures. (A) Three-dimensional illustration (latent dimension 1-3) of the 3 clusters obtained using the variational autoencoder-based deep learning framework. Cluster 1 (red) comprises 146 patients, cluster 2 (green) consists of 138 patients, and cluster 3 (blue) includes 130 patients. (B) Molecular signature profiles for clusters 1, 2, and 3 derived through the intersection of the most significant variables ($q < 0.05$) identified from both standardised mean differences analysis and differential expression analysis within plasma metabolites and miRNA domains, differentiating each cluster.

identified putative miRNA-gene targets using mirDIP [32], identifying 3257, 2211, and 2319 individual genes targeted by the miRNAs in each of the endotype signatures associated with clusters 1 to 3, respectively. Using these gene set lists, we performed enrichment analysis using pathDIP (Supplementary Tables S2-S4) [33]. For metabolites in each endotype signature, pathway annotations were also identified using pathDIP (Supplementary Tables S5-S7). All pathways were also annotated with categories in pathDIP. For each endotype, individual miRNA-gene targets and metabolites were linked to some common as well as unique pathways. The top unique enriched and annotated pathways linked to miRNA-targeted genes or metabolites, respectively, for each endotype are displayed in a network showing individual pathways and categories (Fig 3A, Supplementary Figs S2-S4).

We next used pathway categories to evaluate physiologically relevant mechanisms linked to each endotype. Each enriched miRNA-derived pathway or annotated metabolite pathway was counted based on its category annotation in pathDIP, scaled and visualised using radar plots (Fig 3B). The cluster 1 endotype signature was most linked to pathway categories associated with development and regeneration, membrane transport, metabolism of various molecules, and the nervous system. The cluster 2 endotype signature was most linked to ageing and cellular community categories. Finally, the cluster 3 endotype signature was most linked to transport and catabolism, signal transduction, sensory system, endocrine system, excretory system, immune system, catabolism, and lipid metabolism categories. Overall, these analyses suggested that features associated with each endotype were uniquely associated with distinct physiological pathways.

Table 2

Summary statistics of clinical variables within each cluster identified from variational autoencoder machine learning modelling and K-means clustering

	Cluster 1 (n = 146)	Cluster 2 (n = 138)	Cluster 3 (n = 130)	*P* value between clusters
Sex, n (%)				.9
Female	84 (58)	76 (55)	72 (55)	
Male	62 (42)	62 (45)	58 (45)	
Age (years)				.37
Mean (SD)	66.2 (8.2)	65.4 (8.0)	65.5 (8.9)	
Median (Q1, Q3)	67 (62, 71)	65.0 (60.0, 70.8)	66 (60, 72)	
BMI (kg/m^2)				.55
Mean (SD)	30.7 (6.1)	31.9 (7.7)	31.4 (7.3)	
Median (Q1, Q3)	29.2 (26.4, 33.8)	30.0 (26.5, 35.7)	31.1 (25.3, 34.7)	
HADS anxiety, n (%)				.72
Normal	103 (72)	98 (73)	100 (79)	
Borderline	21 (15)	20 (15)	13 (10)	
Case	19 (13)	17 (13)	14 (11)	
Missing, n	3	3	3	
HADS depression, n (%)				**.037**
Normal	107 (74)	105 (78)	112 (87)	
Borderline,	23 (16)	19 (14)	6 (5)	
Case,	15 (10)	11 (8)	11 (9)	
Missing, n	1	3	1	
painDETECT, n (%)				**.011**
Neuropathic-like	30 (21)	14 (10)	11 (8)	
Nociceptive	86 (59)	82 (59)	87 (67)	
Unclear	27 (18)	31 (22)	23 (18)	
Missing	3 (2)	11 (8)	9 (7)	
WOMAC pain at pre-TKA baseline				.98
Mean (SD)	10.2 (3.5)	10.0 (3.2)	10.0 (3.7)	
Median (Q1, Q3)	10 (8, 12)	10 (8, 12)	10.0 (8.0, 12.4)	
WOMAC pain at 1 year post-TKA				.34
Mean (SD)	3.7 (4.0)	3.7 (3.6)	3.2 (3.6)	
Median (Q1, Q3)	3.0 (1.0, 5.8)	3 (1, 6)	2.0 (0.2, 5.0)	
WOMAC pain change (1 year—baseline)				.55
Mean (SD)	−6.5 (4.1)	−6.3 (3.9)	−6.8 (4.1)	
Median (Q1, Q3)	−7 (−9, −4)	−6.0 (−9.0, −3.2)	−7.0 (−9.8, −4.0)	
WOMAC pain change categorical, n (%)				.48
≤33.3%	27 (18)	33 (24)	22 (17)	
>33.3%	119 (82)	105 (76)	108 (83)	
WOMAC function at pre-TKA baseline				.74
Mean (SD)	34.7 (11.9)	34.9 (11.4)	33.8 (12.3)	
Median (Q1, Q3)	36 (26, 41)	35.0 (26.2, 43.0)	34 (26, 41)	
Missing, n	1	0	1	
WOMAC function at 1 year post-TKA				.24
Mean (SD)	14.8 (13.7)	14.7 (12.9)	12.8 (13.0)	
Median (Q1, Q3)	12.0 (4.2, 21.0)	11.5 (4.0, 20.8)	9.0 (2.2, 19.0)	
WOMAC function change (1 year—baseline)				.76
Mean (SD)	−20.3 (13.4)	−20.0 (13.8)	−20.2 (13.3)	
Median (Q1, Q3)	−20 (−30, −11)	−18.4 (−31.0, −10.0)	−19.0 (−28.8, −11.0)	
WOMAC function change categorical, n (%)				.24
≤33.3%	33 (23)	32 (23)	24 (19)	
>33.3%	112 (77)	106 (77)	105 (81)	
Missing, n	1	0	1	

Frequency (percentage) are provided for categorical variables, whereas median (quartile 1, quartile 3) values are presented for continuous variables according to patients within each cluster. *P* value was computed using Wilcoxon rank sum test for continuous variables and chi-square or Fisher's test as appropriate for categorical variables. *P* values in bold are considered statistically significant ($P < 0.05$).

BMI, body mass index; HADS, hospital anxiety and depression scale; Q, quartile; TKA, total knee arthroplasty; WOMAC, Western Ontario and McMaster Universities Arthritis Index.

Evaluation of classification performance for WOMAC pain and function responses

To determine the classification performance of the clusters for identifying post-TKA WOMAC pain and function response status, we used an integrative ML framework using 5 domains: plasma metabolites, plasma miRNAs, synovial fluid miRNAs, urine miRNAs, and clinical data (age, sex, BMI, anxiety and depression categories and neuropathic-like pain category; Fig 4A). Subject clusters had similar mean pain and function scores 1 year after TKA, change in scores from baseline to 1 year, as well as pain and function response rates (Table 2). We first conducted DE analysis in each cluster, identifying metabolites with a minimum fold change of 1.1 and miRNAs within each biofluid with a minimum fold change of 1.5 between responders and nonresponders. Of the compared ML approaches, random forests consistently outperformed others in each individual domain (Supplementary Table S8) and was used for the unimodal ML models. Subsequently, we employed 10-fold cross-validation to estimate the AUC and 95% CIs obtained while predicting WOMAC pain and function responses (Supplementary Table S9).

After differential analysis–based feature selection, clusters 1 to 3 retained 250, 87, and 49 features, respectively, for the

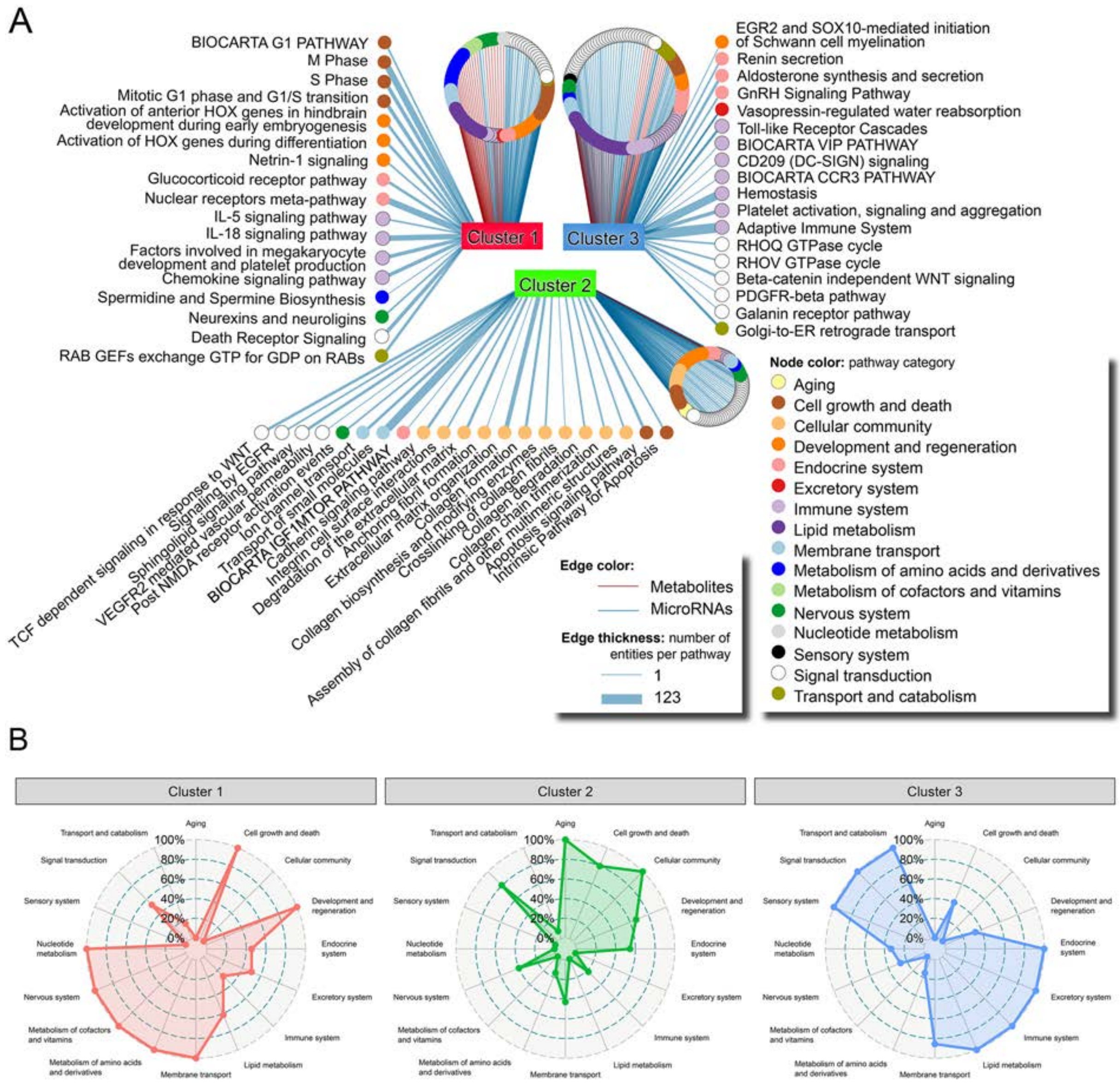

Figure 3. Cluster endotype signatures are associated with different physiological pathways. (A) Network depicting unique enriched pathways from microRNA (miRNA)-gene targets and annotated pathways from metabolites associated with individual cluster endotype signatures. Labels show pathways with lowest q value or highest number of annotated genes. (B) Radar plots of pathway categorisations from enriched pathways of miRNA-gene targets and annotated pathways from metabolites indicating categories most associated to individual clusters endotypes.

ML analysis to classify pain response (Supplementary Table S10). Initially, unimodal models were applied to each domain. Within cluster 1, plasma miRNAs demonstrated the highest unimodal performance with an AUC of 0.735. However, the integrative performance, combining all 4 domains in the meta-classifier, notably improved AUC to 0.841 (highlighted in red in the receiver operating characteristic [ROC] plot). For cluster 2, the clinical domain had the highest unimodal AUC of 0.740, whereas the integrative AUC was 0.816. Cluster 3 achieved the highest integrative AUC of 0.879, with urine miRNAs showing the highest unimodal AUC of 0.786 (Fig 2B).

Based on differential analysis−based feature selection to classify function response, clusters 1 to 3 retained 63, 46, and 46 features, respectively, for the ML analysis (Supplementary Table S11). Across clusters 1 to 3, the clinical data domain consistently exhibited the best performance among unimodal domains, with AUCs of 0.702, 0.791, and 0.722, respectively. In terms of integrative performance, clusters 1 to 3 achieved AUCs of 0.786, 0.808, 0.738 (Fig 2C), respectively.

Identifying key response classification features in our multimodal ML framework

To enhance the interpretability of our model we identified the most important features (molecular and clinical) contributing to response classification in each cluster. The top 20 features contributing to WOMAC pain or function response classification are shown in Supplementary Figures S5 and S6, respectively. Each top 20 list consisted of features from all 4 molecular domains, with a notable absence of clinical features; however, all molecular and clinical features inherently played a role in response classification (Supplementary Tables S12 and S13). Interestingly, only 3 miRNAs overlapped in the top 20 important features for WOMAC pain response between clusters 2 and 3, namely synovial fluid hsa-miR-1265 and hsa-mir-642a-3p, and plasma hsa-3942-5p. In addition, only the metabolite glutamine overlapped in the top 20 important feature lists of clusters 2 and 3 for WOMAC function response. Furthermore, within each cluster, the top 20 predictive features were also primarily different for pain and function outcomes, with only synovial fluid hsa-let-

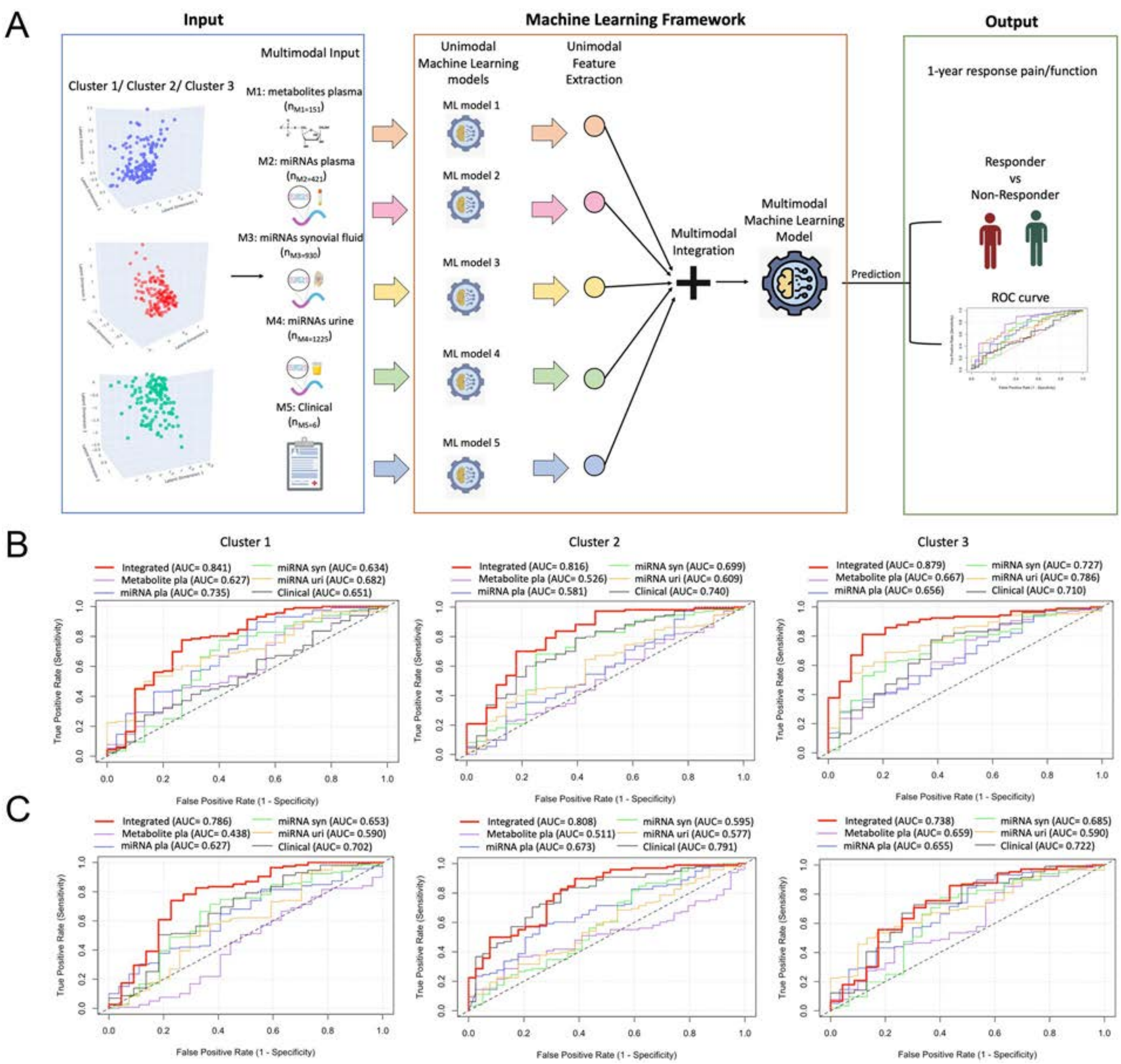

Figure 4. Machine learning modelling for classifying response to 1 year pain and function within each cluster. (A) Comprehensive 2-step machine learning (ML) framework wherein, initially, unimodal ML models extract features from each domain, including metabolites from plasma, microRNAs (miRNAs) from plasma, synovial fluid, and urine as well as clinical data. A second-level multimodal machine learning classifier integrates these features to efficiently classify response vs nonresponse at 1 year. (B) Receiver operating characteristic (ROC) plots illustrating the area under the curve (AUC) for individual domains, alongside the integrated AUC (in red) combining all 5 domains to classify Western Ontario and McMaster Universities Arthritis Index (WOMAC) pain response. (C) ROC plots illustrating the AUC for individual domains, alongside the integrated AUC (in red) combining all 5 domains to classify WOMAC function response. Notably, the integrated AUC outperforms individual AUCs in cluster 1, cluster 2, and cluster 3. Created, in part, with BioRender.com.

7f-1-3p in cluster 1 and plasma hsa-miR-3942-5p in cluster 2 showing overlap between lists. Thus, using our integrative approach, the vast majority of the most important features for response classification were unique for each cluster and were also unique between pain and function outcomes within each cluster, with molecular entities primarily driving classification performance. Overall, these findings highlight the diverse molecular features associated with outcome classification in each cluster, emphasising the importance of integrating multiple domains for classification modelling of WOMAC pain and function responses after TKA.

DISCUSSION

Demographic, anthropometric and clinical characteristics of patients with OA are heterogeneous, influencing outcomes to therapy, including TKA [3,35]. Heterogeneity has also been identified through biofluid data; however, most studies to date have used single biofluids with single molecular type measures to identify endotypes within OA cohorts [13,14]. We developed a novel multimodal deep learning algorithm, *omicVAE*, to cluster a sample of 414 KOA subjects who underwent TKA using preoperative miRNA and metabolite feature sets identified by miRNomics and targeted metabolomics from plasma, synovial fluid, and urine, and uncovered 3 unique cluster endotypes.

OmicVAE, the novel VAE architecture described in this study, was specifically designed for integration and clustering of multimodal, multiomic data. Although VAEs have been applied in other omics settings [36−39], *omicVAE* distinguishes itself by its ability to handle heterogeneous data from distinct modalities: metabolomics and miRNomics. A key innovation lies in its architecture, where a single encoder network generates a shared latent space representation from concatenated multimodal inputs, enabling integrative analysis across these domains. To ensure that modality-specific features are preserved while leveraging shared latent information, *omicVAE* incorporates 4 independent decoder networks, each tasked with reconstructing data from a specific input modality. This modular and integrative design makes *omicVAE* uniquely suited for clustering tasks involving complex, multimodal datasets, where both intermodality relationships and domain-specific reconstruction are critical.

To our knowledge, our study is the first to use a subject-matched multi-biofluid, multiomic approach to endotyping patients with KOA. Not only did we uncover 3 unique multiomic-based cluster endotypes, each was linked to unique pathway categories. Despite a similar clinical phenotype, the cluster 1 endotype was primarily linked to metabolic processes and nervous system pathways, the cluster 2 endotype was primarily associated with ageing pathways, and the cluster 3 endotype was primarily linked to immune, endocrine, and lipid metabolism pathways. Overall, the cluster endotypes uncovered are likely to contribute to, or be the result of, distinct mechanisms associated with patients with KOA.

Using this novel approach to cluster endotyping, combined with integrative multimodal ML, we enhanced classification of patient-reported pain and function responses beyond that achieved using clinical measures alone. Importantly, differences in patient-reported pain and function, or response to surgery, were not found simply between patient clusters. Ultimately, significant differences in clinical measures between clusters were only found in the proportions of patients with suspected depression or neuropathic-like pain. In contrast, we found that differences in molecular and clinical measures across patients within each cluster were able to improve classification response. Although the clusters may not differ in pain or function scores, the ML workflow was designed to identify and leverage more subtle, multidimensional patterns such as biomarkers, clinical characteristics, or other high-dimensional features, that may influence outcomes within each cluster. By focusing on nuanced predictive relationships, the ML workflow adds value by identifying individualised predictors of outcomes, even in the absence of broad differences in traditional clinical scores. Consistent with this, we found that molecular entities primarily drove classification of pain and function responses using our integrative modelling; however, all clinical and molecular features included in the model have some contribution to classification modelling performance. Overall, our unique methodological approach reduced OA patient heterogeneity by defining patient clusters that had intracluster molecular differences that enhanced classifying pain and function responses to TKA. As endotypes are further refined and molecular entities best associated with classification are further characterised, it will be important to understand how these response-based signatures may relate to physiological responses after surgery.

The strength of our methodology lies in developing integrative deep learning and ML techniques for efficient multiomic endotyping and response classification in patients with KOA. VAEs offer advantages to integrating multiple domains for clustering compared to traditional approaches by effectively capturing the underlying structure of heterogeneous data through a joint latent representation. Although traditional approaches such as dimensionality reduction or sequential clustering may provide insights, they often suffer from limitations such as difficulty in capturing nonlinear relationships, and inadequate integration of domain-specific characteristics. Unlike standard VAEs [22], we employed 4 separate decoders, enabling domain-specific reconstruction facilitating robust subject clustering, accounting for the inherent uncertainty in the latent space via the VAE's probabilistic nature. Overall, VAEs effectively leverage complementary information from multiple modalities for a more comprehensive characterisation of KOA patient endotypes.

The integration of multiple data domains through our comprehensive 2-step ML framework represents a significant advancement in response modelling for KOA outcomes by combining complementary information inherent in metabolomics, miRNA, and clinical data domains. Utilisation of unimodal ML models in the first step allowed for extraction of domain-specific features that could classify 1-year TKA pain and function responses, while subsequent integration of these features using a Naïve Bayes meta-classifier enhanced classification accuracy. Naïve Bayes classifiers emulate aspects of clinical decision making by probabilistically combining evidence from multiple sources to make classifications [40]. Importantly, our novel framework demonstrated improvements in classification performance compared to unimodal domain-specific models, underscoring the utility of an integrative approach.

Although we included 3 biofluids to integrate miRNA or metabolite features to identify endotypes among patients with KOA, additional endotypes may exist. Incorporating additional omic technologies (eg, proteomics, genomics and methylomics) in the presented framework, as well as comprehensively evaluating omic measures across all biofluids, may further refine endotypes, or uncover additional endotypes to further improve our understanding of KOA and ability to more accurately classify responses to interventions. Future studies should also focus on easily obtained patient biofluids, such as urine and blood, to determine whether the presented approach can show similar endotyping capability and response classification accuracy. As our methodology sought to identify patient clusters only by molecular features, we did not consider whether clinical/sociodemographic/anthropometric/psychosocial variables (such as age, sex, BMI, diet, medications, race, comorbidities, depression and anxiety) may also influence molecular mediators prior to clustering. However, further understanding associations of these factors with OA clusters may provide insights on their relationships with molecular signatures associated with each cluster. In response classification modelling, we only evaluated a subset of clinical/sociodemographic/anthropometric/psychosocial variables associated with KOA and patient outcomes to TKA, but incorporation of additional patient-related factors, and postsurgical therapies such as rehabilitation, alongside endotype data, may also help improve modelling accuracy. Lastly, similar evaluations in additional patient cohorts, such as those with early KOA, with or without disease progression, having other afflicted joints, or evaluating other response measures, would also be of interest moving forward.

Our study is not without limitations. First, plasma and urine were collected within the 3-month period prior to surgery and synovial fluid collection. Although matching fluid collection on the day of surgery would be ideal, as molecular features may fluctuate over time and have some impact on clustering and classification models, this was not logistically feasible for our cohort on day of surgery. In addition, although we extensively validated our integrative ML unimodal models using a 10-time, 10-fold cross-validation, a lack of external validation remains. For external validation to be accomplished, better patient clinical annotations, omic data and biosample sharing practices, and harmonisation are needed [10,11]. Finally, peptide-based endotypes have been identified in previous studies, including low tissue turnover, structural damage and systemic inflammation endotypes [13];

however, we are currently unable to compare these endotypes with those found in our study. Modelling approaches, biomolecules and omic data examined, and cohort sample characteristics can all impact endotype signatures and associated molecular mechanisms, and must be similar for appropriate comparisons.

Overall, using our novel modelling framework, we were able to unravel some heterogeneity of a sample of late-stage surgical patients with KOA and evaluate post-TKA response classification. We anticipate this methodological approach will aid in understanding underlying molecular contributors and pathways to clusters of patients with OA, and define molecular signatures contributing to intervention response. We wish to emphasise that this is the first step in our approach to complex multiomic data integration to understand patient subsets in OA. We provide the framework and methodology for additional molecular, clinical, sociodemographic, anthropometric and psychosocial variables to be included to refine patient clustering and response classification modelling performance to ultimately help in shared patient–clinician decision making for proceeding with selected therapies, including TKA for KOA, improving precision medicine and aiding in subject selection criteria for future clinical trial designs.

Competing interests

We declare no competing interests.

Acknowledgements

Authors would like to thank the clinical research team within the Division of Orthopedics and members of the Buchan Arthritis Center at the Schroeder Arthritis Institute for their assistance in study recruitment. We also thank Dr Max Kotlyar for his assistance during initial discussions related to the study.

Contributors

JSR, DS, OEG, KH, AS, YRR, AVP, RG and MK conceptualised the study. NNM, K Syed, AVP, YRR, RG and MK supervised patient data and biofluid collection. KP managed biofluid and patient data storage. JSR, DS, OEG, KH, AS, CP, IJ, K Sundararajan, SSL, YRR, AVP, RG and MK processed and curated the data. JSR, DS, OEG, KH, AS, CP, PP, NF, IJ and MK created the methodology and validated the data. DS developed the deep learning and ML algorithms. DS, OEG and KH performed statistical analyses. JSR, DS, CP, IJ and MK created figures and tables. JSR, DS, KH, AS, CP and MK wrote the manuscript. MK supervised and acquired funding for multiomic analysis. All authors had full access to the study data, were involved in manuscript editing, and were responsible for the decision to submit for publication. JSR, DS, OEG, KH, AS and MK are guarantors of the manuscript.

Funding

Funding for this project was provided by the Canada Research Chairs Program (#950-232237, MK), Tony and Shari Fell Platinum Chair in Arthritis Research (MK), Campaign to Cure Arthritis, and University Health Network Foundation. AVP is supported by the Arthritis Society Canada STAR Award-20-0000000012, and YRR is supported by J. Bernard Gosevitz Chair in Arthritis Research at University Health Network. Computational analysis was supported in part by funding from Natural Sciences and Engineering Research Council of Canada (NSERC RGPIN-2024-04314), Canada Foundation for Innovation (CFI #225404, #30865), and Ontario Research Funds (RDI #34876, RE010-020). The funders had no role in study design, data collection and analysis, decision to publish, or preparation of the manuscript.

Ethics approval

Biofluids and patient data were collected from each patient under informed consent and with approval of the Research Ethics Board at University Health Network under REB approval numbers 07-0383-BE and 14-7592-AE.

Patient consent for publication

Not Applicable.

Provenance and peer review

Not comissioned and externally peer-reviewed.

Data availability statement

Deidentified subject primary miRNA sequencing datasets are available on the Gene Expression Omnibus under accession number GSE222979 [41]. Software code and the dataset of processed miRNA counts, metabolite concentrations and demographic, anthropometric and clinical questionnaire responses used in this study is available at https://github.com/divya031090/DeepLearning_KOA [42].

Supplementary materials

Supplementary material associated with this article can be found in the online version at doi:10.1016/j.ard.2025.01.012.

REFERENCES

[1] Long H, Liu Q, Yin H, Wang K, Diao N, Zhang Y, et al. Prevalence trends of site-specific osteoarthritis from 1990 to 2019: findings from the global burden of disease study 2019. Arthritis Rheumatol 2022;74(7):1172–83.
[2] Hunter DJ, Bierma-Zeinstra S. Osteoarthritis. Lancet 2019;393(10182):1745–59.
[3] Bierma-Zeinstra SMA, Verhagen AP. Osteoarthritis subpopulations and implications for clinical trial design. Arthritis Res Ther 2011;13(2):213.
[4] Dell'Isola A, Allan R, Smith SL, Marreiros SS, Steultjens M. Identification of clinical phenotypes in knee osteoarthritis: a systematic review of the literature. BMC Musculoskelet Disord 2016;17(1):425.
[5] Deveza LA, Melo L, Yamato TP, Mills K, Ravi V, Hunter DJ. Knee osteoarthritis phenotypes and their relevance for outcomes: a systematic review. Osteoarthritis Cartilage 2017;25(12):1926–41.
[6] Beswick AD, Wylde V, Gooberman-Hill R, Blom A, Dieppe P. What proportion of patients report long-term pain after total hip or knee replacement for osteoarthritis? A systematic review of prospective studies in unselected patients. BMJ Open 2012;2(1):e000435.
[7] Xie F, Lo NN, Pullenayegum EM, Tarride JE, O'Reilly DJ, Goeree R, et al. Evaluation of health outcomes in osteoarthritis patients after total knee replacement: a two-year follow-up. Health Qual Life Outcomes 2010;8:87.
[8] Lopez-Olivo MA, Landon GC, Siff SJ, Edelstein D, Pak C, Kallen MA, et al. Psychosocial determinants of outcomes in knee replacement. Ann Rheum Dis 2011;70(10):1775–81.
[9] Voskuilen R, Boonen B, Tilman P, Schotanus M, Most J. Demographics are no clinically relevant predictors of patient-reported knee osteoarthritis symptoms - comprehensive multivariate analysis. J Orthop 2023;35:85–92.
[10] Ramos YFM, Rice SJ, Ali SA, Pastrello C, Jurisica I, Rai MF, et al. Evolution and advancements in genomics and epigenomics in OA research: how far we have come. Osteoarthritis Cartilage 2024;32(7):858–68.
[11] Rai MF, Collins KH, Lang A, Maerz T, Geurts J, Ruiz-Romero C, et al. Three decades of advancements in osteoarthritis research: insights from

transcriptomic, proteomic, and metabolomic studies. Osteoarthritis Cartilage 2024;32(4):385–97.
[12] Nielsen RL, Monfeuga T, Kitchen RR, Egerod L, Leal LG, Schreyer ATH, et al. Data-driven identification of predictive risk biomarkers for subgroups of osteoarthritis using interpretable machine learning. Nat Commun 2024 Apr 1;15 (1):2817.
[13] Angelini F, Widera P, Mobasheri A, Blair J, Struglics A, Uebelhoer M, et al. Osteoarthritis endotype discovery via clustering of biochemical marker data. Ann Rheum Dis 2022 May;81(5):666–75.
[14] Werdyani S, Liu M, Zhang H, Sun G, Furey A, Randell EW, et al. Endotypes of primary osteoarthritis identified by plasma metabolomics analysis. Rheumatology (Oxford) 2021;60(6):2735–44.
[15] Rockel JS, Layeghifard M, Rampersaud YR, Perruccio AV, Mahomed NN, Davey JR, et al. Identification of a differential metabolite-based signature in patients with late-stage knee osteoarthritis. Osteoarthr Cartil Open 2022;4 (3):100258.
[16] Ali SA, Espin-Garcia O, Wong AK, Potla P, Pastrello C, McIntyre M, et al. Circulating microRNAs differentiate fast-progressing from slow-progressing and non-progressing knee osteoarthritis in the Osteoarthritis Initiative cohort. Ther Adv Musculoskelet Dis 2022;14 1759720X221082917.
[17] Li YH, Tavallaee G, Tokar T, Nakamura A, Sundararajan K, Weston A, et al. Identification of synovial fluid microRNA signature in knee osteoarthritis: differentiating early- and late-stage knee osteoarthritis. Osteoarthritis Cartilage 2016;24(9):1577–86.
[18] Ali SA, Gandhi R, Potla P, Keshavarzi S, Espin-Garcia O, Shestopaloff K, et al. Sequencing identifies a distinct signature of circulating microRNAs in early radiographic knee osteoarthritis. Osteoarthritis Cartilage 2020;28(11):1471–81.
[19] Beyer C, Zampetaki A, Lin NY, Kleyer A, Perricone C, Iagnocco A, et al. Signature of circulating microRNAs in osteoarthritis. Ann Rheum Dis 2015 Mar;74 (3):e18.
[20] Lin X, Tian T, Wei Z, Hakonarson H. Clustering of single-cell multi-omics data with a multimodal deep learning method. Nat Commun 2022;13 (1):7705.
[21] Kopf A, Fortuin V, Somnath VR, Claassen M. Mixture-of-experts variational autoencoder for clustering and generating from similarity-based representations on single cell data. PLoS Comput Biol 2021;17(6):e1009086.
[22] Rong Z, Liu Z, Song J, Cao L, Yu Y, Qiu M, et al. MCluster-VAEs: An end-to-end variational deep learning-based clustering method for subtype discovery using multi-omics data. Comput Biol Med 2022;150:106085.
[23] Sandhu A, Espin-Garcia O, Rockel JS, Lively S, Perry K, Mohamed NN, et al. Association of synovial fluid and urinary C2C-HUSA levels with surgical outcomes post-total knee arthroplasty. Osteoarthritis Cartilage 2024;32(1):98–107.
[24] Altman R, Asch E, Bloch D, Bole G, Borenstein D, Brandt K, et al. Development of criteria for the classification and reporting of osteoarthritis. Classification of osteoarthritis of the knee. Diagnostic and Therapeutic Criteria Committee of the American Rheumatism Association. Arthritis Rheum 1986;29(8):1039–49.
[25] Bellamy N, Buchanan WW, Goldsmith CH, Campbell J, Stitt LW. Validation study of WOMAC: a health status instrument for measuring clinically important patient relevant outcomes to antirheumatic drug therapy in patients with osteoarthritis of the hip or knee. J Rheumatol 1988;15 (12):1833–40.
[26] Zigmond AS, Snaith RP. The hospital anxiety and depression scale. Acta Psychiatr Scand 1983;67(6):361–70.
[27] Freynhagen R, Baron R, Gockel U, Tölle TR. painDETECT: a new screening questionnaire to identify neuropathic components in patients with back pain. Curr Med Res Opin 2006;22(10):1911–20.
[28] Dworkin RH, Turk DC, Wyrwich KW, Beaton D, Cleeland CS, Farrar JT, et al. Interpreting the clinical importance of treatment outcomes in chronic pain clinical trials: IMMPACT recommendations. J Pain 2008;9(2):105–21.
[29] Conaghan PG, Dworkin RH, Schnitzer TJ, Berenbaum F, Bushmakin AG, Cappelleri JC, et al. WOMAC meaningful within-patient change: results from 3 studies of tanezumab in patients with moderate-to-severe osteoarthritis of the hip or knee. J Rheumatol 2022 Jun;49(6):615–21.
[30] Potla P, Ali SA, Kapoor M. A bioinformatics approach to microRNA-sequencing analysis. Osteoarthr Cartil Open 2021;3(1):100131.
[31] van den Berg RA, Hoefsloot HCJ, Westerhuis JA, Smilde AK, van der Werf MJ. Centering, scaling, and transformations: improving the biological information content of metabolomics data. BMC Genomics 2006;7:142.
[32] Hauschild AC, Pastrello C, Ekaputeri GKA, Bethune-Waddell D, Abovsky M, Ahmed Z, et al. MirDIP 5.2: tissue context annotation and novel microRNA curation. Nucleic Acids Res 2023;51(D1):D217–25.
[33] Pastrello C, Kotlyar M, Abovsky M, Lu R, Jurisica I. PathDIP 5: improving coverage and making enrichment analysis more biologically meaningful. Nucleic Acids Res 2024;52(D1):D663–71.
[34] Brown KR, Otasek D, Ali M, McGuffin MJ, Xie W, Devani B, et al. NAViGaTOR: network analysis, visualization and graphing Toronto. Bioinformatics 2009;25(24):3327–9.
[35] Fernández-de-Las-Peñas C, Florencio LL, de-la-Llave-Rincon AI, Ortega-Santiago R, Cigaran-Mendez M, Fuensalida-Novo S, et al. Prognostic factors for postoperative chronic pain after knee or hip replacement in patients with knee or hip osteoarthritis: an umbrella review. J Clin Med 2023;12(20):6624.
[36] Allesøe RL, Lundgaard AT, Hernández Medina R, Aguayo-Orozco A, Johansen J, Nissen JN, et al. Discovery of drug-omics associations in type 2 diabetes with generative deep-learning models. Nat Biotechnol 2023;41(3):399–408.
[37] Carilli M, Gorin G, Choi Y, Chari T, Pachter L. Biophysical modeling with variational autoencoders for bimodal, single-cell RNA sequencing data. Nat Methods 2024;21(8):1466–9.
[38] Doncevic D, Herrmann C. Biologically informed variational autoencoders allow predictive modeling of genetic and drug-induced perturbations. Bioinformatics 2023;39(6):btad387.
[39] Li M, Guo H, Wang K, Kang C, Yin Y, Zhang H. AVBAE-MODFR: A novel deep learning framework of embedding and feature selection on multi-omics data for pan-cancer classification. Comput Biol Med 2024;177:108614.
[40] Badgeley MA, Zech JR, Oakden-Rayner L, Glicksberg BS, Liu M, Gale W, et al. Deep learning predicts hip fracture using confounding patient and healthcare variables. NPJ Digit Med 2019;2:31.
[41] Rockel JS, Sharma D, Espin-Garcia O, Hueniken K, Sandhu A, Pastrello C, et al. Data From: deep learning-based multimodal clustering model for endotyping and post-arthroplasty response classification using knee osteoarthritis subject-matched multi-omic data [Internet]. Gene Expression Omnibus (GSE222979) 2024 [cited 2024 Dec 29]. Available from: https://www.ncbi.nlm.nih.gov/geo/query/acc.cgi?acc=GSE222979.
[42] Rockel JS, Sharma D, Espin-Garcia O, Hueniken K, Sandhu A, Pastrello C, et al. Data and Code From: Deep learning-based multimodal clustering model for endotyping and post-arthroplasty response classification using knee osteoarthritis subject-matched multi-omic data [Internet]. Github 2024 [cited 2024 May 30]. Available from: https://github.com/divya031090/DeepLearning_KOA.

Ann Rheum Dis 84 (2025) 856−865

Contents lists available at ScienceDirect

Annals of the Rheumatic Diseases

journal homepage: https://www.sciencedirect.com/journal/annals-of-the-rheumatic-diseases

Osteoarthritis

Efficacy, safety and tolerability of GSK3858279, an anti-CCL17 monoclonal antibody and analgesic, in healthy volunteers and patients with knee osteoarthritis pain: a phase I, randomised, double-blind, placebo-controlled, proof-of-mechanism and proof-of-concept study

Jagtar Singh Nijjar[1], Katharine Abbott-Banner[2], Yolanda Alvarez[2], Nicola Aston[1], Damon Bass[3], Jane H. Bentley[2], Joanne Ellis[1], Christian Ellson[1], Edward C. Emery[1], Maria Feeney[1], Disala Fernando[4], David Inman[1], Rejbinder Kaur[1], Louise K. Modis[1], Sam Munoz Vicente[1], Catherine Muya[1], Kiran Nistala[1], Eirini Panoilia[1], Riju Ray[5,*], Sarah Siederer[1], Julia E. Smith[1], Lucinda Weir[1], Nicolas Wisniacki[1]

[1] GSK, Stevenage, Hertfordshire, UK
[2] GSK, Brentford, Middlesex, UK
[3] GSK, Upper Providence, Pennsylvania, USA
[4] GSK, Cambridge, Cambridgeshire, UK
[5] GSK, Research Triangle Park, North Carolina, USA

A R T I C L E   I N F O

Article history:
Received 18 December 2023
Accepted 23 September 2024

Keywords:
Osteoarthritis
Chemokines
Therapeutics

A B S T R A C T

Objectives: The objective of this study was to evaluate efficacy, safety and tolerability of the first-in-class, anti-CCL17 monoclonal antibody, GSK3858279, in treating knee osteoarthritis (OA) pain.
Methods: This was a phase I, randomised, placebo-controlled, two-part, proof-of-mechanism and proof-of-concept study. In part A, healthy participants were randomised 3:1 to receive GSK3858279 as either single intravenous (0.1−10 mg/kg) doses, a subcutaneous (3 mg/kg up to 240 mg maximum) dose, or placebo, to evaluate safety and tolerability. In part B, participants with knee OA pain were randomised 1:1 to receive weekly subcutaneous 240 mg GSK3858279, or placebo, for 8 weeks, to assess safety and change from baseline (CFB) in average and worst knee pain intensity. Exploratory endpoints included CFB in Western Ontario and McMaster Universities Osteoarthritis Index (WOMAC) pain, function and stiffness scores.
Results: GSK3858279 demonstrated greater median CFB (95% credible interval (CrI)) in average and worst knee pain intensity versus placebo (average, −1.18 (−2.15, −0.20); worst, −1.09 (−2.29, 0.12)) at week 8. Median CFB (95% CrI) for GSK3858279 versus placebo in WOMAC pain and function scores were −1.41 (−2.35, −0.46) and −1.29 (−2.28, −0.29), respectively, at week 8. Overall, 72% (26/36; part A) and 88% (21/24; part B) of participants receiving

* **Correspondence to** Dr. Riju Ray.
E-mail address: riju.x.ray@gsk.com (R. Ray).
Handling editor Josef S. Smolen

https://doi.org/10.1136/ard-2023-225434

GSK3858279 experienced adverse events (AEs); with nasopharyngitis being the most common in part A and injection site reactions in part B. No serious AEs or deaths were observed.
Conclusion: GSK3858279 improved pain intensity and WOMAC pain and function scores in adults with knee OA pain and demonstrated favourable safety and tolerability in both healthy participants and adults with knee OA pain.

WHAT IS ALREADY KNOWN ON THIS TOPIC

- C-C motif chemokine ligand 17 (CCL17) is a chemokine involved in immune cell chemotaxis and mediating pain along the peripheral nociceptive pathway through interaction with the G-protein-coupled C-C motif chemokine receptor type 4 (CCR4).
- Current treatment options for chronic pain in patients with osteoarthritis (OA) include non-steroidal anti-inflammatory drugs (NSAIDs) and opioids. These treatments are often associated with inadequate response and undesirable side effects.
- There is a growing need for analgesics that are both safe and effective, with fewer side effects, to manage chronic pain in patients with OA.

WHAT THIS STUDY ADDS

- GSK3858279 is a first-in-class, non-opioid, non-NSAID, high-affinity, peripherally acting, human monoclonal antibody that binds CCL17 to block CCL17-mediated CCR4 signalling.
- GSK3858279 met the primary endpoint by improving average and worst knee pain intensity and demonstrated a favourable safety and tolerability profile in adults with knee OA pain. GSK3858279 also met the exploratory endpoints by improving Western Ontario and McMaster Universities Osteoarthritis Index pain and function scores.

HOW THIS STUDY MIGHT AFFECT RESEARCH, PRACTICE OR POLICY

- The results of this phase I study warrant further investigation of the efficacy and safety of GSK3858279 for treating chronic pain in adults with OA.

INTRODUCTION

Osteoarthritis (OA) is the most common form of arthritis among adults worldwide, impacting approximately 595 million individuals globally in 2020 [1]. Pain is regarded as the defining symptom of OA and contributes to OA-associated functional limitations and a reduced quality of life [2]. In a study of 2170 patients with knee and/or hip OA in the USA and Europe, approximately half of the patients reported moderate or severe pain, which impacted daily life, including impaired work productivity and activity [3]. Common themes among patients with knee OA pain and their caregivers included the emotional and social effects of the condition, as well as a tendency for pain related to OA and its management to dominate their daily lives [4].

C-C motif chemokine ligand 17 (CCL17) is a chemokine principally involved in immune cell chemotaxis and has been implicated in the development of pain through interaction with C-C motif chemokine receptor type 4 (CCR4) in mice [5,6]. Inhibition of CCL17 reduces pain and joint disease in murine models of inflammatory pain, with the mechanism of action yet to be fully elucidated. An unmet need exists for safe and effective analgesics with an acceptable tolerability profile, to treat chronic pain in patients with OA [7,8]. Current treatment options to relieve chronic OA pain include non-steroidal anti-inflammatory drugs (NSAIDs) and opioids. Often, these treatments are insufficient due to inadequate response and undesirable side effects; NSAIDs are associated with an increased risk of gastrointestinal disorders, and cardiovascular and renal side effects, while opioids elevate the risk of side effects including constipation, dizziness, fractures, drowsiness and insomnia, among others [9−12]. Prescription opioids may also be misused, have a dependency risk and represent a potential mortality risk [12,13]. CCL17, thus, represents a potential therapeutic target to control OA pain and a possible option to address the unmet need for safe and effective analgesics to treat chronic pain in patients with OA.

GSK3858279 is a first-in-class, non-opioid, non-NSAID, high-affinity, peripherally acting human monoclonal antibody that binds to CCL17 and prevents downstream signalling via its receptor, CCR4. The primary objectives of this two-part, first-in-human, proof-of-mechanism and proof-of-concept study were to evaluate the safety and tolerability of GSK3858279 in healthy participants (part A) and patients with knee OA pain (part B), and to assess changes in pain among patients with knee OA (Part B).

METHODS

Study design

This was a phase I, randomised, multicentre, double-blind, placebo-controlled, two-part study conducted from May 2018 to September 2022 (NCT03485365). Data from participants in part A (healthy participants) and B (patients with knee OA pain) were collected at clinical units across the UK, Germany and Poland. Part A evaluated the safety, tolerability, pharmacokinetics (PK), immunogenicity and target engagement of either a single ascending intravenous, or single subcutaneous (SC), dose of GSK3858279 in healthy participants (online supplemental figure S1). Single ascending doses of GSK3858279 were administered to six cohorts of healthy participants; in each cohort, eight participants were randomised 3:1 to GSK3858279 or placebo (see online supplement for further randomisation information). The evaluated dose range was from 0.1 mg/kg to 10 mg/kg via 1-hour intravenous infusion in cohorts 1−5; while cohort 6 received a dose of 3 mg/kg (up to a maximum of 240 mg) through SC injections. The follow-up duration was determined based on the predicted exposure for each dose level (range of 85−141 days).

Part B evaluated the efficacy, safety, tolerability, PK, target engagement and immunogenicity of weekly SC GSK3858279 or placebo for 8 weeks (with a 12-week follow-up period) in adult patients with knee OA pain (figure 1). Patients were randomised 1:1 to receive 240 mg of GSK3858279, administered as 4 successive 1.2 mL SC injections (50 mg/mL) weekly (QW), or SC QW placebo (saline (0.9% sodium chloride)). Coprimary efficacy endpoints were assessed at the end of the treatment period (week 8). Pain medication was prohibited from day −10 to day 71 (week 10) (excluding paracetamol ≤3 g/day for use as rescue medication at any time during the study, except 24 hours before a clinical visit). Patients completed a daily pain Numerical

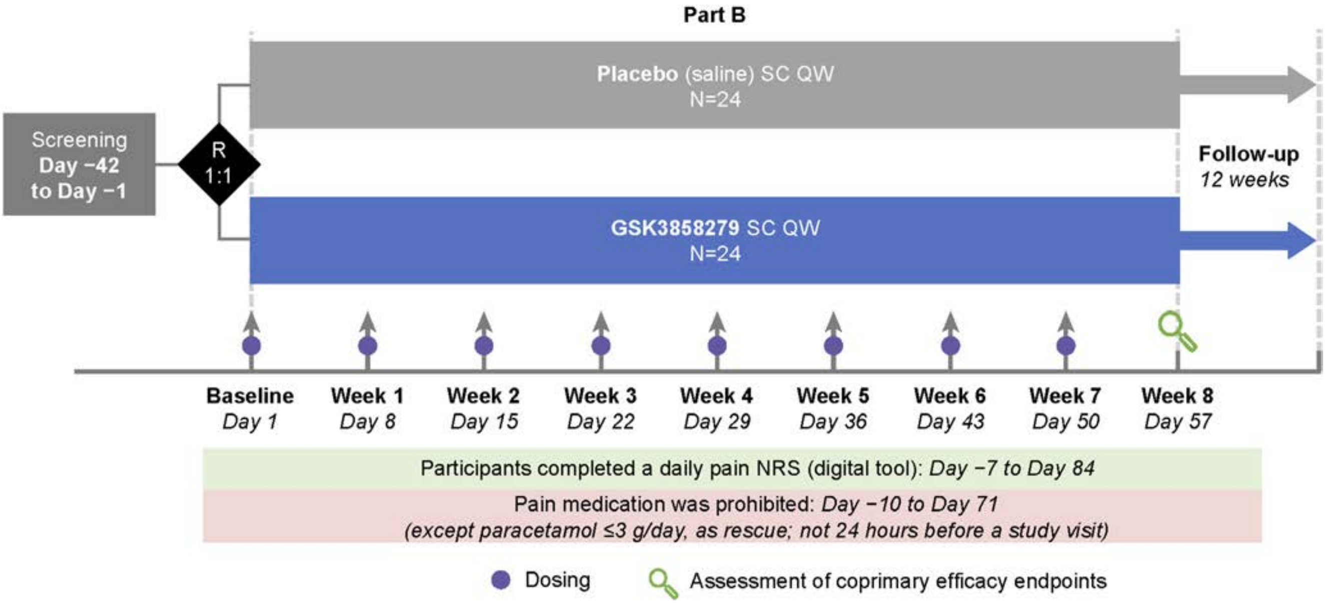

Figure 1. Part B study design. NRS, Numerical Rating Scale; QW, weekly; R, randomisation; SC, subcutaneous.

Rating Scale ((NRS); digital tool) assessing average and worst knee pain from day −7 to day 84 (week 12) on an 11-point scale from 0 to 10, with 0 equating to 'no pain' and 10 equating to 'worst pain and/or difficulty' imaginable. Western Ontario and McMaster Universities Osteoarthritis Index (WOMAC) pain, function and stiffness questionnaires were collected weekly until the end of the follow-up period (week 20).

Participants

In part A, healthy adult participants aged 18–65 years with a body weight of 50–100 kg and body mass index (BMI) of 18–32 kg/m^2 were included if they were either non-smokers or former smokers (cut-off within 6 months prior to screening). In part B, male and female patients with OA of the knee (defined as symptoms for ≥6 months and a clinical diagnosis per American College of Rheumatology criteria) [14] aged 40–75 years and with a BMI of 19–34.9 kg/m^2 were included. Patients were required to have an average daily pain score in the index knee of ≥4 to ≤9 per the 11-point NRS (indicative of moderate-to-severe pain) for the 7 days prior to dosing and a Kellgren and Lawrence (KL) score of ≥2 assessed by X-ray. Patients with a history of insufficient pain relief from, or intolerance to, oral NSAIDs were eligible. See online supplement for further inclusion/exclusion criteria.

Endpoints

The coprimary efficacy endpoints for part B were the change from baseline in (a) average and (b) worst index knee pain intensity at week 8 (per the 11-point NRS) in the intention-to-treat (ITT) population. The primary safety endpoints for parts A and B were the incidence of adverse events (AEs), clinical laboratory measurements (haematology, clinical chemistry and urinalyses), 12-lead ECGs, vital signs (reported from baseline to week 20) and serious AEs (SAEs) in the safety population. Additional endpoints for parts A and B included GSK3858279 PK concentrations and derived parameters (PK population) and free and total CCL17 levels in serum (reported from baseline to week 20; safety population). Exploratory endpoints in parts A and B included the incidence of GSK3858279 antidrug antibodies ((ADAs); reported from baseline to week 20; safety population). Exploratory endpoints in part B included the change from baseline in WOMAC pain, function and stiffness scores (11-point NRS reported from baseline to week 8 and during the follow-up period up to week 20; ITT population; part B).

Populations

The safety and ITT populations included all randomised participants who received at least one dose of the study treatment. The PK population was based on the treatment each participant received and included all participants in the safety population who had at least one reportable serum PK assessment.

Statistical analyses

The sample size for part A was based on a sufficient number of patients needed to assess safety, pharmacokinetics and immunogenicity evaluation. In part B, the planned sample size of approximately 50 participants was chosen to give a 75% probability of declaring a positive conclusion when the true treatment difference in pain NRS score is −1, and >80% probability of declaring a negative conclusion if the true treatment difference is 0, assuming an SD of 1.8, where a more negative value denotes a greater analgesic response. A positive conclusion was to be declared for part B if there was ≥90% probability that the treatment difference versus placebo was better than 0; a negative conclusion was to be declared if there was ≥85% probability that the difference versus placebo was worse than −1.

For parts A and B, AEs, SAEs, clinical laboratory measurements (haematology, clinical chemistry and urinalyses), 12-lead ECGs and vital signs were summarised using descriptive statistics.

For part A, a non-compartmental analysis (NCA) was performed (WinNonlin, V.8.1.0.3530) to estimate the systemic exposure to GSK3858279 expressed as the maximum concentration (C_{max}) and the area under the curve (AUC). NCA is a model-independent method that is less complex and requires fewer assumptions about body compartments than a compartmental PK analysis. An NCA relies almost exclusively on simple algebraic equations to estimate PK parameters directly from the observed concentration-time data [15–17]. PK parameters

(C_{max} and AUC) were summarised descriptively by treatment. Dose proportionality was assessed for the C_{max} and AUC using a log-linear power model, which is a linear regression model of the log of the PK parameters and the log of the dose.

For part B, a Bayesian repeated-measures model using non-informative priors (adjusting for treatment, week, baseline, as well as the treatment-by-week and baseline-by-week interactions) was fitted to the efficacy change from baseline data from week 1 to week 8. Medians and 95% credible intervals (CrI) for treatment differences were calculated. Total GSK3858279 and CCL17 parameters in participants with OA of the knee were predicted from a population pharmacokinetic/target engagement model developed from time-matched serum concentrations of total GSK3858279 and total CCL17 using non-linear mixed effects modelling with the currently supported version of NON-linear Mixed Effects Modeling software (V.7.4).

Patient and public involvement

Patients were involved in the design of this study through consultation interviews.

RESULTS

Participant disposition

In part A, of the 49 healthy participants who were randomised, 2 were withdrawn due to protocol deviations (equipment failure for one participant receiving placebo and out of visit window for one participant receiving 3 mg/kg intravenous GSK3858279) (online supplemental figure S2). In part B, of the 214 patients screened, 48 (22%) were enrolled and randomised (patients were from Germany (n = 25, 52%); UK (n = 18, 38%); Poland (n = 5, 10%)) (figure 2). Two patients who received placebo were withdrawn from study treatment due to AEs.

Baseline characteristics

Baseline characteristics for parts A and B are summarised in table 1. Participants were predominantly male (part A, 88%; part B, 56%) and white (part A, 92%; part B, 98%). The median (range) age of healthy participants in part A was 47 (28−66) years and the median (range) BMI was 25.8 (20−31) kg/m^2. The baseline characteristics of patients in part B were relatively balanced between treatment arms, but more patients were male in the GSK3858279 arm (n = 16 (67%) vs n = 11 (46%) in the placebo arm) and more patients in the GSK3858279 arm had a grade 4 KL score (n = 8 (33%) vs n = 4 (17%) in the placebo arm).

Efficacy in knee OA pain (part B only)

GSK3858279 was associated with a greater change from baseline in both average (figure 3A) and worst (figure 3B) index knee pain intensity scores versus placebo. At week 8, the median difference (95% CrI) in change from baseline for patients receiving GSK3858279 versus placebo for (a) average knee pain intensity was −1.18 (−2.15, −0.20) (probability (true difference<0) >99%; probability (true difference <−0.6) = 88%) and (b) worst knee pain intensity was −1.09 (−2.29, 0.12) (probability (true difference<0) = 96%; probability (true difference <−0.6) = 79%).

Patients who received GSK3858279 had an increased improvement in WOMAC pain and function scores compared with those who received placebo at all post-baseline time points up to and including week 8 (figure 4A,B). At week 8, the median difference (95% CrI) in change from baseline for patients receiving GSK3858279 versus placebo for (a) WOMAC pain score was −1.41 (−2.35, −0.46) (probability of true difference: >99%; <−0.6 = 95%) and (b) WOMAC function score was −1.29 (−2.28, −0.29) (probability of true difference: >99%; <−0.6 = 91%). Numerical differences between treatment groups were observed in WOMAC stiffness scores; at week 8, the median difference (95% CrI) in change from baseline WOMAC stiffness score for patients receiving GSK3858279 versus placebo was −0.57 (−1.71, 0.55) (probability of true difference: <0 = 85%) (figure 4C).

Prior and concomitant medications are shown in table 1 and online supplemental table 1, respectively. In part B, 42% (n = 10/24) of patients receiving GSK3858279 and 29% (n = 7/24) of patients receiving placebo were taking rescue medication (paracetamol) for ≥1 day at baseline. At week 8, 25% (n = 6) and 5% (n = 1) of patients receiving GSK3858279 and placebo, respectively, reported taking paracetamol as rescue medication for ≥1 day. Post hoc sensitivity analyses demonstrated that the overall efficacy signal observed in the study was not an artefact of the reported use of rescue medication (data are not shown).

Safety

No SAEs or deaths were reported in this study. No safety signals were observed for haematology, clinical chemistry or urinalysis, and no clinically relevant changes in vital signs (systolic blood pressure, diastolic blood pressure and heart rate) were detected. In addition, no clinically significant ECG abnormalities were noted.

A summary of treatment-emergent AEs for parts A and B is provided in table 2. All doses of GSK3858279 in part A were administered by intravenous infusion except for the SC 3 mg/kg group. Of the 49 healthy participants recruited, 38 (78%) reported any treatment-emergent AE (GSK3858279: intravenous 0.1 mg/kg, n = 2/6 (33%); intravenous 0.3 mg/kg, n = 2/6 (33%); intravenous 1 mg/kg, n = 4/6 (67%); intravenous 3 mg/kg, n = 6/6 (100%); intravenous 10 mg/kg, n = 6/6 (100%); SC 3 mg/kg, n = 6/6 (100%); intravenous placebo n = 12/13 (92%)). The most common AE across all GSK3858279 treatment arms in part A was nasopharyngitis (n = 7/36; 19%), followed by contact dermatitis (n = 6/36; 17%) and headache (n = 4/36; 11%). The most common AEs in the placebo group were headache (n = 3/13, 23%), nasopharyngitis (n = 3/13, 23%) and contact dermatitis (2/13, 15%). A total of three participants in part A (6%) reported at least one treatment-related AE, determined by the investigator, while receiving GSK3858279 and none of the AEs led to treatment discontinuation.

In part B, weekly doses of 240 mg GSK3858279 showed a favourable safety profile over 8 weeks. Of the 48 participants in the safety population, 36 (75%) had any treatment-emergent AE (GSK3858279, n = 21 (88%); placebo, n = 15 (63%)). The most common AE reported in the placebo group was headache (n = 5/24, 21%), while the most common AEs reported in the GSK3858279 group were injection site reactions (ISR; n = 10/24, 42%) and arthralgia (n = 3/24, 16%) (table 2). In the placebo group, 13% (n = 3/24) of patients experienced ISRs with 4 events, compared with 42% (n = 10/24) of patients in the GSK3858279 group, with 24 events; all ISRs were mild and recovered fully without the need for dose changes. One patient who received GSK3858279 reported 11 ISRs (out of a possible 32 site injections), accounting for 46% of all ISRs. In part B, two patients (8%) from the placebo group discontinued due to AEs; however, no patients in the GSK3858279 group discontinued treatment due to AEs.

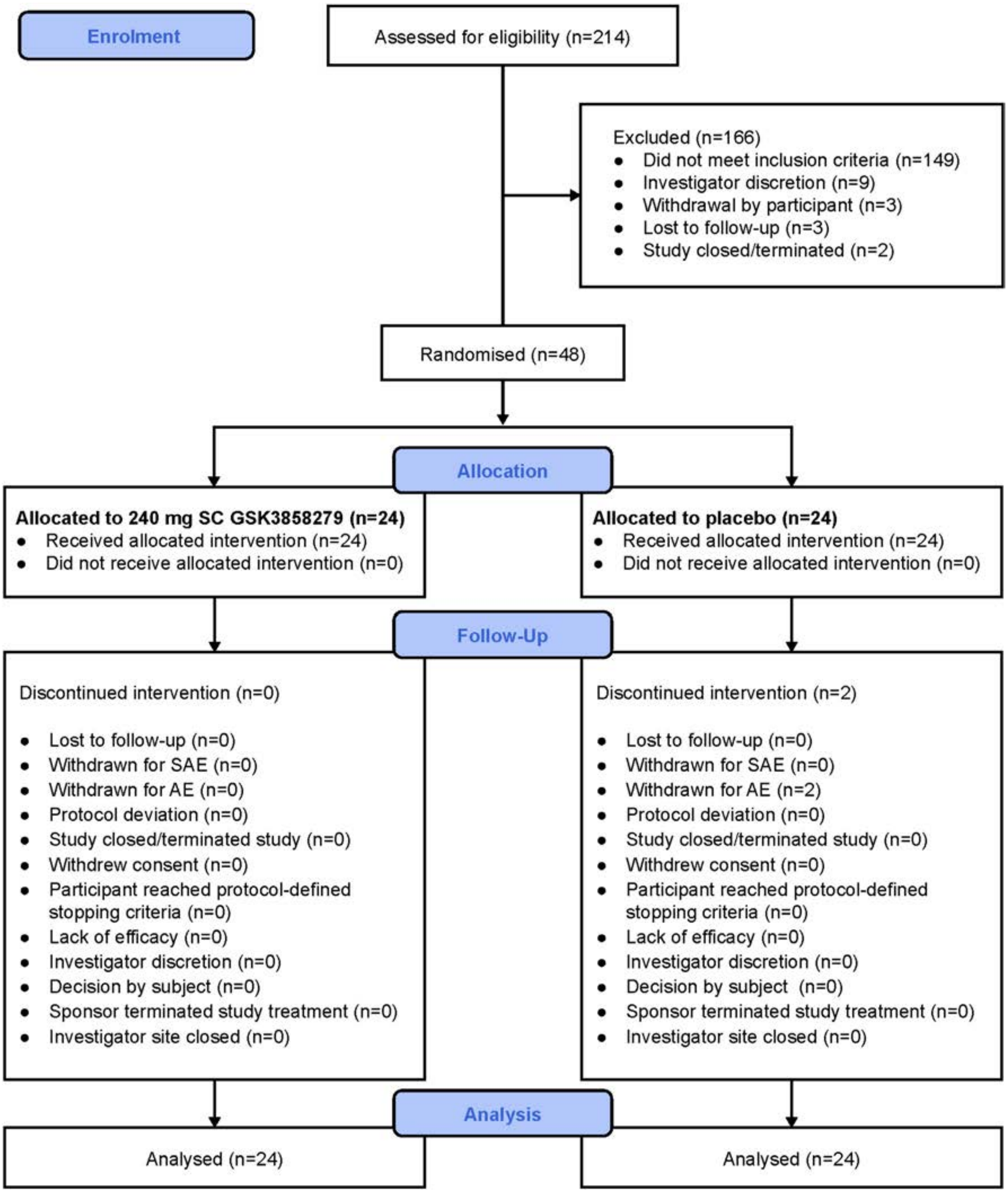

Figure 2. CONSORT diagram (part B). AE, adverse event; CONSORT, consolidated standards of reporting trials; SAE, serious adverse event; SC, subcutaneous.

PK, target engagement and immunogenicity

In part A, systemic exposure to GSK3858279 (C_{max} (maximum concentration of GSK3858279) and AUC increased in an approximately dose-proportional manner with increasing intravenous doses. There appeared to be saturation of CCL17 at all GSK3858279 doses within 1-day postdose, with prolonged reductions in free CCL17 achieved with increasing doses (based on the semiquantitative free target assay). In part A, 2 of 36 (6%) healthy participants in the GSK3858279 arm (1 each in the 1 mg/kg intravenous and 3 mg/kg SC dose arms) were confirmed positive for ADAs, which were considered treatment-emergent ADAs. No participants were positive for ADAs in the placebo arm.

In part B, large percentage reductions in free CCL17 relative to baseline were observed from baseline to week 8 (based on the semiquantitative free target assay) and were maintained over the weekly dosing interval following SC administration. In part B, 5 of 24 (21%) participants in the treatment arm were positive for ADAs, which were considered treatment-emergent ADAs. In the placebo arm, 1 of 24 (4%) participants were positive for ADAs, which were considered not related to treatment and likely non-specific. No safety, efficacy or PK impact was observed for participants with treatment-emergent ADAs versus those without.

DISCUSSION

The challenges associated with current OA pain therapies, such as NSAIDs and opioids, are well documented [9–12]. Nevertheless, the potential application of biologics to

Table 1
Baseline characteristics of ITT population

	Part A								Part B		
		GSK3858279									
Characteristic	Placebo (n = 13)	0.1 mg/kg IV (n = 6)	0.3 mg/kg IV (n = 6)	1 mg/kg IV (n = 6)	3 mg/kg IV (n = 6)	10 mg/kg IV (n = 6)	3 mg/kg SC (n = 6)	Total (n = 49)	Placebo (n = 24)	GSK3858279 240 mg SC (n = 24)	Total (n = 48)
Male, n (%)	13 (100)	5 (83)	6 (100)	4 (67)	6 (100)	5 (83)	4 (67)	43 (88)	11 (46)	16 (67)	27 (56)
Age, years, median (range)	47.0 (28 to 60)	52.0 (28 to 59)	40.5 (31 to 59)	56.5 (39 to 66)	36.5 (32 to 57)	47.0 (28 to 61)	47.0 (29 to 56)	47.0 (28 to 66)	59.0 (51 to 75)	58.5 (46 to 74)	59.0 (46 to 75)
Race, n (%)											
White	13 (100)	6 (100)	5 (83)	6 (100)	4 (67)	5 (83)	6 (100)	45 (92)	24 (100)	23 (96)	47 (98)
Asian	0 (0)	0 (0)	1 (17)	0 (0)	1 (17)	1 (17)	0 (0)	3 (6)	0 (0)	1 (4)	1 (2)
BMI, kg/m^2, median (range)	25.5 (20 to 29)	24.5 (20 to 30)	26.9 (20 to 30)	25.6 (25 to 30)	26.8 (23 to 30)	26.7 (23 to 29)	27.6 (24 to 31)	25.8 (20 to 31)	28.3 (24 to 35)	29.7 (23 to 34)	29.2 (23 to 35)
Kellgren and Lawrence score, n (%)											
Grade 2	N/A	N/A	N/A	N/A	N/A	N/A	N/A	N/A	12 (50)	8 (33)	20 (42)
Grade 3									8 (33)	8 (33)	16 (33)
Grade 4									4 (17)	8 (33)	12 (25)
Average knee pain intensity*, median (range)	N/A	N/A	N/A	N/A	N/A	N/A	N/A	N/A	5.5 (4.0 to 7.8)	5.3 (4.0 to 7.4)	5.3 (4.0 to 7.8)
Worst knee pain intensity*, median (range)	N/A	N/A	N/A	N/A	N/A	N/A	N/A	N/A	6.0 (4.0 to 8.0)	6.2 (4.2 to 8.6)	6.1 (4.0 to 8.6)
WOMAC pain score*, median (range)	N/A	N/A	N/A	N/A	N/A	N/A	N/A	N/A	5.3 (2.6 to 9.0)	5.5 (2.8 to 7.0)	5.4 (2.6 to 9.0)
WOMAC function score*, median (range)	N/A	N/A	N/A	N/A	N/A	N/A	N/A	N/A	5.2 (1.6 to 9.4)	5.5 (1.7 to 7.5)	5.4 (1.6 to 9.4)
WOMAC stiffness score*, median (range)	N/A	N/A	N/A	N/A	N/A	N/A	N/A	N/A	5.8 (2.0 to 9.5)	5.5 (1.0 to 9.0)	5.5 (1.0 to 9.5)
Prior medications (>5% total), n (%)											
Ibuprofen	N/A	N/A	N/A	N/A	N/A	N/A	N/A	N/A	11 (46)	5 (21)	16 (33)
Paracetamol									2 (8)	2 (8)	4 (8)
Diclofenac									1 (4)	2 (8)	3 (6)
Diclofenac sodium									2 (8)	1 (4)	3 (6)
Tramadol hydrochloride									2 (8)	1 (4)	3 (6)
Chondroitin sulfate sodium									2 (8)	0 (0)	2 (4)
Tozinameran									2 (8)	0 (0)	2 (4)
Pregabalin									1 (4)	0 (0)	1 (2)
Any concomitant medication (>5% total), n (%)	6 (46)	1 (17)	1 (17)	5 (83)	3 (50)	3 (50)	5 (83)	24 (49)	22 (92)	21 (88)	43 (90)

BMI, body mass index; ITT, intention to treat; IV, intravenous; N/A, not applicable; NRS, Numerical Rating Scale; SC, subcutaneous; WOMAC, Western Ontario and McMaster Universities Osteoarthritis Index.
*11-point NRS, where 0 is no pain/difficulty and 10 is worst imaginable pain/difficulty.

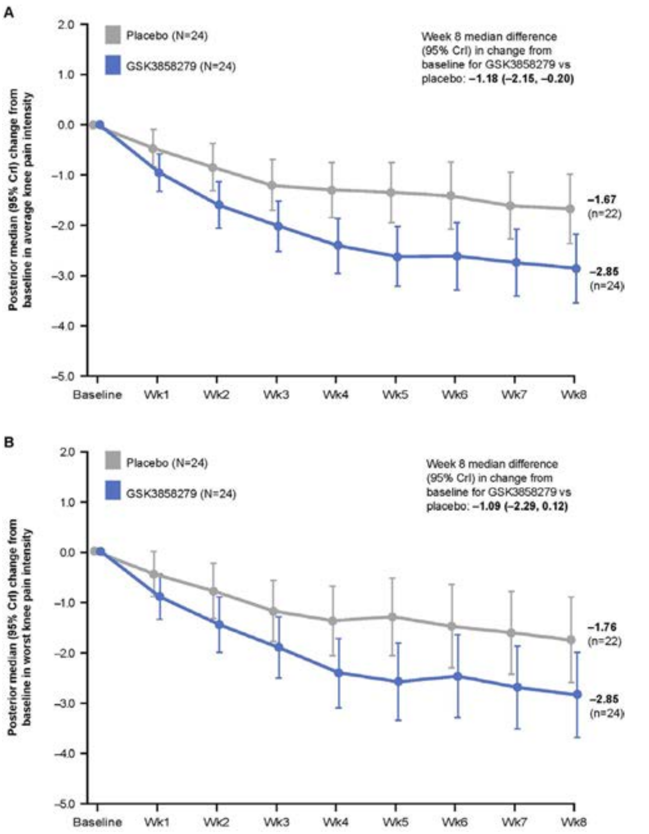

Figure 3. Coprimary endpoints in part B: change from baseline to week 8 in (A) average and (B) worst index knee pain intensity. CrI, credible interval; SC, subcutaneous; Wk, week.

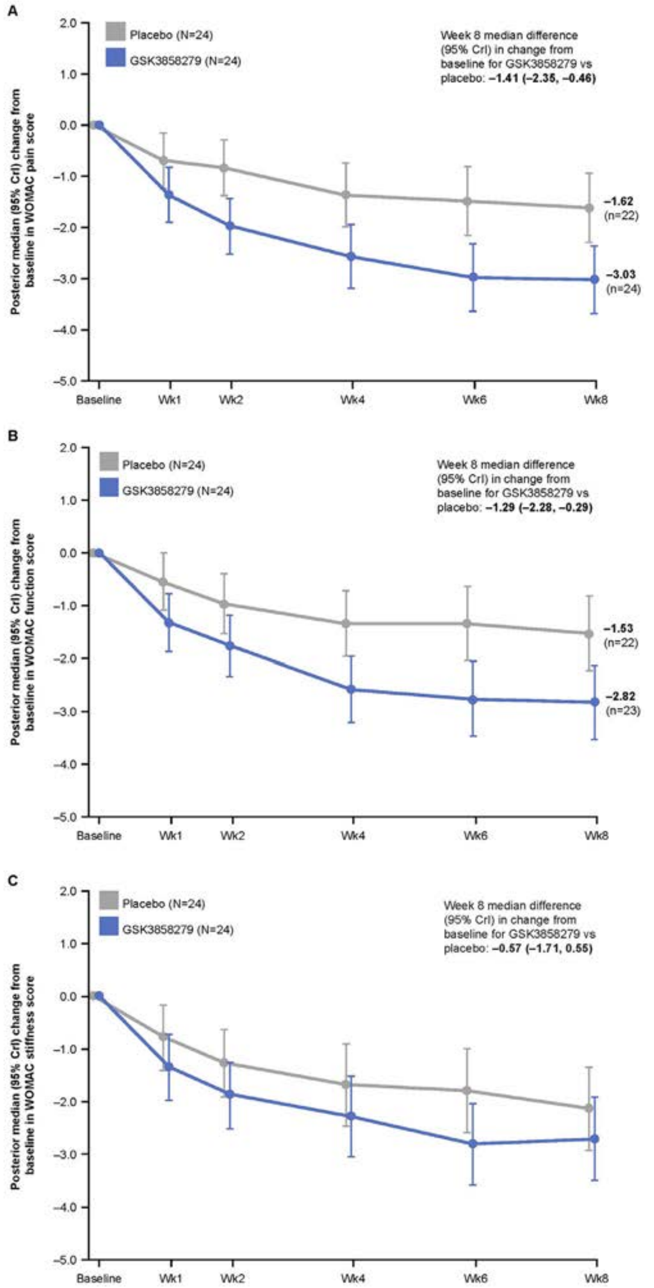

Figure 4. Key exploratory efficacy endpoints: change from baseline to week 8 in WOMAC (A) pain, (B) function and (C) stiffness scores. CrI, credible interval; Wk, week; WOMAC, Western Ontario and McMaster Universities Osteoarthritis Index.

specifically target chemokine pathways of OA pain has not been fully explored [7,18]. This two-part, first-in-human study investigated the efficacy, safety and tolerability of the anti-CCL17 antibody, GSK3858279, in healthy participants and patients with OA-associated knee pain. GSK3858279 induced greater clinically important improvement in both average and worst knee pain intensity than placebo and was also associated with clinically meaningful changes from baseline in WOMAC pain and function scores versus placebo.

In this study, patients who received GSK3858279 showed greater improvements in both average and worst knee pain intensity compared with placebo, indicating that GSK3858279 improved their pain on a daily basis, as well as the worst pain they experienced. Therefore, using both measures of pain offered deeper insights into the impact of GSK3858279 on the patients' pain. In a separate study conducted in the USA, 20 healthcare providers treating patients with chronic pain were interviewed to understand their perspectives on different clinical measurements of pain [19]. The study found that worst pain intensity was the most important measure for healthcare providers, as it reflects the pain experienced during physical activities (eg, pain that occurs when performing specific activities), which can influence treatment decisions [19]. Worst pain intensity is also recommended by the Food and Drug Administration as the primary outcome for clinical trials measuring pain [20]. The study also found that average pain intensity, while considered less important than worst pain intensity, was still necessary to understand the overall impact of patients' average pain [19]. However, given that pain does not remain constant over time, average pain intensity alone may not be sufficient; healthcare providers confirmed they often used more than one measure, such as average and worst pain intensity, to gain a better understanding of patient functioning [19].

In addition to focusing on worst and average knee pain, this study used the WOMAC pain score, which provides a broader assessment of pain and physical functioning. The WOMAC pain score is the standard measure used for self-reported pain in knee OA clinical trials [21]. The current study reported a greater benefit of GSK3858279 with WOMAC pain compared with average pain intensity. The WOMAC pain score requires patients to rate their pain experienced for certain physical activities, for example, walking, climbing stairs and weight bearing [21], while the average pain intensity is rated on a scale of 0−10, (where 0 is no pain and 10 is the worst pain possible). Therefore, the lower WOMAC pain scores may be attributed to differences in how patients rated their pain for each score; specifically, they may

Table 2
Summary of AEs (baseline to week 20)

	Part A								Part B		
		GSK3858279									
	Placebo (n = 13)	0.1 mg/kg IV (n = 6)	0.3 mg/kg IV (n = 6)	1 mg/kg IV (n = 6)	3 mg/kg IV (n = 6)	10 mg/kg IV (n = 6)	3 mg/kg SC (n = 6)	Total (N = 49)	Placebo (n = 24)	GSK3858279 240 mg SC (n = 24)	Total (N = 48)
Any AE, n (%)	12 (92)	2 (33)	2 (33)	4 (67)	6 (100)	6 (100)	6 (100)	38 (78)	15 (63)	21 (88)	36 (75)
Most common AEs (≥3 participants)											
Headache	3 (23)	0 (0)	0 (0)	0 (0)	2 (33)	1 (17)	1 (17)	7 (14)	5 (21)	2 (8)	7 (15)
Arthralgia	1 (8)	0 (0)	0 (0)	0 (0)	0 (0)	0 (0)	0 (0)	1 (2)	2 (8)	4 (17)	6 (13)
Injection site bruising	0 (0)	0 (0)	0 (0)	0 (0)	0 (0)	0 (0)	0 (0)	0 (0)	2 (8)	3 (13)	5 (10)
COVID-19	0 (0)	0 (0)	0 (0)	0 (0)	0 (0)	0 (0)	0 (0)	0 (0)	2 (8)	3 (13)	5 (10)
Nasopharyngitis	3 (23)	0 (0)	0 (0)	0 (0)	3 (50)	1 (17)	3 (50)	10 (20)	2 (8)	3 (13)	5 (10)
Contact dermatitis	2 (15)	0 (0)	0 (0)	1 (17)	3 (50)	1 (17)	1 (17)	8 (16)	0 (0)	2 (8)	2 (4)
Injection site reactions (ISRs) (no. of events)*	N/A	N/A	N/A	N/A	N/A	N/A	N/A	N/A	3 (13) (4)	10 (42) (24)	13† (27) (28)
Injection site erythema	N/A	N/A	N/A	N/A	N/A	N/A	N/A	N/A	0 (0)	4 (17)	4 (8)
Treatment-related AEs	0 (0)	0 (0)	0 (0)	1 (17)	1 (17)	1 (17)	0 (0)	3 (6)	3 (13)	7 (29)	10 (21)
AE leading to treatment discontinuation	0 (0)	0 (0)	0 (0)	0 (0)	0 (0)	0 (0)	0 (0)	0 (0)	2‡ (8)	0 (0)	2 (4)
Any SAE, n (%)	0 (0)	0 (0)	0 (0)	0 (0)	0 (0)	0 (0)	0 (0)	0 (0)	0 (0)	0 (0)	0 (0)
Deaths, n (%)	0 (0)	0 (0)	0 (0)	0 (0)	0 (0)	0 (0)	0 (0)	0 (0)	0 (0)	0 (0)	0 (0)

AE, adverse event; IV, intravenous; SAE, serious adverse event; SC, subcutaneous.

* For part B, AEs were classified as injection site reactions based on a list of preferred terms; classification of AEs as ISRs was not performed for part A.

† Includes injection site bruising (n = 2) and injection site haematoma (n = 1) in the placebo arm, and injection site erythema (n = 4), injection site bruising (n = 3), injection site pain (n = 2), injection site haematoma, administration site bruise, injection site induration, injection site pruritus, injection site rash, and injection site swelling (n = 1 each) in the GSK3858279 arm.

‡ One patient with COVID-19 and one with pruritus and urticaria.

not have considered factors such as climbing stairs when assessing their average pain intensity score.

GSK3858279 was well tolerated, with a favourable safety and tolerability profile in both healthy participants and patients with knee OA pain. Reductions in free CCL17 relative to baseline were observed and maintained between SC doses. Although ADAs were noted in some patients, they were not associated with discernible differences in efficacy, safety or PK. Overall, 72% (part A) and 88% (part B) of participants receiving GSK3858279 experienced AEs, most commonly nasopharyngitis (part A) and ISRs (part B). Specifically, 42% of patients receiving GSK3858279 experienced ISRs (part B); these findings are consistent with previous studies (NCT04114656). No deaths or SAEs were observed.

This study was not without its limitations. This was a first-in-human study and, as such, was both of a small sample size and of a minimum (8-week) duration which was, however, deemed sufficient to make a preliminary evaluation on pain. Given the short time period, future studies are needed to determine the duration of efficacy after the last administration of GSK3858279 and to evaluate if repeat administrations or a longer treatment duration is needed to maintain efficacy, as well as whether these would elicit the same degree of response. The population of OA patients in this phase I study was a relatively small sample size compared with the general OA population, in terms of age and severity of pain at baseline, but the degree of joint damage (as measured by KL grade) and BMI were aligned with general OA patients [22]. The study population was predominantly white, and understanding the treatment effect of GSK3858279 in an ethnically diverse population is important [23]. Finally, although not a study limitation, of note is the magnitude of the placebo effect in the current study. Previous randomised, placebo-controlled clinical trials in OA have shown improvements in knee pain scores and function for patients receiving only placebo [24,25]. The magnitude of the placebo effect in the current study is consistent with previous studies in OA [24−26].

This study provides promising results regarding the potential of GSK3858279 to treat knee OA pain. Future studies will expand on these findings by enrolling a more diverse population, extending the GSK3858279 treatment duration and evaluating different dose regimens. Importantly, the observed efficacy of GSK3858279 in this study confirms the human relevance of prior preclinical findings [5,27−31] and opens the door to a potential new treatment paradigm for OA pain.

CONCLUSION

Weekly SC dosing for 8 weeks with 240 mg of GSK3858279 showed clinically meaningful efficacy in adults with knee OA pain, as indicated by improved average and worst knee pain intensity scores and WOMAC pain and function scores versus placebo. GSK3858279 also demonstrated a favourable safety and tolerability profile. These promising data warrant further study of the efficacy and safety of GSK3858279 for treating chronic pain in adults with OA.

Acknowledgments

The authors would like to acknowledge Patricia Coyle, Jane Temple, Nicola Williams, Sheina Santos, Jessica Renaux, Emma Greening, Stefano Zamuner and John Connell, along with all principal investigators, clinical staff and study participants, for their contributions to the study. Medical writing support, under the guidance of the authors, was provided by Niamh Southern, MPhil, and Ellen McKenna, MSc, of Ashfield MedComms, an Inizio company, and was funded by GSK

Contributors

All authors had access to the study data, took responsibility for the accuracy of the analysis, contributed to data interpretation, reviewed and contributed to the content of the manuscript, and had the authority to decide on the submission of the manuscript. JSN served as guarantor.

Funding

This study, including study design, data collection, analysis and interpretation, and medical writing and submission support for the manuscript, was funded by GSK (study 207804)

Competing interests

JSN, JE, KA-B, RR, SMV, JHB, CM, SS, EP, YA, DB, DF, RK, DI, CE, MF, JES, LW and NW are employed by GSK and hold financial equities in GSK. NA was employed by GSK and held financial equities in GSK at the time of study conduct. ECE was employed by GSK and held financial equities in GSK at the time of the study conduct; and is currently employed by, and holds shares in, AstraZeneca. LKM was employed by GSK and held financial equities in GSK at the time of study conduct; and is currently employed by, and holds shares in, Amphista Therapeutics. KN was employed by GSK and held financial equities in GSK at the time of study conduct and was a previous employee of and shareholder in AstraZeneca.

Patient and public involvement

Patients and/or the public were involved in the design, or conduct, or reporting, or dissemination plans of this research. Refer to the Methods section for further details.

Patient consent for publication

Not applicable.

Ethics approval

The study protocol, all amendments, informed consent and other information that required preapproval was submitted to a national, regional or investigational centre ethics committee or Institutional Review Board, in accordance with the International Council on Harmonisation of Technical Requirements for Registration of Pharmaceuticals for Human Use (ICH) Good Clinical Practice (GCP) and applicable country-specific requirements. The study was performed in accordance with ICH GCP and all applicable privacy requirements and ethical principles outlined in the Declaration of Helsinki. Signed, informed consent was obtained from each participant prior to the performance of any study procedures.

Data availability statement

Data are available on reasonable request. Information on GSK's data sharing commitments and requesting access to anonymised individual participant data and associated data can be found at www.clinicalstudydatarequest.com.

Supplementary materials

Supplementary material associated with this article can be found in the online version at doi:10.1136/ard-2023-225434.

Orcid

Jagtar Singh Nijjar: http://orcid.org/0000-0003-4947-6299

REFERENCES

[1] GBD. Osteoarthritis Collaborators. Global, regional, and national burden of osteoarthritis, 1990-2020 and projections to 2050: a systematic analysis for the global burden of disease study 2021. Lancet Rheumatol 2023;5:e508–22. doi: 10.1016/S2665-9913(23)00163-7.

[2] Neogi T. The epidemiology and impact of pain in osteoarthritis. Osteoarthritis Cartilage 2013;21:1145–53. doi: 10.1016/j.joca.2013.03.018.

[3] Jackson J, Iyer R, Mellor J, et al. The burden of pain associated with osteoarthritis in the hip or knee from the patient's perspective: a multinational cross-sectional study. Adv Ther 2020;37:3985–99. doi: 10.1007/s12325-020-01445-4.

[4] Wallis JA, Taylor NF, Bunzli S, et al. Experience of living with knee osteoarthritis: a systematic review of qualitative studies. BMJ Open 2019;9: e030060. doi: 10.1136/bmjopen-2019-030060.

[5] Lee M-C, Saleh R, Achuthan A, et al. CCL17 blockade as a therapy for osteoarthritis pain and disease. Arthritis Res Ther 2018;20:62. doi: 10.1186/s13075-018-1560-9.

[6] Imai T, Baba M, Nishimura M, et al. The T cell-directed CC chemokine TARC is a highly specific biological ligand for CC chemokine receptor 4. J Biol Chem 1997;272:15036–42. doi: 10.1074/jbc.272.23.15036.

[7] Grässel S, Muschter D. Recent advances in the treatment of osteoarthritis. F1000Res 2020;9:F1000–325. doi: 10.12688/f1000research.22115.1.

[8] Malfait AM, Schnitzer TJ. Towards a mechanism-based approach to pain management in osteoarthritis. Nat Rev Rheumatol 2013;9:654–64. doi: 10.1038/nrrheum.2013.138.

[9] Yu SP, Hunter DJ. Managing osteoarthritis. Aust Prescr 2015;38:115–9. doi: 10.18773/austprescr.2015.039.

[10] Fuggle N, Curtis E, Shaw S, et al. Safety of opioids in osteoarthritis: outcomes of a systematic review and meta-analysis. Drugs Aging 2019;36:129–43. doi: 10.1007/s40266-019-00666-9.

[11] Moore RA, McQuay HJ. Prevalence of opioid adverse events in chronic non-malignant pain: systematic review of randomised trials of oral opioids. Arthritis Res Ther 2005;7:R1046–51. doi: 10.1186/ar1782.

[12] Solomon DH, Rassen JA, Glynn RJ, et al. The comparative safety of analgesics in older adults with arthritis. Arch Intern Med 2010;170:1968–76. doi: 10.1001/archinternmed.2010.391.

[13] Ivers N, Dhalla IA, Allan GM. Opioids for osteoarthritis pain: benefits and risks. Can Fam Physician 2012;58:e708.

[14] Kolasinski SL, Neogi T, Hochberg MC, et al. 2019 American College of Rheumatology/Arthritis Foundation guideline for the management of osteoarthritis of the hand, hip, and knee. Arthritis Care Res 2020;72:149–62. doi: 10.1002/acr.24131.

[15] Marques L, Costa B, Pereira M, et al. Advancing precision medicine: a review of innovative in silico approaches for drug development, clinical pharmacology and personalized healthcare. Pharmaceutics 2024;16:332. doi: 10.3390/pharmaceutics16030332.

[16] Gabrielsson J, Weiner D. Non-compartmental analysis. Methods Mol Biol 2012;929:377–89. doi: 10.1007/978-1-62703-050-2_16.

[17] Nakashima E, Benet LZ. An integrated approach to pharmacokinetic analysis for linear mammillary systems in which input and exit may occur in/from any compartment. J Pharmacokinet Biopharm 1989;17:673–86. doi: 10.1007/BF01062124.

[18] Chen D, Shen J, Zhao W, et al. Osteoarthritis: toward a comprehensive understanding of pathological mechanism. Bone Res 2017;5:16044. doi: 10.1038/boneres.2016.44.

[19] Goldman RE, Broderick JE, Junghaenel DU, et al. Beyond average: providers' assessments of indices for measuring pain intensity in patients with chronic pain. Front Pain Res (Lausanne) 2021;2:692567. doi: 10.3389/fpain.2021.692567.

[20] U.S Department of health and human services food and drug administration: guidance for industry analgesic indications: developing drug and biological products 2014. Available: https://www.fdanews.com/ext/resources/files/02/02-05-14-Analgesic.pdf.

[21] Bellamy N, Buchanan WW, Goldsmith CH, et al. Validation study of WOMAC: a health status instrument for measuring clinically important patient relevant

outcomes to antirheumatic drug therapy in patients with osteoarthritis of the hip or knee. J Rheumatol 1988;15:1833–40.

[22] Arsenault P, Chiche D, Brown W, et al. NEO6860, modality-selective TRPV1 antagonist: a randomized, controlled, proof-of-concept trial in patients with osteoarthritis knee pain. Pain Rep 2018;3:e696. doi: 10.1097/PR9.0000000000000696.

[23] Vaughn IA, Terry EL, Bartley EJ, et al. Racial-ethnic differences in osteoarthritis pain and disability: a meta-analysis. J Pain 2019;20:629–44. doi: 10.1016/j.jpain.2018.11.012.

[24] Bennell KL, Paterson KL, Metcalf BR, et al. Effect of intra-articular platelet-rich plasma vs placebo injection on pain and medial tibial cartilage volume in patients with knee osteoarthritis: the RESTORE randomized clinical trial. JAMA 2021;326:2021–30. doi: 10.1001/jama.2021.19415.

[25] Paget LDA, Reurink G, de Vos R-J, et al. Effect of platelet-rich plasma injections vs placebo on ankle symptoms and function in patients with ankle osteoarthritis: a randomized clinical trial. JAMA 2021;326:1595–605. doi: 10.1001/jama.2021.16602.

[26] Zhang W. The powerful placebo effect in osteoarthritis. Clin Exp Rheumatol 2019;37(Suppl 120):118–23.

[27] Lee KM-C, Jarnicki A, Achuthan A, et al. CCL17 in inflammation and pain. J Immunol 2020;205:213–22. doi: 10.4049/jimmunol.2000315.

[28] Achuthan A, Cook AD, Lee M-C, et al. Granulocyte macrophage colony-stimulating factor induces CCL17 production via IRF4 to mediate inflammation. J Clin Invest 2016;126:3453–66. doi: 10.1172/JCI87828.

[29] Cook AD, Lee M-C, Saleh R, et al. TNF and granulocyte macrophage-colony stimulating factor interdependence mediates inflammation via CCL17. JCI Insight 2018;3:e99249. doi: 10.1172/jci.insight.99249.

[30] Bogacka J, Popiolek-Barczyk K, Pawlik K, et al. CCR4 antagonist (C021) influences the level of nociceptive factors and enhances the analgesic potency of morphine in a rat model of neuropathic pain. Eur J Pharmacol 2020;880:173166. doi: 10.1016/j.ejphar.2020.173166.

[31] Shin H, Prasad V, Lupancu T, et al. The GM-CSF/CCL17 pathway in obesity-associated osteoarthritic pain and disease in mice. Osteoarthritis Cartilage 2023;31:1327–41. doi: 10.1016/j.joca.2023.05.008.

Ann Rheum Dis 84 (2025) 866−876

Contents lists available at ScienceDirect

Annals of the Rheumatic Diseases

journal homepage: https://www.sciencedirect.com/journal/annals-of-the-rheumatic-diseases

Connective tissue diseases

AI-driven histologic analysis of human Achilles tendinopathy provides a roadmap to unravel pathogenesis

Guillaume Planckaert[1,2,3,4], Arne Burssens[1,3,4], Flore Stappers[1,2], Julie Coudenys[1,2], Sofía Demolder[1,2], Irem Kaya[5,6], Malaïka Van der Linden[5,6], Amanda Gonçalves[7], Kelly Lemeire[7], Benjamin Pavie[7], Edwin Van Ovost[8], Peter Burssens[9], Amber Vanhaecke[5,6], Jo Van Dorpe[5,6], Lauren Pringels[10], Evi Wezenbeek[11], Jess Snedeker[12], Katrien De Bock[12], Fiona Bonar[13], Jill Cook[14], Jan Victor[3,4], Dirk Elewaut[1,2,15,*], Eric Gracey[1,2,*]

[1] *Unit for Molecular Immunology and Inflammation, Center for Inflammation Research, Flanders Institute for Biotechnology (VIB), Ghent, Belgium*
[2] *Department of Internal Medicine and Paediatrics, Faculty of Medicine and Health Sciences, Ghent University, Ghent, Belgium*
[3] *Department of Human Structure and Repair, Faculty of Medicine and Health Sciences, Ghent University, Ghent, Belgium*
[4] *Department of Orthopaedics and Traumatology, Ghent University Hospital, Ghent, Belgium*
[5] *Department of Pathology, Ghent University Hospital, Ghent, Belgium*
[6] *Department of Diagnostic Sciences, Faculty of Medicine and Health Sciences, Ghent University, Ghent, Belgium*
[7] *Bioimaging Core, Center for Inflammation Research, Flanders Institute for Biotechnology (VIB), Ghent, Belgium*
[8] *Department of Orthopaedics and Traumatology, General Hospital (AZ) Sint-Lucas, Ghent, Belgium*
[9] *Department of Orthopaedics and Traumatology, General Hospital (AZ) Jan-Palfijn, Ghent, Belgium*
[10] *Department of Rehabilitation Sciences, Faculty of Medicine and Health Sciences, Ghent University, Ghent, Belgium*
[11] *Movement Antwerp (MOVANT) Research Group, Department of Rehabilitation Sciences and Physiotherapy (REVAKI), University of Antwerp, Wilrijk, Belgium*
[12] *Department of Health Sciences and Technology, Federal Institute of Technology (ETH) Zürich, Zürich, Switzerland*
[13] *Douglass Hanly Moir Pathology, Macquarie Park, Sydney, NSW, Australia*
[14] *Sport and Exercise Medicine Research Centre, La Trobe University, Melbourne, Victoria, Australia*
[15] *Department of Rheumatology, Ghent University Hospital, Ghent, Belgium*

ARTICLE INFO

Article history:
Received 7 October 2024
Received in revised form 20 November 2024
Accepted 25 November 2024

ABSTRACT

Objectives: Achilles tendinopathy is a common source of pain and dysfunction, yet its pathogenesis remains poorly understood. Research on human tendons is hampered by lack of standardisation in tissue sample validation, making interpretation of results challenging. We sought to develop an automated and operator-independent approach to histologically score human tendons.

Methods: We assembled a cohort of 15 tendinopathic and 10 normal control Achilles tendon samples. We stained longitudinal sections with haematoxylin and eosin and Alcian blue and developed a low temperature epitope-retrieval protocol for immunostaining of blood vessels. Histologic sections were scored by pathologists using the current gold standard Bonar score. Whole sections were then analysed with open-source software (QuPath). Histologic features

***Correspondence to** Professor Dirk Elewaut and Dr Eric Gracey.

E-mail addresses: dirk.elewaut@ugent.be (D. Elewaut), eric.gracey@ugent.be (E. Gracey).

Handling editor Josef S. Smolen.

https://doi.org/10.1016/j.ard.2025.01.027

were automatically quantified across the entire section and summarised in the BonAIr score. Tissue from the same patients was subsequently analysed by quantitative polymerase chain reaction and flow cytometry to validate elements of the BonAIr score.
Results: We observed increased cell roundness, collagen disarrangement, ground substance, and vascularity in tendinopathy using both the Bonar and BonAIr scores. Increased cellularity was only detected by the BonAIr score. Cellular and transcriptomic analyses corroborated tendinopathic shifts in all elements of the BonAIr score and further identified elevated THY1/CD90 expression in tendinopathy. $CD90^+$ cells were found to localise to areas of low collagen alignment. These results align with the concept of stromal cell dysregulation in tendinopathy.
Conclusions: Automated analysis of whole tendon sections refines conventional histopathologic scoring and predicts cellular and molecular changes found in tendinopathy. The BonAIr score should be further developed for standardised assessment of tendons samples across other anatomical locations and different research centres.

WHAT IS ALREADY KNOWN ON THIS TOPIC

- Histologic sample validation is a cornerstone of translational research but is rarely done in tendon research. Current histology score systems for tendons are manual and only examine the worst field of view, which fails to account for heterogeneity in tissue pathology and inflates the final pathology score.

WHAT THIS STUDY ADDS

- This study provides a digital, automated, whole-section histologic analysis pipeline for human Achilles tendon samples, using accessible laboratory staining techniques. The resulting score, the BonAIr, is quantitative and objective.

HOW THIS STUDY MIGHT AFFECT RESEARCH, PRACTICE OR POLICY

- Future use of the BonAIr score to validate human tendon samples in a standardised way will improve interpretation of translational research results and allow for more effective comparison of tendon studies.

INTRODUCTION

Tendinopathy is a condition involving pain and loss of tendon function following excessive mechanical loading [1]. The Achilles tendon is one the most commonly affected tendons [1,2].

Multiple treatment options are available for tendinopathy, with varying degrees of success. Exercise is the frontline therapy to which most patients respond [3]. A number of additional therapies exist; however, the quality of evidence related to the effectiveness of these interventions is limited [4,5]. Surgery is the final treatment option for those failing therapy, but even this does not guarantee clinical improvement [6]. Therefore, there is an unmet need for effective therapies against therapy-resistant tendinopathy.

A deep biological understanding has led to the development of disease-modifying therapeutics in other musculoskeletal diseases [7]. In contrast, no targeted therapeutics exist for tendinopathy, due in part to a poor understanding of the underlying biology. Recent studies have pushed the boundaries of tendon research through the use of cutting edge technologies such as single-cell sequencing [8−10], albeit with some caveats. First, only a few studies compare diseased tendon tissue with anatomically matched healthy tissue [11,12]. Second, formal histopathologic validation of tendon tissues is rarely reported. Therefore, when interpreting, data assumptions must be made that pathogenic cells or gene signatures reflect biological shifts with tendon disease and not technical variation unrelated to tissue pathology. Indeed, a recent consensus article highlighted the importance of histology in tendon research but noted that hurdles exist in tissue processing and analysis [13]. Despite this, there have not been major advancements in tendon histology scoring since the revisited Bonar score in 2013 [14].

This study aimed to address the limitations of conventional histopathologic scoring of tendons, in order to facilitate the easy and efficient incorporation of histologic features in tendon research, thereby enabling more consistent and reliable comparisons between different studies. We use digital microscopy to develop the automated, quantitative, and objective BonAIr score. Histologic features of tendinopathy are validated with complementary analyses of cellular content and gene expression levels in tendinopathy.

METHODS

See Supplemental Material for extended methods.

Human sample collection

The study protocol was approved by the local ethical committees of the participating centres (B.U.N.: B6702020000966). Human midportion tendon samples were collected during surgical procedures in patients experiencing longstanding Achilles tendinopathy or from patients with acquired spastic paresis, after written informed consent was given. Normal midportion Achilles tendon samples were obtained from organ donors, shortly after circulatory arrest.

Statistical analysis

Statistical analyses were performed in GraphPad Prism using tests indicated in the figure legends. Before statistical testing, the distribution of the data was evaluated with a Q-Q Plot; if the data were not normally distributed, nonparametric testing was performed or the data were transformed before parametric testing. Nonparametric Kruskal-Wallis test and Dunn posttest was used to compare differences among normal control, tendinopathy, and acquired spasticity in histologic scores, in cellularity after tissue digestion and in RNA properties after extraction. Nonparametric Mann-Whitney test was used to compare differences between normal control and tendinopathic samples in cell frequencies of major tendon cell populations and in collagen alignment. Simple linear regression and Spearman correlation test was used to examine the association between cell yield after tissue digestion and histologic cell density as well as the association between gene expression levels and relevant histologic variables. Further, *t* tests with correction for multiple testing (2-stage step-up method of Benjamini, Krieger, and Yekutieli) were used to compare expression levels of individual genes between normal control and tendinopathy samples, after logarithmic transformation of the data points. Two-way analysis of variance and Fisher least significant difference testing was conducted to evaluate differences in $CD90^+$, $CD45^+$, and $CD68^+$ cell density based on patient status and collagen alignment, after logarithmic transformation of the data points. For all data, ns = not significant ($P > .05$), *$P < .05$, **$P < .01$, and ***$P < .001$.

Patient and public involvement statement

This work is the start of a project initiated by a clear clinical need. Physicians involved in this study (DE, AB, and GP) are confronted daily in clinical practice with questions from patients about tendon pain, function, and treatment. There is a clear unmet medical need in the treatment of tendinopathy, and this work lays the foundations for human sample selection in translational tendinopathy research that has to goal to define new biological therapeutical targets in tendinopathy. After publication of this work, we will share our insights to the general public via online symposia of patient groups.

RESULTS

Assembling a cohort of Achilles midportion tendinopathy with anatomically matched controls

Cellular and molecular studies of human often assemble cohorts from tendinopathy of mixed anatomical locations. In this study, we followed ICON consensus guidelines to recruit 15 patients with midportion Achilles tendinopathy from 3 orthopaedic centres in Ghent, Belgium [15]. Briefly, all patients had a clinical diagnosis of tendinopathy, based on painful palpable thickening of the tendon midportion (2-7 cm proximal from insertion), confirmed by magnetic resonance imaging. The patients had symptoms for more than 6 months and had at least 18 physiotherapy sessions. Patients were excluded if taking statins or quinolones, if there was diagnosis or suspicion of rheumatic disease, if there was a history of tendon surgery, or if a macroscopic rupture was present. For the tendinopathic patients, VISA-A scores ranged from 4 to 78, with a mean of 40. Samples were obtained during debridement surgery to promote tendon healing (Fig 1A-C, Table).

One particular strength of this cohort is the inclusion of 2 anatomically matched control groups. Our primary control group are 10 normal Achilles tendons from tissue donors that were age- and sex-matched to the tendinopathy patients. Normal donors had no history of musculoskeletal disease and were not immobilised for more than 1 week before death. The Achilles tendon was visually inspected by an orthopaedic surgeon (GP, AB, EV, and PB) during dissection to ensure it was not macroscopically tendinopathic. A second control group constituted samples from 4 patients undergoing tendon lengthening surgery following acquired spastic paresis of the lower limb. This tendon was collected during surgery and therefore acted as a qualitative control for the normal tendon group, which was subjected to warm ischaemia.

Bonar histopathologic validation of tendinopathic tissue

Two histology stains are commonly used to assess tendinopathic tissue: hematoxylin and eosin (H&E) stain for general architecture and cell morphology and Alcian blue for proteoglycan deposition [13]. Before formally scoring, it was clear that tendinopathic tissue was distinct from control tissues, with a loss of interfascicular matrix (IFM) boundaries and extensive regions of collagen disarrangement and proteoglycan deposition (Fig 1D-F).

The Bonar score is the gold standard for histologic analysis of tendinopathy [14]. Five elements within fascicles were scored within a single field of view in the worst region of each section: cellularity, cell morphology, vascularity, proteoglycan deposition, and collagen arrangement (Supplemental Fig S1). Intratendinous adipocytes and calcification were not observed in any sample. The fascicle cellularity was not significantly different between patients and controls, as all samples scored hypercellular as defined by the semiquantitative Bonar system, with more than 30 cells per 100 × field of view. Fascicular nuclei in the tendinopathic samples were rounder and had visible cytoplasm, but no lacuna formation was observed. Normal and acquired spasticity controls had cells with elongated, spindle-shaped nuclei, and no visible cytoplasm. Blood vessels were not readily detectable in most control tendon fascicles, and in tendinopathic tendons, it was not possible to determine whether blood vessels were fascicular owing to the aforementioned loss of tissue architecture. In control tendons, proteoglycan deposition was restricted to the IFM, but in tendinopathy, there was ample deposition in fascicles. Complete loss of collagen architecture (grade 3) was only observed in 3 of 15 tendinopathic samples, which is unsurprising as this grade is typical of macroscopic ruptures [16,17], which were excluded from our cohort. In summary, our tendinopathic samples scored significantly higher than either control group with the Bonar score (Fig 1G), confirming their pathogenic status.

Despite achieving clear separation of our patients and controls, the Bonar score system has some limitations. First, only the worst area is scored. This region is manually selected and can result in observer bias and inflated scores, especially in tendinopathic tissues with large areas of healthy architecture. A second limitation is that the IFM boundaries are lost with tendinopathy, making it difficult to select fascicular regions. To overcome these limitations, we decided to use machine learning to automate scoring. We chose to use quPath as it has user-friendly interface, built in machine learning tools, and is open source [18].

The fascicle-IFM boundary is lost in tendinopathy

As the Bonar score focuses on the fascicle, we first used machine learning to distinguish fascicle from IFM. As the IFM was clearly distinct from the fascicles in normal tendons, we trained a pixel classifier on 5 samples (Supplemental Fig S2A). To determine how our trained model performed compared with the ground truth, the pixel classifier was applied to 5 additional normal controls, for which all fascicles were manually annotated. We assessed the precision and recall of our pixel classifier by calculating the F1 score. The average F1 score of our validation samples was 0.88 (Supplemental Fig S2B), which was close to a perfect model score of 1.0 [19].

We quantified the number of cells using a nuclei identifier. As reported [20], the IFM of normal tendons is significantly richer

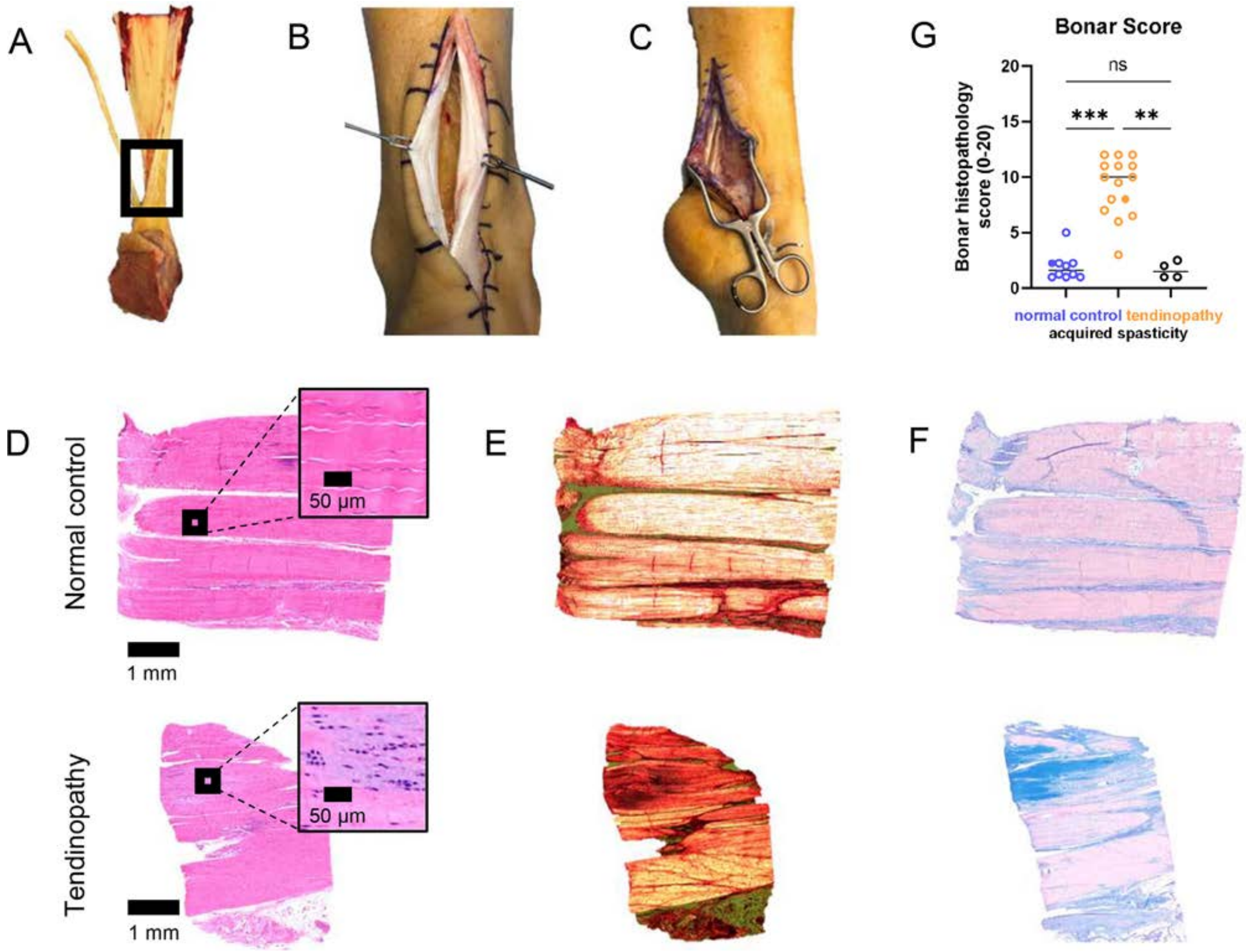

Figure 1. Histological validation of human Achilles tendons using the Bonar score. Midportion tendon tissue was collected from (A) organ donors, (B) during surgical debridement of tendinopathic tissue, and (C) during tendon lengthening surgery for acquired spastic paresis (spasticity). Sections were stained with hematoxylin and eosin, which was imaged with (D) bright field and (E) polarised light. (F) Sequential sections were stained with Alcian blue. (G) For each specimen, 2 trained pathologists selected the most severe region to perform conventional Bonar scoring. Each data point is representative of an individual patient. The solid data points indicate the subjects for which the representative histology is shown. Kruskal-Wallis test was used to analyse the difference among normal control, tendinopathic, and acquired spasticity samples ($P < .001$), with Dunn posttest showing specific comparisons.

Table
Patient demographics

Clinical parameter	Normal control	Tendinopathy	Acquired spasticity
Number of patients	10	15	4
Mean age, y (SD)	56.3 (10.0)	54.2 (7.8)	41 (10)
Sex (M/F)	6/4	7/8	1/3
Mean VAS (SD)	NA	81 (9.9)	NA
Mean VISA-A (SD)	NA	40.3 (20.9)	NA
Mean BMI, kg/m^2 (SD)	NA	27.6 (4.2)	26.4 (4.0)
Mean symptom duration in months (SD)	NA	32.5 (32.7)	NA
Previous injection (yes/no)	NA	7/8	NA
Mean warm ischaemia time, hh:mm (SD)	4:38 (4:55)	0:10 (0:12)	0:13 (0:03)

BMI, body mass index; F, female; M, male; NA, not available; VAS, visual analogue score; VISA-A, Victorian institute of sport assessment-achilles.

in cells than the fascicle (Supplemental Fig S2C). In addition, cells of the IFM are rounder than those of the fascicles.

We then applied our fascicle pixel classifier to tendinopathic samples. The model identified degraded fascicles as IFM, reflecting our aforementioned observations of the lack of fascicle/IFM boundary. This is perhaps not surprising as these areas have high cellularity and an H&E staining profile indicative of disorganised extracellular matrix (ECM). We therefore decided to automate the Bonar scoring on entire sections, including IFM, to avoid excluding highly degenerated fascicles.

BonAIr: automating tendon histopathology with artificial intelligence

We used quPath to automate the core elements of the Bonar score across the entire section. The area examined was on average 15.6 mm^2 per sample. The cell detection tool was used on H&E sections (Fig 2A), which revealed a doubling of cell density in tendinopathy vs both control groups. Tendinopathic cells were also significantly rounder.

We used machine learning to assess collagen arrangement and proteoglycan deposition. Eighty tiles of 0.23 mm^2 were randomly generated from polarised light–imaged H&E-stained and Alcian blue–stained sections from normal and tendinopathic samples and graded by 2 independent assessors (GP and FB) based on the Bonar grades of 0 to 3. Only the image tiles that were independently given the same score by both assessors were then used to train a pixel classifier (Fig 2B,C). The average grade of the entire section was then calculated. Tendinopathic samples

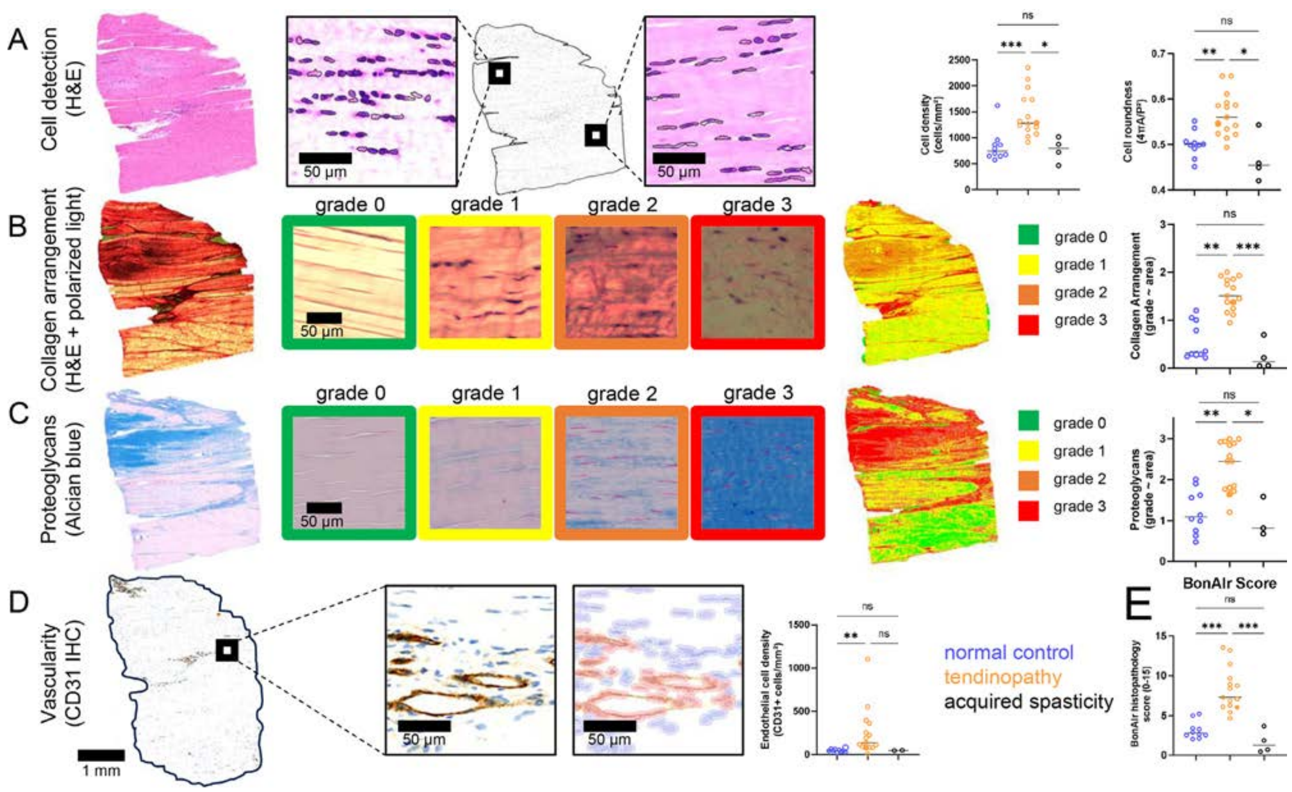

Figure 2. Development of the BonAIr score for automated, whole-section histopathology scoring of human Achilles tendon. (A) QuPath was used to detect all nuclei per section to quantify the cell density (cellularity) and cell roundness (morphology). Machine learning was used on tiles representative of the classical Bonar grades (0-3) to train models for (B) collagen arrangement and (C) ground substance (proteogylcans). The average grade was calculated over the entire section for the respective features. (D) Formalin-fixed paraffin-embedded sections underwent low temperature (58 °C) epitope retrieval overnight before immunohistochemical staining for CD31, a marker of endothelial cells. Continuous data for cell density, cell roundness, and endothelia cell density was converted to a 0-3 grade using *Z*-score normalisation. These normalised features were added to collagen arrangement and ground substance to create (E) the BonAIr score, an artificial intelligence−driven composite histopathology score for human tendons. Each data point is representative of an individual patient. The solid data point in the tendinopathy group indicates the sample used for representative images. Kruskal-Wallis test was used to analyse the difference among normal control, tendinopathic, and acquired spasticity samples (all data $P < .001$), with Dunn posttest showing specific comparisons.

had significantly worse collagen arrangement and more proteoglycan deposition than both control groups. It is noteworthy that many tendinopathic samples had regions of extreme degeneration adjacent to relatively normal regions, as shown in the representative images. As a result, such heterogeneous sections had moderate histologic grades.

To overcome the limitations of detecting small blood vessels in H&E-stained sections, we opted to include an additional stain. Specifically, we performed chromogenic immunohistochemistry (IHC) for the blood vessel marker, CD31 (Fig 2D). We used a cell detection tool and object classifier to automatically detect CD31$^+$ cells. This allowed for clear quantification of CD31$^+$ endothelial cells in the entire section, in which more were observed in tendinopathic samples than controls. A noteworthy limitation of using CD31 as a marker is that it can be expressed on some immune cells [21]. Indeed, in 1 tendinopathic sample with microscopic ruptures, regions were seen with intense CD31 staining outside of blood vessels, indicative of immune cell infiltration (Supplemental Fig S2D).

Having automated the 5 features of the Bonar score, we next set out to create a composite score with each element contributing up to 3 points. The sum of these 5 graded features was significantly higher in our tendinopathic samples than that in controls (Fig 2E). We termed this artificial intelligence (AI)−assisted, full-section tendon grading system the BonAIr score.

To assess the performance of the BonAIr score system, we analysed additional sections from the same cohort. For selected samples, we cut new sections from the same tissue blocks. For some samples we also cut sections from separate tissue blocks. In both cases, there was good correlation of BonAIr scores from the same patient (Supplemental Fig S2E), indicating that it is sufficient to analyse a single section to get a representative histopathologic score for a given patient. We next sought to benchmark the BonAIr score against complimentary laboratory techniques.

CD90$^+$ stromal cells are a hallmark of tendinopathy

To assess the cellularity of our tendon samples, we performed enzymatic digestions. A cocktail of collagenases supplemented with hyaluronidase and DNase was found to release an abundant number of viable cells (Fig 3A,B), although it should be noted that certain cells will be lost during digestion either by death (eg, neutrophils) or due to buoyancy (eg, adipocytes). The cell count obtained by digestion of tissue moderately correlated with the BonAIr cell density (Fig 3C). Based on this, we conclude that our estimation of cell numbers by histology matches the cell count of larger tendon samples.

With methods in place to obtain single tendon cells, we decided to examine broad cell types by flow cytometry on a subset of our tendinopathy and normal controls (Fig 3D, Supplemental Fig S3). In this study, we could clearly distinguish cells from ECM debris using MHC class 1 (HLA-ABC), following which immune cells and endothelial cells could be readily

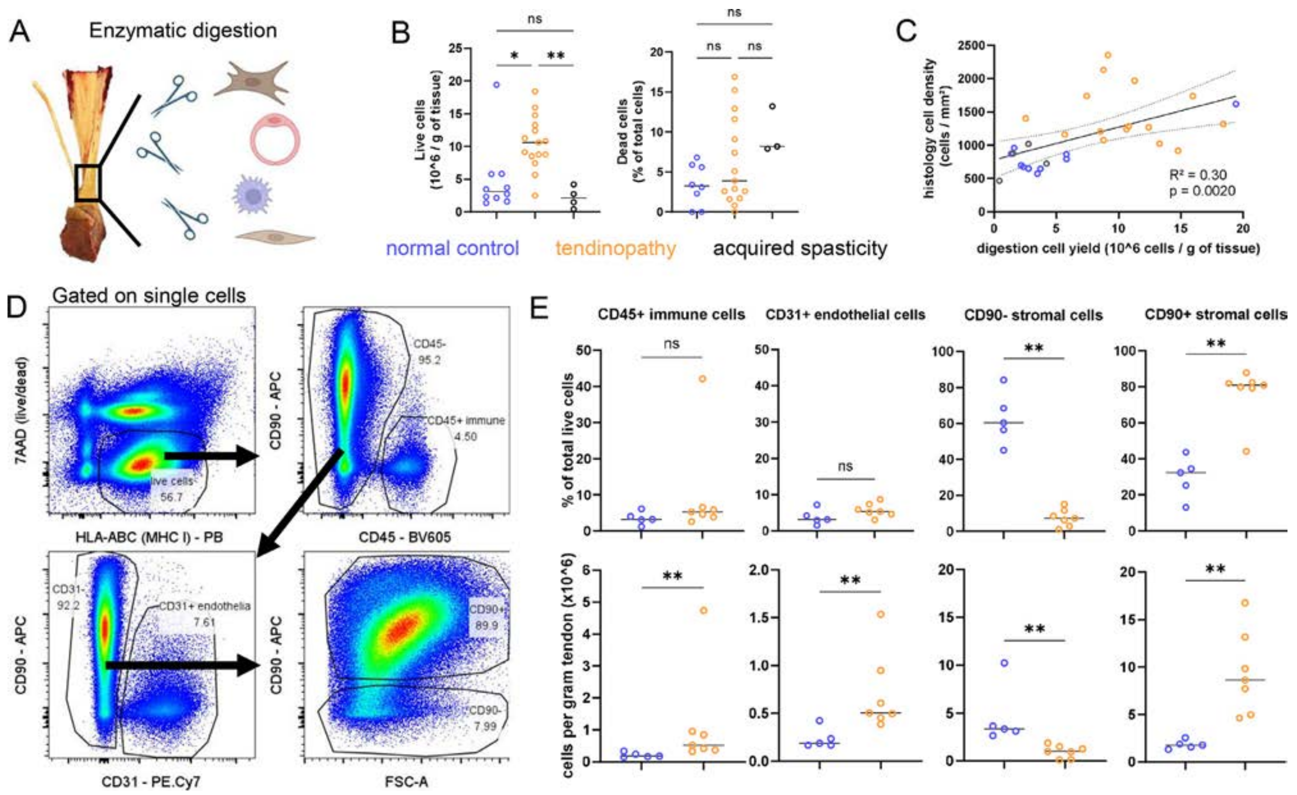

Figure 3. Analysis of enzymatically digested Achilles tendons confirms elevated cellularity in tendinopathy and reveals an expansion of CD90$^+$ cells. (A) Midportions were cleaned of peritendinous tissue, diced, and enzymatically digested. (B) Samples were counted with trypan blue to assess the viability of cells and absolute number of live cells. C) Cell density calculated by automated analysis of hematoxylin and eosin sections correlated with cell yield from digested tissue. (D, E) Cells from tendinopathy and healthy controls were stained with a 5-marker flow cytometry panel to identify and quantify the major tendon cell populations. Each data point is representative of an individual patient. Kruskal-Wallis test was used to analyse the data shown in (B) live cell (P = .0013) and dead cell (P = nonsignificant [ns]), with Dunn posttest showing specific comparisons. A simple linear regression with 95% confidence bands was used to calculate the slope in (C), and the correlation calculated with a Spearman test. Mann-Whitney tests were used in (D).

identified by CD45 and CD31, respectively. We found no difference in the frequency of these cell populations between our groups but did see a slight increase in the absolute number with tendinopathy (Fig 3E), reflecting the large increase in total tendon cellularity with disease.

Based on existing single-cell data sets from human tendons, fibroblasts make up the majority of nonimmune, nonendothelial tendon stromal cells [10], thus likely account for most of our CD31$^-$CD45$^-$ cells. We chose to focus on CD90, as it has been found to be a marker of tendinopathy [22]. We observed a major shift in the expression of CD90, with both frequency and absolute number of CD90$^+$ stromal cells being higher in tendinopathy (Fig 3E). Further, CD90$^+$ stromal cells were larger than their CD90$^-$ counterparts, especially in tendinopathy (Supplemental Fig S3C), suggestive of activation. These data support the hypothesis that tendinopathy is mediated by fibroblasts dysregulation [23], which we sought to confirm by gene expression.

Gene expression analysis of whole tissue indicates matrix dysregulation in tendinopathy

Because of the highly fibrous, acellular nature of tendons, specialised techniques are required to extract RNA [24]. We opted to cryopreserve RNA in whole tissue using an RNA-stabilising solution, allowing us to extract RNA in a single batch. Homogenisation in TRIZol with a hand-held blender coupled with column extraction provided good RNA yield and quality (Fig 4A-D). The integrity of RNA following extraction was comparable with that reported in the literature [24]. We noted that the RNA integrity was superior in tendinopathic samples. This was likely because normal and acquired spasticity tendons required slightly longer homogenisation to disrupt the tissue owing to them being tougher than degenerated tendinopathic tissue. Further, we found tendinopathic tissue contained higher concentrations of RNA than control tissues. This increased RNA load was likely due to the high cellularity of tendinopathic tendons as RNA yield was not higher on a per-cell basis.

We used quantitative polymerase chain reaction (qPCR) to assess gene expression. As qPCR rests on the assumption that housekeeper genes are stable, we first assessed the stability of 10 candidate housekeeper genes using geNorm [25] in open source software, qBase [26]. Candidate housekeepers were selected from commonly used housekeepers, housekeepers used in tendon literature [27,28], and those found to be stable in musculoskeletal tissues [29,30]. Importantly, this analysis revealed that commonly used housekeepers such as *ACTB* (β actin) and *GAPDH* are poor housekeepers for tendinopathic tissue (Supplemental Fig S4A,B). geNorm predicted the most stable housekeeper genes to be *RPL13A* and *RPL4* based on the low geNorm M value that represents the average pairwise variation of that gene compared with that of all other genes, so we used both housekeepers in subsequent analyses.

We examined the level of gene expression of 29 genes by qPCR, to broadly probe ECM composition and the presence of major cell types. We found significant differential expression in all gene categories (Fig 4E), with the largest fold changes occurring in ECM and stromal genes. Importantly, *THY1* (CD90) was

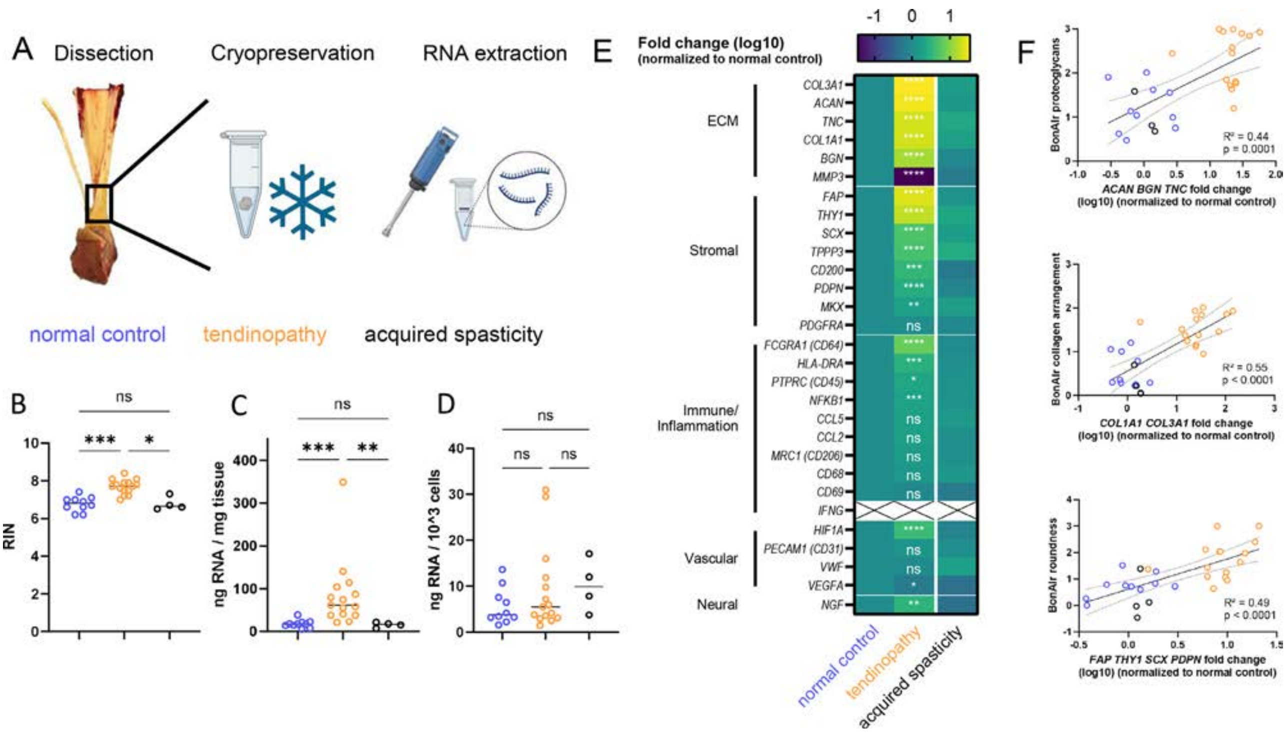

Figure 4. Gene expression analysis reveals activation of the major cell compartments in tendinopathy. (A) RNA was extracted from cryopreserved Achilles tendon midportions through combined homogenisation of tissue in TRIzol and column purification. (B) RNA integrity was assessed by electrophoresis. RNA yield calculated in (C) whole tissue and (D) per cell using the counts obtained from enzymatic digestion of tissue for flow cytometry. (E) qPCR used to assess the expression of genes representative of the respective tendon extracellular and cellular components. Two stable housekeepers (*RPL4* and *RPL13A*) were used as internal controls. (F) Average expression of selected genes correlated with their respective histology parameters. Each data point is representative of an individual patient. Data analysed with Kruskal-Wallis test in (B, C) $P < .001$ and (D) P = nonsignificant (ns), with Dunn posttest showing specific comparisons. Normal control and tendinopathy data in (E) analysed with *t* tests corrected for multiple testing. A simple linear regression with 95% confidence bands was used to calculate the slopes in (F), and the correlations were calculated with a Spearman test.

strongly upregulated in tendinopathy, consistent with our flow cytometry results. Principal component analysis of all genes revealed separation of tendinopathic and control samples, with a complete overlap of acquired spasticity and normal tendons (Supplemental Fig S4C). Sex did not contribute to the variation in expression of the genes we assessed (Supplemental Fig S4D).

To determine the relationship between gene expression and histopathology, we correlated BonAIr features with their respective genes (Fig 4F). Significant correlations were seen between the extent of proteoglycan deposition and the proteoglycan genes *ACAN, BGN* and *TNC*. Likewise, there was a positive correlation between the degree of collagen disarrangement and the expression of collagen genes *COL1A1* and *COL3A1*. Finally, cell roundness correlated with markers of fibroblast activation (*FAP, THY1, SCX*, and *PDPN*). Thus, our BonAIr score appears to reflect the underlying pathophysiologic changes of the tendon tissue.

One caveat with analysis of genes and cells in bulk tissue was that information on the spatial distribution of potentially pathogenic factors was lost. We therefore chose to examine CD90 spatially in our tendon samples.

CD90$^+$ cells localise to areas of ECM degeneration in tendinopathy

Chromogenic IHC was performed using low temperature epitope retrieval to detect CD90. Consistent with our flow cytometry, CD90$^+$ cells were more abundant in tendinopathic tendons (Fig 5A,B).

To formally assess the spatial distribution of CD90$^+$ cells, we imaged the immunohistochemical sections using polarised light. The BonAIr collagen arrangement grading was confounded by DAB staining; instead, we divided the collagen alignment into 2 bins using quPath's thresholder tool (Fig 5C). It was clear that regions of low collagen alignment, likely IFM, were rare in normal tendons but dominated in tendinopathy (Fig 5D). Subsequent analyses revealed CD90$^+$ cell density to be the highest in the areas of low collagen alignment regardless of disease status (Fig 5E). In contrast, areas of high collagen alignment (fascicles) had an increase in CD90$^+$ cell density in tendinopathy.

Recently, interest has grown in the role of the immune system in tendinopathy. The spatial distribution of immune cells (CD45$^+$) and macrophages (CD68$^+$) were quantified in the regions of high and low collagen alignment (Fig 5F). Higher numbers over CD45$^+$ and CD68$^+$ cells were found in areas with low collagen alignment, irrespective of disease status (Fig 5E-G). The IFM localisation of immune cells matches that of the CD90$^+$ fibroblast, indicating potential cellular interactions, which should be followed up in future studies.

DISCUSSION

Many factors contribute to insightful translational research, from careful patient recruitment to technical expertise in processing samples. During this process, effective sample validation is crucial. In this body of work, we present a framework for automated histologic assessment of human tendons for the purpose of sample validation, which facilitates unravelling the

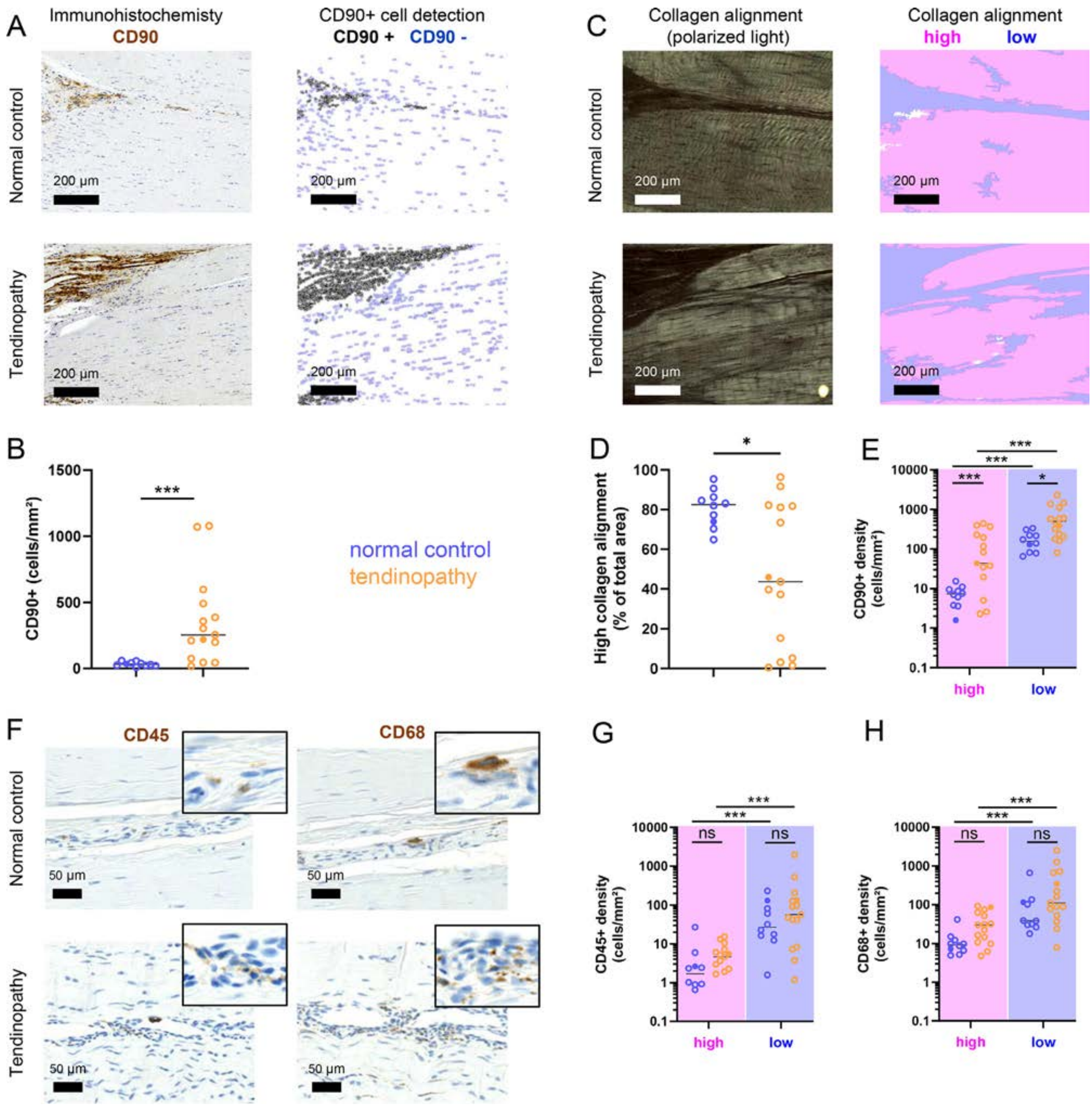

Figure 5. CD90$^+$, CD45$^+$, and CD68$^+$ cells are enriched in areas of low collagen alignment. Formalin-fixed paraffin-embedded human Achilles tendon sections were subjected to low temperature epitope retrieval before staining for CD90 (*THY1*), CD45 (*PTPRC*), and CD68. (A) Representative sections from normal control and tendinopathic Achilles tendons stained with CD90 and imaged with brightfield. quPath used to detect CD90$^+$ cells across entire sections to calculate (B) the density of CD90$^+$ cells. (C) The same CD90-stained slides were imaged with polarised light to identify regions of low versus high collagen alignment to calculate (D) the relative amount of collagen alignment and (E) the density of CD90$^+$ cells in each region. (F) Representative sections stained with CD45 and CD68 and imaged with brightfield. quPath used to detect CD45$^+$ and CD68$^+$ cells across the entire sections to calculate the density of (G) CD45$^+$ and H) CD68$^+$ cells across regions with high and low collagen alignment. The solid data points indicate the subjects for which the representative histology is shown. Data in (B) and (D) analysed with Mann-Whitney test. Data in (E, G, H) were analysed with 2-way analysis of variance after logarithmic transformation: (E) *P* value for variation from: patient = .0060, disease status = .0012, collagen alignment < .0001, interaction between disease status and collagen alignment = .0483; (G) *P* value for variation from: patient < .001, disease status = .652, collagen alignment < .0001, interaction between disease status and collagen alignment = .824; (H) *P* value for variation from: patient < .0001, disease status = .0450, collagen alignment < .0001, interaction between disease status and collagen alignment = .9837. Selected pairs are compared with Fisher least significant difference posttest.

pathogenesis of human tendinopathy. We validated histologic findings using complementary techniques.

Obtaining effective control tissue is a challenge in tendon research. In this study, we provide 2 levels of anatomically matched control tissue. Our normal control tissue, obtained from post mortem tissue donors, provides a unique reference point to identify pathogenic shifts in tendinopathic samples. A limitation when working with donor tissue is long warm ischaemia times. The addition of acquired spasticity controls provides evidence that tendon tissue is not strongly affected by ischaemia, as cell yield, viability and gene expression are comparable with that in normal donors. Thus, obtaining tendons from tissue donors or acquired spasticity patients are effective controls for Achilles tendinopathy studies.

Histology remains the gold standard to assess the pathologic status of tendons. In our hands, the original Bonar score performs well for Achilles tendinopathy; however, a plateau effect is seen in the scores. This is common with conventional histologic scores, such as the Bonar or Movin [13,31,32], due to measurement binning and scoring of the most pathologic areas.

By leveraging recent advancements in digital microscopy [18,33], our whole section BonAIr score overcomes these limitations. For example, we observed binning errors in the Bonar cellularity: all control tendons were found to be hypercellular, as defined as >30 cells per 10 × field of view in human gluteus medius tendon [14]. By quantitatively assessing cellularity, a significant difference was seen between patients and controls. Another example lies in scoring the most pathogenic area, which introduces sampling bias by ignoring tissue heterogeneity. We reduce this bias by moving from a single field of view of approximately 3 mm^2, to a whole section of at average 15 mm^2. An 'average' histopathologic evaluation that takes into account tissue heterogeneity should be a better predictor of pathologic cellular and molecular analyses done on larger portions of tissue. For example, single-cell sequencing data usually comes from large portions of digested/processed tissue, not the 'worst' region, and will therefore are likely contain some 'normal' cells.

In order to validate our BonAIr score, we compared features of the score to relevant cellular and biological readouts. In this study, we found the histology cell count to reflect the cell count of digested tissue. We further found other features of the BonAIr score to correlate well with the expression of relevant genes. Thus, we provide evidence that the BonAIr score is a good reflection of the biological status of human Achilles tendons.

Beyond supporting the BonAIr score, our data also generated insight into the biology of tendinopathy. First, we provide some evidence through IHC that immune cells in the tendon are found mostly in the IFM, regardless of the disease status. This spatial localisation is important when predicting cell-cell interactions, especially when proposing to manipulate the interactions as a therapeutic target. Second, in contradiction to the literature [34] some immune genes were not differentially expressed or were even undetectable. It is possible that immune involvement in Achilles tendinopathy is low relative to other tendons studied. It is also possible that the fibrotic stage of the disease has limited immune involvement relative to that seen during acute damage to tendons [35]. Third, persistent fibroblast activation has been reported to be a hallmark of tendinopathy [22,36]. Here we support this hypothesis by showing CD90+ stromal cells are expanded in Achilles tendinopathy, and that additional genes associated with fibroblast activation, such as *FAP, PDPN* and *TPPP3* are upregulated. We speculate that IFM-originating CD90 + fibroblasts play a pathogenic role in tendinopathy through ECM degeneration, as is seen in ECM degrading, invasive CD90 + synovial fibroblasts in arthritis [37]. Our CD90 IHC supports this notion by demonstrating $CD90^+$ cell enrichment in IFM-like regions. Future studies should deeply characterise these cells, as their presence may act as a prognostic biomarker, and targeting them may allow for regeneration of tendon tissue.

Our study is not without limitations. First, only end-stage tendinopathic samples were analysed, so the sensitivity of the BonAIr score to detect more subtle changes in the early stages of the disease has yet to be determined. Second, we could not find any correlation with patient-reported outcomes, especially with patient-reported pain, partially because not only our cohort is underpowered for this, but also because pain is mediated by nociceptors, whose cell body is located outside of the tendon proper, and are thus invisible to our analyses [38]. Despite this, we did see an upregulation of nerve growth factor, which is known to regulate nociceptor growth and subsequent pain [39].

In summary, we have automated histopathology analysis of human Achilles tendon tissue using AI integrated into open source software, quPath. This can be used to objectively score tendon samples before investment of costly molecular analyses. Future studies will need to determine whether this new method can be applied to other regions of the Achilles tendon, like the enthesis, or to tendons/ligaments of other anatomical locations. We propose using an automated, unbiased histology score system like the BonAIr for all fundamental research of tendons, as such an approach will greatly aid in the interpretation of molecular data, the results of which will be essential for therapeutic target identification for the treatment of tendinopathy.

Competing interests

AB receives consulting fees from CurveBeamAI and Cousin Surgery, honoraria from Newclip Techniques and DePuy Synthes (J&J MedTech) and is the vice-president of the International Weigh-bearing CT Society. All other authors have no competing interests to declare relevant to the content of this work.

Acknowledgements

We would like to thank the patients who participated in this study and Hilde Beele and Sarah Glorieux (Center for Human Body Material, University Hospital Ghent) for providing normal control human tendon tissue. This work was previously presented at the 1st TENET General Meeting & Conference (Salzburg, Austria) on March 11, 2024, and at the ORS Tendon Conference (Rochester, MN, USA) on May 30, 2024.

Contributors

GP (first author) conceptualised and designed this work; acquired, analysed, and interpreted the; data and wrote the first version of the manuscript. FS, JC, SD, IK, MV, and KL contributed to the design and execution of this work and reviewed the manuscript. AG and BP contributed to data analysis and interpretation and reviewed the manuscript. AV and JV contributed to data acquisition, analysis, and interpretation and reviewed the manuscript. AB, EV, and PB contributed to the conceptualisation of this work, data acquisition and interpretation, and reviewed the manuscript. EW, LP, JS, and KD contributed to the conceptualisation of this work and reviewed the manuscript. JC and FB contributed to conceptualisation and design of this work, data interpretation, and manuscript writing. DE and EG (shared last authors) shared the supervision of this work and equally contributed to the conceptualisation of this project, the interpretation of the data, and manuscript writing and revising and are the guarantors of this work.

Funding

This work has been funded by the following: Fonds Wetenschappelijk Onderzoek (FWO) Vlaanderen predoctoral mandate in fundamental research (grant number 11A2721N) (to GP) and research project (grant number G082023N) (to DE and EG), Fonds voor Wetenschappelijk Reumaonderzoek (FWRO) and King Baudouin Foundation (KBF) project funding (grant number 2020-J5820590-E010), and the Swiss National Science Foundation (SNSF) sinergia project grant (grant number 10000132). GP, EG, LP, EW, and JS acknowledge support from TENET COST Action CA22170 for fostering collaboration, networking opportunities, and for providing funds for attending conferences. The funders had no involvement in study design, collection, analysis, and interpretation of the data, in the writing of the report, or in the decision to submit the paper for publication.

Patient consent for publication

Only entirely anonymized images from which the individual cannot be identified are used. All patients gave written informed consent that anonymized information will be used in scientific publications.

Ethics approval

This work was approved by the central ethical board of the University Hospital Ghent and the local ethical board of the General Hospital (AZ) Sint-Lucas, Ghent and the General Hospital (AZ) Maria-Middelares, Ghent, before inclusion of the first patient. The Belgian Unique Number of this project is B6702020000966.

Provenance and peer review

Not commissioned; externally peer reviewed.

Data availability statement

All data relevant to the study are included in the article or uploaded as supplemental information. Raw, deidentified data available upon reasonable request made to the corresponding authors. Detailed protocols that allow to replicate this work are made available in the supplementary materials.

Supplementary materials

Supplementary material associated with this article can be found in the online version at doi:10.1016/j.ard.2025.01.027.

REFERENCES

[1] Albers IS, Zwerver J, Diercks RL, Dekker JH, Van den Akker-Scheek I. Incidence and prevalence of lower extremity tendinopathy in a Dutch general practice population: a cross sectional study. BMC Musculoskelet Disord 2016;17:16. doi: 10.1186/s12891-016-0885-2.
[2] Riel H, Lindstrøm CF, Rathleff MS, Jensen MB, Olesen JL. Prevalence and incidence rate of lower-extremity tendinopathies in a Danish general practice: a registry-based study. BMC Musculoskelet Disord 2019;20:239. doi: 10.1186/s12891-019-2629-6.
[3] Irby A, Gutierrez J, Chamberlin C, Thomas SJ, Rosen AB. Clinical management of tendinopathy: a systematic review of systematic reviews evaluating the effectiveness of tendinopathy treatments. Scand J Med Sci Sports 2020;30:1810–26. doi: 10.1111/sms.13734.
[4] Millar NL, Silbernagel KG, Thorborg K, Kirwan PD, Galatz LM, Abrams GD, et al. Tendinopathy. Nat Rev Dis Primers 2021;7:1. doi: 10.1038/s41572-020-00234-1.
[5] Van Der Vlist AC, Winters M, Weir A, Ardern CL, Welton NJ, Caldwell DM, et al. Which treatment is most effective for patients with Achilles tendinopathy? A living systematic review with network meta-analysis of 29 randomised controlled trials. Br J Sports Med 2021;55:249–55. doi: 10.1136/bjsports-2019-101872.
[6] Maffulli N, Longo UG, Kadakia A, Spiezia F. Achilles tendinopathy. Foot Ankle Surg 2020;26:240–9. doi: 10.1016/J.FAS.2019.03.009.
[7] Feldmann M, Maini RN, Soriano ER, Strand V, Takeuchi T. 25 years of biologic DMARDs in rheumatology. Nat Rev Rheumatol 2023;19:761–6 2023 19:12. doi: 10.1038/s41584-023-01036-x.
[8] Garcia-Melchor E, Cafaro G, MacDonald L, Crowe LAN, Sood S, McLean M, et al. Novel self-amplificatory loop between T cells and tenocytes as a driver of chronicity in tendon disease. Ann Rheum Dis 2021;80:1075–85. doi: 10.1136/annrheumdis-2020-219335.
[9] Kendal AR, Layton T, Al-Mossawi H, Appleton L, Dakin S, Brown R, et al. Multi-omic single cell analysis resolves novel stromal cell populations in healthy and diseased human tendon. Sci Rep 2020;10:1–14. doi: 10.1038/s41598-020-70786-5.
[10] Mimpen JY, Ramos-Mucci L, Paul C, Kurjan A, Hulley PA, Ikwuanusi CT, et al. Single nucleus and spatial transcriptomic profiling of healthy human hamstring tendon. FASEB J 2024;38:e23629. doi: 10.1096/fj.202300601RRR.
[11] Fu W, Yang R, Li J. Single-cell and spatial transcriptomics reveal changes in cell heterogeneity during progression of human tendinopathy. BMC Biol 2023;21:1–22. doi: 10.1186/s12915-023-01613-2.
[12] Mimpen JY, Baldwin MJ, Paul C, Ramos-Mucci L, Kujan A, Cohen CJ, et al. Exploring cellular changes in ruptured human quadriceps tendons at single-cell resolution. bioRxiv:2024.09.06.611599 [Preprint]. 2024 [cited 2024 Sep 8] [32p]. doi:10.1101/2024.09.06.611599
[13] Chatterjee M, Evans MK, Bell R, Nguyen PK, Kamalitdinov TB, Korntner S, et al. Histological and immunohistochemical guide to tendon tissue. J Orthop Res 2023;41:2114–32. doi: 10.1002/jor.25645.
[14] Fearon A, Dahlstrom JE, Twin J, Cook J, Scott A. The Bonar score revisited: region of evaluation significantly influences the standardized assessment of tendon degeneration. J Sci Med Sport 2014;17:346–50. doi: 10.1016/j.jsams.2013.07.008.
[15] Rio EK, Mc Auliffe S, Kuipers I, Girdwood M, Alfredson H, Bahr R, et al. ICON PART-T 2019-International Scientific Tendinopathy Symposium Consensus: recommended standards for reporting participant characteristics in tendinopathy research (PART-T). Br J Sports Med 2019;54:627–30. doi: 10.1136/bjsports-2019-100957.
[16] Maffulli N, Barrass V, Ewen SWB. Light microscopic histology of achilles tendon ruptures: A comparison with unruptured tendons. Am J Sports Med 2000;28:857–63. doi: 10.1177/03635465000280061401.
[17] Sethi PM, Sheth CD, Pauzenberger L, McCarthy MBR, Cote MP, Soneson E, et al. Macroscopic rotator cuff tendinopathy and histopathology do not predict repair outcomes of rotator cuff tears. Am J Sports Med 2018;46:779–85. doi: 10.1177/0363546517746986.
[18] Bankhead P, Loughrey MB, Fernández JA, Dombrowski Y, McArt DG, Dunne PD, et al. QuPath: open source software for digital pathology image analysis. Sci Rep 2017;7:16878. doi: 10.1038/S41598-017-17204-5.
[19] Reinbigler M, Cosette J, Guesmia Z, Jimenez S, Fetita C, Brunet E, et al. Artificial intelligence workflow quantifying muscle features on Hematoxylin–Eosin stained sections reveals dystrophic phenotype amelioration upon treatment. Sci Rep 2022;12:1–12. doi: 10.1038/s41598-022-24139-z.
[20] Patel D, Zamboulis DE, Spiesz EM, Birch HL, Clegg PD, Thorpe CT, et al. Structure-function specialisation of the interfascicular matrix in the human Achilles tendon. Acta Biomater 2021;131:381–90. doi: 10.1016/j.actbio.2021.07.019.
[21] Marelli-Berg FM, Clement M, Mauro C, Caligiuri G. An immunologist's guide to CD31 function in T-cells. J Cell Sci 2013;126:2343–52. doi: 10.1242/JCS.124099.
[22] Malmgaard-Clausen NM, Kjaer M, Dakin SG. Pathological tendon histology in early and chronic human patellar tendinopathy. Transl Sports Med 2022;2022:2799665. doi: 10.1155/2022/2799665.
[23] Dakin SG, Buckley CD, Al-Mossawi MH, Hedley R, Martinez FO, Wheway K, et al. Persistent stromal fibroblast activation is present in chronic tendinopathy. Arthritis Res Ther 2017;19:16. doi: 10.1186/s13075-016-1218-4.
[24] Ramos-Mucci L, Sarmiento P, Little D, Snelling S. Research perspectives—pipelines to human tendon transcriptomics. J Orthop Res 2022;40:993. doi: 10.1002/JOR.25315.
[25] Vandesompele J, De Preter K, Pattyn F, Poppe B, Roy NV, De Paepe A, et al. Accurate normalization of real-time quantitative RT-PCR data by geometric averaging of multiple internal control genes. Genome Biol 2002;3:1–12. doi: 10.1186/GB-2002-3-7-RESEARCH0034/COMMENTS.
[26] Hellemans J, Mortier G, De Paepe A, Speleman F, Vandesompele J. qBase relative quantification framework and software for management and automated analysis of real-time quantitative PCR data. Genome Biol 2007;8:R19. doi: 10.1186/gb-2007-8-2-r19.
[27] Viganò M, Perucca Orfei C, De Girolamo L, Pearson JR, Ragni E, De Luca P, et al. Housekeeping gene stability in human mesenchymal stem and tendon cells exposed to tenogenic factors. Tissue Eng Part C Methods 2018;24:360–7. doi: 10.1089/TEN.TEC.2017.0518.
[28] Sarver DC, Kharaz YA, Sugg KB, Gumucio JP, Comerford E, Mendias CL. Sex differences in tendon structure and function. J Orthop Res 2017;35:2117–26. doi: 10.1002/JOR.23516.

[29] Panina Y, Germond A, Masui S, Watanabe TM. Validation of common housekeeping genes as reference for qPCR gene expression analysis during iPS reprogramming process. Sci Rep 2018;8:8716. doi: 10.1038/S41598-018-26707-8.

[30] Quiñonez-Flores CM, López-Loeza SM, Pacheco-Tena C, Muñoz-Morales PM, Acosta-Jiménez S, González-Chávez SA. Stability of housekeeping genes in inflamed joints of spontaneous and collagen-induced arthritis in DBA/1 mice. Inflamm Res 2021;70:619–32. doi: 10.1007/S00011-021-01453-2.

[31] Movin T, Gad A, Reinholt FP, Rolf C. Tendon pathology in long-standing achillodynia. Biopsy findings in 40 patients. Acta Orthop Scand 1997;68:170–5. doi: 10.3109/17453679709004002.

[32] Cook JL, Feller JA, Bonar SF, Khan KM. Abnormal tenocyte morphology is more prevalent than collagen disruption in asymptomatic athletes' patellar tendons. J Orthop Res 2004;22:334–8. doi: 10.1016/j.orthres.2003.08.005.

[33] Aeffner F, Zarella MD, Buchbinder N, Bui MM, Goodman MR, Hartman DJ, et al. Introduction to digital image analysis in whole-slide imaging: a white paper from the Digital Pathology Association. J Pathol Inform 2019;10. doi: 10.4103/jpi.jpi_82_18.

[34] Akbar M, MacDonald L, Crowe LAN, Carlberg K, Kurowska-Stolarska M, Ståhl PL, et al. Single cell and spatial transcriptomics in human tendon disease indicate dysregulated immune homeostasis. Ann Rheum Dis 2021;80:1494. doi: 10.1136/ANNRHEUMDIS-2021-220256.

[35] Crosio G, Huang A. Innate and adaptive immune system cells implicated in tendon healing and disease. Eur Cell Mater 2022;43:39–52. doi: 10.22203/ECM.V043A05.

[36] Dakin SG, Newton J, Martinez FO, Hedley R, Gwilym S, Jones N, et al. Chronic inflammation is a feature of Achilles tendinopathy and rupture. Br J Sports Med 2018;52:359–67. doi: 10.1136/bjsports-2017-098161.

[37] Mizoguchi F, Slowikowski K, Wei K, Marshall JL, Rao DA, Chang SK, et al. Functionally distinct disease-associated fibroblast subsets in rheumatoid arthritis. Nat Commun 2018;9:789. doi: 10.1038/s41467-018-02892-y.

[38] Ackermann PW, Alim MA, Pejler G, Peterson M. Tendon pain − what are the mechanisms behind it? Scand J Pain 2023;23:14–24. doi: 10.1515/sjpain-2022-0018.

[39] Barker PA, Mantyh P, Arendt-Nielsen L, Viktrup L, Tive L. Nerve growth factor signaling and its contribution to pain. J Pain Res 2020;13:1223. doi: 10.2147/JPR.S247472.

Ann Rheum Dis 84 (2025) 877−878

Contents lists available at ScienceDirect

Annals of the Rheumatic Diseases

journal homepage: https://www.sciencedirect.com/journal/annals-of-the-rheumatic-diseases

Images in rheumatology

Hardening of the skin on neck and back

Ran Cui[1], Yan-Li Luo[2], Shu Qin[3], Sheng-Ming Dai[1,*]

[1] Department of Rheumatology and Immunology, Shanghai Sixth People's Hospital Affiliated to Shanghai Jiao Tong University School of Medicine, Shanghai, China
[2] Department of Pathology, Shanghai Sixth People's Hospital Affiliated to Shanghai Jiao Tong University School of Medicine, Shanghai, China
[3] Department of Plastic Surgery, Shanghai Sixth People's Hospital Affiliated to Shanghai Jiao Tong University School of Medicine, Shanghai, China

A man in his 60s presented to the rheumatology clinic complaining of a 10-year history of progressively hardening of the skin on neck and back. There had been no preceding fever, skin infection, or history of chemical product exposure. Physical examination revealed the skin of his posterior neck and entire back was thickened and firm (Fig A). There was associated erythema and peau d'orange appearance (Fig B,C). The neck mobility was limited. The patient had no skin changes elsewhere or sclerodactyly, and the nailfold capillaroscopy evaluation was normal (Fig D). Laboratory examinations showed that serum protein electrophoresis, antinuclear antibodies, erythrocyte sedimentation rate, syphilis, and HIV were all normal or negative. Given the presentation, morphea (localised scleroderma) and eosinophilic fasciitis were discussed. It is noteworthy that the

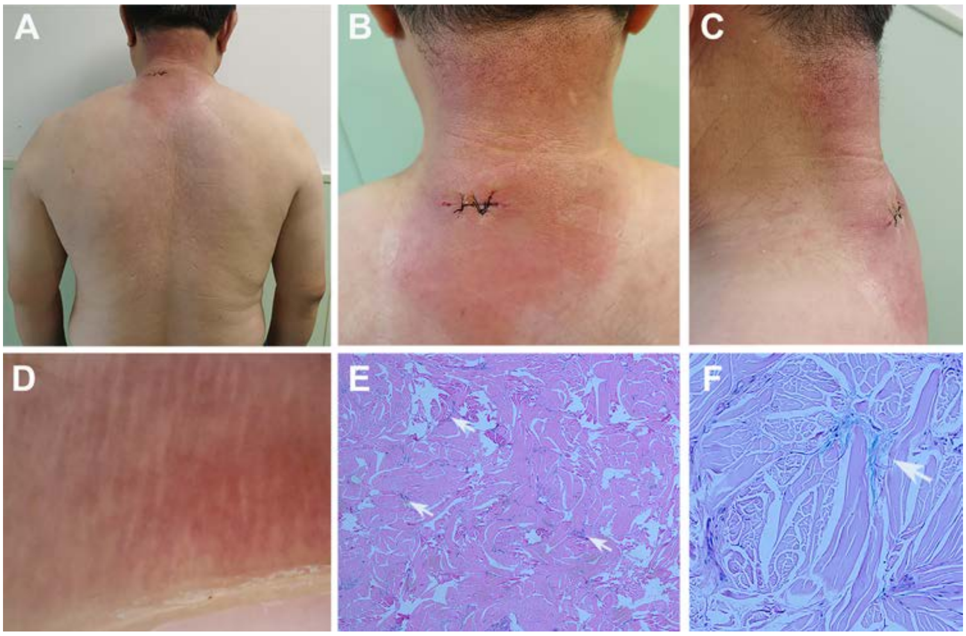

Figure. Diabetes-associated scleredema. (A-C) Hardening of the skin on neck and entire back; (D) Nailfold capillaroscopy evaluation for microvascular was normal; (E) Skin histopathology analysis revealed widened spaces between the thickening collagen bundles (H&E, × 200) and (F) mucin deposits (Alcian Blue PAS staining, × 400).

*Correspondence to Dr. Sheng-Ming Dai, Department of Rheumatology and Immunology, Shanghai Sixth People's Hospital Affiliated to Shanghai Jiao Tong University School of Medicine, Shanghai, China.

E-mail address: shengmingdai@163.com (S.-M. Dai).

Handling editor Josef S. Smolen.

https://doi.org/10.1016/j.ard.2025.02.003
Received 10 November 2024; Revised 27 January 2025; Accepted 2 February 2025

patient had a 26-year history of diabetes mellitus that was complicated by diabetic retinopathy, and his glycated haemoglobin level had been in the range of 8.7% to 13% (reference value, <6.5%). He had been treated with oral hypoglycaemic drugs and subcutaneous insulin for decades. Scleredema of Buschke was, therefore, suspected. A skin biopsy of the posterior neck showed markedly thickening of the collagen bundles (Fig E), separated from one another by prominent mucin-filled spaces (Fig F, arrows).

A diagnosis of scleredema of Buschke was made. It is a rare connective tissue disease and belongs to the spectrum of scleroderma-like disorders. The scleredema of Buschke is classified into three types. Type 1 occurs in patients with infections, particularly streptococcal [1]. Type 2 is usually caused by paraproteinaemia, monoclonal gammopathy, multiple myeloma. and amyloidosis [2]. Type 3 is referred to as diabetes-associated scleredema since it involves around 2.5% to 14% of diabetic patients [3]. It was hypothesised that high glucose levels induce nonenzymatic glycosylation of collagen in the dermis. Histological features include dermal fibrosis with thickened collagen bundles and variable amounts of mucin deposits. Tight control of diabetes is vital for diabetes-associated scleredema. Other therapies include phototherapy, intravenous immunoglobulin, corticosteroids, cyclosporine, and cyclophosphamide [3]. The patient received oral mycophenolate mofetil treatment (1 g twice a day), and was referred to the endocrinology clinic to improve his glycaemic control. Three months later, the patient reported that his symptoms were gradually subsided, and the glycated haemoglobin level was 8.3%.

Competing interests

All authors declare they have no competing interests.

Acknowledgements

We acknowledge the patient for giving his consent to this publication.

Contributors

RC, YLL, and SQ prepared the clinical image and the medical description of the case. All the authors were in charge of the patient during his hospitalisation. All authors discussed the manuscript and contributed to the final manuscript.

Funding

This project was supported by grant Shanghai Jiao Tong University School of Medicine Affiliated Sixth People's Hospital (No. ynhg202115).

Patient consent for publication

Consent obtained directly from the patient.

Ethics approval

As required for the publication of a clinical image, the patient had access to the manuscript and gave his written consent to the *BMJ* publication of images and/or information.

Provenance and peer review

Not commissioned; externally peer reviewed.

Orcid

Ran Cui: http://orcid.org/0000-0003-4923-5882
Sheng-Ming Dai: http://orcid.org/0000-0001-8876-4205

REFERENCES

[1] Jung SE, Kim YC. Scleredema of Buschke following streptococcal infection. Ann Dermatol 2015;27:478–80.
[2] Stables GI, Taylor PC, Highet AS. Scleredema associated with paraproteinaemia treated by extracorporeal photopheresis. Br J Dermatol 2000;142:781–3.
[3] Kennemer C, Pavlidakey P, Sami N. Successful treatment with IVIg therapy of diabetes-associated scleredema severe progressive case and review of the literature. Dermatol Ther 2017;30. doi: 10.1111/dth.12504.

Ann Rheum Dis 84 (2025) 879−880

Contents lists available at ScienceDirect

Annals of the Rheumatic Diseases

journal homepage: https://www.sciencedirect.com/journal/annals-of-the-rheumatic-diseases

Letter

Refractory MDA-5 dermatomyositis rapidly progressive interstitial lung disease successfully treated with emapalumab

Anti-melanoma antigen 5 antibody (MDA-5) dermatomyositis (DM) is a rare autoimmune disease that can be associated with rapidly progressive interstitial lung disease (RP-ILD) and a hyperferritinemic state [1]. Mortality rates remain high despite aggressive attempts at immunosuppression.

We present a 54-year-old female who developed gum swelling and rash on the lateral face and forehead. She worsened for 2 months and was admitted with fever, severe hepatic injury (aspartate aminotransferase 2442 unit/L, alanine aminotransferase 1482 unit/L, alkaline phosphatase 200 unit/L, gamma-glutamyl transferase 258 unit/L, bilirubin 0.5 mg/dL), and elevated ferritin levels (11,502 ng/mL). Aldolase was elevated, presumed secondary to liver injury, as she had no weakness. Infectious work-up was unrevealing. Liver biopsy showed lobular disarray and extensive hepatocyte ballooning without significant inflammation. She was given steroids for hemophagocytic lymphohistiocytosis (HLH) of presumed viral aetiology with mild improvement and discharged.

During hospitalisation, chest computed tomography (CT) was concerning for early interstitial lung disease (ILD). Outpatient labs showed positive anti-MDA-5 antibody (83 SI) and anti-Ro52 antibody. Now, 6 months from initial symptoms, she had lower extremity weakness and dysphagia. Creatinine kinase and aldolase levels were normal. Ferritin levels remained high (1000s-2000s ng/mL), and liver enzymes remained elevated with fluctuating severity. She had Gottron's sign and was diagnosed with MDA-5 DM. She was admitted for steroids, intravenous immunoglobulin, cyclophosphamide, and tacrolimus. Although her dysphagia and weakness improved, she developed new oxygen requirements and continued to have elevated levels of ferritin, liver enzymes, and lactate dehydrogenase.

MDA-5 DM has been associated with hyperferritinemic states, satisfying criteria for secondary HLH (macrophage activation syndrome) in its most severe form [1]. Liver biopsies commonly show hepatic ballooning, as in our patient [2]. We started anakinra and ruxolitinib (transitioned to tofacitinib for insurance purposes). However, inflammatory markers minimally responded, and respiratory status continued to worsen. Plasmapheresis achieved an unsustained response in inflammatory markers. She had increasing oxygen requirements with worsening pulmonary infiltrates suggestive of RP-ILD.

Emapalumab is an anti-interferon-gamma monoclonal antibody that is approved for use in HLH. De Benedetti et al [3] demonstrated efficacy of emapalumab in patients with refractory macrophage activation syndrome secondary to systemic

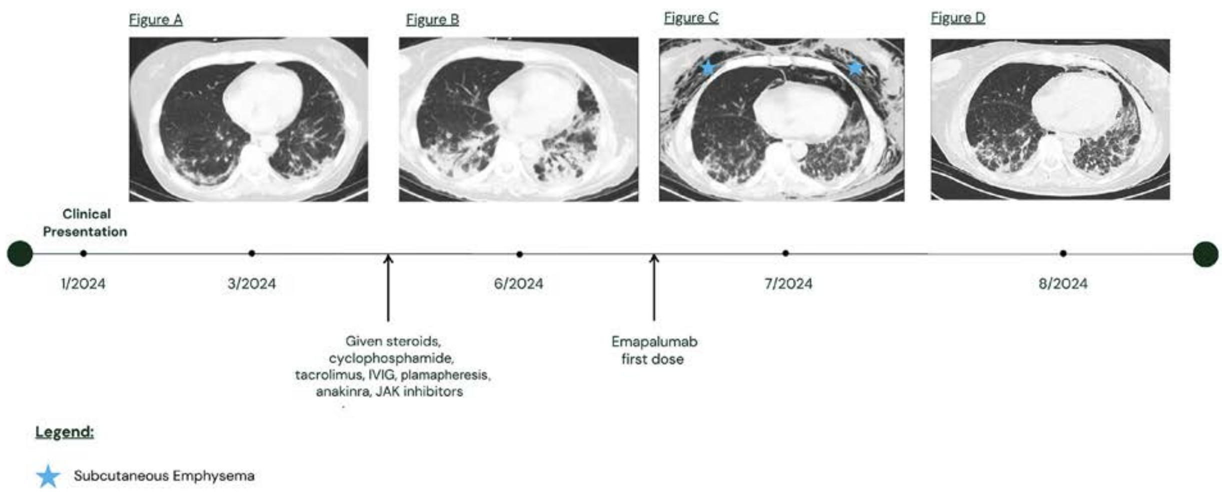

Figure. CT chest findings. A, Early disease onset with nonspecific interstitial pneumonia (NSIP) features that preceded respiratory symptoms. B, Rapidly progressive ILD with features of NSIP and organising pneumonia (OP) in bilateral lower lobes despite aggressive combination treatment of immunosuppression. C, Improvement of the lower lobe OP infiltrates after emapalumab dose but with pneumomediastinum and left pneumothorax complicated by extensive subcutaneous emphysema (marked with blue stars). D, Sustained radiographic improvement of OP with resolution of left pneumothorax and minimal residual pneumomediastinum and subcutaneous emphysema. CT, computed tomography; ILD, interstitial lung disease; IVIG, intravenous immunoglobulin.

https://doi.org/10.1016/j.ard.2025.01.010
Received 5 October 2024; Revised 2 December 2024; Accepted 23 December 2024

juvenile idiopathic arthritis or adult-onset still's disease. Interferon-gamma has been implicated in the pathophysiology of MDA-5-associated RP-ILD. A retrospective study found MDA-5 DM patients produce antibodies that directly stimulate interferon-gamma production [4]. Moreover, a case−control study evaluated the association of cytokines with CT scores in DM patients with RP-ILD and found interferon-gamma correlated with severity of ground glass opacities. Immunohistochemical staining from MDA-5 DM RP-ILD lung tissue showed numerous interferon-gamma positive histiocytes compared with other DM phenotypes [5].

Given these findings, we started emapalumab utilising dosing described by De Benedetti et al [3]. By the second dose, there was significant improvement in cutaneous vasculopathy, respiratory symptoms, and oxygen requirements. Radiographically, there was marked improvement in consolidations by week 4 (Fig). Her course was complicated by significant spontaneous pneumomediastinum, which has been described in MDA-5 DM with RP-ILD, which eventually resolved over 1 month [6]. The patient was discharged to continue the emapalumab taper outpatient; remains on tofacitinib, a prednisone taper; and was transitioned from cyclophosphamide to rituximab for a better safety profile. Her inflammatory markers continue to improve slowly with her ferritin level now 352 ng/mL (6 months from her MDA-5 DM diagnosis).

To our knowledge, this is the first report of emapalumab used for MDA-5 DM with RP-ILD. As interferon-gamma may be involved in the pathogenesis of MDA-5 DM ILD, further research by way of clinical trials would be beneficial. With effective treatment strategies limited, particularly in advanced presentations, this novel treatment may improve outcomes in an otherwise deadly disease.

Contributors

All authors contributed by drafting, revising, and approving the final manuscript for submission. All listed authors accept full responsibility for the accuracy of this reports, had access to all relevant clinical data, and approved this submission for publication. All listed authors will be guarantors.

Competing interests

None declared.

Funding

No funding was obtained for this article.

Patient consent for publication

Patient consent obtained for publication.

Ethics approval

Ethics approval via patient consent for publication.

Provenance and peer review

Not commissioned; externally peer reviewed.

REFERENCES

[1] Fuzzi E, Gatto M, Zen M, Franco C, Zanatta E, Ghirardello A, Doria A. Anti-MDA5 dermatomyositis: an update from bench to bedside. Curr Opin Rheumatol 2022;34:365–73.
[2] Nagashima T, Kamata Y, Iwamoto M, Okazaki H, Fukushima N, Minota S. Liver dysfunction in anti-melanoma differentiation-associated gene 5 antibody-positive patients with dermatomyositis. Rheumatol Int 2019;39:901–9.
[3] De Benedetti F, Grom AA, Brogan PA, Bracaglia C, Pardeo M, Marucci G, et al. Efficacy and safety of emapalumab in macrophage activation syndrome. Ann Rheum Dis 2023;82:857–65.
[4] Coutant F, Bachet R, Pin JJ, Alonzo M, Miossec P. Monoclonal antibodies from B cells of patients with anti-MDA5 antibody-positive dermatomyositis directly stimulate interferon gamma production. J Autoimmun 2022;130:102831.
[5] Ishikawa Y, Iwata S, Hanami K, Nawata A, Zhang M, Yamagata K, et al. Relevance of interferon-gamma in pathogenesis of life-threatening rapidly progressive interstitial lung disease in patients with dermatomyositis. Arthritis Res Ther 2018;20:240.
[6] Yang J, Yan B. Rare complications of anti-melanoma differentiation-associated gene 5 antibody-positive dermatomyositis: time to nip them in the bud. Front Immunol 2022;13:1009546.

Jennifer Concepcion[1], Miriam Marti[3], Susan Vehar[2], Kelly Corbitt[3,*]
[1] *Internal Medicine, University of Miami Department of Medicine, Miami, Florida, USA*
[2] *Division of Pulmonary, Critical Care and Sleep Medicine, University of Miami Miller School of Medicine, Miami, Florida, USA*
[3] *Division of Rheumatology, University of Miami Miller School of Medicine, Miami, Florida, USA*
*__Correspondence to__ Dr. Kelly Corbitt, Division of Rheumatology, University of Miami Miller School of Medicine, Miami, Florida, USA.
E-mail address: KKC51@med.miami.edu (K. Corbitt).

Ann Rheum Dis 84 (2025) 881−882

Contents lists available at ScienceDirect

Annals of the Rheumatic Diseases

journal homepage: https://www.sciencedirect.com/journal/annals-of-the-rheumatic-diseases

Letter

Anti-myxovirus resistance protein 1: a novel biomarker for autoimmune myositis and interstitial lung disease in systemic lupus erythematosus

Given the heterogeneous nature of systemic lupus erythematosus (SLE), identification and subclassification of patients with uncommon but highly morbid manifestations could help identify subsets of patients with distinct pathophysiologic mechanisms. Autoimmune myopathy (AIM) and interstitial lung disease (ILD) in SLE are associated with significant morbidity and poor outcomes [1]. Human myxovirus resistance protein 1 (MxA) is an interferon-induced GTPase, which is upregulated during myxovirus infections and inhibits viral transcription and replication [2]. MxA is also upregulated in muscle, blood, and skin in patients with SLE-related AIM and dermatomyositis [3,4]. Antibodies directed against MxA (anti-MxA) have recently been reported in idiopathic interstitial pneumonia [5]. We hypothesized that dysregulated interferon activity and upregulated MxA expression, possibly in the setting of a viral trigger, could result in anti-MxA antibodies in SLE-associated AIM and ILD and that anti-MxA antibodies may be a promising biomarker in this SLE subset.

In our recently published case-cohort study (N = 550), we identified Krebs von den Lungen-6 (KL-6), as well as autoantibodies to Ro52/tripartite motif containing-21 (anti-Ro52/TRIM21) and Ku (anti-Ku), as potential biomarkers in SLE-associated AIM and/or ILD [6]. In this cohort, 13 patients developed AIM and/or ILD (13/550, 2.4%, as previously defined in the article by Cotton et al [6]; Supplementary Table S1). To determine how anti-MxA antibodies compared with these previously identified biomarkers in this SLE cohort, we tested for anti-MxA antibodies by addressable laser bead immunoassay (ALBIA) using full-length human recombinant protein on (1) baseline samples (first visit starting from January 2000, or enrolment if after this date) and (2) one follow-up sample (randomly selected between baseline and the date of AIM and/or ILD diagnosis or December 31, 2017, in those who did not develop AIM and/or ILD; Supplementary Table S1). We validated our ALBIA results using a dot blot immunoassay (Supplementary Fig 1). In total, there were 19 (19/84, 22.6%) SLE patients who expressed anti-MxA antibodies (clinical features and serologic profiles are described in Supplementary Table S2). SLE patients who developed AIM and/or ILD on follow-up (12 cases; 1 case did not have available sera for testing; the mean [SD] time between SLE diagnosis and AIM and/or ILD onset was 18.8 [18.9] years) were compared with a randomly selected subcohort of SLE patients (72 controls; the mean [SD] duration between SLE diagnosis and the end of the study period was 15.9 [5.9] years) (Supplementary Table S3).

At baseline, we noted a greater proportion of anti-MxA antibody positivity among patients with AIM and/or ILD compared with other SLE controls (50.0% vs 9.7%, respectively; crude odds ratio, 9.3; 95% CI, 2.3-36.7). When anti-MxA antibodies were assessed at baseline and follow-up, almost all AIM and/or ILD cases (11/12, 91.7%) were anti-MxA antibody-positive during their disease course (ILD alone 7/8, 87.5%; AIM alone 2/2, 100%; AIM and ILD 2/2, 100%), while only 11.1% (8/72) of SLE controls expressed anti-MxA antibodies. Anti-MxA antibody positivity was highly sensitive (91.7%; 95% CI, 61.5%-99.9%) and specific (88.9%; 95% CI, 79.3%-95.1%) for developing AIM and/or ILD, with a receiver operating characteristic area under the curve (ROC AUC) of 0.90 (95% CI, 0.81-0.99), which outperformed the ROC AUC of previously identified biomarkers KL-6 (0.65; 95% CI, 0.50-0.80), anti-Ku (0.53; 95% CI, 0.45-0.62), and anti-Ro52/TRIM21 (0.60; 95% CI, 0.44-0.75) (Fig).

In summary, anti-MxA antibodies appear to be a highly sensitive and specific biomarker for the development of AIM and/or ILD in SLE, outperforming other reported biomarkers. Interestingly, MxA functions as an antiviral protein that is upregulated in the setting of myxovirus infections [2]. The expression of anti-MxA antibodies hints at the possibility that aberrant interferon activity in the setting of a viral infection may act as the stimulus for autoimmunity in this subgroup of SLE; however, further studies are needed to explore this hypothesis. As a future direction, we will evaluate anti-MxA antibodies in patients with idiopathic inflammatory myopathies, including dermatomyositis and other systemic autoimmune rheumatic diseases with and without ILD. We will also validate the performance of our ALBIA results using alternate assays for anti-MxA antibody testing, as well as assess for sarcoplasmic MxA protein expression in muscle biopsies from anti-MxA antibody-positive SLE patients with AIM. Furthermore, the clinical utility of anti-MxA antibodies in AIM and ILD will need to be investigated in a larger SLE cohort and non-SLE patients.

Competing interests

MJF is the medical director of Mitogen Diagnostics Corporation and a consultant for Werfen. MYC is the associate director of MitogenDx and a consultant for Werfen, AstraZeneca, GlaxoSmithKline Inc, Celltrion, Organon, and Mallinckrodt Pharmaceuticals.

https://doi.org/10.1016/j.ard.2025.01.031

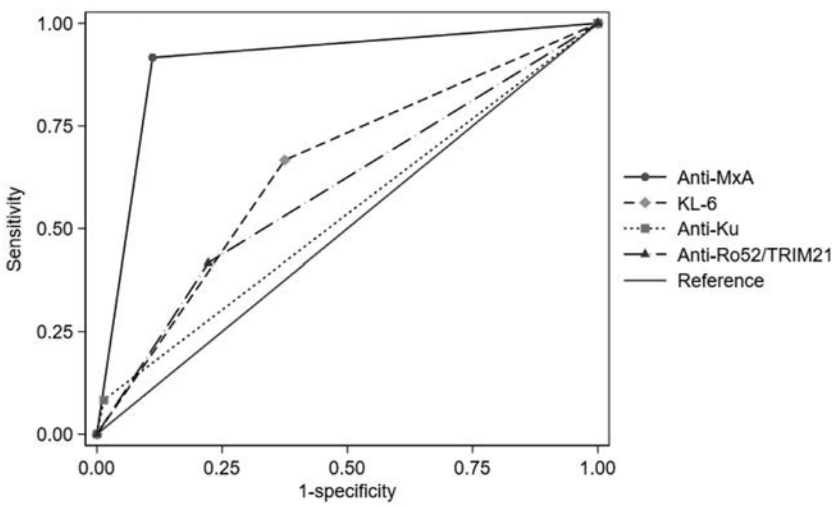

Figure. Antibodies directed against myxovirus resistance protein 1 (anti-MxA) expression studied over the disease course was highly associated with the development of autoimmune myositis (AIM) and/or interstitial lung disease (ILD) in systemic lupus erythematosus (N = 550). The receiver operating characteristic area under the curve (ROC AUC) for predicting the development of AIM and/or ILD for anti-MxA was 0.90 (95% CI, 0.81-0.99), which was significantly higher than the ROC AUC for Krebs von den Lungen-6 (KL-6; 0.65 [95% CI, 0.50-0.80]), autoantibodies to Ku (anti-Ku; 0.53 [95% CI, 0.45-0.62]), and autoantibodies to Ro52/tripartite motif containing-21 (anti-Ro52/TRIM21; 0.60 [95% CI, 0.44-0.75]).

Acknowledgements

We thank Meifeng Zhang and Jean Kawasoe for their technical assistance.

Contributors

EK conceptualized the study, contributed to the study design, and drafted the manuscript. MJF and SB contributed to the study design and reviewed the manuscript. YSP performed statistical analysis and reviewed the manuscript. MYC was the principal investigator and the guarantor for this study, conceptualized the study, contributed to the study design, and reviewed the manuscript. The remaining authors were involved in patient recruitment and data collection and reviewed the manuscript.

Funding

This work was supported by the McGill University Health Center Lupus Clinic; research activities are funded by the Singer Family Fund for Lupus Research.

Patient consent for publication

Patients or the public were not involved in the design, conduct, reporting, or dissemination plans of our research.

Ethics approval

Approval for our study was obtained from the research ethics board of McGill University Health Centre Research Institute.

Provenance and peer review

Not commissioned; externally peer reviewed.

Data availability statement

Data are available upon request from the corresponding author.

Supplementary materials

Supplementary material associated with this article can be found in the online version at doi:10.1016/j.ard.2025.01.031.

REFERENCES

[1] Dayal NA, Isenberg DA. SLE/myositis overlap: are the manifestations of SLE different in overlap disease? Lupus 2002;11(5):293–8.
[2] Haller O, Kochs G. Human MxA protein: an interferon-induced dynamin-like GTPase with broad antiviral activity. J Interferon Cytokine Res 2011;31(1):79–87.
[3] Xing C, Trivedi J, Bitencourt N, Burns DK, Reisch JS, Cai C. Myxovirus resistance protein A (MxA) expression in myositides: sarcoplasmic expression is common in both dermatomyositis and lupus myositis. Muscle Nerve 2024;69(5):548–55.
[4] Lambers WM, de Leeuw K, Doornbos-van der Meer B, Diercks GFH, Bootsma H, Westra J. Interferon score is increased in incomplete systemic lupus erythematosus and correlates with myxovirus-resistance protein A in blood and skin. Arthritis Res Ther 2019;21(1):260.
[5] Arai T, Hirose M, Hamano Y, Kagawa T, Murakami A, Kida H, et al. Anti-myxovirus resistance protein-1 immunoglobulin A autoantibody in idiopathic pulmonary fibrosis. Can Respir J 2022;2022:1107673.
[6] Cotton T, Fritzler MJ, Choi MY, Zheng B, Niaki OZ, Pineau CA, et al. Serologic phenotypes distinguish systemic lupus erythematosus patients developing interstitial lung disease and/or myositis. Lupus 2022;31(12):1477–84.

Eugene Krustev[1], Marvin J. Fritzler[1], Sasha Bernatsky[2], Yvan St. Pierre[1], Paul J. Sciore[3], Evelyne Vinet[2,4], Christian A. Pineau[2], Arielle Mendel[2,4], Fares Kalache[2], Louis-Pierre Grenier[2], Thaisa Cotton[2], Omid Zahedi Niaki[5], May Y. Choi[1,6,*]

[1] *Department of Medicine, Cumming School of Medicine, University of Calgary, Calgary, AB, Canada*
[2] *Division of Rheumatology, Department of Medicine, McGill University, Montreal, QC, Canada*
[3] *MitogenDx, Calgary, AB, Canada*
[4] *Centre for Outcomes Research and Evaluation, McGill University Health Centre, Montreal, QC, Canada*
[5] *Division of Rheumatology, University of British Columbia, Vancouver, BC, Canada*
[6] *McCaig Institute for Bone and Joint Health, University of Calgary, Calgary, AB, Canada*

*__Correspondence to__ Dr May Y. Choi, Division of Rheumatology, Department of Medicine, Cumming School of Medicine, University of Calgary, Calgary, AB, Canada.
E-mail address: may.choi@ucalgary.ca (M.Y. Choi).